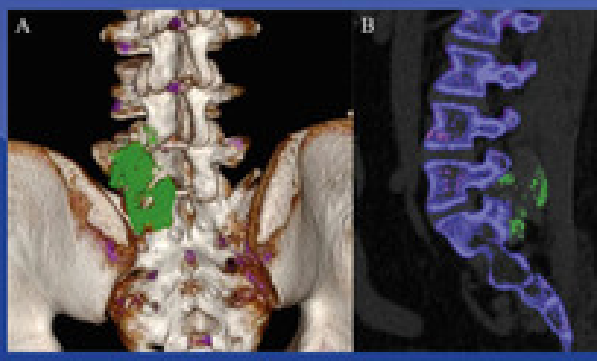
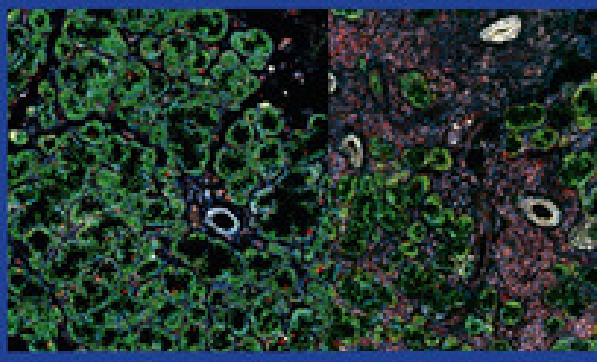
AUGUST 2025
VOLUME 84
ISSUE
8

# ANNALS OF THE RHEUMATIC DISEASES

THE EULAR JOURNAL



ELSEVIER

eular
EUROPEAN ALLIANCE OF ASSOCIATIONS FOR RHEUMATOLOGY

The home of innovative rheumatology research

Ann Rheum Dis 84 (2025) 1287–1292

Contents lists available at ScienceDirect

Annals of the Rheumatic Diseases

journal homepage: https://www.sciencedirect.com/journal/annals-of-the-rheumatic-diseases

Review

# Pseudogout, chondrocalcinosis, CPPD et al: crystal clear. . . or clear as mud?—The time has come to reconsider the nomenclature of calcium pyrophosphate deposition

Silvia Sirotti[1,2], Charlotte Jauffret[3,4], Antonella Adinolfi[5], Edoardo Cipolletta[6,7], Daniele Cirillo[8], Luca Ingrao[8], Alessandro Lucia[8], Emilio Filippucci[6], Tristan Pascart[3], Sara K Tedeschi[9,10], Robert Terkeltaub[11], Nicola Dalbeth[12], Georgios Filippou[1,2,*]

[1] *Department of Rheumatology, IRCCS Galeazzi –Sant'Ambrogio Hospital, Milan, Italy*
[2] *Department of Biomedical and Clinical Sciences, Università degli Studi di Milano, Milan, Italy*
[3] *Rheumatology Department, Lille Catholic University, Saint Philibert Hospital, EA 7446 - ETHICS, Lille, France*
[4] *University of Lille, ULR 2694 –METRICS, CERIM, Lille, France*
[5] *Rheumatology Unit, ASST Grande Ospedale Metropolitano Niguarda, Milan, Italy*
[6] *Rheumatology Unit, Department of Clinical and Molecular Sciences, Polytechnic University of Marche, Ancona, Italy*
[7] *Academic Rheumatology, University of Nottingham, Nottingham, UK*
[8] *Department of Clinical Sciences and Community Health, Università degli Studi di Milano, Milan, Italy*
[9] *Division of Rheumatology, Inflammation and Immunity, Brigham and Women's Hospital, Boston, MA, USA*
[10] *Harvard Medical School, Boston, MA, USA*
[11] *Department of Medicine, Division of Rheumatology, Autoimmunity, and Inflammation, University of California San Diego, La Jolla, CA, USA*
[12] *Department of Medicine, University of Auckland, Auckland, New Zealand*

ARTICLE INFO

ABSTRACT

Scientific interest in calcium pyrophosphate deposition (CPPD) has been limited by several challenges. These include difficulties in diagnosis due to diverse clinical presentations, the lack of classification criteria, the absence of standardised diagnostic modalities, underrecognition in clinical care, and, most significantly, the lack of evidence-based treatments. Consequently, CPPD was often regarded as the 'poor cousin' of gout. Fortunately, in recent years, CPPD has garnered increased attention from the rheumatology community. Milestones such as the first American College of Rheumatology/European Alliance of Association for Rheumatology classification criteria, the European Alliance of Association for Rheumatology recommendations for the use of imaging in clinical practice, validated OMERACT ultrasound definitions and scoring system, and the OMERACT core domain sets for CPPD have significantly advanced the field. Yet, unresolved issues regarding CPPD nomenclature hold back advancement in both research and clinical practice. The terminology surrounding CPPD remains inconsistent in the scientific literature, with numerous terms and acronyms used to describe the condition and its manifestations. For example, many 'pseudosyndromes' (eg, pseudogout) and purely radiographic descriptors (eg, chondrocalcinosis) are still commonly used by clinicians and researchers interchangeably,

*Correspondence to Dr Georgios Filippou, Department of Biomedical and Clinical Sciences, Università degli Studi di Milano, Milan, Italy.
*E-mail address:* georgios.filippou@unimi.it (G. Filippou).
**Handling editor** Josef S Smolen

https://doi.org/10.1016/j.ard.2025.04.004

0003-4967/© 2025 The Authors. Published by Elsevier B.V. on behalf of European Alliance of Associations for Rheumatology (EULAR). This is an open access article under the CC BY license (http://creativecommons.org/licenses/by/4.0/)

as either the name of the condition or one of its clinical or radiographic manifestations. This lack of standardisation complicates communication among health care professionals, researchers, and between doctors and patients, creating insurmountable barriers to effective care and research advances. In this viewpoint, we highlight the value of standardised terminology, drawing parallels with other rheumatic diseases. We aimed to explore the historical evolution of CPPD nomenclature, assess the impact of previous standardisation efforts, and propose a possible way for a common language.

Language is the most essential tool for communication. When different terms are used to describe the same disease or aspect of a condition, especially with inconsistent or inhomogeneous terminology, clarity is diminished, and effective communication is compromised [1]. This issue affects not only technical terminology to be used among health care professionals but, even more critically, communication with patients. In the case of calcium pyrophosphate deposition (CPPD), the problem extends beyond inconsistent terminology to include the multiple abbreviations used to refer to both the crystals and the condition itself [2]. The situation mirrors the biblical Tower of Babel, where fragmented language created confusion and hindered understanding [3].

## THE VALUE OF A COMMON TERMINOLOGY: INSIGHTS FROM OTHER RHEUMATIC DISEASES

The importance of clear and consistent terminology is underscored by other examples in rheumatology. One notable shift is the transition from ankylosing spondylitis to axial spondyloarthritis, which reflects a deliberate effort to adopt a more precise language for describing disease by emphasising the anatomic focus of disease (axial) and removing the term ankylosing, which carries a negative prognostic connotation, as the associated degree of structural damage may take years to develop or may not occur at all [4]. The standardisation of the nomenclature of axial spondyloarthritis has been supported by numerous publications on the topic and has been embraced by international scientific groups. For instance, the ASAS working group renamed itself from 'ASsessment of Ankylosing Spondylitis' working group to 'Assessment of SpondyloArthritis International Society'. Furthermore, there has been a proposal to officially redefine the ASDAS acronym, changing its meaning from 'Ankylosing Spondylitis Disease Activity Score' to 'Axial Spondyloarthritis Disease Activity Score'. These initiatives have significantly increased the use of the term axial spondyloarthritis in both clinical practice and scientific literature, promoting greater alignment in the field.

## CPPD TERMINOLOGY: FROM THE ORIGINS TO THE CURRENT DISARRAY

In 1962, McCarty et al [5] coined the term pseudogout to describe acute arthritis flares resembling gout but caused by non-urate crystals. They later identified these crystals as calcium pyrophosphate dihydrate and introduced the term CPPD to refer to the crystals [6]. They proposed 5 clinical phenotypes, many of which were labelled with the prefix pseudo due to their resemblance to other rheumatic conditions [7]. The condition was defined as calcium pyrophosphate dihydrate crystal deposition disease [7], although some called it pyrophosphate arthropathy [8] or pyrophosphate synovitis [9]. Moreover, the term chondrocalcinosis, initially used to describe the radiographic appearance of CPPD [10], became common to describe the condition itself [11] (Fig).

In 2011, a European Alliance of Association for Rheumatology (EULAR) CPPD task force attempted to standardise CPPD nomenclature via a consensus paper based on expert opinion

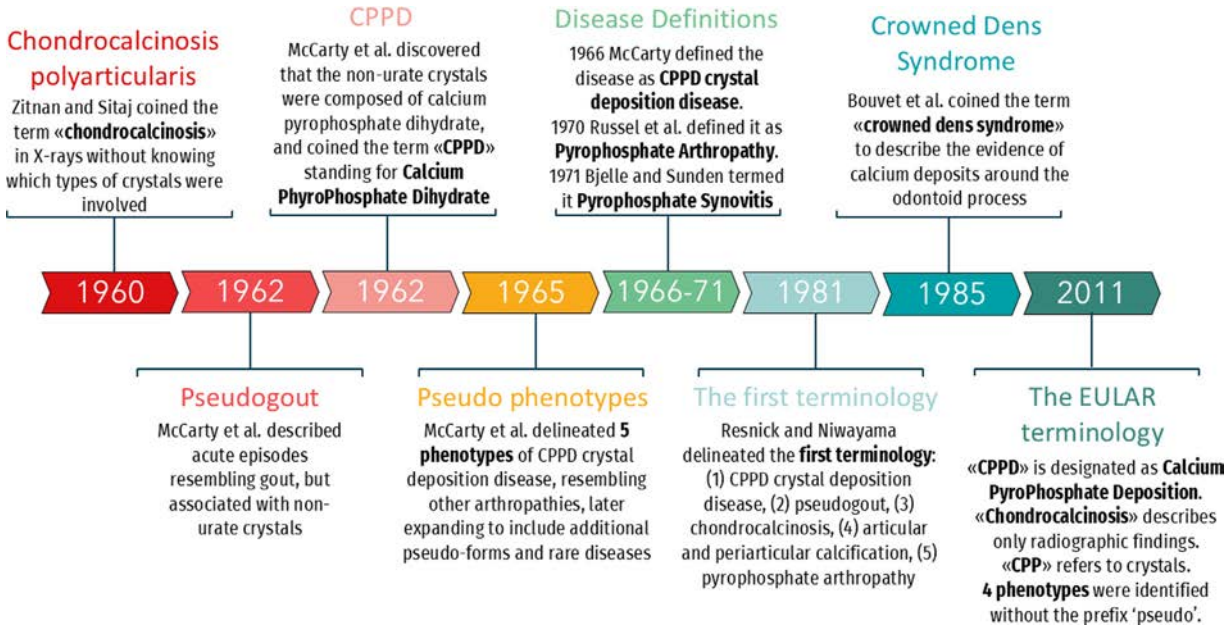



**Figure.** Timeline of the fundamental steps in calcium pyrophosphate deposition description. Adapted from Sirotti et al [3]. CPDD, calcium pyrophosphate deposition disease; CPP, calcium pyrophosphate; EULAR, European Alliance of Association for Rheumatology.

[12]. Their recommendations aimed to eliminate the pseudo prefix and restrict the term chondrocalcinosis to describe radiographic findings (Fig). For the first time, CPPD was specified to stand for calcium pyrophosphate (CPP) deposition, referring to the umbrella term for all instances of CPP crystal occurrence, including the asymptomatic form, while the pathogenic crystals were referred to as CPP crystals. Moreover, the task force outlined 4 distinct phenotypes: (i) asymptomatic CPPD, (ii) osteoarthritis with CPPD, (iii) acute CPP crystal arthritis, and (iv) chronic CPP crystal inflammatory arthritis.

A recent systematic literature review (SLR) examined the terminology commonly used to describe CPPD, revealing significant inconsistencies across the literature [13]. Among 886 articles analysed from 2000 to 2022, the most frequent label used to designate the condition remains pseudogout, appearing in nearly half of the article, followed by chondrocalcinosis and calcium pyrophosphate deposition disease (CPDD). Controversy also surrounds the appropriate abbreviation for the condition −CPPD or CPDD? Although CPPD was the most used abbreviation, it predominantly referred to calcium pyrophosphate deposition disease, rather than calcium pyrophosphate deposition as recommended by the EULAR. This reflects ongoing confusion on the significance of the final letter 'D'. Another key issue identified was the inconsistent use of the term chondrocalcinosis, which has been applied variably to describe the condition itself, its elements, and its states. Furthermore, the frequent use of pseudoterms to describe different condition's states remains prevalent in the literature.

## IMPACT OF THE 2011 EULAR TERMINOLOGY RECOMMENDATION

The SLR demonstrated that terms such as chondrocalcinosis and pseudogout are still deeply rooted in the terminology despite the 2011 EULAR recommendations [12]. To evaluate the impact of these recommendations, a comparison of data from before and after 2011 was conducted, driving this viewpoint (Table). Between 2000 and 2011, the most frequently used term to describe the condition was pseudogout (52%), followed by chondrocalcinosis (33%) and calcium pyrophosphate dihydrate crystal deposition disease (19.7%). Unfortunately, only a slight improvement was observed after 2011. While the use of pseudogout decreased to 43.7%, it remained the most used term, followed by calcium pyrophosphate deposition disease (31.5%) and chondrocalcinosis (22.8%). The term proposed by the EULAR taskforce, calcium pyrophosphate deposition, was scarcely adopted, appearing in just 1.1% of articles before 2011 and increasing to only 5% after 2011.

The abbreviation CPPD also exhibited a shift in usage before and after 2011. Before 2011, it predominantly referred to calcium pyrophosphate dihydrate in the context of crystals, whereas after 2011, it was used to describe the condition as calcium pyrophosphate deposition disease. However, this usage still does not align precisely with the EULAR recommendation, which advocated for calcium pyrophosphate deposition, omitting the term disease, as CPPD was meant to include also the asymptomatic form.

In contrast, terms referring to crystals showed better adherence to the recommendations. Before 2011, calcium pyrophosphate dihydrate (abbreviated as CPPD) was the most frequently used term, but it transitioned to calcium pyrophosphate with the abbreviation CPP after 2011, in line with EULAR's guidance.

The use of pseudoterminology has lessened for describing certain phenotypes following the publication of the EULAR recommendations. Nevertheless, pseudogout remained the most used term to describe 'an episode of acute arthritis' and 'recurrent acute arthritis' both before and after 2011. The recommended term, acute CPP crystal arthritis, was found in only 1.2% of articles before 2011 and increased to 32.9% of articles after 2011−reflecting the research community's openness to new terminology for this condition state. A more significant shift occurred in the terminology for 'persistent inflammatory arthritis'. Before 2011, this was predominantly referred to as pseudorheumatoid arthritis, whereas after the EULAR recommendations, it was more frequently labelled as chronic CPP crystal arthritis. Similarly, 'osteoarthritis related to CPP crystals' underwent a terminological change. Before 2011, it was described using the pseudoterm pseudo-osteoarthritis. After 2011, it was more commonly referred to as CPPD-related/associated osteoarthritis, a term more closely aligned with EULAR's recommendations.

These analyses revealed that the EULAR recommendations had a moderate impact on scientific language and have failed to replace entrenched habits. The reason for this may be attributed to several factors: the absence of subsequent articles emphasising the importance of standardising terminology, insufficient endorsement of the recommendations by other scientific societies, the absence of an alignment in the International Classification of Diseases (ICD) coding system, or a lack of intervention by peer reviewers to correct the terminology used in submitted papers and promote greater alignment with the recommendations.

## THE GOUT, HYPERURICEMIA AND CRYSTAL-ASSOCIATED DISEASE NETWORK NOMENCLATURE PROJECT FOR CPPD

An international initiative developed by the Gout, Hyperuricemia and Crystal-Associated Disease Network (G-CAN), is underway to agree on standardised terminology for CPPD, aiming to update inconsistencies and varied meanings of existing terms. Launched in 2022, the project began with an SLR to identify existing definitions and terms used to describe CPPD [13]. Following this, a Delphi consensus process involving leading experts is in progress to refine and standardise the scientific terminology. Moreover, the project also includes a third step for creating lay-friendly language, ensuring accurate, clear, and consistent communication with patients. This step seeks to overcome the linguistic barriers that have hindered the broader adoption of EULAR-recommended terminology in clinical practice.

As previously mentioned, the EULAR recommendations on CPPD terminology have faced challenges in gaining widespread acceptance, likely due to several factors. First, since 2011, CPPD has seen a remarkable advance in research [14–17], and as understanding of its clinical manifestations and pathogenetic mechanisms grows [18,19], more precise terms are required to accurately describe the condition. For instance, while the condition itself is referred to as calcium pyrophosphate deposition, no consensus exists for its symptomatic form, which has been spontaneously termed calcium pyrophosphate deposition disease in recent publications. Another area of imprecision lies in the use of the term chondrocalcinosis, which is often applied broadly to

Table
**The most frequently used labels representing the condition, the crystal, the condition element, and the condition states, presented in comparison before and after the 2011 EULAR recommendations on CPPD terminology**

| Concept | Before 2011 | | After 2011 | |
|---|---|---|---|---|
| | Total no. of distinct labels | Most used labels, no. of papers (%) | Total no. of distinct labels | Most used labels, no. of papers (%) |
| The condition | | | | |
| Condition name | 46 | Pseudogout, 145/279 (52.0)<br>Chondrocalcinosis, 92/279 (33.0)<br>Calcium pyrophosphate dihydrate crystal deposition disease, 55/279 (19.7) | 51 | Pseudogout, 220/504 (43.7)<br>Calcium pyrophosphate deposition disease, 159/504 (31.5)<br>Chondrocalcinosis, 115/504 (22.8) |
| Condition acronym | 10 | CPPD, 60/97 (61.9)<br>CPDD, 12/97 (12.4)<br>CC, 12/97 (12.4) | 13 | CPPD, 252/293 (86.0)<br>CPDD, 27/293 (9.2)<br>CC, 19/293 (6.5) |
| Condition acronym meaning | 24 | Calcium pyrophosphate dihydrate, 44/123 (35.8)<br>Calcium pyrophosphate deposition disease, 15/123 (12.2)<br>Calcium pyrophosphate dihydrate deposition disease, 11/123 (8.9) | 24 | Calcium pyrophosphate deposition disease, 89/298 (29.9)<br>Calcium pyrophosphate deposition, 66/298 (22.1)<br>Calcium pyrophosphate dihydrate, 29/298 (9.7) |
| The crystal | | | | |
| Crystal name | 7 | Calcium pyrophosphate dihydrate, 206/271 (76.0)<br>Calcium pyrophosphate, 47/271 (17.3)<br>Calcium pyrophosphate dehydrate, 16/271 (5.9) | 10 | Calcium pyrophosphate, 233/446 (52.2)<br>Calcium pyrophosphate dihydrate, 166/446 (37.2)<br>Calcium pyrophosphate dehydrate, 45/446 (10.1) |
| Crystal acronym | 8 | CPPD, 196/210 (93.3)<br>CPP, 10/210 (4.8)<br>CCP, 1/210 (0.5) | 7 | CPP, 203/341 (59.5)<br>CPPD, 138/341 (11.1)<br>CCP, 2/341 (0.6) |
| The condition element | | | | |
| Evidence of crystal deposition on radiography | 13 | Chondrocalcinosis, 106/153 (69.3)<br>Calcification, 56/153 (36.6)<br>Deposit, 6/153 (3.9) | 15 | Chondrocalcinosis, 179/246 (72.8)<br>Calcification, 83/246 (33.7)<br>Deposit, 11/246 (4.5) |
| The condition states | | | | |
| Asymptomatic evidence of crystal deposition on radiography | 9 | Chondrocalcinosis, 4/13 (30.8)<br>Asymptomatic chondrocalcinosis, 4/13 (30.8)<br>Incidental radiographic finding, 1/13 (7.7) | 13 | Chondrocalcinosis, 11/25 (44.0)<br>Asymptomatic chondrocalcinosis, 7/25 (28.0)<br>Incidental radiographic finding, 1/25 (4.0) |
| Acute peripheral articular inflammation triggered by the presence of crystals | 22 | Pseudogout, 44/86 (51.2)<br>Acute pseudogout, 10/86 (11.6)<br>Acute arthritis, 5/86 (5.8) | 36 | Pseudogout, 69/164 (42.1)<br>Acute CPP crystal arthritis, 54/164 (32.9)<br>Acute arthritis, 16/164 (9.8) |
| Recurrent acute peripheral articular inflammation triggered by the presence of crystals | 9 | Pseudogout, 6/18 (33.3)<br>Pseudorheumatoid arthritis, 3/18 (16.7)<br>Pseudogout attacks, 3/18 (16.7) | 12 | Pseudogout, 10/28 (35.7)<br>Acute recurrent CPP arthritis, 4/28 (14.3)<br>Recurrent arthritis, 3/28 (10.7) |
| Persistent peripheral articular inflammation triggered by the presence of crystals | 12 | Pseudorheumatoid arthritis, 12/30 (40.0)<br>Chronic arthritis, 8/30 (26.7)<br>Chronic arthropathy, 1/30 (3.3) | 19 | Chronic CPP crystal arthritis, 27/58 (46.6)<br>Pseudorheumatoid arthritis, 13/58 (22.4)<br>Chronic arthritis, 7/58 (12.1) |
| Symptomatic osteoarthritis related to crystal deposits | 24 | Pseudo-osteoarthritis, 13/51 (25.5)<br>CPP crystals deposits with osteoarthritis, 7/51 (13.7) | 30 | CPPD-related/associated osteoarthritis, 31/77 (40.3)<br>Pseudo-osteoarthritis, 12/77 (15.6) |

CPDD, calcium pyrophosphate deposition disease; CPP, calcium pyrophosphate; CPPD, calcium pyrophosphate deposition; CC: ChondroCalcinosis; CCP: CalCium Pyrophosphate.
Proportion and percentage refer to the articles in which at least 1 label is identified for each concept, with multiple labels possible per article.

describe any imaging features of articular calcification. This is particularly relevant now that more precise definitions of CPPD-related imaging findings are available on both plain radiography and other imaging modalities [20–22].

Further, any change in nomenclature must be widely supported by the scientific community, which requires broad expert involvement. To achieve this, the G-CAN initiative has invited all its members—over 250 experts from across the globe specialising in crystal-induced arthropathies—to contribute. This ensures comprehensive input into the Delphi surveys, and hopefully the new terminology should be able to foresee and cover also future directions of the research.

## CONCLUSIONS

Achieving widespread changes in medical nomenclature is a gradual process, often requiring years to overcome entrenched habits and inconsistent practices. In the case of CPPD, the persistent use of outdated terms underscores the challenges of adopting standardised terminology, as noted in the SLR. The 2011

EULAR terminology represented an important step forward; however, its partial adoption reflects the ongoing need for greater consensus and implementation. While several terms were valuable when first introduced, advances in knowledge necessitate updates to language. The G-CAN nomenclature project will play a pivotal role in revising and promoting standardised terminology for CPPD. The full implementation of consistent terminology will require revisions to systems like the ICD coding, endorsement by major scientific societies, and active efforts from editors and peer reviewers to support alignment in publications. These changes, driven by the efforts of researchers and clinicians, will enhance communication, research, and improve patient care. Progress may be incremental, but it is an essential and transformative journey.

## Competing interests

GF has received a research grant from Eli Lilly for an Investigator Initiated Trial in CPPD. All other authors have no competing interests regarding this article.

## CRediT authorship contribution statement

**Silvia Sirotti:** Writing – review & editing, Writing – original draft, Visualization, Validation, Data curation, Conceptualization. **Charlotte Jauffret:** Writing – review & editing, Visualization, Validation, Methodology, Formal analysis. **Antonella Adinolfi:** Writing – review & editing, Visualization, Validation. **Edoardo Cipolletta:** Writing – review & editing, Visualization, Validation. **Daniele Cirillo:** Writing – review & editing, Visualization, Validation. **Luca Ingrao:** Writing – review & editing, Visualization, Validation. **Alessandro Lucia:** Writing – review & editing, Visualization, Validation. **Emilio Filippucci:** Writing – review & editing, Visualization, Validation. **Tristan Pascart:** Writing – review & editing, Visualization, Validation. **Sara K Tedeschi:** Writing – review & editing, Visualization, Validation. **Robert Terkeltaub:** Writing – review & editing, Visualization, Validation. **Nicola Dalbeth:** Writing – review & editing, Visualization, Validation. **Georgios Filippou:** Writing – review & editing, Writing – original draft, Visualization, Validation, Supervision, Data curation, Conceptualization.

## Contributors

SS and GF drafted the first version of the manuscript. CJ performed data analysis. All authors reviewed and approved the final version of the manuscript before submission. GF accepts full responsibility for the work, had access to the data, and controlled the decision to publish.

## Funding

This work was supported by the Italian Ministry of Health, 'Ricerca Corrente.'

## Patient consent for publication

Not applicable.

## Ethics approval

Not applicable.

## Provenance and peer review

Not commisioned, externally peer revied.

## Patient and public involvement

Patients and/or the public were not involved in the design, or conduct, or reporting, or dissemination plans of this research.

## Orcid

Silvia Sirotti: http://orcid.org/0000-0001-9795-131X
Charlotte Jauffret: http://orcid.org/0000-0002-0973-5797
Antonella Adinolfi: http://orcid.org/0000-0002-4034-7186
Edoardo Cipolletta: http://orcid.org/0000-0002-6881-8197
Daniele Cirillo: http://orcid.org/0009-0004-1255-0824
Luca Ingrao: http://orcid.org/0009-0003-2046-9316
Alessandro Lucia: http://orcid.org/0009-0002-7262-8545
Emilio Filippucci: http://orcid.org/0000-0002-7251-7784
Tristan Pascart: http://orcid.org/0000-0002-8395-826X
Sara K Tedeschi: http://orcid.org/0000-0001-9475-1363
Robert Terkeltaub: http://orcid.org/0000-0001-5368-7473
Nicola Dalbeth: http://orcid.org/0000-0003-4632-4476
Georgios Filippou: http://orcid.org/0000-0002-1647-2083

## REFERENCES

[1] van der Heijde D, Daikh DI, Betteridge N, Burmester GR, Hassett AL, Matteson EL, et al. Common language description of the term rheumatic and musculoskeletal diseases (RMDs) for use in communication with the lay public, healthcare providers and other stakeholders endorsed by the European League Against Rheumatism (EULAR) and the American College of Rheumatology (ACR). Ann Rheum Dis 2018;77:829–32. doi: 10.1136/annrheumdis-2017-212565.
[2] Tedeschi SK. Issues in CPPD nomenclature and classification. Curr Rheumatol Rep 2019;21:49. doi: 10.1007/s11926-019-0847-4.
[3] Sirotti S, Terkeltaub R, Filippou G. Describing calcium pyrophosphate deposition: undoing the tower of Babel!. Curr Opin Rheumatol 2024;36:241–50. doi: 10.1097/BOR.0000000000001001.
[4] Van Der Heijde D, Molto A, Ramiro S, Braun J, Dougados M, van Gaalen FA, et al. Goodbye to the term 'ankylosing spondylitis', hello 'axial spondyloarthritis': time to embrace the ASAS-defined nomenclature. Ann Rheum Dis 2024;83:547–9. doi: 10.1136/ard-2023-225185.
[5] McCarty DJ, Kohn NN, Faires JS. The significance of calcium phosphate crystals in the synovial fluid of arthritic patients: the "pseudogout syndrome. Ann Intern Med 1962;56:711–37. doi: 10.7326/0003-4819-56-5-711.
[6] Kohn NN, Hughes RE, McCarty DJ, Faires JS. The significance of calcium phosphate crystals in the synovial fluid of arthritic patients: the "pseudogout syndrome". II. Identification of crystals. Ann Intern Med 1962;56:738–45. doi: 10.7326/0003-4819-56-5-738.
[7] McCarty DJ. Calcium pyrophosphate dihydrate crystal deposition disease—1975. Arthritis Rheum 1976;19:275–85. doi: 10.1002/1529-0131(197605/06)19:3+<275::AID-ART1780190702>3.0.CO;2-0.
[8] Russell RG, Bisaz S, Fleisch H, Currey HL, Rubinstein HM, Dietz AA, et al. Inorganic pyrophosphate in plasma, urine, and synovial fluid of patients with pyrophosphate arthropathy (chondrocalcinosis or pseudogout). Lancet 1970;2:899–902. doi: 10.1016/s0140-6736(70)92070-2.
[9] Sundén G, Bjelle A. Pyrophosphate synovitis. Acta Orthop Scand 1971;42:443–4.
[10] Zitnan D, Sitaj S. [Chondrocalcinosis polyarticularis (familiaris): roentgenological and clinical analysis]. Cesk Rentgenol 1960;14:27–34.
[11] McCarty D. Crystals, joints, and consternation. Ann Rheum Dis 1983;42:243–53.
[12] Zhang W, Doherty M, Bardin T, Barskova V, Guerne PA, Jansen TL, et al. European League Against Rheumatism recommendations for calcium pyrophosphate deposition. Part I: terminology and diagnosis. Ann Rheum Dis 2011;70:563–70. doi: 10.1136/ard.2010.139105.
[13] Jauffret C, Adinolfi A, Sirotti S, Cirillo D, Ingrao L, Lucia A, et al. Systematic literature review on calcium pyrophosphate deposition (CPPD) nomenclature: condition elements and clinical states—a Gout, Hyperuricaemia and

Crystal-Associated Disease Network (G-CAN) consensus project. RMD Open 2025;11:e004847. doi: 10.1136/rmdopen-2024-004847.
[14] Abhishek A, Tedeschi SK, Pascart T, Latourte A, Dalbeth N, Neogi T, et al. The 2023 ACR/EULAR classification criteria for calcium pyrophosphate deposition disease. Ann Rheum Dis 2023;82:1248–57. doi: 10.1136/ard-2023-224575.
[15] Abhishek A, Tedeschi SK, Pascart T, Latourte A, Dalbeth N, Neogi T, et al. The 2023 ACR/EULAR classification criteria for calcium pyrophosphate deposition disease. Arthritis Rheum 2023;75:1703–13. doi: 10.1002/art.42619.
[16] Mandl P, D'Agostino MA, Navarro-Compán V, Geßl I, Sakellariou G, Abhishek A, et al. 2023 EULAR recommendations on imaging in diagnosis and management of crystal-induced arthropathies in clinical practice. Ann Rheum Dis 2024;83:752–9. doi: 10.1136/ard-2023-224771.
[17] Zhang Y, Tedeschi S, Abhishek A, Hensey O, Grossberg D, Cai K, et al. Core domain set for long-term studies of calcium pyrophosphate deposition disease: Omeract Delphi Survey to Establish Consensus. 2024. doi:10.2139/ssrn.4952538
[18] Pascart T, Filippou G, Lioté F, Sirotti S, Jauffret C, Abhishek A. Calcium pyrophosphate deposition disease. Lancet Rheumatol 2024;6:e791–804. doi: 10.1016/S2665-9913(24)00122-X.
[19] Tedeschi SK. A new era for calcium pyrophosphate deposition disease research: the first-ever calcium pyrophosphate deposition disease classification criteria and considerations for measuring outcomes in calcium pyrophosphate deposition disease. Gout Urate Cryst Depos Dis 2024;2:52–9. doi: 10.3390/gucdd2010005.
[20] Sirotti S, Terslev L, Filippucci E, Iagnocco A, Moller I, Naredo E, et al. Development and validation of an OMERACT ultrasound scoring system for the extent of calcium pyrophosphate crystal deposition at the joint level and patient level. Lancet Rheumatol 2023;5:e474–82. doi: 10.1016/S2665-9913(23)00136-4.
[21] Filippou G, Scirè CA, Damjanov N, Adinolfi A, Carrara G, Picerno V, et al. Definition and reliability assessment of elementary ultrasonographic findings in calcium pyrophosphate deposition disease: a study by the OMERACT Calcium Pyrophosphate Deposition Disease Ultrasound Subtask Force. J Rheumatol 2017;44:1744–9. doi: 10.3899/jrheum.161057.
[22] Tedeschi SK, Becce F, Pascart T, Guermazi A, Budzik JF, Dalbeth N, et al. Imaging features of calcium pyrophosphate deposition disease: consensus definitions from an international multidisciplinary working group. Arthritis Care Res (Hoboken) 2023;75(4):825–34. doi: 10.1002/acr.24898.

Ann Rheum Dis 84 (2025) 1293–1300

Contents lists available at ScienceDirect

Annals of the Rheumatic Diseases

journal homepage: https://www.sciencedirect.com/journal/annals-of-the-rheumatic-diseases

Rheumatoid arthritis

# Adalimumab serum concentration to choose a subsequent biological DMARD in patients with rheumatoid arthritis (ADDORA-switch): results of a blinded randomised test-treatment trial

Maike H.M. Wientjes[1,*], Sadaf Atiqi[2], Gerrit J. Wolbink[2,3], Michael T. Nurmohamed[2,4], Maarten Boers[5], Femke Hooijberg[2], Theo Rispens[3,4,6], Annick de Vries[4], Ronald F. van Vollenhoven[2,7], Sofia Ramiro[8], Noortje van Herwaarden[1,9], Bart J.F. van den Bemt[9,10], Alfons A. den Broeder[1,11]

[1] *Department of Rheumatology, Sint Maartenskliniek, Nijmegen, the Netherlands*
[2] *Department of Rheumatology, Amsterdam Rheumatology and Immunology Centre, Reade, Amsterdam, the Netherlands*
[3] *Sanquin Research, Sanquin, Amsterdam, the Netherlands*
[4] *Antibodies and Immunogenicity, R&D, Sanquin Diagnostic Services, Amsterdam, the Netherlands*
[5] *Department of Epidemiology and Data Science, Amsterdam UMC, Amsterdam, the Netherlands*
[6] *Amsterdam Institute for Infection and Immunity, Amsterdam, the Netherlands*
[7] *Department of Clinical Immunology and Rheumatology, Amsterdam UMC, Amsterdam, the Netherlands*
[8] *Department of Rheumatology, Zuyderland Medical Centre, Heerlen, and Leiden University Medical Centre, Leiden, the Netherlands*
[9] *Department of Pharmacy, Radboud University Medical Centre, Nijmegen, the Netherlands*
[10] *Department of Pharmacy, Sint Maartenskliniek, Nijmegen, the Netherlands*
[11] *Department of Rheumatology, Radboud University Medical Centre, Nijmegen, the Netherlands*

ARTICLE INFO

*Article history:*
Received 11 November 2024
Received in revised form 26 March 2025
Accepted 28 March 2025

ABSTRACT

*Objectives:* A substantial proportion of patients with rheumatoid arthritis (RA) discontinue adalimumab due to ineffectiveness. The next treatment step can be another tumour necrosis factor inhibitor (TNFi) or a biological/targeted synthetic disease-modifying antirheumatic drug (b/tsDMARD). Therapeutic drug monitoring (TDM) of serum drug levels may help guide this choice. This study evaluated whether switching treatments based on adalimumab trough levels is more effective than random switching.

*Methods:* In this 24-week, multicentre, triple-blinded, randomised controlled trial, patients with RA who stopped adalimumab due to inefficacy (disease activity score based on 28 joint count and C-reactive protein [DAS28-CRP] >2.9) were enrolled. Participants were randomly assigned (1:1) to a TDM-based or random switching (control) strategy. The primary outcome was the difference in mean time-weighted DAS28-CRP between groups at 24 weeks.

*Results:* From July 2020 to November 2023, 83 consecutive patients with RA were included, with 78 initiating a new b/tsDMARD (TDM-based group: n = 38; control: n = 40). The mean time-weighted DAS28-CRP was 3.15 in both groups (TDM: SD, 0.99; control: SD, 1.01; 95% CI of difference: −0.46 to 0.47). There were no significant differences between the groups in flare rates,

*Correspondence to Maike H.M. Wientjes, Department of Rheumatology, Sint Maartenskliniek, Nijmegen, the Netherlands.
*E-mail address:* m.wientjes@maartenskliniek.nl (M.H.M. Wientjes).
**Handling editor** Josef S. Smolen.

https://doi.org/10.1016/j.ard.2025.03.015

0003-4967/© 2025 European Alliance of Associations for Rheumatology (EULAR). Published by Elsevier B.V. All rights are reserved, including those for text and data mining, AI training, and similar technologies.

escape medication use, disease activity, or adverse events. Receiver operating characteristic analyses in the control group found no predictive value of adalimumab levels for response to TNFi or non-TNFi.

*Conclusions:* Switching treatments based on adalimumab trough levels was not more effective than random switching in patients with RA who failed adalimumab treatment. Therefore, serum drug level measurements to guide therapy choices in this context is not recommended.

**WHAT IS ALREADY KNOWN ON THIS TOPIC**

- Adalimumab is a widely used and effective treatment for rheumatoid arthritis (RA), but many patients discontinue due to inefficacy.
- Recommendations suggest switching to another tumour necrosis factor inhibitor (TNFi) or a non-TNFi such as biological/targeted synthetic disease-modifying antirheumatic drug (DMARD) when adalimumab fails.
- Therapeutic drug monitoring (TDM) has been suggested to guide treatment decisions, but its effectiveness in patients with RA failing adalimumab has not been tested in a controlled trial.

**WHAT THIS STUDY ADDS**

- To our knowledge, this is the first trial comparing TDM-based switching with random switching in patients with RA after adalimumab failure.
- Switching based on serum drug levels was not superior to random switching in reducing disease activity.
- Adalimumab serum levels did not help distinguish between subsequent DMARD responders and nonresponders.

**HOW THIS STUDY MIGHT AFFECT RESEARCH, PRACTICE OR POLICY**

- These findings do not support the use of serum drug level measurements in guiding treatment decisions after adalimumab failure.

## INTRODUCTION

Adalimumab is a fully human monoclonal antibody tumour necrosis factor inhibitor (TNFi) that is among the most frequently prescribed biologic disease-modifying antirheumatic drugs (bDMARDs) worldwide. It is effective and safe for treating rheumatoid arthritis (RA). Still, a substantial proportion of patients with RA discontinue treatment due to intolerance and/or inefficacy. When treatment fails, the European Alliance of Associations for Rheumatology (EULAR) recommends switching to another TNFi or to another biologic or targeted synthetic disease-modifying antirheumatic drugs (b/tsDMARDs) with a different mode of action [1]. Implicitly, these 2 approaches are thus assumed to have similar chances of response on a group level.

Therapeutic drug monitoring (TDM), involving serum drug concentration or antidrug antibody (ADA) measurement, may aid in determining the subsequent treatment choice between a TNFi and a non-TNFi [2–4]. This is based on the notion that adalimumab failure can have multiple causes. The hypothesis is that a subset of patients is insensitive to TNF inhibition, making a switch to a non-TNFi conceptually superior. Another subset of patients, about 30% of patients with RA failing adalimumab, develops substantial and prolonged ADAs that adversely affect pharmacokinetics, which may lead to immediate (primary) or delayed (secondary) nonresponse [4,5]. Patients developing ADAs may experience drug failure but this is not necessarily class failure, so they may still respond adequately to a second TNFi, especially secondary nonresponders who were initially responsive to TNFis.

A systematic review identified 3 studies that explored the use of TDM markers to predict response to a new bDMARD after failure of the first bDMARD [3]. Two studies reported that presence of ADAs in patients who did not respond to an initial TNFi predicted a better response to a second TNFi, while a third study with similar results did not reach statistical significance [5–7]. Subsequently, 2 additional studies examined this concept. One study found that patients with RA with high adalimumab levels, despite nonresponse, benefitted less from switching to etanercept compared with those with low adalimumab levels [4]. However, another study found no predictive value in ADA presence or drug concentrations for response to either a second TNFi or a non-TNFi [8]. All these studies had limitations regarding clinical applicability, including small sample sizes, incomplete reporting of test characteristics (such as sensitivity and specificity), and reliance on random rather than trough-level sampling. The available prospective studies also only addressed switching between TNFis, leaving the predictive value of TDM for response to non-TNFi drugs after TNFi failure unclear. Therefore, it is unclear whether TDM can differentially predict response to a second TNFi vs a non-TNFi.

In patients with RA failing adalimumab, the clinical effectiveness of TDM to select the optimal subsequent b/tsDMARDs has not been tested in a controlled trial. This study aimed to assess whether a switching strategy based on adalimumab trough serum concentration at the time of failure is superior to random switching in reducing disease activity for patients with RA who have failed adalimumab treatment.

## METHODS

### *Study design and participants*

ADDORA-switch was a triple-blinded, superiority, randomised, controlled, test-treatment trial conducted across 3 centres in the Netherlands (Reade, Zuyderland MC, and Sint Maartenskliniek). The study rationale and design have been previously detailed and are summarised in this study [9]. We recruited adult patients with RA (according to 1987 and/or 2010 criteria by American College of Rheumatology (ACR) and/or clinical diagnosis) who recently failed adalimumab treatment (defined as disease activity score based on 28 joint count and C-reactive protein [DAS28-CRP] >2.9). Patients were included if they had received adalimumab (originator or biosimilar) for at least the last 10 weeks (time point at which steady-state concentrations are reached) in standard dosing (40.0 mg subcutaneously every other week, either as monotherapy or in combination with methotrexate or leflunomide) and were due to stop adalimumab owing to lack of efficacy, regardless of concurrent side effects. Patients were excluded if they had been treated with another TNFi before adalimumab, had a contraindication to receive either etanercept or any of the non-TNFi b/tsDMARDs allowed by the study protocol, or had preplanned

reasons for treatment discontinuation during follow-up. The study received ethical review board approval (number NL69841.091.19) and has been registered (Dutch Trial Register NL8210). All participants provided written informed consent. Patients and/or the public were not involved in the design, or conduct, or reporting, or dissemination plans of this research.

### *Randomisation and blinding*

Patients were randomised in a 1:1 ratio to either the TDM-guided intervention group, where the next treatment was guided by adalimumab concentration in addition to usual care, or a control group, where a random switching strategy was applied alongside usual care. Randomisation blocks were generated by an online programme and had variable block sizes of 2 or 4 per block. The allocation was performed by an independent researcher, and the sequence was concealed from all participants, including patients, physicians, and assessors (triple-blinded). In the TDM-guided intervention group, subsequent treatment was determined by adalimumab trough concentration. Patients with a trough concentration of <1.0 mg/L were switched to another TNFi, etanercept, while those with a concentration of 1.0 mg/L or higher were switched to a non-TNFi bDMARD. The specific non-TNFi bDMARD was chosen by the treating health care provider in shared decision making with the patient. This could be abatacept, rituximab, sarilumab, tocilizumab, or a Janus kinase inhibitor (JAKi). The treating physician received a concrete treatment recommendation (etanercept or non-TNFi b/tsDMARD) from an independent researcher, without knowing whether this recommendation was based on therapeutic drug monitoring (TDM-guided intervention group) or chance (control group). Allocation of TNFi or non-TNFi in the control group was standardised by directly basing the assignment of subsequent treatment on the allocation in the TDM-guided intervention group. When operationalised, this means that when a patient in the intervention group was receiving etanercept, the subsequent patient randomised to the control group was also assigned to etanercept. In case of temporary imbalance with an excess of patients allocated to the control group, these patients were randomised in a ratio of 1:2 to etanercept or a non-TNFi. This procedure was selected to maintain the same TNFi to non-TNFi ratio in both groups, as described more detailed previously, thus autobalancing this ratio [9]. Everyone involved (including the patient, physician, and researcher) knew which specific treatment the patient was using, but no one knew whether this allocation was based on the serum drug level or usual care.

### *Study procedures*

At the first visit (screening, while the patient was still on adalimumab), serum samples were collected to measure trough adalimumab concentrations and antiadalimumab antibodies. Trough concentrations were taken before the next adalimumab injection within a 3-day window. In both groups, patients were randomised, started treatment as described earlier, and visited the clinic 4, 12 and 24 weeks after treatment initiation. Disease activity was measured at each visit, and the treating rheumatologists treated participants to the target of DAS28-CRP <2.9. If disease activity increased or remained high between visits, patients were encouraged to contact the clinic for an additional visit. Antirheumatic comedication was allowed and managed by the rheumatologist, with efforts to keep comedication disease-modifying antirheumatic drugs (DMARDs) stable. Changes in comedication were permitted during flares (defined as DAS28-CRP increase >1.2, or >0.6 if current DAS28-CRP ≥2.9) [10] or adverse events. In case of active disease, bridging treatment could be offered, which included nonsteroidal anti-inflammatory drugs, methylprednisolone 120.0 mg intramuscularly, triamcinolone 80.0 mg intramuscularly, or oral prednisone (usually 15.0 mg, tapered over 2-6 weeks). In case of a persistent flare, the rheumatologist and participant together could decide to switch the b/tsDMARDs to any other b/conventional synthetic/tsDMARD treatment. All adverse events were recorded.

Serum adalimumab trough concentrations were measured by enzyme-linked immunosorbent assay, with a detection limit of 0.001 mg/L [11]. A threshold of 1.0 mg/L was selected based on previous studies [4,12]. Baseline ADAs were measured by radioimmunoassay; ADA were expressed in arbitrary units (AUs) per millilitre. Patients were positive for ADA if ADA were above the cutoff of 12 AU/mL (limit of detection); ADA are quantifiable above 30 AU/mL (lower limit of quantification). Assays were conducted by Sanquin Diagnostic Services in the Netherlands.

### *Outcomes*

The primary outcome was the between-group difference in mean time-weighted (MTW) DAS28-CRP after 24 weeks. This outcome was chosen since patients were treated to target and therefore no difference in DAS28 scores might be found only at study end, despite a potentially higher flare frequency in 1 group. Switching DMARDs or bridging treatment longer than 6 weeks was considered treatment failure. Secondary outcomes included the percentage of patients with good or moderate EULAR response after 12 and 24 weeks, low disease activity (defined as DAS28-CRP <2.9) [13] after 24 weeks, number of patients with a flare after 24 weeks, (serious) adverse events, and use of comedication/rescue medication.

### *Statistical analyses*

The sample size calculation was based on the superiority principle and has been described previously in more detail [9]. The primary outcome was anticipated to be a MTW DAS28-CRP of 2.8 with an SD of 0.9 based on other RA studies [14,15]. The clinically relevant difference was defined as a change in MTW-DAS28 of ≥0.6. With a 2-sided 5% significance level, 80% power, and a 15% dropout rate, the sample size was set at 84 patients.

Data were primarily analysed with an intention-to-treat (ITT) approach. In cases where treatment failed, a participant dropped out during follow-up, or a disease activity measure was missing, the most recent DAS28-CRP measurement recorded before the start of bridging or escape medication (or before dropout) was used, following the last observation carried forward method. Additionally, a per-protocol (PP) analysis was conducted, which included only participants who completed the full study follow-up. The difference in the primary outcome between the 2 study arms was tested with *t* test. Prespecified adjusted analyses were performed on the primary ITT outcome, adjusting for rheumatoid factor/anticitrullinated protein antibody status and baseline DAS28-CRP using linear regression. Additional adjusted analyses were conducted to investigate confounding and effect modification by use of concomitant conventional synthetic DMARDs (csDMARDs). A 2-sided *P* value of <.05 was considered statistically significant. Secondary outcomes were compared in the ITT population using Fisher exact test or were described

numerically. Subgroup analyses were conducted to assess differences in the effect of the intervention for patients experiencing primary (≤6 months) or secondary (>6 months) failure to adalimumab. The predictive value of baseline serum drug levels for achievement of moderate or good EULAR response after 24 weeks was evaluated with receiver operating characteristic (ROC) curves. The area under the ROC curve was calculated to quantify the overall ability of adalimumab serum levels to predict EULAR (non)response in the control group, separately for patients randomised to TNFi or non-TNFi DMARDs. Data were collected with paper case report forms or recorded in the participants' electronic health records. All study data were entered into an electronic data capture database (Castor EDC) and exported to RStudio version 4.4.0 for statistical analysis.

## RESULTS

Between July 31, 2020, and November 6, 2023, 83 patients with RA were included in the study and randomised to the TDM-guided intervention (n = 40) or control (n = 43). Of these 83 patients, 5 were excluded (2 belonging to the TDM-guided intervention arm, 3 to control) directly after baseline visit due to cancer diagnosis (n = 2) and withdrawal of consent (n = 3). The ITT population consisted of 78 patients who started a new b/tsDMARD based on random assignment to either the TDM-guided intervention (n = 38) or control (n = 40). Of 78 randomised participants, 7 were lost to follow-up. These patients were excluded from the PP population, which included 71 participants. Baseline patient disease and treatment characteristics of the ITT population are summarised in Table 1. A flow diagram of the randomisation process, trough levels and subsequent treatment is shown in Figure 1. Data of the study have been reported according to Consolidated Standards of Reporting Trials reporting guidelines (Supplementary File 1) [16].

### *Disease activity outcomes*

Key outcomes for both groups are presented in Table 2. MTW DAS28-CRPs over 24 weeks were 3.15 (SD, 0.99) and 3.15 (SD, 1.01) in the TDM-guided intervention and control groups, respectively (95% CI of difference, −0.46 to 0.47). PP analyses showed similar results (between-group difference, 0.005; 95% CI, −0.46 to 0.47). Prespecified adjusted analyses showed that baseline DAS28-CRP was significantly associated with MTW DAS28-CRP; however, this did not influence the primary outcome ($P$ = .68). The use of concomitant csDMARD was neither a confounder nor an effect modifier ($P$ = 0.62). Mean differences between absolute DAS28-CRP at week 24 and baseline were −1.05 (SD, 1.37) and −1.31 (SD, 1.22) for the TDM-guided intervention and control groups, respectively (Fig 2).

### *Secondary outcomes*

A total of 26 patients (33%) experienced a flare during follow-up: 14 (37%) in the intervention group and 12 (30%) in the control group. Three (8%) patients in the intervention group and 4 (10%) patients in the control group started another b/tsDMARD during follow-up. One (3%) patient in the intervention group and 2 in the control group (5%) started or switched a concomitant csDMARD during the study period. One (3%) in the intervention and 2 (5%) patients in the control group received ≥2 injections with glucocorticoids, and 4 (10%) intervention and 2 (5%) control patients received oral prednisone during follow-up. Low disease activity was achieved in 18 (47%) participants in the TDM-guided intervention group and 22 (55%) participants in the control group. Four patients, all belonging to the control group, reported serious adverse events during follow-up (Table 2), comprising newly diagnosed squamous cell carcinoma with metastases, chronic obstructive pulmonary disease, pulmonary embolism, and stroke. A total of 89 nonserious adverse events were registered, mostly infections and gastrointestinal complaints. Fifty (64%) participants reported at least 1 adverse event. Fifteen (39%) and 22 (55%) patients in the TDM-guided intervention and control groups, respectively, experienced primary failure to adalimumab. Subgroup analyses did not identify differences in primary outcome between patients experiencing primary (difference, −0.14; 95% CI, −0.96 to 0.68) or secondary (difference, 0.10; 95% CI, −0.46 to 0.67) failure to adalimumab. The area under the ROC curves in the control group were 0.62 (95% CI, 0.31-0.94) for patients receiving TNFi and 0.58 (95% CI, 0.39-0.78) for patients receiving a non-TNFi (Fig 3).

## DISCUSSION

In this study, we showed that in patients with RA who had failed adalimumab treatment, a switching strategy based on adalimumab trough serum concentration did not prove superior in reducing disease activity over 24 weeks compared with random switching. There were also no significant differences observed in flare rates, the need for escape medication, absolute disease activity scores, or adverse events, and adalimumab serum levels showed no discriminative power in distinguishing between subsequent DMARD responders and nonresponders. These findings do not support the use of serum drug level measurements in guiding treatment decisions after adalimumab failure.

To our knowledge, the ADDORA-switch is the first randomised controlled test-treatment trial to investigate the added value of TDM in the context of drug switching following treatment failure in RA. A previous study examined a similar mechanism and reported comparable results; however, it was a retrospective study with random timed serum levels [8]. Neither study shows a predictive value for adalimumab serum levels for achieving response to the next (TNFi or non-TNFi) treatment. These results differ from those in previous cohort studies showing lower response rates to the second TNFi in patients with sufficient TNFi drug levels or without ADAs against the first TNFi [4−7]. Tentative explanations for these contradictory results include differences in design (only focusing on response to the second TNFi), in drug (infliximab, etanercept, or adalimumab) and in disease (RA or axial spondyloarthritis).

There are several potential reasons why adalimumab serum levels may not reliably guide patients towards the most effective treatment option (TNFi or non-TNFi). Firstly, there might be differences in the relation between the drug concentrations in the central compartment compared with those in the peripheral compartment. Secondly, it might be that lower adalimumab drug levels are also associated with better response to non-TNFi, not only to the TNFi, thus negating any differential prediction. However, this does not seem to be the case, as ROC analyses in both this study and 1 previous study including both TNFi and non-TNFi showed no predictive value of adalimumab serum levels for predicting response to subsequent therapy. This lack of association might be attributed to variability in the pharmacokinetic and pharmacodynamic relation between patients, which causes a drug level of 1.0 mg/L to be too high for 1 patient and too low for another, diluting the predictive effect. In addition, lower drug levels can be associated with less exposure of the

Table 1
**Patient, disease, and treatment characteristics**

| Characteristic | TDM-guided (n = 38) | Control (n = 40) | Overall (N = 78) |
|---|---|---|---|
| Age (y) | 57 ± 12 | 56 ± 11 | 56 ± 11 |
| Sex (female)[h] | 19 (50) | 25 (62) | 44 (56) |
| Disease duration (y) | 8.3 ± 9.1 | 5.5 ± 5.5 | 6.9 ± 7.5 |
| RF + | 26 (68) | 25 (62)[a] | 51 (65)[a] |
| ACPA + | 28 (74) | 30 (75) | 58 (74) |
| Erosive | 4 (11) | 6 (15)[b] | 10 (13)[b] |
| Previous b/tsDMARDs | | | |
| 0 | 7 (18) | 7 (18) | 14 (18) |
| 1 | 29 (76) | 31 (78) | 60 (77) |
| ≥2 | 2 (5) | 2 (4) | 4 (5) |
| Previous csDMARDs | | | |
| 1 | 10 (26) | 11 (28) | 21 (27) |
| 2 | 12 (32) | 13 (32) | 25 (32) |
| ≥3 | 16 (42) | 16 (40) | 32 (41) |
| Duration of adalimumab use (d) | 216 (143-311) | 173 (132-378) | 185 (138-348) |
| Primary nonresponse to adalimumab[c] | 15 (39) | 22 (55) | 37 (47) |
| Baseline csDMARD use | 29 (76) | 29 (72) | 58 (74) |
| Baseline DAS28-CRP | 4.0 ± 1.2 | 4.2 ± 1.0 | 4.1 ± 1.1 |
| Baseline tender joint count | 5 (2-7) | 4 (2-7) | 4 (2-7) |
| Baseline swollen joint count | 2 (1-5) | 3 (1-5) | 3 (1-5) |
| Baseline VAS patient global | 60 (43-77) | 63 (54-75) | 61.5 (50-75) |
| Baseline CRP | 5.5 (1-11)[a] | 3.1 (1-13) | 3.6 (1-11) |
| Baseline adalimumab trough level (mg/L) | 3.9 (0.1-6.7) | 3.7 (0.9-7.3) | 3.7 (0.1-7.1) |
| In patients with <1.0 mg/L | 0.04 (0.01-0.1) | 0.02 (0.01-0.4) | 0.03 (0.01-0.1) |
| In patients with ≥1.0 mg/L | 6.1 (4.3-9.0) | 6.4 (2.7-7.7) | 6.2 (3.7-8.1) |
| Baseline antidrug antibody positivity[d] | | | |
| >12 AU/mL | 17[e] (54) | 11[f] (38) | 28[g] (47) |
| >100 AU/mL | 8[e] (26) | 5[f] (17) | 13[g] (22) |
| Treatment after randomisation | | | |
| TNFi | 14 (37) | 16 (40) | 30 (39) |
| Non-TNFi | 24 (63) | 24 (60) | 48 (62) |

ACPA, anticitrullinated protein antibody; AU, arbitrary unit; b/tsDMARD, biologic or targeted synthetic disease-modifying antirheumatic drug; csDMARD, conventional synthetic disease-modifying antirheumatic drug; DAS28 CRP, Disease Activity Score based on 28 joint count and C-reactive protein; RF, rheumatoid factor; TDM, therapeutic drug monitoring; TNFi, tumour necrosis factor inhibitor; VAS, visual analogue scale.
Data are mean ± SD, n (%), or median (Q1-Q3).
[a] 1 missing.
[b] 2 missing.
[c] Primary nonresponse defined as failure ≤6 months after start of adalimumab.
[d] Antidrug antibodies to adalimumab were positive if above the cutoff of 12 AU/mL (limit of detection); however, all values below 100 AU/mL were considered low.
[e] 7 missing.
[f] 11 missing.
[g] 18 missing.
[h] Sex is defined as biological sex, encompassing the physiological and genetic traits that typically categorize individuals as male or female.

antigen to the drug, meaning that the antigen may not be fully neutralised, leading to a reduced therapeutic effect. Conversely, when the drug concentration is very low, the drug may have a higher likelihood of binding to the available antigen. In this case, the drug is quickly depleted by binding to its target antigen, further reducing the free drug available in the system (also known as target-mediated drug disposition). This creates a complex relationship between the amount of drug and its interaction with the target, as low drug levels can paradoxically both decrease and increase effectiveness due to insufficient antigen exposure and rapid binding.

The only other available randomised controlled test-treatment studies regarding TDM demonstrated some benefit of TDM in a somewhat similar context. Two large trials, NOR DRUM A and B, assessed the added value of TDM in different settings [17,18]. NOR DRUM A found no improvement in clinical remission rates with TDM during the induction phase of infliximab treatment, but NOR DRUM B demonstrated that proactive TDM was more effective than standard therapy in maintaining disease control without worsening during the maintenance phase of infliximab therapy. The NOR DRUM studies included multiple diseases (both rheumatic and gastroenterologic) and did not include a treat-to-target treatment strategy. Additionally, effect sizes varied across diseases and were low and not statistically significant for RA. Finally, infliximab, and not adalimumab, was the study drug. This suggests that the added value of TDM may depend on type of drug, clinical decision context, and disease.

Our study has several strengths, including its design, which is a rare example of a test-treatment trial where a fully blinded approach was feasible [19]. The trial also was designed with automatic balancing of TNFi and non-TNFi treatment in mind, to prevent between-group differences being caused by imbalance in drugs with possible different efficacy. It should be noted that the test delay was present in both groups because the secondary randomisation depended on this. In clinical practice, patients would have been treated 2 weeks earlier in the control arm. Additionally, the trial was conducted at multiple centres across the country, enhancing its generalisability. However, the study also had limitations, such as a longer-than-expected inclusion period, partly due to the COVID-19 pandemic during the trial phase. This led to a deviation from the original protocol [9], as we incorporated JAKi as a non-TNFi option due to

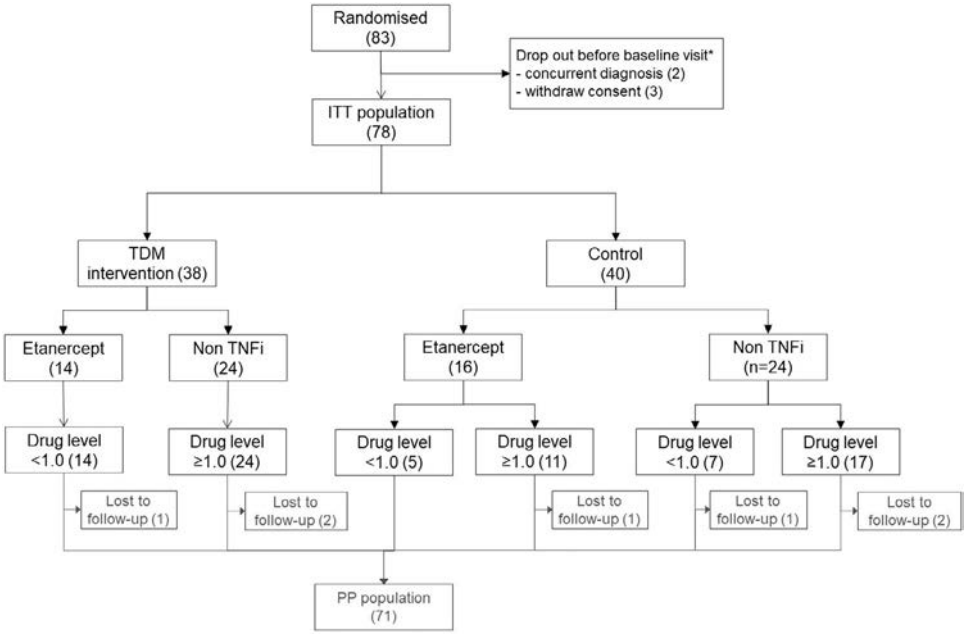



**Figure 1.** Flow diagram. *Two patients randomised to intervention and 3 to control. Numbers within brackets are number of patients. ITT, intention-to-treat; PP, per-protocol; TDM, therapeutic drug monitoring; TNFi, tumour necrosis factor inhibitor.

Table 2
**Key outcomes at 24 weeks of follow-up**

| Outcome variable | TDM-guided (n = 38) | Control (n = 40) |
|---|---|---|
| MTW DAS28-CRP | 3.15 ± 0.99 | 3.15 ± 1.01 |
| DAS28-CRP | 3.0 ± 1.1 | 2.9 ± 1.2 |
| Tender joint count | 1 (0-3) | 1 (0-5) |
| Swollen joint count | 0 (0-2) | 1 (0-3) |
| VAS patient global | 40 (20-69) | 30 (15-50) |
| CRP | 3.8 (1.0-8.5) | 1.2 (0.8-3.7) |
| DAS28-CRP <2.9 | 18 (47) | 22 (55) |
| EULAR response[a] | 21 (55) | 30 (75) |
| No. of patients with flare[b] | 14 (37) | 12 (30) |
| Serious adverse events | 3 (8) | 1 (3) |

CRP, C-reactive protein; EULAR, European Alliance of Associations for Rheumatology; MTW DAS28-CRP, mean time-weighted disease activity score based on 28-joint count and CRP; TDM, therapeutic drug monitoring.
Data are mean ± SD, n (%), or median (Q1-Q3).
[a] Good or moderate response according to the EULAR response criteria.
[b] Flare defined as an increase in DAS28-CRP compared with that in DAS28-CRP at the former visit with >1.2, or >0.6 when current DAS28-CRP ≥2.9.

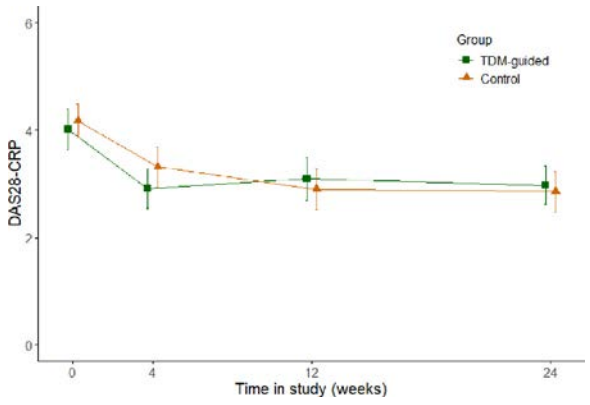



**Figure 2.** Disease activity during the study period. Data are mean (95% CIs). DAS28-CRP, disease activity score based on 28 joint count and C-reactive protein; TDM, therapeutic drug monitoring.

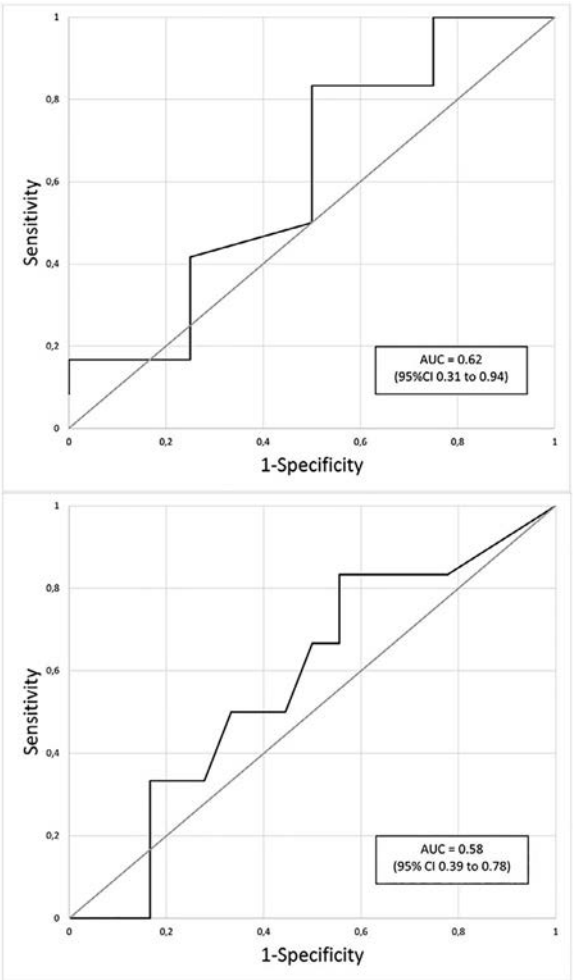



**Figure 3.** Receiver operating characteristic curve of the predictive value of adalimumab serum levels for achievement of EULAR response for patients in the control group receiving TNFi (upper) or non-TNFi (bottom). AUC, area under receiver operating characteristic curve; EULAR, European Alliance of Associations for Rheumatology; TNFi, tumour necrosis factor inhibitor.

COVID-19–related shortages or safety concerns with other non-TNFi options, which included rituximab, tocilizumab, sarilumab, and abatacept.

In conclusion, our study found no clinical benefit in the use of adalimumab trough serum concentrations to guide treatment switching in patients with RA who failed adalimumab.

## Competing interests

MB has received payment for expert testimony from Celltrion. TR has received research grants from Genmab and KyronBio. RFvV has received research grants to the institution from BMS, educational grants to institution from Alfasigma, AstraZeneca, Galapagos, MSD, Novartis, Pfizer, Roche, Sanofi, and UCB and consulting fees/honoraria from AbbVie, AstraZeneca, Biogen, Galapagos, BMS, GSK, Janssen, Pfizer, RemeGen, and UCB. SR has received research grants and/or consultancy fees from AbbVie, Eli Lilly, Galapagos/Alfasigma, MSD, Novartis, Pfizer, Sanofi, and UCB and is a member of the Executive Committee of the Assessment of Spondyloarthritis international society and of the EULAR Quality of Care Committee. NvH has received grants to the institution from Novartis, Lilly, Celltrion. BJFvdB has received research grants from Novartis/Fresenius and speaker fee from Lilly, Amgen, AbbVie, UCB, and Novartis. AAdB has received research grants to the institution from Celltrion, Lilly, Pfizer, AbbVie, Gilead, Sanofi, Janssen, Novartis, and Alfasigma/Galapagos. All other authors declare no competing interests.

## CRediT authorship contribution statement

**Maike H.M. Wientjes:** Writing – review & editing, Writing – original draft, Visualization, Project administration, Methodology, Investigation, Formal analysis, Data curation, Conceptualization. **Sadaf Atiqi:** Writing – review & editing, Project administration, Investigation, Data curation, Conceptualization. **Gerrit J. Wolbink:** Writing – review & editing, Writing – original draft, Supervision, Methodology, Investigation, Funding acquisition, Data curation. **Michael T. Nurmohamed:** Writing – review & editing, Writing – original draft, Supervision, Methodology, Investigation, Funding acquisition, Data curation, Conceptualization. **Maarten Boers:** Writing – review & editing, Visualization, Methodology, Funding acquisition, Conceptualization. **Femke Hooijberg:** Writing – review & editing, Project administration, Methodology, Data curation, Conceptualization. **Theo Rispens:** Writing – review & editing. **Annick de Vries:** Writing – review & editing. **Ronald F. van Vollenhoven:** Writing – review & editing, Funding acquisition, Conceptualization. **Sofia Ramiro:** Writing – review & editing, Project administration, Data curation. **Noortje van Herwaarden:** Writing – review & editing, Methodology. **Bart J.F. van den Bemt:** Writing – review & editing, Writing – original draft, Methodology, Investigation, Funding acquisition, Data curation, Conceptualization. **Alfons A. den Broeder:** Writing – review & editing, Writing – original draft, Supervision, Project administration, Methodology, Investigation, Funding acquisition, Formal analysis, Data curation, Conceptualization.

## Funding

The study is funded by Netherlands Organisation for Health Research and Development (ZonMw, grant number 8481 01 006) and Sanquin Diagnostic Services. There are no other financial or nonfinancial conflicts of interest other than specified. The Department of Rheumatology at Reade fulfils the role as sponsor, and the Department of Rheumatology at Sint Maartenskliniek is the coordinating study centre.

## Patient consent for publication

All participants provided written informed consent.

## Ethics approval

The study received ethical review board approval (number NL69841.091.19) and has been registered (Dutch Trial Register NL8210).

## Provenance and peer review

Not commissioned; externally peer reviewed.

## Data availability statement

The sponsor will consider requests for clinical trial data from qualified researchers with an appropriate and clearly defined scientific objective, following the publication of the primary results of the trial. Data considered for sharing can include anonymised aggregate clinical trial data not covered by relevant privacy legislation, clinical study reports, statistical analysis plan, informed consent forms, and protocol. Researchers will be required to sign a Data Use Agreement before receiving study documents. Data requests can be submitted to a.denbroeder@maartenskliniek.nl.

## Patient and public involvement

Patients and/or the public were not involved in the design, or conduct, or reporting, or dissemination plans of this research.

## Supplementary materials

Supplementary material associated with this article can be found in the online version at doi:10.1016/j.ard.2025.03.015.

## Orcid

Maike H.M. Wientjes: http://orcid.org/0000-0002-6666-9378
Michael T. Nurmohamed: http://orcid.org/0000-0002-6274-1934
Maarten Boers: http://orcid.org/0000-0002-6969-283X
Sofia Ramiro: http://orcid.org/0000-0002-8899-9087

## REFERENCES

[1] Smolen JS, Landewé RBM, Bergstra SA, Kerschbaumer A, Sepriano A, Aletaha D, et al. EULAR recommendations for the management of rheumatoid arthritis with synthetic and biological disease-modifying antirheumatic drugs: 2022 update. Ann Rheum Dis 2023;82(1):3–18.
[2] Krieckaert CL, van Tubergen A, Gehin JE, Hernández-Breijo B, Le Mélédo G, Balsa A, et al. EULAR points to consider for therapeutic drug monitoring of biopharmaceuticals in inflammatory rheumatic and musculoskeletal diseases. Ann Rheum Dis 2023;82(1):65–73.
[3] Van Herwaarden N, Van Den Bemt BJF, Wientjes MHM, Kramers C, Den Broeder AA. Clinical utility of therapeutic drug monitoring in biological disease modifying anti-rheumatic drug treatment of rheumatic disorders: a systematic narrative review. Expert Opin Drug Metab Toxicol 2017;13(8):843–57.
[4] L'Ami MJ, Ruwaard J, Krieckaert C, Nurmohamed MT, van Vollenhoven RF, Rispens T, et al. Serum drug concentrations to optimize switching from

adalimumab to etanercept in rheumatoid arthritis. Scand J Rheumatol 2019;48(4):266–70.
[5] Jamnitski A, Bartelds GM, Nurmohamed MT, van Schouwenburg PA, van Schaardenburg D, Stapel SO, et al. The presence or absence of antibodies to infliximab or adalimumab determines the outcome of switching to etanercept. Ann Rheum Dis 2011;70(2):284–8.
[6] Bartelds GM, Wijbrandts CA, Nurmohamed MT, Stapel S, Lems WF, Aarden L, et al. Anti-infliximab and anti-adalimumab antibodies in relation to response to adalimumab in infliximab switchers and anti-tumour necrosis factor naive patients: a cohort study. Ann Rheum Dis 2010;69(5):817–21.
[7] Plasencia C, Pascual-Salcedo D, Garcia-Carazo S, Lojo L, Nuno L, Villalba A, et al. The immunogenicity to the first anti-TNF therapy determines the outcome of switching to a second anti-TNF therapy in spondyloarthritis patients. Arthritis Res Ther 2013;15(4):R79.
[8] Ulijn E, den Broeder N, Wientjes M, van Herwaarden N, Meek I, Tweehuysen L, et al. Therapeutic drug monitoring of adalimumab in RA: no predictive value of adalimumab serum levels and anti-adalimumab antibodies for prediction of response to the next bDMARD. Ann Rheum Dis 2020;79(7):867–73.
[9] Wientjes MHM, Atiqi S, Wolbink GJ, Nurmohamed MT, Boers M, Rispens T, et al. Using adalimumab serum concentration to choose a subsequent biological DMARD in rheumatoid arthritis patients failing adalimumab treatment (ADDORA-switch): study protocol for a fully blinded randomised superiority test-treatment trial. Trials 2021;22(1):406.
[10] van der Maas A, Lie E, Christensen R, Choy E, de Man YA, van Riel P, et al. Construct and criterion validity of several proposed DAS28-based rheumatoid arthritis flare criteria: an OMERACT cohort validation study. Ann Rheum Dis 2013;72(11):1800–5.
[11] Pouw MF, Krieckaert CL, Nurmohamed MT, van der Kleij D, Aarden L, Rispens T, et al. Key findings towards optimising adalimumab treatment: the concentration-effect curve. Ann Rheum Dis 2015;74(3):513–8.
[12] Bartelds GM, Wijbrandts CA, Nurmohamed MT, Stapel S, Lems WF, Aarden L, et al. Clinical response to adalimumab: relationship to anti-adalimumab antibodies and serum adalimumab concentrations in rheumatoid arthritis. Ann Rheum Dis 2007;66(7):921–6.
[13] Fleischmann R, van der Heijde D, Koenig AS, Pedersen R, Szumski A, Marshall L, et al. How much does Disease Activity Score in 28 joints ESR and CRP calculations underestimate disease activity compared with the Simplified Disease Activity Index? Ann Rheum Dis 2015;74(6):1132–7.
[14] Bouman CA, van Herwaarden N, van den Hoogen FH, Fransen J, van Vollenhoven RF, Bijlsma JW, et al. Long-term outcomes after disease activity-guided dose reduction of TNF inhibition in rheumatoid arthritis: 3-year data of the DRESS study – a randomised controlled pragmatic non-inferiority strategy trial. Ann Rheum Dis 2017;76(10):1716–22.
[15] Fautrel B, Pham T, Alfaiate T, Gandjbakhch F, Foltz V, Morel J, et al. Step-down strategy of spacing TNF-blocker injections for established rheumatoid arthritis in remission: results of the multicentre non-inferiority randomised open-label controlled trial (STRASS: Spacing of TNF-blocker injections in Rheumatoid ArthritiS Study). Ann Rheum Dis 2016;75(1):59–67.
[16] Schulz KF, Altman DG, Moher D. CONSORT 2010 statement: updated guidelines for reporting parallel group randomized trials. Obstet Gynecol 2010;115(5):1063–70.
[17] Syversen SW, Goll GL, Jørgensen KK, Sandanger Ø, Sexton J, Olsen IC, et al. Effect of therapeutic drug monitoring vs standard therapy during infliximab induction on disease remission in patients with chronic immune-mediated inflammatory diseases: a randomized clinical trial. JAMA 2021;325(17):1744–54.
[18] Syversen SW, Jørgensen KK, Goll GL, Brun MK, Sandanger Ø, Bjørlykke KH, et al. Effect of therapeutic drug monitoring vs standard therapy during maintenance infliximab therapy on disease control in patients with immune-mediated inflammatory diseases: a randomized clinical trial. JAMA 2021;326(23):2375–84.
[19] Ferrante di Ruffano L, Dinnes J, Sitch AJ, Hyde C, Deeks JJ. Test-treatment RCTs are susceptible to bias: a review of the methodological quality of randomized trials that evaluate diagnostic tests. BMC Med Res Methodol 2017;17(1):35.

Ann Rheum Dis 84 (2025) 1301–1312

Contents lists available at ScienceDirect

Annals of the Rheumatic Diseases

journal homepage: https://www.sciencedirect.com/journal/annals-of-the-rheumatic-diseases

Rheumatoid arthritis

# Time-independent disease state identification defines distinct trajectories determined by localised vs systemic inflammation in patients with early rheumatoid arthritis

Nils Steinz[1,*], Tjardo D. Maarseveen[1], Erik B. van den Akker[2,3], Andrew P. Cope[4], John D. Isaacs[5], Aaron R. Winkler[6], Tom W. J. Huizinga[1], Yann Abraham[7], Rachel Knevel[1,3,8]

[1] *Department of Rheumatology, Leiden University Medical Centre, Leiden, the Netherlands*
[2] *Leiden Computational Biology Centre, Leiden University Medical Center, Leiden, the Netherlands*
[3] *The Delft Bioinformatics Lab, Pattern Recognition and Bioinformatics, Delft University of Technology, Delft, the Netherlands*
[4] *Centre for Rheumatic Diseases, School of Immunology and Microbial Sciences, Faculty of Life Sciences and Medicine, King's College London, London, UK*
[5] *Musculoskeletal Unit, Newcastle Upon Tyne Hospitals NHS Foundation Trust, Newcastle upon Tyne, UK*
[6] *Inflammation and Immunology Research Unit, Pfizer Inc, Cambridge, MA, USA*
[7] *Janssen Research and Development, Beerse, Belgium*
[8] *Translational and Clinical Research Institute, Newcastle University, Newcastle upon Tyne, UK*

ARTICLE INFO

*Article history:*
Received 8 November 2024
Received in revised form 14 March 2025
Accepted 8 April 2025

ABSTRACT

*Objectives:* Patients with rheumatoid arthritis (RA) display different trajectories towards improvement of disease. We aimed to disentangle the heterogeneity of RA disease trajectories from the first clinical visit onwards using graph-based pseudotime analysis.

*Methods:* We studied early patients with RA over 1.5 years in 2 data sets: Leiden (Netherlands), n = 1237, with 5017 visits, and Towards a Cure for Early Rheumatoid Arthritis (TACERA) (United Kingdom), n = 243, with 750 visits. We created a pipeline for time-independent clustering of clinical and haematologic features to identify disease states. Sequence analyses of these states defined the trajectories. We studied the predictability of the trajectories with baseline features.

*Results:* Clustering identified 8 disease states with localised inflammation (joints) and systemic inflammation (erythrocyte sedimentation rate [ESR] or leucocytes) as the main discriminating factors. The disease state sequences consisted of 4 trajectories, which we independently replicated in TACERA: A, high ESR; B, rapid progression from many inflamed joints towards remission; C, high leucocytes; and D, many inflamed joints with poor prognosis. Systemic vs local inflammation patterns showed moderate predictability at baseline (sensitivity of 71% and precision of 0.73 for trajectory A, although lower precision of 0.52 for trajectory B), while other trajectories were less predictable. Trajectories C and D had strong resemblance with B at baseline but deteriorated into less favourable trajectories. Patients in trajectory A were more often female and on average older. The trajectories were not explained by time till disease-modifying antirheumatic drug, baseline disease activity, or symptom duration. The suboptimal trajectories coincided with worse patient-reported outcomes, even when the inflammation was mainly systemic.

*Correspondence to Nils Steinz.
*E-mail address:* n.steinz@lumc.nl (N. Steinz).
**Handling editor** Josef S. Smolen.

https://doi.org/10.1016/j.ard.2025.04.011

0003-4967/© 2025 The Author(s). Published by Elsevier B.V. on behalf of European Alliance of Associations for Rheumatology (EULAR). This is an open access article under the CC BY license (http://creativecommons.org/licenses/by/4.0/)

*Conclusions:* We identified 4 distinct trajectories in early RA, differentiating RA into localised vs systemic inflammation. Our results highlight potential differences in disease pathology and opportunities for further targeted treatment. Inevitably, patterns without linkage to our selected features could not be detected.

**WHAT IS ALREADY KNOWN ON THIS TOPIC**

- The course of early rheumatoid arthritis (RA) after disease-modifying antirheumatic drug (DMARD) initiation differs in slow, moderate, and rapid progressors.
- Longer symptoms duration before DMARD initiation, older age, female sex, and seropositivity are associated with worse outcomes.

**WHAT THIS STUDY ADDS**

- Early RA consists of at least 4 different trajectories characterised by systemic inflammation (elevated erythrocyte sedimentation rate [ESR] or leucocytes) and localised inflammation (either fast or no/bad responders to treatment).
- Patients with mainly systemic inflammation (elevated ESR or leucocytes) are less likely to reach remission and have worse patient-reported outcomes.
- Most patients' trajectories are predictable with baseline joint and blood measurements and are not further explained by symptom duration, baseline disease activity, or timing of methotrexate prescription.

**HOW THIS STUDY MIGHT AFFECT RESEARCH, PRACTICE OR POLICY**

- To achieve optimal disease control, it is important to suppress inflammation in both the joints and systemic circulation.
- The trajectories underline the relevance of studies to the pathological differences of systemic vs local inflammation.
- Our study highlights a subgroup who deviates from the favourable trajectory who might benefit from more intensive treatment.

## INTRODUCTION

Despite advances in RA treatment, disease trajectories from first clinical visit to remission vary significantly [1–5]. Furthermore, the path to remission is rarely linear, with patients frequently experiencing fluctuations in disease activity over time [5]. To identify optimal moments for intervention and improve overall treatment outcomes, it is crucial to capture and analyse real-life trajectories of patients with early-treated RA.

Previous research identified 3 trajectories: rapid, gradual, and slow progressors [6,7]. These studies categorised patients exhibiting comparable disease activity difference at equivalent postbaseline time points [8]. By design, these studies could not have detected the granularity of disease trajectories where patients can move back to previous disease states. To further improve the knowledge on disease trajectory, we need to capture the granularity, apply methods that do not assume linear or polynomial relationships, and allow for variable transition speeds through disease states.

Unsupervised clustering methods are able to uncover unknown or invisible structures. They use functions and mathematical equations to separate data points, rather than using labels to differentiate data. These equations establish either linear or nonlinear correlations between data points, thereby forming clusters primarily based on the similarity between variables [9–11]. Specifically, graph-based pseudotime analysis has proven its value to discern the order of cell states in single-cell analyses [12]. Clinical patient data are different from single-cell data as there are no clear markers, highlighting whether a state is early or late, with the potential exception of the remission state. Certain states (eg, modest amount of joint inflammation) can occur either early or late during the disease course. Luckily, with the accessibility of electronic health records and observational cohorts, longitudinal data are available where the sequence of disease states can be deducted from the chronology of clinical visits.

In this study, we aimed to capture the real-world disease trajectories of patients with RA during their first 1.5 year at the outpatient clinic. First, we identified existing disease states independent of time integrating swollen joint counts (SJCs) and tender joint counts (TJCs) with multiple standard laboratory measurements. Subsequently, we defined disease trajectories by grouping patients with similar disease state sequences. The ultimate goal of this research was to elucidate distinct, explainable patient trajectories that elucidate the heterogeneity of early RA.

## METHODS

### *Data*

Our retrospective study contained 2 independent longitudinal datasets: the Dutch Leiden electronic health records (EHR) and the Towards a Cure for Early Rheumatoid Arthritis (TACERA) cohort from the United Kingdom. Both data sets consist of new/recent onset adult patients with RA (≥18 years), disease-modifying antirheumatic drug (DMARD) naive at baseline.

The Leiden EHR cohort contains patients who were newly referred to the Leiden outpatient clinic between 2011 and 2022 and received a diagnosis of RA within the first 1.5 years of follow-up by their rheumatologist [13]. Our data contains the first 1.5 years of records from patients who had at least 2 visits, including baseline. A single visit was defined as a haematologic laboratory test and a consultation with a rheumatologist within a 10-day window and incomplete visits were disregarded. A total of 1237 patients met the inclusion criteria for the study and collectively had 5017 visits. The treatment of patients reflects clinical care.

The Towards A Cure for Eary Rheumatiod Arthritis (TACERA) cohort consists of newly diagnosed patients with RA (European Alliance of Associations for Rheumatology (EULAR) 1987 or American College of Rheumatology (ACR) 2010) [14,15] with a maximum of 12-month symptom duration who were DMARD naive and seropositive (243 patients with 750 total visits) [7]. They were recruited in 2014 at time of DMARD initiation and the follow-up ranged from 0.5 to 1.5 years. Treatment changes were in accordance with the National Institute for health and Care Excellence guidelines [16].

### *Feature selection for clustering*

Feature selection was guided by 3 key principles: (1) focus on direct measures of disease activity that can change over time, (2) availability of consistent measurements across routine clinical visits, and (3) exclusion of treatments and their related variables and measurements. This led us to include SJC28 and TJC28,

erythrocyte sedimentation rate (ESR), leucocyte count, haemoglobin (Hb), mean corpuscular volume (MCV), and thrombocyte counts as measures of systemic inflammation. These variables capture the core clinical presentation of disease stages of RA and represent features routinely used in clinical decision-making. Anti-cyclic citrullinated peptide (aCCP) and rheumatoid factor (RF) were not part of the clustering as they did not meet the principles. In accordance with the third principle, the clustering excluded medication, dosage, and liver enzymes.

### *Clustering of independent visits to identify disease states*

Figure 1 provides a schematic representation of the study's pipeline from raw data to identification of disease states and disease trajectories. Visits were excluded if they missed clustering variables, occurred beyond 1.5 years after initial rheumatologist visit, or when leucocytes exceeded $25 \times 10^9$ (as this was most likely not RA related). Patients were excluded if they lacked complete baseline data or had fewer than 2 visits within 1.5 years of follow-up. The input data were the SJC28, TJC28, ESR, leucocyte count, Hb, MCV, and thrombocyte counts at each visit. C-reactive protein was not included due to low availability, and for the TACERA, the MCV was excluded due to its absence in the data set. The features were normalised using minimum to maximum normalisation between 0 and 1. For identification of the disease states, we clustered the visits using the Phenograph [17] with the cosine similarity metric and the Leiden algorithm. The time of the visits, sex, age, and seropositivity were not used for clustering.

We determined the number of clusters (disease states) based on data clustering consistency and cluster size. For this, we set the optimal $k$ for the $k$-nearest neighbours algorithm in the Phenograph package by testing a range of $k$ values between 10 and 400, with increments of 10. We compared the different configurations for the clustering model to find the most stable region in the adjusted Rand index between $k$ values. For transferability testing, we used machine learning algorithms (logistic regression, support vector machine, and random forest) to classify the clusters based on the features.

### *Defining patient trajectories*

With the real timing of visits, we could order the disease states for each patient creating individual trajectories. We identified commonalities in patients' trajectories with the adjusted Bobroske algorithm [18] to disallow transposition. Matches were calculated as the inverse logarithm of the frequency of the disease state occurrence and further normalised to within a range between 1 and 5. Mismatches were transformed by multiplying the matches by −0.5, and indels were calculated as mismatches multiplied by 0.75. The sequence score was transformed using the same calculation as in the original article. Pairwise sequence similarity was applied to all patients, resulting in a similarity matrix. The Phenograph package's clustering algorithm was then applied to cluster similar trajectories.

After identifying trajectories, we performed post hoc analyses to characterise these patterns using variables excluded from the clustering analysis. This included examining medication usage, treatment survival, and patient characteristics (eg, age, CCP, and RF) across the different trajectories.

### *Clinical differences between trajectories*

To compare differences in patient-reported outcome measure (PROM), we created a linear mixed effect model with random intercept. The model was fitted with fixed-effects age, sex, months, and trajectory cluster with an interaction between months and trajectory cluster. We tested whether the interactions between month and trajectory clusters were significant.

### *Baseline features used to predict the future trajectory*

In order to predict the trajectory that a patient would take, we trained an support vector machine (SVM) model using crossvalidation on 80% of the data and used a 20% test set for final results. The model used the baseline features that were used to cluster the data. We then analysed the discrepancies between the baseline trajectory assignment and their true trajectory. To investigate the impact of age, sex, seropositivity, days until medication, and symptom duration on the

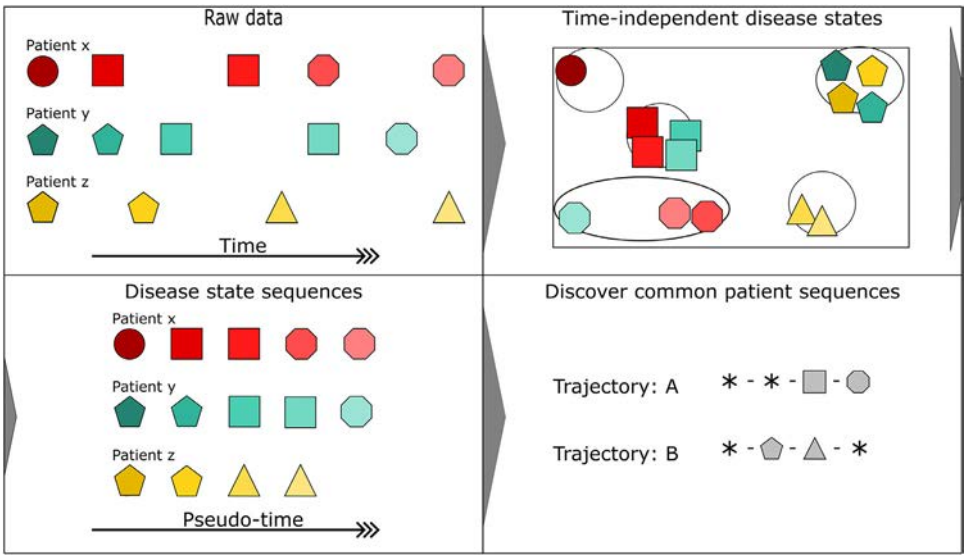



**Figure 1.** Individual patient visits are clustered based on similar phenotypic characteristics, irrespective of patient, treatment, or time. Next, the sequence of patient states is inferred from the date of visits, leading to individual patient trajectories. Disease trajectories are defined based on a shared sequence of states across patients using sequence similarity and clustering. The colours indicate different patients, and the hue decreases with time in a patient visit sequence. Different shapes indicate different disease states.*Any cluster could be in that time point.

prediction of trajectories, we used logistic regression on the subset of patients with known symptom duration.

### *Treatment survival analysis*

To assess whether differences in outcomes between trajectories reflect patterns of treatment response, we performed survival analyses of DMARD persistence. We performed 2 analyses: first DMARD survival and second DMARD survival. For the first DMARD analysis, time zero was set at DMARD initiation, and events were defined as switching to or adding another DMARD. For the second DMARD analysis, we calculated survival until the start of the third DMARD change event if patients had a second DMARD. In both analyses, patients were censored at the last follow-up visit if no switch occurred. We used Kaplan–Meier to estimate survival probabilities and compared trajectories using log-rank tests.

## RESULTS

### *Baseline description and general patient trajectory*

The 2 data sets had some differences due to inclusion criteria (Table 1). The Leiden patients were slightly older and less often female. As per study design, patients in TACERA were seropositive. The overall seropositivity rate was 55.2% in Leiden. At the first visit, the majority of patients in Leiden (53%) received a DMARD, which rapidly increased over the follow-up visits (Supplementary Fig S1). In TACERA, this was 100%, by design. On average, both the Leiden and TACERA populations improved over time on all features (Table 1). Patient characteristics of those excluded from the Leiden cohort due to missing data are presented and compared in Supplementary Table S1.

### *Patient disease states during the first 1.5 years of RA*

We used a data-driven approach as outlined earlier to define the optimal number of disease states (clusters). This clearly showed 8 clusters over any other number of clusters (Supplementary Fig S2). We then further confirmed the stability of the clusters with an SVM algorithm, which predicted the clusters with 94.8% accuracy on a holdout test set (Supplementary Fig S3).

The 8 identified clusters described the disease states exhibited by patients during their visits to the clinic (Fig 2A and Supplementary Table S2). Although time of visit was not part of the clustering, the disease states exhibited significant temporal differences (Fig 2B). The disease state that contained the most late-time visits was L1. At this disease state, patients had the lowest disease activity with near-zero number of swollen and tender joints, lowest ESR, and within normal range leucocytes and Hb. L8 is predominantly an early visit state that contains no visits after 1 year. At this disease state, patients have low swelling and tenderness and low Hb.

For the in-between disease states, the main differentiation is based on the amount of swollen and tender joints vs systemic inflammation (ESR or leucocytes).

Among the high joint inflammation states, L7 is the most severe state. Patients in this state have a high number of swollen and tender joints and a moderately elevated ESR. The L7 disease state not only is frequently observed at baseline but also occurred less frequently at later stages of disease course. A similar but more moderate disease state L4 is characterised by numerous swollen and tender joints and without elevated ESR. L4 is common early in the disease course and common after 1 year of follow-up.

The inflamed disease states could be further differentiated into elevated ESR or leucocytes. The elevated ESR states were L6, L5, and L2. L6 contains patients who have moderately swollen and tender joints and a highly elevated ESR. Patients with L6 disease were commonly seen at baseline, and some may present with the disease state later on in their treatment. Patients in disease state L5 have similar disease characteristics, visit frequency, and time after baseline to L6, but with a less elevated ESR. L2 contains patients at a low disease state: low to no swollen and/or tender joints but still a modestly elevated ESR. This elevated ESR coincides with a subtle increase in leucocytes, thrombocytes, and decreased Hb. This condition could be

Table 1
**General data description of the Leiden cohort and the TACERA cohort**

| | Leiden | | TACERA | | *P* | |
|---|---|---|---|---|---|---|
| Features | Baseline | Last visit | Baseline | Last visit | Baseline | Last visit |
| No. of patients | 1237 | | 243 | | | |
| No. of visits | 4 (2-5) | | 3 (2-4) | | | |
| Female | 797 (64.4) | | 177 (72.8) | | <.05 | |
| RF positive | 570 (46.1) | | 207 (85.2) | | <.05 | |
| aCCP positive | 571 (46.2) | | 223 (91.8) | | <.05 | |
| Seropositive | 683 (55.2) | | 243 (100) | | <.05 | |
| Age (y), mean (SD) | 59.8 (14.7) | | 53.0 (14.9) | | <.05 | |
| TJC28[a] | 4 (2-8) | 1 (0-3) | 9 (4-14) | 2 (0-5) | <.05 | <.05 |
| SJC28[a] | 3 (1-7) | 0 (0-2) | 6 (3-10) | 1 (0-3) | <.05 | .786 |
| ESR[a] | 28 (11-45) | 14 (6-29) | 27 (12-43) | 12 (6-24) | .228 | <.05 |
| Leucocytes[a] | 7.9 (6.3-9.6) | 7.2 (6.0-8.8) | 7.8 (6.6-9.2) | 6.3 (5.1-7.8) | .299 | <.05 |
| Haemoglobulin[a] | 8.2 (7.5-8.8) | 8.3 (7.7-8.8) | 8.2 (7.5-8.8) | 8.2 (7.6-8.8) | <.05 | .221 |
| MCV[a] | 90 (87-93) | 92 (89-96) | NA | NA | NA | NA |
| Thrombocytes[a] | 290 (246-352) | 264 (225-314) | 293 (255-365) | 267 (226-312) | .199 | .885 |
| DAS28 | 4.3 (3.3-5.3) | 2.9 (2.1-3.9) | 5.0 (4.1-5.8) | 3.0 (2.0-4.0) | <.05 | .651 |
| DMARD assignment | 650 (52.5) | 1148 (92.8) | 243 (100) | 243 (100) | <.05 | <.05 |

aCCP, anticyclic citrullinated peptide; DAS, disease activity score; DMARD, disease-modifying antirheumatic drug; ESR, erythrocyte sedimentation rate; MCV, mean corpuscular volume; RF, rheumatoid factor; SJC, swelling joint count; TACERA, Towards a Cure for Early Rheumatoid Arthritis; TJC, tender joint count.
Values are median (IQR) or n (%) unless specified. Welch t test was applied for the P values.
[a] Features included for clustering.

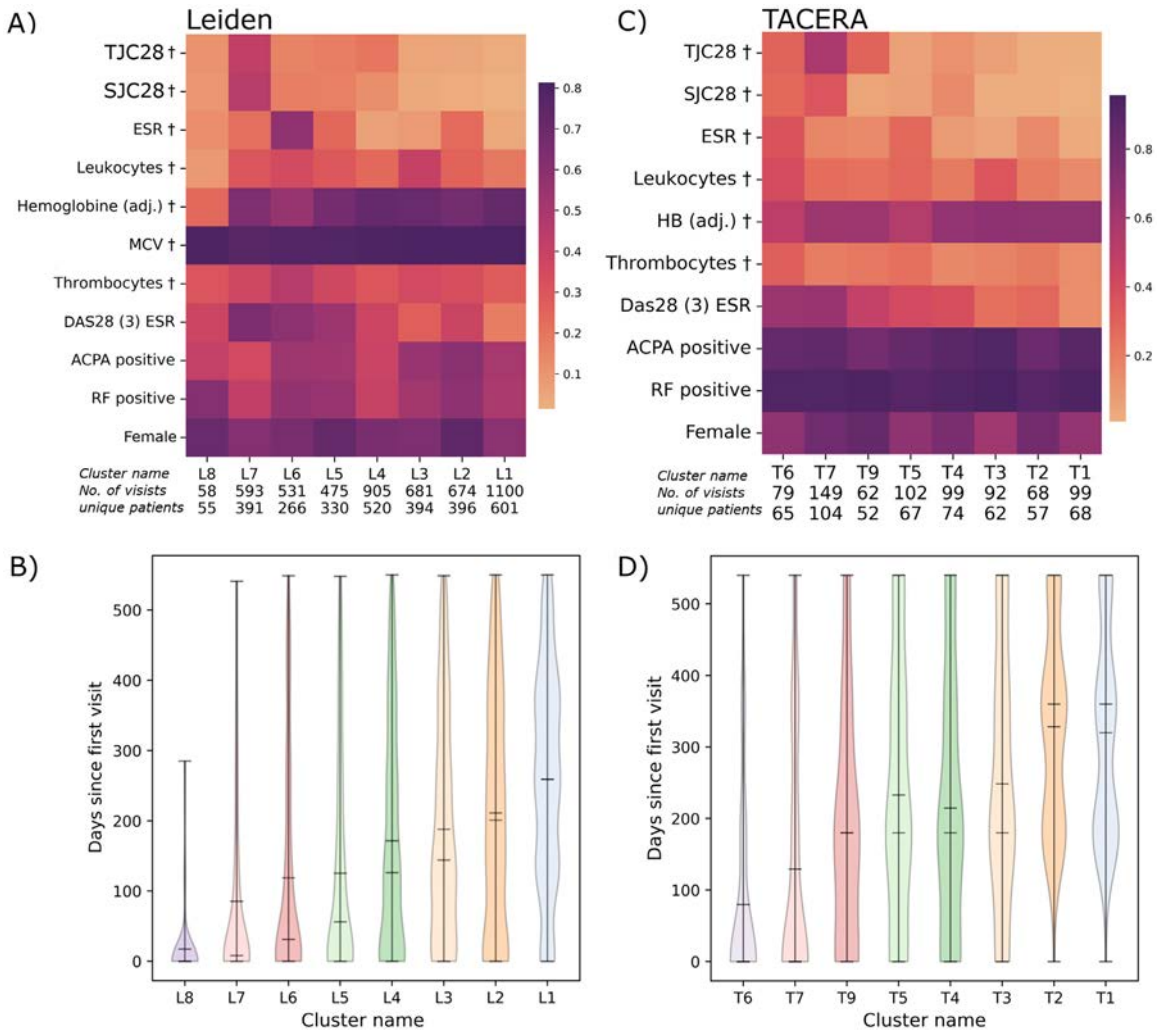



**Figure 2.** Results of the clustering and sequence analyses on the Leiden or TACERA data. (A,C) Heatmap of mean characteristics of the disease states (clusters). All values are scaled between 0 and 1 (orange–purple). (B,D) Number of days the visit took place after baseline for each cluster. †Variables used for clustering. TACERA, Towards a Cure for Early Rheumatoid Arthritis.

observed in the clinic in all states within the first 1.5 years, but the majority of the L2 assigned visits were after 200 days of first visit.

L3 describes a phenotype with a leucocyte count above the upper reference values (mean, 11.0 × $10^9$; SD, 2.69; reference = 4.0-10.0 × $10^9$) and a low amount of joint and blood inflammation. This state of the disease was most prevalent 1 year after the baseline.

### *Similar disease states observed in independent replication in TACERA*

For the TACERA data set, we applied the same normalisation and unsupervised clustering pipeline as used for Leiden. To facilitate comparability of cluster content with Leiden, we set the *k* to find 8 clusters in TACAERA. The content of the clusters were defined in an unsupervised manner, without using any knowledge from the findings in the Leiden data.

Within TACERA, we saw that the disease states resembled those from the Leiden data (Fig 2C). The optimal disease state L1 was also present in TACERA which we named T1. T1 shows no active disease with a near-zero amount of swollen and tender joints and no elevation in ESR.

All first 7 disease state (L1-L7) were also present in TACERA. We identified a distinct state characterised by patients with tender joints and mildly elevated ESR (<30) in TACERA. While this state shares some features with L4 (tender joints), it represents a unique intermediate phenotype not observed in the Leiden cohort. To avoid confusion with L8 (the early disease state unique to Leiden), we designated this TACERA-specific state as T9. Similar as in the Leiden data, the main differentiating factor in TACERA is based on local (joints) vs systemic inflammation (ESR and leucocytes).

### *Different disease trajectories in patients with early RA*

At the group level, we observed a clear pattern of reduction of disease activity towards reaching remission; 47.0% and 28.0% of the patients reached the optimal disease state L1/T1 within 1.5 years, and 31.4% and 23.5% got close to the optimal state and ended in L2/T2. This suboptimal end state appears optimal based on SJCs and TJCs, but the ESR was still elevated. This deviation from the optimal disease state was rather subtle as most values were within the normal range.

To find subsets of trajectories, we independently clustered the patient-level sequences of Leiden and TACERA and found 4 separate trajectories in Leiden and 5 in TACERA (Fig 3 and Supplementary Fig S4). These revealed a more granular pattern of disease improvement and flare than the average patterns. At baseline, patients across the trajectories differed in age, sex, seropositivity, baseline disease activity score (DAS)28, and symptom duration (Tables 2 and 3).

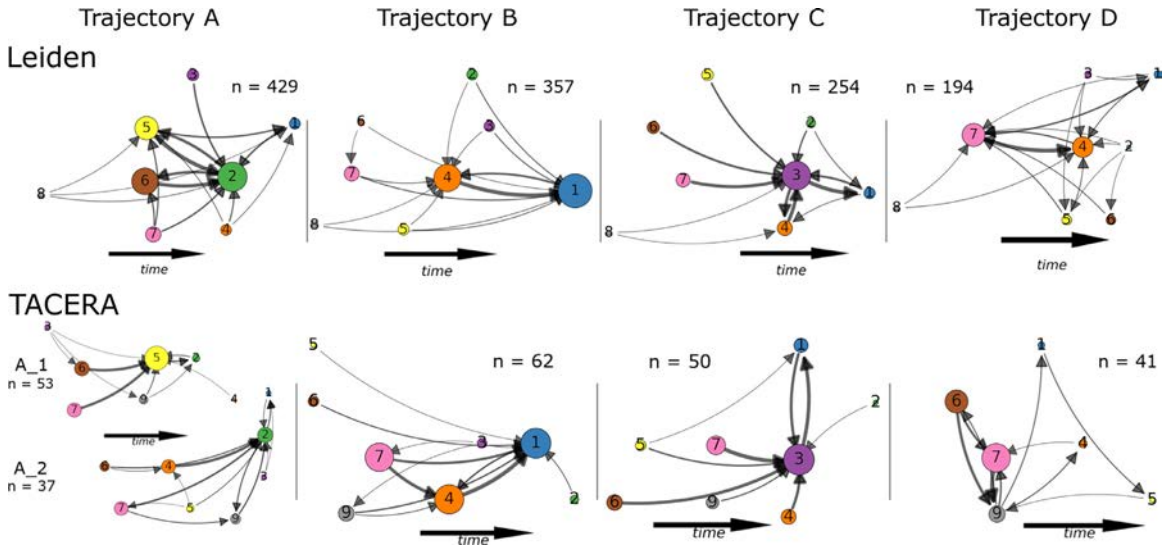



**Figure 3.** Trajectories based on the cluster sequence per patient. Four common trajectories were identified and were distinguished by (A) erythrocyte sedimentation rate, (B) good trajectory, (C) leucocytes, and (D) bad trajectory. The nodes are the disease states with the size of the node marking the number of patient visits. The edge thickness reflects the transition frequency. The nodes on the left side of the graph are, on average, more prevalent at an earlier state of the trajectory, while the nodes on the right side are more common at a later state. TACERA, Towards a Cure for Early Rheumatoid Arthritis.

Although independently analysed, the trajectories from Leiden and TACERA exhibited strong similarities as summarised further.

### *Leiden-A, TACERA-A.1, and TACERA-A.2—high ESR clusters at start and end (L6 to L5 to L2, and T6 to T5 to T2)*

While patients following this trajectory could start in any disease state, it was most common for them to start in the active disease state L/T6 or L/T5 with elevated ESR and active swollen and tender joints and end up in the suboptimal disease state L/T2. A small subset of patients reached the optimal final state (L/T1), but most moved back to L/T2. Within TACERA, trajectory A was subdivided into 2 similar trajectories marked by elevated ESR, where patients in TACERA-A.1 have the worse outcome by remaining in the modestly active disease T5, instead of moving towards T2. Trajectory A was predominantly female. The prevalence of CCP and RF was higher than average in Leiden and more evenly distributed in TACERA.

### *Leiden-B and TACERA-B—rapid progression from primarily joint inflammation towards the ideal cluster (L1 and T1)*

Patients can start from any cluster and reached L/T1 within a year, either directly or via L/T4. Trajectory B had the most marked DAS28 improvement. They were more frequently male were younger. On average, it took patients in trajectory B

Table 2
**Descriptive characteristics of Leiden patients and trajectories**

| Feature | Leiden patients | Leiden trajectory A | Leiden trajectory B | Leiden trajectory C | Leiden trajectory D |
|---|---|---|---|---|---|
| No. of patients | 1237 | 429 | 357 | 254 | 197 |
| Visits | 4 (2-5) | 3 (2-5) | 4 (3-5) | 4 (3-5) | 3 (2-5) |
| Female | 797 (64.4) | 309 (72.0) | 214 (59.9) | 155 (61.0) | 119 (60.4) |
| Age (y), mean (SD) | 59.8 (14.7) | 63.01 (13.8) | 56.03 (14.27) | 58.76 (16.45) | 61.1 (13.45) |
| Rheumatoid factor | 570 (46.1) | 217 (50.6) | 162 (45.4) | 123 (48.4) | 68 (34.5) |
| aCCP | 571 (46.2) | 227 (52.9) | 160 (44.8) | 130 (51.2) | 54 (27.4) |
| Seropositive | 683 (55.2) | 263 (61.3) | 195 (54.6) | 145 (57.1) | 80 (40.6) |
| Baseline TJC28[a] | 4 (2-8) | 4 (2-7) | 3 (1-6) | 3 (1-7) | 9 (5-15) |
| Baseline SJC28[a] | 3 (1-7) | 3 (1-6) | 2 (0-5) | 2 (1-6) | 7 (4-13) |
| Baseline ESR[a] | 28 (11-45) | 43 (31-67) | 14 (6-25) | 19 (11-36) | 19 (9-36) |
| Baseline DAS28(3) ESR, mean (SD) | 4.27 (1.38) | 4.71 (1.12) | 3.61 (1.3) | 3.94 (1.4) | 4.89 (1.39) |
| Last visit TJC28[a] | 1 (0-3) | 2 (0-4) | 1 (0-2) | 1 (0-2) | 4 (1-7) |
| Last visit SJC28[a] | 0 (0-2) | 1 (0-3) | 0 (0-1) | 1 (0-2) | 3 (0-5) |
| Last visit ESR[a] | 14 (6-29) | 32 (19-45) | 6 (2-11) | 11 (6-19) | 9 (6-17) |
| Last visit DAS28(3) ESR, mean (SD) | 3.01 (1.29) | 3.72 (1.15) | 2.13 (0.95) | 2.76 (1.15) | 3.37 (1.23) |
| Symptom duration at baseline (d) | 155 (62-548) | 154 (62-730.0) | 180 (62-546) | 233 (80-730) | 115 (42-276) |
| Time till first DMARD (d) | 28 (14-105) | 28 (14-120) | 28 (14-101) | 28 (14-147) | 28 (14-65) |
| Prednisolone used ever (%) | 72.8 | 77.2 | 65.5 | 74.6 | 78.3 |
| Most prevalent first DMARD (%) | MTX (80.0) | MTX (81.0) | MTX (82.5) | MTX (80.6) | MTX (78.6) |
| Remission[b] (%) | 56.9 | 25.4 | 90.5 | 72.4 | 44.7 |

aCCP, anticyclic citrullinated peptide; DAS(3), 3-component disease activity score for the 28 joint scheme; DMARD, disease-modifying antirheumatic drug; ESR, erythrocyte sedimentation rate; MTX, methotrexate; SJC, swollen joint count; TJC, tender joint count.
Values are median (IQR) or n (%) unless specified.
[a] Features included for clustering.
[b] Reached DAS28(3) ESR < 2.6 at some point in the trajectory.

208 days to reach low disease activity or remission, while starting with an average of 3 tender and swollen joints at baseline.

### *Leiden-C and TACERA-C—transition through or ending at high leucocyte state (L3 and T3)*

Patients in trajectory C experience difficulty reaching cluster L1 and may divert from L3 to L4, which can be considered a worsening disease activity. Time between symptom onset and the first visit was the longest for this group, while other aspects of the data set were average. The main difference between trajectory C and the optimal trajectory B was an increase in leucocytes. Patients in trajectory C had the highest leucocyte count before and after prednisone (Supplementary Fig S5).

### *Leiden-D and TACERA-D—poor prognosis (L7 to L4 and T7 to T4)*

Trajectory D was the most severe trajectory, as patients do not reach the optimal disease state L/T1 or even the low disease states L/T2 and L/T3. Instead, they end up in an active disease state of L/T4 with inflamed joints but low levels of blood inflammation. Trajectory D had the worst baseline TJC and SJC. The DAS decreased from 4.65 to 3.54 in Leiden and 5.75 to 4.60 in TACERA, indicating a moderate disease activity state, over the course of 1.5 years. The patients in this trajectory exhibited the shortest symptom duration until their first visit to the clinic, with an average of 101 days. Additionally, trajectory D exhibited the lowest prevalence of seropositive patients. At the start, patients in trajectory D were similar to those in trajectory B.

Most patients in the trajectories received DMARDs within the first month, with a median time to DMARD of 15 (14-19) days. In all trajectories, methotrexate (MTX) was the primary DMARD, with only slight variations in average usage. In addition, compared with the other trajectories, patients in trajectory B receive least frequently prednisolone. A comparable proportion of patients within the TACERA cohort receive MTX at baseline, with the remainder receiving other conventional synthetic DMARDs. However, TACERA patients were less likely than Leiden patients to receive steroids (triamcinolone or prednisone), with the highest percentage being trajectory D.

### *Patient-reported outcomes differ between trajectories*

The trajectories differed in both the disease states patients' transition through as well as the final disease state. The question arises whether the differences between the trajectories in systemic or localised inflammation are clinically relevant, particularly when the difference was driven by ESR or leucocytes and not per se the joints. To analyse the differences in patient-perceived progressions and correlation with trajectories, we examined the PROMs from the TACERA cohort, which were available for 72.4% of the visits. Our findings showed that the trajectories that do not lead to the optimal state (L/T1) also resulted in worse outcomes in the PROMs (Fig 4). The disease progression and activity described by DAS28 (A) and simplified disease activity index (SDAI) (B) showed similar trajectories with the SDAI being worse overall. In addition, in PROMs, trajectory B was the most favourable trajectory. Here, patients start with clear impairment and steadily improve over time as measured in health assessment questionnaire (HAQ), fatigue, and global assessment. Trajectory A_1 and A_2 (the trajectories characterised by increased ESR) have fairly good improvement in HAQ, but their fatigue remains unchanged. Trajectory D, the poorest trajectory with highly inflamed joints, starts with the poorest HAQ, slightly improving in the first year, but returns to HAQ levels similar to baseline. This trajectory differs significantly from B (Supplementary Table S4). For the fatigue score, the plot lines were stable, with only groups B and C demonstrating a distinct downwards trend in the first 6 months. Surprisingly, trajectory C returns to the initial values, while B continues to improve. For both patient global assessment (PGA) and evaluator global assessment (EGA), trajectory C showed a significantly different

Table 3
**Descriptive characteristics of TACERA patients and trajectories**

| Feature | TACERA patients | TACERA trajectory A_1 | TACERA trajectory A_2 | TACERA trajectory B | TACERA trajectory C | TACERA trajectory D |
|---|---|---|---|---|---|---|
| No. of patients | 243 | 53 | 37 | 62 | 50 | 41 |
| Visits | 3 (2-4) | 3 (2-4) | 3 (2-4) | 4 (3-4) | 3 (2-4) | 3 (2-4) |
| Female | 177 (73.5) | 36 (67.9) | 30 (81.1) | 45 (72.6) | 32 (64.0) | 34 (82.9) |
| Age (y), mean (SD) | 53.4 (15.00) | 60.23 (12.4) | 53.41 (13.77) | 49.58 (15.00) | 50.48 (16.23) | 51.24 (14.56) |
| Rheumatoid factor | 223 (91.8) | 47 (88.7) | 34 (91.9) | 58 (93.5) | 48 (96.0) | 36 (87.8) |
| aCCP | 207 (85.5) | 43 (81.1) | 30 (81.1) | 53 (85.5) | 45 (90.0) | 37 (90.2) |
| Seropositive | 100 | 100 | 100 | 100 | 100 | 100 |
| Baseline TJC28[a] | 9 (4-14) | 7 (3-13) | 8 (4-15) | 9 (5.2-14) | 6.5 (3-10) | 13 (9-17) |
| Baseline SJC28[a] | 6 (3-10) | 6 (3-10) | 7 (5-9) | 6 (4-9.8) | 4 (2-7) | 8 (4-10) |
| Baseline ESR[a] | 27 (12-43) | 40 (27-52) | 26 (14-44) | 17 (8-32) | 15 (7-31) | 30 (17-65) |
| Baseline DAS28(3) ESR, mean (SD) | 5.18 (1.37) | 5.2 (1.12) | 5.02 (1.38) | 5.11 (1.32) | 4.17 (1.27) | 5.75 (1) |
| Last visit TJC28[a] | 2 (0-5) | 1 (0-3) | 0 (0-2) | 1 (0-3) | 1 (0-3.8) | 8 (6-13) |
| Last visit SJC28[a] | 1 (0-3) | 1 (0-2) | 0 (0-2) | 0 (0-2) | 0 (0-1.8) | 4 (2-6) |
| Last visit ESR[a] | 12 (6-24) | 27 (17-33) | 21 (10-24) | 7 (2-11) | 6 (2.2-9.8) | 16 (8-25) |
| Last visit DAS28(3) ESR, mean (SD) | 3.04 (1.36) | 3.36 (0.91) | 2.93 (0.99) | 2.40 (1.33) | 2.30 (1.10) | 4.60 (1.00) |
| Symptom duration at baseline (d) | 137 (87-198) | 119 (84-159) | 138 (93-182) | 146 (92-199) | 153 (93-218) | 173 (83-259) |
| Time till first DMARD (d) | 0 (0-0) | 0 (0-0) | 0 (0-0) | 0 (0-0) | 0 (0-0) | 0 (0-0) |
| Steroid used ever (%) | 72.4 | 81.1 | 64.9 | 72.6 | 68.0 | 73.2 |
| Remission[b] (%) | 38.4 | 20.8 | 32.4 | 62.9 | 62 | 0 |

aCCP, anticyclic citrullinated peptide; DAS(3), 3-component disease activity score for the 28 joint scheme; DMARD, disease-modifying antirheumatic drug; ESR, erythrocyte sedimentation rate; SJC, swollen joint count; TACERA, Towards a Cure for Early Rheumatoid Arthritis; TJC is tender joint count.
Values are median (IQR) or n (%) unless specified.
[a] Features included for clustering.
[b] Reached DAS28(3) ESR < 2.6 at some point in the trajectory.

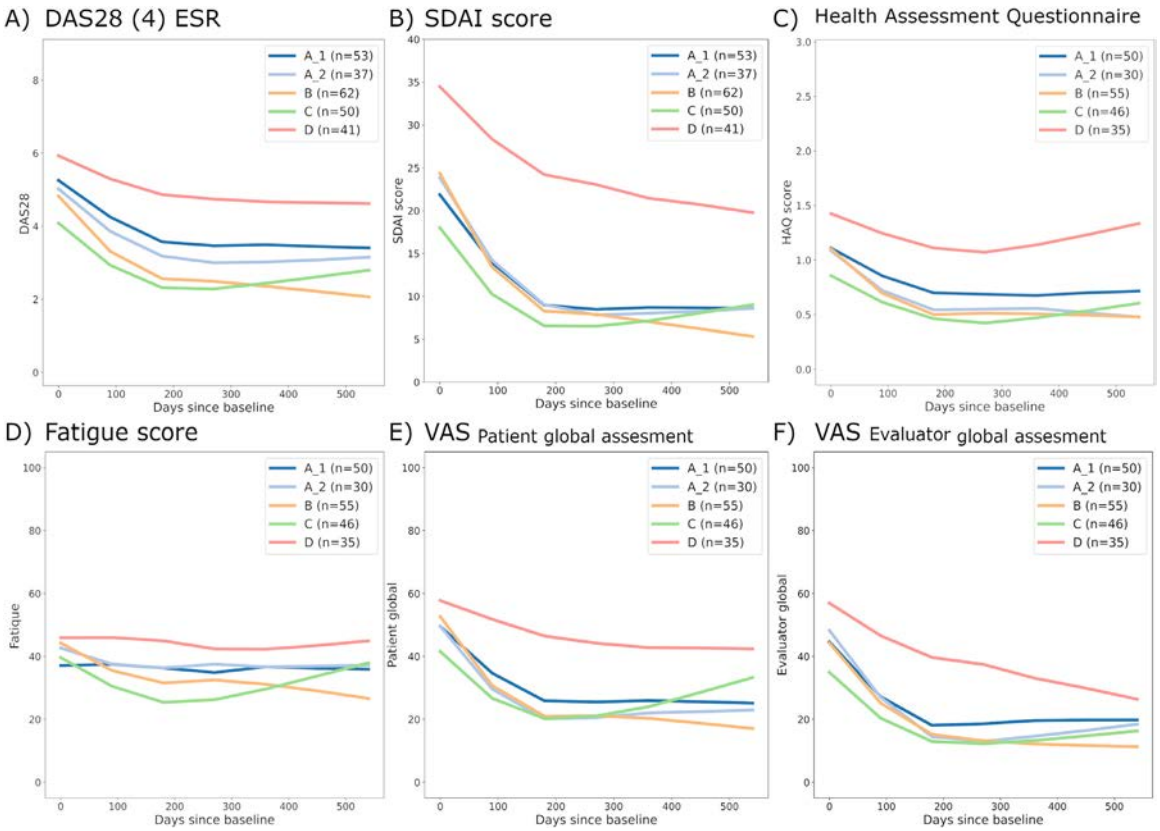



**Figure 4.** Evolution of patient-reported outcomes over time. Trajectories A_1 and A_2 are characterised by elevated erythrocyte sedimentation rate (ESR) levels, with A_1 associated with an unfavourable prognosis. Trajectory B represents the optimal outcome, while Trajectory C is categorised by elevated leucocyte counts. Trajectory D represents the least favourable progression group. The graphs depict (A) disease activity score (DAS)28 ESR trend, (B) simplified disease activity index (SDAI) trend, (C) the trend of health assessment questionnaire score, (D) fatigue reported by patients, (E) disease activity experienced by patients; (F) disease activity assessed by the rheumatologist. VAS, visual analogue scale.

path after 1 year compared with B. For trajectory D, only PGA was significantly different.

### *Predicting trajectories based on baseline features*

We built a classifier to predict patients' trajectory using baseline value of the features that were used for defining the disease states. This model exhibited an overall accuracy of 60%. Particularly trajectories A and B could be accurately predicted with a sensitivity (recall) of 71% for both (Fig 5 and Supplementary Table S3), while trajectory B was less precise with a precision of 0.52 vs 0.73 for trajectory A. The prediction of D and, to a lesser extent C, at baseline had lower sensitivity rates (26% and 48%, respectively), with D additionally not being precise (0.38) compared with C (0.71). Patients who ultimately end up in trajectory C or D were frequently labelled or predicted to follow trajectory B or even A. Many patients at baseline exhibited characteristics similar to those of patients following trajectory B. Yet, they ultimately deviate towards the less favourable trajectories C and D. Similarly, approximately 15% of patients in different trajectories have a similar baseline compared with those in trajectory A. Women, older people, and people with anti-CCP (aCCP) were more likely to end up in trajectory A than B (Supplementary Fig S6). Age, sex, and aCCP improved the predictive model, while MTX, time to DMARD, and symptom duration until the first visit did not significantly improved the prediction of any of the trajectories at baseline (Supplementary Tables S5 and S6).

### *Treatment persistence across trajectories*

To understand treatment patterns across trajectories, we analysed both first and second DMARD survival (Fig 6). First DMARD survival at 1.5 years varied significantly between trajectories, with trajectory B showing the highest persistence (62% remaining on initial DMARD) compared to trajectories A (54%; $P = .002$), C (58%; $P = .924$), and D (47%; $P = .001$). Notably, while trajectories B and C showed similar persistence ($P = .924$), both demonstrated significantly better drug survival than trajectory D (C vs D: $P = .002$) and trajectory A (C vs A: $P = .008$). Trajectories A and D showed comparable persistence rates ($P = .278$).

This pattern was largely maintained for second DMARD survival, where trajectory B again showed superior persistence (68%) compared with trajectories A (58%; $P < .001$), C (60%; $P = .559$), and D (51%; $P = .003$). Trajectory C maintained significantly better persistence than both trajectories A ($P = .009$) and D ($P = .030$), while trajectories A and D showed similar survival rates ($P = .920$).

## DISCUSSION

Our findings confirm the existence of distinct disease trajectories in early RA. We uncovered 4 RA trajectories: (A) elevated ESR, (B) localised joint inflammation with favourable outcome, (C) elevated leucocyte count, and (D) persistent localised joint inflammation. These trajectories can be broadly categorised into localised inflammation and systemic inflammation patterns,

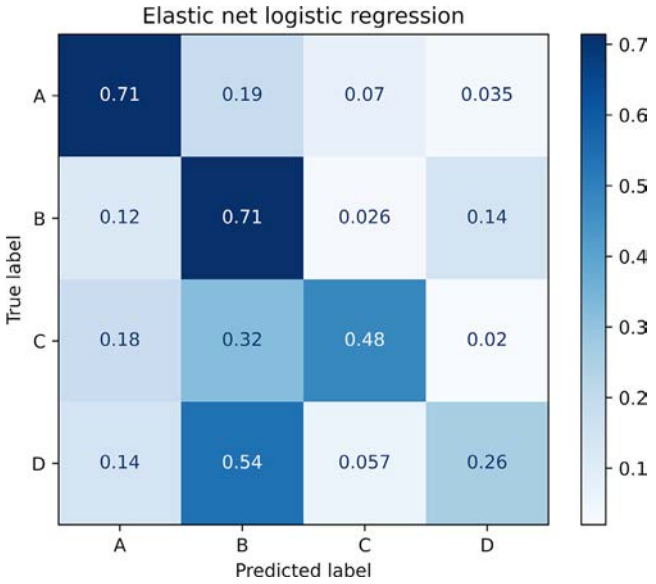



**Figure 5.** The confusion matrix on the test set illustrates the predictive accuracy of the trajectory based on the features used in the clustering process at baseline. The predictions for A and B are generally accurate, while those for C are less accurate and those for D are not predictable based on the baseline characteristics and features (tender joint count 28, swollen joint count 28, erythrocyte sedimentation rate, and other laboratory values).

with systemic inflammation generally associated with poorer outcomes. The study's strengths include a reasonable sample size of patients with DMARD-naïve early RA, independent replication in a second data set, additional validation with PROMs, and the use of widely available model parameters.

Replication was crucial to validate our unsupervised clustering and avoid detecting spurious patterns. Our replication data, TACERA, differed by containing only seropositive patients fulfilling RA classification criteria at baseline, resulting in a more severe RA population. Applying the unsupervised clustering to TACERA allowed for the potential discovery of entirely different clusters. That we identified 7 of the 8 similar disease states and all 4 trajectories strongly confirms the robustness and generalisability of the identified structure.

Previous studies on RA trajectories focused on recovery speed and identified factors like age, sex, and baseline ESR as influential [19]. Our findings provide more nuanced insights, revealing elevated ESR vs joint inflammation as characteristics of distinct patient subgroups. We observed both favourable and unfavourable trajectories within seropositive cohorts, and symptom duration varied among trajectories across data sets. These results challenge established notions about predictive factors in RA outcomes and offer a more detailed perspective on disease progression. The divergent disease states at 1.5 years highlight potential areas for clinical improvement, with over 50% of patients ending with elevated ESR or leucocytes. This co-occurs with decreased Hb and elevated thrombocytes within the limits of normal. This suboptimal outcome is mirrored in PROMs and suggests that blood inflammation is not merely a bystander effect.

While the distinction between systemic and localised inflammation emerges as an overarching pattern, it represents a simplification of complex inflammatory processes that likely interact and overlap. This framework, derived from unsupervised clustering rather than imposed a priori hypothesis, provides a clinically interpretable foundation for understanding disease heterogeneity while acknowledging that the underlying biology is more nuanced.

The different patterns observed in the various trajectories may indicate the existence of multiple RA subtypes. Further studies are required to substantiate this hypothesis. The main disease states, trajectories A and B, show a consistent difference in having either predominantly elevated ESR or joint inflammation. Women, older people, and people with aCCP were more likely to end up in trajectory A than those in B. Possibly, the A subtype is more B cell driven, while the B subtype is more driven by innate immunity. This is supported by the higher prevalence

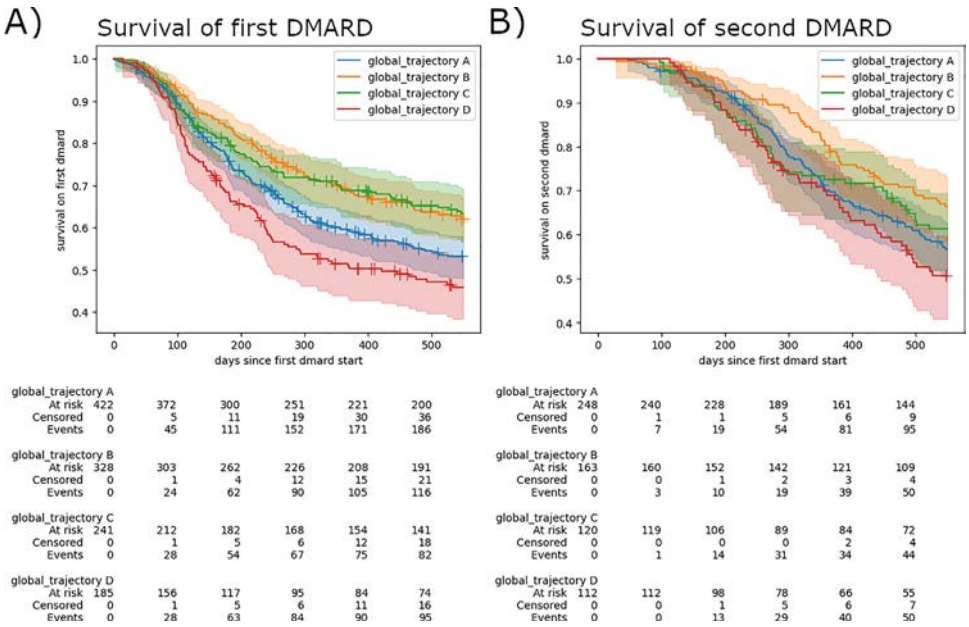



**Figure 6.** Kaplan–Meier curves for disease-modifying antirheumatic drug (DMARD) survival across disease trajectories. (A) First DMARD survival and (B) second DMARD survival over 500 days from first DMARD initiation. Shaded areas represent 95% CIs. Tables below each plot show the number of patients at risk, censored cases, and events at 100-day intervals. Trajectory B shows superior drug survival for both first and second DMARDs, while trajectory D shows accelerated discontinuation rates.

of seropositivity within the A subtype. Although we have named the inflammation in trajectory A systemic inflammation, it is possible that the elevated ESR is an inflammation from elsewhere in the body, for instance in the lungs or gums, both of which are known to be correlated to aCCP-positive disease [20,21].

The leucocytosis in trajectory C suggests an IL-8–driven subtype. We cannot definitively conclude that trajectory C is not caused by prednisone prescriptions, as we lack data on prednisone use before baseline, although our analyses show high leucocytes in trajectory C patients with and without prednisone.

Trajectory D resembles the pauci-immune or fibroid subtypes described in recent biopsy studies [22,23]. Patients in trajectory D show low ESR, high SJC and TJC early in the disease, low seropositivity, poor treatment response, and a discrepancy between PROMs and physician global assessment. Despite differences in study populations, these features align with suggestions of aCCP-negative RA being more pauci-immune [24,25]. In the seropositive TACERA cohort, trajectory D patients still display these features, suggesting that also within this group, a pauci-immune-like subset might exist. Further study to the 54% patients from trajectory D, who at start resemble the more favourable outcome group of trajectory B, might underpin important treatment opportunities for this difficult-to-treat group.

By excluding previously established predictors (age, sex, and seropositivity) from our clustering algorithm, we could independently validate their relationship with the identified trajectories. Analysing how established predictors like RF status and sex related to our identified trajectories, provided valuable validation of our approach. For example, we found that women and seropositive patients were indeed more likely to follow trajectory A, confirming the relevance of these factors, while demonstrating that they emerge naturally from inflammation-based clustering. Importantly, our analysis also revealed that traditional subset markers may be imperfect proxies for underlying disease patterns, as we observed women and seropositive patients across all trajectories. This suggests that our inflammation-based clustering approach might capture more fundamental disease mechanisms that are only partially reflected by conventional patient characteristics. This observation aligns with the growing recognition that RA is a heterogeneous disease with complex pathophysiological patterns that may not perfectly align with traditional patient subsets. Finally, finding the same clusters within the completely seropositive replication data set of TACERA, confirms our choice of not including serology.

The differential patterns of DMARD survival across trajectories provide additional validation of our clustering approach. The poor DMARD survival in trajectory D aligns with its overall worse outcomes, while the superior persistence in trajectory B supports its identification as a favourable disease course. Notably, the consistency of these patterns across both first and second DMARDs suggests these trajectories represent fundamental disease characteristics rather than simply treatment response categories. The similar DMARD survival between trajectories A and D, despite their different inflammatory patterns (systemic vs local), suggests that both forms of persistent inflammation may similarly impact treatment durability. These findings suggest that early trajectory identification might help inform expectations about treatment durability and could guide decisions about treatment intensity.

Our study has several limitations. First, trajectories may be influenced by deviations from treatment guidelines, leading to indication bias, especially for patients resembling trajectory A or B but later shifting to C or D. However, 48% and 26% of patients were correctly predicted to follow trajectories C and D at baseline, respectively. While these findings enhance our understanding of disease patterns, the prediction model's clinical utility is limited when using only baseline features. Optimising the algorithm for practical implementation remains a goal for future research beyond this study's scope. Another possible limitation is phenotypical misclassification, such as by relying on rheumatologists' diagnoses in the Leiden data. Despite this, the same trajectories were observed in TACERA, where all patients met RA criteria at baseline.

The third key principle of the feature selection was to exclude medications from the clustering algorithm, with the aim of avoiding the creation of clusters that primarily reflect treatment decisions rather than underlying disease phenotypes. The incorporation of medication data has the potential to introduce bias from unknown factors influencing prescription patterns and treatment alterations over time. The approach adopted in this study separates phenotype identification from treatment variables, enabling subsequent analysis of differential treatment responses across the identified clusters. This, in turn, has the potential to reveal how distinct patient subgroups respond to various interventions. This methodologic decision is one of the cornerstones of the development of more targeted, personalised treatment strategies based on objectively defined disease phenotypes.

There are missing disease states between patients' first visits and the 1.5-year cutoff, which may result in an incomplete or incorrect trajectory. The methodology used partly overcomes this problem. The sequence similarity approach inherently accommodates temporal irregularities by focusing on the pattern of disease states rather than the precise timing of transitions. This results in the possibility that while patients might have a missing visit, the sequence is still similar in the comparison made.

The unsupervised clustering design could present a limitation. More than 4 trajectories may exist, as clustering depends on the number of clusters chosen. In the Leiden data, 8 disease states and 4 trajectories were optimal, and the TACERA analysis was aligned to maintain comparability. Forcing 8 clusters in TACERA resulted in a new cluster, T9, likely a mix of disease states L4 and L7. This suggests that with more extensive data, additional trajectories could emerge, as seen with substantial overlap in trajectory C with trajectories A and B. Trajectory C might even be subdivided further.

In conclusion, our study identified the existence of 4 distinct disease trajectories in early RA, categorised into patterns of localised and systemic inflammation. These trajectories were replicated, demonstrating the robustness of our findings. The results provide a more nuanced understanding of RA progression, challenging traditional predictors and suggesting the presence of multiple RA subtypes. While systemic inflammation was associated with poorer outcomes, localised inflammation also presented challenges, particularly in trajectory D, which may align with the pauci-immune subtype. Future studies should explore further subdivision of trajectories and potential treatment strategies for difficult-to-treat subgroups, particularly those transitioning from more favourable to less favourable outcomes.

## Competing interests

All authors declare they have no competing interests.

## CRediT authorship contribution statement

**Nils Steinz:** Writing – review & editing, Writing – original draft, Visualization, Validation, Software, Methodology, Investigation, Formal analysis, Data curation. **Tjardo D. Maarseveen:** Writing – review & editing, Validation, Methodology, Data curation. **Erik B. van den Akker:** Writing – review & editing, Visualization, Validation, Supervision, Methodology. **Andrew P. Cope:** Writing – review & editing, Funding acquisition, Conceptualization. **John D. Isaacs:** Writing – review & editing, Funding acquisition, Data curation, Conceptualization. **Aaron R. Winkler:** Writing – review & editing, Funding acquisition, Conceptualization. **Tom W. J. Huizinga:** Writing – review & editing, Supervision, Resources, Project administration, Funding acquisition. **Yann Abraham:** Writing – review & editing, Supervision, Methodology, Investigation, Funding acquisition, Data curation, Conceptualization. **Rachel Knevel:** Writing – review & editing, Writing – original draft, Visualization, Validation, Supervision, Project administration, Methodology, Investigation, Funding acquisition, Formal analysis, Data curation, Conceptualization.

## Acknowledgements

We thank Samantha Jurado-Zapata and David Steeman for their help in extracting and processing the electronic health record data from Leiden University Medical Centre. Additional thanks to Daan van der Bijl for making the first steps in the study. The results in this paper were presented at EULAR 2024 under abstract number OP0018 (doi:10.1136/annrheumdis-2024-eular.1512).

## Funding

This project has received funding from Horizon Europe programme [101095052] (SQUEEZE), [101080711] (SPIDERR), and [777357] (RTCure); MRC/ABPI Inflammation and Immunology Initiative Grant [MRC reference numbers: G1001516 and G1001518] Towards a Cure for Early Rheumatoid Arthritis (TACERA); ZonMw klinische fellow [40-00703-97-19069]; and ZonMw Open Competitie 2021 [09120012110075].

## Patient consent for publication

Not applicable.

## Ethics approval

Ethics committee approved.

## Provenance and peer review

Not commissioned; externally peer reviewed

## Data availability statement

We have made our scripts available in a public repository at: https://github.com/nilssteinz/Early_RA_Trajectories. Study data are available upon reasonable request.

## Declaration of generative AI and AI-assisted technologies in the writing process

During the preparation of this work, the authors used Claude.ai in order to improve the text and the readability of the text. After using this tool/service, the authors reviewed and edited the content as needed and take(s) full responsibility for the content of the published article.

## Supplementary materials

Supplementary material associated with this article can be found in the online version at doi:10.1016/j.ard.2025.04.011.

## Orcid

Nils Steinz: http://orcid.org/0009-0009-4314-8228
Erik B. van den Akker: http://orcid.org/0000-0002-7693-0728
John D. Isaacs: http://orcid.org/0000-0002-6103-7056
Aaron R. Winkler: http://orcid.org/0000-0001-7365-795X
Yann Abraham: http://orcid.org/0000-0001-5600-5896

## REFERENCES

[1] Watanabe R, Hashimoto M, Murata K, Murakami K, Tanaka M, Ohmura K, et al. Prevalence and predictive factors of difficult-to-treat rheumatoid arthritis: the KURAMA cohort. Immunol Med 2022 Jan;45(1):35–44.
[2] Ni J, Wang P, Yin KJ, Yang XK, Cen H, Sui C, et al. Novel insight into the aetiology of rheumatoid arthritis gained by a cross-tissue transcriptome-wide association study. RMD Open 2022 Sep;8(2):e002529.
[3] van der Kooij SM, Goekoop-Ruiterman YPM, de Vries-Bouwstra JK, Peeters AJ, van Krugten MV, Breedveld FC, et al. Probability of continued low disease activity in patients with recent onset rheumatoid arthritis treated according to the disease activity score. Ann Rheum Dis 2008 Feb;67(2):266–9.
[4] Studenic P, Radner H, Smolen JS, Aletaha D. Discrepancies between patients and physicians in their perceptions of rheumatoid arthritis disease activity. Arthritis Rheum 2012;64(9):2814–23.
[5] Singh JA, Saag KG, Bridges Jr SL, Akl EA, Bannuru RR, Sullivan MC, et al. 2015 American College of Rheumatology guideline for the treatment of rheumatoid arthritis. Arthritis Rheumatol 2016;68(1):1–26.
[6] Movahedi M, Cesta A, Li X, Bombardier C, investigators OBRI. Disease activity trajectories for early and established rheumatoid arthritis: real-world data from a rheumatoid arthritis cohort. PLoS One 2022 Sep;17(9):e0274264.
[7] RA-MAP Consortium. Characterization of disease course and remission in early seropositive rheumatoid arthritis: results from the TACERA longitudinal cohort study. Ther Adv Musculoskelet Dis 2021;13:1759720X211043977.
[8] Barnabe C, Sun Y, Boire G, Hitchon CA, Haraoui B, Thorne JC, et al. Heterogeneous disease trajectories explain variable radiographic, function and quality of life outcomes in the Canadian Early Arthritis Cohort (CATCH). PLoS One 2015 Aug;10(8):e0135327.
[9] Ahlqvist E, Storm P, Käräjämäki A, Martinell M, Dorkhan M, Carlsson A, et al. Novel subgroups of adult-onset diabetes and their association with outcomes: a data-driven cluster analysis of six variables. Lancet Diabetes Endocrinol 2018 May;6(5):361–9.
[10] Ma EY, Kim JW, Lee Y, Cho SW, Kim H, Kim JK. Combined unsupervised-supervised machine learning for phenotyping complex diseases with its application to obstructive sleep apnea. Sci Rep 2021 Feb;11(1):4457.
[11] Maurits MP, Korsunsky I, Raychaudhuri S, Murphy SN, Smoller JW, Weiss ST, et al. A framework for employing longitudinally collected multicenter electronic health records to stratify heterogeneous patient populations on disease history. J Am Med Inform Assoc 2022 May;29(5):761–9.
[12] Heumos L, Schaar AC, Lance C, Litinetskaya A, Drost F, Zappia L, et al. Best practices for single-cell analysis across modalities. Nat Rev Genet 2023 Aug;24(8):550–72.
[13] Maarseveen TD, Maurits MP, Niemantsverdriet E, van der Helm-van Mil AHM, Huizinga TWJ, Knevel R. Handwork vs machine: a comparison of rheumatoid arthritis patient populations as identified from EHR free-text by diagnosis extraction through machine-learning or traditional criteria-based chart review. Arthritis Res Ther 2021 Jun;23(1):174.

[14] Arnett FC, Edworthy SM, Bloch DA, Mcshane DJ, Fries JF, Cooper NS, et al. The American Rheumatism Association 1987 revised criteria for the classification of rheumatoid arthritis. Arthritis Rheum 1988;31(3):315–24.
[15] Aletaha D, Neogi T, Silman AJ, Funovits J, Felson DT, Bingham III CO, et al. 2010 Rheumatoid arthritis classification criteria: an American College of Rheumatology/European League Against Rheumatism collaborative initiative. Arthritis Rheum 2010 Sep;62(9):2569–81.
[16] Deighton C, O'Mahony R, Tosh J, Turner C, Rudolf M, Guideline Development Group. Management of rheumatoid arthritis: summary of NICE guidance. BMJ 2009 Mar;338:b702.
[17] Levine JH, Simonds EF, Bendall SC, Davis KL, el-AD Amir, Tadmor MD, et al. Data-driven phenotypic dissection of AML reveals progenitor-like cells that correlate with prognosis. Cell 2015 Jul;162(1):184–97.
[18] Bobroske K, Larish C, Cattrell A, Bjarnadóttir MV, Huan L. The bird's-eye view: a data-driven approach to understanding patient journeys from claims data. J Am Med Inform Assoc 2020 Jun;27(7):1037–45.
[19] Nilsson J, Andersson MLE, Hafström I, Svensson B, Forslind K, Ajeganova S, et al. Influence of age and sex on disease course and treatment in rheumatoid arthritis. Open Access Rheumatol 2021;13:123–38.
[20] Holers VM, Demoruelle MK, Kuhn KA, Buckner JH, Robinson WH, Okamoto Y, et al. Rheumatoid arthritis and the mucosal origins hypothesis: protection turns to destruction. Nat Rev Rheumatol 2018 Sep;14(9):542–57.
[21] Demoruelle MK, Deane KD, Holers VM. When and where does inflammation begin in rheumatoid arthritis? Curr Opin Rheumatol 2014 Jan;26(1):64–71.
[22] Zhang F, Jonsson AH, Nathan A, Millard N, Curtis M, Xiao Q, et al. Deconstruction of rheumatoid arthritis synovium defines inflammatory subtypes. Nature 2023 Nov;623(7987):616–24.
[23] Matthijssen XME, Niemantsverdriet E, Huizinga TWJ, van der Helm–van Mil AHM. Enhanced treatment strategies and distinct disease outcomes among autoantibody-positive and -negative rheumatoid arthritis patients over 25 years: a longitudinal cohort study in the Netherlands. PLoS Med 2020 Sep;17(9):e1003296.
[24] Nerviani A, Di Cicco M, Mahto A, Lliso-Ribera G, Rivellese F, Thorborn G, et al. A pauci-immune synovial pathotype predicts inadequate response to TNF$\alpha$-blockade in rheumatoid arthritis patients. Front Immunol 2020;11:845.
[25] Li K, Wang M, Zhao L, Liu Y, Zhang X. ACPA-negative rheumatoid arthritis: from immune mechanisms to clinical translation. EBioMedicine 2022 Sep;83:104233.

Ann Rheum Dis 84 (2025) 1313–1323

Contents lists available at ScienceDirect

Annals of the Rheumatic Diseases

journal homepage: https://www.sciencedirect.com/journal/annals-of-the-rheumatic-diseases

Rheumatoid arthritis

# Mosaic loss of chromosome Y characterises late-onset rheumatoid arthritis and contrasting associations of polygenic risk score based on age at onset

Shunsuke Uchiyama[1,2], Yuki Ishikawa[2], Katsunori Ikari[3], Suguru Honda[4], Keiko Hikino[5], Eiichi Tanaka[4], Yoichiro Kamatani[6], Takahisa Gono[1], Giulio Genovese[7,8], Masataka Kuwana[1,*], Chikashi Terao[2,9,*]

[1] *Department of Allergy and Rheumatology, Nippon Medical School Graduate School of Medicine, Tokyo, Japan*
[2] *Laboratory for Statistical and Translational Genetics, RIKEN Center for Integrative Medical Sciences, Yokohama, Japan*
[3] *Department of Orthopedic Surgery, Tokyo Women's Medical University School of Medicine, Tokyo, Japan*
[4] *Division of Rheumatology, Department of Internal Medicine, Tokyo Women's Medical University School of Medicine, Tokyo, Japan*
[5] *Laboratory for Pharmacogenomics, RIKEN Center for Integrative Medical Sciences, Yokohama, Japan*
[6] *Department of Computational Biology and Medical Sciences, Graduate School of Frontier Sciences, The University of Tokyo, Japan*
[7] *Program in Medical and Population Genetics, Broad Institute of MIT and Harvard, Cambridge, MA, USA*
[8] *Department of Genetics, Harvard Medical School, Boston, MA, USA*
[9] *Clinical Research Center, Shizuoka General Hospital, Shizuoka, Japan*

ARTICLE INFO

ABSTRACT

*Objectives:* Mosaic chromosomal alterations (mCAs) increase with age and are associated with age-related diseases. The association between mCAs and rheumatoid arthritis (RA), particularly late-onset RA (LORA), has not been explored.

*Methods:* mCAs were detected in peripheral blood samples from 2 independent Japanese datasets (Set 1: 2107 RA cases and 86,998 controls; Set 2: 2359 RA cases and 86,998 controls). The associations between mCAs and RA were evaluated in each dataset using logistic regression models and meta-analysis. In each dataset, the effect sizes of mosaic loss of Y (mLOY) and polygenic risk score (PRS) of RA in males was evaluated, and a meta-analysis was subsequently performed. The interaction between mLOY and PRS was assessed. These models were applied separately to RA, LORA, and young-onset RA (YORA).

*Results:* mLOY increased significantly in LORA (odds ratio [OR] = 1.43, $P$ = .0070). We observed a negative association between mLOY and YORA (OR = 0.66, $P$ = .0034). On the other hand, we found consistently negative associations of autosomal mCAs or mosaic loss of X with RA, LORA, and YORA. The PRS effect sizes were lower for LORA than for YORA. mLOY with a high cell fraction strengthened the association between PRS and LORA ($P$ = .0036), whereas the association with YORA was independent of mLOY.

*Conclusions:* LORA was characterised by the presence of a high burden of mLOY. The observed interaction between mLOY and PRS in LORA, but not in YORA, supports different gene-environment interactions between the subsets. These data suggest that distinct pathophysiological mechanisms underlie the development of LORA and YORA.

*Correspondence to Prof. Masataka Kuwana, Department of Allergy and Rheumatology, Nippon Medical School Graduate School of Medicine, Tokyo, Japan and Dr Chikashi Terao, Laboratory for Statistical and Translational Genetics, Center for Integrative Medical Sciences, Riken, Yokohama 230-0045, Japan.

*E-mail addresses:* kuwanam@nms.ac.j (M. Kuwana), chikashi.terao@riken.jp (C. Terao).

**Handling editor** Josef S. Smolen.

https://doi.org/10.1016/j.ard.2025.01.034

0003-4967/© 2025 European Alliance of Associations for Rheumatology (EULAR). Published by Elsevier B.V. All rights are reserved, including those for text and data mining, AI training, and similar technologies.

**WHAT IS ALREADY KNOWN ON THIS TOPIC**

- The prevalence of late-onset rheumatoid arthritis (LORA) in ageing societies is increasing worldwide.
- LORA has unique clinical characteristics, including higher prevalence in males, acute onset of the disease, and lower proportion of seropositivity compared with young-onset RA (YORA), suggesting distinct genetic and environmental components between the rheumatoid arthritis (RA) subsets.
- Mosaic chromosomal alterations (mCAs) accumulate with age and are associated with age-related disorders. mCAs occur in both autosomes and sex chromosomes and may reflect the clonal expansion of dysregulated immune cells.

**WHAT THIS STUDY ADDS**

- Mosaic loss of Y (mLOY) is increased in male patients with LORA.
- While mLOY is positively associated with LORA, mLOY is negatively associated with YORA.
- The association of the RA polygenic risk score with LORA was more apparent in the presence of mLOY, while the association with YORA was independent of mLOY.

**HOW THIS STUDY MIGHT AFFECT RESEARCH, PRACTICE OR POLICY**

- mLOY causes an acquired risk for RA in males by modifying the contribution of the genetic risk to RA development depending on age at onset.
- Further investigation of the different effects of mLOY on LORA and YORA may lead to a better understanding of the pathological basis of RA influenced by ageing and sex.

## INTRODUCTION

Rheumatoid arthritis (RA) is the most common form of inflammatory arthritis in adults and can lead to joint destruction and disability [1]. Genetic and environmental factors are associated with RA development [1]. Elderly patients with RA include those who present with young-onset RA (YORA) earlier in life and those with late-onset RA (LORA), in whom the disease begins after age 60 to 65 years, depending on the definition [2,3]. The prevalence of LORA has been increasing worldwide, especially in Japan, due to accelerated global ageing, particularly in developed countries [4–6].

Previous studies have suggested that genetic and environmental factors may differ between patients with LORA and those with YORA. LORA is characterised by higher prevalence in males, acute onset, large joint involvement, and lower prevalence of rheumatoid factor (RF) or anti-cyclic citrullinated peptide antibody (ACPA) positivity than YORA [6,7]. The *HLA-DRB1* allele, such as shared epitope alleles, is the strongest genetic risk factor for RA; several studies have shown different associations of *HLA-DRB1* alleles between LORA and YORA [8]. Regarding environmental factors, current LORA patients may have been exposed to smoking for a longer period than YORA patients, given that the prevalence of smoking, one of the major environmental factors for RA, has been decreasing worldwide over the last 20 years (data from the World Health Organization; https://www.who.int).

Mosaic chromosomal alterations (mCAs) are clonal cellular expansions associated with somatic mutations, particularly large-scale chromosomal rearrangements [9]. mCAs can occur in autosomes and sex chromosomes, and the impact on health outcomes appears to differ between autosomal and sex chromosomal mCAs. Previous studies have found that autosomal mCAs are associated with haematological malignancies and ageing disorders, such as infections and cardiovascular diseases [10–12]. Sex chromosomal mCAs include mosaic loss of Y (mLOY) in males and mosaic loss of X (mLOX) in females. mLOY is a highly polygenic trait associated with multiple age-related diseases such as malignancy and cardiovascular diseases [13–15], and mLOX is associated with genes related to autoimmunity [16]. While mCAs have been discussed primarily in the context of haematological malignancies and age-related diseases [17], recent studies have reported that mCAs can also be observed in healthy individuals, especially in males and the elderly [10,13,16,18,19]. Given that mCAs accumulate with age, especially in males, and reflect the clonal expansion of dysregulated immune cells, similar to non-mCA somatic mutations [10,20], we hypothesised that mCAs have a substantial impact on the development of LORA compared to YORA. Knowledge of the association between mCAs, including mLOX and mLOY, and RA is lacking.

Here, we analysed the associations of mCAs (autosome, mLOX, and mLOY) with RA or its subsets (LORA and YORA) in 4466 patients with RA derived from 2 independent datasets. Our findings suggest that mCAs substantially affect RA development, emphasising the possible different effects of mLOY between LORA and YORA.

## METHODS

### *Study participants and study design*

We recruited 4875 RA cases and 176,923 non-RA controls from the BioBank Japan cohort (BBJ cohort [21]) and the Institute of Rheumatology, Rheumatoid Arthritis (IORRA) cohort [22], and detected mCAs in peripheral blood samples (Fig 1A). The present study comprised of 2 independent datasets: Set 1 (discovery dataset) and Set 2 (validation dataset). Set 1 consisted of 2107 BBJ RA cases and 86,998 non-RA controls. Set 2 consisted of 2,359 IORRA cases and 86,998 non-RA controls (Fig 1B). The BBJ cohort included 2452 RA patients and 176,923 non-RA disease controls with targeted diseases [21], except for RA. For subjects from the BBJ, the diagnosis of RA was made by the attending physicians as described elsewhere [21], and only subjects with definitive RA were enrolled. In the IORRA cohort, RA was diagnosed by physicians according to the 1987 American College of Rheumatology (ACR) criteria [23] and/or the 2010 ACR/European Alliance of Associations for Rheumatology classification criteria for RA [24]. We defined LORA and YORA as RA with onset at ≥60 and <60 years of age, respectively [3]. All patients provided informed consent, and this study was approved by the local ethics committee of each institute.

### *Genotyping*

DNA was extracted from blood samples of all individuals. Details of genotyping of the BBJ samples have been described elsewhere [10]. Briefly, BBJ samples were genotyped using Illumina Human OmniExpress Exome v1.0 (OEEv1.0), Human OmniExpress Exome v1.2 (OEEv1.2), or a combination of Illumina Human OmniExpress v1.0 and HumanExome v1.0, 1.1. IORRA samples were genotyped using Human OmniExpress Exome v1.2. The variants in the HumanExome were not used in detection of mCAs and included to construct the PRS (see below).

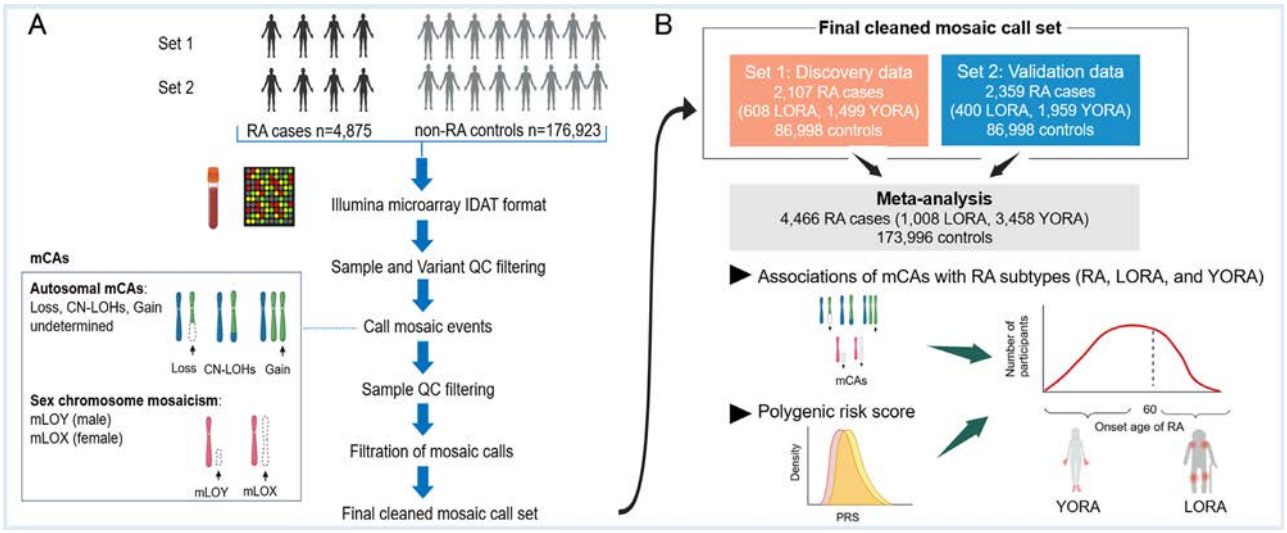



**Figure 1.** Schematic view of mosaic calling and study subjects in the current study. (A) Method of mosaic calling by the MoChA. (B) Study subjects in each dataset (Set 1: discovery dataset and Set 2: validation dataset). Created using Bio-Render.com. CN-LOH, copy-neutral loss of heterozygosity; LORA, late-onset rheumatoid arthritis; mCA, mosaic chromosomal alteration; mLOX, mosaic loss of chromosome X; mLOY, mosaic loss of chromosome Y; MoChA, Mosaic Chromosomal Alterations; PRS, polygenic risk score; QC, quality control; RA, rheumatoid arthritis; YORA, young-onset rheumatoid arthritis.

### *Variant- and sample-level quality controls*

The details of quality control (QC) steps for the variants and samples are shown in Supplementary Methods and Supplementary Figure S1. According to the Mosaic Chromosomal Alterations (MoChA) [18,19] protocols, we excluded variants that met any of the following criteria: genotyping call rate <97%, variants falling in segmental duplications with low divergence (<2%), variants with excess heterozygosity ($P < 1\times10^{-6}$, Hardy-Weinberg equilibrium test), and variants with allele frequency difference >3.0% from those in the imputation panel. For the sample QCs, we removed genetically identical samples and outliers from East Asian clusters using principal component analysis. We also excluded subjects with sample call rate <0.97 and samples with phased B-allele frequency (BAF) autocorrelation >0.03.

### *Detection of mosaic events*

A schematic view of the detection of mosaic events is shown in Figure 1A, and the detailed methods are described in Supplementary Methods. Briefly, mosaic events were identified using the MoChA [18,19]. The raw intensity data (IDAT) files of the subjects were used as inputs. After sample- and variant-level QC as described above, phasing was performed using SHAPEIT4 [25], and mCAs were detected. The samples were filtered after mosaic calling based on the medical history of haematological malignancies in the BBJ samples. We also removed samples that met other criteria (details are presented in Supplementary Methods). After filtering the mosaic calls, the final cleaned mosaic call set was obtained. We detected autosomal mCA events by copy number state (loss, copy-neutral loss of heterozygosity [CN-LOH], or gain) and by p versus q arm for loss and CN-LOH events. mCAs for which we could not determine the copy number state were categorised as undetermined. In addition to loss, CN-LOH, and gain events, we included undetermined calls in the presence of autosomal mCAs. mLOY and mLOX were detected in males and females, respectively. For each mLOY that passed QC, the cell fraction (CF) was calculated as 4×bdev/(1 +2×bdev), where bdev represents the BAF deviation estimated from 0.5.

### *Construction of PRS for RA*

To evaluate the difference in genetic impact and effect sizes of mLOY on RA subsets (RA, LORA, and YORA) in males, we constructed a PRS. We previously conducted a multi-ancestry genome-wide association study (GWAS) meta-analysis for RA [26] and constructed the best-performing PRS model, which was based on a multi-ancestry GWAS and included variants for the binding motif of T-bet in $CD4^+$ T cells annotated by IMPACT [27]. The best-performing model was based on 2576 autosomal variants outside the human leukocyte antigen region. The imputed genotypes were used to calculate the PRS. For single nucleotide polymorphism (SNP) imputation, we conducted SNP QC by excluding those with genotyping call rate <0.97, Hardy-Weinberg equilibrium $P$ value $<1.0\times10^{-6}$, or minor allele frequency (MAF) <0.005. We also excluded variants with MAFs >3.0% different from those of the imputation panel to achieve high imputation accuracy. Variants with low imputation accuracy ($R^2 < 0.3$) were excluded. For an imputation panel, we used a previously constructed imputation panel from the phase 3 1000 Genomes Project version 5 (http://www.internationalgenome.org/data) [28] combined with high-depth whole-genome sequencing data from 3265 Japanese subjects from BBJ, which enabled rare variant detection [29]. We extracted the SNPs shared among BBJ, IORRA, and the best-performing model (2046 SNPs). The effect size estimates of the risk alleles from the best-performing model were then multiplied by the corresponding genotype dosages of the risk alleles and summed for each individual. We calculated the PRS for subjects who passed the sample-level QC as described above.

### *Statistical analysis*

We performed logistic regression analyses to evaluate the association between RA and detectable mosaicism as follows:

$$RA\ subsets \sim mCA + Sex + age + genotyping\ arrays \quad (1)$$

where the RA subsets are RA, LORA, and YORA, and sex, age, and types of genotyping array (OEEv1.0 and OEEv1.2) are the covariate terms. We separately assessed the following mosaic

events: autosomal mCAs, mLOX, and mLOY. Only female and male samples were analysed for mLOX and mLOY, respectively, without sex as a covariate. We also analysed samples for which smoking information was available, adding smoking history (never or previous/current) to the covariates, and compared the results with those without smoking information. We also analysed the association between genotyping array and mCA to evaluate the mCA detection performance among different arrays, setting OEEv1.2 as a reference. We further assessed the associations between RA subsets and the CF of mLOY (mLOY-CF) >5% in the same manner as described above to evaluate whether the associations between RA subsets and mLOY increased in a CF-dependent manner. We also assessed the association between age at disease onset and mLOY among RA subjects adjusted for age, age$^2$, and array types. The 2 analyses to evaluate the association between RA subsets and mCA were also conducted without samples genotyped on the OmniExpress (OE) array.

Associations between genetic risk factors for RA and RA subsets in the presence of mLOY were examined in each dataset using logistic regression models adjusted for age using the following formula:

$$RA\ subsets \sim mLOY + RA - PRS + smoking + age \quad (2)$$

where the PRS for RA (RA-PRS) and smoking history were included as risk factors. To avoid overfitting, we removed first- or second-degree relatives showing PIHAT >0.25 by identity-by-descent detection. We conducted this analysis on the RA, LORA, and YORA groups. We also assessed the association between mLOY and PRS, adjusting for age, age$^2$, and smoking status, to ensure no associations between them. Furthermore, we evaluated the impact of risks on LORA by referring to YORA and applying the same logistic regression models to RA subjects. Only male participants with available smoking information were included in the 3 analyses to evaluate the association between PRS and mLOY.

We investigated the interactive association between mLOY and RA-PRS in male patients with LORA using a logistic regression model. First- or second-degree relatives with PIHAT >0.25 were excluded from this analysis. We stratified the patients into 6 subgroups according to the PRS and mLOY status. The PRS was divided into low (<25%) and high (≥25%) based on the distribution of PRS across the RA subjects from both datasets. We set 3 mLOY statuses: mLOY negative, mLOY positive, and mLOY-CF >5%. Setting low genetic risk subgroups, which did not have mLOY, as a reference, we analysed the risk of LORA in each group adjusted for age in each dataset using logistic regression models and combined the results by adding the dataset (Set 1 or Set 2) as a covariate as follows:

$$LORA \sim subgroup + age + dataset \quad (3)$$

We did not include smoking as a covariate to maximise the sample size. We assessed the interactive association between mLOY and PRS among male patients with YORA in the same manner. To further evaluate the interaction between mLOY-CF >5% and RA-PRS, we compared the goodness of fit between the following 2 logistic regression models using 1-way analysis of variance (ANOVA):

$$model1:\ LORA \sim mLOY + PRS\ group \quad (4)$$

$$model2:\ LORA \sim mLOY + PRS\ group + PRS\ group \times mLOY - CF > 5\% \quad (5)$$

where LORA (0: non-RA, 1: LORA), PRS group (0: low, 1: high), and mLOY-CF >5% (0: mLOY negative or mLOY-CF <5%, 1: mLOY-CF >5%) are all binary traits; hence, PRS group × mLOY-CF >5% is an interaction term in Equation (5). We also analysed the interaction analyses shown above using samples for which smoking information was available, adding smoking history to the covariates.

All statistical analyses were conducted using the R software (version 3.3.3). All analyses, except for the interactive association between mLOY and PRS, were performed separately for the 2 datasets (Sets 1 and 2), and the results were meta-analysed. Meta-analyses were performed using an inverse variance fixed-effects model using metafor (Meta-Analysis Package for R). We set non-RA subjects as a reference in the analyses to evaluate the associations between mCAs or mLOY-CF >5% with RA subsets (RA, LORA, and YORA) and the associations between mLOY and risk factors for RA. All the analyses with smoking history as a covariate were also evaluated with pack-years as an alternative covariate (Supplementary Methods). The statistical significance of the associations between mCAs or mLOY-CF >5% and RA subsets (RA, LORA, and YORA) was based on the Bonferroni correction ($P < .05/3 = .016$). The statistical significance of the interactive associations between mLOY and PRS among the 5 subgroups was also based on Bonferroni correction ($P < .05/5 = .010$). In other logistic regression models, we set the significance threshold at a 2-sided $P$ value < .05.

### *Patient and public involvement statement*

Patients were not involved in any part of this research, including the study design, formal analyses, result interpretation, writing, or editing of the manuscript for readability or accuracy.

## RESULTS

### *Characteristics of study participants*

The demographic features of the participants in Sets 1 (discovery dataset) and 2 (validation dataset) are listed in Table 1. Patients with RA were younger than controls in both datasets. Female sex rates were higher in patients with RA than in controls in both datasets (Set 1: 81.5% vs 45.6%; Set 2: 85.5% vs 45.6%). The age of patients with LORA was higher than that of the controls. In contrast, the age of patients with YORA was lower than that of controls in both datasets (Supplementary Tables S1 and S2). Consistent with previous findings [6,7], the prevalence of LORA was higher in males, and autoantibody positivity (RF or ACPA) was lower in LORA than in YORA in both datasets (Supplementary Table S3).

### *Broadly consistent mCA detection rate among different genotyping arrays*

To evaluate possible confounding across genotyping arrays, we compared the association between array types and mCA. As expected [10], the mCA detection rate was broadly consistent across genotyping arrays with slightly lower rates in the OE array (Supplementary Table S4).

### *Significant negative associations of autosomal mCAs and mLOX with RA*

Consistent with previous studies, the prevalence of autosomal mCA events increased with age in patients with RA and controls in both datasets (Fig 2). We found that autosomal mCAs

Table 1
**Demographic features of subjects in each dataset**

| Datasets | Set 1: Discovery data | | Set 2: Validation data | |
|---|---|---|---|---|
| | RA | Controls | RA | Controls |
| Number of subjects | 2107 | 86,998 | 2359 | 86,998 |
| Age (y), median (IQR) | 63.0 (55.0-70.0) | 65.0 (55.0-73.0) | 60.0 (51.0-67.0) | 65.0 (55.0-73.0) |
| Sex, n (%) | | | | |
| Male | 389 (18.5%) | 47,302 (54.4%) | 343 (14.5%) | 47,302 (54.4%) |
| Female | 1718 (81.5%) | 39,696 (45.6%) | 2016 (85.5%) | 39,696 (45.6%) |
| Smoking status, n (%) | | | | |
| Smokers | 692 (32.8%) | 43,194 (49.6%) | 770 (32.7%) | 43,205 (49.7%) |
| Never smokers | 1386 (65.8%) | 42,531 (48.9%) | 1494 (63.3%) | 42,568 (48.9%) |
| No information | 29 (1.4%) | 1273 (1.5%) | 95 (4.0%) | 1225 (1.4%) |
| Types of RA, n (%) | | | | |
| LORA | 608 (28.9%) | - | 400 (17.0%) | - |
| YORA | 1499 (71.1%) | - | 1959 (83.0%) | - |
| Types of arrays, n (%) | | | | |
| OEE v1.0 | 129 (6.1%) | 17,152 (19.7%) | - | 16,951 (19.5%) |
| OEE v1.2 | 1913 (90.8%) | 53,752 (61.8%) | 2359 (100.0%) | 54,074 (62.1%) |
| OE v1.0 and HE v1.0, 1.1 | 65 (3.1%) | 16,094 (18.5%) | - | 15,973 (18.4%) |

HE, HumanExome; LORA, late-onset rheumatoid arthritis; OE, OmniExpress; OEE, OmniExpress Exome; RA, rheumatoid arthritis; YORA, young-onset rheumatoid arthritis.

showed consistent negative associations with RA and its subsets in both datasets, even after adjusting for covariates, including age, and significant associations were confirmed by meta-analyses (Table 2; Figs 2 and 3A). As observed for autosomal mCAs, mLOX increased with age (Fig 2). A logistic regression model adjusted for covariates, including age, revealed consistent negative associations between mLOX and RA and its subsets, and significant associations were confirmed by the meta-analysis (Table 2; Figs 2 and 3B). These results were consistent in the logistic regression models without samples genotyped on the OE array, which showed a lower mCA detection rate (Fig 3A,B; Supplementary Table S5). Because cigarette smoking is associated with mCAs [14], we included smoking history as a covariate in the statistical model, in which we confirmed significant negative associations between autosomal mCAs or mLOX and RA or its subsets, even at the expense of decreased sample sizes (Supplementary Fig S2A,B; Supplementary Table S6). We observed a similar trend in the logistic regression models using smoking pack-years as a covariate (Supplementary Fig S2A,B; Supplementary Table S7).

### *Significant positive association between mLOY and LORA*

When we analysed the association of mLOY with RA and its subsets in male samples, mLOY was positively associated with LORA in each dataset and meta-analysis. However, no consistent

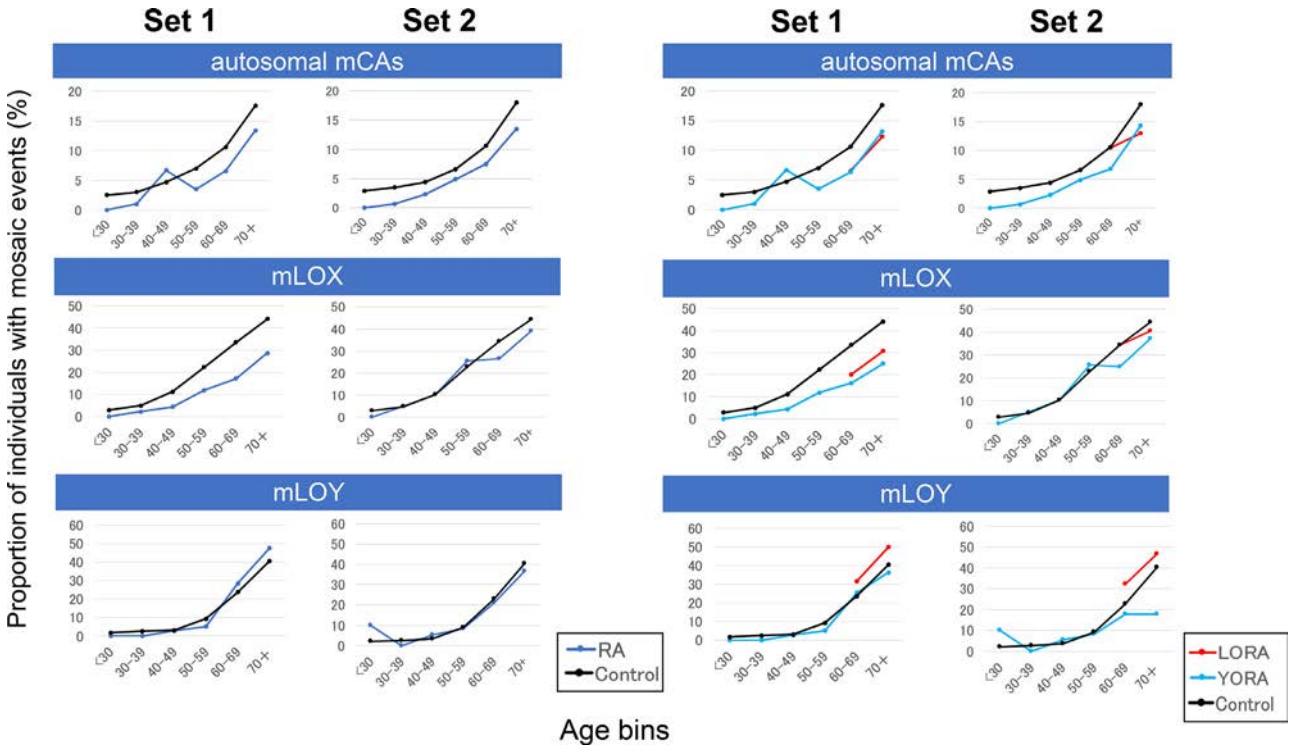



**Figure 2.** Frequency of detectable mosaic events stratified by age. The frequencies (means) are indicated for Set 1 (2107 RA and 86,998 controls) and Set 2 (2359 RA and 86,998 controls). LORA, late-onset rheumatoid arthritis; mCA, mosaic chromosomal alteration; mLOX, mosaic loss of chromosome X; mLOY, mosaic loss of chromosome Y; RA, rheumatoid arthritis; YORA, young-onset rheumatoid arthritis.

Table 2
**The associations between different types of mCAs and RA subsets (RA, LORA, and YORA) in each dataset corresponding to Figure 3, upper panel**

| Datasets | | Set 1: Discovery data | | | | Set 2: Validation data | | | | Meta-analysis (Sets 1 and 2) | |
|---|---|---|---|---|---|---|---|---|---|---|---|
| | | mCA carriers/participants (prevalence) | | | | mCA carriers/participants (prevalence) | | | | | |
| | | RA cases | non-RA controls | OR (95% CI) | *P* | RA cases | non-RA controls | OR (95% CI) | *P* | OR (95% CI) | *P* |
| autosomal mCAs | RA | 157/2107 (7.45%) | 9890/86,998 (11.4%) | 0.72 (0.61-0.85) | **$9.5\times10^{-5}$** | 157/2359 (6.66%) | 9977/86,998 (11.5%) | 0.72 (0.61-0.85) | **.00011** | 0.72 (0.64-0.81) | **$4.0\times10^{-8}$** |
| | LORA | 69/608 (11.3%) | 9890/86,998 (11.4%) | 0.75 (0.58-0.97) | .029 | 48/400 (12.0%) | 9977/86,998 (11.5%) | 0.83 (0.61-1.12) | .22 | 0.78 (0.64-0.95) | **.014** |
| | YORA | 88/1499 (5.87%) | 9890/86,998 (11.4%) | 0.65 (0.52-0.81) | **.00015** | 109/1959 (5.56%) | 9977/86,998 (11.5%) | 0.66 (0.54-0.80) | **$3.4\times10^{-5}$** | 0.66 (0.57-0.76) | **$1.9\times10^{-8}$** |
| mLOX | RA | 290/1718 (16.9%) | 12,104/39,696 (30.5%) | 0.43 (0.37-0.49) | **$3.1\times10^{-36}$** | 489/2016 (24.3%) | 12,207/39,696 (30.8%) | 0.79 (0.70-0.88) | **$2.4\times10^{-5}$** | 0.61 (0.56-0.67) | **$1.3\times10^{-29}$** |
| | LORA | 120/443 (27.1%) | 12,104/39,696 (30.5%) | 0.53 (0.43-0.66) | **$6.4\times10^{-9}$** | 118/310 (38.1%) | 12,207/39,696 (30.8%) | 0.89 (0.70-1.13) | .33 | 0.67 (0.57-0.78) | **$7.5\times10^{-7}$** |
| | YORA | 170/1275 (13.3%) | 12,104/39,696 (30.5%) | 0.38 (0.32-0.45) | **$1.1\times10^{-29}$** | 371/1706 (21.7%) | 12,207/39,696 (30.8%) | 0.76 (0.67-0.87) | **$2.4\times10^{-5}$** | 0.60 (0.54-0.66) | **$3.9\times10^{-24}$** |
| mLOY | RA | 102/389 (26.2%) | 11,366/47,302 (24.0%) | 1.15 (0.90-1.46) | .27 | 68/343 (19.8%) | 11,172/47,302 (23.6%) | 0.88 (0.66-1.17) | .37 | 1.03 (0.85-1.23) | .79 |
| | LORA | 71/165 (43.0%) | 11,366/47,302 (24.0%) | 1.47 (1.07-2.04) | .020 | 38/90 (42.2%) | 11,172/47,302 (23.6%) | 1.36 (0.87-2.11) | .17 | 1.43 (1.10-1.86) | **.0070** |
| | YORA | 31/224 (13.8%) | 11,366/47,302 (24.0%) | 0.73 (0.49-1.09) | .12 | 30/253 (11.9%) | 11,172/47,302 (23.6%) | 0.59 (0.39-0.88) | **.0094** | 0.66 (0.49-0.87) | **.0034** |

LORA, late-onset rheumatoid arthritis; mCA, mosaic chromosomal alteration; mLOX, mosaic loss of chromosome X; mLOY, mosaic loss of chromosome Y; OR, odds ratio referring to non-RA controls; RA, rheumatoid arthritis; YORA, young-onset rheumatoid arthritis.
*P* values in bold indicate statistical significance based on Bonferroni correction ($P < .016$).

association was observed between mLOY and RA. Notably, we observed a protective association between mLOY and YORA, which is in stark contrast to that observed for LORA (Table 2; Figs 2 and 3C). The directions of the effect sizes of mLOY on both LORA and YORA were concordant for both datasets (Fig 3C; Table 2). The observed associations were not affected by the OE array (Fig 3C; Supplementary Table S5). We confirmed robust associations in the statistical models that included smoking history or pack-years as a covariate (Supplementary Fig S2C; Supplementary Tables S6 and S7). Because the age definition of LORA varied among different populations [6], we also evaluated the association between age at RA onset and mLOY, which showed a significant positive association in the meta-analysis adjusted for covariates, including age (Supplementary Fig S3; Supplementary Table S8), further supporting a positive association between mLOY and LORA, regardless of the definition of age for LORA.

### *Significant and CF-dependent association between mLOY and LORA*

Because the CF of mLOY varies among individuals, we hypothesised that the higher the CF of mLOY, the larger the effect size of mLOY on LORA. To test this hypothesis, we extracted subjects with RA or its subsets whose CF of mLOY was >5% (mLOY-CF >5%) (Supplementary Fig S4). We examined their association with mLOY using a logistic regression model adjusted for covariates, including age. We found that the effect sizes of mLOY-CF >5% were higher than those of mLOY without the CF threshold on LORA in both the datasets and the meta-analysis (Fig 4; Supplementary Table S9), indicating that the effect size of mLOY on LORA increases in a CF-dependent manner. In contrast, we did not observe consistent CF-dependent changes in the effect sizes of YORA, whereas the same nonsignificant trends were observed in RA (Fig 4). We found that these associations were consistent even after excluding the samples genotyped on the OE array (Fig 4; Supplementary Table S10). The observed associations were not affected by the adjustment for smoking status or pack-years (Supplementary Fig S5; Supplementary Tables S11 and S12).

### *Distinct associations of RA-PRS and mLOY between LORA and YORA*

The PRS measures the collection of associations between heritable genetic components, causal SNPs, or their proxies, while mosaic events occur after birth and accumulate with age. Accordingly, we evaluated the associations of mLOY and PRS for RA with RA subsets (RA, LORA, and YORA) using a model adjusted for smoking status in each dataset (Sets 1 and 2; Supplementary Table S13) and meta-analysis. Notably, mLOY was not associated with the PRS in patients with RA (Supplementary Table S14). The effect size of PRS was higher in the YORA group ($\beta = 0.61$; 95% CI, 0.55-0.66; $P = 3.0\times10^{-111}$) than in the LORA group ($\beta = 0.44$; 95% CI, 0.37-0.51; $P = 1.7\times10^{-32}$) in the individual datasets and meta-analysis (Fig 5A; Supplementary Table S15). We also confirmed a positive association between mLOY and LORA ($\beta = 0.32$, $P = .017$) and a negative association between mLOY and YORA ($\beta = -0.41$, $P = .0047$) during conditioning on the PRS for RA (Fig 5B; Supplementary Table S15). We observed the same trend in the statistical models using smoking pack-years as a covariate (Supplementary Fig S6; Supplementary Table S16). Among the RA subjects, the PRS was lower in LORA than in YORA ($\beta = -0.16$, $P = .014$). mLOY

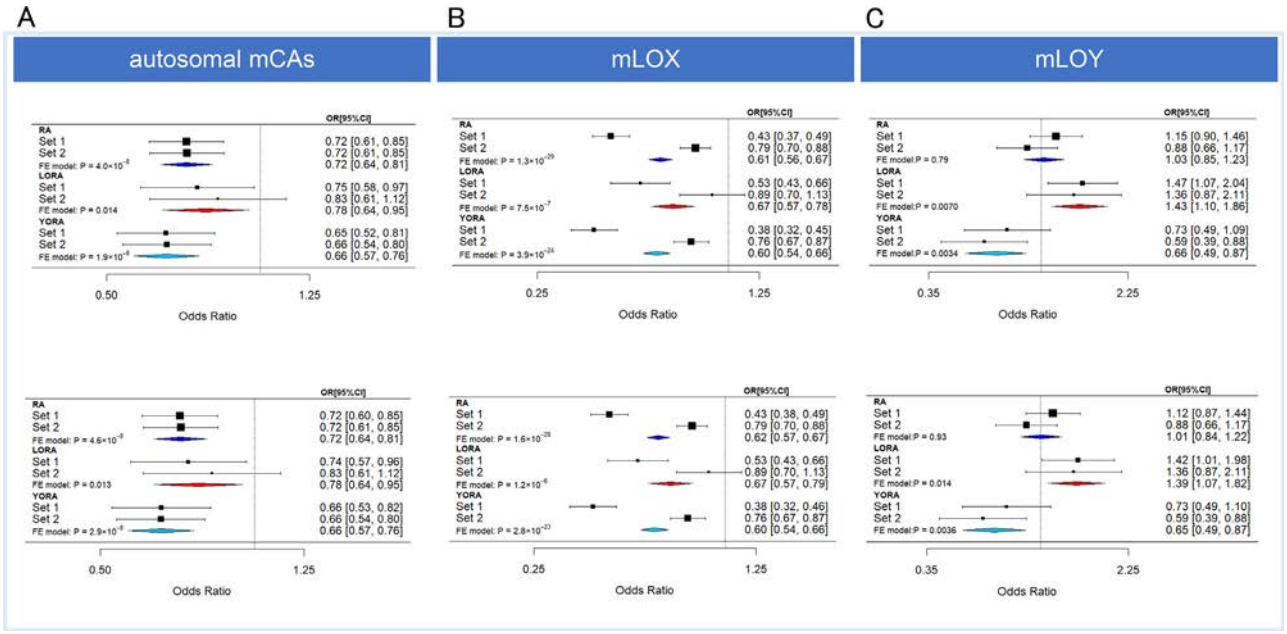



**Figure 3.** Associations between autosomal mCAs, mLOX, or mLOY and RA subsets. Associations between detectable mosaicism [autosomal mCAs (A), mLOX (B), and mLOY (C)] and RA subsets (RA, LORA, and YORA) were evaluated by comparison with non-RA controls. Forest plots of the meta-analysis for each association analysis using 2 datasets (Sets 1 and 2) are shown. The results for the samples including and excluding those genotyped on the OE array are presented in the upper and lower panels, respectively. ORs are indicated by squares and 95% CIs are indicated by 2-sided lines. The corresponding data are listed in Table 2 and Supplementary Table S5. FE, fixed-effects; LORA, late-onset rheumatoid arthritis; mCA, mosaic chromosomal alteration; mLOX, mosaic loss of chromosome X; mLOY, mosaic loss of chromosome Y; OR, odds ratio; RA, rheumatoid arthritis; YORA, young-onset rheumatoid arthritis.

demonstrated a borderline significant positive association with LORA compared with YORA ($\beta = 0.46$, $P = .067$) (Supplementary Fig S7; Supplementary Table S17). These data suggest distinct underlying somatic architectures between LORA and YORA, in addition to their different genetic backgrounds.

### *Dose-dependent association of mLOY and a potential interactive association of mLOY and RA-PRS on LORA*

Finally, we evaluated the dose-dependent association of mLOY and the potential interactive association between RA-PRS and mLOY in LORA and YORA (Supplementary Table S13). Patients were stratified into 6 subgroups based on PRS (low or high) and mLOY status (positive, negative, or mLOY-CF >5%); a subgroup of patients with low PRS and mLOY(−) was used as a reference. Among the low PRS subgroups, both the mLOY(+) and mLOY-CF >5% subgroups showed a nonsignificant slight increase in the risk of LORA (Fig 6A, upper panel). Interestingly, among the high PRS subgroups, the risk of LORA sharply and significantly increased in a CF-dependent manner (Fig 6A, lower panel). In contrast, for YORA, we observed a significant increase in the risk among high PRS subgroups but in a CF-independent manner or rather in a trend of a CF-dependent protective manner (Fig 6B, lower panel), highlighting a different association of mLOY-CF on LORA and YORA. These associations were consistent in each dataset (Supplementary Figs S8 and S9). The observed associations were not affected by the adjustment for smoking status (Fig 6C,D). We observed the same trend in the statistical model including pack-years as a covariate, although the CF-dependent effects were not obvious among the low PRS subgroup because of the small sample size in patients with RA in this subgroup (Supplementary Figure S10). To further investigate the potential interaction between RA-PRS and mLOY-CF >5% in LORA, we introduced an interaction term (PRS group × mLOY-CF >5%) into the model. We compared the goodness of fit between the models with and without the interaction term using a 1-way ANOVA. We found that the model with the interaction term fit significantly better than the model without the interaction term ($P = .0036$) (Supplementary Table S18), supporting a possible interaction between mLOY-CF >5% and the PRS in the LORA. The additive interaction between PRS and mLOY-CF >5% in LORA was also confirmed by a 1-way ANOVA adding smoking as a covariate ($P = .0032$) (Supplementary Table S19).

## DISCUSSION

The association between somatic mutations in peripheral blood mononuclear cells and RA has been previously investigated. Savola et al [30] explored a possible association between clonal haematopoiesis of indeterminate potential (CHIP) and the expansion of cells with somatic point mutations. However, a significant association between CHIP and RA was not found. In contrast, our previous study observed a trend towards a protective association between RA and autosomal mCAs [10]. In the present study, we investigated the association between mCAs and RA or its subsets (LORA and YORA) and found that mLOY was positively associated with LORA, while mLOY was negatively associated with YORA. We also found consistent negative associations between autosomal mCAs (as reported in our previous study [10]) and mLOX in RA, LORA, and YORA. Although PRS was weakly associated with LORA compared to YORA, the association between PRS and LORA was augmented by mLOY in a dose-dependent manner. In contrast, the positive associations between PRS and YORA were independent of mLOY or showed a trend of protective associations in the presence of mLOY.

It is well known that genetic and environmental factors, as well as their interaction, play significant roles in the development of RA [1]. Previous studies have identified both genetic and environmental risks of RA susceptibility, seropositivity of

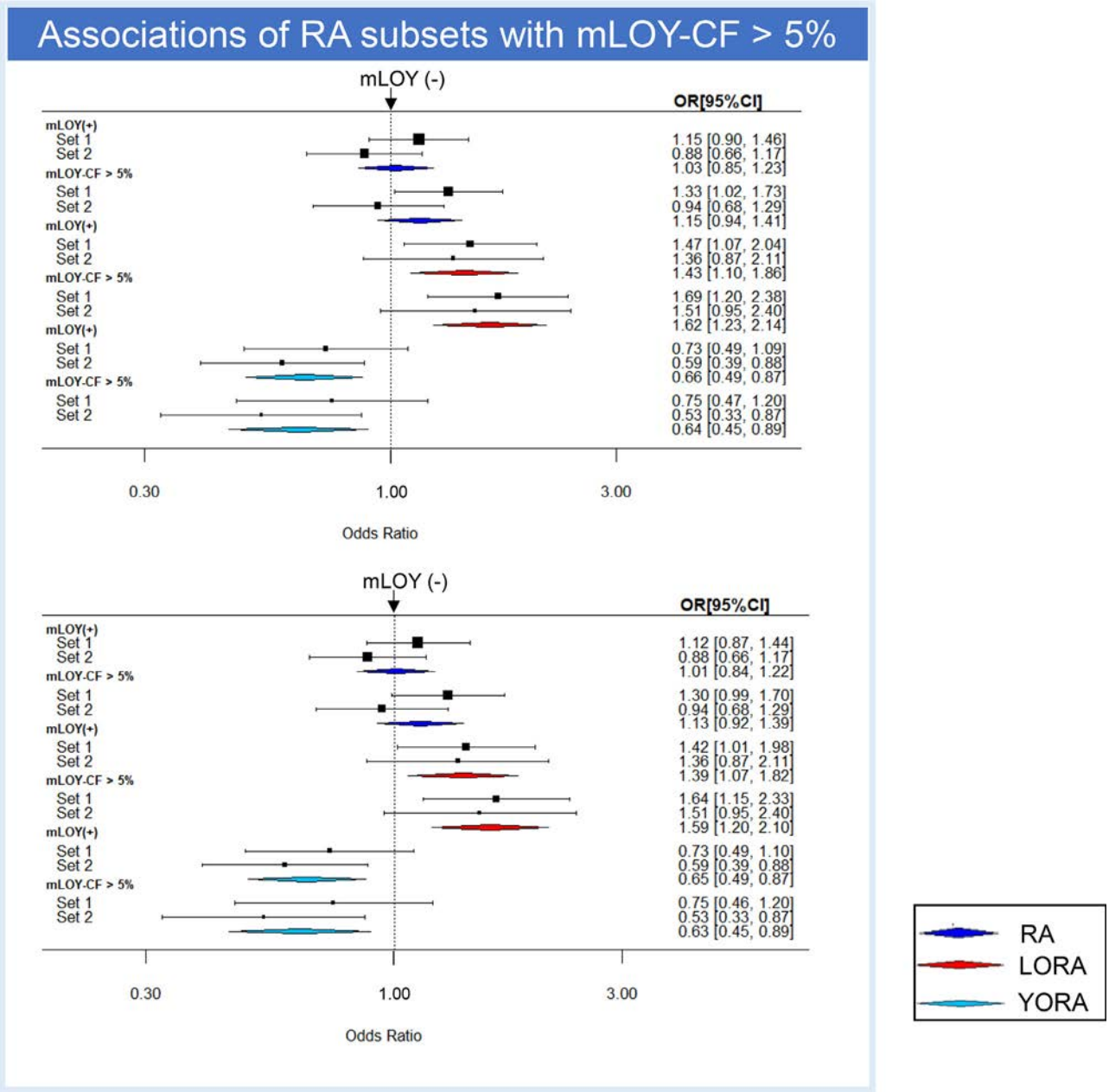



**Figure 4.** Associations of CF of mLOY >5% with RA and its subsets. Associations between mLOY-CF >5% and the RA subsets (RA, LORA, and YORA) were evaluated referring to non-RA controls. The associations of mLOY without the CF threshold with the RA subsets (RA, LORA, and YORA) are also shown. Forest plots of the meta-analysis for each association analysis using 2 datasets (Sets 1 and 2) are shown. The results for the samples including and excluding those genotyped on the OE array are presented in the upper and lower panels, respectively. ORs are indicated by squares and 95% CIs are indicated by two-sided lines. The corresponding data are listed in Supplementary Tables S9 and S10. CF, cell fraction; LORA, late-onset rheumatoid arthritis; mLOY, mosaic loss of chromosome Y; OE, OmniExpress; OR, odds ratio; RA, rheumatoid arthritis; YORA, young-onset rheumatoid arthritis.

autoantibodies (RF or ACPA), and joint destruction [1]. However, the target samples in most studies were YORA subjects; hence, neither the genetic nor the environmental risks specific to LORA have been thoroughly investigated. The smaller PRS effect sizes in LORA than in YORA observed in the present study suggest that the heritable components of disease risk, or at least their contributions, differ between LORA and YORA. Regarding environmental (somatic) components in LORA, acquired age-related alterations of the immune system, including immunosenescence and inflammageing, have recently been implicated in the development of LORA [31]. We hypothesised that acquired immune alterations could be caused by mCAs and their subsequent gene-environment interactions. The observed significant positive association between mLOY and LORA, along with the accumulation of mLOY with age and the possible interaction between PRS and mLOY, supports the idea that mLOY may play a pivotal role in the development of LORA. Indeed, recent studies have found that in addition to the heritable germline variants, the acquired somatic mutations lead to the development of autoimmune and autoinflammatory diseases later in life [32,33]. Overall, these results suggest that the underlying genetic and environmental (somatic) architecture of the LORA is distinct from that of the YORA.

Regarding the biological mechanisms, mLOY is known to be associated with age-related disorders, such as cardiovascular disease or Alzheimer's disease [15,34], by directly altering gene functions in particular immune cell subsets [35] or causing genetic instability, leading to clonal expansion of dysregulated

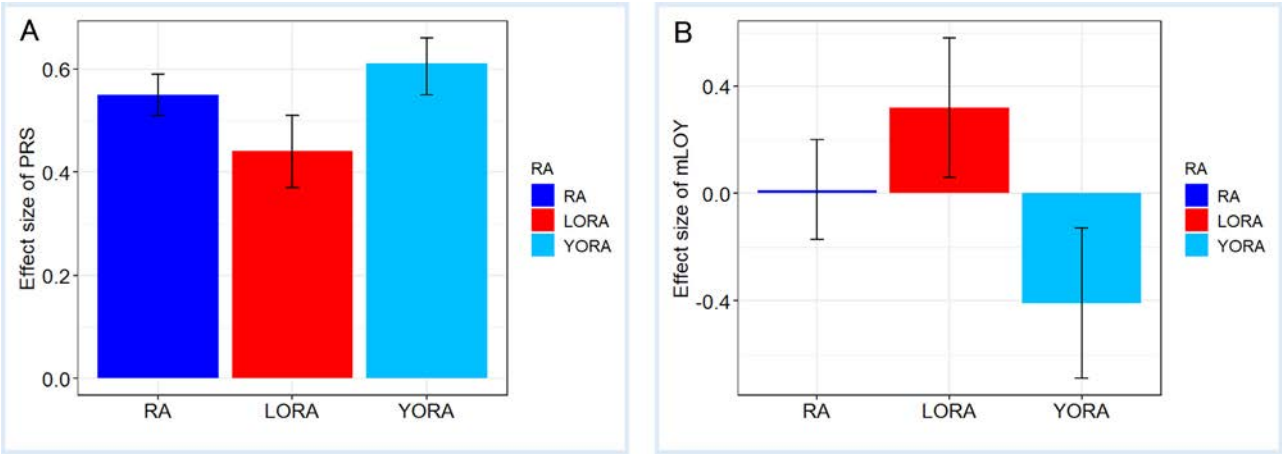



**Figure 5.** Comparison of effect sizes of PRS and mLOY among RA and its subsets. The effect sizes of the PRS (A) or mLOY (B), referring to non-RA controls, were compared among the RA subsets (RA, LORA, and YORA). The effect sizes of the PRS (A) and mLOY (B) of the meta-analysis for each association analysis using the 2 datasets (Sets 1 and 2) are shown. Effect sizes are indicated in vertical columns and 95% CIs of effect sizes are indicated by 2-sided lines. The corresponding data are presented in Supplementary Table S15. LORA, late-onset rheumatoid arthritis; mLOY, mosaic loss of chromosome Y; PRS, polygenic risk score; RA, rheumatoid arthritis; YORA, young-onset rheumatoid arthritis.

immune cells [13,36]. Hence, LORA may also develop in dysregulated immune systems because of the accumulation of mLOY in certain immune cell types. In contrast, we observed consistent protective associations between autosomal mCAs, mLOX, and RA. Future studies, such as single-cell RNA sequencing of patient-derived immune cells, will clarify the downstream effects of mLOY in a cell type-specific manner.

Several epidemiological studies have shown an increase in the prevalence of LORA in recent years [5,6], reflecting the acceleration of ageing societies, especially in developed countries. Males are more susceptible to LORA, whereas females are more likely to develop autoimmune diseases in general, including YORA [37], probably because of the effects of oestrogen or progesterone on immune cells [38]. The significant positive association between mLOY and LORA partly but reasonably explains the male predominance of LORA susceptibility. Because not all women are protected from LORA, the male predominance needs to be further addressed in future studies.

Our study had several limitations. First, the sample size was limited, especially for male patients with LORA. At this point, most of the analyses were conducted separately in independent datasets, which were then meta-analysed to evaluate robustness. Although we admit that not all the tests fulfilled the stringent thresholds, such as Bonferroni-corrected *P* values, we still observed similar trends in individual datasets, even with relatively small sample sizes. Further validation with mCA detection from whole-genome sequencing data using a large sample size is needed to strengthen these findings. Second, because we did not test the causality of mLOY on LORA or vice versa owing to the sample size limitation, causality needs to be tested by enrolling

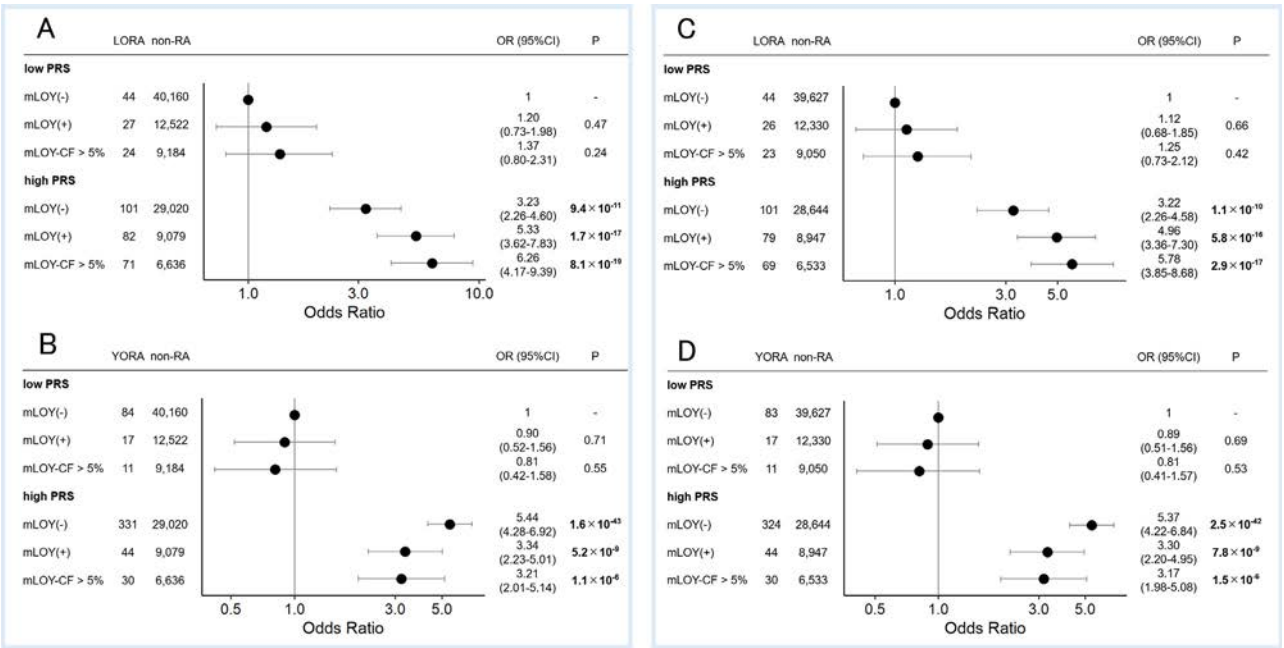



**Figure 6.** Combinatory associations of PRS and mLOY on LORA and YORA. The associations of the PRS subgroups with LORA (A) or YORA (B) stratified by mLOY status were evaluated referring to the low PRS subgroup without mLOY. The right panels (C and D) show the associations adjusted for smoking status. ORs are indicated by dots, and 95% CIs are indicated by two-sided lines. CF, cell fraction; LORA, late-onset rheumatoid arthritis; mLOY, mosaic loss of chromosome Y; OR, odds ratio; PRS, polygenic risk score; YORA, young-onset rheumatoid arthritis.

more subjects to enable us to construct a reliable PRS specifically for LORA. Finally, the association between PRS and RA might be inflated owing to partial sample overlap between the subjects in the present study and those in the previous GWAS [26]. Although testing the replicability of the datasets completely independent of the previous GWAS is warranted, the aim of this analysis was not to evaluate the PRS performance; thus, the impact of sample overlap on our analyses would be minimal, if any.

To the best of our knowledge, this is the first study to demonstrate distinct associations of mCAs between LORA and YORA, which may explain the different pathophysiological mechanisms and clinical manifestations between the RA subsets.

## Competing interests

SU, YI, KI, SH, KH, ET, and CT have no conflicts of interest. YK has research grants from Takeda Pharmaceuticals. TG received speaking fees from Asahi Kasei Pharma, Astellas, Boehringer-Ingelheim, Bristol-Myers Squibb, Chugai, Eisai, Eli Lily, Gilead Sciences, Ono Pharmaceuticals, Pfizer, and Tanabe Mitsubishi. GG declared competing interests, and patent application PCT/WO2019/079493 has been filed for the mosaic chromosomal alteration detection method used in this study. MK has received consulting fees, speaking fees, and/or research grants from Argenx, Asahi Kasei Parma, AstraZeneca, Boehringer-Ingelheim, Chugai, GSK, Janssen, Kissei, MBL, Mochida, MSD, Novartis, Ono Pharmaceuticals, and Tanabe Mitsubishi.

## Acknowledgements

We thank the staff of BioBank Japan for collecting and managing the samples and clinical information.

## Contributors

MK and CT conceived and supervised the project equally. SU and CT analysed the data. KH shared the statistical codes. YK managed the BioBank Japan data. KI, SH, and ET generated the Institute of Rheumatology, Rheumatoid Arthritis data. GG developed Mosaic Chromosomal Alterations pipelines for mosaic calling. TG participated in discussions related to this project. SU, YI, and CT wrote the manuscript. All authors have critically reviewed and approved the final version of the manuscript. CT is guarantor.

## Funding

This work was supported by the Japan Agency for Medical Research and Development grants 21ek0109555, 21tm0424220, 21ck0106642, 23ek0410114, and 23tm0424225; the Japan Society for the Promotion of Science KAKENHI grant JP20H00462; and Takeda Hosho Grants for Research in Medicine.

## Patient consent for publication

Not applicable.

## Ethics approval

All patients provided informed consent, and this study was approved by the local ethics committee of each institute.

## Provenance and peer review

Not commissioned: externally peer reviewed.

## Data availability

Statistical codes are available from Chikashi Terao (ORCID 0000-0002-6452-4095) at any time, only on reasonable request. The Mosaic Chromosomal Alterations pipelines used for mosaic calling (mocha.wdl) are available at (https://github.com/freeseek/mochawdl).

## Supplementary materials

Supplementary material associated with this article can be found in the online version at doi:10.1016/j.ard.2025.01.034.

## REFERENCES

[1] Rheumatoid arthritis. Nat Rev Dis Primers 2018;4:18002.
[2] Kobak S, Bes C. An autumn tale: geriatric rheumatoid arthritis. Ther Adv Musculoskelet Dis 2018;10:3–11.
[3] Deal CL, Meenan RF, Goldenberg DL, Anderson JJ, Sack B, Pastan RS, et al. The clinical features of elderly-onset rheumatoid arthritis. A comparison with younger-onset disease of similar duration. Arthritis Rheum 1985;28:987–94.
[4] GBD 2021. Rheumatoid Arthritis Collaborators. Global, regional, and national burden of rheumatoid arthritis, 1990-2020, and projections to 2050: a systematic analysis of the Global Burden of Disease Study 2021. Lancet Rheumatol. 2023;5:e594–610.
[5] Kato E, Sawada T, Tahara K, Hayashi H, Tago M, Mori H, et al. The age at onset of rheumatoid arthritis is increasing in Japan: a nationwide database study. Int J Rheum Dis 2017;20:839–45.
[6] Uchiyama S, Takanashi S, Takeno M, Gono T, Kaneko Y, Takeuchi T, et al. Should we reconsider the definition of elderly-onset rheumatoid arthritis in an ageing society? Mod Rheumatol 2022;32:323–9.
[7] Serhal L, Lwin MN, Holroyd C, Edwards CJ. Rheumatoid arthritis in the elderly: characteristics and treatment considerations. Autoimmun Rev 2020;19:102528.
[8] Gonzalez-Gay MA, Hajeer AH, Dababneh A, Makki R, Garcia-Porrua C, Thomson W, et al. Seronegative rheumatoid arthritis in elderly and polymyalgia rheumatica have similar patterns of HLA association. J Rheumatol 2001;28:122–5.
[9] Liu X, Kamatani Y, Terao C. Genetics of autosomal mosaic chromosomal alteration (mCA). J Hum Genet 2021;66:879–85.
[10] Terao C, Suzuki A, Momozawa Y, Akiyama M, Ishigaki K, Yamamoto K, et al. Chromosomal alterations among age-related haematopoietic clones in Japan. Nature 2020;584:130–5.
[11] Zekavat SM, Lin SH, Bick AG, Liu A, Paruchuri K, Wang C, et al. Hematopoietic mosaic chromosomal alterations increase the risk for diverse types of infection. Nat Med 2021;27:1012–24.
[12] Evans MA, Walsh K. Clonal hematopoiesis, somatic mosaicism, and age-associated disease. Physiol Rev 2023;103:649–716.
[13] Thompson DJ, Genovese G, Halvardson J, Ulirsch JC, Wright DJ, Terao C, et al. Genetic predisposition to mosaic Y chromosome loss in blood. Nature 2019;575:652–7.
[14] Terao C, Momozawa Y, Ishigaki K, Kawakami E, Akiyama M, Loh PR, et al. GWAS of mosaic loss of chromosome Y highlights genetic effects on blood cell differentiation. Nat Commun 2019;10:4719.
[15] Sano S, Horitani K, Ogawa H, Halvardson J, Chavkin NW, Wang Y, et al. Hematopoietic loss of Y chromosome leads to cardiac fibrosis and heart failure mortality. Science 2022;377:292–7.
[16] Liu A, Genovese G, Zhao Y, Pirinen M, Zekavat MM, Kentistou K, et al. Population analyses of mosaic X chromosome loss identify genetic drivers and widespread signatures of cellular selection. Nature 2024;631:134–41.
[17] Laurie CC, Laurie CA, Rice K, Doheny KF, Zelnick LR, McHugh CP, et al. Detectable clonal mosaicism from birth to old age and its relationship to cancer. Nat Genet 2012;44:642–50.
[18] Loh PR, Genovese G, McCarroll SA. Monogenic and polygenic inheritance become instruments for clonal selection. Nature 2020;584:136–41.
[19] Loh PR, Genovese G, Handsaker RE, Finucane HK, Reshef YA, Palamara PF, et al. Insights into clonal haematopoiesis from 8,342 mosaic chromosomal alterations. Nature 2018;559:350–5.

[20] Alriyami M, Polychronakos C. Somatic mutations and autoimmunity. Cells 2021;10:2056. doi: 10.3390/cells10082056.
[21] Nagai A, Hirata M, Kamatani Y, Muto K, Matsuda K, Kiyohara Y, et al. Overview of the BioBank Japan project: study design and profile. J Epidemiol 2017;27:S2–8.
[22] Yamanaka H, Tanaka E, Nakajima A, Furuya T, Ikari K, Taniguchi A, et al. A large observational cohort study of rheumatoid arthritis, IORRA: providing context for today's treatment options. Mod Rheumatol 2020;30:1–6.
[23] Arnett FC, Edworthy SM, Bloch DA, McShane DJ, Fries JF, Cooper NS, et al. The American Rheumatism Association 1987 revised criteria for the classification of rheumatoid arthritis. Arthritis Rheum 1988;31:315–24.
[24] Aletaha D, Neogi T, Silman AJ, Funovits J, Felson DT. Bingham CO 3rd, et al. 2010 rheumatoid arthritis classification criteria: an American College of Rheumatology/European League Against Rheumatism collaborative initiative. Ann Rheum Dis 2010;69:1580–8.
[25] Delaneau O, Zagury JF, Robinson MR, Marchini JL, Dermitzakis ET. Accurate, scalable and integrative haplotype estimation. Nat Commun 2019;10:5436.
[26] Ishigaki K, Sakaue S, Terao C, Luo Y, Sonehara K, Yamaguchi K, et al. Multi-ancestry genome-wide association analyses identify novel genetic mechanisms in rheumatoid arthritis. Nat Genet 2022;54:1640–51.
[27] Amariuta T, Ishigaki K, Sugishita H, Ohta T, Koido M, Dey KK, et al. Improving the trans-ancestry portability of polygenic risk scores by prioritizing variants in predicted cell-type-specific regulatory elements. Nat Genet 2020;52:1346–54.
[28] 1000 Genomes Project Consortium, Auton A, Brooks LD, Durbin RM, Garrison EP, Kang HM, et al. A global reference for human genetic variation. Nature 2015;526:68–74.
[29] Ito S, Liu X, Ishikawa Y, Conti DD, Otomo N, Kote-Jarai Z, et al. Androgen receptor binding sites enabling genetic prediction of mortality due to prostate cancer in cancer-free subjects. Nat Commun 2023;14:4863.
[30] Savola P, Lundgren S, Keränen MAI, Almusa H, Ellonen P, Leirisalo-Repo M, et al. Clonal hematopoiesis in patients with rheumatoid arthritis. Blood Cancer J 2018;8:69.
[31] Bauer ME. Accelerated immunosenescence in rheumatoid arthritis: impact on clinical progression. Immun Ageing 2020;17:6.
[32] Sikora KA, Wells KV, Bolek EC, Jones AI, Grayson PC. Somatic mutations in rheumatological diseases: VEXAS syndrome and beyond. Rheumatology (Oxford) 2022;61:3149–60.
[33] Beck DB, Ferrada MA, Sikora KA, Ombrello AK, Collins JC, Pei W, et al. Somatic mutations in *UBA1* and severe adult-onset autoinflammatory disease. N Engl J Med 2020;383:2628–38.
[34] Dumanski JP, Lambert JC, Rasi C, Giedraitis V, Davies H, Grenier-Boley B, et al. Mosaic loss of chromosome Y in blood is associated with Alzheimer disease. Am J Hum Genet 2016;98:1208–19.
[35] Dumanski JP, Halvardson J, Davies H, Rychlicka-Buniowska E, Mattisson J, Moghadam BT, et al. Immune cells lacking Y chromosome show dysregulation of autosomal gene expression. Cell Mol Life Sci 2021;78:4019–33.
[36] Guo X, Dai X, Zhou T, Wang H, Ni J, Xue J, et al. Mosaic loss of human Y chromosome: what, how and why. Hum Genet 2020;139:421–46.
[37] Klein SL, Flanagan KL. Sex differences in immune responses. Nat Rev Immunol 2016;16:626–38.
[38] Moulton VR. Sex hormones in acquired immunity and autoimmune disease. Front Immunol 2018;9:2279.

Ann Rheum Dis 84 (2025) 1324–1334

Contents lists available at ScienceDirect

Annals of the Rheumatic Diseases

journal homepage: https://www.sciencedirect.com/journal/annals-of-the-rheumatic-diseases

Axial spondyloarthritis

# Evaluation of instruments assessing peripheral arthritis in spondyloarthritis: an analysis of the ASAS-PerSpA study

Dafne Capelusnik[1,2,*], Clementina Lopez-Medina[3,4], Désirée van der Heijde[5], Robert Landewé[6,7], Maxime Dougados[8,9], Joachim Sieper[10], Anna Molto[8,9], Sofia Ramiro[5,7]

[1] *Care and Public Health Research Institute (CAPHRI), Maastricht University, Maastricht, The Netherlands*
[2] *Department of Rheumatology, Tel Aviv Sourasky Medical Center, Tel Aviv, Israel*
[3] *Rheumatology, Reina Sofia University Hospital, Cordoba, Spain*
[4] *Maimonides Biomedical Research Institute of Cordoba, University of Cordoba, Cordoba, Spain*
[5] *Department of Rheumatology, Leiden University Medical Center, Leiden, The Netherlands*
[6] *Department of Rheumatology & Clinical Immunology, Amsterdam University Medical Centers, University of Amsterdam, Amsterdam, The Netherlands*
[7] *Department of Rheumatology, Zuyderland Medical Center, Heerlen, The Netherlands*
[8] *Rheumatology Department, Hospital Cochin, APHP, Paris, France*
[9] *INSERM U-1153, Center for Research in Epidemiology and Statistics, Université Paris Cité, Paris, France*
[10] *Department of Gastroenterology, Infectious Diseases and Rheumatology, Charité Universitatsmedizin Berlin, Berlin, Germany*

ARTICLE INFO

ABSTRACT

*Objectives:* To assess construct validity, including known-group discrimination, of the currently available disease activity instruments assessing peripheral arthritis in spondyloarthritis (SpA).
*Methods:* In this analysis from the Assessment of SpondyloArthritis International Society (ASAS)-PerSpA study, patients with a diagnosis of axial SpA, peripheral SpA, or psoriatic arthritis (PsA) were included. The disease activity instruments evaluated were the Patient Global Assessment (PGA), Bath Ankylosing Spondylitis Disease Activity Index, Axial Spondyloarthritis Disease Activity Score, Disease Activity Index for PsA (DAPSA), Swollen Joint Count (SJC), Tender Joint Count, Disease Activity Score (DAS) 28, DAS44, and C-reactive protein (CRP). Construct validity was assessed through correlations with external constructs (Bath Ankylosing Spondylitis Functional Index, ASAS Health Index, and Euro Quality of Life 5 Dimensions) and known-group discrimination (active/inactive disease based on a combination of PGA [≥5/<5]), and SJC (≥1/0 and ≥2/<2) was analysed using standardised mean differences (SMDs).
*Results:* In total, 4121 patients were included (mean age 45 [SD, 14] years, 61% males). When assessing the construct validity through correlations with external constructs, all instruments performed excellently (100% hypotheses confirmed). When assessing known-group discrimination, all disease activity measures, except CRP, presented SMDs ≥ 0.8 (good discrimination), with higher SMDs observed for DAS28 followed by DAPSA. Results were similar across disease phenotypes. Considering all combinations of PGA and SJC to discriminate between active/inactive disease, a better performance was observed for the composite scores, including joint counts.

*Correspondence to Dr Dafne Capelusnik, Care and Public Health Research Institute (CAPHRI), Maastricht University, Maastricht, The Netherlands.
*E-mail address:* capelusnikdafne@gmail.com (D. Capelusnik).
Anna Molto and Sofia Ramiro contributed equally to this work.
**Handling editor** Josef S. Smolen.

https://doi.org/10.1016/j.ard.2025.02.011

0003-4967/© 2025 The Author(s). Published by Elsevier B.V. on behalf of European Alliance of Associations for Rheumatology (EULAR). This is an open access article under the CC BY license (http://creativecommons.org/licenses/by/4.0/)

*Conclusions:* In our construct validity analysis, all disease activity instruments assessing peripheral arthritis had a good performance as reflected in the correlations with external constructs and the known-group discrimination. The highest discriminatory capacity to distinguish between 'active/inactive disease' was observed for composite scores, including joint counts, like DAS28 and DAPSA.

**What is already known on this topic**

- The current instrument endorsed in the Assessment of SpondyloArthritis International Society core outcome set for the assessment of peripheral arthritis in trials is the 44 Swollen Joint Count.
- The performance of other instruments or composite scores in evaluating disease activity related to peripheral arthritis has been scarcely studied.

**WHAT THIS STUDY ADDS**

- In this study, aiming to identify the optimal instrument to assess peripheral arthritis and related disease activity in spondyloarthritis (SpA), all disease activity instruments had a good construct validity reflected in the correlations with external constructs and known-group discrimination.
- Composite scores, such as Disease Activity Score 28 and Disease Activity Index for Psoriatic Arthritis, which incorporate joint counts, showed the highest capacity to discriminate between active and inactive disease.

**HOW THIS STUDY MIGHT AFFECT RESEARCH, PRACTICE OR POLICY**

- Composite scores seem to be more promising tools for assessing disease activity in peripheral arthritis.
- Future analyses should focus on identifying the most suitable composite scores for assessing peripheral arthritis in SpA.

## INTRODUCTION

Spondyloarthritis (SpA) is a heterogeneous disease that can present with several phenotypes or clinical forms, such as axial SpA (axSpA) and peripheral SpA (pSpA). Moreover, peripheral rheumatological manifestations (ie, arthritis, dactylitis, and peripheral enthesitis) can occur either concomitantly with the axial disease, before or independently [1,2].

Recently, the Assessment of SpondyloArthritis International Society (ASAS) core outcome set (COS) for axSpA, which describes the minimum set of outcome measures that should be collected in all studies, has been updated, and for the 'peripheral manifestations domain,' only 2 instruments were assessed for peripheral arthritis, namely the Swollen Joint Count (SJC) with 66 and 44 joints (SJC66 and SJC44, respectively) [3]. Although psychometric properties were comparable for both, with inadequate performance of both for clinical trial discrimination, both were endorsed by ASAS members to facilitate future assessment of their performance by promoting standardised data collection. Finally, the SJC44 was chosen as the preferred instrument for inclusion in the COS [3]. Nevertheless, no composite score was assessed for the peripheral manifestations domain. Although scarce, there is some evidence of the good performance of composite scores when assessing disease activity in the pSpA population [4]. In a previous study from our group [4] addressing the sensitivity to change and discriminatory aspects of different measurement instruments, the Axial Spondyloarthritis Disease Activity Score (ASDAS) [5], Bath Ankylosing Spondylitis Disease Activity Index (BASDAI) [6], Patient Global Assessment (PGA), and Physician Global Assessment showed the highest sensitivity to change and the highest level of discriminatory capacity, while the performance of SJC, Tender Joint Count (TJC), and C-reactive protein (CRP) was not good enough. In another study assessing the construct validity of measurement instruments in pSpA in clinical practice, Beckers et al [7] found a good performance of the Disease Activity Index for Psoriatic Arthritis (DAPSA) [8], PsA Disease Activity Score [9], and ASDAS, although agreement among the 3 instruments when classifying disease activity states was not sufficient.

Recently, the ASAS-PerSpA study has focused on the peripheral involvement in patients with SpA, answering some of the previous research questions, such as the prevalence of 'isolated' (ie, without axial disease) pSpA, the clinical presentation of peripheral rheumatological SpA features with regard to the presence or absence of skin psoriasis, and the intercountry variability in the clinical presentation of SpA, among others [10]. One of ASAS-PerSpA's main objectives was to evaluate the validity of existing outcome measures of peripheral rheumatological features and to explore the possibility of improving them. Indeed, the optimal instrument to assess disease activity in patients with peripheral arthritis has not yet been identified. While the SJC is the measurement instrument included in the ASAS COS for axSpA, the use of composite scores validated for other forms of SpA (ie, ASDAS, BASDAI, and DAPSA) or even in other rheumatic and musculoskeletal diseases (RMDs) (eg, Disease Activity Score [DAS]) has also been proposed. Still, little is known regarding the actual performance of these outcome measures in the assessment of peripheral arthritis, as well as their performance across SpA phenotypes.

The objectives of this study were to assess the construct validity, including discriminatory capacity between known groups, of the currently available disease activity measurement instruments in patients with SpA with peripheral arthritis and to investigate whether there are differences across SpA phenotypes.

## METHODS

### *Study design and population*

Data from the ASAS-PerSpA study were used. Briefly, the ASAS-PerSpA study is an international, multicentre study with 24 participating countries (23 actively involved), in which data of consecutive patients with SpA (axSpA, pSpA, or PsA based on the physician's diagnosis) were cross-sectionally collected between July 2018 and February 2020. Patients without missing data on all the instruments of interest (described below) were included in the analysis.

Written informed consent was obtained from all patients before enrolment, and ethics committees from the individual participating centres approved the study.

### Outcomes measures

The following disease activity measures evaluating peripheral articular involvement (ie, arthritis, not enthesitis or dactylitis) were assessed.

The PGA was adapted from the question of 'Global assessment of well-being: *Considering all the ways your spondyloarthritis has affected you during the last 48 hours, tick the box that best describes how you are doing*' on a numeric rating scale (NRS) (range, 0-10) (10 = worse well-being).

The SJC66 and *68-joint TJC* (TJC68) include the respective number of peripheral joints from the upper and lower limbs, as well as the temporomandibular, sternoclavicular, and acromioclavicular joints.

The BASDAI [6] includes patient-reported levels of fatigue, back pain, peripheral joint pain/swelling, localised tenderness, and severity and duration of morning stiffness. Each question uses an NRS (range, 0-10) (10 = very severe), and the scores are averaged (questions 5 and 6 first and then the remaining 4), giving a final score from 0 to 10 (10 = maximal disease activity).

The ASDAS [5,11] includes patient-reported overall back pain, peripheral pain/swelling, duration of morning stiffness, global assessment of disease activity ranging from 0 to 10 on NRS, and the CRP as a measure of inflammation. All these elements are combined in a weighted equation with higher values indicating higher disease activity.

The DAPSA [7] is calculated by simply summing up the PGA, pain assessment (0-10), SJC66, TJC68, and CRP (mg/dL). As the overall pain assessment was not collected in PerSpA, the third BASDAI question on peripheral pain/swelling was used instead.

The *28-joint and 44-joint DAS* [12,13] are composite scores measuring disease activity in rheumatoid arthritis that combine information on swollen joints, tender joints, acute phase reactants, and PGA. Both scores are calculated using a weighted equation with higher values indicating higher disease activity.

The acute phase reactant CRP (mg/dL) was also assessed as a potential separate outcome measurement instrument for disease activity.

### External constructs

The following outcomes were used as external constructs in the construct validity analysis of each instrument: the Bath Ankylosing Spondylitis Functional Index (BASFI) [14], which assesses functional ability (range, 0-10) (10 = worse functional capacity); the rating scale of the Euro Quality of Life 5 Dimensions (EuroQoL) [15] used to measure health-related quality of life (range, 0-100) (0 = worst imaginable health); and the ASAS Health Index (ASAS-HI) [16], assessing the overall functioning and health (range, 0-17) (17 = worse health status).

### Statistical analysis

Descriptive statistics were used for the overall population and each of the individual populations of patients with axSpA, pSpA, and PsA.

Following the Outcome Measures in Rheumatology (OMERACT) filter for instrument selection [17], construct validity (as part of the 'Truth pillar') was assessed through 2 different approaches:

#### Construct validity analysis through correlations of strength

As the first step, hypotheses for the strength of the correlation between the assessed instruments and external constructs were established. Previously, such hypotheses were established by the steering committee for the ASAS COS exercise [3] (when these were available, they were used). However, some of them were missing, namely for the peripheral composite scores and, therefore, a group of 12 rheumatologists, experts in SpA, was consulted to decide on the hypothetical strength of the correlation. Then, we proceeded with the analysis through Spearman correlation, evaluating whether the hypothesis for the strength of each correlation (between the assessed instruments and the external constructs) was accepted/rejected. Construct validity was considered 'good' if ≥75% of the hypotheses were confirmed, 'adequate' if 50% to 75% of the hypotheses were confirmed, or poor if <50% of the hypotheses were confirmed, as per the OMERACT and ASAS COS procedures [3,17]. The correlation cutoffs were weak if <0.30, moderate if 0.30 to 0.69, and strong if ≥0.70 [17,18].

#### Construct validity through discrimination between known groups

Finally, we measured the discriminatory capacity of these instruments between 2 states of peripheral disease activity. No gold standard is available to define disease activity states concerning peripheral articular involvement; thus, we used 2 disease activity instruments: PGA (as a patient subjective outcome that includes the perception of both axial and peripheral involvement) and SJC (as an objective and exclusive peripheral outcome) to stratify the population. The stratification of PGA was based on the middle of the scale, so it had a value of 5. Due to the high frequency of patients without arthritis, the stratification of SJC was performed in 2 ways: (1) no swollen joints vs any (≥1) swollen joint and (2) SJC below the median SJC vs equal or above the median SJC. Combining both stratifications of PGA and SJC, patients were considered to be in 'low disease activity' in case they had a PGA < 5 and no swollen joints vs in 'high disease activity' in case they had a PGA ≥ 5 and at least 1 swollen joint. Subsequently, comparisons were made across all possible subgroups combining the stratifications based on PGA and SJC: (1) PGA < 5 and SJC < median vs PGA < 5 and SJC ≥ median; (2) PGA < 5 and SJC = 0 vs PGA < 5 and SJC ≥ 1; (3) PGA ≥ 5 and SJC < median vs PGA ≥ 5 and SJC ≥ median; (4) PGA > 5 and SJC = 0 vs PGA > 5 and SJC ≥ 1. Finally, an additional stratification was performed based solely on SJC to minimise the potential influence of axial manifestations on the PGA. Then, the standardised mean difference (SMD) was calculated as the difference between the group means divided by the pooled SD. The SMD has no units, which facilitates comparison across disease measures. An SMD with a higher absolute value indicates better discriminatory ability, and an SMD above 0.8 is considered 'good' [17,19,20].

### Sensitivity analysis

Additionally, the same analyses (*correlations of strength* and *discrimination between known groups)* were conducted as sensitivity analyses individually in the different subpopulations (axSpA, pSpA, and PsA) and also in the population of non-PsA SpA, including axSpA and pSpA (so excluding PsA). This last analysis was conducted to ensure that including PsA in the analysis did not drive the results, as PsA is often polyarticular, and the stratifications used in our analyses were often based on SJC.

All the analyses were performed using Stata SE V.17 (StataCorp LLC).

## RESULTS

From the 4185 patients included in the ASAS-PerSpA study, 4121 had complete data on all the disease activity measures assessed and were thus included in the analysis. According to the rheumatologist, 2679 (65%) patients had a diagnosis of axSpA, 428 (10%) of pSpA, and 1014 (25%) of PsA. From the entire population, 2291 (56%) patients had a history of peripheral arthritis, mainly with oligo- or polyarticular involvement (43% and 45%, respectively). Across the disease phenotypes, the percentage of patients with a history of peripheral articular involvement was lower in axSpA (36% vs 95% in pSpA and 91% in PsA) with a predominant oligoarticular involvement, while in pSpA and PsA, there was a similar distribution between oligo and polyarticular involvement. The population characteristics and mean values for each disease activity instrument assessed can be found in Table 1.

### *Construct validity analysis through correlations of strength*

When looking at the construct validity through correlations with external constructs (BASFI, ASAS-HI, and EuroQoL), all the assessed disease activity instruments had a good performance, with 100% of the hypotheses confirmed. When stratifying by disease phenotype, all the instruments remained with good performance, except for BASDAI and SJC in pSpA and BASDAI and ASDAS in PsA, where they had only adequate performance (67% of the hypotheses confirmed). Nevertheless, the reason for the 'rejection' of the hypotheses was due to a better correlation than hypothesised (Table 2).

### *Discrimination between known groups*

In the entire population, all disease activity measures, except for CRP (SMD, 0.51), were highly discriminatory as they presented SMDs above 0.8, with the highest SMD being observed for DAS28 (SMD, 3.11), followed by DAPSA (SMD, 2.62), DAS44 (SMD, 2.51), BASDAI (SMD, 2.40), and ASDAS (SMD, 2.40) (Fig).

In the pSpA and PsA subgroups, DAS28 also had the highest SMD, followed by ASDAS and BASDAI, while the highest SMD in the axSpA population was also DAS28, but followed by DAPSA and DAS44 (Table 3).

When stratifying by both PGA and SJC and considering all the possible strata and not only the most extreme ones, a better performance was observed for composite scores that include joint counts, ie, DAS28, DAS44, and DAPSA. With a higher SJC

Table 1
**Patient characteristics in the total population and according to spondyloarthritis phenotype**

| Patients characteristics | Total PerSpA n = 4121, mean (SD) or n (%) | axSpA n = 2679, mean (SD) or n (%) | pSpA n = 428, mean (SD) or n (%) | PsA n = 1014, mean (SD) or n (%) |
|---|---|---|---|---|
| Age (y) | 45 (14.0) | 42 (13.0) | 44.1 (14.3) | 51.8 (12.9) |
| Male sex | 2521 (61) | 1829 (68) | 203 (47) | 489 (48) |
| Symptom duration (y) | 20.9 (18.3) | 20.1 (16.6) | 14.2 (14.6) | 26.0 (22.3) |
| Disease duration (y) | 14.5 (11.4) | 14.3 (11.0) | 10.0 (9.4) | 16.8 (12.3) |
| Diagnosis delay (y) | 6.4 (8.7) | 5.8 (7.6) | 4.2 (6.6) | 9.2 (11.2) |
| BMI (kg/m$^2$) | 26.4 (5.4) | 25.9 (5.1) | 26.4 (5.4) | 28.0 (5.9) |
| Axial involvement[a] | 3215 (78) | 2614 (98) | 238 (56) | 363 (36) |
| Peripheral arthritis[a] | 2291 (56) | 965 (36) | 405 (95) | 921 (91) |
| Dactylitis[a] | 632 (15) | 161 (6) | 98 (23) | 373 (37) |
| Enthesitis[a] | 1812 (44) | 1099 (41) | 246 (57) | 467 (46) |
| History of | | | | |
| Monoarticular[b] involvement | 275 (12) | 192 (20) | 44 (11) | 39 (4) |
| Oligoarticular[b] involvement | 979 (43) | 472 (49) | 180 (44) | 327 (36) |
| Polyarticular[b] involvement | 1037 (45) | 301 (31) | 181 (45) | 555 (40) |
| CRP (mg/L) | 11.9 (27.1) | 11.7 (26.6) | 14.1 (25.5) | 11.5 (28.8) |
| BASFI (0-10) | 3.0 (2.7) | 3.0 (2.6) | 2.80 (2.6) | 3.1 (2.7) |
| ASAS-HI (0-17) | 6.6 (4.6) | 6.3 (4.5) | 6.63 (4.4) | 7.3 (4.7) |
| EuroQoL (0-100) | 65 (20) | 67 (20) | 63 (20) | 63 (25) |
| PGA (0-10) | 4.4 (2.7) | 4.3 (2.7) | 4.6 (2.7) | 4.6 (2.7) |
| BASDAI (0-10) | 3.9 (2.4) | 3.7 (2.4) | 4.0 (2.4) | 4.3 (2.5) |
| ASDAS | 2.5 (1.1) | 2.5 (1.1) | 2.6 (1.2) | 2.6 (1.1) |
| DAPSA | 12.3 (11.6) | 10.2 (9.5) | 14.6 (11.8) | 16.8 (14.7) |
| SJC (0-66) | 0.8 (3.1) | 0.3 (2.0) | 1.2 (2.9) | 1.9 (4.8) |
| TJC (0-68) | 2.5 (6.1) | 1.5 (4.4) | 3.4 (6.2) | 4.8 (8.7) |
| DAS28 | 2.6 (1.1) | 2.4 (0.9) | 2.9 (1.2) | 3.0 (1.2) |
| DAS44 | 1.2 (0.8) | 1.1 (0.6) | 1.5 (0.8) | 1.6 (1.0) |
| NSAIDs (last month) | 2817 (68) | 1903 (71) | 307 (72) | 607 (60) |
| Current steroids | 486 (12) | 199 (7) | 88 (21) | 199 (20) |
| cDMARDs (since diagnosis) | 1452 (35) | 616 (23) | 229 (54) | 607 (60) |
| b/tsDMARDs (since diagnosis) | 1945 (47) | 1275 (48) | 156 (36) | 514 (51) |

ASAS, Assessment of SpondyloArthritis International Society; ASAS-HI, ASAS Health Index; ASDAS, Axial Spondyloarthritis Disease Activity Score; axSpA, axial spondyloarthritis; BASDAI, Bath Ankylosing Spondylitis Disease Activity Score; BASFI, Bath Ankylosing Spondylitis Functional Index; BMI, body mass index; c/b/tsDMARDs, conventional/biologic/targeted synthetic disease-modifying antirheumatic drug; CRP, C-reactive protein; DAPSA, Disease Activity in Psoriatic Arthritis; DAS, Disease Activity Score; EuroQoL, Euro Quality of Life 5 Dimensions; NSAID, nonsteroidal anti-inflammatory drug; PGA, Patient Global Assessment; PsA, psoriatic arthritis; pSpA, peripheral spondyloarthritis; SJC, Swollen Joint Count; TJC, Tender Joint Count.
Disease phenotype was defined by the physician. Data were incomplete for BMI (n = 15), ASAS-HI (n = 2), and EuroQoL (n = 14).
[a] Manifestation ever-present.
[b] History of type of involvement: monoarticular, 1 swollen joint; oligoarticular, 2 to 4 swollen joints; polyarticular, 5 or more swollen joints.

Table 2
**Correlation between disease activity measures and external comparators**

| External comparators | | Spearman correlations (Weak – Moderate – Strong)§ | | | | | | | | |
|---|---|---|---|---|---|---|---|---|---|---|
| ***Entire ASAS-perSpA population (n=4121)*** | | | | | | | | | | |
| | | PGA | BASDAI | ASDAS | DAPSA | SJC | TJC | DAS28 | DAS44 | CRP |
| BASFI (0-10) | **Hypothesis±** | **Moderate** | **Strong** | **Moderate** | **Moderate** | **Weak** | **Moderate** | **Moderate** | **Moderate** | **Weak** |
| | Correlation coefficient | 0.653 | 0.733 | 0.697 | 0.637 | 0.199 | 0.367 | 0.566 | 0.412 | 0.273 |
| ASAS-HI | **Hypothesis±** | **Moderate** | **Moderate** | **Moderate** | **Moderate** | **Weak** | **Moderate** | **Moderate** | **Moderate** | **Weak** |
| | Correlation coefficient | 0.601 | 0.682 | 0.619 | 0.600 | 0.208 | 0.364 | 0.527 | 0.399 | 0.208 |
| EuroQoL | **Hypothesis±** | **Moderate** | **Moderate** | **Moderate** | **Moderate** | **Weak** | **Moderate** | **Moderate** | **Moderate** | **Weak** |
| | Correlation coefficient | -0.632 | -0.680 | -0.652 | -0.622 | -0.250 | -0.377 | -0.561 | -0.419 | -0.261 |
| **Construct validity*** | | 100% | 100% | 100% | 100% | 100% | 100% | 100% | 100% | 100% |
| **axSpA (n=2679)** | | | | | | | | | | |
| BASFI (0-10) | **Hypothesis±** | **Moderate** | **Strong** | **Moderate** | **Moderate** | **Weak** | **Moderate** | **Moderate** | **Moderate** | **Weak** |
| | Correlation coefficient | 0.665 | 0.727 | 0.691 | 0.678 | 0.215 | 0.372 | 0.594 | 0.421 | 0.284 |
| ASAS-HI | **Hypothesis±** | **Moderate** | **Moderate** | **Moderate** | **Moderate** | **Weak** | **Moderate** | **Moderate** | **Moderate** | **Weak** |
| | Correlation coefficient | 0.602 | 0.663 | 0.612 | 0.608 | 0.192 | 0.328 | 0.531 | 0.377 | 0.221 |
| EuroQoL | **Hypothesis±** | **Moderate** | **Moderate** | **Moderate** | **Moderate** | **Weak** | **Moderate** | **Moderate** | **Moderate** | **Weak** |
| | Correlation coefficient | -0.633 | -0.672 | -0.649 | -0.632 | -0.225 | -0.342 | -0.569 | -0.402 | -0.264 |
| **Construct validity*** | | 100% | 100% | 100% | 100% | 100% | 100% | 100% | 100% | 100% |
| **pSpA (n=428)** | | | | | | | | | | |
| BASFI (0-10) | **Hypothesis±** | **Moderate** | **Strong** | **Moderate** | **Moderate** | **Weak** | **Moderate** | **Moderate** | **Moderate** | **Weak** |
| | Correlation coefficient | 0.614 | 0.716 | 0.651 | 0.600 | 0.229 | 0.381 | 0.492 | 0.380 | 0.242 |
| ASAS-HI | **Hypothesis±** | **Moderate** | Moderate | **Moderate** | **Moderate** | **Weak** | **Moderate** | **Moderate** | **Moderate** | **Weak** |
| | Correlation coefficient | 0.610 | 0.711 | 0.609 | 0.591 | 0.251 | 0.375 | 0.469 | 0.373 | 0.171 |
| EuroQoL | **Hypothesis±** | **Moderate** | **Moderate** | **Moderate** | **Moderate** | Weak | **Moderate** | **Moderate** | **Moderate** | **Weak** |
| | Correlation coefficient | -0.631 | -0.676 | -0.654 | -0.637 | -0.345 | -0.428 | -0.559 | -0.444 | -0.296 |
| **Construct validity*** | | 100% | 67% | 100% | 100% | 67% | 100% | 100% | 100% | 100% |
| ***PsA (n=1014)*** | | | | | | | | | | |
| BASFI (0-10) | **Hypothesis±** | **Moderate** | **Strong** | Moderate | **Moderate** | **Weak** | **Moderate** | **Moderate** | **Moderate** | **Weak** |
| | Correlation coefficient | 0.669 | 0.767 | 0.734 | 0.622 | 0.216 | 0.412 | 0.568 | 0.456 | 0.265 |
| ASAS-HI | **Hypothesis±** | **Moderate** | Moderate | **Moderate** | **Moderate** | **Weak** | **Moderate** | **Moderate** | **Moderate** | **Weak** |
| | Correlation coefficient | 0.592 | 0.714 | 0.641 | 0.588 | 0.200 | 0.422 | 0.526 | 0.447 | 0.203 |
| EuroQoL | **Hypothesis±** | **Moderate** | **Moderate** | **Moderate** | **Moderate** | **Weak** | **Moderate** | **Moderate** | **Moderate** | **Weak** |
| | Correlation coefficient | -0.627 | -0.697 | -0.658 | -0.604 | -0.246 | -0.430 | -0.551 | -0.452 | -0.244 |
| **Construct validity*** | | 100% | 67% | 67% | 100% | 100% | 100% | 100% | 100% | 100% |

ASAS, Assessment of SpondyloArthritis International Society; ASAS-HI, ASAS Health Index; ASDAS, Axial Spondyloarthritis Disease Activity Score; axSpA, axial spondyloarthritis; BASDAI, Bath Ankylosing Spondylitis Disease Activity Score; BASFI, Bath Ankylosing Spondylitis Functional Index; CRP, C-reactive protein; DAPSA, Disease Activity in Psoriatic Arthritis; DAS, Disease Activity Score; EuroQoL, Euro Quality of Life 5 Dimensions; PGA, Patient Global Assessment; PsA, psoriatic arthritis; pSpA, peripheral spondyloarthritis; SJC, Swollen Joint Count; TCJ, Tender Joint Count.
Hypotheses are in bold when they were met.
[a]Weak < 0.30; moderate, 0.30 to 0.69; strong ≥ 0.70.
[b]Hypothesis for the strength of correlation.
[c]Construct validity: ≥75% of the hypotheses confirmed: good (green); 50%-75% of the hypotheses confirmed: adequate (orange); <50% of the hypotheses confirmed: poor (red).

cutoff (median SJC vs presence of arthritis [≥1]), the performance of the composite scores, including joint counts, was better. ASDAS showed worse performance than the composite scores with joint counts across all groups (Tables 4 and 5). Lastly, the results from the analysis stratified solely by SJC were consistent with the main findings (Supplementary Table S1).

## *Sensitivity analysis*

In the sensitivity analysis, after excluding PsA patients, similarly to the main analysis, all disease activity measures met 100% of the hypotheses (good performance) (Supplementary Table S2). Similar to the main analysis, all the measures except for CRP presented SMDs above 0.8, but in this case, ASDAS discriminated slightly better than BASDAI between active/inactive disease (Supplementary Table S3). When stratifying by the different combinations of PGA and SJC, better performance of composite scores with joint counts was also observed, except for PGA < 5 dichotomising by the SJC median, where BASDAI and ASDAS performed well, though still worse than the composite scores with joint counts. With a higher SJC cutoff, the performance of the composite scores, including joint count, was better or worse than that of a lower cutoff of SJC (Supplementary Table S4).

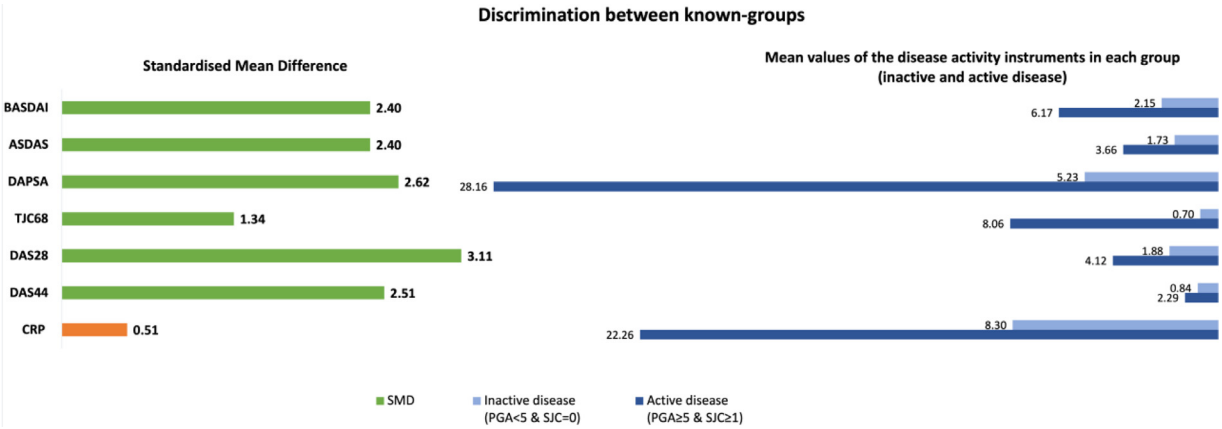



**Figure.** Discriminatory capacity of the disease activity measurement instruments. Analyses are stratified by extreme groups of inactive and active disease according to the Patient Global Assessment (PGA) and Swollen Joint Count (SJC) in the entire ASAS-PerSpA population, ie, inactive disease (PGA $< 5$ and SJC $= 0$) vs active disease (PGA $\geq 5$ and SJC $= 1$). Bars are coloured in green when the standardised mean difference (SMD) $\geq 0.8$ and in orange when SMD $\geq 0.5$ but $<0.8$. ASAS, Assessment of SpondyloArthritis International Society; ASDAS, Axial Spondyloarthritis Disease Activity Score; BASDAI, Bath Ankylosing Spondylitis Disease Activity Index; CRP, C-reactive protein; DAPSA, Disease Activity in Psoriatic Arthritis; DAS, Disease Activity Score; TCJ, Tender Joint Count.

## DISCUSSION

To our knowledge, the present study is the first to analyse and compare the construct validity between different instruments, particularly the discrimination between known groups, when assessing the impact of peripheral arthritis on disease activity in SpA patients and across the whole spectrum of SpA. In this comprehensive analysis of the ASAS-PerSpA study, all assessed disease activity instruments showed good construct validity reflected in the strength of the correlations with external constructs. Furthermore, when discriminating between known groups, all of them had good performance, and the highest discriminatory capacity to discriminate between 'active and inactive disease' was observed for the composite scores with joint counts, like DAS28 and DAPSA, with consistent results across all disease phenotypes.

Recently, the core set for axSpA was updated, and the SJC44 was selected for the peripheral domain assessment. However, no composite score was assessed. Currently, in almost all RMDs, the use of composite DAS is recommended over separate instruments in both clinical trials and clinical practice. Unlike individual outcomes, composite scores can capture the multiple facets of disease, resulting in more reliability and responsiveness to change instruments [21–23].

The correlation of strength with external constructs is the most commonly used construct validity analysis. With this first approach, when assessing the entire population, all the instruments met 100% of the hypotheses, and that was also true for the axSpA subgroup, which represented more than 60% of the entire population. In pSpA, however, BASDAI and SJC only achieved 'adequate' performance, while in PsA, the 2 specific axSpA scores, BASDAI and ASDAS, had lower performance ('adequate'). As the reason for the 'rejection' of the hypotheses was, in all the cases, a higher correlation than hypothesised, it could be argued that a better correlation than expected should also meet the hypothesis. However, for the time being, there is no agreement on how to handle these cases of better correlations than the ones hypothesised.

By performing discrimination between known-group analyses, we could additionally assess and compare the performance of each instrument when discriminating between 'active and

Table 3
**Discriminatory capacity of the disease activity measurement instruments. Analyses are stratified by extreme groups according to PGA and SJC in the entire ASAS-PerSpA population, and the different phenotypes**

| | Entire population (axSpA, pSpA and PsA) | | | axSpA | | | pSpA | | | PsA | | |
|---|---|---|---|---|---|---|---|---|---|---|---|---|
| Assessment measure | PGA<5 & SJC=0 (n=1823) | PGA≥5 & SJC ≥1 (n=577) | SMD | PGA<5 & SJC=0 (n=1335) | PGA≥5 & SJC ≥1 (n=197) | SMD | PGA<5 & SJC=0 (n=144) | PGA≥5 & SJC ≥1 (n=120) | SMD | PGA<5 & SJC=0 (n=344) | PGA≥5 & SJC ≥1 (n=260) | SMD |
| BASDAI (0-10) | 2.15 (1.57) | 6.17 (1.95) | 2.40 | 2.12 (1.51) | 6.44 (1.96) | 2.73 | 2.05 (1.8) | 5.65 (1.88) | 1.96 | 2.32 (1.68) | 6.21 (1.94) | 2.17 |
| ASDAS | 1.73 (0.75) | 3.66 (0.96) | 2.40 | 1.74 (0.74) | 3.95 (1.01) | 2.83 | 1.65 (0.74) | 3.51 (0.95) | 2.20 | 1.72 (0.77) | 3.52 (0.89) | 2.18 |
| DAPSA | 5.23 (4.85) | 28.16 (15.67) | 2.62 | 4.83 (4.34) | 26.33 (14.11) | 3.32 | 6.02 (5.69) | 25.52 (13.5) | 1.94 | 6.44 (5.97) | 30.76 (17.30) | 1.99 |
| TJC (0-68) | 0.70 (2.34) | 8.06 (10.40) | 1.34 | 0.48 (1.68) | 6.32 (8.48) | 1.71 | 1.35 (3.4) | 6.66 (8.68) | 0.83 | 1.26 (3.53) | 10.01 (12.01) | 1.05 |
| DAS28 | 1.88 (0.57) | 4.12 (1.07) | 3.11 | 1.86 (0.54) | 4.03 (0.98) | 3.54 | 1.92 (0.63) | 4 (1.06) | 2.43 | 1.94 (0.64) | 4.24 (1.12) | 2.61 |
| DAS44 | 0.84 (0.40) | 2.29 (0.93) | 2.51 | 0.81 (0.35) | 2.17 (0.86) | 3.03 | 0.96 (0.52) | 2.2 (0.89) | 1.75 | 0.92 (0.50) | 2.42 (0.99) | 1.98 |
| CRP (mg/L) | 8.30 (22.59) | 22.26 (38.67) | 0.51 | 8.09 (20.54) | 28.38 (45.17) | 0.81 | 7.46 (16.98) | 24.97 (36.94) | 0.63 | 9.48 (30.81) | 16.38 (32.99) | 0.22 |

ASDAS, Axial Spondyloarthritis Disease Activity Score; axSpA, axial spondyloarthritis; BASDAI, Bath Ankylosing Spondylitis Disease Activity Index; CRP, C-reactive protein; DAPSA, Disease Activity in Psoriatic Arthritis; DAS, Disease Activity Score; PGA, Patient Global Assessment; PsA, psoriatic arthritis; pSpA, peripheral spondyloarthritis; SJC, Swollen Joint Count; SMD, standardised mean difference; TCJ, Tender Joint Count.
Values are shown as mean (SD).
Cells are coloured according to the following system: SMD ≥ 0.8 (green); ≥0.5 (orange); <0.5 (red).

Table 4

**Discriminatory capacity of the disease activity measurement instruments. Analyses are stratified by both PGA and SJC[a] in the entire ASAS-PerSpA population (n = 4121)**

| | Patient global assessment <5 (n=2100) | | | | | | Patient global assessment ≥5 (n=2021) | | | | | |
|---|---|---|---|---|---|---|---|---|---|---|---|---|
| Assessment measure | SJC<2 (n=1947) | SJC≥2 (n=153) | SMD | SJC=0 (n=1823) | SJC≥1 (n=277) | SMD | SJC<2 (n=1624) | SJC≥2 (n=397) | SMD | SJC=0 (n=1444) | SJC≥1 (n=577) | SMD |
| BASDAI (0-10) | 2.2 (1.6) | 3.18 (1.87) | 0.60 | 2.15 (1.57) | 3.03 (1.86) | 0.54 | 5.37 (1.96) | 6.21 (1.91) | 0.43 | 5.28 (1.93) | 6.17 (1.95) | 0.46 |
| ASDAS | 1.75 (0.76) | 2.29 (0.89) | 0.70 | 1.73 (0.75) | 2.16 (0.89) | 0.56 | 3.22 (0.86) | 3.71 (0.99) | 0.55 | 3.18 (0.84) | 3.67 (0.96) | 0.55 |
| DAPSA | 5.5 (4.98) | 19.51 (15.93) | 2.18 | 5.23 (4.85) | 15.02 (13.3) | 1.48 | 14.99 (7.84) | 31.45 (16.96) | 1.60 | 14.25 (7.39) | 28.16 (15.67) | 1.33 |
| TJC (0-68) | 0.78 (2.4) | 6.74 (10.46) | 1.64 | 0.7 (2.34) | 4.62 (8.34) | 1.05 | 2.53 (5.42) | 9.54 (11.26) | 1.01 | 2.25 (5.09) | 8.06 (10.4) | 0.83 |
| DAS28 | 1.92 (0.59) | 3.34 (0.97) | 2.26 | 1.88 (0.57) | 2.97 (0.94) | 1.73 | 2.95 (0.79) | 4.32 (1.13) | 1.58 | 2.86 (0.75) | 4.12 (1.07) | 1.48 |
| DAS44 | 0.88 (0.43) | 2.02 (0.88) | 2.41 | 0.84 (0.4) | 1.72 (0.8) | 1.86 | 1.25 (0.67) | 2.5 (0.97) | 1.70 | 1.18 (0.64) | 2.29 (0.93) | 1.50 |
| CRP (mg/L) | 8.4 (22.25) | 14.48 (20.28) | 0.28 | 8.3 (22.59) | 12.43 (18.72) | 0.19 | 12.83 (26.69) | 24.53 (43.5) | 0.38 | 12.28 (26.94) | 22.26 (38.67) | 0.32 |

ASDAS, Axial Spondyloarthritis Disease Activity Score; BASDAI, Bath Ankylosing Spondylitis Disease Activity Index; CRP, C-reactive protein; DAPSA, Disease Activity in Psoriatic Arthritis; DAS, Disease Activity Score; PGA, Patient Global Assessment; SJC, Swollen Joint Count; SMD, standardised mean difference.
Values are shown as mean (SD).
Cells are coloured according to the following system: SMD ≥ 0.8 (green); ≥0.5 (orange); <0.5 (red).
[a] The population was stratified by PGA and SJC in different ways, showing all the groups of such stratification, allowing us to evaluate the performance of the indices in the complete population and according to the different levels of disease activity (including 2 different cutoffs of SJC).

Table 5

**Discriminatory capacity of the disease activity measurement instruments. Analyses are stratified by both PGA and SJC[a] for each disease phenotype**

| axSpA population (n=2679) | | | | | | | | | | | | |
|---|---|---|---|---|---|---|---|---|---|---|---|---|
| | Patient global assessment <5 (n=1414) | | | | | | Patient global assessment ≥5 (n=1265) | | | | | |
| Assessment measure | SJC<2 (n=1377) | SJC≥2 (n=37) | SMD | SJC=0 (n=1335) | SJC≥1 (n=79) | SMD | SJC<2 (n=1139) | SJC≥2 (n=126) | SMD | SJC=0 (n=1068) | SJC≥1 (n=197) | SMD |
| BASDAI (0-10) | 2.14 (1.54) | 3.65 (2.41) | 0.96 | 2.12 (1.51) | 3.17 (2.29) | 0.67 | 5.25 (1.93) | 6.54 (1.9) | 0.67 | 5.19 (1.9) | 6.44 (1.96) | 0.65 |
| ASDAS | 1.75 (0.75) | 2.57 (1) | 1.08 | 1.74 (0.74) | 2.33 (0.97) | 0.78 | 3.25 (0.86) | 4.04 (1.05) | 0.91 | 3.21 (0.84) | 3.95 (1.01) | 0.86 |
| DAPSA | 4.99 (4.47) | 21.96 (24.1) | 2.90 | 4.83 (4.34) | 15.56 (17.92) | 1.80 | 13.83 (6.94) | 30.03 (15.68) | 1.97 | 13.44 (6.75) | 26.33 (14.11) | 1.55 |
| TJC (0-68) | 0.53 (1.75) | 8.49 (15.43) | 2.64 | 0.48 (1.68) | 5.11 (11.16) | 1.50 | 1.83 (4.27) | 7.91 (9.33) | 1.22 | 1.72 (4.13) | 6.32 (8.48) | 0.91 |
| DAS28 | 1.88 (0.55) | 3.54 (0.99) | 2.92 | 1.86 (0.54) | 2.97 (0.99) | 1.95 | 2.86 (0.75) | 4.23 (1.09) | 1.72 | 2.81 (0.72) | 4.03 (0.98) | 1.58 |
| DAS44 | 0.83 (0.37) | 2.26 (1.06) | 3.55 | 0.81 (0.35) | 1.82 (0.91) | 2.52 | 1.14 (0.6) | 2.42 (0.91) | 2.00 | 1.1 (0.59) | 2.17 (0.86) | 1.68 |
| CRP (mg/L) | 8.23 (20.49) | 17.97 (23.96) | 0.47 | 8.09 (20.54) | 15.19 (21.24) | 0.34 | 13.31 (27.52) | 33.96 (53.5) | 0.66 | 12.96 (27.87) | 28.38 (45.17) | 0.49 |
| pSpA population (n=428) | | | | | | | | | | | | |
| | Patient global assessment <5 (n=201) | | | | | | Patient global assessment ≥5 (n=227) | | | | | |
| Assessment measure | SJC<2 (n=179) | SJC≥2 (n=22) | SMD | SJC=0 (n=144) | SJC≥1 (n=57) | SMD | SJC<2 (n=150) | SJC≥2 (n=77) | SMD | SJC=0 (n=107) | SJC≥1 (n=120) | SMD |
| BASDAI (0-10) | 2.29 (1.88) | 3.26 (1.68) | 0.52 | 2.05 (1.8) | 3.27 (1.79) | 0.68 | 5.37 (1.91) | 5.58 (1.88) | 0.11 | 5.21 (1.9) | 5.65 (1.88) | 0.23 |
| ASDAS | 1.76 (0.83) | 2.48 (0.95) | 0.86 | 1.65 (0.74) | 2.31 (0.99) | 0.80 | 3.19 (0.83) | 3.51 (1.05) | 0.36 | 3.06 (0.83) | 3.51 (0.95) | 0.50 |
| DAPSA | 7 (6.07) | 14.8 (6.56) | 1.27 | 6.02 (5.69) | 12.49 (6.43) | 1.10 | 16.49 (7.55) | 28.36 (15.38) | 1.09 | 14.89 (7.24) | 25.52 (13.5) | 0.97 |
| TJC (0-68) | 1.55 (3.46) | 3.73 (3.01) | 0.64 | 1.35 (3.4) | 2.89 (3.43) | 0.45 | 3.11 (5.54) | 8.1 (9.72) | 0.69 | 2.72 (5.47) | 6.66 (8.68) | 0.54 |
| DAS28 | 2.07 (0.72) | 3.32 (0.88) | 1.69 | 1.92 (0.63) | 2.93 (0.85) | 1.44 | 3.08 (0.8) | 4.19 (1.17) | 1.18 | 2.85 (0.72) | 4 (1.06) | 1.26 |
| DAS44 | 1.04 (0.55) | 1.93 (0.63) | 1.59 | 0.96 (0.52) | 1.6 (0.61) | 1.18 | 1.44 (0.7) | 2.42 (0.96) | 1.22 | 1.3 (0.7) | 2.2 (0.89) | 1.12 |
| CRP (mg/L) | 8.54 (17.87) | 19.41 (22.9) | 0.59 | 7.46 (16.98) | 15.46 (21.69) | 0.43 | 13.92 (22.1) | 25.77 (39.76) | 0.40 | 10.06 (15.39) | 24.97 (36.94) | 0.52 |
| PsA population (n=1014) | | | | | | | | | | | | |
| | Patient global assessment <5 (n=485) | | | | | | Patient global assessment ≥5 (n=529) | | | | | |
| Assessment measure | SJC<2 (n=391) | SJC≥2 (n=94) | SMD | SJC=0 (n=344) | SJC≥1 (n=141) | SMD | SJC<2 (n=335) | SJC≥2 (n=194) | SMD | SJC=0 (n=269) | SJC≥1 (n=260) | SMD |
| BASDAI (0-10) | 2.36 (1.66) | 2.97 (1.64) | 0.37 | 2.32 (1.68) | 2.86 (1.6) | 0.32 | 5.75 (2.05) | 6.24 (1.88) | 0.25 | 5.66 (2.03) | 6.21 (1.94) | 0.28 |
| ASDAS | 1.73 (0.76) | 2.13 (0.81) | 0.53 | 1.72 (0.77) | 2.01 (0.78) | 0.37 | 3.17 (0.88) | 3.58 (0.87) | 0.47 | 3.12 (0.86) | 3.52 (0.89) | 0.46 |
| DAPSA | 6.62 (5.78) | 19.65 (13.13) | 1.68 | 6.45 (5.97) | 15.75 (12.25) | 1.12 | 18.27 (9.64) | 33.6 (18.12) | 1.14 | 17.25 (8.97) | 30.76 (17.3) | 0.98 |
| TJC (0-68) | 1.31 (3.4) | 6.76 (9.01) | 1.09 | 1.26 (3.54) | 5.05 (7.84) | 0.73 | 4.62 (7.8) | 11.16 (12.71) | 0.66 | 4.13 (7.44) | 10.01 (12.01) | 0.59 |
| DAS28 | 2 (0.65) | 3.27 (0.98) | 1.74 | 1.94 (0.64) | 2.98 (0.95) | 1.39 | 3.17 (0.88) | 4.44 (1.14) | 1.29 | 3.05 (0.85) | 4.24 (1.12) | 1.20 |
| DAS44 | 0.96 (0.51) | 1.94 (0.85) | 1.67 | 0.92 (0.5) | 1.72 (0.8) | 1.31 | 1.53 (0.77) | 2.6 (1.01) | 1.23 | 1.44 (0.75) | 2.42 (0.99) | 1.11 |
| CRP (mg/L) | 8.95 (29.03) | 11.96 (17.73) | 0.11 | 9.48 (30.81) | 9.65 (15.36) | 0.01 | 10.72 (25.66) | 17.92 (36.1) | 0.24 | 10.44 (26.71) | 16.38 (32.99) | 0.20 |

ASDAS, Axial Spondyloarthritis Disease Activity Score; axSpA, axial spondyloarthritis; BASDAI, Bath Ankylosing Spondylitis Disease Activity Index; CRP, C-reactive protein; DAPSA, Disease Activity in Psoriatic Arthritis; DAS, Disease Activity Score; PGA, Patient Global Assessment; PsA, psoriatic arthritis; pSpA, peripheral spondyloarthritis; SJC, Swollen Joint Count; SMD, standardised mean difference; TCJ, Tender Joint Count.
Values are shown as mean (SD).
Cells are coloured according to the following system: SMD ≥ 0.8 (green); ≥0.5 (orange); <0.5 (red).
[a] The population was stratified by PGA and SJC in different ways, showing all the groups of such stratification, allowing us to evaluate the performance of the indices in the complete population and according to the different levels of disease activity (including 2 different cutoffs of SJC).

inactive' disease constructs. Starting with the most extreme groups, ie, comparing patients with low PGA and no SJC with patients with high PGA and arthritis, allows us to identify the performance of the instruments in these most extreme situations with more certainty about peripheral disease activity. However, when making decisions about the performance of an instrument, it is important also to consider its performance and discriminatory capacity in less contrasting situations like the discrimination between patients with and without peripheral arthritis when the PGA is low. Therefore, both analyses were conducted so that they could inform on the overall performance of the instruments together.

According to the OMERACT handbook for instrument selection [24], before moving forward with the OMERACT filter, the instruments of interest should pass through a 'Domain match and feasibility' assessment. In this regard, some concerns may be raised about the different joint counts used in the different instruments assessed. For example, the 28-joint count does not include the joints of the feet, which are frequently affected in SpA, and it has, therefore, been considered to not meet the domain match in PsA [25]. For the same reason, the 28-joint count may be problematic in axSpA. This raises concerns about the validity of the DAS28 in SpA.

Continuing with the OMERACT filter, the last pillar, 'Discrimination' (including test–retest reliability, longitudinal construct validity, and ability to discriminate in randomized controlled trials (RCTs), should also be compared across the composite scores. Unfortunately, composite scores nonspecific to axSpA, like the DAS and DAPSA, have not been assessed in trials of axSpA or pSpA so far. Given the positive results obtained in our study for the discriminatory capacity of composite scores, post hoc analyses of RCTs calculating these composite scores and their psychometric properties could provide further valuable insights.

The lower performance of measurement instruments without joint counts, like BASDAI and ASDAS, could be explained by an incomplete appraisal of peripheral arthritis. A previous analysis identified both peripheral arthritis and ASDAS as factors independently contributing to explaining physical function, as measured by BASFI, also confirming that the assessment of peripheral arthritis is not fully captured by ASDAS [26]. A physician's examination reflected on joint count seems to be more accurate and additionally informative.

A key finding of our study is that in the sensitivity analysis, in which patients with PsA were excluded, disease activity measures, including joint counts, performed persistently better, independent of the type of peripheral articular involvement, ie, there were no differences regardless of patients presenting with oligo- or polyarthritis. Similar performance of disease activity measurements, reflecting peripheral arthritis across the SpA phenotypes, reinforces the idea of the spectrum of SpA as a whole.

It is important to emphasise that this study was not intended to provide recommendations on the use of any specific instrument, as proper validation would be required for that. Rather, our aim was to assess all available instruments for measuring disease activity in peripheral arthritis, regardless of whether they had been previously validated for the diseases of interest. The findings of this study underscored the need for a more formal evaluation process, which led to the initiation of the ASAS-SPARADISE (Spondyloarthritis and Peripheral Arthritis Disease Activity Instrument Selection and Evaluation) project. This new initiative aims to systematically evaluate and compare the psychometric properties of different measurement instruments, with the ultimate goal of identifying the most suitable and best-performing instrument to be recommended for evaluating disease activity due to peripheral arthritis in clinical trials involving patients with axSpA or pSpA.

One of the limitations of the discrimination analysis based on the SMD is that it assumes normally distributed data. The lack of normal distribution, as in the case of DAPSA, makes methods like the SMD less suitable to assess discrimination. However, in the absence of a better methodology, the SMD is often used despite this limitation, as there is no consensus on how to analyse discrimination in a different way [3,17]. Notwithstanding, we still believe that this analysis has some strengths worth mentioning. First of all, it is more informative and more robust than the sole comparison of the mean scores between the 2 groups (active/inactive patients) through a simple t-test or analysis of variance. Second and more importantly, the SMD allows a fair comparison across the instruments and their performance. On the other hand, besides the above-mentioned linear score limitation, the same simplicity of DAPSA also becomes a significant advantage over the other more complex instruments that require the calculation of complex formulas or the use of an online tool. Finally, the similarity in SMD values between instruments with normally distributed (DAS28 and DAS44) and nonnormally distributed values (DAPSA) suggests that the nonnormality of DAPSA did not introduce meaningful bias or impact the conclusions.

Another point to consider is the use of external constructs primarily oriented towards axSpA rather than those specifically tailored for pSpA or PsA. This was due to data availability in the ASAS-PerSpA study, where only these instruments were collected. However, given the known overlap between these diseases [27] and the absence of alternative instruments in the study, applying the same constructs was a necessary approach.

To summarise, the present construct validity analysis showed that all disease activity measurement instruments assessing peripheral arthritis have a good performance, reflected in the correlations of strength with external constructs. Furthermore, when discriminating between known groups, all of them have a good performance, with composite scores with joint counts, particularly DAS28 and DAPSA, standing out as having the best discriminatory capacity. Future analyses comparing psychometric properties across composite scores, mainly discrimination in clinical trials, should be performed to identify the most adequate and best-performing measurement instrument to assess peripheral arthritis in SpA (including axSpA and pSpA).

## Competing interests

DC declares no conflict of interest. CL-M received consultant fees/speaker from UCB Novartis Janssen Lilly MSD AbbVie. DvH received consultant fees from AbbVie, Argenx, BMS, Galapagos, Glaxo-Smith-Kline, Janssen, Lilly, Novartis, Pfizer, Takeda, and UCB Pharma. RL received consultant fees from AbbVie, BMS, Galapagos, Eli Lilly, Novartis, Jansen, Pfizer, and UCB. MD received grants or consultant fees from UCB, Novartis, Eli Lilly, Pfizer, and AbbVie. JS received consulting fees or honoraria from UCB, AbbVie, MSD, Novartis, and UCB. AM received grants from Biogen, Pfizer, and UCB and honoraria from AbbVie, UCB, Viatris, Amgen, BMS, Biogen, Galapagos, Janssen, Lilly, and Novartis. SR received research grants from AbbVie, Galapagos, MSD, Novartis, Pfizer, and UCB and honoraria or consultancy/speaker fees from AbbVie, Eli Lilly, Galapagos, Janssen, MSD, Novartis, Pfizer, UCB, and Sanofi.

## CRediT authorship contribution statement

**Dafne Capelusnik:** Writing – original draft, Formal analysis, Data curation, Conceptualization. **Clementina Lopez-Medina:** Writing – original draft, Visualization, Data curation, Conceptualization. **Désirée van der Heijde:** Writing – original draft, Visualization, Supervision, Conceptualization. **Robert Landewé:** Writing – original draft, Visualization, Supervision, Conceptualization. **Maxime Dougados:** Writing – original draft, Visualization, Conceptualization. **Joachim Sieper:** Writing – original draft, Supervision, Conceptualization. **Anna Molto:** Writing – original draft, Visualization, Supervision, Conceptualization. **Sofia Ramiro:** Writing – original draft, Visualization, Supervision, Conceptualization.

## Acknowledgements

We would like to thank all the collaborators who participated in the study: José Maldonado-Cocco (Buenos Aires University School of Medicine, Buenos Aires, Argentina), Hernán Maldonado Ficco (Hospital San Antonio de Padua, Rio Cuarto, Argentina), Rodolfo Pérez Alamino (Hospital Dr Nicolás Avellaneda, Tucumán, Argentina), Emilio Buschiazzo (Hospital Señor del Milagro, Salta, Argentina), Romina Calvo (Hospital Provincial Dr José M Cullen, Santa Fé, Aregntina), Vanesa Duarte (Clínica Monte Grande, Buenos Aires, Argentina), Maria Victoria Martire (Instituto Médico Platense, La Plata, Argentina), Diego Baenas (Hospital Privado de Córdoba, Córdoba, Argentina), Dora Pereira (Hospital Ricardo Gutiérrez, La Plata, Argentina), Adrian Salas (Consultorio Reumatológico, La Plata, Argentina), Juan Manuel Bande (Hospital General de Agudos Dr E Tornú, Buenos Aires, Argentina), Alberto Berman (Centro Médico Privado de Tucumán, Tucumán, Argentina), Walter P Maksymowych (University of Alberta, Canada), Stephanie Belton (University of Alberta, Alberta, Canada), Sebastián Ibáñez (Facultad de Medicina Clínica Alemana−Universdidad del Desarrollo, Santiago de Chile, Chile), María Paz Poblete (Facultad de Medicina Clínica Alemana−Universidad del Desarrollo, Santiago de Chile, Chile), Francisca Valenzuela (Facultad de Medicina Clínica Alemana −Universidad del Desarrollo, Santiago de Chile, Chile), Wilson Bautista-Molano (University Hospital Fundación Santa Fé de Bogotá, Bogotá, Colombia), Jieruo Gu (Third Affiliated Hospital of Sun Yat-Sen University, Guangzhou, China), Min Xiao (Third Affiliated Hospital of Sun Yat-Sen University, Guangzhou, China), CS Lau (Hong-Kong University, China), Ho Yin Chung (Hong-Kong University, China), Bassel Elzorkany (Cairo University, Cairo, Egypt), Sherif Gamal (Cairo University, Cairo, Egypt), Catherine Lebourlout (Cochin Hospital, Paris, France), Daniel Wendling (CHU Besançon, Besançon, France), Clément Prati (CHU Besançon, Besançon, France), Frank Verhoeven (CHU Besançon, Besançon, France), Martin Soubrier (CHU Clermont-Ferrand, Clermont-Ferrand, France), Carine Savel (CHU Clermont-Ferrand, Clermont-Ferrand, France), Trigui Alia (CHU Clermont-Ferrand, Clermont-Ferrand, France), Fan Angélique (CHU Clermont-Ferrand, Clermont-Ferrand, France), Pascal Claudepierre (Henri Mondor Hospital, Créteil, France), Valerie Farrenq (Henri Mondor Hospital, Créteil, France), Kamelia Faramarz (Henri Mondor Hospital, Créteil, France), Uta Kiltz (Rheumazentrum Ruhrgebiet, Herne, Germany), Isabella Sieber (Rheumazentrum Ruhrgebiet, Herne, Germany), Dories Morzeck (Rheumazentrum Ruhrgebiet, Herne, Germany), Fabian Proft (Charité University, Berlin, Germany), Pál Geher (Semmelweis University, Budapest, Hungary), Edit Toth (Flór Ferenc Hospital, Kistarcsa, Hungary), Katalin Nagy (Markhot Ferenc Hospital, Eger, Hungary), Attila Kovacs (MÁV Hospital, Szolnok, Hungary), Meghna Gavali (Nizam's Institute of Medical Sciences, Hyderabad, India), Liza Rajasekhar (Nizam's Institute of Medical Sciences, Hyderabad, India), Sapan Pandya (Smt NHL Medical College and Sardar Vallabhbhai Patel Hospital and Vedanta Institute of Medical Sciences, Ahmedabad, India), Bhowmik Meghnathi (Sri Sai Siri Hospital and Prathima Institue of Medical Sciences, Karimnagar, India), Carlomaurizio Montecucco (Fondazione IRCCS Policlinico San Matteo, Pavia, Italia), Sara Monti (Fondazione IRCCS Policlinico San Matteo, Pavia, Italia), Alessandro Biglia (Fondazione IRCCS Policlinico San Matteo, Pavia, Italia), Mitsumasa Kishimoto (Kyorin University School of Medicine, Tokyo, Japan), Akihiko Asahina (The Jikei University School of Medicine, Japan), Masato Okada (St Luke`s International University and Hospital, Japan), Tadashi Okano (Osaka City University, Japan), Yuko Kaneko (Keio University School of Medicine, Japan), Hideto Kameda (Toho University, Japan), Yoshinori Taniguchi (Kochi University, Japan), Naoto Tamura (Juntendo University School of Medicine, Japan), Shigeyoshi Tsuji (National Hospital Organization Osaka Minami Medical Center, Japan), Hiroaki Dobashi (Kagawa University Faculty of Medicine, Japan), Yoichiro Haji (Daido Hospital, Japan), Akimichi Morita (Nagoya City University, Japan), Nelly Ziade (Saint-Joseph University, Beirut, Lebanon), Nelly Salloum (Saint-Joseph University, Beirut, Lebanon), Rubén Burgos-Vargas (Hospital General de México Eduardo Liceaga, Mexico City, Mexico), Graciela Meza (CLIDITER), Julio Casasola-Vargas (Hospital General de Mexico, Mexico), César Pacheco-Tena (Hospital General Dr Salvador Zubirán, Chihuahua, Mexico), Greta Reyes-Cordero (Hospital General Dr Salvador Zubirán, Chihuahua, Mexico), César Ramos-Remus (Unidad de Investigación de Enfermedades Crónico Degenerativas, Jalisco, Mexico), J Dionisio Castillo (Unidad de Investigación de Enfermedades Crónico Degenerativas, Jalisco, Mexico), Laura González-López (Universidad de Guadalajara, Jalisco, Mexico), Iván Gámez-Nava (Unidad de Investigación Biomédica 02, Hospital de Especialidades, Centro Médico Nacional de Occidente, IMSS Guadalajara, Jalisco, Mexico), Najia Hajjaj-Hassouni (International University of Rabat [UIR], Rabat, Morocco), Fadoua Allali (University Mohammed V, CHU Ibn Sina, Rabat, Morocco), Hanan Rkain (University Mohammed V, CHU Ibn Sina, Rabat, Morocco), Lahcen Achemlal (University Mohammed V, CHU Ibn Sina, Rabat, Morocco), Taoufik Harzy (University Sidi Mohammed Benabdellah, CHU Hassan II, Fès, Morocco), Fernando M Pimentel-Santos (Universidade NOVA de Lisboa, Lisboa, Portugal), Santiago Rodrigues-Manica (Universidade NOVA de Lisboa, Portugal), Agna Neto (Universidade NOVA de Lisboa, Portugal), Jose Marona (Universidade NOVA de Lisboa, Portugal), Mª Joao Gonçalves (Universidade NOVA de Lisboa, Portugal), Ana Filipa Mourao (Universidade NOVA de Lisboa, Portugal), Rita Pinheiro Torres (Universidade NOVA de Lisboa, Portugal), Ruxandra Schiotis (Iuliu Hatieganu University of Medicine, Cluj-Napoca, Romania), Simona Rednic (Iuliu Hatieganu University of Medicine, Cluj-Napoca, Romania), Siao-Pin Simon (Iuliu Hatieganu University of Medicine, Cluj-Napoca, Romania), Laura Muntean (Iuliu Hatieganu University of Medicine, Cluj-Napoca, Romania), Ileana Filipescu (Iuliu Hatieganu University of Medicine, Cluj-Napoca, Romania), Maria Tamas (Iuliu Hatieganu University of Medicine, Cluj-Napoca, Romania), Laura Damian (Iuliu Hatieganu University of Medicine, Cluj-Napoca, Romania), Ioana Felea (Iuliu Hatieganu University of Medicine, Cluj-Napoca, Romania), Dana Fodor (Second Medical Clinic, Emergency Conty Hospital, Cluj-Napoca, Romania), Tae-Jong Kim (Chonnam National University Medical School and Hospital,

South Korea), Hyun-Yi Kook (Chonnam National University Medical School and Hospital, South Korea), Hyun-Ju Jung (Chonnam National University Medical School and Hospital, South Korea), Tae-Hwan Kim (Hanyang University Hospital for Rheumatic Diseases, South Korea), Victoria Navarro-Compan (University Hospital La Paz, Madrid, Spain), Mireia Moreno (Hospital Parc Taulí, Barcelona, Spain), Eduardo Collantes-Estévez (Hospital Universitario Reina Sofía de Córdoba, Spain), M Carmen Castro-Villegas (Hospital Universitario Reina Sofía, Córdoba, Spain), Cristina Fernández-Carballido (Hospital Universitario San Juan de Alicante, Alicante, Spain), Elizabeth Fernández (Hospital Universtario La Paz, Madrid, Spain), Marta Arévalo (Hospital Parc Taulí, Barcelona, Spain), Shue-Fen Luo (Chang Gung Memorial Hospital-Linkou, Taoyuan, Taiwan), Yeong-Jian Jan Wu (Chang Gung Memorial Hospital at Kee-Lung, Taiwan), Tian-Tsai Cheng (Chang Gung Memorial Hospital at Kao-Hsiung, Taiwan), Cheng-Chung Wei (Chung Sun Medical University, Taiwan), Tuncay Duruöz (Marmara University School of Medicine, Istanbul, Turkey), Servet Akar (Izmir Katip Çelebi University School of Medicine, Turkey), Ilhan Sezer (Akdeniz University School of Medicine), Umut Kalyoncu (Hacettepe University School of Medicine, Turkey), Sebnem Ataman (Ankara University School of Medicine, Turkey), Meltem Alkan Melikoglu (Erzurum Atatürk University School of Medicine, Turkey), Sami Hizmetli (Sivas Cumhuriyet University School of Medine, Turkey), Ozgur Akgul (Manisa Celal Bayar University School of Medicine, Turkey), Nilay Sahin (Balikesir University School of Medicine, Turkey), Erhan Capkin (Karadeniz Teknik University School of Medicine, Turkey), Fatima Gluçin Ural (Ankara Yildirim Beyazit University School of Medicine, Turkey), Figen Yilmaz (Istanbul Sisli Etfal Training and Research Hospital), Ilknur Aktas (Istanbul Fatih Sultan Mehmet Training and Research Hospital, Turkey), Floris van Gaalen (Leiden University Medical Center, The Netherlands), Anne Boel (Leiden University Medical Center, The Netherlands), Mirian Starmans-Kool (Zuyderland Medical Center, The Netherlands), Femke Hoekstra-Drost (Zuyderland Medical Center, The Netherlands), Maha Abdelkadir (Maasstad Hospital in Rotterdam, The Netherlands), Angelique Weel (Maasstad Hospital, Rotterdam, The Netherlands), Pedro M Machado (University College of London, London, UK), Marina Magrey (Cases Western Reserve University School of Medicine, Cleveland, Ohio, USA), and Darerian Schueller (Cases Western Reserve University School of Medicine, Cleveland, Ohio, USA).

## Contributors

DC, CL-M, SR, AM, DvH, RL, MD, and JS designed the study. DC and CL-M collected and/or prepared the data. DC analysed the data. DC, CL-M, SR, AM, DvH, RL, MD, and JS critically interpreted the results. DC, CL-M, SR, and AM were involved in drafting the manuscript. All authors revised the manuscript critically for important intellectual content and approved the final manuscript.

## Funding

No funding was provided for the current analysis. The ASAS-perSpA study was funded by the ASAS with an unrestricted grant from AbbVie, Pfizer, Lilly, Novartis, UCB, Janssen and Merck. The funders did not have any role in the design or conduct of the study; collection, manegement, analysis or interpretation of the data; preparation, review or approval of the manuscript; or decision to submit the manuscript for publication.

## Patient consent for publication

Not required.

## Ethics approval

The ethics committees from all participating hospitals have approved the study.

## Provenance and peer review

Not commissioned; externally peer reviewed.

## Data availability statement

No additional data are available.

## Supplementary materials

Supplementary material associated with this article can be found in the online version at doi:10.1016/j.ard.2025.02.011.

## Orcid

Dafne Capelusnik: http://orcid.org/0000-0001-9336-0416
Clementina Lopez-Medina: http://orcid.org/0000-0002-2309-5837
Désirée van der Heijde: http://orcid.org/0000-0002-5781-158X
Robert Landewé: http://orcid.org/0000-0002-0577-6620
Maxime Dougados: http://orcid.org/0000-0003-3009-6229
Joachim Sieper: http://orcid.org/0000-0003-0285-9890
Anna Molto: http://orcid.org/0000-0003-2246-1986
Sofia Ramiro: http://orcid.org/0000-0002-8899-9087

## REFERENCES

[1] Rudwaleit M, van der Heijde D, Landewé R, Akkoc N, Brandt J, Chou CT, et al. The Assessment of SpondyloArthritis International Society classification criteria for peripheral spondyloarthritis and for spondyloarthritis in general. Ann Rheum Dis 2011;70(1):25–31.
[2] Molto A, Sieper J. Peripheral spondyloarthritis: concept, diagnosis and treatment. Best Pract Res Clin Rheumatol 2018;32(3):357–68.
[3] Navarro-Compán V, Boel A, Boonen A, Mease PJ, Dougados M, Kiltz U, et al. Instrument selection for the ASAS core outcome set for axial spondyloarthritis. Ann Rheum Dis 2023;82(6):763–72.
[4] Turina MC, Ramiro S, Baeten DL, Mease P, Paramarta JE, Song IH, et al. A psychometric analysis of outcome measures in peripheral spondyloarthritis. Ann Rheum Dis 2016;75(7):1302–7.
[5] Lukas C, Landewé R, Sieper J, Dougados M, Davis J, Braun J, et al. Development of an ASAS-endorsed disease activity score (ASDAS) in patients with ankylosing spondylitis. Ann Rheum Dis 2009;68(1):18–24.
[6] Garrett S, Jenkinson T, Kennedy LG, Whitelock H, Gaisford P, Calin A. A new approach to defining disease status in ankylosing spondylitis: the Bath Ankylosing Spondylitis Disease Activity Index. J Rheumatol 1994;21(12):2286–91.
[7] Beckers E, Been M, Webers C, Boonen A, Ten Klooster PM, Vonkeman HE, et al. Performance of 3 composite measures for disease activity in peripheral spondyloarthritis. J Rheumatol 2022;49(3):256–64.
[8] Schoels M, Aletaha D, Funovits J, Kavanaugh A, Baker D, Smolen JS. Application of the DAREA/DAPSA score for assessment of disease activity in psoriatic arthritis. Ann Rheum Dis 2010;69(8):1441–7.
[9] Tillett W, FitzGerald O, Coates LC, Packham J, Jadon DR, Massarotti M, et al. Composite measures for clinical trials in psoriatic arthritis: testing pain and fatigue modifications in a UK multicenter study. J Rheumatol 2021;52(3) jrheum.201674.
[10] López-Medina C, Molto A, Sieper J, Duruöz T, Kiltz U, Elzorkany B, et al. Prevalence and distribution of peripheral musculoskeletal manifestations in

spondyloarthritis including psoriatic arthritis: results of the worldwide, cross-sectional ASAS-PerSpA study. RMD Open 2021;7(1):e001450.
[11] van der Heijde D, Molto A, Ramiro S, Braun J, Dougados M, van Gaalen FA, et al. Goodbye to the term 'ankylosing spondylitis', hello 'axial spondyloarthritis': time to embrace the ASAS-defined nomenclature. Ann Rheum Dis 2024;83(5):547–9.
[12] Fuchs HA, Brooks RH, Callahan LF, Pincus T. A simplified twenty-eight-joint quantitative articular index in rheumatoid arthritis. Arthritis Rheum 1989;32(5):531–7.
[13] van der Heijde DM, van't Hof MA, van Riel PL, Theunisse LA, Lubberts EW, van Leeuwen MA, et al. Judging disease activity in clinical practice in rheumatoid arthritis: first step in the development of a disease activity score. Ann Rheum Dis 1990;49(11):916–20.
[14] Calin A, Garrett S, Whitelock H, Kennedy LG, O'Hea J, Mallorie P, et al. A new approach to defining functional ability in ankylosing spondylitis: the development of the Bath Ankylosing Spondylitis Functional Index. J Rheumatol 1994;21(12):2281–5.
[15] EuroQol Group. EuroQol—a new facility for the measurement of health-related quality of life. Health Policy 1990;16(3):199–208.
[16] Kiltz U, van der Heijde D, Boonen A, Cieza A, Stucki G, Khan MA, et al. Development of a health index in patients with ankylosing spondylitis (ASAS HI): final result of a global initiative based on the ICF guided by ASAS. Ann Rheum Dis 2015;74(5):830–5.
[17] Maxwell LJ, Beaton DE, Boers M, D'Agostino MA, Conaghan PG, Grosskleg S, et al. The evolution of instrument selection for inclusion in core outcome sets at OMERACT: filter 2.2. Semin Arthritis Rheum 2021;51(6):1320–30.
[18] Mukaka MM. Statistics corner: a guide to appropriate use of correlation coefficient in medical research. Malawi Med J 2012;24(3):69–71.
[19] Cohen J. Statistical power analysis for the behavioral sciences. Lawrence Erlbaum Associates; 1988.
[20] Murad MH, Wang Z, Chu H, Lin L. When continuous outcomes are measured using different scales: guide for meta-analysis and interpretation. BMJ 2019;364:k4817.
[21] Smolen JS, Aletaha D. Scores for all seasons: SDAI and CDAI. Clin Exp Rheumatol 2014;32(5 Suppl 85) S-75-9.
[22] Landewé RBM, van der Heijde D. Use of multidimensional composite scores in rheumatology: parsimony versus subtlety. Ann Rheum Dis 2021;80(3):280–5.
[23] Navarro-Compán V, Gherghe AM, Smolen JS, Aletaha D, Landewé R, van der Heijde D. Relationship between disease activity indices and their individual components and radiographic progression in RA: a systematic literature review. Rheumatology (Oxford) 2015;54(6):994–1007.
[24] Beaton D, Maxwell L, Grosskleg S, Shea B, Tugwell P. The OMERACT handbook version 2.1 [Internet]. 2021. Available from: https://omeract.org/handbook/ Accessed January, 2019.
[25] Duarte-García A, Leung YY, Coates LC, Beaton D, Christensen R, Craig ET, et al. Endorsement of the 66/68 joint count for the measurement of musculoskeletal disease activity: OMERACT 2018 psoriatic arthritis workshop report. J Rheumatol 2019;46(8):996–1005.
[26] Capelusnik D, Ramiro S, Schneeberger EE, Citera G. Peripheral arthritis and higher disease activity lead to more functional impairment in axial spondyloarthritis: longitudinal analysis from ESPAXIA. Semin Arthritis Rheum 2021;51(3):553–8.
[27] Feld J, Chandran V, Haroon N, Inman R, Gladman D. Axial disease in psoriatic arthritis and ankylosing spondylitis: a critical comparison. Nat Rev Rheumatol 2018;14(6):363–71.

Ann Rheum Dis 84 (2025) 1335–1341

Contents lists available at ScienceDirect

Annals of the Rheumatic Diseases

journal homepage: https://www.sciencedirect.com/journal/annals-of-the-rheumatic-diseases

Axial spondyloarthritis

# Radiographic structural damage in axial spondyloarthritis: is there a preferred way to quantify progression over time? Comparison of blinded versus unblinded mSASSS scoring

Xenofon Baraliakos[1], Mikhail Protopopov[2,*], Valeria Rios Rodriguez[2], Murat Torgutalp[2], Ani Dilbaryan[3], Hildrun Haibel[2], Joachim Sieper[2], Juergen Braun[4], Martin Rudwaleit[5], Denis Poddubnyy[2,6]

[a] *Rheumazentrum Ruhrgebiet Herne, Ruhr-University Bochum, Herne, Germany*
[b] *Charité-Universitätsmedizin Berlin, Department of Gastroenterology, Infectiology and Rheumatology (including Nutrition Medicine), Berlin, Germany*
[3] *Medsi Clinics, Moscow, Russia*
[4] *Rheumatologisches Versorgungszentrum Steglitz, Berlin, Germany*
[5] *Klinikum Bielefeld Rosenhöhe, University clinic for internal medicine and rheumatology, Bielefeld, Germany*
[6] *University of Toronto and University Health Network, Division of Rheumatology, Toronto, ON, Canada*

ARTICLE INFO

ABSTRACT

*Objectives:* Structural progression in spine in axial spondyloarthritis (axSpA) is assessed by conventional radiographs and quantified by the modified Stoke Ankylosing Spondylitis Spine Score (mSASSS). Blinded mSASSS scoring might be associated with 'background noise,' and for assessing a slow-progressing disease such as axSpA, high sensitivity to change without loss of specificity is crucial. The aim of this study was to compare the sensitivity to change of blinded vs unblinded application of mSASSS for identification of a preferred way of assessing radiographic damage in axSpA over time.
*Methods:* Cervical and lumbar radiographcs of axSpA patients participating in a national inception cohort (GErman SPondyloarthritis Inception Cohort) obtained at baseline and after 2 years were scored using the mSASSS by 5 experienced readers, 2 blinded and 3 unblinded to chronology. Mean scores were used for calculations.
*Results:* Overall, 210 patients (37.3 years, 51% male, 79% human leukocyte antigen B27 positive) were included. The mean baseline mSASSS was 4.2 ± 8.3 vs 3.4±7.9 and mean mSASSS progression was 0.7 ± 2.3 vs 1.0 ± 1.9 for the blinded vs unblinded scoring method, respectively ($P = .005$). Progression of ≥2 mSASSS units was found in 30 (14.3%) vs 37 (17.6%) patients in blinded and unblinded scoring. In the shift analysis, mSASSS worsening was found in 35 (0.8%) vs 109 (2.2%) and improvement in 4 (0.1%) vs 2 (0.04%) of a total of 4.373 and 4914 vertebral edges in the blinded vs unblinded group, respectively. The majority of progression was found for the development of syndesmophytes in both groups.
*Conclusions:* More mSASSS progression was detected using unblinded vs blinded scoring. Scoring spinal radiographs with known chronological order seems to be more sensitive to changes.

*Correspondence to Dr. Mikhail Protopopov.
*E-mail address:* Mikhail.Protopopov@charite.de (M. Protopopov).
Xenofon Baraliakos and Mikhail Protopopov contributed equally.
**Handling editor** Josef S. Smolen.

https://doi.org/10.1016/j.ard.2025.03.017

0003-4967/© 2025 The Authors. Published by Elsevier B.V. on behalf of European Alliance of Associations for Rheumatology (EULAR). This is an open access article under the CC BY license (http://creativecommons.org/licenses/by/4.0/)

**WHAT IS ALREADY KNOWN ON THIS TOPIC**

- Radiographic progression in axial spondyloarthritis (axSpA) is commonly assessed using the modified Stoke Ankylosing Spondylitis Spine Score (mSASSS), typically scored in a blinded manner to avoid bias, despite concerns about low sensitivity to change in slowly progressing diseases. In rheumatoid arthritis, it has been demonstrated that scoring with a known chronological order might be preferred over the blinded method.

**WHAT THIS STUDY ADDS**

- This study shows that unblinded mSASSS scoring (with known chronological order of radiographs) detects more structural progression than blinded scoring, with better inter-reader agreement and minimal loss of specificity. How this study might affect research, practice or policy. Adopting unblinded radiographic reading in axSpA clinical trials and cohort studies could improve sensitivity to progression, interreader reliability, reduce negative noice and enhance trial efficiency by reducing sample size requirements.

## INTRODUCTION

Axial spondyloarthritis (axSpA) is a chronic inflammatory disease that involves predominantly the axial skeleton, such as the sacroiliac joints and the spine. New bone formation is one of the key events in the pathophysiology of axSpA [1]. Together with disease activity, irreversible structural damage in the spine, ie, presence of syndesmophytes and ankylosis, is associated with worse spinal mobility in patients with axSpA [2–4]. A significant proportion of patients with axSpA tends to exponentially develop more radiographic spinal damage over time [5–7], with currently available treatment modalities able to slow this process down [6,8,9].

Structural damage and radiographic progression in the spine are usually assessed by conventional radiographs, with the modified Stokes Ankylosing Spondylitis Scoring System (mSASSS) being the most commonly reported outcome for quantification of structural damage in the spine of patients with axSpA [10]. This method includes the assessment of the anterior portion of the cervical and lumbar spine using a nominal scoring system (0 = no abnormality; 1 = erosion, sclerosis or squaring; 2 = syndesmophyte; and 3 = bridging syndesmophyte). The mSASSS is also used for the quantification of progression of radiographic damage, quantified as a change in the mSASSS score. However, the reliability of such radiographic assessment of spinal progression is limited [11]. Nevertheless, radiographic progression is widely considered a key treatment outcome reflecting structural damage progression in clinical trials [12], where it is commonly scored in a 'blinded' manner, with readers being blinded to the time points of assessments when scoring sets of radiographs of the same patient. From an epidemiological point of view, this method seems to be less susceptible to bias and avoids overestimation of progression. However, this approach has been accompanied by questions about the influence of patients showing improvement in the mSASSS, reflecting the chance of a possible disappearance of syndesmophytes over time, which is something that is not naturally expected.

It has previously been reported that reading of radiographs in rheumatoid arthritis with a known chronological order might be preferred over the blinded method due to the better signal-to-noise ratio, decreased variability around the estimation of the progression rate and, therefore, smaller sample sizes required to detect small differences [13,14]. Scoring of mSASSS with a known chronology was previously explored by Wanders et al [10]. However, the number of patients in that data set was limited, and no comparison between blinded and unblinded reading was performed.

The present study compared the performance of mSASSS in assessing radiographic damage in the spine with a known chronologic order of radiographs against the blinded assessment, with a focus on the sensitivity to change, for identification of a preferred way of assessing radiographic damage in axSpA over time.

## METHODS

### *Cohort description and selection of patients*

A detailed description of the GErman SPondyloarthritis Inception Cohort (GESPIC) has been reported previously [15–17]. Briefly, this prospective cohort study included patients with recently diagnosed axSpA (radiographic [r-] axSpA with a symptom duration of ≤10 years or nonradiographic [nr-] axSpA with a symptom duration of ≤5 years). Clinical assessments were performed at baseline and every 6 months thereafter until year 2. Lateral and anteroposterior radiographs of the cervical and lumbar spine were performed at baseline and year 2. Overall, 210 patients (115 with r-axSpA and 95 with nr-axSpA) were included in the present analysis based on the availability of spinal radiographs at baseline and after 2 years of follow-up.

### *Radiographic assessments*

Lateral radiographs of the cervical and lumbar spine were obtained locally at baseline and after 2 years of follow-up. Images were digitised (if not available in digital form), anonymised and subsequently scored by 5 different experienced readers, of whom 2 were blinded to the timepoint of radiography (baseline or follow-up) and 3 were aware of the timepoint the imaging was performed. All readers were blinded to all clinical data. The images were assessed using the mSASSS, summarising the scores for the lumbar and cervical spine (range 0-72) [18]. The final mSASSS score was calculated as a mean of 2 (blinded) or 3 (unblinded exercise) readers.

The following definitions of progression were implemented:

- mean radiographic progression, calculated as the difference in mean mSASSS score between baseline and year 2;
- number of patients with progression of mean mSASSS score by ≥2 mSASSS units at year 2 compared with baseline;
- change of the mean mSASSS score between baseline and year 2, considering only 'definite' radiographic findings (only scores of 2 for syndesmophytes or 3 for ankylosis; corners with a score of 1 were recoded to 0);
- shift analysis, performed on a vertebral corner level, exploring whether the mSASSS score between baseline and year 2 had increased (upwards shift) or decreased (downwards shift);
- progression group, based on a previously established data-based definition [7], in which fast progression was calculated as a change >5 mSASSS units or >2 new syndesmophytes; moderate progression as a change of 2.0 to 5.0 mSASSS units or 2 new syndesmophytes; and slow progression as a change of <2 mSASSS units or ≤1 new syndesmophyte within 2 years [7].

### *Statistical analysis*

Descriptive statistics, cumulative probability plots and shift analyses (agreement of 2/2 readers in the blinded group and at least 2/3 readers in the unblinded group on the score change at the level of single vertebral edges) were performed by each reader group. Results on the status and the change of the mSASSS scores over 2 years were calculated by the blinded and unblinded reader groups separately. The change of the mSASSS scores over time as well as the difference in mSASSS progression was compared between the blinded and unblinded scoring groups using the Wilcoxon signed-rank test. The difference in the number of progressors was measured using the chi-square test. The agreement between the readers was measured using the intraclass correlation coefficient (ICC).

## RESULTS

A total of 210 patients (mean age 37.3 years, 51% male, 79% human leukocyte antigen B27 positive) with axSpA (115 r-axSpA and 95 nr-axSpA at baseline) were included in the analysis. The main baseline disease characteristics of the study sample are presented in Table 1.

The mean mSASSS status scores were assessed as 4.2 ± 8.3 and 3.4 ± 7.9 units at baseline and 5.0 ± 9.6 and 4.4 ± 9.1 at the follow-up by the blinded and unblinded readers, respectively ($P < .001$ for both blinded and unblinded readers). The mSASSS score was higher in the r-axSpA group (5.9 ± 10.3 vs 4.9 ± 9.9 at baseline, 6.8 ± 11.7 vs 6.3 ± 11.2 at the follow-up for the blinded vs the unblinded readers) than in nr-axSpA patients (2.3 ± 4.2 vs 1.6 ± 3.8 at baseline, 2.8 ± 5.3 vs 2.2±4.7 at the follow-up for the blinded vs unblinded readers).

The mean radiographic progression was assessed as 0.7 ± 2.3 vs 1.0 ± 1.9 mSASSS units for the blinded vs the unblinded group, respectively ($P = .005$; r-axSpA: 1.0 ± 2.8 vs 1.4 ± 2.3, $P = .006$; nr-axSpA: 0.5 ± 1.6 vs 0.6 ± 1.1, $P = .34$). The change in the mean mSASSS score at the patient level for both reading approaches is presented in the Figure.

Table 1
**Baseline disease characteristics of 210 patients with axial spondyloarthritis**

| Baseline parameters | nr-axSpA (n = 95) | r-axSpA (n = 115) | All patients (n = 210) |
|---|---|---|---|
| Age, y | 38.7 ± 9.9 | 36.1 ± 11.0 | 37.3 ± 10.6 |
| Male sex, n (%) | 32 (33.7) | 75 (65.2) | 107 (51.0) |
| HLA-B27 positive, n (%) | 69 (72.6) | 97 (84.3) | 166 (79.0) |
| Duration of symptoms, y | 3.1 ± 2.2 | 5.0 ± 2.8 | 4.2 ± 2.7 |
| BASDAI, points NRS (0-10) | 4.2 ± 2.0 | 3.8 ± 2.2 | 4.0 ± 2.1 |
| BASFI, points NRS (0-10) | 2.8 ± 2.2 | 3.0 ± 2.4 | 2.9 ± 2.3 |
| BASMI, points (0-10) | 1.5 ± 1.5 | 2.0 ± 1.7 | 1.8 ± 1.6 |
| CRP, mg/L | 6.5 ± 12.8 | 12.4 ± 16.6 | 9.7 ± 15.2 |
| Current smoking, n (%) | 24 (25.3) | 39 (33.9) | 63 (30.0) |
| NSAID intake, n (%) | 64 (67.4) | 76 (66.1) | 140 (66.7) |
| Systemic steroids intake, n (%) | 6 (6.3) | 6 (5.2) | 12 (5.7) |
| DMARD intake, n (%) | 26 (27.4) | 35 (30.4) | 61 (29.0) |
| TNF$\alpha$ inhibitor intake, n (%) | 1 (1.1) | 4 (3.5) | 5 (2.4) |

BASDAI, Bath Ankylosing Spondylitis Disease Activity Index; BASFI, Bath Ankylosing Spondylitis Functional Index; BASMI, Bath Ankylosing Spondylitis Metrology Index; CRP, C-reactive protein; DMARD, disease-modifying antirheumatic drug; HLA, human leukocyte antigen; nr-axSpA, nonradiographic axial spondyloarthritis; NRS, numeric rating scale; NSAID, nonsteroidal anti-inflammatory drug; r-axSpA, radiographic axial spondyloarthritis; TNF$\alpha$, tumour necrosis factor alpha.
Continuous variables are presented as mean ± SD.

At the patient level, progression of ≥2 mSASSS units was observed in 30 (14.3%) vs 37 (17.6%) patients as assessed by the blinded vs the unblinded group (r-axSpA: 23 [20.0%] vs 30 [26.1%] patients, nr-axSpA: 7 [7.4%] vs 7 [7.4%]), while agreement between both groups on the progression of ≥2 mSASSS points was seen in 179 (85.2%) patients (18 [8.9%] patients for progression and 161 [76.7%] for no progression). Negative progression (reduction of mean mSASSS score on year 2 compared to baseline) was observed in 46 patients (21.9%) in the blinded reading as compared with 2 (1.0%) patients in the unblinded reading.

In the shift analysis, mSASSS worsening was found in 35 (0.8%) and mSASSS improvement in only 4 (0.1%) of the total of 4373 vertebral edges analysed by the blinded group and in 109 (2.2%) and 2 (0.0%), respectively, of the total of 4914 vertebral edges analysed by the unblinded group (Table 2). The majority of progression (shifts) was found for the development of definite signs of progression (development of syndesmophytes or ankylosis) by both the blinded (25/35, 71.4%) and unblinded (61/109, 56.0%) groups, while fewer vertebral edges showing minor signs of progression (no syndesmophytes or ankylosis) were detected by the blinded (10/35, 28.6%) group than the unblinded (48/109, 44.0%). The change in the mSASSS score on the vertebral level is presented in Table 2.

In the progression speed analysis, 9 (4.3%, 6 r-axSpA, 3 nr-axSpA) patients were classified as fast progressors and 21 (10.0%, 17 r-axSpA, 4 nr-axSpA) as moderate progressors by blinded readers, and 10 (4.8%, 9 r-axSpA, 1 nr-axSpA) and 27 (12.9%, 21 r-axSpA, 6 nr-axSpA), respectively, by unblinded readers. The distribution of fast, moderate and slow progressors in a blinded and unblinded scoring approach is shown in Table 3.

There was excellent agreement within both groups regarding status scores (mSASSS) of spinal radiographic damage. For the blinded group, the ICC between both readers was 0.96 (95% CI, 0.95-0.97) at baseline and 0.96 (95% CI, 0.95-0.97) at year 2. For the unblinded group, the ICC for all 3 readers was 0.97 (95% CI, 0.96-0.98) at baseline and 0.97 (95% CI, 0.97-0.98) at year 2. The agreement regarding the mSASSS score change was also very good for the unblinded group, with an ICC coefficient of 0.87 (95% CI, 0.84-0.90), and moderate for the blinded group, with an ICC coefficient of 0.60 (95% CI, 0.47-0.69).

## DISCUSSION

To our knowledge, our study is the first to compare mSASSS reading in a blinded and unblinded manner in patients with the entire spectrum of axSpA (both nr-axSpA and r-axSpA). Wanders et al [10] previously explored the performance of unblinded mSASSS reading. However, their data set was limited to 131 patients with r-axSpA only. All images were assessed by one reader, whereas a second reader scored only 20 patients; therefore, the ability to assess intraobserver reliability was limited. Most importantly, no comparison between blinded and unblinded reading was performed due to the peculiarities of the data set because the format of the radiographs was changed in some centres during the study. This made it possible for the observer to identify the time of the imaging, so all radiographs were scored with known chronology.

Measuring radiographic spinal progression in axSpA remains pivotal for multiple reasons. As radiographic damage is linked with functional limitations and might also indirectly reflect increased disease activity [19], recognising the radiographic progression is important in the clinical context for assessing

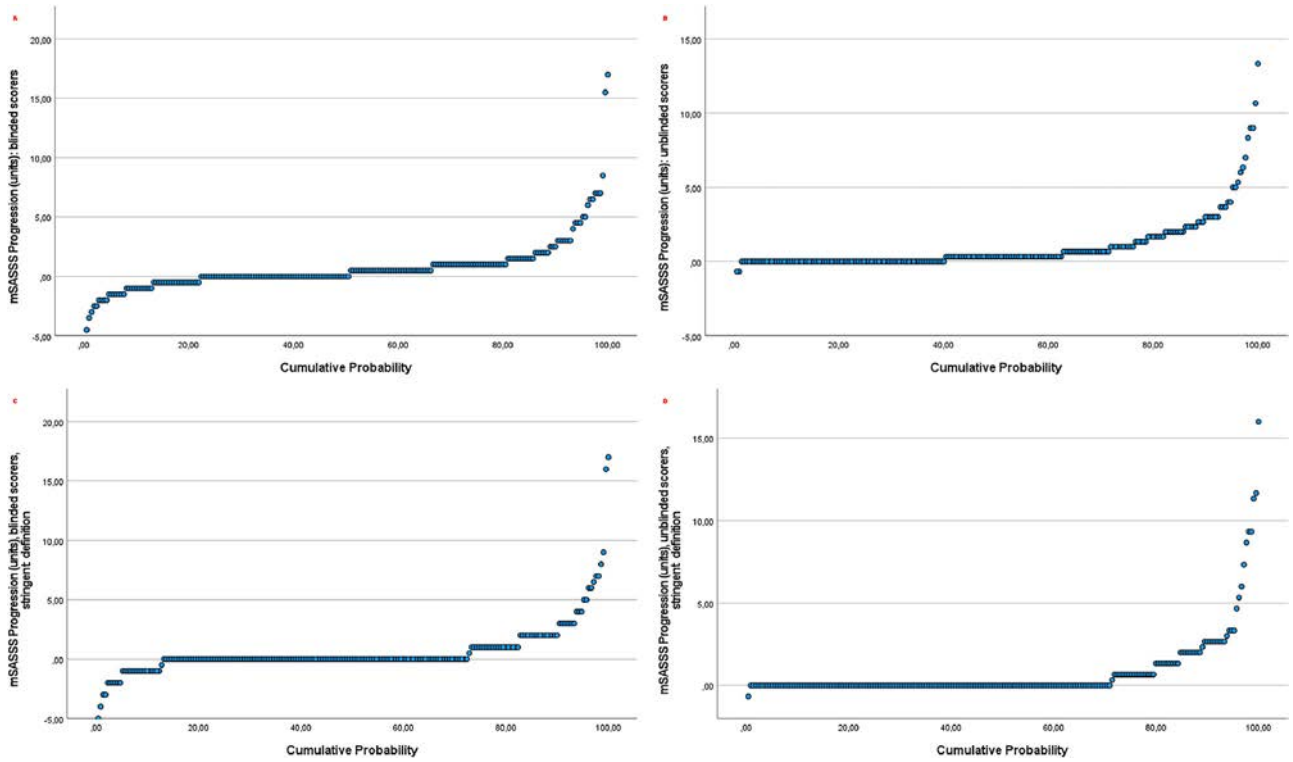



**Figure.** (A,B) Cumulative probability plots for mean mSASSS score change for all scores in blinded (A) and unblinded (B) scoring. (C,D) Cumulative probability plots for mean mSASSS score change considering only 'definite' scores in blinded (C) and unblinded (D) scoring. Definite scores were scores of 2 for syndesmophytes or 3 for ankylosis, and corners with a score of 1 were recoded as 0. mSASSS, modified Stoke Ankylosing Spondylitis Spine Score.

treatment efficacy and making treatment decisions. Reliable tracking of radiographic spinal progression in spondyloarthritis (SpA) patients also contributes valuable data to research efforts. It aids in understanding the natural history of the disease, identifying factors influencing progression, and developing new therapeutic approaches to slow or prevent structural damage, and is therefore included as a necessary component in the Assessment of SpondyloArthritis international Society–Outcomes Measures in Rheumatology Core Outcome Set for axSpA [12]. In this context, sensitive recognition of changes is vital because radiographic spinal progression is a slow process. Emerging data suggest that the radiographic spinal progression observed in SpA could potentially be attenuated through the administration of biologic therapies [6], as evidenced by recent trials revealing only marginal progression in individuals undergoing biologic treatments [20,21]. Hence, the significance of discerning and acknowledging minimal changes becomes pivotal to comprehensively assess the efficacy of these interventions. Having a method with better sensitivity to change is also important for designing clinical studies, as the availability of more sensitive methods might result in a lower number of patients necessary

Table 2
**Change in mSASSS score between baseline and year 2 at the vertebral corner level**

| Blinded reading | | | | | | |
|---|---|---|---|---|---|---|
| mSASSS scores | | 2-y follow-up | | | | Total |
| | | 0 | 1 | 2 | 3 | |
| Baseline | 0 | 4.166 | 10 | 8 | 9 | 4.193 |
| | 1 | 0 | 29 | 4 | 0 | 33 |
| | 2 | 3 | 1 | 48 | 4 | 56 |
| | 3 | 0 | 0 | 0 | 92 | 92 |
| Total | | 4.169 | 40 | 60 | 105 | 4.374 |

| Unblinded reading | | | | | | |
|---|---|---|---|---|---|---|
| mSASSS scores | | 2-y follow-up | | | | Total |
| | | 0 | 1 | 2 | 3 | |
| Baseline | 0 | 4.575 | 48 | 14 | 3 | 4.640 |
| | 1 | 1 | 75 | 16 | 8 | 100 |
| | 2 | 0 | 0 | 69 | 20 | 89 |
| | 3 | 0 | 1 | 0 | 84 | 85 |
| Total | | 4.576 | 124 | 99 | 115 | 4.914 |

mSASSS, modified Stoke Ankylosing Spondylitis Spine Score.

Table 3
**Fast, moderate and slow progressors in a blinded and unblinded scoring approach**

| Blinded reading | | | | |
|---|---|---|---|---|
| | | nr-axSpA | r-axSpA | Total |
| Progression category | Slow | 88 | 92 | 180 |
| | Moderate | 4 | 17 | 21 |
| | Fast | 3 | 6 | 9 |
| Total | | 95 | 115 | 210 |

| Unblinded reading | | | | |
|---|---|---|---|---|
| | | nr-axSpA | r-axSpA | Total |
| Progression category | Slow | 88 | 85 | 173 |
| | Moderate | 6 | 21 | 27 |
| | Fast | 1 | 9 | 10 |
| Total | | 95 | 115 | 210 |

nr-axSpA, nonradiographic axial spondyloarthritis; r-axSpA, radiographic axial spondyloarthritis.

for recruitment to demonstrate statistically and clinically significant differences in the radiographic progression. The current treatment paradigm in axSpA favours early diagnosis and early treatment of patients, including the early initiation of treatment with biologics in axSpA patients with persistently high disease activity, optimally before significant radiographic damage occurs [22]. It has previously been reported that the presence of baseline radiographic damage strongly predicts the development of further structural damage early in the disease [23]. As the initial mSASSS scores in such patients are typically low and the progression limited compared to those of patients in the advanced stage, the availability of a sensitive approach to measuring radiographic progression is important.

The idea behind this study was that reading images with a known chronology might be more sensitive to change and would theoretically result in higher sensitivity at the cost of lower specificity, but the increase in sensitivity might be due to expectation bias rather than a reduction in measurement error. At the same time, the findings from rheumatoid arthritis studies indicate that sequential assessment of hand radiographs in a known chronological order not only did not yield notable reductions in specificity but was favoured over blinded readings, making it a more reliable and preferred method for comprehensive evaluation [14]. Our results confirm that the same might be true for mSASSS scoring in axSpA. The cumulative probability plots (Fig) indicate that in the unblinded group, negative progression (which is probably associated with noise or measurement error) was almost fully cut off, resulting in higher mSASSS progression scores. However, the estimation of positive progression (mSASSS increase) was only marginally influenced compared to the blinded group. In fact, the mean mSASSS status scores at both baseline and follow-up were lower for the unblinded group than for the blinded group. The right halves of the cumulative probability plots were also very similar between the groups regardless of the definition. Scoring mSASSS with a known time sequence resulted in more progression being observed in r-axSpA patients, whereas no differences were seen in nr-axSpA patients. We attribute this disparity to the enhanced detection of genuine progression and the reduction of noise, as it is known that r-axSpA patients tend to progress more than nr-axSpA patients [24]. Advanced transition analyses (shift analysis as well as progression group analysis) have indicated more transitions and a higher number of patients categorised to the fast and moderate progression groups in the unblinded reading, reflecting either more confident detection of the radiographic progression with a known chronologic order or an added expectation bias. However, the majority of the shifts reflected definite signs of progression. Those definite changes, roughly corresponding with the 2-point threshold in the mSASSS scoring system, are important in the clinical context, as they indicate a clinically significant change in spinal damage, such as the formation of syndesmophytes or worsening of existing structural changes. To further reduce the possible expectation bias in unblinded scoring in clinical trials, we believe it will be essential to score the admixture of patients treated and not treated with the drug under investigation in a single data set, as the duration of the placebo-controlled trial over 2 years is very unlikely at this stage. In addition, the choice between blinded and unblinded scoring becomes even more relevant in observational cohorts with multiple imaging time points available. Based on our findings, we speculate that in such settings, noise reduction plays an even greater role, supporting the use of unblinded readings. However, this assumption requires further confirmation.

The agreement between the unblinded readers regarding the change of the mSASSS score was also significantly improved compared to that of the blinded readers, primarily due to the cutoff of the negative noise, although a higher number of readers was involved (therefore creating more potential room for variability).

Our study has some limitations. Firstly, no gold standard was available to verify the scores of both blinded and unblinded scoring because the mSASSS score itself is used as the gold standard. As a complementary imaging modality, spinal computed tomography could potentially serve as a reference for validating mSASSS-based radiographic assessments.. However, this examination would lead to significant (and probably unnecessary) radiation exposure, and such images were not available in our cohort. The second possible limitation is the quality of the conventional radiographs. GESPIC was established in 2000 [16] and much of the imaging performed at that time was available as hard films, which were digitised for the analysis. Since progression over the first 2 years was analysed, pictures were available for central reading only for a subset of patients included in the cohort. However, the quality of the films was good to excellent in the vast majority of cases. Previous analyses have also not detected any significant differences between the study subset and the entire cohort [15,17]. In addition, only 2% of the study population were receiving advanced therapies, such as biologics. This is a limitation for validation of these results in current common clinical practice or trials because a large proportion of patients receive this type of therapy. However, as advanced therapies are likely reducing the chance of radiographic progression, having a group of patients generally naïve to advanced treatments probably allowed more differences to be demonstrated, as these patients would presumably have higher progression rates than patients treated with advanced therapies. Furthermore, previous studies have suggested that in the first 2 years of advanced therapy, there is no substantial retardation of radiographic progression.

In summary, our results suggest that the assessment of spinal radiographs in chronological order in clinical trials of SpA seems more efficient due to the reduction of negative noise, better detection of clinically significant progression of structural changes, and better interreader reliability.

## Competing interests

XB declares that he has received grants from Novartis; consultant fees from AbbVie, Alphasigma, Amgen, BMS, Cesas, Celltrion, Galapagos, Janssen, Lilly, Moonlake, Novartis, Pfizer, Roche, Sandoz, Springer, Stada, Takeda, UCB, and Zuellig; speakers honoraria from AbbVie, Alphasigma, Amgen, BMS, Cesas, Celltrion, Galapagos, Janssen, Lilly, Moonlake, Novartis, Pfizer, Roche, Sandoz, Springer, Stada, Takeda, UCB, and Zuellig; received support for attending meetings and/or travel from AbbVie, Alphasigma, Amgen, BMS, Cesas, Celltrion, Galapagos, Janssen, Lilly, Moonlake, Novartis, Pfizer, Roche, Sandoz, Springer, Stada, Takeda, UCB, and Zuellig; participated in advisory boards sponsored by AbbVie, Alphasigma, Amgen, BMS, Cesas, Celltrion, Galapagos, Janssen, Lilly, Moonlake, Novartis, Pfizer, Roche, Sandoz, Springer, Stada, Takeda, UCB, and Zuellig; and is an Editorial Board member of *Annals of Rheumatic Diseases*, ASAS President, and EULAR President-Elect. MP declares that he has received consulting fees from Janssen and Novartis and support for attending meetings and/or travel from Novartis, AbbVie, Janssen and UCB. VRR declares that she has received grants from AbbVie, Eli Lilly, Jansen, UCB and Pfizer; consulting fees from AbbVie and Takeda; and support for attending meetings and/or travel from Novartis,

Pfizer and UCB. HH declares that she has received a grant from Sobi; consulting fees from AbbVie, Janssen, MSD, Novartis, Pfizer, Roche, and UCB; and support for attending meetings and/or travel from Novartis, AbbVie, Pfizer and UCB. JS declares that he has received speakers honoraria form AbbVie, Merck, Novartis and UCB. DP declares that he has received grants from AbbVie, Eli Lilly, MSD, Novartis and Pfizer; consulting fees from AbbVie, Biocad, Bristol Myers Squibb, Eli Lilly, Janssen, Moonlake, Novartis, Pfizer and UCB; speakers honoraria from AbbVie, Canon, DKSH, Eli Lilly, Janssen, MSD, Medscape, Novartis, Peervoice, Pfizer, and UCB; and is a member of the executive committee of ASAS and a member of steering committee of GRAPPA. The other authors (MT, AD, JB, MR) declare no competing interests.

## CRediT authorship contribution statement

**Xenofon Baraliakos:** Writing – review & editing, Writing – original draft, Supervision, Project administration, Methodology, Investigation, Formal analysis, Data curation, Conceptualization. **Mikhail Protopopov:** Writing – review & editing, Writing – original draft, Supervision, Project administration, Methodology, Investigation, Formal analysis, Data curation, Conceptualization. **Valeria Rios Rodriguez:** Writing – review & editing, Investigation, Data curation. **Murat Torgutalp:** Writing – review & editing, Investigation, Formal analysis, Data curation. **Ani Dilbaryan:** Writing – review & editing, Investigation, Formal analysis, Data curation. **Hildrun Haibel:** Writing – review & editing, Investigation, Formal analysis, Data curation. **Joachim Sieper:** Writing – review & editing, Supervision, Project administration, Methodology, Funding acquisition, Data curation, Conceptualization. **Juergen Braun:** Writing – review & editing, Supervision, Project administration, Funding acquisition, Formal analysis, Data curation, Conceptualization. **Martin Rudwaleit:** Writing – review & editing, Project administration, Funding acquisition, Data curation, Conceptualization. **Denis Poddubnyy:** Writing – review & editing, Writing – original draft, Supervision, Software, Resources, Project administration, Methodology, Investigation, Funding acquisition, Formal analysis, Data curation, Conceptualization.

## Acknowledgements

We thank Prof M Leirisalo-Repo, Finland, Prof D van der Heijde, The Netherlands, and Prof M Dougados, France, for scientific advice on the design of the cohort. We are grateful to Beate Buss and Petra Tietz for monitoring the cohort; Johanna Callhoff, Anja Weiss, and Martina Niewerth for the data management support; Joachim Listing for statistical advice; Janis Vahldiek and Georg Heine for the x-ray image handling and for the development of the image scoring interface; and to all patients who voluntarily participated in this cohort. We further thank the following rheumatologists for inclusion and follow-up of their patients: J Brandt, H Brandt, J Braun, G-R Burmester, H Deister, E Edelmann, J Emmerich, M Enderlein, E Feist, A Gauliard, E Gromnica-Ihle, F Heldmann, S Hermann, U von Hinüber, Ü Hübner, K Karberg, C Kedor, E Märker-Hermann, H Nüßlein, R Pelle-Lohfink, D Pick, G Reichmuth, E Riehers, M Rihl, R Schmidt, S Schnarr, U Schneider, I-H Song, I Spiller, U Syrbe, V Walz, S Wassenberg, H M Wisseler, H Zeidler, and S Zinke. We also thank Maryna Verba for her contribution to data management.

## Contributors

All authors made substantial contributions to the conception or design of the work or the acquisition, analysis, or interpretation of data for the work; drafting the work or revising it critically for important intellectual content; approved the final version to be published; and agree to be accountable for all aspects of the work in ensuring that questions related to the accuracy or integrity of any part of the work are appropriately investigated and resolved. MP and XB are both responsible for the overall content as the guarantors and accept full responsibility for the work, had access to the data, and controlled the decision to publish.

## Funding

GESPIC has been financially supported by the German Federal Ministry of Education and Research (Bundesministerium für Bildung und Forschung–BMBF). As funding by BMBF was reduced according to schedule in 2005 and stopped in 2007, complementary financial support has been obtained also from Abbott/AbbVie, Amgen, Centocor, Schering-Plough, and Wyeth. Since 2010, GESPIC has been supported by AbbVie. Additional support was also obtained from the ANCYLOSS (grant number FKZ 01EC1002D), ArthroMark (grant numbers FKZ 01EC1009A and FKZ 01EC1401A) and METARTHROS (grant number FKZ 01EC1407A) projects funded by BMBF.

## Patient consent for publication

Not applicable.

## Ethics approval

The study protocol was approved by the ethics committee of the coordinating centre (Charité—Universitätsmedizin Berlin, Germany/ethics approval number 188-19) and by local ethical committees of participating centres. Participants gave informed consent to participate in the study before taking part.

## Provenance and peer review

Not comissioned; externally peer reviewed.

## Data availability statement

Data are available upon reasonable request. The original study data can be made available upon reasonable request, which should be directed to the corresponding author.

## Patient and public involvement

Patients and/or the public were not involved in the design, or conduct, or reporting, or dissemination plans of this research.

## Orcid

Xenofon Baraliakos: http://orcid.org/0000-0002-9475-9362
Mikhail Protopopov: http://orcid.org/0000-0003-4840-5069
Valeria Rios Rodriguez: http://orcid.org/0000-0001-5612-043X
Murat Torgutalp: http://orcid.org/0000-0003-4600-9484
Denis Poddubnyy: http://orcid.org/0000-0002-4537-6015

## REFERENCES


[1] Navarro-Compán V, Sepriano A, Capelusnik D, Baraliakos X. Axial spondyloarthritis. Lancet 2025;405(10473):159–72.

[2] Landewé R, Dougados M, Mielants H, van der Tempel H, van der Heijde D. Physical function in ankylosing spondylitis is independently determined by both disease activity and radiographic damage of the spine. Ann Rheum Dis 2009;68(6):863–7.

[3] Wanders A, Landewé R, Dougados M, Mielants H, van der Linden S, van der Heijde D. Association between radiographic damage of the spine and spinal mobility for individual patients with ankylosing spondylitis: can assessment of spinal mobility be a proxy for radiographic evaluation? Ann Rheum Dis 2005;64(7):988–94.

[4] Baraliakos X, Listing J, Rudwaleit M, Haibel H, Brandt J, Sieper J, et al. Progression of radiographic damage in patients with ankylosing spondylitis: defining the central role of syndesmophytes. Ann Rheum Dis 2007;66(7):910–5.

[5] Poddubnyy D, Fedorova A, Listing J, Haibel H, Baraliakos X, Braun J, et al. Physical function and spinal mobility remain stable despite radiographic spinal progression in patients with ankylosing spondylitis treated with TNF-$\alpha$ inhibitors for up to 10 years. J Rheumatol 2016;43(12):2142–8.

[6] Torgutalp M, Rios Rodriguez V, Dilbaryan A, Proft F, Protopopov M, Verba M, et al. Treatment with tumour necrosis factor inhibitors is associated with a time-shifted retardation of radiographic spinal progression in patients with axial spondyloarthritis. Ann Rheum Dis 2022;81(9):1252–9.

[7] Baraliakos X, Listing J, von der Recke A, Braun J. The natural course of radiographic progression in ankylosing spondylitis—evidence for major individual variations in a large proportion of patients. J Rheumatol 2009;36(5):997–1002.

[8] Ajrawat P, Touma Z, Sari I, Taheri C, Diaz Martinez JP, Haroon N. Effect of TNF-inhibitor therapy on spinal structural progression in ankylosing spondylitis patients: a systematic review and meta-analysis. Int J Rheum Dis 2020;23(6):728–43.

[9] Baraliakos X, Haibel H, Listing J, Sieper J, Braun J. Continuous long-term anti-TNF therapy does not lead to an increase in the rate of new bone formation over 8 years in patients with ankylosing spondylitis. Ann Rheum Dis 2014;73(4):710–5.

[10] Wanders AJB, Landewé RBM, Spoorenberg A, Dougados M, van der Linden S, Mielants H, et al. What is the most appropriate radiologic scoring method for ankylosing spondylitis? A comparison of the available methods based on the outcome measures in rheumatology clinical trials filter. Arthritis Rheum 2004;50(8):2622–32.

[11] Aydin SZ, Kasapoglu Gunal E, Kurum E, Akar S, Mungan HE, Alibaz-Oner F, et al. Limited reliability of radiographic assessment of spinal progression in ankylosing spondylitis. Rheumatology (Oxford) 2017;56(12):2162–9.

[12] Navarro-Compán V, Boel A, Boonen A, Mease PJ, Dougados M, Kiltz U, et al. Instrument selection for the ASAS core outcome set for axial spondyloarthritis. Ann Rheum Dis 2023;82(6):763–72.

[13] van Tuyl LHD, van der Heijde D, Knol DL, Boers M. Chronological reading of radiographs in rheumatoid arthritis increases efficiency and does not lead to bias. Ann Rheum Dis 2014;73(2):391–5.

[14] Bruynesteyn K, Van Der Heijde D, Boers M, Saudan A, Peloso P, Paulus H, et al. Detecting radiological changes in rheumatoid arthritis that are considered important by clinical experts: influence of reading with or without known sequence. J Rheumatol 2002;29(11):2306–12.

[15] Poddubnyy D, Rudwaleit M, Haibel H, Listing J, Märker-Hermann E, Zeidler H, et al. Rates and predictors of radiographic sacroiliitis progression over 2 years in patients with axial spondyloarthritis. Ann Rheum Dis 2011;70(8):1369–74.

[16] Rudwaleit M, Haibel H, Baraliakos X, Listing J, Märker-Hermann E, Zeidler H, et al. The early disease stage in axial spondylarthritis: results from the German Spondyloarthritis Inception Cohort. Arthritis Rheum 2009;60(3):717–27.

[17] Poddubnyy D, Rudwaleit M, Haibel H, Listing J, Märker-Hermann E, Zeidler H, et al. Effect of non-steroidal anti-inflammatory drugs on radiographic spinal progression in patients with axial spondyloarthritis: results from the German Spondyloarthritis Inception Cohort. Ann Rheum Dis 2012;71(10):1616–22.

[18] Creemers MCW, Franssen MJAM, van't Hof MA, Gribnau FWJ, van de Putte LBA, van Riel PLCM. Assessment of outcome in ankylosing spondylitis: an extended radiographic scoring system. Ann Rheum Dis 2005;64(1):127–9.

[19] Machado P, Landewé R, Braun J, Hermann KGA, Baker D, van der Heijde D. Both structural damage and inflammation of the spine contribute to impairment of spinal mobility in patients with ankylosing spondylitis. Ann Rheum Dis 2010;69(8):1465–70.

[20] van der Heijde D, Østergaard M, Reveille JD, Baraliakos X, Kronbergs A, Sandoval DM, et al. Spinal radiographic progression and predictors of progression in patients with radiographic axial spondyloarthritis receiving ixekizumab over 2 years. J Rheumatol 2022;49(3):265–73.

[21] Braun J, Baraliakos X, Deodhar A, Poddubnyy D, Emery P, Delicha EM, et al. Secukinumab shows sustained efficacy and low structural progression in ankylosing spondylitis: 4-year results from the MEASURE 1 study. Rheumatology (Oxford) 2019;58(5):859–68.

[22] Ramiro S, Nikiphorou E, Sepriano A, Ortolan A, Webers C, Baraliakos X, et al. ASAS-EULAR recommendations for the management of axial spondyloarthritis: 2022 update. Ann Rheum Dis 2023;82(1):19–34.

[23] Ramiro S, van der Heijde D, Sepriano A, van Lunteren M, Moltó A, Feydy A, et al. Spinal radiographic progression in early axial spondyloarthritis: five-year results from the DESIR cohort. Arthritis Care Res (Hoboken) 2019;71(12):1678–84.

[24] Hebeisen M, Micheroli R, Scherer A, Baraliakos X, de Hooge M, van der Heijde D, et al. Spinal radiographic progression in axial spondyloarthritis and the impact of classification as nonradiographic versus radiographic disease: data from the Swiss clinical quality management cohort. PLoS One 2020;15(3):e0230268.

Ann Rheum Dis 84 (2025) 1342–1353

Contents lists available at ScienceDirect

Annals of the Rheumatic Diseases

journal homepage: https://www.sciencedirect.com/journal/annals-of-the-rheumatic-diseases

Systemic lupus erythematosus

# Enhanced B cell and complement cascade gene signatures in patients with neuropsychiatric systemic lupus erythematosus

Dionysis Nikolopoulos[1,2,3,*], George Sentis[2], Iasonas Kitsios[2], Panagiotis Garantziotis[2,4], Noemin Kapsala[3], Antigone Pieta[3], Sofia Flouda[3], Theodora Manolakou[1,5], Myrto Nikoloudaki[6], Aggelos Banos[2], Katerina Chavatza[3], Ioannis Parodis[1,7], Anastasia Filia[2], George Bertsias[6,8], Antonis Fanouriakis[3], Dimitrios T. Boumpas[2,3,9,*]

[1] *Division of Rheumatology, Department of Medicine Solna, Karolinska Institutet, Karolinska University Hospital, and Center for Molecular Medicine (CMM), Stockholm, Sweden*
[2] *Laboratory of Autoimmunity and Inflammation, Center of Clinical, Experimental Surgery and Translational Research, Biomedical Research Foundation Academy of Athens, Athens, Greece*
[3] *4th Department of Internal Medicine, Attikon University Hospital, National and Kapodistrian University of Athens Medical School, Athens, Greece*
[4] *Department of Internal Medicine 3—Rheumatology and Immunology, Friedrich Alexander University Erlangen-Nuremberg and Universitätsklinikum Erlangen, Erlangen, Germany*
[5] *Science for Life Laboratory, Department of Oncology and Pathology, Karolinska Institute, Stockholm, Sweden*
[6] *Rheumatology, Clinical Immunology and Allergy Department, Medical School University of Crete, Heraklion, Greece*
[7] *Department of Rheumatology, Faculty of Medicine and Health, Örebro University, Örebro, Sweden*
[8] *Laboratory of Autoimmunity-Inflammation, Institute of Molecular Biology and Biotechnology, Heraklion, Greece*
[9] *Joint Academic Rheumatology Program, Medical School, National and Kapodistrian University of Athens, Athens, Greece*

ARTICLE INFO

*Article history:*
Received 9 January 2025
Received in revised form 15 March 2025
Accepted 4 April 2025

ABSTRACT

*Objectives:* The management of neuropsychiatric systemic lupus erythematosus (NPSLE) remains challenging because of clinical heterogeneity and the complexity of pathophysiologic mechanisms involved. We sought to determine the molecular signature of NPSLE and its endotypes towards novel biomarkers and targeted therapies.

*Methods:* Whole-blood RNA sequencing from 308 patients with systemic lupus erythematosus (119 with NPSLE, 189 non-NPSLE) and 72-matched healthy controls (HCs) were performed. Supervised pathway enrichment analysis and unsupervised weighted gene coexpression network analysis were applied to distinguish clinically and molecularly defined NPSLE endotypes.

*Results:* Compared with HCs, patients with NPSLE demonstrated dysregulation of adaptive immune responses along with upregulation of interleukin (IL)-1, IL-6, IL-17, and IL-12/IL-23 signalling pathways. The comparison between NPSLE and non-NPSLE groups revealed a robust upregulation of complement cascade, DNA damage response, adaptive immunity, and IL-1 and IL-6 signalling. Furthermore, active NPSLE exhibited a strong autophagy signature. The B cell and complement cascade signatures exhibited a gradual upregulation across the non-NPSLE, inactive NPSLE, and active NPSLE subgroups. Within NPSLE, diffuse syndromes correlated

*Correspondence to Dr Dionysis Nikolopoulos and Prof. Dimitrios T. Boumpas.
*E-mail addresses:* dionysis.nikolopoulos@ki.se (D. Nikolopoulos), boumpasd@uoc.gr (D.T. Boumpas).
GB, A. Fanouriakis and DTB contributed equally to this work.
**Handling editor** Josef S. Smolen.

https://doi.org/10.1016/j.ard.2025.04.006

0003-4967/© 2025 The Author(s). Published by Elsevier B.V. on behalf of European Alliance of Associations for Rheumatology (EULAR). This is an open access article under the CC BY license (http://creativecommons.org/licenses/by/4.0/)

positively with the oxidative phosphorylation module, while antiphospholipid antibody–positive NPSLE was not associated with specific signatures by unsupervised analysis. NPSLE endotypes such as cognitive dysfunction, seizures, psychosis, and optic neuritis were associated with distinct transcriptomic signatures namely IL-6 signalling and leukocyte migration, DNA damage response, inflammation, and type-I interferon, respectively.
*Conclusions:* The clinical heterogeneity of NPSLE appears to be associated with molecular diversity, with certain endotypes or syndromes exhibiting distinct gene signatures. Upregulation of adaptive immune response and complement cascade suggests that complement inhibitors and B cell–targeted therapies could be further explored in NPSLE.

**WHAT IS ALREADY KNOWN ON THIS TOPIC**

- Because of the limited access to human tissue, our understanding of neuropsychiatric systemic lupus erythematosus (NPSLE) is based mainly on murine and neuroimaging studies.

**WHAT THIS STUDY ADDS**

- In a large cohort of patients with systemic lupus erythematosus, the clinical heterogeneity of NPSLE is mirrored by its molecular diversity by blood transcriptome profiling, with specific NPSLE endotype/syndromes characterised by distinct molecular perturbations.
- Upregulation of adaptive immune response and complement cascade-in a step-wise, gradient fashion from inactive to active disease correlated with NPSLE.

**HOW THIS STUDY MIGHT AFFECT RESEARCH, PRACTICE OR POLICY**

- Complement inhibitors and B cell–targeted therapies may be further explored for the targeted therapy of NPSLE.

## INTRODUCTION

The clinical heterogeneity of neuropsychiatric systemic lupus erythematosus (NPSLE) complicates the establishment of well-defined patient cohorts for research purposes, resulting in gaps regarding its pathogenesis and management [1]. Importantly, the limited access to human tissue increases the reliance on murine models; however, they do not exhibit the full spectrum of NPSLE manifestations [2]. This limitation hampers efforts to extrapolate findings from murine models to explain the mechanisms driving major NPSLE, underlying the need for studies using human material. Recent advancements in neuroimaging techniques have expanded our knowledge, yet these techniques are limited in revealing precise pathogenetic mechanisms, and thus, our insight remains incomplete [3]. Despite the establishment of large NPSLE cohorts to study the natural history, translational studies remain scarce in the literature [4]. Accordingly, there has been limited progress in developing novel therapies, and thus, current therapeutic approaches remain empirical extrapolated from non-NPSLE manifestations [5].

High throughput omic studies, particularly transcriptomics, have been instrumental in elucidating the complexities of rare diseases like NPSLE [6]. These studies provide critical evidence for the underlying mechanisms and may offer valuable insights for drug discovery [7]. While NPSLE primarily manifests as inflammation within the nervous system, its pathogenesis is rooted in systemic autoimmunity, including dysregulated immune cell activity and peripheral inflammatory mediators, which infiltrate the central nervous system (CNS), leading to sustained neuroinflammation [8]. Investigating whole blood provides an unbiased approach to studying immune cells' dysregulation, offering insights into the early mechanisms driving NPSLE and potential therapeutic and preventative implications.

In this study, we aimed to report a comprehensive RNA sequencing analysis to profile the blood transcriptome of NPSLE in a large systemic lupus erythematosus (SLE) cohort. We analysed their transcriptomic signatures across distinct neuropsychiatric (NP) syndromes and NPSLE endotypes such as focal vs diffuse NPSLE. Our findings demonstrated molecular diversity, with each NPSLE syndrome/endotype characterised by distinct molecular signatures, while enhanced adaptive immune response and complement cascade signatures were associated with active NP disease within patients with SLE. These data may have implications for the pathogenesis and targeted therapy of NPSLE.

## METHODS

### *Patients and healthy individuals*

Patients were recruited from the Attikon Lupus cohort in Athens [9] and Leto Lupus registry in Crete [10]. We recruited 308 patients with SLE fulfilling the Systemic Lupus Erythematosus International Collaborating Clinics 2012 criteria [11] and 72 matched healthy controls (HCs). Among patients with SLE, 119 were diagnosed with at least 1 NP syndrome attributed to SLE according to the 1999 American College of Rheumatology (ACR) nomenclature (patients with NPSLE) [12]. The attribution of each NP event to SLE was based on expert physician judgement (AF, GB, and DTB) combined with clinical, serologic, and imaging data as previously descripted [13]. The remaining 189 patients with SLE had never been diagnosed with any NP syndrome (patients with non-NPSLE) nor had they received any specific drug for either neurologic or psychiatric diseases. Subgroups of the participants are shown in Supplementary Figure S1.

Patients with NPSLE were further divided into those with (i) diffuse (psychosis, acute confusional state [ACS], aseptic meningitis, demyelinating syndrome, anxiety, depression, headache, and cognitive dysfunction) and focal (seizures, cerebrovascular events, myelopathy, movement disorder, cranial neuropathy) NPSLE with CNS involvement based on 1999 ACR nomenclature; (ii) active and inactive NPSLE; and (iii) antiphospholipid (aPL) antibody–positive NPSLE defined as persistent positivity of at least 1 aPL (LA, anti-CL, and anti-$\beta$2GPI; either IgG or IgM) and aPL-negative NPSLE [14]. We investigated potential transcriptomic differences between patients with aPL-positive and patients with aPL-negative NPSLE because (i) aPL positivity in NPSLE is associated with an increased predisposition to underlying thrombotic mechanisms, as opposed to inflammatory mechanisms, and (ii) aPL is a strong independent predictor of NP involvement in SLE and is strongly associated with specific

NPSLE manifestations presumed to result from thrombotic underlying mechanisms [15]. NP manifestations and demographic, clinical, and serologic characteristics were recorded for each patient at the time of sampling are summarised in Supplementary Tables S1-S5.

All participants were asked to withhold daily medications on the day of sample collection. Only 2 patients (inactive) were on rituximab at the time of sampling. For the active cohort, all samples were collected before initiation of induction therapy for active NPSLE. The study was approved by the Ethics Committee of 'Attikon' University Hospital, Athens (protocol number 103/06-03-2014). Following the acquisition of written informed consent from all participants, blood samples were collected, and RNA extraction was performed and analysed.

### *Definitions*

#### *Attribution of NPSLE*

NPSLE attribution was based on physician judgement through a comprehensive evaluation of multiple factors. These include the ACR exclusion and association criteria and traditional NPSLE risk factors: (i) aPL antibodies, (ii) previous NP events, (iii) generalised disease activity, (iv) timing in relation to SLE diagnosis, and (v) type of NP manifestation according to the definition by Ainalia et al [16]. Findings from brain imaging and other diagnostic tests (eg, cerebrospinal fluid [CSF] analysis) were considered to rule out SLE-unrelated NP manifestations. For CNS manifestations, atherosclerotic risk factors (eg, hypertension, diabetes, smoking, and dyslipidaemia) are also assessed. In complex cases, a multidisciplinary approach was used involving physicians from different disciplines (eg, neurologists, radiologists, and rheumatologists) and attribution was further corroborated by prospective follow-up [13–15].

#### *NP activity in SLE*

Active NPSLE was defined as the onset of new NP symptoms attributed to SLE (ie, SLE-related NP manifestations) that necessitate hospitalisation and/or an intensification of immunosuppressive therapy. Inactive NPSLE refers to a history of SLE-related NP manifestations without current NP symptoms requiring intensive treatment or with symptoms attributed to irreversible nervous system damage due to past NPSLE.

### *RNA sequencing*

RNA was extracted from whole blood using the Paxgene Blood miRNA kit (PreAnalytiX), and libraries were prepared according to the Illumina Truseq mRNA protocol for stranded mRNA sequencing [17]. Paired-end mRNA sequencing with read lengths of 67/100 bp was carried out on Illumina HiSeq4000 platform at the Department of Genetic Medicine and Development, University of Geneva Medical School [6]. The library preparation and sequencing procedures followed previously established protocols. Quality assessment of the sequencing data was performed using FastQC software [18]. Sorting of bam files was accomplished using Samtools, and gene expression counts were obtained using HTSeq [19].

### *Computational analysis of the gene expression data*

The edgeR package (v:3.40.2,RRID: SCR_012802) was used to identify differential expressed genes (DEGs) following raw counts normalisation [20]. DEGs with fold change (|FC|) of >1.5 and $P$ value of <.05 were considered significant. The gProfiler was used for gene ontology analysis, as previously described. Gene set enrichment analysis (GSEA) was performed using the software (v:4.3.2) against the gene sets of MsigDB database as previously descripted [17,21]. CIBERSORTx was used for deconvolution analysis as previously described [17]. Unsupervised cluster analysis was performed with weighted gene coexpression network analysis (WGCNA) R package (v:1.72-1, RRID: SCR_003302) to identify molecular groups (modules) of coexpressed genes as previously described [22,23]. Networks of interactions were created with StringDB using the STRINGdb R package and visualised using packages ggraph and igraph as previously described [24–26]. All analyses were performed in R (v:4.2.0, RRID: SCR_001905).

### *Druggability analysis*

#### *L1000CDS2*

The resulting sets of DEGs with their corresponding |logFC| values used as inputs for the L1000CDS2 signature search engine as previously descripted [7]. The top 50 signatures exhibiting the largest cosine distances, indicating perturbations with potential phenotype-reversing effects, were extracted.

#### *Connectivity map*

The clue.io web portal was used to access Connectivity Map 2.0 (CMAP2) and query compounds with reversal potential of the NPSLE subgroups transcriptomic signatures. Only the top upregulated and downregulated valid genes were provided after being ranked according to their logFC values. CMAP2 results were filtered keeping only compounds with at least 3 nonmissing exemplar signature normalised connectivity scores among cell lines THP1, K562, KMS34, OCILY19, and HBL1.

## RESULTS

### *Patients with NPSLE demonstrate extensive aberrancies in blood transcriptome*

We first investigated what distinguishes the NPSLE transcriptome from both the non-NPSLE transcriptome and the healthy transcriptome. Unsupervised principal component analysis of patients with NPSLE, patients with non-NPSLE, and HCs is illustrated in Figure 1A. A total of 938 upregulated and 354 downregulated DEGs were found in the NPSLE group compared with that in HCs (Fig 1B). Gene ontology analysis revealed dysregulation of multiple pathways, including adaptive immune response, immunoglobulin-mediated immune response, and classical autoantibody-mediated complement activation between NPSLE and HC groups (Fig 1C). GSEA identified enhanced interleukin (IL)-1, IL-6, IL-17, and IL-12/IL-23 signalling in the former group (Fig 1D, Supplementary Fig S2A). The most enriched upregulated pathways in NPSLE vs HC groups included neuroinflammatory response, oxidative phosphorylation, interferon-$\alpha$, and neutrophil degranulation (Fig 1E). Key dysregulated genes associated with each pathway are highlighted in Figure 1D,E. Next, we performed deconvolution analysis to examine changes in the proportion of circulating myeloid and lymphoid immune cells. We observed significantly increased monocyte, memory B cell, and activated memory CD4 T cell proportions in the NPSLE group compared with those in the HC group, indicating that both myeloid and lymphoid subpopulation are expanded in NPSLE (Fig 1F). Altogether, the NPSLE transcriptome demonstrates extensive aberrancies with quantitative and qualitative differences associated mainly with both innate and adaptive

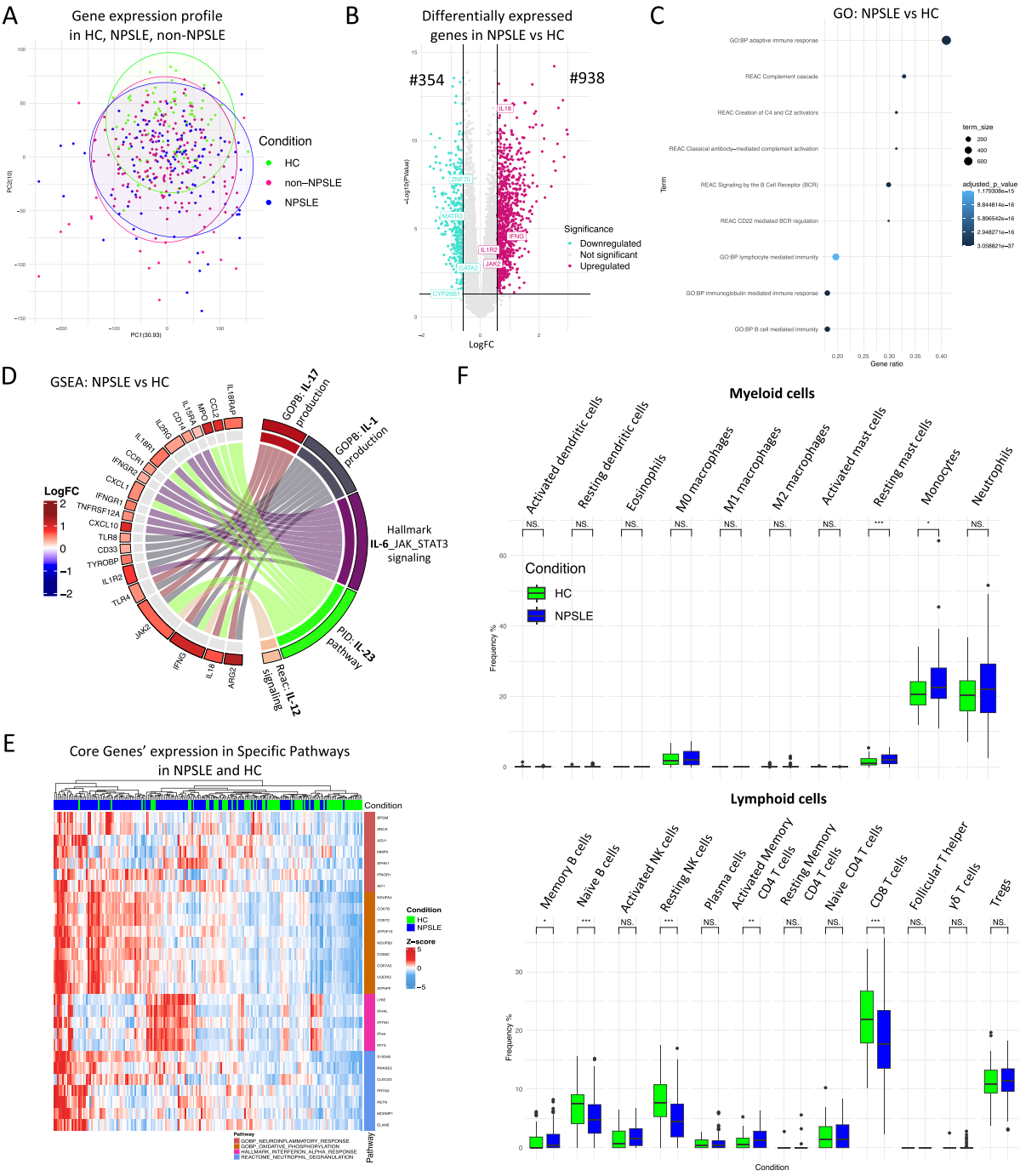



**Figure 1.** Transcriptomic signature in patients with neuropsychiatric systemic lupus erythematosus (NPSLE) vs healthy individuals demonstrates extensive aberrancies in blood transcriptome. A total of 1292 dysregulated differentially expressed genes (DEGs) in NPSLE compared with healthy controls (HCs) revealed enhanced interleukin (IL)-1, IL-6, IL-17, and IL-12/IL-23 signalling. (A) Principal component analysis of blood gene expression profiles from patients with NPSLE (n = 119) and HCs (n = 72). (B) Volcano plot highlighting the DEGs (|log2FC| > 0.58; $P < .05$) in NPSLE vs HCs. (C) Dot plot shows the results of gene ontology (GO) analysis representing biological pathways that are deregulated in NPSLE vs HCs. (D) Chord plot shows the results of gene set enrichment analysis (GSEA) including significantly enriched pathways (false discovery rate < 0.25) in NPSLE vs HCs and key deregulated genes of each pathway. (E) Heatmap shows the expression profile of the 28 genes belonging to specific pathways (neuroinflammatory response, oxidative phosphorylation, interferon-$\alpha$, and neutrophil degranulation). (F) Deconvolution analysis using CIBERSORTx shows the estimated proportions of different myeloid (up) and lymphoid (down) cell subsets in NPSLE and HCs.

immune response, proinflammatory IL signalling, and complement activation.

### *B cell and T cell signatures differentiate patients with NPSLE from those with non-NPSLE*

We next searched for unique transcriptomic perturbations in the NPSLE but not the non-NPSLE group. We found 17 upregulated and 22 downregulated DEGs in NPSLE vs non-NPSLE groups, mainly involving pathways related to immune system process B cell activation and complement cascade (Fig 2A,B). GSEA revealed a robust upregulation of immunoglobulin complex, complement cascade, DNA damage response (DDR), B cell activation signatures coupled with increased IL-1 and IL-6 signalling in NPSLE. Conversely, the non-NPSLE group was significantly associated with upregulation of T cell receptor

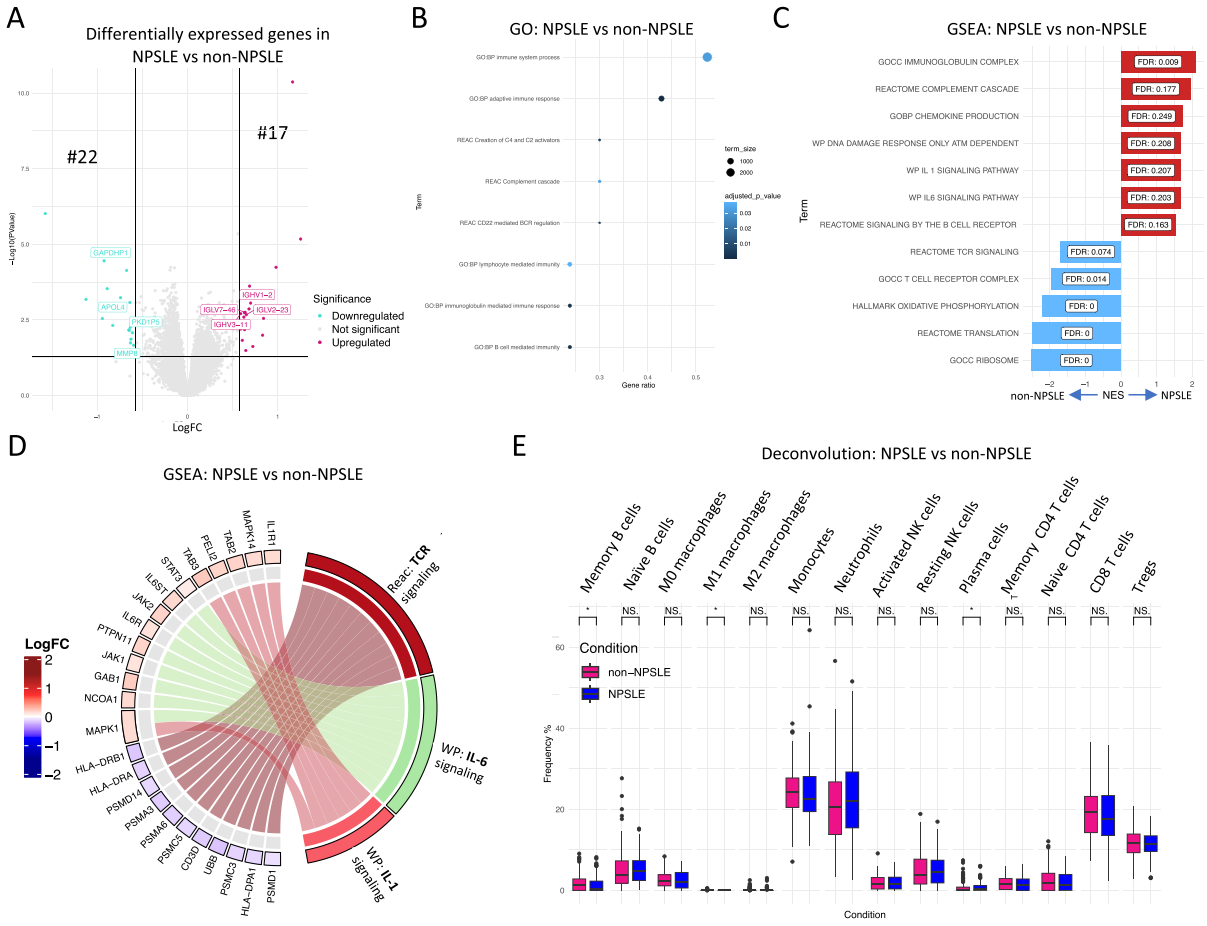



**Figure 2.** Transcriptomic signature in patients with neuropsychiatric systemic lupus erythematosus (NPSLE) vs non-NPSLE: B cell and T cell signatures differentiate patients with NPSLE from those with non-NPSLE. (A) Volcano plot highlighting the differentially expressed genes (DEGs; |log2FC| > 0.58; $P < .05$) in NPSLE vs non-NPSLE. (B) Dot plot shows the results of gene ontology (GO) analysis representing biological pathways that are deregulated in NPSLE vs non-NPSLE. (C) Bar plot shows the results of gene set enrichment analysis (GSEA) including the positively (red) and negatively (blue) enriched pathways (false discovery rate [FDR] < 0.25) in NPSLE vs non-NPSLE. (D) Chord plot shows the results of GSEA including significantly enriched pathways (FDR < 0.25) in NPSLE vs non-NPSLE and key deregulated genes of each pathway. (E) Deconvolution analysis using CIBERSORTx shows the estimated proportions of immune cell subsets in NPSLE and non-NPSLE.

signalling and noninflammatory pathways including ribosome/translation and oxidative phosphorylation (Fig 2C,D, Supplementary Fig S2B). To further explore these findings, we performed deconvolution analysis, which showed that patients with NPSLE exhibited significantly higher frequency of plasma cells and lower frequency of memory B cells (Fig 2E). These findings may suggest that within the SLE population, NPSLE is marked by increased B cell activation and decreased T cell –mediated immune response.

### *Adaptive immune response and complement activation are enhanced in active compared with inactive NPSLE in a step-wise, gradient pattern*

To provide a more comprehensive understanding of the transcriptomic landscape of NPSLE, we performed a comparison between patients with active and inactive NPSLE, which revealed 114 upregulated and 128 downregulated DEGs mainly involved in adaptive immune response and classical antibody-mediated complement activation (Fig 3A,B). In addition to upregulation of B cell and complement activation in active NPSLE, GSEA revealed significantly enriched pathways related to T cells, oxidative phosphorylation, and mTORC signalling (Fig 3C, D, Supplementary Fig S2C). No differences were captured with regards to the proportions of circulating immune cells (Fig 3E), suggesting that qualitative disparities within immune cells may account for inflammatory signatures of active NPSLE. Taken together, our data indicate a hierarchical upregulation of B cell and complement cascade signatures in NPSLE, which are even more pronounced in patients with active NPSLE.

### *Unsupervised analysis reveals distinct pathogenetic mechanisms across the various NPSLE endotypes*

To further elucidate the complexity of NPSLE beyond the gene signatures and the 'gradient' molecular deregulations identified through supervised approaches, we proceeded with unsupervised analysis. This allowed us to explore the transcriptomic landscape in relation to specific endotypes (diffuse vs focal), NP activity, and aPLs (eg, positive vs negative), capturing the molecular associations of multiple and diverse clinical subgroups within NPSLE. We performed WGCNA (unsupervised analysis) using transcriptomic data from the entire SLE cohort; 16 modules of coexpressed genes were identified. Comparison between diffuse and focal NPSLE revealed a significant upregulation of *Magenta* module (oxidative phosphorylation) in diffuse

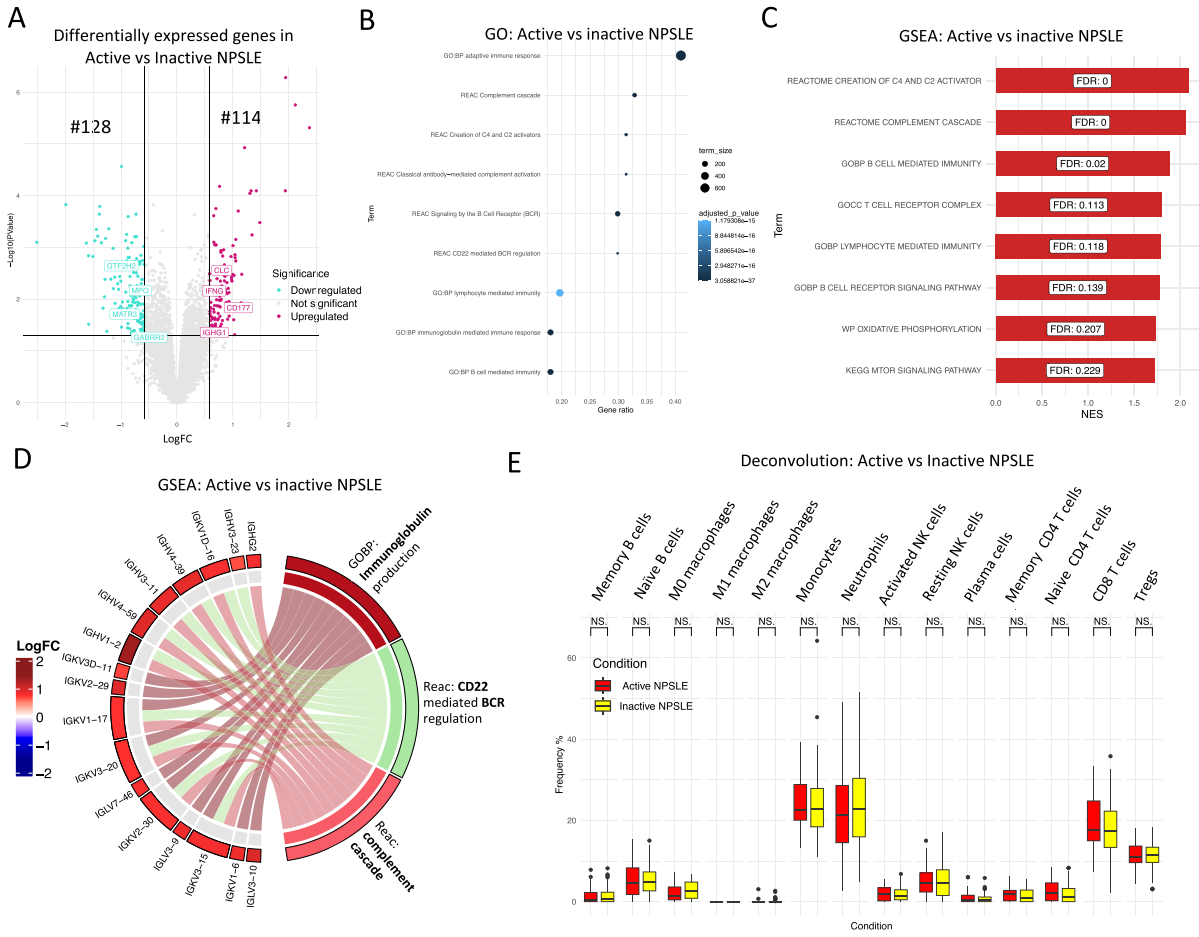



**Figure 3.** Transcriptomic signature in patients with active neuropsychiatric systemic lupus erythematosus (NPSLE) vs those with inactive NPSLE: adaptive immune response and complement activation are more pronounced in active vs inactive NPSLE. (A) Volcano plot highlighting the differentially expressed genes (DEGs; $|\log2FC| > 0.58$; $P < .05$) in active vs inactive NPSLE. (B) Dot plot shows the results of gene ontology (GO) analysis representing biological pathways that are deregulated in active vs inactive NPSLE. (C) Bar plot shows the results of gene set enrichment analysis (GSEA) of the positively (red) enriched pathways (false discovery rate [FDR] < 0.25) active vs inactive NPSLE. (D) Chord plot shows the results of GSEA including significantly enriched pathways (FDR < 0.25) in active vs inactive NPSLE and key deregulated genes of each pathway. (E) Deconvolution analysis using CIBERSORTx shows the estimated proportions of immune cell subsets in active and inactive NPSLE.

NPSLE. *Greenyellow* (autophagy) module was significantly upregulated in active NPSLE group compared with that in inactive NPSLE group. Comparing different patients with NPSLE and different aPL profiles with those with aPL-negative NPSLE, only anti-b2GPI$^+$ NPSLE group positively correlated with *Brown* (adaptive immunity) and *Grey* (cell cycle) modules (Fig 4A). Next, we performed enrichment analysis to identify deregulated pathways in each module. *Magenta* module was annotated to oxidative phosphorylation signature, supporting that diffuse NPSLE is mediated by mechanisms beyond inflammation (Fig 4B). The *Greenyellow* module was associated with autophagy, suggesting that increased autophagic activity may account for the transition from the inactive to active phase of NPSLE. To further evaluate these findings, we constructed a protein–protein interaction (PPI) network based on deregulated coding genes in *Greenyellow* module, and we found key orchestrators of diffuse NPSLE including *MAGOH* (essential for cell proliferation), *MRPL47* (involved in mitochondrial translation), and *ELOC* (Fig 4C). The active NPSLE PPI network demonstrated *PINK1* (a serine/threonine protein kinase that protects cells from stress-induced mitochondrial dysfunction), *CDC34* (ubiquitin-conjugating enzyme that controls cellular proliferation), and *KLF1* (modulator of PD-L1–mediated immune suppression in CD4$^+$ T cells) as significant upstream regulators of active NPSLE (Fig 4D). To this end, *Brown* and *Grey* modules were linked to adaptive immunity and mitotic cell cycle signatures indicating that anti-$\beta$2GPI$^+$ NPSLE may exhibit distinct pathogenetic properties. Taken together, these data suggest that NPSLE endotypes may exhibit distinct transcriptomic profiles.

Next, we performed the same analysis comparing the NPSLE endotypes with patients with non-NPSLE to gain insights on molecular perturbations within the SLE (Supplementary Fig S3A,B). *Black* and *Magenta* modules, which are associated with protein metabolism and oxidative phosphorylation pathways, respectively, negatively correlated with most of NPSLE endotypes. *Blue* module, annotated to DDR pathways, was negatively associated with aPL-negative, focal, and inactive NPSLE. Conversely, *Pink* module, characterised with innate immunity and myeloid leukocyte migration, positively correlated with most of the NPSLE endotypes. Both focal and aPL-negative NPSLE groups were positively associated with *Turquoise* module, which was annotated to DNA metabolism pathways (Supplementary Fig S3A,B). These data suggest that NPSLE endotypes as a whole may display unique transcriptional features compared with non-NPSLE.

Omic data are increasingly used to identify new therapeutic targets for complex diseases with limited treatment options [7]. Although a comprehensive druggability analysis was beyond the

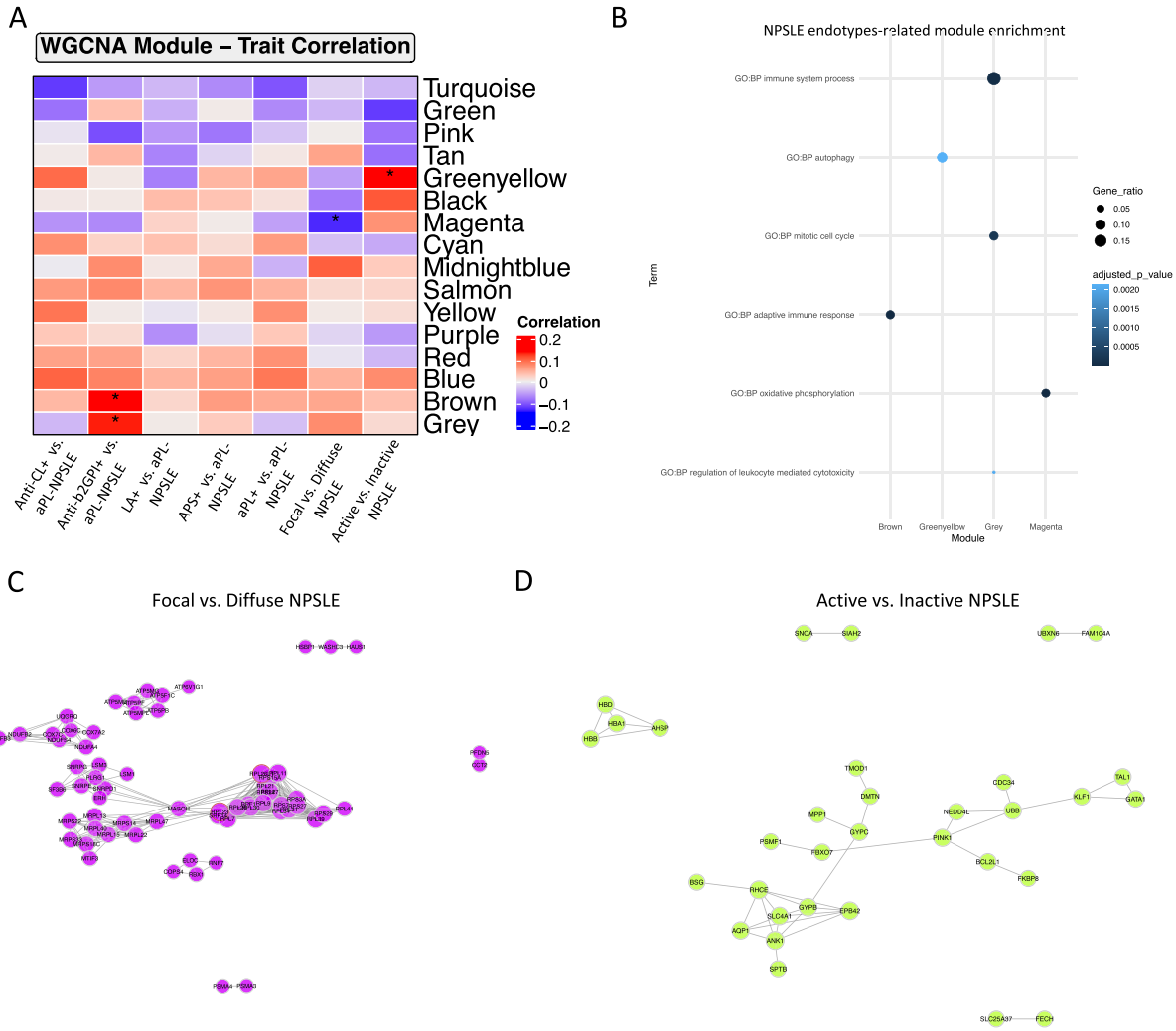



**Figure 4.** Unsupervised cluster analysis reveals distinct pathogenetic mechanisms implicated in patients with different neuropsychiatric systemic lupus erythematosus (NPSLE) endotypes: oxidative phosphorylation signature differentiates diffuse from focal NPSLE, while autophagy signature differentiates active from inactive NPSLE. (A) Heatmap showing gene modules derived from weighted gene coexpression network analysis using transcriptomic data of the entire systemic lupus erythematosus cohort. *Statistically significant correlations between modules (rows) and NPSLE endotypes (columns). (B) Bubble plot of gene ontology terms found as significantly enriched in the correlated modules (*brown, greenyellow, grey,* and *magenta*). Colour represents adjusted false discovery rate, and size represents the number of genes related to a term found in each module. (C) Network from protein−protein interactions of proteins derived from *Magenta* (*magenta*) module. Node fill colour corresponds to the module. (D) Network from protein−protein interactions of proteins derived from greenyellow (*greenyellow*) module. Node fill colour corresponds to the module. The network layouts were created using Davidson and Harels simulated annealing algorithm from the package *igraph*.

scope of this work, we performed a preliminary analysis to identify FDA-approved or investigational drugs with potential to reverse the active transcriptomic signature of NPSLE, using 2 computational tools, L1000CDS2 and CMAP. Our analysis highlighted Aurora kinase inhibitors (barasertib), mTOR inhibitors (everolimus), and PI3K inhibitors (alpelisib) as candidates capable of reversing the active NPSLE transcriptomic signature (Supplementary Fig S4A,B). The diffuse NPSLE signature, characterised by oxidative phosphorylation pathways, was found to be potentially reversible by mTOR/PI3K inhibitors (everolimus and SB-2343) and the Aurora kinase inhibitor barasertib. The focal NPSLE signature, dominated by inflammatory pathways, appeared responsive to multikinase inhibitors such as regorafenib, the tyrosine kinase inhibitor dasatinib (noted for its senolytic and anti-inflammatory properties), PI3K inhibitors (alpelisib), Janus kinase inhibitors, and Bruton's tyrosine kinase inhibitors such as ibrutinib (Supplementary Fig S4C-F). Further research with advanced tools is required to validate these results and identify novel therapeutic targets.

### *Unsupervised analysis reveals pathogenetic mechanisms underlying distinct NPSLE manifestations*

Taking the advantage of the large NPSLE cohort, we proceeded with unsupervised analysis to explore whether specific NPSLE manifestations are associated with distinct transcriptomic signatures. We used WGCNA to investigate this question; 8 NP syndromes were significantly associated with at least 1 gene module (Fig 5A). *Turquoise* (DNA metabolism) and *Blue* (DDR) modules correlated with seizures, while the later also correlated with ACS. Both modules were related to DDR and DNA metabolism, indicating shared pathogenetic mechanisms between seizures and ACS mediated by aberrant DDR (Fig 5A, B). Psychosis was positively associated with the *Grey* module, which was characterised by robust inflammation (Fig 5A,B). The *Pink* module, which was annotated to innate immune response, was positively linked to impaired cognition and headache (Fig 5A,B). The *Tan* module (chromatin organisation) was associated with both impaired cognition and myelitis (Fig 5A,

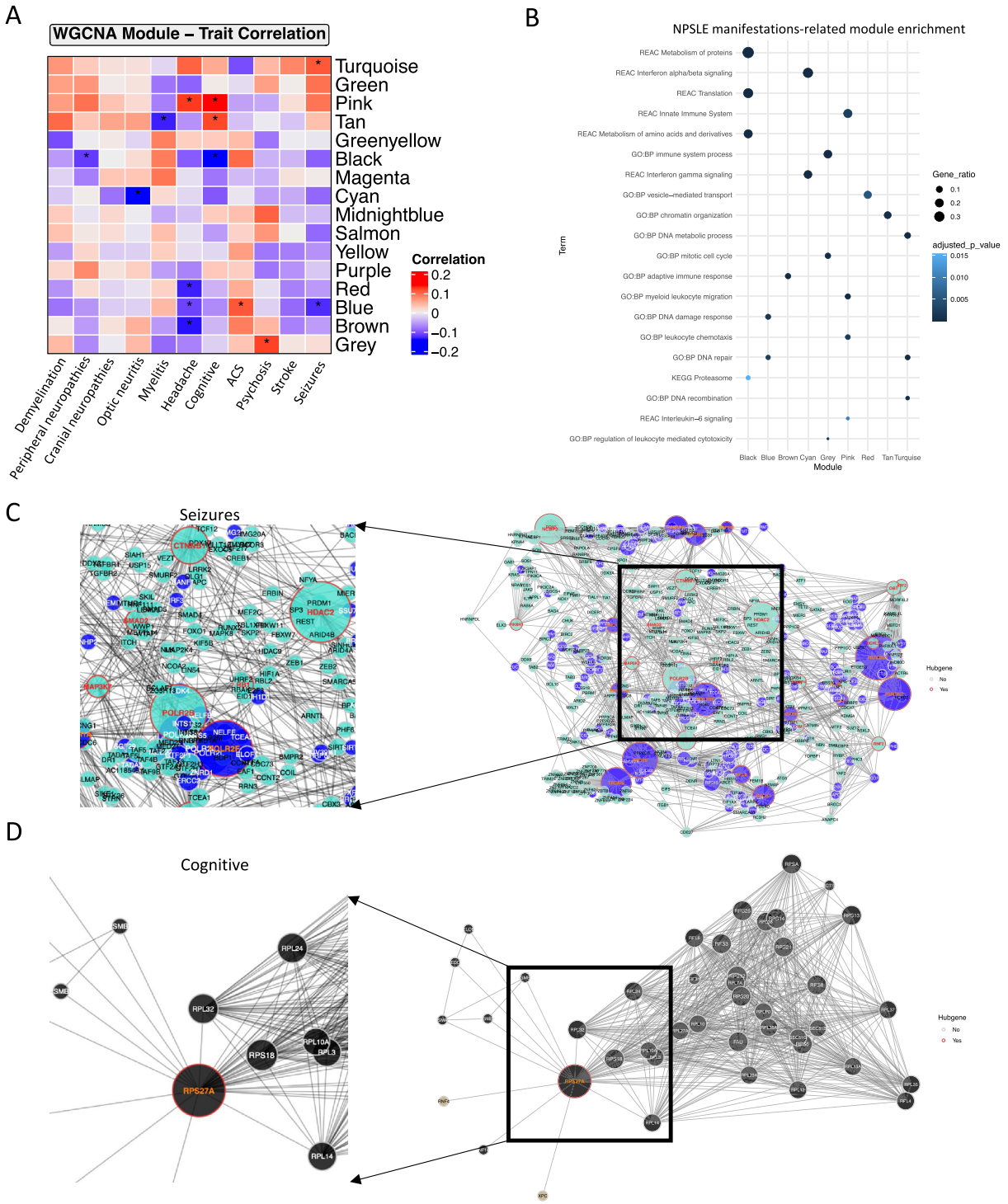



**Figure 5.** Unsupervised cluster analysis reveals distinct pathogenetic mechanisms implicated in patients with neuropsychiatric systemic lupus erythematosus (NPSLE) with different neuropsychiatric manifestations: NPSLE is heterogeneous not only from a clinical standpoint but also from a molecular perspective. (A) Heatmap showing gene modules derived from weighted gene coexpression network analysis (WGCNA) using transcriptomic data of the entire systemic lupus erythematosus cohort. *Statistically significant correlations between modules (rows) and NPSLE manifestations (columns). (B) Bubble plot of gene ontology terms found as significantly enriched in the correlated modules (*black, blue, brown, cyan, grey, pink, red, tan,* and *turquoise*). Colour represents adjusted false discovery rate, and size represents the number of genes related to a term found in each module. (C) Network from protein−protein interactions of proteins derived from *Turquoise* module. (D) Network from protein−protein interactions of proteins derived from *Grey* module. (E) Network from protein−protein interactions of proteins derived from *Pink* and *Tan* modules. Node fill colour corresponds to the modules. The network layouts were created using Davidson and Harels simulated annealing algorithm from the package *igraph*.

B). Moreover, the *Black* module, related to protein metabolism, negatively associated with impaired cognition and peripheral neuropathies (Fig 5A,B). Finally, the interferon module (*Cyan*) significantly correlated only with optic neuritis (Fig 5A,B). The 'seizures' PPI network based on deregulated coding genes in *blue* (DDR) and *Turquoise* (DNA metabolism) modules revealed *HDAC2, POLR2B,* and *CTNNB1* as key orchestrators of seizures (Fig 5C). The 'cognition' PPI network (*Tan* module) revealed *RPS27A* as significant gene that are associated with cognitive impairment (Fig 5D). Taken together, these data justify that

NPSLE is heterogeneous from not only a clinical standpoint but also a molecular perspective.

## DISCUSSION

Our study provides a comprehensive characterisation of the blood molecular profile of patients with NPSLE compared with those of patients with non-NPSLE and healthy individuals. NPSLE is associated with a significant upregulation of adaptive immune response and complement cascade signatures within the SLE population. Notably, these signatures are more pronounced during the active phase of NPSLE compared with those during the inactive phase. Of note, we also detected unique transcriptomics signatures that characterise the different NP syndromes of SLE and differentiate the diffuse from focal NPSLE endotypes. Finally, we exploited the active NPSLE and endotypes molecular fingerprints to identify potential therapeutic targets and demonstrated that NPSLE endotypes display differential anticipated response to targeted therapies towards personalised medicine (Fig 6).

One of the challenges in elucidating the NPSLE pathogenesis is the involvement of different mechanisms across various manifestations as supported by clinical experience including inflammation, neurotoxicity due to autoantibodies or complement activation, microvasculopathy, demyelination, and immune thrombosis. Specifically, manifestations such as psychosis and transverse myelitis often occur during flares and are driven by robust peripheral inflammation that penetrates the brain following blood–brain barrier disruption [15]. Conversely, other manifestations, such as cognitive impairment, appear to be driven by low-grade chronic brain inflammation [27]. In this study, we demonstrated that sustained signalling by proinflammatory cytokines in the periphery of a large NPSLE with various NP manifestation, including IL-1, IL-6, IL-17, and IL-12/23. Both serum and CSF IL-6 levels have been reported to be elevated in patients with NPSLE compared with those in patients with non-NPSLE, with IL-6 proposed as potential biomarker of NPSLE, whereas the other cytokines have been found to be elevated in a few studies, but their roles remain poorly investigated [15,28,29]. Increasing evidence from 2 different murine models of NPSLE supports the pathogenetic role of IL-6 in NPSLE. In the MRL/lpr model, IL-6 promotes behavioural deficits through the activation of astrocytes [30], whereas in NZB/W-F1 mice, locally increased IL-6 mediates NP symptoms by disrupting hippocampal neurogenesis [27]. Our data confirm the upregulation of IL-6 signalling at the transcriptome level in human NPSLE, providing further evidence to support testing IL-6 inhibition.

The clinical heterogeneity of NPSLE is mirrored by molecular diversity, with each NPSLE endotype or syndrome displaying distinct molecular profiles. Following unsupervised analysis, we identified significant associations between specific transcriptomic signatures and certain NP events, findings that are – at least in part – consistent with previous evidence. Lupus psychosis, known for its rapid response to immunosuppressants [31], was associated with an inflammation molecular signature. Seizures, which are often self-limited or can occur in the absence of generalised disease activity [15], were associated with an aberrant DDR [32]. The association of the IL-6 signature with cognitive impairment aligns with our understanding that IL-6 is pivotal in murine NPSLE, resulting in cognitive decline as a prominent manifestation [27,30]. Above and beyond the syndromes, we also identified signatures that differentiate active from inactive and diffuse from focal NPSLE, while patients with NPSLE with and without aPL do not seem to differ at the transcriptome level. The upregulation of the autophagy signature was associated with the transition from inactive to active NPSLE. Hydroxychloroquine, which inhibits autophagy by preventing the fusion of autophagosomes with lysosomes [33], prevents flares – including NP flares [34] and thrombotic events in SLE [35]. Although there is a lack of dedicated clinical studies showing its protective effect against NP events, this may be attributed to the number of patients with NPSLE included in SLE studies [36]. The protective effect of hydroxychloroquine on NPSLE is further supported by its antithrombotic properties

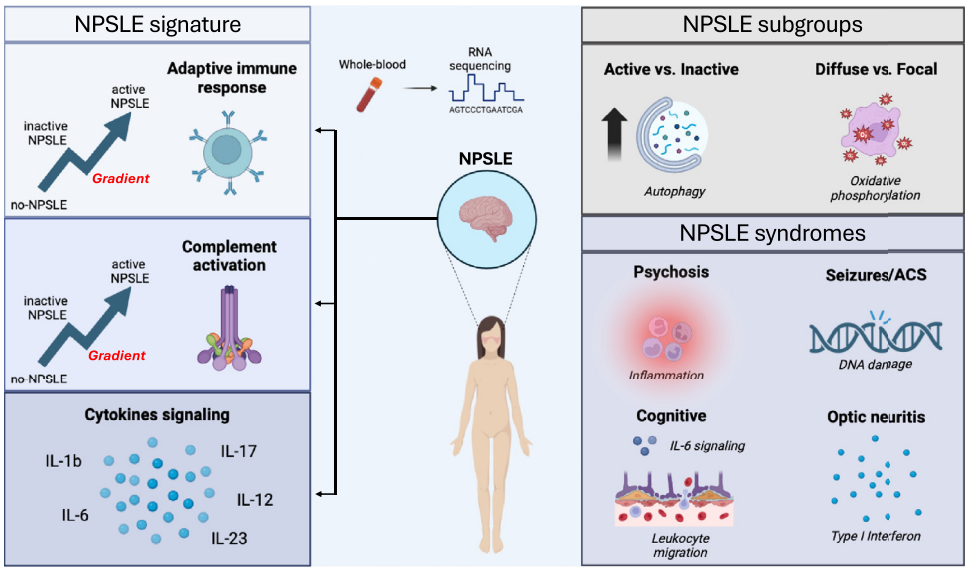



**Figure 6.** Schematic overview of deregulated mechanisms in neuropsychiatric systemic lupus erythematosus (NPSLE). The NPSLE transcriptome demonstrates extensive aberrancies with quantitative and qualitative differences characterised mainly by adaptive immune response, immunoglobulin-mediated immune response and classical autoantibody-mediated complement activation along with enhanced interleukin (IL)-1, IL-6, IL-17, and IL-12/IL-23 signalling. Diffuse vs focal NPSLE is characterised by enhanced ribosome/metabolism pathways, while active NPSLE was associated with enhanced autophagy pathways compared with inactive NPSLE. Within systemic lupus erythematosus, complement cascade and adaptive immune response signatures are more upregulated in NPSLE in a gradient fashion. Unsupervised analysis revealed distinct molecular signatures underlying each neuropsychiatric syndrome.

[37], as some NP events are mediated by thrombotic mechanisms [2]. Interestingly, PI3K inhibitors, which inhibit autophagy [38], have emerged as potential treatment capable of reversing the aberrant transcriptomic signature of active NPSLE.

Our findings have possible therapeutic implications. Our findings align with previous studies in both murine and human NPSLE [39,40], which have demonstrated the crucial role of the complement pathway. Activated microglia promote synaptic pruning in a C1q-depedent manner [40]. Complement deposition is evident in the MRL/lpr model of NPSLE, and the use of complement inhibitors has been shown to improve the brain inflammatory burden in this model, highlighting their therapeutic potential [41]. More importantly, brain autopsies of patients with NPSLE revealed diffuse vasculopathy, vasculitis, microinfarction, and macroinfarction, accompanied by C4d-associated and C5b-9–associated microthrombi [42]. Recent data using functional magnetic resonance imaging informed single-nucleus RNA sequencing in multiple sclerosis have identified complement component 1q (C1q) as a critical mediator of 'microglia inflamed' activation, suggesting that C1q inhibition is a potential therapeutic avenue to address chronic white matter inflammation [43]. Over the past decade, the C5a receptor antagonist avacopan and the monoclonal antibody eculizumab, targeting C5b, have been introduced into clinical practice for treating severe inflammatory conditions like antineutrophil cytoplasmic antibody–associated vasculitis [44,45]; however, their effectiveness in treating severe SLE, including NPSLE, has yet to be determined. Taken together, our data support further assessment of complement inhibitors in clinical trials, to treat patients with SLE with major NP involvement.

The management of NPSLE remains largely empirical, and thus, intravenous cyclophosphamide is recommended for severe NP cases based on observational studies and 1 clinical trial [46]. Our data demonstrated a hierarchical upregulation and, likely, dependence on adaptive immune response in NPSLE with the highest B cell signature observed in patients with active disease. The crucial role of B cells is further supported by murine studies indicating that B cells infiltrate the brain of lupus-prone mice during the early phase of the disease [27]. Currently, B cell –depleting agents such as rituximab are not recommended, unless conventional immunosuppressive agents are contraindicated, due to paucity of randomised evidence. However, observational studies in patients with active NPSLE have demonstrated that rituximab is effective in treating refractory disease, and in few cases, it has been used as a first-line therapy for severe neurologic manifestations [47–49]. These data are more promising in view of recently introduced B cell–depleting therapies such obinutuzumab [50] and CD19-CAR T cell therapy for the treatment of refractory SLE [51]. Of note, NPSLE were not included in this study. As opposed to rituximab, CD19-CAR T cell therapy induces deep tissue and sustain depletion of B cells, which recur after approximately 3 months after CAR T cell exposure [52]. Preliminary evidence demonstrated that this treatment results in sustained and drug-free remission, with good short-term and long-term safety [53]. Accordingly, controlled clinical trials have been designed to further investigate the efficacy in patients with severe autoimmune diseases. To this end, our data provide rationale for including patients with major NPSLE in clinical trials aimed at evaluating the effectiveness of these interventions in severe SLE.

The major strength of this study lies in its large sample size and the inclusion of well-characterised cases of major and severe NPSLE manifestations with stringent attribution to SLE. This is further supported by the very low frequency of 'minor' NPSLE manifestations within the cohort. A key limitation is the inherent heterogeneity of SLE regarding disease activity, non-NP manifestations, and administered medications, which could potentially influence the findings. Notably, the 2 main groups—NPSLE and non-NPSLE—did not differ significantly in terms of treatments received. All patients were off medications for 1 day before sample collection for research purposes. The 2 groups were also well-matched with respect to disease activity, autoantibody profiles including complement consumption, and active extra-NP manifestations at the time of sampling other than lupus nephritis. Moreover, their clinical phenotypes (defined as ever manifestations) were similar across all manifestations, except for lupus nephritis, which was higher in patients with non-NPSLE as expected [1]. The differences in extra-NP characteristics of the various NPSLE endotypes did not reach statistical significance, due to the limited sample size of each endotype; matching or adjusting for the NPSLE endotypes was not feasible given the small sample size. Taken together, although we cannot entirely exclude the possibility of minor confounding factors within the subgroups, the 2 main groups (NPSLE and non-NPSLE) were well-matched, and no major differences were observed across endotypes. Comprehensive data on mental and cognitive function, CSF samples, as well as magnetic resonance imaging findings were not available.

To this end, a major limitation of the study lies in reproducibility of data, as our findings are derived from a single SLE cohort, without validation in an independent cohort, limiting the generalisability of our results. The absence of publicly available NPSLE transcriptomic data further constrained our effort to externally validate our findings. This limitation, in addition to small sample size of each NP manifestation per se, necessitates cautious interpretation of our results. Thus, our study should be viewed as hypothesis generating, providing preliminary data to enhance our understanding of the underlying mechanisms of NPSLE and guide future research. Further studies including replication in larger, independent cohorts is essential to confirm and extend these findings.

In summary, our findings demonstrate that NP involvement within SLE is associated with distinct transcriptomic signatures with complement cascade and adaptive immune response showing the most pronounced upregulation. Furthermore, each NP syndrome in SLE is associated by unique transcriptomic signature, further supporting that distinct pathogenetic mechanisms may account for specific NPSLE manifestations. Further translational research is essential to validate these findings and integrate them into therapeutic and precision medicine applications.

## Competing interests

All authors declare they have no competing interests.

## Acknowledgements

We thank patients and their referring physicians for participating in this study and physicians and nurses from Attikon University hospital and PAGNI University Hospital for superb patient care. Figure 6 was created with Biorender.com.

## Contributors

DN and DTB conceived the project and guarantee for overall content. DN recruited and took care of patients, collected blood samples, and extracted clinical data. GS, IK, and PG, performed

analysis. GS supervised the analysis. PG, AFi, and TM performed data interpretation and visualisation. NK, MN, AP, KC, and SF contributed to recruitment of patients and healthy individuals and extracted clinical data from the medical charts. AB and IP data interpretation and manuscript editing. DN, GB, and DTB drafted the manuscript with contributions from all authors. GB, AFa, and DTB supervised the study and the writing. All authors read and approved the final manuscript for publication.

## Funding

This work was supported by grants from EU (SYSCID grant agreement number 733100) and ERC (LUPUSCARE grant agreement number 742390), all to DTB. DN has received grants from Ulla o Roland Gustafssons Donationsfond (2024-49), Ulla och Gustaf af Ugglas stiftelse (2023-025029), Reumatikerförbundet (2024 R-995557), Åke Wiberg stiftelse, King Gustaf V's 80-year Foundation (FAI-2023-1006), and Karolinska Institutet.

## Patient consent for publication

Written informed consent was obtained from all participants.

## Ethics approval

The study was approved by the Ethics Committee of the 'Attikon' University Hospital of Athens (protocol number 103/06-03-2014).

## Provenance and peer review

Not commissioned; externally peer reviewed.

## Data availability statement

The RNA sequencing presented in this study can be found in EGA online repository. The accession number is EGAS00001007750. Data are available on reasonable request.

## Supplementary materials

Supplementary material associated with this article can be found, in the online version, at doi:10.1016/j.ard.2025.04.006.

## Orcid

Dionysis Nikolopoulos: http://orcid.org/0000-0002-9894-6966
George Sentis: http://orcid.org/0009-0002-0331-3910
Panagiotis Garantziotis: http://orcid.org/0009-0006-9432-1228
Antigone Pieta: http://orcid.org/0000-0003-2361-0525
Aggelos Banos: http://orcid.org/0000-0002-5647-6505
Katerina Chavatza: http://orcid.org/0000-0002-1274-0909
Ioannis Parodis: http://orcid.org/0000-0002-4875-5395
George Bertsias: http://orcid.org/0000-0001-5299-1406

## REFERENCES

[1] Nikolopoulos D, Kostopoulou M, Pieta A, Karageorgas T, Tseronis D, Chavatza K, et al. Evolving phenotype of systemic lupus erythematosus in Caucasians: low incidence of lupus nephritis, high burden of neuropsychiatric disease and increased rates of late-onset lupus in the 'Attikon' cohort. Lupus 2020;29(5):514–22.
[2] Nikolopoulos D, Fanouriakis A, Boumpas DT. Update on the pathogenesis of central nervous system lupus. Curr Opin Rheumatol 2019;31(6):669–77.
[3] Luyendijk J, Steens SCA, Ouwendijk WJN, Steup-Beekman GM, Bollen ELEM, van der Grond J, et al. Neuropsychiatric systemic lupus erythematosus: lessons learned from magnetic resonance imaging. Arthritis Rheum 2011;63(3):722–32.
[4] Padovan M, Castellino G, Bortoluzzi A, Caniatti L, Trotta F, Govoni M. Factors and comorbidities associated with central nervous system involvement in systemic lupus erythematosus: a retrospective cross-sectional case-control study from a single center. Rheumatol Int 2012 Jan;32(1):129–35.
[5] Bertsias GK, Boumpas DT. Pathogenesis, diagnosis and management of neuropsychiatric SLE manifestations. Nat Rev Rheumatol 2010 Jun;6(6):358–67.
[6] Frangou E, Garantziotis P, Grigoriou M, Banos A, Nikolopoulos D, Pieta A, et al. Cross-species transcriptome analysis for early detection and specific therapeutic targeting of human lupus nephritis. Ann Rheum Dis 2022;81(10):1409–19.
[7] Nikolakis D, Garantziotis P, Sentis G, Fanouriakis A, Bertsias G, Frangou E, et al. Restoration of aberrant gene expression of monocytes in systemic lupus erythematosus via a combined transcriptome-reversal and network-based drug repurposing strategy. BMC Genomics 2023 Dec 1;24(1):207.
[8] Makinde HM, Winter DR, Procissi D, Mike EV, Stock AD, Kando MJ, et al. A novel microglia-specific transcriptional signature correlates with behavioral deficits in neuropsychiatric lupus. Front Immunol 2020 Feb 26;11:230.
[9] Nikolopoulos DS, Kostopoulou M, Pieta A, Flouda S, Chavatza K, Banos A, et al. Transition to severe phenotype in systemic lupus erythematosus initially presenting with non-severe disease: implications for the management of early disease. Lupus Sci Med 2020;7(1):e000394.
[10] Adamichou C, Nikolopoulos D, Genitsaridi I, Bortoluzzi A, Fanouriakis A, Papastefanakis E, et al. In an early SLE cohort the ACR-1997, SLICC-2012 and EULAR/ACR-2019 criteria classify non-overlapping groups of patients: use of all three criteria ensures optimal capture for clinical studies while their modification earlier classification and treatment. Ann Rheum Dis 2020;79(2):232–41.
[11] Petri M, Orbai AM, Alarcón GS, Gordon C, Merrill JT, Fortin PR, et al. Derivation and validation of the Systemic Lupus International Collaborating Clinics classification criteria for systemic lupus erythematosus. Arthritis Rheum 2012 Aug;64(8):2677–86.
[12] Liang MH, Corzillius M, Bae SC, Lew RA, Fortin PR, Gordon C, et al. The American College of Rheumatology nomenclature and case definitions for neuropsychiatric lupus syndromes. Arthritis Rheumatol 1999 Apr;42(4):599–608.
[13] Fanouriakis A, Pamfil C, Rednic S, Sidiropoulos P, Bertsias G, Boumpas DT. Is it primary neuropsychiatric systemic lupus erythematosus? Performance of existing attribution models using physician judgment as the gold standard. Clin Exp Rheumatol 2016;34(5):910–7.
[14] Fanouriakis A, Kostopoulou M, Alunno A, Aringer M, Bajema I, Boletis JN, et al. 2019 update of the EULAR recommendations for the management of systemic lupus erythematosus. Ann Rheum Dis 2019;78(6):736–45.
[15] Nikolopoulos D, Fanouriakis A, Bertsias G. Treatment of neuropsychiatric systemic lupus erythematosus: clinical challenges and future perspectives. Expert Rev Clin Immunol 2021;17(4):317–30.
[16] Ainiala H, Hietaharju A, Loukkola J, Peltola J, Korpela M, Metsänoja R, et al. Validity of the new American College of Rheumatology criteria for neuropsychiatric lupus syndromes: a population-based evaluation. Arthritis Rheum 2001 Oct;45(5):419–23.
[17] Nikolopoulos D, Loukogiannaki C, Sentis G, Garantziotis P, Manolakou T, Kapsala N, et al. Disentangling the riddle of systemic lupus erythematosus with antiphospholipid syndrome: blood transcriptome analysis reveals a less-pronounced IFN-signature and distinct molecular profiles in venous versus arterial events. Ann Rheum Dis 2024;83(9):1132–43.
[18] Babraham Bioinformatics. FastQC: a quality control tool for high throughput sequence data [Internet]. [cited 2023 Dec 23]. Available from: https://www.bioinformatics.babraham.ac.uk/projects/fastqc/
[19] Anders S, Pyl PT, Huber W. HTSeq—a Python framework to work with high-throughput sequencing data. Bioinformatics 2015;31(2):166–9.
[20] Robinson MD, McCarthy DJ, Smyth GK. edgeR: a Bioconductor package for differential expression analysis of digital gene expression data. Bioinformatics 2010;26(1):139–40.
[21] Liberzon A, Birger C, Thorvaldsdóttir H, Ghandi M, Mesirov JP, Tamayo P. The Molecular Signatures Database (MSigDB) hallmark gene set collection. Cell Syst 2015 Dec 23;1(6):417–25.
[22] Sentis G, Loukogiannaki C, Malissovas N, Nikolopoulos D, Manolakou T, Flouda S, et al. A network-based approach reveals long non-coding RNAs associated with disease activity in lupus nephritis: key pathways for flare and potential biomarkers to be used as liquid biopsies. Front Immunol 2023;14:1203848.

[23] Langfelder P, Horvath S. WGCNA: an R package for weighted correlation network analysis. BMC Bioinformatics 2008;9:559.
[24] Szklarczyk D, Kirsch R, Koutrouli M, Nastou K, Mehryary F, Hachilif R, et al. The STRING database in 2023: protein-protein association networks and functional enrichment analyses for any sequenced genome of interest. Nucleic Acids Res 2023;51(D1):D638–46.
[25] Thomas M, Pedersen L. Package 'ggraph' 2022.
[26] Csardi G, Nepusz T. The igraph software package for complex network research. InterJournal Complex Systems 2006:1695. [Internet]Complex Sy (1695)Available from: http://igraph.sf.net.
[27] Nikolopoulos D, Manolakou T, Polissidis A, Filia A, Bertsias G, Koutmani Y, et al. Microglia activation in the presence of intact blood-brain barrier and disruption of hippocampal neurogenesis via IL-6 and IL-18 mediate early diffuse neuropsychiatric lupus. Ann Rheum Dis 2023;82(5):646–57.
[28] Asano T, Ito H, Kariya Y, Hoshi K, Yoshihara A, Ugawa Y, et al. Evaluation of blood-brain barrier function by quotient alpha2 macroglobulin and its relationship with interleukin-6 and complement component 3 levels in neuropsychiatric systemic lupus erythematosus. PLoS One 2017 Oct 1;12(10):e0186414.
[29] Hirohata S, Kikuchi H. Role of serum IL-6 in neuropsychiatric systemic lupus erythematosus. ACR Open Rheumatol 2021 Jan 1;3(1):42–9.
[30] Reynolds J, Huang M, Li Y, Meineck M, Moeckel T, Weinmann-Menke J, et al. Constitutive knockout of interleukin-6 ameliorates memory deficits and entorhinal astrocytosis in the MRL/lpr mouse model of neuropsychiatric lupus. J Neuroinflammation 2024 Dec 1;21(1):89.
[31] Hanly JG, Li Q, Su L, Urowitz MB, Gordon C, Bae SC, et al. Psychosis in systemic lupus erythematosus: results from an international inception cohort study. Arthritis Rheumatol 2019 Feb 1;71(2):281–9.
[32] Manolakou T, Nikolopoulos D, Gkikas D, Filia A, Samiotaki M, Stamatakis G, et al. ATR-mediated DNA damage responses underlie aberrant B cell activity in systemic lupus erythematosus. Sci Adv 2022;8(43):eabo5840.
[33] Xu R, Ji Z, Xu C, Zhu J. The clinical value of using chloroquine or hydroxychloroquine as autophagy inhibitors in the treatment of cancers: a systematic review and meta-analysis. Medicine (Baltimore) 2018;97(46):e12912.
[34] Group Canadian Hydroxychloroquine Study. A randomized study of the effect of withdrawing hydroxychloroquine sulfate in systemic lupus erythematosus. N Engl J Med 1991 Jan 17;324(3):150–4.
[35] Dörner T. Therapy: hydroxychloroquine in SLE: old drug, new perspectives. Nat Rev Rheumat 2010;6(1):10–1.
[36] Palazzo L, Lindblom J, Cetrez N, Ala H, Parodis I. Determinants of neuropsychiatric flares in patients with systemic lupus erythematosus: results from five phase III trials of belimumab. Rheumatology (Oxford) 2024 Mar 1;63(3):798–808.
[37] Petri M, Konig MF, Li J, Goldman DW. Association of higher hydroxychloroquine blood levels with reduced thrombosis risk in systemic lupus erythematosus. Arthritis Rheumatol 2021 Jun 1;73(6):997–1004.
[38] Iershov A, Nemazanyy I, Alkhoury C, Girard M, Barth E, Cagnard N, et al. The class 3 PI3K coordinates autophagy and mitochondrial lipid catabolism by controlling nuclear receptor PPAR$\alpha$. Nat Commun 2019 Apr 5;10(1):1566.
[39] Cohen D, Rijnink EC, Nabuurs RJA, Steup-Beekman GM, Versluis MJ, Emmer BJ, et al. Brain histopathology in patients with systemic lupus erythematosus: identification of lesions associated with clinical neuropsychiatric lupus syndromes and the role of complement. Rheumatology (Oxford) 2017 Jan;56 (1):77–86 [cited 2019 Jun 1]Available from: https://academic.oup.com/rheumatology/article-lookup/doi/10.1093/rheumatology/kew341.
[40] Nestor J, Arinuma Y, Huerta TS, Kowal C, Nasiri E, Kello N, et al. Lupus antibodies induce behavioral changes mediated by microglia and blocked by ACE inhibitors. J Exp Med 2018;215(10):2554–66.
[41] Alexander JJ, Jacob A, Bao L, Macdonald RL. Quigg RJ. Complement-dependent apoptosis and inflammatory gene changes in murine lupus cerebritis. J Immunol 2005;175(12):8312–9.
[42] Cohen D, Rijnink EC, Nabuurs RJA, Steup-Beekman GM, Versluis MJ, Emmer BJ, et al. Brain histopathology in patients with systemic lupus erythematosus: identification of lesions associated with clinical neuropsychiatric lupus syndromes and the role of complement. Rheumatology (Oxford) 2017;56(1):77–86.
[43] Absinta M, Maric D, Gharagozloo M, Garton T, Smith MD, Jin J, et al. A lymphocyte-microglia–astrocyte axis in chronic active multiple sclerosis. Nature 2021 Sep 8;597(7878):709–14 [Internet][cited 2025 Jan 8]Available from: https://www.nature.com/articles/s41586-021-03892-7.
[44] Osman M, Cohen Tervaert JW, Pagnoux C. Avacopan for the treatment of ANCA-associated vasculitis: an update. Expert Rev Clin Immunol 2023;19(5):461–71.
[45] Wright RD, Bannerman F, Beresford MW, Oni L. A systematic review of the role of eculizumab in systemic lupus erythematosus-associated thrombotic microangiopathy. BMC Nephrol 2020;21(1):245.
[46] Pamfil C, Fanouriakis A, Damian L, Rinzis M, Sidiropoulos P, Tsivgoulis G, et al. EULAR recommendations for neuropsychiatric systemic lupus erythematosus vs usual care: results from two European centres. Rheumatology (Oxford) 2015;54(7):1270–8.
[47] Angeletti A, Baraldi O, Chiocchini AL, Comai G, Cravedi P, La Manna G. Rituximab as first-line therapy in severe lupus erythematosus with neuropsychiatric and renal involvement: a case-report and review of the literature. J Clin Case Rep 2017;7(10):1033.
[48] Tokunaga M, Saito K, Kawabata D, Imura Y, Fujii T, Nakayamada S, et al. Efficacy of rituximab (anti-CD20) for refractory systemic lupus erythematosus involving the central nervous system. Ann Rheum Dis 2007 Apr 19;66 (4):470–5 [Internet][cited 2019 Jun 1]Available from: http://ard.bmj.com/cgi/doi/10.1136/ard.2006.057885.
[49] McCarthy EM, Sutton E, Nesbit S, White J, Parker B, Jayne D, et al. Short-term efficacy and safety of rituximab therapy in refractory systemic lupus erythematosus: results from the British Isles Lupus Assessment Group Biologics Register. Rheumatology (Oxford) 2018 Mar 1;57(3):470–9.
[50] Furie RA, Aroca G, Cascino MD, Garg JP, Rovin BH, Alvarez A, et al. B-cell depletion with obinutuzumab for the treatment of proliferative lupus nephritis: a randomised, double-blind, placebo-controlled trial. Ann Rheum Dis 2022 Jan 1;81(1):100–7.
[51] Mackensen A, Müller F, Mougiakakos D, Böltz S, Wilhelm A, Aigner M, et al. Anti-CD19 CAR T cell therapy for refractory systemic lupus erythematosus. Nat Med 2022 Oct 1;28(10):2124–32.
[52] Tur C, Eckstein M, Velden J, Rauber S, Bergmann C, Auth J, et al. CD19-CAR T-cell therapy induces deep tissue depletion of B cells. Ann Rheum Dis 2025;84(1):106–14.
[53] Müller F, Taubmann J, Bucci L, Wilhelm A, Bergmann C, Völkl S, et al. CD19 CAR T-cell therapy in autoimmune disease—a case series with follow-up. N Engl J Med 2024 Feb 22;390(8):687–700.

Ann Rheum Dis 84 (2025) 1354–1362

Contents lists available at ScienceDirect

Annals of the Rheumatic Diseases

journal homepage: https://www.sciencedirect.com/journal/annals-of-the-rheumatic-diseases

Sjögren Syndrome

# A cross-sectional observational study of patients with sicca with salivary autoantibodies defines a potential new phenotype of Sjögren's disease

Martha Tsaliki[1,2,3], Joshua Cavett[1,3], Biji T. Kurien[1,3], Christina Bruxvoort[1,2,3], Valerie M. Lewis[1,3], John A. Ice[1,3], Devavrat Dave[1,4], Sina Khosravani[1], Kiely Grundahl[1,5], Christopher J. Lessard[2,5], Astrid Rasmussen[5], Kathy L. Sivils[1], Amy Darise Farris[1], Kristi A. Koelsch[1], Robert Hal Scofield[1,3,4,*]

[1] *Arthritis and Clinical Immunology Research Program, Oklahoma Medical Research Foundation, Oklahoma City, Oklahoma*
[2] *Department of Pathology, University of Oklahoma Health Sciences Center, Oklahoma City, Oklahoma*
[3] *Oklahoma City US Department of Veterans Affairs Medical Center, Oklahoma City, Oklahoma*
[4] *Departments of Medicine and Pathology, College of Medicine, University of Oklahoma Health Sciences Center, Oklahoma City, Oklahoma*
[5] *Genes and Human Diseases Research Program, Oklahoma Medical Research Foundation, Oklahoma City, Oklahoma*

ARTICLE INFO

ABSTRACT

*Objectives:* Diagnosis of Sjögren's disease (SjD) consists of clinical examinations that include invasive studies such as lower lip biopsies and blood collection to identify presence of serum autoantibodies. Salivary glands of patients with SjD are sites where antibody-secreting cells accumulate and secrete immunoglobulins. Many patients with dry manifestations who do not meet classification criteria are grouped as non-Sjögren's sicca (NSS) and are heavily understudied. We undertook this cross-sectional observational study to investigate the role of salivary autoantibodies as a diagnostic tool and determine presence of salivary autoantibodies in patients with NSS.

*Methods:* In this cross-sectional observational study, we screened whole unstimulated saliva from 446 subjects by direct enzyme-linked immunosorbent assays and capillary western blotting for anti-Ro60, anti-La, and rheumatoid factor (immunoglobulin (Ig)G and IgA) antibodies. All subjects were classified following the ACR/EULAR classification at the Oklahoma Medical Research Foundation Sjögren's Research Clinic.

*Results:* Patients with SjD were significantly more likely to have salivary antibodies compared with those with NSS and healthy control subjects. In this cohort, there were 88 subjects with NSS with seronegative profiles who had detectable salivary autoantibodies and objective measures of dryness.

*Conclusions:* Of these 88 subjects with NSS, we identified 75 subjects that had positive objective examinations of dryness and could belong to an early-onset SjD group. Alternatively, these 75 subjects with NSS could belong to a distinct phenotype of SjD that will remain seronegative while being saliva positive for anti-Ro60. These data showed a relationship between ocular and oral dryness and the presence of salivary anti-Ro60 antibodies in subjects with NSS.

*Correspondence to Dr. R. Hal Scofield, Arthritis & Clinical Immunology Program, Oklahoma Medical Research Foundation, 825 NE 13th Street, Oklahoma City, OK 73104, USA.

*E-mail address:* hal-scofield@omrf.ouhsc.edu (R.H. Scofield).

**Handling editor** Josef S. Smolen.

https://doi.org/10.1016/j.ard.2025.03.012

0003-4967/Published by Elsevier B.V. on behalf of European Alliance of Associations for Rheumatology (EULAR).

**WHAT IS ALREADY KNOWN ON THIS TOPIC**

- Salivary autoanibodies are known to be present in some SjD patients.

**WHAT THIS STUDY ADDS**

- We studied salivary autoantibodies in patients with sicca but who did not meet the classification criteria and were not diagnosed with SjD.

**HOW THIS STUDY MIGHT AFFECT RESEARCH, PRACTICE OR POLICY**

- Patients with clinical features of SjD who have salivary anti-Ro60, but no serum autoantibody, constitute a new phenotype of SjD. The mechanisms by which salivary autoantibodies are produced without serum autoantibodies needs investigation.

## INTRODUCTION

Sjögren's disease (SjD) is a chronic inflammatory exocrinopathy characterised by autoimmune-related involvement of the lacrimal and salivary glands. The most common manifestations are persistent dry mouth (xerostomia) and dry eyes (xerophthalmia) [1]. A third of patients experience systemic disease, developing extraglandular complications involving many organ systems, some of which can be debilitating or even life threatening [1,2]. SjD is the second most common rheumatic disease, estimated to affect 1% of the world population [1]. Although this disease affects individuals of all age groups, postmenopausal women specifically demonstrate higher risk for developing SjD [3]. Currently, there is no cure or disease-modifying therapy for SjD. Typical symptomatic treatments include application of artificial saliva and tears, anti-inflammatory eye drops, pain relief, cholinergic agents, glucocorticoids, and antifungals [4]. SjD is a complex and multifactorial disease in which patients must often consult with multiple specialists, adding complexity in diagnosing and managing SjD [1].

Clinical diagnosis and/or research classification of SjD involves invasive examinations, like minor salivary gland lip biopsies to evaluate salivary gland immune infiltrates, along with serologic testing as well as dental and ophthalmologic examinations, to determine the severity of dryness [5]. Patients are then classified as either those with SjD alone or those with overlap disease of SjD plus an existing autoimmune disease, most commonly, rheumatoid arthritis or systemic lupus erythematosus [5,6]. Many patients who present into the clinic with dry manifestations do not meet the ACR/EULAR SjD classification criteria, and these patients are grouped in non-Sjögren's sicca (NSS), sicca refering to their dry symptoms [5]. These patients with NSS have a large unmet health need, and although they have increased subjective dryness, they are understudied and commonly excluded from clinical trials [7]. Within our Oklahoma Medical Research Foundation (OMRF) Sjögren's clinic cohort, subjects who belong to NSS group (48%) are more common than patients with SjD (38%).

Histologic assessment of labial salivary gland biopsy frequently shows the presence of lymphocytic infiltrates in SjD salivary glands; these mononuclear cell infiltrates are counted in defined areas with inflammatory foci, defined by the presence of at least 50 inflammatory cells, per 4.0 $mm^2$ glandular section (focus score), which is used to classify and diagnose disease [5,6,8]. The most commonly observed autoantibodies in SjD sera are anti-Ro60, (or Sjögren's syndrome A (SSA), found in 60%-80% of patients) and anti-La (or Sjögren's syndrome B (SSB), found in 40%-60% of patients) [9]. Anti-Ro60 and anti-La have shown association with glandular dysfunction and disease severity, with anti-Ro60 constituting a biological measurement for purposes of SjD research classification [6]. Furthermore, rheumatoid factor (RF) is very common in SjD sera, found in 40% to 60% of patients, and is also associated with other rheumatic disorders [9,10].

Studies have shown the presence of autoantibodies in SjD sera years before clinical onset of the disease [11,12]. In addition, antibody-secreting cells (ASCs) localise in the salivary glands of patients with SjD and play an important role in disease pathogenesis [13–16]. Studies have shown decreases in peripheral blood memory B cells of patients with SjD that are specific to anti-Ro60 and anti-La memory B cells; furthermore, these cells target the inflamed salivary glands [17]. These ASCs infiltrating the salivary glands of patients with NSS and those with SjD could be the source of the autoantibodies observed in peripheral plasma and saliva. In a cohort of 269 patients with SjD, 28% had germinal centre-like architecture in their minor salivary gland biopsies; the presence of these structures was associated with high serum titres of anti-Ro60 and anti-La autoantibodies [14]. In an independent cohort of 25 patients with SjD, 21 had salivary anti-La (IgA) antibodies that were secreted by ASCs localised to inflamed salivary gland tissue [18].

A previous study screened tears of 28 patients with SjD and found positive correlation between tear and serum titres of anti-Ro60 and anti-La antibodies [19]. In the same study, the authors reported a significant positive correlation ($r = 0.56$; $P = .002$) between tear anti-La concentrations and dry eye symptoms [19]. Furthermore, in a similar study, investigators screened tears of seronegative patients and detected anti-Ro60 and/or anti-La antibodies [20].

Tears and saliva are both direct products of inflamed lacrimal and salivary glands in SjD. It is possible that autoantibodies will be present in such bodily fluids prior or even without being detectable in serum. Saliva and tears could be key biofluids for SjD classification, diagnosis, and research, and these fluids can be collected via noninvasive methods. In this study, we aimed to investigate the presence of common autoantibodies in the saliva of SjD and subjects with NSS while comparing them with those of healthy controls (HCs). Further, we aimed to associate their salivary immunoglobulin profiles (IgG vs IgA) to the clinical manifestations of SjD.

## METHODS

### *Human subject sample collection*

In this cross-sectional observational study, we screened previously collected and frozen whole unstimulated saliva samples from 175 patients with SjD, 225 patients with NSS, and 46 HC subjects under blinded conditions (Table), obtained from the OMRF Sjögren's Research Clinic repository. All study participants gave informed consent. This study was approved by the University of Oklahoma Health Sciences Center and OMRF Institutional Review Boards. There was no public or SjD patient involvement in the development of the study. All participants were evaluated at the OMRF Sjögren's Research Clinic and classified based on the 2016 ACR/EULAR Sjögren's Classification criteria [6]. Eligibility for inclusion of participants was based on classification criteria for SjD, NSS, or HC [6], along with availability of sufficient saliva volumes and clinical data. Owing to

Table
**Subject demographics, clinical criteria, and characteristics**

| Classification | Healthy controls (n = 46), n (%) | NSS (n = 225), n (%) | SjD (n = 175), n (%) | NSS vs SjD, *P* |
|---|---|---|---|---|
| Sex (F/M; ratio) | 36/10 (4:1)[a,b] | 213/12 (18:1) | 159/16 (10:1) | NS |
| Race (%) | | | | |
| White | 39 (85)[a,b] | 128 (57) | 95 (54) | NS |
| Black | 1 (2) | 6 (3) | 7 (4) | NS |
| American Indian/Alaskan Native | 0 (0) | 7 (3) | 13 (7) | NS |
| Asian | 2 (4) | 4 (2) | 3 (2) | NS |
| More than 1 race | 3 (7)[a,b] | 77 (34) | 56 (32) | NS |
| Unknown | 1 (2) | 3 (1) | 1 (0.5) | NS |
| Age (y), mean/median/SD | 42/42/±14.55[a,b] | 49/49/±13.32 | 55/56/±13.60 | <.0001 |
| Subjective criteria (% positive) | | | | |
| Dry eyes | 0 (0)[a,b] | 217 (96) | 172 (98) | NS |
| Dry mouth | 0 (0)[a,b] | 219 (97) | 173 (99) | NS |
| Objective criteria (% positive) | | | | |
| Lissamine green/van Bijsterveld positive | 0 (0)[a,b] | 84 (37) | 101 (58) | <.0001 |
| Schirmer positive | 0 (0)[a,b] | 59 (26) | 75 (43) | .0006 |
| WUSF positive | 0 (0)[a,b] | 105 (47) | 111 (63) | .0012 |
| Focus score positive | 0 (0)[a,b] | 17 (7.5) | 153 (87) | <.0001 |
| Serum anti-Ro60 | 0 (0)[a,b] | 3 (1) | 83 (47) | <.0001 |
| Serum anti-La | 0 (0)[a,b] | 15 (7) | 47 (27) | <.0001 |
| Clinical measures (% positive) | | | | |
| Serum rheumatoid factor | 1 (2) | 18 (8) | 47 (27) | <.0001 |
| ANA positive | NA | 148 (66) | 143 (82) | .0004 |
| IgG (mg/dL), mean ± SD | NA | 974 ± 250 | 1155 ± 353 | <.0001 |
| IgM (mg/dL), mean ± SD | NA | 113 ± 58 | 124 ± 77 | NS |
| IgA (mg/dL), mean ± SD | NA | 216 ± 94 | 233 ± 102 | NS |
| Concurrent disease (% positive) | | | | |
| Any concurrent disease | 1 (2)[a] | 62 (27) | 44 (25) | NS |
| Fibromyalgia | 0 (0)[a] | 29 (13) | 17 (10) | NS |
| AITD | 0 (0)[a] | 24 (11) | 20 (11) | NS |
| T1D | 0 (0) | 2 (1) | 0 (0) | NS |
| Psoriasis | 1 (2) | 7 (3) | 7 (4) | NS |
| Neuromyelitis optica | 0 (0) | 0 (0) | 1 (1) | NS |
| Celiac disease | 0 (0) | 0 (0) | 1 (1) | NS |

AITD, autoimmune thyroid disease; ANA, antinuclear antibody; F/M, female/male, NA, not applicable; NS, not significant; NSS, non-Sjögren's sicca; SjD, Sjögren's disease; T1D, Type 1 diabetes; WUSF, whole unstimulated salivary flow.
[a] Difference in values between HC and NSS.
[b] Difference in values between HC and pSS.

our participant recruitment qualification design, the subjective criteria (patient reported dry eyes and mouth) were comparable between the NSS and SjD groups. The clinical data of this cohort were available for our analysis. Serum antibodies were assessed using data from the OMRF Sjögren's Research Clinic, where detection is routinely performed using validated commercial assays, including BioPlex, Inno-Lia, ELISA, and double immunodiffusion [21]. The individuals who performed the analyses and experiments were unaware of the sample identities or group assignments (eg, SjD, NSS, and HC) to ensure unbiased interpretation of data.

### *Saliva enzyme-linked immunosorbent assay*

Whole unstimulated saliva samples were screened to detect presence of anti-Ro60, anti-La, and RF autoantibodies, IgG and IgA, by direct enzyme-linked immunosorbent assays (ELISAs). The anti-Ro60 and anti-La ELISAs were developed in-house using Enhanced Binding Immuno Breakable Module plates (ThermoFisher). These plates were coated overnight at 4 °C, with 50 $\mu$L of either Ro60 (1 unit/well) or La (2 units/well; 1 unit of activity is defined as the amount of antigen that will generate an absorbance of 1.2; ImmunoVision) using carbonate coating buffer. The plates were washed and blocked for 1 hour at 37 °C. Saliva samples (1:20 dilution) run in duplicate were incubated for 2 hours at 37 °C. Binding was detected following 1 hour incubation, at 37 °C with alkaline phosphatase-conjugated secondary antibodies, goat antihuman IgA (#109-055-088) and goat antihuman IgG (#109-055-011), respectively (Jackson ImmunoResearch). We used *p*-nitrophenylphosphate as the substrate and read the plates (405 nm, approximately 60 minutes) until the positive control reached an optical density (OD) signal of 1.0 [22]. To correct for potential nonspecific absorption, the OD signal at 650 nm was subtracted from the substrate-specific signal at 405 nm. The OD of each sample was corrected by subtracting the blank OD at 405 nm. Each sample's mean OD was normalised by dividing it by the mean OD of the positive control on the same plate, with the result expressed as units. Positive thresholds were determined by calculating the mean units plus 3 SDs of the HCs.

The IgA and IgG RF ELISAs were performed using commercial serum-based QUANTA Lite RF ELISA kits (#708695 and #708685; Inova Diagnostics) according to manufacturer's protocols with minor modifications to accommodate saliva samples. Specifically, samples were diluted 1:20 using the kit diluent and tested in duplicate. The positive thresholds were determined by calculating the mean absorbance (450 nm) + 3SD of the HC samples.

### *Salivary western blot testing*

Capillary western blot testing was performed on samples that were positive for Ro60 and/or La binding by ELISA using recombinant human Ro60 and La proteins (#A174 and #A128; Surmodics IVD). The assay was carried out with Jess from Protein Simple (Bio-Techne Brands) according to manufacturer's

instructions using 25-capillary cartridges, assay plates containing milk-free blocking/diluent, separating and stacking matrix, as well as wash buffers, all purchased from Protein Simple. Salivary anti-Ro60 or anti-La IgG or IgA were then detected in individual capillaries. Briefly, Ro60 or La was separated at 375 V for 25 minutes on a reducing matrix at 20.0 $\mu$g/mL in individual capillaries. After the run, the separated proteins are crosslinked to the wall of the capillary tube by ultraviolet light and the matrix is eluted from the capillary. The wall of the capillary now behaves as a membrane does in traditional western blots. The capillaries aspirate and hold milk-free diluent for 5 minutes to block nonspecific binding sites. After ejection of the blocking, the capillaries aspirate and hold human saliva as the primary antibody (diluted at 1:25 with milk-free diluent), along with goat antihuman IgA $\alpha$-chain−specific biotin conjugate (diluted 1:100), for 60 minutes. We used goat antihuman IgA biotin conjugate as a signal amplification method to augment the IgA anti-Ro60 and anti-La signal response. Next, the primary antibody were flushed out of the capillaries by washing with diluent and then the secondary antibody was incubated for 30 minutes. This secondary antibody is a mixture of streptavidin-conjugated horseradish peroxidase (1:100) and goat antihuman IgG horseradish peroxidase conjugate (1:100). Signal was detected by the chemiluminescence method using luminol and hydrogen peroxide provided (Protein Simple; Bio-Techne Brands). Results obtained were analysed using the Compass software by Protein Simple.

### *Statistical analysis*

To analyse the presence of autoantibodies and their associations with clinical measures, we used descriptive statistics. All statistical analyses were performed using GraphPad Prism software (version 9.4, GraphPad Software) and Microsoft Excel (version 19.89.1, Microsoft Corporation, Redmond, WA). Data points with a coefficient of variation over the allowable threshold of 10% were removed from the analysis, which resulted in sample totals that may differ from the original group totals.

We categorised antibody presence into binary outcomes (positive vs negative) using thresholds set at the mean + 3 SDs of HCs. For clinical measures like salivary flow and ocular staining, we grouped the data based on clinically relevant cutoffs (eg, normal vs impaired function).

To compare antibody presence between 2 or more groups (eg, SjD, NSS, and HC), we used nonparametric tests, including the Mann−Whitney $U$ test for 2-group comparisons and the Kruskal−Wallis test for 3-group comparisons. For categorical comparisons (eg, positive vs negative autoantibody status), we used $\chi^2$ or Fisher exact tests. Correlations between antibody levels and clinical scores (such as whole unstimulated salivary flow [WUSF]; BioPlex) were assessed using Spearman rank correlation coefficient ($r$), and 95% CIs were calculated to evaluate the strength and direction of associations. Statistical significance was determined using a 2-tailed $P$ value, with the significance threshold set at $\alpha = 0.05$. We considered $P$ values of <.05 to be statistically significant.

## RESULTS

We examined saliva from 175 patients with SjD, 225 patients with NSS, and 46 HC subjects for the presence of autoantibodies and then compared their presence with clinical criteria and disease severity. We have summarised relevant demographics and clinical characteristics of this cohort in Table. As expected, in both patients with NSS and those with SjD, the objective criteria mirrored the larger OMRF Sjögren's cohort. Of note, 17 subjects in the NSS group demonstrated a positive focus score (≥1 foci on minor salivary gland histology). Serum immunoglobulin levels were available for most of these subjects (Table). The clinical serum IgG levels decreased significantly in subjects with NSS compared with those in patients with SjD ($P < .001$, Mann−Whitney test), but we found no difference in serum IgM levels between the 2 groups (Table). The rates and types of concurrent diseases were comparable between the NSS and SjD groups (Table).

Salivary anti-Ro60 autoantibodies, combining IgG and IgA, showed a significant higher prevalence among SjD (71%) compared with those with NSS (40%), and both NSS and SjD groups showed significantly higher levels than the HC (7%) group ($P <$ .0001) (Fig 1A). Similarly, salivary anti-La autoantibodies, of IgG and IgA combined, were significantly more common among patients with SjD (50%) than those among patients with NSS (38%; Fisher exact, $P = .02$) and HC (2%) subjects (Fisher exact, $P <$ .0001) (Fig 1B). In turn, subjects with NSS had significantly more anti-La antibodies compared with HCs (Fisher exact, $P <$ .0001) (Fig 1B). RF IgG and IgA ELISAs showed significant prevalence of autoantibodies in SjD (31%) compared with that in those with NSS (12%; Fisher exact, $P < .0001$) and HCs (4%; Fisher exact, $P = .0002$), while there was no significant difference between patients with NSS and HCs (Fisher exact, $P = .18$) (Fig 1C).

In further analysis, we focused exclusively on anti-Ro60−positive subjects, as the presence of serum anti-Ro60 is a key component of the classification criteria [6]. Combined ELISA and capillary western blot results showed that 122 of 175 (70%) patients with SjD and 89 of 225 (40%) subjects with NSS showed positive results for salivary anti-Ro60 antibodies (IgG/IgA). Of those subjects with salivary anti-Ro60 antibodies, 51 of 122 (42%) patients with SjD and 88 of 89 (99%) patients with NSS were seronegative for these autoantibodies (Supplementary Figs S1 and S2). There were 12 of 53 (23%) patients with SjD and 2 of 136 (1.5%) subjects with NSS who showed negative results for salivary anti-Ro60 but positive results in the sera (Fig 2, Supplementary Fig S3). From the HC group, 3 of the 46 (6.5%) subjects had salivary autoantibodies and were seronegative. No subject in the HC group had anti-Ro60 antibodies in their serum.

We then compared subjects with NSS with or without the presence of salivary anti-Ro60, in terms of their clinical objective examinations of dryness. Ocular staining scores were similar between subjects with NSS with salivary anti-Ro60 antibodies (NSS+; 39%) and those without (NSS-; 38%; Fisher exact, $P = .78$; odds ratio [OR], 1.1; 95% CI, 0.64-1.92) (Fig 3A). There was a significant difference in Schirmer test results, indicating ocular dryness, between NSS+ subjects (34%) and NSS- subjects (21%; Fisher exact test, $P = .045$; OR, 1.88; 95% CI, 1-3.37) (Fig 3B). WUSF scores showed no significant difference between NSS+ subjects (53%) and NSS- subjects (43%; Fisher exact test, $P = .17$; OR, 1.5; 95% CI, 0.9-2.56) (Fig 3C). These results indicate a distinction between NSS+ and NSS- subjects in terms of their objective measures of lacrimal gland function, with those having salivary anti-Ro60 significantly more likely to have abnormal Schirmer test results.

Several patients with NSS (n = 88) with salivary anti-Ro60 but negative sera were abnormal in their objective examinations of dryness (Fig 2, Supplementary Fig S1). Of these 88 subjects with NSS, we identified 75 seronegative subjects with NSS with salivary anti-Ro60 and positive objective examinations that

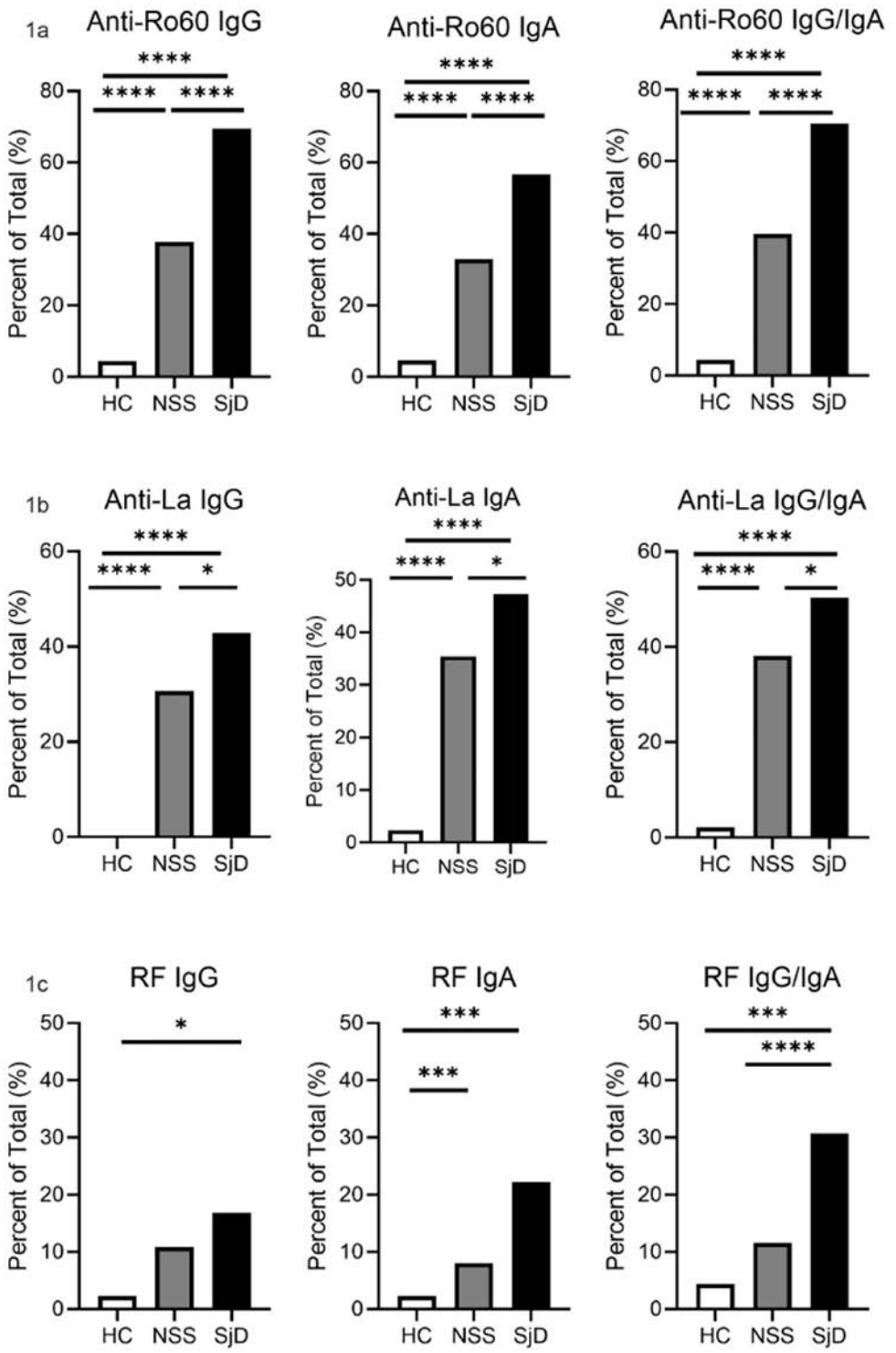



**Figure 1.** Combined ELISA and capillary western blot results representing the presence of anti-Ro60, anti-La, and rheumatoid factor (RF) autoantibodies in healthy controls (HCs) and in patients with non-Sjögren's sicca (NSS) and Sjögren's disease (SjD). A, Patients with SjD (67%) were significantly more likely to test positive for anti-Ro60 IgG compared with those with NSS (38%) and HCs (4%; $P$ <.0001). Additionally, subjects with NSS were significantly more likely to test positive compared with HCs ($P < .0001$). Patients with SjD (57%) were significantly more likely to test positive for anti-Ro60 IgA compared with those with NSS (33%) and HCs (5%; $P < .0001$). However, subjects with NSS were significantly more likely to test positive compared with HCs ($P < .0001$). When combining IgG and IgA results, patients with SjD (71%) were significantly more likely to test positive for anti-Ro60 antibodies compared with those with NSS (40%) and HCs (7%; $P < .0001$). Moreover, subjects with NSS were significantly more likely to test positive compared with HCs ($P < .0001$). B, Patients with SjD (43%) were significantly more likely to test positive for anti-La IgG compared with those with NSS (38%; $P = .02$) and HCs (0%; $P < .0001$). Additionally, subjects with NSS were significantly more likely to test positive compared with HCs ($P < .0001$). Patients with SjD (47%) were significantly more likely to test positive for anti-La IgA compared with those with NSS (35%; $P = .02$) and HCs (2%; $P < .0001$). However, subjects with NSS were significantly more likely to test positive compared with HCs ($P < .0001$). When combining IgG and IgA results, patients with SjD (50%) were significantly more likely to test positive for anti-La antibodies compared with those with NSS (38%; $P = .02$) and HCs (2%; $P < .0001$). Subjects with NSS were significantly more likely to test positive compared with HCs ($P < .0001$). C, Patients with SjD (17%) showed no significant difference in RF IgG positivity compared with those with NSS (11%; $P = .09$) but were significantly more likely to test positive compared with HCs (4%; $P = .0002$). Subjects with NSS were not significantly different from HCs ($P = .18$). Patients with SjD (22%) were significantly more likely to test positive for RF IgA compared with those with NSS (8%; $P < .0001$) and HCs (2%; $P = .0008$). Subjects with NSS

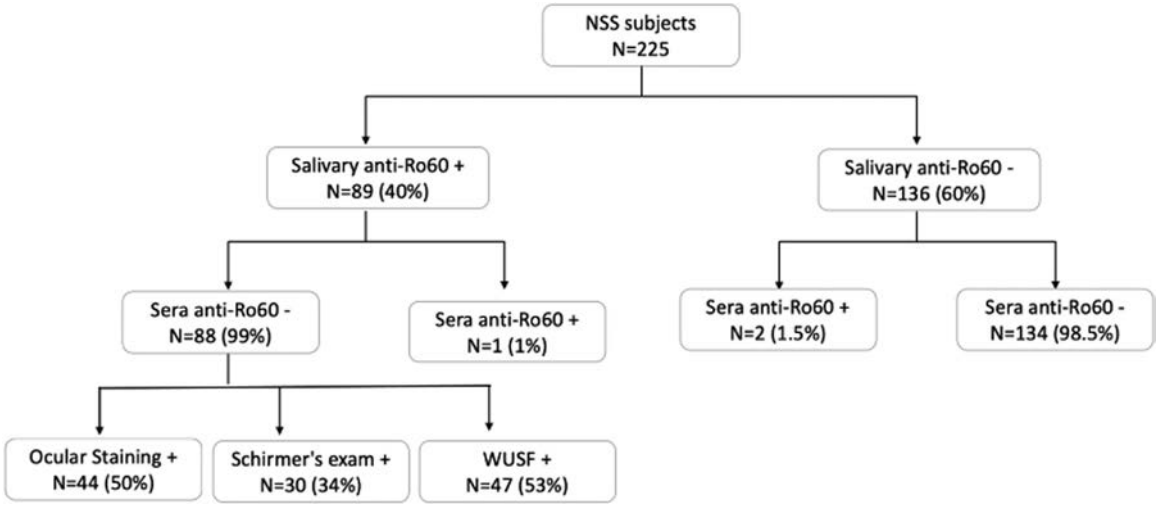



**Figure 2.** Breakdown of subjects with non-Sjögren's sicca (NSS) according to their salivary and sera anti-Ro60 positivity. Data represent results of combined ELISA and capillary western blot assays. Representation of subjects with NSS that had sera and/or saliva anti-Ro60 antibody presence. Of the 225 subjects with NSS, 89 (40%) were positive for salivary anti-Ro60. Of these 89 subjects with NSS, 88 (99%) were seronegative but had positive objective examinations, such as ocular staining score (n = 44, 50%), Schirmer examination (n = 30, 34%), and whole unstimulated salivary flow (WUSF; n = 47, 53%).

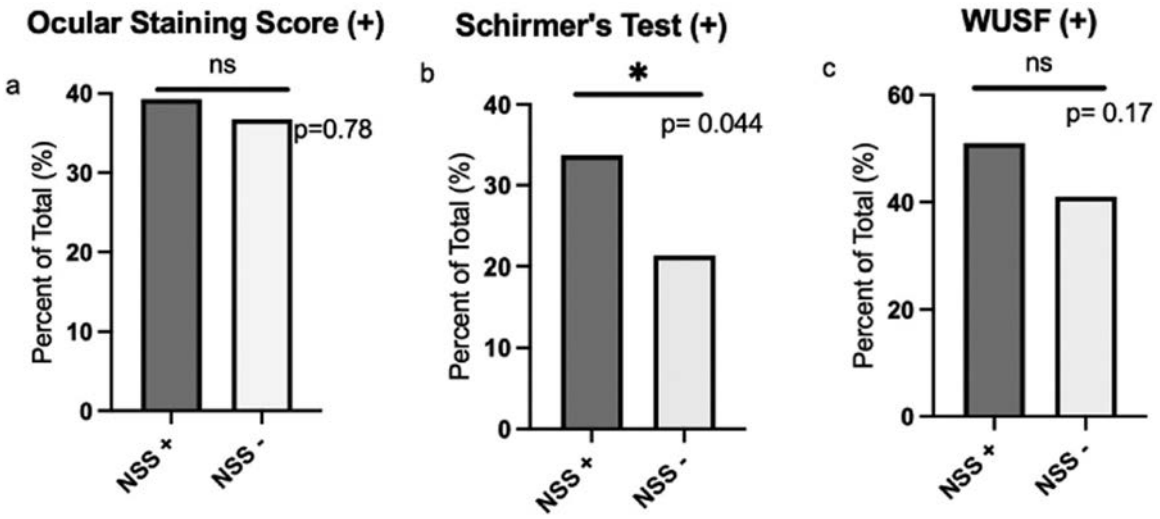



**Figure 3.** Comparison of subjects with non-Sjögren's sicca (NSS) with (+) or without (−) salivary anti-Ro60 antibodies and their positive scores on objective clinical examinations assessing dryness. Data represent the results of combined ELISA and capillary western blot assays. A, Ocular staining scores were similar between NSS+ (39%) and NSS- (38%; $P$ = .78; OR, 1.1; 95% CI, 0.64-1.92). B, Subjects with NSS+ (34%) were significantly more likely to have abnormal Schirmer test results compared with those with NSS- (21%; $P$ = .045; OR, 1.88; 95% CI, 1-37). C, Whole unstimulated salivary flow (WUSF) scores showed no significant difference between NSS+ (53%) and NSS- (43%; $P$ = .17; OR, 1.5; 95% CI, 0.9-2.56).

could have been classified as SjD if salivary anti-Ro60 was part of the ACR/EULAR classification (Supplementary Fig S1). For the following analysis, these 75 subjects with NSS are described as reclassified Sjögren's disease (R-SjD). Subjects with R-SjD exhibited distinct objective examinations of dryness compared with the rest of the NSS group, closely resembling those scores observed in the SjD group (Fig 3). The R-SjD (43%) group tend to be more likely to have a positive ocular staining examination compared with the NSS (36%) group ($P$ = .4975), with an OR of 0.57 (95% CI, 0.33-0.99) (Fig 4A). SjD (58%) and NSS groups showed a significant difference ($P$ < .0001) with an OR of 0.35 (95% CI, 0.22-0.54) (Fig 4A), while R-SjD and SjD groups were not significantly different ($P$ = .27), with an OR of 0.61 (95% CI, 0.35-1.00) (Fig 4A). Interestingly, when assessing Schirmer test, the R-SjD (40%) group was significantly more likely to have an abnormal tear flow compared with NSS(19%; $P$ = .001; OR, 0.36; 95% CI, 0.2-0.7). Likewise, patients with SjD (43%) were significantly more likely to have positive Schirmer test compared with subjects with NSS ($P$ < .0001) with an OR of 0.32 (95% CI, 0.19-0.52) (Fig 4B). We did not find statistical differences between SjD and R-SjD groups ($P$ = .78), with OR being 0.89 (95% CI, 0.52-1.53) (Fig 4B). Subjects with R-SjD (63%) were significantly more likely to have an abnormal WUSF score compared with those with NSS (39%) ($P$ = .001), with an OR of 0.38 (95% CI, 0.21-0.67); similar to patients with SjD (63%), who were also significantly more likely to have abnormal WUSF

were not significantly different from HCs ($P$ = .21). When combining IgG and IgA results, patients with SjD (31%) were significantly more likely to test positive compared with those with NSS (12%; $P$ < .0001) and HCs (4%; $P$ = .0002). Subjects with NSS were not significantly different from HC ($P$ = .18). All RF data derived from ELISA assays.

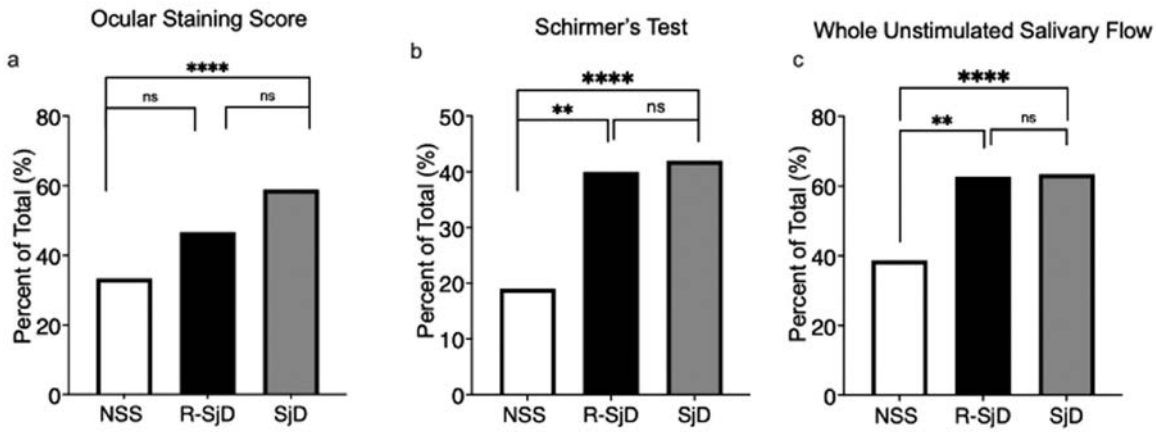



**Figure 4.** Subjects with non-Sjögren's sicca (NSS) classified as reclassified Sjögren's disease (R-SjD), based on the presence of salivary anti-Ro60 autoantibodies, exhibit clinical objective examinations of dryness that are nearly identical to those of subjects with SjD. A, Ocular staining scores were higher in patients with R-SjD (43%) compared with those in subjects with NSS (36%; $P = .4975$). R-SjD and Sjögren's disease (SjD; 58%) groups were not significantly different ($P = .27$), while scores of SjD group were significantly higher than those of NSS group ($P < .0001$). B, Schirmer test scores were significantly higher in patients with R-SjD (40%) compared with those in patients with NSS (19%; $P = .001$). SjD group (43%) scores were also significantly higher than NSS group scores ($P < .0001$), with no difference between R-SjD and SjD groups ($P = .78$). C, Whole unstimulated salivary flow (WUSF) scores were significantly higher in patients with R-SjD (63%) compared with those in patients with NSS (39%; $P = .001$). SjD group (63%) scores were also higher than NSS group scores ($P < .0001$) and identical to R-SjD group scores ($P > .9999$).

compared with those with NSS ($P < .0001$), with an OR of 0.36 (95% CI, 0.23-0.56) (Fig 4C). Subjects with R-SjD were almost identical to patients with SjD in regards of their WUSF scores ($P > .9999$), with an OR of 0.97 (95% CI, 0.55-1.67) (Fig 4C). All subjects with NSS with salivary anti-Ro60 antibodies that were seronegative for anti-Ro60 had negative focus scores, except for 7 individuals (Supplementary Fig S1). No significant correlation was observed between focus scores and salivary antibodies in either NSS or SjD groups. Overall, these data indicate that R-SjD exocrine gland dysfunction appears more similar to SjD than to the NSS group, without salivary anti-Ro60.

## DISCUSSION

In this study, we investigated the presence of salivary autoantibodies in patients with SjD, patients with NSS, and HC subjects to better elucidate their relationship to the pathogenesis of Sjögren's and dryness severity. All antibody panels (anti-Ro60, anti-La, and RF) were tested for both IgG and IgA isotypes. As expected, SjD saliva bound most antigens, and salivary anti-Ro60 showed concordance with the serum presence of anti-Ro60 antibodies (Table, Fig 1). Most importantly, we identified a cohort of 75 subjects with NSS with salivary antibodies who had similar objective measurements of dryness to patients with SjD. We postulate that these 75 subjects with NSS belong to a new and distinct phenotype of the disease. These results support the premise that in some patients with sicca and SjD, salivary glands are sites of antibody production and that these antibodies travel from the salivary glands to the oral cavity.

Research classification of SjD involves both subjective criteria of dryness, where patients answer questionnaires regarding their symptom severity, and objective criteria for which ascertainment can be invasive and unpleasant. Objective examinations include minor salivary gland biopsies to identify the presence of lymphocytic foci and in later stages, atrophy, and fibrosis of the tissue; phlebotomy to screen for autoantibodies; ocular staining; tear flow measurements to assess xerophthalmia; and assessments of both unstimulated and stimulated of salivary flow [5,6]. It is important to note that lower lip minor salivary gland biopsies do not necessarily correlate to the inflammation and fibrosis found in the major salivary glands of most patients with SjD [23]. Focus scores also do not necessarily correlate with measures of dryness and do not capture all forms of immune infiltrations [23]. Immune cells, including ASCs, can localise within salivary glands without forming the dense, organised architecture required to be classified as a focus score but they may be part of ectopic germinal centres [13]. This distinction is critical in understanding the 82 subjects with NSS in our study with salivary anti-Ro60 antibodies and negative focus scores (Supplementary Fig S1). These patients may have ASCs actively producing autoantibodies in their glands, contributing to localised immune activity and dysfunction, despite the absence focus scores. The presence of salivary anti-Ro60 antibodies has shown significant correlation to oral dryness [24]. This supports the notion that salivary autoantibodies, particularly anti-Ro60, may reflect glandular immune processes independent of traditional markers like focus scores, offering an alternative and potentially more sensitive diagnostic tool [25].

Ectopic germinal centres can be present in the salivary glands of patients with dry symptoms, and 25% of patients with SjD have germinal center formation in their exocrine glands [26]. ASCs, such as plasmablasts and memory B cells, are among the most common cell types found in ectopic germinal centres [27]. Salivary glands in patients with NSS and patients with SjD are sites where ASCs accumulate to secrete anti-Ro60 and anti-La antibodies that are then detected in saliva and sera [13]. We previously evaluated single ASCs collected from salivary gland biopsies of patients with SjD and showed that the autoantibodies present in both saliva and sera mirror the ASC humoral immune response in the salivary glands [28].

In this study, we identified 7 of 88 subjects with NSS who showed positive results for salivary anti-Ro60 positive and negative results for serum anti-Ro60 but had positive focus scores, suggesting localised immune activity. Additionally, we observed cases in which salivary anti-Ro60 antibodies were present despite negative focus scores. This finding may reflect underlying immune processes not captured by traditional histopathologic scoring. Potential mechanisms include early or small ectopic lymphoid aggregates,

localised ASC activity, or glandular immune activation below the detection threshold of conventional focus scoring. Further studies using immunohistochemistry and single-cell approaches are needed to explore the immunoarchitecture in these subjects.

Characterisation and analysis of salivary samples in this study revealed a correlation between salivary anti-Ro60 presence and objective examinations of dryness in subjects with NSS. If salivary anti-Ro60 autoantibodies were included in the classification criteria, these 68 subjects with NSS (R-SjD) would not have escaped classification. However, with the previous American-European Consensus Group (AECG) classification criteria and the newer ACR/EULAR classification criteria [6], both of which require serum anti-Ro60, these subjects are excluded from the SjD group.

Clinical diagnosis of SjD does not rely on research criteria but is based entirely on expert opinion. However, similar to research classification, virtually, no patient would be diagnosed without autoantibodies or focal lymphocytic infiltrates of the exocrine glands. In our experience, patients with sicca and/or other characteristic clinical features of the disease and serum autoantibodies are diagnosed with SjD. However, without the presence of autoantibodies, diagnosis is difficult and tentative without a biopsy. Clinical determination of salivary autoantibodies may make diagnosis and classification easier and more definitive in patients without serum autoantibodies. In fact, 51 of 122 (42%) patients with SjD had salivary anti-Ro60 but no serum autoantibody (Supplementary Figs S2 and S3). If salivary anti-Ro60 could be measured clinically, then patients such as these might avoid a lip biopsy.

The limitations of our study include the small size of the cohort we screened, consisting of 175 patients with SjD, 225 patients with NSS, and 49 HC subjects. SjD is heterogeneous and can affect multiple organ systems, with each patient presenting a variety of manifestations. In the future, there should be more cohorts screened for salivary anti-Ro60 antibodies to clarify the role of these autoantibodies in SjD management, diagnosis, and classification. Additionally, we did not evaluate anti-R052, an important biomarker in SjD that is commonly associated with systemic and overlap disease [29]. While detecting anti-Ro52 was not part of the original scope of this study, we acknowledge the importance of investigating its presence in future research, particularly in relation to disease severity. Our analysis focused on the frequency or positivity of specific antibodies rather than the absolute concentrations of immunoglobulins. Future studies could benefit from investigating the levels of these autoantibodies or even screening for total IgG levels in saliva to provide a more comprehensive picture of the immunopathologies in these patients. Lastly, since we used previously collected and frozen saliva samples, some samples could have lost antigen reactivity over time.

It is possible that ASCs that accumulate in the inflamed salivary glands produce antibodies that present in the saliva before the sera. In our cohort, we identified 89 subjects with NSS having salivary anti-Ro60 antibodies, and of these, 88 were seronegative. Of the 88 subjects with NSS, we identified 75 R-SjD that could be classified as SjD if salivary anti-Ro60 was a classifier in ACR/EULAR criteria and would receive 3 points, same as serum anti-Ro60. These results suggest a possibly distinct and stable new phenotype of SjD (R-SjD), consisting of subjects with seronegative but salivary-positive anti-Ro60 antibody profiles. Alternatively, these serum anti-Ro60 negative, salivary-positive patients could have an early or evolving form of the disease and go on to develop autoantibodies in their sera over time. Given that autoantibodies are known to appear in serum long before the onset of clinical illness in SjD we favour the former possibility. Namely, that this work has identified a new phenotype of the disease. The relationship between salivary and serum antibodies in this context raises the intriguing question of whether these autoantibodies recognise the same epitopes or reflect epitope spreading, where immune responses evolve to target additional epitopes over time. Investigating this through epitope mapping studies could provide insights into the mechanisms driving disease progression and the potential distinctiveness of the R-SjD phenotype. This distinction can be answered by follow-up with longitudinal studies that we are planning, where these patients will be called back for re-evaluation and potentially reclassification. Salivary anti-Ro60 antibodies could play an important role in the early diagnosis and classification of SjD.

## Competing interests

MT reports financial support was provided by Alexander S Onassis Public Benefit Foundation. KAK reports financial support was provided by Sjogrens Syndrome Foundation. RHS reports financial support was provided by National Institutes of Health and consulting or advisory fees from Jenssen Pharmaceuticals, IQVIA, and Merck & Co. All other authors declare they have no competing interests.

## CRediT authorship contribution statement

**Martha Tsaliki:** Writing – review & editing, Writing – original draft, Visualization, Validation, Supervision, Software, Resources, Project administration, Methodology, Investigation, Formal analysis, Data curation. **Joshua Cavett:** Writing – review & editing, Writing – original draft, Visualization, Validation, Supervision, Software, Project administration, Methodology, Investigation, Funding acquisition, Formal analysis, Data curation. **Biji T. Kurien:** Writing – review & editing, Visualization, Validation, Supervision, Software, Resources, Project administration, Methodology, Investigation, Formal analysis, Data curation. **Christina Bruxvoort:** Visualization, Validation, Software, Project administration, Formal analysis. **Valerie M. Lewis:** Supervision. **John A. Ice:** Formal analysis. **Devavrat Dave:** Writing – original draft, Validation. **Sina Khosravani:** Validation. **Kiely Grundahl:** Resources. **Christopher J. Lessard:** Resources. **Astrid Rasmussen:** Writing – review & editing. **Kathy L. Sivils:** Resources. **Amy Darise Farris:** Writing – review & editing, Resources. **Kristi A. Koelsch:** Writing – original draft, Visualization, Validation, Supervision, Software, Resources, Project administration, Methodology, Investigation, Funding acquisition, Formal analysis, Data curation, Conceptualization. **Robert Hal Scofield:** Writing – review & editing, Writing – original draft, Validation, Supervision, Resources, Project administration, Methodology, Investigation, Funding acquisition, Formal analysis, Conceptualization.

## Funding

This work was funded in part by NIH grants AR053483, AI082714, GM104938, AR060804, and DE028001 as well as a Sjögren's Foundation High Impact Research Award grant to KAK. MT is supported in part by the Onassis Foundation (Scholarship ID: J ZK 011-2/2019-2020).

## Patient consent for publication

All study participants gave written informed consent.

## Ethics approval

This study was approved by the University of Oklahoma Health Sciences Center and OMRF Institutional Review Boards.

## Provenance and peer review

Not commissioned; externally peer reviewed.

## Supplementary materials

Supplementary material associated with this article can be found in the online version at doi:10.1016/j.ard.2025.03.012.

## Orcid

Martha Tsaliki: http://orcid.org/0000-0001-9615-6699
Biji T. Kurien: http://orcid.org/0000-0002-7877-6859
Christina Bruxvoort: http://orcid.org/0000-0002-1796-7782
Valerie M. Lewis: http://orcid.org/0000-0002-5496-7132
Devavrat Dave: http://orcid.org/0000-0002-8745-1431
Christopher J. Lessard: http://orcid.org/0000-0003-2440-3843
Astrid Rasmussen: http://orcid.org/0000-0001-7744-2948
Robert Hal Scofield: http://orcid.org/0000-0003-1015-5850

## REFERENCES

[1] Negrini S, Emmi G, Greco M, Borro M, Sardanelli F, Murdaca G, et al. Sjogren's syndrome: a systemic autoimmune disease. Clin Exp Med 2022;22 (1):9–25. doi: 10.1007/s10238-021-00728-6.
[2] Ramos-Casals M, Brito-Zerón P, Seror R, Bootsma H, Bowman SJ, Dörner T, et al. Characterization of systemic disease in primary Sjogren's syndrome: EULAR-SS Task Force recommendations for articular, cutaneous, pulmonary and renal involvements. Rheumatology (Oxford) 2015;54(12):2230–8. doi: 10.1093/rheumatology/kev200.
[3] Brandt JE, Priori R, Valesini G, Fairweather D. Sex differences in Sjogren's syndrome: a comprehensive review of immune mechanisms. Biol Sex Differ 2015;6:19. doi: 10.1186/s13293-015-0037-7.
[4] Ramos-Casals M, Brito-Zerón P, Bombardieri S, Bootsma H, De Vita S, Dörner T, et al. EULAR recommendations for the management of Sjogren's syndrome with topical and systemic therapies. Ann Rheum Dis 2020;79(1):3–18. doi: 10.1136/annrheumdis-2019-216114.
[5] Vitali C, Del Papa N. Classification and diagnostic criteria in Sjogren's syndrome: a long-standing and still open controversy. Ann Rheum Dis 2017;76 (12):1953–4. doi: 10.1136/annrheumdis-2017-211378.
[6] Shiboski CH, Shiboski SC, Seror R, Criswell LA, Labetoulle M, Lietman TM, et al. 2016 American College of Rheumatology/European League Against Rheumatism classification criteria for primary Sjogren's syndrome: a consensus and data-driven methodology involving three international patient cohorts. Ann Rheum Dis 2017;76(1):9–16. doi: 10.1136/annrheumdis-2016-210571.
[7] Tashbayev B, Garen T, Palm Ø, Chen X, Herlofson BB, Young A, et al. Patients with non-Sjogren's sicca report poorer general and oral health-related quality of life than patients with Sjogren's syndrome: a cross-sectional study. Sci Rep 2020;10(1):2063. doi: 10.1038/s41598-020-59078-0.
[8] Segerberg-Konttinen M. Focus score in sialolithiasis. A pitfall in differential diagnosis of Sjogren's syndrome. Scand J Rheumatol 1988;17(2):87–9. doi: 10.3109/03009748809098767.
[9] Fayyaz A, Kurien BT, Scofield RH. Autoantibodies in Sjogren's syndrome. Rheum Dis Clin North Am 2016;42(3):419–34. doi: 10.1016/j.rdc.2016.03.002.
[10] Malladi AS, Sack KE, Shiboski SC, Shiboski CH, Baer AN, Banushree R, et al. Primary Sjogren's syndrome as a systemic disease: a study of participants enrolled in an international Sjogren's syndrome registry. Arthritis Care Res (Hoboken) 2012;64(6):911–8. doi: 10.1002/acr.21610.
[11] Jonsson R, Theander E, Sjöström B, Brokstad K, Henriksson G. Autoantibodies present before symptom onset in primary Sjogren syndrome. JAMA 2013;310(17):1854–5.
[12] Theander E, Jonsson R, Sjöström B, Brokstad K, Olsson P, Henriksson G. Prediction of Sjogren's syndrome years before diagnosis and identification of patients with early onset and severe disease course by autoantibody profiling. Arthritis Rheumatol 2015;67(9):2427–36. doi: 10.1002/art.39214.
[13] Tengnér P, Halse AK, Haga HJ, Jonsson R, Wahren-Herlenius M. Detection of anti-Ro/SSA and anti-La/SSB autoantibody-producing cells in salivary glands from patients with Sjogren's syndrome. Arthritis Rheum 1998;41(12): 2238–48.
[14] Jonsson MV, Skarstein K, Jonsson R, Brun JG. Serological implications of germinal center-like structures in primary Sjogren's syndrome. J Rheumatol 2007;34(10):2044–9.
[15] Daridon C, Pers JO, Devauchelle V, Martins-Carvalho C, Hutin P, Pennec YL, et al. Identification of transitional type II B cells in the salivary glands of patients with Sjogren's syndrome. Arthritis Rheum 2006;54(7):2280–8.
[16] Reksten TR, Jonsson MV, Szyszko EA, Brun JG, Jonsson R, Brokstad KA. Cytokine and autoantibody profiling related to histopathological features in primary Sjogren's syndrome. Rheumatology (Oxford) 2009;48(9):1102–6.
[17] Aqrawi LA, Skarstein K, Bredholt G, Brun JG, Brokstad KA. Autoantigen-specific memory B cells in primary Sjogren's syndrome. Scand J Immunol 2012;75(1):61–8. doi: 10.1111/j.1365-3083.2011.02625.x.
[18] Horsfall AC, Rose LM, Maini RN. Autoantibody synthesis in salivary glands of Sjogren's syndrome patients. J Autoimmun 1989;2(4):559–68. doi: 10.1016/0896-8411(89)90189-3.
[19] Toker E, Yavuz S, Direskeneli H. Anti-Ro/SSA and anti-La/SSB autoantibodies in the tear fluid of patients with Sjogren's syndrome. Br J Ophthalmol 2004;88(3):384–7. doi: 10.1136/bjo.2003.028340.
[20] Zandbelt M, te Boome L, Klasen I, van de Putte L, van den Hoogen F. Tear fluid measurement of anti-SS-A and anti-SS-B antibody in anti-SS-A and anti-SS-B seronegative Sjogren's syndrome patients. Clin Exp Rheumatol 2009;27 (3):536.
[21] Longobardi S, Lopez-Davis C, Khatri B, Georgescu C, Pritchett-Frazee C, Lawrence C, et al. Autoantibodies identify primary Sjogren's syndrome in patients lacking serum IgG specific for Ro/SS-A and La/SS-B. Ann Rheum Dis 2023;82(9):1181–90. doi: 10.1136/ard-2022-223105.
[22] Harley JB, Alexander EL, Bias WB, Fox OF, Provost TT, Reichlin M, et al. Anti-Ro (SS-A) and anti-La (SS-B) in patients with Sjogren's syndrome. Arthritis Rheum 1986;29(2):196–206.
[23] Bookman AA, Shen H, Cook RJ, Bailey D, McComb RJ, Rutka JA, et al. Whole stimulated salivary flow: correlation with the pathology of inflammation and damage in minor salivary gland biopsy specimens from patients with primary Sjogren's syndrome but not patients with sicca. Arthritis Rheum 2011;63 (7):2014–20. doi: 10.1002/art.30295.
[24] Chatzis LG, Stergiou IE, Goules AV, Pezoulas V, Tsourouflis G, Fotiadis D, et al. Clinical picture, outcome and predictive factors of lymphoma in primary Sjogren's syndrome: results from a harmonized dataset (1981-2021). Rheumatology (Oxford) 2022;61(9):3576–85. doi: 10.1093/rheumatology/keab939.
[25] Jin Y, Li J, Chen J, Shao M, Zhang R, Liang Y, et al. Tissue-specific autoantibodies improve diagnosis of primary Sjogren's syndrome in the early stage and indicate localized salivary injury. J Immunol Res 2019;2019:3642937. doi: 10.1155/2019/3642937.
[26] Salomonsson S, Jonsson MV, Skarstein K, Brokstad KA, Hjelmström P, Wahren-Herlenius M, et al. Cellular basis of ectopic germinal center formation and autoantibody production in the target organ of patients with Sjogren's syndrome. Arthritis Rheum 2003;48(11):3187–201.
[27] Aqrawi LA, Skarstein K, Øijordsbakken G, Brokstad KA. Ro52- and Ro60-specific B cell pattern in the salivary glands of patients with primary Sjogren's syndrome. Clin Exp Immunol 2013;172(2):228–37. doi: 10.1111/cei.12058.
[28] Maier-Moore JS, Koelsch KA, Smith K, Lessard CJ, Radfar L, Lewis D, et al. Antibody-secreting cell specificity in labial salivary glands reflects the clinical presentation and serology in patients with Sjogren's syndrome. Arthritis Rheumat 2014;66(12):3445–56.
[29] Espinosa A, Hennig J, Ambrosi A, Anandapadmanaban M, Abelius MS, Sheng Y, et al. Anti-Ro52 autoantibodies from patients with Sjogren's syndrome inhibit the Ro52 E3 ligase activity by blocking the E3/E2 interface. J Biol Chem 2011;286(42):36478–91. doi: 10.1074/jbc.M111.241786.

Ann Rheum Dis 84 (2025) 1363–1374

Contents lists available at ScienceDirect

Annals of the Rheumatic Diseases

journal homepage: https://www.sciencedirect.com/journal/annals-of-the-rheumatic-diseases

Systemic sclerosis

# Integrative exome sequencing and machine learning identify *MICB* and interferon pathway genes as contributors to SSc risk

Shamika Ketkar[1], Hongzheng Dai[1], Lindsay Burrage[1], David Murdock[2], Brian Dawson[1], Marialbert Acosta-Herrera[3], Martin Kerick[3], Javier Martin[3], Kevin Wilhelm[4], Jennifer Kay Asmussen[4], Olivier Lichtarge[4], Regeneron Genetics Center[5], Shervin Assassi[6], Maureen D. Mayes[6], Brendan H. Lee[1,*]

[1] *Department of Molecular and Human Genetics, Baylor College of Medicine, Houston, TX, USA*
[2] *Department of Internal Medicine, McGovern Medical School, University of Texas, Houston, TX, USA*
[3] *Institute of Parasitology and Biomedicine López-Neyra, CSIC, Granada, Spain*
[4] *Computational and Integrative Biomedical Research Center, Baylor College of Medicine, Houston, TX, USA*
[5] *Regeneron Pharmaceuticals Inc, Tarrytown, NY, USA*
[6] *Department of Internal Medicine, Division of Rheumatology, McGovern Medical School, University of Texas, Houston, TX, USA*

ARTICLE INFO

*Article history:*
Received 30 January 2025
Received in revised form 28 April 2025
Accepted 10 May 2025

ABSTRACT

*Objectives:* Systemic sclerosis (SSc) is a complex autoimmune disease with both known and unidentified genetic contributors. While genome-wide association studies (GWAS) have implicated multiple loci, many reside in noncoding regions. We aimed to identify novel protein-coding variants and pathogenic pathways using exome sequencing (ES) integrated with an Evolutionary Action-Machine Learning (EAML) framework, single-cell RNA sequencing (scRNA-seq), and expression quantitative trait locus (eQTL) analysis.

*Methods:* GWAS was conducted in 2,559 SSc cases and 893 controls of Caucasian ancestry, with replication in 9,846 cases and 18,333 controls of European ancestry. EAML prioritized genes with high-impact missense variants predictive of disease. Public scRNA-seq data from SSc and control skin biopsies were analyzed to localize gene expression across cell types. Whole blood eQTL data were used to identify regulatory effects of risk variants.

*Results:* A novel SSc risk locus at *MICB* (rs2516497, $P = 3.66 \times 10^{-13}$) was identified and replicated. EAML highlighted 284 genes enriched in interferon signaling. scRNA-seq localized *MICB* and *NOTCH4* to fibroblasts and endothelial cells, while *HLA* class II genes were enriched in macrophages and fibroblasts. eQTL analysis confirmed regulatory effects at *MICB*, *NOTCH4*, and other prioritized genes, linking SSc-associated variants to transcriptional dysregulation.

*Conclusions:* This integrative genomic study identifies novel risk loci and mechanistic pathways in SSc, highlighting *MICB*, *NOTCH4*, and interferon-related genes. The findings provide insight into the cellular and regulatory architecture of SSc and support the utility of combining ES, machine learning, scRNA-seq, and eQTL data in complex disease genetics.

*Correspondence to Dr. Brendan H. Lee.
*E-mail address:* blee@bcm.edu (B.H. Lee).
**Handling editor** Josef S. Smolen.

https://doi.org/10.1016/j.ard.2025.05.009

0003-4967/© 2025 European Alliance of Associations for Rheumatology (EULAR). Published by Elsevier B.V. All rights are reserved, including those for text and data mining, AI training, and similar technologies.

**WHAT IS ALREADY KNOWN ON THIS TOPIC**

- Genome-wide association studies (GWAS) have identified both human leucocyte antigen (HLA) and non-HLA loci contributing to systemic sclerosis (SSc) susceptibility.
- Most GWAS hits map to noncoding regions, limiting functional interpretation.

**WHAT THIS STUDY ADDS**

- Using exome sequencing and an evolutionary action–machine learning (EAML) framework, we identified *MICB* as a novel coding risk locus for SSc, independent of classical HLA alleles.
- We further prioritised interferon pathway genes (*IFI44L* and *IFIT5*) contributing to disease risk through rare, deleterious missense variants.
- Single-cell RNA sequencing and expression quantitative trait locus analyses linked risk loci to fibroblast, endothelial, and immune cell dysfunction in SSc tissues.

**HOW THIS STUDY MIGHT AFFECT RESEARCH, PRACTICE OR POLICY**

- These findings enhance the genetic and functional understanding of SSc pathogenesis.
- Integration of loci such as *MICB* and rare interferon-related variants into future polygenic risk score models could improve early prediction and precision medicine strategies in SSc.
- The EAML approach is broadly applicable to gene discovery in other complex autoimmune diseases.

## INTRODUCTION

Systemic sclerosis (SSc, scleroderma) is a chronic autoimmune disease leading to systemic vasculopathy and fibrosis. It has the highest mortality among major systemic autoimmune diseases. The pathogenesis of SSc involves extensive fibrosis of the skin and internal organs, vascular damage, and immune imbalance, including autoantibody production [1]. The causes of SSc are unknown, and it is generally considered to result from a combination of external triggers operating in the context of genetic susceptibility, similar to other complex genetic autoimmune diseases. SSc shows one of the highest mortality rates among rheumatic diseases, and 25% of patients with SSc have an additional autoimmune disease [2].

In the United States, the estimated incidence of SSc is 20 cases per 1 million, and its prevalence has been estimated at 276 cases per 1 million [3]. The risk of SSc is 4 to 9 times higher in women than that in men [1,4].

With the advent of sequencing studies, genome-wide association studies (GWAS) were used to analyse the frequency of common genetic variants in several thousand genomic positions located throughout the whole genome and compare large cohorts of cases and controls in a hypothesis-free fashion [5]. Early GWAS identified the strongest genetic contribution to the disease thus far as coming from the human leucocyte antigen (HLA) region [6,7]. Several non-HLA loci have been identified including *STAT4* [8], *IRF5* [9], CD247 [10], and *ATP8B4* [11], which contribute to SSc risk. A strong role for genetic etiologic factors has been suggested in SSc by family studies showing an absolute risk of 1.6% in families when compared with 0.026% in the general population [12]. It is evident that genetic component plays an important role for pathogenesis of SSc; however, more studies are needed to estimate precise heritability and to clarify an exact genetic mechanism. One possible source of missing heritability is the potential for variants to have nonadditive effects on disease risk [13] based on their functional impact. Association methods could be augmented by the fact that variants have different levels of impact on protein structure and function across evolution. Together, this argues that new approaches are needed to identify more direct, functional connections between genetic factors and SSc.

In this study, using exome sequencing (ES) data from Scleroderma Registry patients, our goal was to comprehensively identify novel potential common or rare causal variants and to identify putative causative pathways to gain an understanding of the complex aetiology of SSc. To that end, we conducted association analyses for common and rare variants (RVs) as well as incorporated a novel evolutionary action–machine learning (EAML) framework that scores the relative contribution of a gene's mutations in distinguishing individuals affected by a complex trait from healthy controls [14,15]. By incorporating the evolutionary action (EA) functional impact score [16], derived from a systematic analysis of evolutionary information on protein sequence variations and divergences [17], into association testing and focusing on protein–coding variants, the method includes a larger portion of variance in the association modelling that is directly related to biological importance. Additionally, the use of machine learning allows us to address nonlinear patterns of variation within potential risk genes in SSc. To further elucidate the functional relevance of prioritized loci, we incorporated publicly available single-cell RNA sequencing (scRNA-seq) data from SSc skin biopsies to resolve cell type-specific expression patterns of genetic risk genes, and performed expression quantitative trait locus (eQTL) analysis using publicly available whole blood datasets to establish regulatory connections between disease-associated variants and transcriptomic alterations. Together, these integrative genomic approaches bridge genetic variation with gene function and cellular context, providing mechanistic insights into SSc pathogenesis.

## METHODS

### *Subjects and methods*

An overview of the analytic workflow, including sample numbers at each step, is provided in Supplementary Figure S1. To identify novel SSc susceptibility loci and complex aetiology of SSc, we performed GWAS using ES data in a population of Caucasian ancestry including 2559 cases and 893 controls enrolled in the Scleroderma Family Registry and DNA Repository at the University of Texas Health Science Center at Houston. The inclusion of patients was based on the classification standards available at the time of enrollment. Specifically, patient recruitment began in 1998, pre-dating the 2013 American College of Rheumatology (ACR)/European Alliance of Associations for Rheumatology (EULAR) classification criteria for SSc. Therefore, the majority of early cases were included based on the 1980 ACR preliminary classification criteria [18]. For a subset of patients in whom complete classification data could not be retrieved from the medical record, inclusion was permitted if the individual had a physician-confirmed diagnosis of SSc and met at least 3 of the 5 clinical features of CREST syndrome (calcinosis, Raynaud phenomenon, oesophageal dysfunction, sclerodactyly, or telangiectasia), with sclerodactyly being mandatory. This strategy reflected expert clinical judgement during the earlier enrollment period, being consistent with methods previously reported by our group [4,19]. Following the publication of the 2013 ACR/EULAR classification criteria [20], we performed a retrospective assessment of clinical and serological data available in our registry to evaluate alignment with these

updated criteria. Although capillaroscopy data were not available, over 99% of enrolled patients met the 2013 ACR/EULAR criteria based on available clinical manifestations and serologic profiles. All study participants provided written informed consent, and the study was approved by the Institutional Review Board at the University of Texas Health Science Center at Houston. Healthy control participants had no history of autoimmune rheumatologic disease and were not related to enrolled patients with SSc.

We further performed genotype imputation using Minimac4 [21] algorithm with the 1000 genomes Phase 3 v5 release as a reference [22,23]. Imputation involves the prediction of genotypes not directly assayed in a sample of individuals. Genotype imputation yielded 5,522,961 variants that passed quality control (QC). QC measures were applied as follows: include only single-nucleotide polymorphisms (SNPs) with a 90% genotyping rate with minor allele frequency (MAF) of ≥0.01 and exclude those that deviated from Hardy–Weinberg equilibrium ($P < .05$ in both cases and control subjects). Principal component (PC) analysis (PCA) based on the variance-standardised relationship matrix was performed using PLINK v1.9 [24] (–pca) for dimension reduction. Case–control association analysis was performed using PLINK logistic regression model (–logistic) of additive effects, including biological sex and first 3 PCs as covariates.

### *Replication cohort*

The replication cohort was investigated by our collaborators (JM, MK, and MA-H). The genetic association data included 9095 SSc cases and 17,584 controls of European ancestry meta-analysis previously published by López-Isac et al [25]. This study included 14 independent epidemiologic cohorts, 2 each from Spain, the Netherlands, Germany, and USA and 1 each from France, Italy, UK, Sweden, Norway, and Australia/UK. All patients fulfilled the 1980 ACR classification criteria for SSc. SNPs identified in our discovery cohort were evaluated for replication and external validation in all meta-analysis cohorts and in a smaller subset of the overall, which excluded the USA cohorts for an unbiased analysis. Variants were considered replicated if they achieved genome-wide level of significance ($P < 5 \times 10^{-8}$). We also obtained chromosome 6 data from the Spanish 2 cohort (949 patients with SSc and 998 controls) for investigating our findings in an independent homogeneous cohort. The logistic regressions were conducted for each replication analysis adjusted by sex (Spanish cohort and meta-analysis cohort) and 5 PCs and country of origin (meta-analysis cohort). To identify independent signals within the region, sequential conditional association analyses were performed with the software GCTA-COJO [26–28] using the summary statistics.

### *Exome sequencing*

ES was performed for the entire cohort in collaboration with the Regeneron Genetics Center. In brief, ES was conducted using Integrated DNA Technologies (IDT) xGen Exome Research Panel v1.0. The standard processing and bioinformatics (SPB) pipeline maps raw reads to a flat version of the GRCh38 reference genome that does not include alternative contigs. Human reference version Hg38 was used for alignment.

Filtering was done in 2 major steps: (1) samples were filtered at particular variant sites: sample genotype calls at sites carrying SNP variants were filtered using 1 criterion: (i) samples with depth of coverage at a particular SNP site (read depth [DP]) of <7 were changed to 'No-call" (./.). Sample genotype calls at sites carrying INDEL variants were filtered using 1 criterion: (i) samples with depth of coverage at a particular INDEL site (DP) of <10 were changed to No-call (./.). (2) Sites were filtered based on allele balance (AB) filters that were applied to all samples at a variant site. Variant sites were omitted from the data set after sample specific filters were applied and all appropriate samples were changed to No-call (./.). Only sites where all samples carrying variation had heterozygous (0/1) genotype calls and all samples carrying the Het variation failed the AB cutoff were removed from the dataset. (i) SNP variant sites required at least 1 sample to carry an alternate AB of ≥15%.

### *Preparation of sequencing data for EAML*

#### *Quality control*

Variant-level and sample-level QC was applied to the full SSc cohort (n = 3527). For variant-level QC, SNPs with a DP of <10, genotype quality of <20, non-PASS flag, allele quality of <230, percentage of genotypes missing of <5%, and Hardy–Weinberg equilibrium $P$ value of $<5 \times 10^{-20}$ were excluded. For sample-level QC, we used Kinship-based INference for Genome-wide association studies (KING) [29] to predict ancestry and relatedness and excluded samples with mismatched ancestry prediction and kinship of >0.0884. Additional sample outliers were excluded by the following thresholds: total variants >21,500; number of genotypes missing >200; number of indels >700; number of singletons >400; and a heterozygous/homozygous ratio >2.05. After QC, a subset of 2267 non-Hispanic White index cases and 794 unrelated healthy controls were selected for analysis. Random sampling, with sex ratio matching, was used to obtain equal cohorts comprising 663 index cases and 663 healthy controls (male = 276, female = 387).

#### *Variant annotation*

Single-nucleotide variants and indels were annotated for gene, consequence, and transcript information with Ensembl's Variant Effect Predictor (v94, GRCh38) [30]. Nonsynonymous variants were then assigned an EA score [16] ranging from 0 (benign) to 100 (loss of function). Frameshift indels were assumed to be loss-of-function variants and assigned an EA score of 100.

### *Risk gene discovery with EAML*

The EAML algorithm was applied to all nonsynonymous variants (without an allele frequency threshold) from the previously described 663 index cases and 663 healthy controls. EAML is an ensemble machine learning method that evaluates each gene's ability to successfully predict cases from controls [14]. Genes with a $q$ value of <0.1 were prioritised as SSc risk genes (n = 284).

### *Validation of novel EAML risk genes*

A series of criteria for success experiments were performed to assess the relationship of the EAML risk genes to SSc.

#### *Scleroderma reference set*

When possible, the EAML-prioritised genes were compared with a set of in-house curated gene list most known for SSc associations (92-SS) (Supplementary Table S1).

### Network connectivity

The connectivity within the EAML-prioritised risk genes was assessed using the STRING protein–protein interaction (PPI) network website and default parameters [31]. The general network connectedness of the EAML genes to the 92-SS set was tested using network diffusion across the STRING PPI v11 network with 100 random degree-matched gene sets [32]. First neighbour connectivity enrichment between the 2 sets was assessed using the STRING PPI v11 network and bootstrapping of 100 random gene sets of equal size, limited to highest confidence (weight >0.9) edges and all evidence types.

### Pathway enrichment

GWAS catalog enrichment was performed using the GENE2FUNC tool within the Functional Mapping and Annotation of Genome-Wide Association Studies website [33], with protein-coding genes as the background set.

### Odds ratios

Variant-based odds ratios were calculated for variants with a cohort allele frequency of >1% using a Fisher exact test with a multiple hypothesis testing correction for the false discovery rate (FDR). Gene-based odds ratios were calculated using RVs (cohort allele frequency <1%) by aggregating allele counts across genes and using a Fisher exact test with a multiple hypothesis testing correction [34]. The significance threshold for both the variant and gene-based odds ratios was FDR of <0.1.

### Literature comentions

PubMed comentions were obtained using the BioPython package's Entrez module, with the search query "({gene}) AND ('Systemic Sclerosis') AND ('gene' or 'protein')" and no field filters [35].

### Functional clustering

Functional clustering was generated using the STRING PPI v11 network, limiting the network to medium confidence edges (weight >0.4) and all evidence types. The markov_clustering package in Python was used for network clustering with an inflation parameter of 1.5 (Allard, Guy; Markov_clustering; GitHub). A pathway enrichment analysis was performed across each cluster using a hypergeometric enrichment test (with multiple hypothesis correction) with Gene Ontology [36,37] and Reactomes [38] gene sets. Significant terms had a $q$ value of <0.01.

### Structural variant clustering

We performed structural clustering for FZD1 using the AlphaFold structure AF-Q9UP38-F1-model_v4 [39,40] and the structural clustering weight (SCW) method [41,42]. The SCW method tested adjacency distances between atoms of rare allele frequency (AF) <1%) mutated protein residues in cases and controls across 4 to 12 Å using adjusted distance, giving more weight to structurally close residues. $Z$ scores were calculated from a closed form solution and compared with a null distribution.

### Prioritisation of novel EAML risk genes

The novel EAML risk genes were ranked using a scoring system based on the previously mentioned criteria for success experiments (see validation of novel EAML risk genes section). For functional clustering experiments, genes received 1 point if they were included in a functional cluster and an additional point if that cluster achieved significance ($q < 0.01$) for any pathway enrichment. To score the PubMed comentions, 1 point was assigned for 1 to 5 comentions with SSc, 2 points for 6 to 15 comentions, 3 points for 16 to 50 comentions, and 4 points for 50+ comentions. To score the interconnections with the 92-SS set, 1 point was given for direct connections to 1 to 3 gold standards, 2 points for 4 to 6 gold standards, and 3 points for 7 to 9 gold standards. To score the odds ratios, 1 point was awarded if the variant-based or gene-based odds ratio reached significance (FDR < 0.1) and had an odds ratio between 2 and 0.5, 2 points for odds between 2 to 10 and 0.1 to 5, and 3 points for an odds ratio of 10 or more or <0.1. The maximum score a gene could attain was 12 points.

Correlation of EAML priority genes with skin expression profiles was performed as part of our effort to validate novel risk genes using independent transcriptomic data. Differential expression analysis was conducted using publicly available RNA sequencing data from the Prospective Registry for Early Systemic Sclerosis (PRESS) cohort, including skin biopsies from 48 patients with SSc (mean disease duration ~1.3 years) and 33 matched healthy controls, as published by Skaug et al [43]. We downloaded the processed differential expression data ($\log_2$fold change and FDR-adjusted $P$ values) and intersected it with the list of EAML-prioritised genes. For validation, we considered genes to be transcriptionally relevant if they met an FDR of <0.05 in skin tissue.

### Single-cell transcriptomic profiling

Single-cell RNA sequencing data from Tabib et al [44] were downloaded from Gene Expression Omnibus using accession GSE138669. Gene expression matrices were processed in R using Seurat [45] (v4.0). Individual samples were read with Read10X and filtered to retain cells with >100 detected transcripts and >500 expressed features. LogNormalisation was performed with a scale factor of 10,000. Highly variable features were identified using the vst method (n = 2000). Data were scaled, subjected to PCA analysis, and visualised via Uniform Manifold Approximation and Projection (UMAP) based on the top 10 PCs. Cell clusters were annotated based on the expression of well-established marker genes: endothelial cells (*PECAM1* and *VWF*), fibroblasts (*COL1A1, COL1A2*, and *PDGFRA*), T cells (*CD3D* and *CD3E*), macrophages (*CD68* and *C1QA*), keratinocytes (*KRT5* and *KRT14*), and pericytes (*RGS5* and *PDGFRB*).

### Patient and public involvement

Patients and/or the public were not involved in the design, or conduct, or reporting, or dissemination plans of this research.

## RESULTS

### GWAS identifies MICB as a novel SSc susceptibility locus

We performed GWAS using the ES data in a population of Caucasian ancestry including 3527 samples comprising of 2749 females and 778 males. As expected, the number of females was higher in the patients with SSc than those in the controls. We further performed genotype imputation with the 1000 Genome Project Phase 3 panel. Genotype imputation on 121,866 genotyped variants yielded 5,522,961 imputed variants. After extensive QC, GWAS was run on 877,343 variants from 3452 samples (2559 cases and 893 controls). Case–control association analysis was performed using PLINK v1.9 logistic regression model of

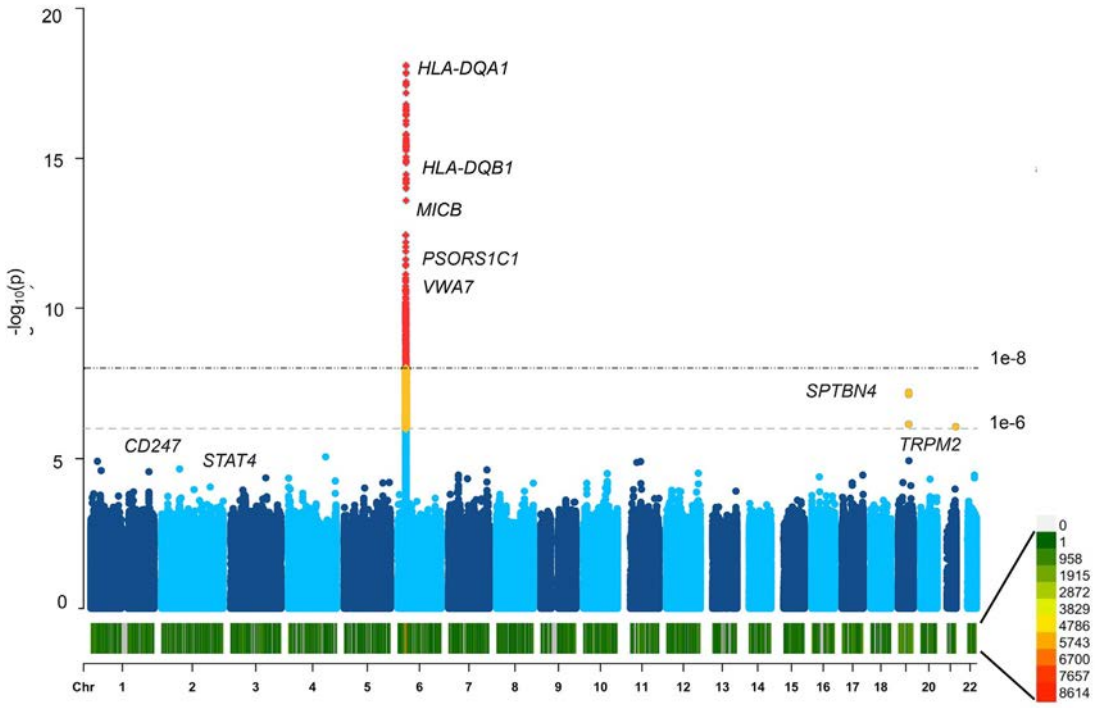



**Figure 1.** Manhattan plot of genome-wide association study analysis performed in PLINK using a logistic regression model of additive effects, including the first 3 principal components as covariates. Top panel (in blue) shows Manhattan plot of the imputed data, whereas bottom panel (in green) shows single-nucleotide polymorphism density for each chromosome on x-axis. The y-axis plots $-\log_{10}(P)$. Dotted lines shows the genome-wide significant cutoff of *P* value $10^{-8}$ and $10^{-6}$.

additive effects, including sex and first 3 PCs as covariates (Supplementary Fig S2).

Within the MHC region, we identified a novel susceptibility locus for SSc at MHC class I chain-related gene B (*MICB*) locus (rs2516497; $P = 3.66 \times 10^{-13}$) independent of *HLA-B*0801* (Figs 1 and 2). Additionally, we observed previously identified associations signals such as *HLA-DQA1* (rs1048372; $P = 8.00 \times 10^{-19}$) and *HLA-DQB1* (rs1049130; $P = 9.72 \times 10^{-15}$) as SSc genetic risk factors. Supplementary Table S2 lists the genome-wide significant results for all variants with *P* value of $<10^{-8}$ with the nearest genes. Most of the genome-wide significant values are from chromosome 6 MHC region including psoriasis susceptibility 1 candidate 1 (*PSORS1C1*) gene [46], tenascin XB (*TNXB*) [47], notch 4 (*NOTCH4*) [48], and von Willebrand factor A domain containing 7 (*VWA7*). Other non-MHC SNPs are in the intronic region of *SPTBN4* gene (rs208027265;

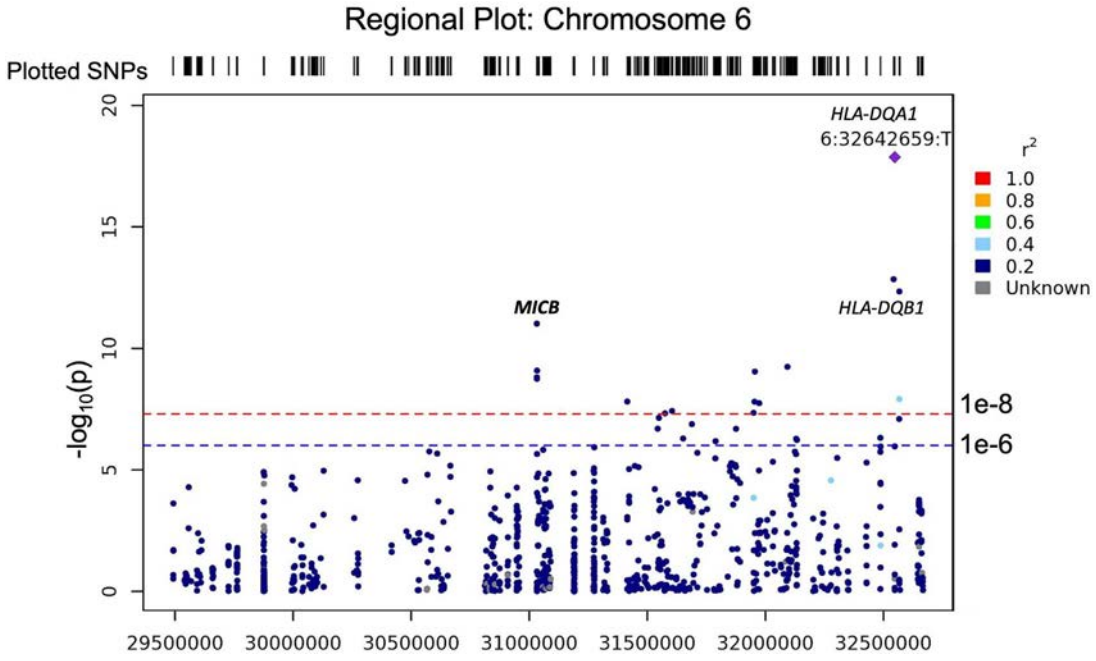



**Figure 2.** Regional plot of chromosome 6 including the MICB region. Regional association plot for the top hits on chromosome 6. The plot was constructed using LocusZoom (http://locuszoom.org/). The −log10 transformed *P* values are plotted on the y-axis. The x-axis shows the position of the variants (dots) on chromosome 6 and the genes in this region. The most significant variant (rs1048372) is shown by the purple diamond, and the colour of the dots indicates whether the top hits are linkage disequilibrium ($r^2$) with *MICB* variant. SNP, single-nucleotide polymorphism.

Table 1
**ExWAS identified *MICB* SNPs associated with SSc and replication in previously published independent meta-analysis cohort [26]**

| MICB SNPs | | | | Discovery cohort | | Replication cohort | |
|---|---|---|---|---|---|---|---|
| rs_ID | SNP | Chr | Position | GWAS (logistic) *P* | OR | SSc_Meta GWAS *P* | OR |
| rs2246986 | 6:31514426:A:G | 6 | 31514426 | $2.49 \times 10^{-5}$ | 0.6968 | $9.41 \times 10^{-10}$ | 0.7239 |
| rs2516398 | 6:31513749:G:T | 6 | 31513749 | $4.40 \times 10^{-7}$ | 0.7426 | $4.19 \times 10^{-10}$ | 0.8362 |
| rs2516497 | 6:31498128:G:T | 6 | 31498128 | $3.66 \times 10^{-13}$ | 0.4575 | $7.17 \times 10^{-9}$ | 0.6493 |
| rs2844494 | 6:31515638:C:A | 6 | 31515638 | $2.09 \times 10^{-7}$ | 0.7364 | $7.17 \times 10^{-9}$ | 0.8092 |

Chr, chromosome; GWAS, genome-wide association study; OR, odds ratio; SNP, single-nucleotide polymorphism; SSc, systemic sclerosis; ExWAS, exome-wide association analysis.

$P = 7.22 \times 10^{-8}$, and rs1254667230; $P = 6.14 \times 10^{-8}$). *MICB* SNPs have been found to be associated with systemic lupus erythematosus (SLE) [49,50] but not with scleroderma. So far, there are no reports of association between *SPTBN4* and any other rheumatic autoimmune diseases.

### *Replication analysis confirms MICB association in independent cohorts*

For replication analysis, we used array data from previously published large-scale meta-analyses of 14 independent epidemiologic cohorts from European ancestry. The data comprised 28,179 unrelated and genome-wide genotyped individuals (9846 patients with SSc and 18,333 healthy controls) [10,25,46]. Meta-analysis for the SNPs in the *MICB* region (chr6:31440928-31494023) was performed for all cohorts (Supplementary Table S3) and on a smaller subset excluding the USA cohorts for a completely unbiased analysis (Supplementary Table S4). To assess significance in an independent cohort, we obtained Spanish 2 cohort.

Replication testing confirmed association of *MICB* SNP (rs2516497; meta-analysis, $P = 7.17 \times 10^{-9}$; Spanish 2 cohort, $P = 2.33 \times 10^{-7}$) with SSc. In addition, the replication cohort also confirmed that the association of *MICB* SNP is an independent event (adjusted by the *HLA-B*0801*), that is, it is not in linkage disequilibrium with other HLA class genes (Supplementary Figs S3–S5). The meta-analysis replication cohort yielded genome-wide significance for 4 other *MICB* SNPs, which were only borderline significant in the SSc ES data (Table 1) [26].

### *RV burden analysis highlights additional risk genes in SSc*

RVs are known to play an important role in human disease. RVs have also largely remained unexplored in the GWAS era of genetic association analysis. GWASs mostly identifies the common variants, but it is plausible that low frequency and RVs could explain disease risk or trait variability. To help understand the extent to which more variants (including low frequency [1% ≤ MAF < 5%] and RVs [<1%]) can enhance previously identified associations and identify novel loci, we performed RV tests using the rare variant test tool (RVTEST) [51]. Burden tests were performed on variants grouped by a single gene via a collapsing test. Table 2 (*P* value cutoff of $< P = 5 \times 10^{-5}$) and Supplementary Table S5 (*P* value cutoff of $< P = .01$) lists the significant results for the sequence kernel association test analysis. Most of the significant gene–phenotype associations were identified in the HLA region on chromosome 6 and found to be consistent with the current knowledge in the SSc field (Fig. 3) [44]. RVs in *HLA-DRB1* [52], *ATF6B* [53], *TNXB* [47], *NOTCH4* [48], *STAT4* [54], and *MICB* (this publication) were associated with SSc risk.

### *EA equation for the fitness effect of missense mutations*

To explore the impact of variation beyond the level of independent SNP and gene, we augmented it by the fact that variants have different levels of impact on protein structure and function across evolution. We used a novel method that combines machine learning with evolutionary data in the form of EA scores that predict the effect of coding mutations on protein function by measuring the fitness effect based on phylogenetic distances and substitution odds in homologous gene sequences [16]. For a given mutation, EA is calculated by using the evolutionary importance of the residue in the protein by the magnitude of the amino acid substitution. For example, an alanine to serine transition represents a small substitution magnitude, while an alanine to tryptophan is a large one. Importantly, the EA distributions can be used to identify genes under selection, where these genes deviate from the expected, exponential decay is observed (Supplementary Fig S6) [14]. We next applied the EAML method to the SSc ES data. After variant and sample QC, all single-nucleotide variants were given an EA functional impact score based on the residue's evolutionary importance and amino acid substitution. These scores are used to train an ensemble machine learning model that ranks each gene's disease association. The schematic on the right side in Supplementary Figure S6 shows EAML as it uses variants and inheritance hypotheses to identify genes associated with SSc. EAML identified 284 prioritised genes (Supplementary Table S6) by aggregating evidence related to relative risk, GWAS, and PubMed co-occurrences. EAML list includes *MICB, NOTCH4, GLIS2*, and interferon (IFN)-induced proteins (*IFI44L* and *IFIT5*). To assess whether these EAML genes were functionally connected with genes linked to SSc, we matched them to the list of differentially expressed genes identified in the PRESS cohort [43]. Skin biopsy RNA from 48 patients in the PRESS cohort (mean disease duration, 1.3 years) and 33 matched healthy controls were examined by next-generation RNA sequencing. Table 3 lists the EAML genes that were found to be dysregulated in the PRESS RNA seq data at the FDR cutoff of <0.05.

### *Cell type–specific expression patterns of genetic risk loci in SSc skin tissue*

To investigate the cellular localisation of *MICB* and related genes in SSc, we analysed publicly available scRNA-seq data from Tabib et al [44] (GSE138669). This study compared scRNA-seq of single-cell suspensions from mid-forearm skin biopsies of 12 discrete samples from patients with SSc with the

Table 2
**Rare variant burden analysis: significant gene results (sequence kernel association test *P* value cutoff of $<P = 5 \times 10^{-5}$)**

| Gene | N_INFORMATIVE | NumVar | NumPolyVar | Q | *P* | NumPerm | ActualPerm | Stat | NumGreater | NumEqual | Perm*P* |
|---|---|---|---|---|---|---|---|---|---|---|---|
| *HLA-DRB1* | 3452 | 23 | 22 | 844,484 | $1.59 \times 10^{-13}$ | 10,000 | 10,000 | 844,484 | 0 | 0 | 0 |
| *ATF6B* | 3452 | 106 | 72 | $1.70 \times 10^{6}$ | $3.78 \times 10^{-12}$ | 10,000 | 10,000 | $1.70 \times 10^{6}$ | 0 | 0 | 0 |
| *TNXB* | 3452 | 597 | 397 | $8.00 \times 10^{6}$ | $1.29 \times 10^{-11}$ | 10,000 | 10,000 | $8.00 \times 10^{6}$ | 0 | 0 | 0 |
| *MPIG6B* | 3452 | 24 | 15 | $1.46 \times 10^{6}$ | $3.76 \times 10^{-11}$ | 10,000 | 10,000 | $1.46 \times 10^{6}$ | 0 | 0 | 0 |
| *PRKRA* | 3452 | 118 | 79 | $2.48 \times 10^{6}$ | $1.37 \times 10^{-10}$ | 10,000 | 10,000 | $2.48 \times 10^{6}$ | 0 | 0 | 0 |
| *PPT2-EGFL8* | 3452 | 128 | 90 | $3.69 \times 10^{6}$ | $3.87 \times 10^{-10}$ | 10,000 | 10,000 | $3.69 \times 10^{6}$ | 0 | 0 | 0 |
| *LY6G6F* | 3452 | 32 | 24 | 599,869 | $4.61 \times 10^{-10}$ | 10,000 | 10,000 | 599,869 | 0 | 0 | 0 |
| *NOTCH4* | 3452 | 310 | 183 | $3.72 \times 10^{6}$ | $9.34 \times 10^{-10}$ | 10,000 | 10,000 | $3.72 \times 10^{6}$ | 0 | 0 | 0 |
| *C4A* | 3452 | 3 | 3 | 359,777 | $1.12 \times 10^{-9}$ | 10,000 | 10,000 | 359,777 | 0 | 0 | 0 |
| *LOC110384692* | 3452 | 3 | 3 | 359,777 | $1.12 \times 10^{-9}$ | 10,000 | 10,000 | 359,777 | 0 | 0 | 0 |
| *C4B_2* | 3452 | 3 | 3 | 359,777 | $1.12 \times 10^{-9}$ | 10,000 | 10,000 | 359,777 | 0 | 0 | 0 |
| *C4B* | 3452 | 3 | 3 | 359,777 | $1.12 \times 10^{-9}$ | 10,000 | 10,000 | 359,777 | 0 | 0 | 0 |
| *HCP5* | 3452 | 36 | 26 | 854,597 | $1.68 \times 10^{-9}$ | 10,000 | 10,000 | 854,597 | 0 | 0 | 0 |
| *EHMT2* | 3452 | 194 | 135 | $2.74 \times 10^{6}$ | $5.48 \times 10^{-9}$ | 10,000 | 10,000 | $2.74 \times 10^{6}$ | 0 | 0 | 0 |
| *PPT2* | 3452 | 79 | 56 | $2.80 \times 10^{6}$ | $7.14 \times 10^{-9}$ | 10,000 | 10,000 | $2.80 \times 10^{6}$ | 0 | 0 | 0 |
| *DXO* | 3452 | 25 | 20 | 878,466 | $8.98 \times 10^{-9}$ | 10,000 | 10,000 | 878,466 | 0 | 0 | 0 |
| *FKBPL* | 3452 | 8 | 6 | 929,520 | $2.10 \times 10^{-8}$ | 10,000 | 10,000 | 929,520 | 0 | 0 | 0 |
| *LOC100507547* | 3452 | 10 | 9 | 852,522 | $1.55 \times 10^{-7}$ | 10,000 | 10,000 | 852,522 | 0 | 0 | 0 |
| *EGFL8* | 3452 | 46 | 33 | $1.01 \times 10^{6}$ | $2.86 \times 10^{-7}$ | 10,000 | 10,000 | $1.01 \times 10^{6}$ | 0 | 0 | 0 |
| *AGPAT1* | 3452 | 73 | 46 | $1.15 \times 10^{6}$ | $1.04 \times 10^{-6}$ | 10,000 | 10,000 | $1.15 \times 10^{6}$ | 0 | 0 | 0 |
| *TSBP1* | 3452 | 755 | 571 | $1.13 \times 10^{7}$ | $2.78 \times 10^{-6}$ | 10,000 | 10,000 | $1.13 \times 10^{7}$ | 0 | 0 | 0 |
| *LOC100287329* | 3452 | 110 | 83 | $1.64 \times 10^{6}$ | $4.27 \times 10^{-6}$ | 10,000 | 10,000 | $1.64 \times 10^{6}$ | 0 | 0 | 0 |
| *LSM2* | 3452 | 95 | 69 | 980,442 | $7.60 \times 10^{-6}$ | 10,000 | 10,000 | 980,442 | 0 | 0 | 0 |
| *DBR1* | 3452 | 53 | 32 | 394,804 | $1.27 \times 10^{-5}$ | 10,000 | 10,000 | 394,804 | 0 | 0 | 0 |
| *RRP7BP* | 3452 | 13 | 5 | 38,497.5 | $2.16 \times 10^{-5}$ | 10,000 | 10,000 | 38,497.5 | 0 | 0 | 0 |
| *KIF22* | 3452 | 36 | 11 | 647,070 | $2.65 \times 10^{-5}$ | 10,000 | 10,000 | 647,070 | 0 | 0 | 0 |
| *TSBP1-AS1* | 3452 | 1781 | 1438 | $2.40 \times 10^{7}$ | $3.92 \times 10^{-5}$ | 10,000 | 10,000 | $2.40 \times 10^{7}$ | 0 | 0 | 0 |
| *STK19* | 3452 | 81 | 58 | $1.11 \times 10^{6}$ | $5.29 \times 10^{-5}$ | 10,000 | 10,000 | $1.11 \times 10^{6}$ | 2 | 0 | 0.0002 |
| *SLC44A4* | 3452 | 160 | 115 | $1.45 \times 10^{6}$ | $5.80 \times 10^{-5}$ | 10,000 | 10,000 | $1.45 \times 10^{6}$ | 1 | 0 | 0.0001 |
| *DDX39B* | 3452 | 126 | 88 | $1.10 \times 10^{6}$ | $6.20 \times 10^{-5}$ | 10,000 | 10,000 | $1.10 \times 10^{6}$ | 0 | 0 | 0 |
| *IER3-AS1* | 3452 | 6 | 5 | 398,849 | $6.53 \times 10^{-5}$ | 10,000 | 10,000 | 398,849 | 1 | 0 | 0.0001 |
| *IER3* | 3452 | 9 | 6 | 259,677 | $6.68 \times 10^{-5}$ | 10,000 | 10,000 | 259,677 | 0 | 0 | 0 |
| *TMEM121B* | 3452 | 27 | 17 | 79,530.7 | $8.27 \times 10^{-5}$ | 10,000 | 10,000 | 79,530.7 | 1 | 0 | 0.0001 |
| *BMP7-AS1* | 3452 | 1 | 1 | 23,202.1 | $9.13 \times 10^{-5}$ | 10,000 | 10,000 | 23,202.1 | 1 | 0 | 0.0001 |
| *PLEKHG2* | 3452 | 121 | 76 | 882,110 | $9.51 \times 10^{-5}$ | 10,000 | 10,000 | 882,110 | 2 | 0 | 0.0002 |

10 control mid-forearm biopsies. Using scRNA-seq, the authors identified *SFRP2*$^{hi}$ fibroblasts as progenitor-like cells that differentiate into myofibroblasts, with progressive upregulation of *SFRP4* during fibrotic transition, implicating Wnt and TGF-$\beta$ signalling in SSc pathogenesis. We performed unsupervised clustering and UMAP to identify distinct populations of endothelial cells, keratinocytes, fibroblasts, macrophages, and pericytes (Fig 4A). Comparison of UMAPs between SSc cases and controls revealed notable shifts in cell population distribution. In SSc cases, there was an apparent expansion of fibroblast and endothelial cell clusters relative to controls. These findings are consistent with known pathophysiologic mechanisms in SSc, where fibroblast activation leads to excessive extracellular matrix (ECM) deposition and fibrosis and endothelial dysfunction contributes to vasculopathy and tissue ischaemia. Figure 4B,C,E,F shows UMAPs for top GWAS hits. *MICB* expression was predominantly localised to fibroblasts, with lower-level expression observed in endothelial cells, consistent with its known upregulation in stressed stromal and vascular compartments [56]. Similarly, *NOTCH4* was enriched in fibroblast and

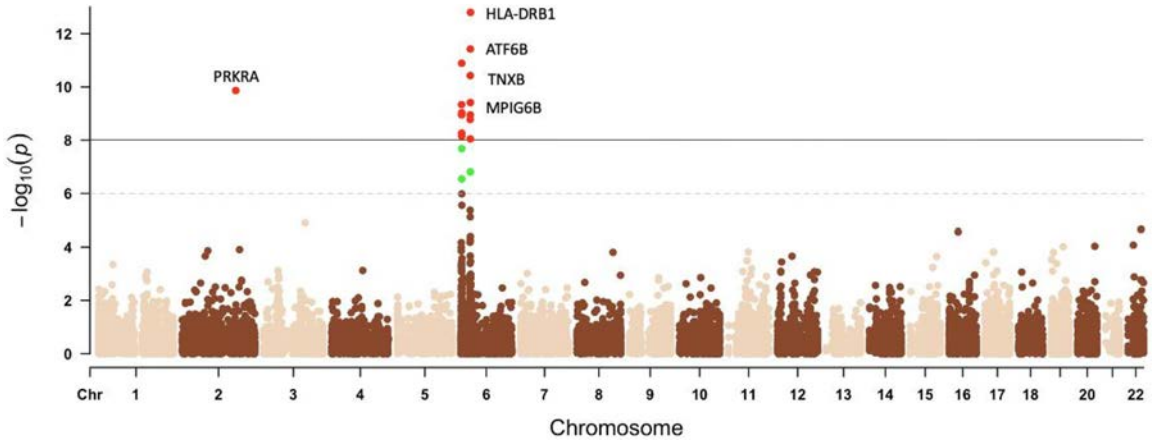



**Figure 3.** Manhattan plot of the rare variants (minor allele frequency < 0.05) for each chromosome on x-axis. The y-axis plots $-\log_{10}(P)$. Dotted line shows the genome-wide significant cutoff of *P* value $10^{-8}$.

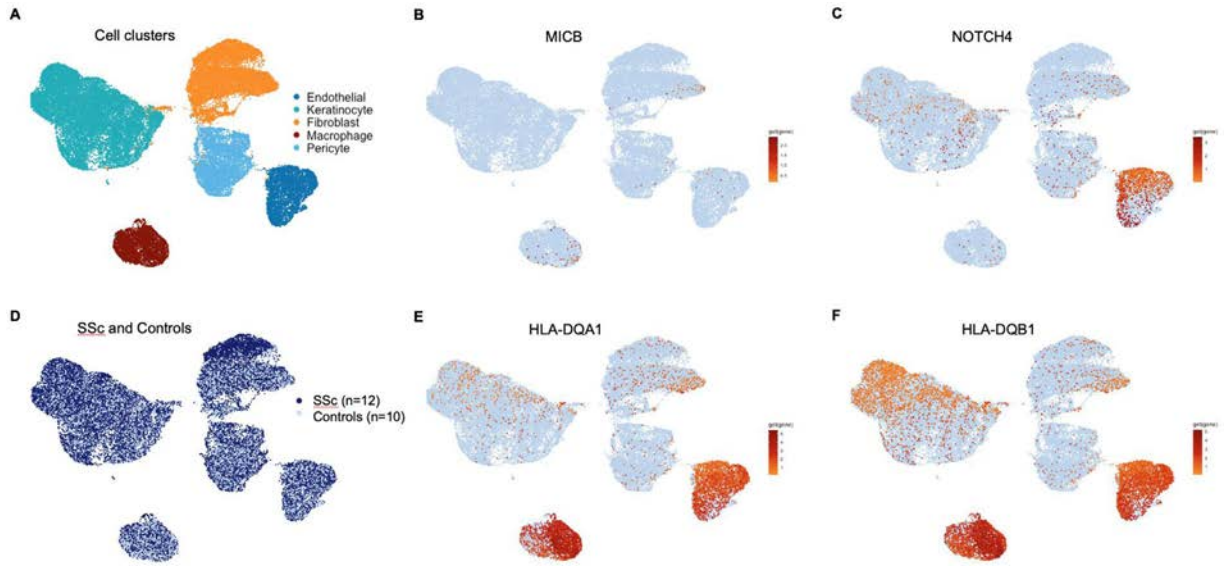



**Figure 4.** Uniform Manifold Approximation and Projection plot of scRNA-seq data from control and systemic sclerosis (SSc) skin biopsies in the study by Tabib et al [44]. Transcriptomes of all cells obtained after enzymatic digestion of dorsal mid-forearm skin biopsies from 10 healthy controls and 12 patients with SSc, showing each Smart Local Moving (SLM) cluster [55] by colour (A), by source from SSc (darkblue) or control (lightblue) biopsies (D). (B, C, E, F) Feature plots for genome-wide association study top hits.

endothelial clusters, supporting previous findings of Notch pathway activation in fibrotic vasculopathy [57]. In contrast, HLA class II genes, including *HLA-DQA1* and *HLA-DQB1*, showed prominent expression in macrophages and fibroblasts, reflecting the activation of antigen presentation pathways previously implicated in SSc pathogenesis [58,59]. UMAPs for RVs and EAML hits are shown in Supplementary Figure S7. *IFI44L, IFIT5, STAT4*, and *PSORS1C1* displayed heterogeneous patterns across keratinocytes, fibroblasts, and macrophages, mirroring previous transcriptomic studies of skin fibrosis [60]. *TNXB* expression is primarily localised to fibroblast clusters it is an ECM glycoprotein that plays a crucial role in collagen organisation and tissue integrity. In SSc, fibroblasts are central to the pathogenesis, contributing to excessive ECM deposition and fibrosis. *GLIS2* expression is more scattered and heterogeneous. GLIS2 is known as a transcriptional repressor implicated in fibrosis attenuation; loss of GLIS2 enhances fibrotic responses in kidney and skin models [61].

## *Functional regulatory evidence for SSc risk variants through expression quantitative trait locus analysis*

To further investigate the functional impact of our findings, we systematically analysed publicly available expression quantitative trait locus (eQTL) data from SSc study by Kerick et al [62]. In this study, genome-wide eQTL analyses were performed in whole blood from patients with SSc and controls, identifying 49,123 validated cis-eQTLs and prioritising genes (eGenes) whose expression is influenced by disease-associated variants. Importantly, the study integrated eQTL findings with SSc GWAS loci to highlight genes where genetic variation likely alters gene expression relevant to disease mechanisms.

We crossreferenced our top candidates from GWAS, EAML prioritisation, and RV burden testing against the data set from the study by Kerick et al [62]. Supplementary Figure S8 is adapted from the study by Kerick et al [62] to highlight our most significant genes; briefly, the figure compares the variance in gene expression explained by SSc-associated SNPs (x-axis) versus the variance explained by all SNPs (y-axis) across identified eGenes. For each gene, the percentage of expression variance attributable to SSc-specific risk variants was calculated using linear regression models and plotted against the total genetic contribution to expression variance from genome-wide SNPs. Genes were colour coded based on the degree of SSc SNP influence, with additional highlighting for loci associated with GWAS signals or RVs. Notably, both *MICB* and *NOTCH4* were identified as high-confidence eGenes with strong SSc SNP effects on expression (classified in the high genetic impact category). This finding is particularly significant because regulatory variation at these loci meaningfully alters gene expression levels in SSc, providing a mechanistic link between genetic susceptibility and transcriptional dysregulation. We additionally annotated genes identified in our RV analysis (*PPT2, ATF6B, TNXB, LY6G6F*, and *HLA-DRB1*), highlighting convergence between common and RV signals.

To further investigate the functional relevance of our top candidate genes, we examined differential expression data from the study by Kerick et al [62]. Figure 5 [62] shows heatmap depicting log-fold changes in gene expression across key immune and stromal cell types for our candidate genes identified as eGenes through eQTL analysis. Positive values (red) indicate upregulation, while negative values (blue) indicate downregulation compared with controls. *HLA-DQA1* and *HLA-DQB1* were markedly

Table 3
**EAML-prioritised genes–expression changes in PRESS cohort**

| Gene | Score | Common with differentially expressed genes in skin | *P* (FDR) | Fold change |
|---|---|---|---|---|
| *FCGR3A* | 3 | *FCGR3A* | $2.56 \times 10^{-26}$ | 7.747806944 |
| *GLIS2* | 4 | *GLIS2* | .002142908 | 1.817664922 |
| *IFI44L* | 3 | *IFI44L* | .000513493 | 2.233049764 |
| *ISG15* | 4 | *ISG15* | .0000007 | 2.412856645 |
| *IYD* | 3 | *IYD* | .011703777 | 0.551341742 |
| *XAF1* | 3 | *XAF1* | .000021 | 1.780835945 |

EAML, evolutionary action–machine learning; FDR, false discovery rate; PRESS, Prospective Registry for Early Systemic Sclerosis.

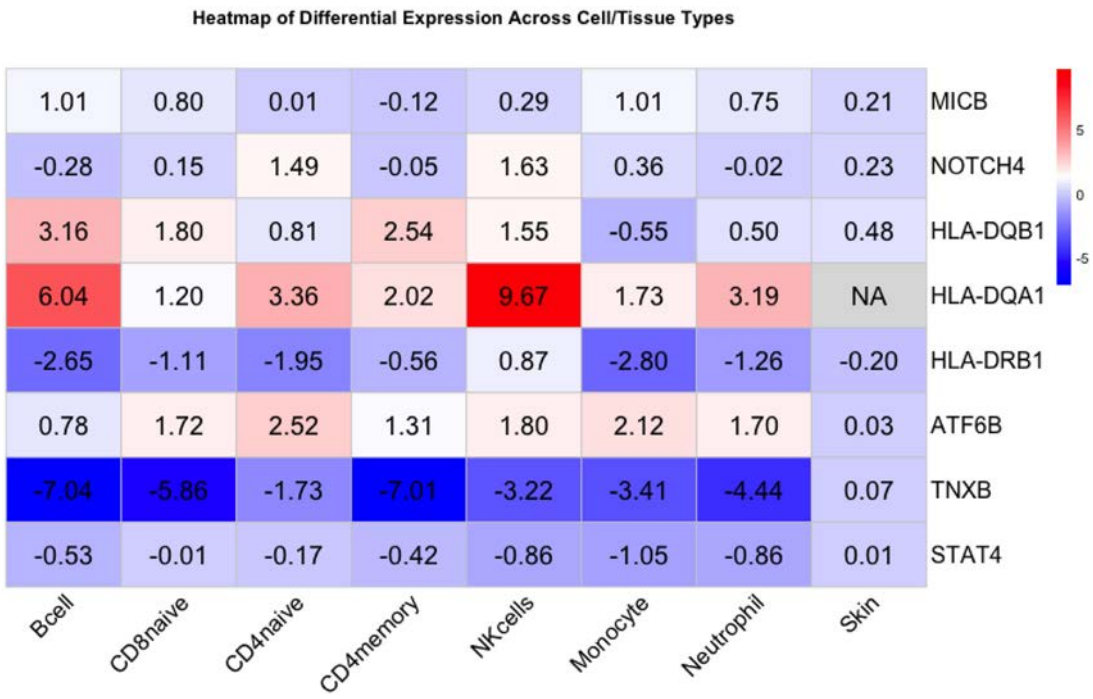



**Figure 5.** Differential gene expression across immune and stromal cell types in systemic sclerosis [62]. Heatmap depicting log-fold changes in gene expression across key immune and stromal cell types for candidate genes identified through expression quantitative trait locus analysis. Positive values (red) indicate upregulation, while negative values (blue) indicate downregulation compared with controls.

upregulated across multiple immune cell types, including B cells, natural killer (NK) cells, and $CD4^+$ T cells, consistent with activation of antigen presentation pathways in SSc. *MICB* and *NOTCH4* showed moderate upregulation in NK cells and $CD4^+$ T cells, supporting roles in innate immune activation and vascular remodelling. In contrast, *TNXB* exhibited strong downregulation across most immune subsets, reflecting its association with ECM disorganisation. These cell type–specific expression patterns provide mechanistic insight into how genetic risk variants may contribute to fibrosis and immune dysregulation across affected tissues in SSc.

## DISCUSSION

In this study, we presented a large GWAS scan using the ES data from the Scleroderma Registry patients. We identified novel *MICB* SNPs associated with SSc along with several known hits (*HLA-DQA1, HLA-DQB1*, and *PSORS1C1*). *MICB* is a protein-coding gene in the MHC region whose gene product is a stress-inducible cell surface molecule that labels malfunctioning cells for targeting by cytotoxic lymphocytes such as natural killer cells.

A recent study by Hartman et al [63] showed association of *MICB* with Raynaud phenomenon in a large cohort. While Raynaud phenomenon is present in 95% of patients with SSc [64], the study did not make a distinction between primary Raynaud phenomenon, which is not associated with autoimmune disease, and secondary Raynaud phenomenon, which is associated with the autoimmune disease. A previous report of high-density SNP screening of *MHC* in SLE demonstrated strong evidence for independent susceptibility regions within *MICB*, in a Caucasian population [49]. While SSc and SLE are both autoimmune conditions, they are clinically, immunologically, and pathophysiologically distinct. Although certain genetic variants may be shared across autoimmune diseases due to common immune regulatory pathways, the presence of a variant previously reported in SLE does not preclude its independent relevance in SSc. Given the distinct phenotypic and serologic profiles of SSc, identifying this variant in the context of SSc contributes important insights into disease-specific and potentially shared mechanisms of autoimmunity. Thus, the association of this variant with SSc remains of scientific interest and may enhance our understanding of the genetic architecture underlying this complex disease. Despite recent HLA fine-mapping studies, *MICB* association has not been previously directly reported in SSc.

Additionally, we replicated our results in a large European cohort, where a significant association of *MICB* SNP was identified as an independent event. The replication cohort also identified 4 additional *MICB* SNPs to be associated with SSc.

GWAS is an unbiased approach as it scans the entire genome for SNPs associated with a certain disease without any assumptions, the method still only provides approximately 80% coverage for common polymorphisms in the human genome and often misses unusual or RVs [65]. RVs are known to play an important role in human disease and could explain disease risk or trait variability. RVs are low frequency ($1\% \leq MAF < 5\%$) and RVs (<1%) variants, which have largely remained unexplored in the GWAS era of genetic association analysis. Our analysis observed RVs in *HLA-DRB1, ATF6B, TNXB*, and *NOTCH4* to be associated with SSc risk. Despite the fact that RV association tests have low statistical power and need a very large sample size to observe RVs with a high probability, our results are promising and highly consistent with the current knowledge in the field. A larger sample size might allows us to pick novel RVs associated with SSc.

To discover novel risk genes associated with SSc using evolutionary information, we applied an EA method to identify deleterious variants. Previous applications of this method have predicted disease risk using functional variants annotated with EA. Therefore, we postulated that an evolutionary history would improve the power of SSc case–control genome analyses. While the full data set included a larger number of cases and controls,

a carefully curated subset was selected for EAML analysis to ensure optimal model performance. EAML is specifically designed to prioritise functionally informative variation, and its accuracy is maximised when applied to high-confidence, well-matched training sets. This subset represents samples that passed stringent QC filters including sequencing depth, ancestry prediction, and mutation load consistency necessary to generate robust and interpretable results. EAML identified several genes associated with SSc, including a subset involved in the type I interferon pathway (IFN-I), such as *IFI44L* and *IFIT5*. While only 6 of the EAML-prioritised genes demonstrated significant differential expression in skin biopsies from the PRESS cohort, this is consistent with previous studies in SSc and other autoimmune diseases where small sets of sentinel genes are sufficient to mark pathway dysregulation and stratify disease subtypes [19,54]. Moreover, IFN-I play a central role in SSc pathogenesis, particularly in early disease stages, and their overactivity has been documented in both skin and peripheral blood [54]. Patients with higher IFN signatures often show more severe disease, including increased risk of interstitial lung disease and digital ulcers [66,67]. Additionally, a recent phase II trial of anifrolumab, a monoclonal antibody targeting the type I IFN receptor, demonstrated efficacy in SLE, a disease with overlapping IFN dysregulation [68]. This supports the feasibility of targeting the IFN axis in autoimmune diseases and justifies exploration in SSc, namely future mechanistic and interventional studies to assess IFN blockade in selected SSc patient subsets with molecular IFN activation. Despite the limited number of differentially expressed EAML genes in this data set, the functional coherence and pathway enrichment observed highlight biologically meaningful signal. Importantly, IFN-related pathways are often marked by changes in a restricted set of high-impact genes with strong regulatory functions, which may serve as therapeutic targets or biomarkers. Thus, our findings suggest that EAML can successfully capture disease-relevant biology beyond gene expression thresholds alone.

Cell type–specific expression patterns of genetic risk loci in SSc skin tissue were interrogated in a publicly available scRNA-seq data set. The results highlight fibroblasts and endothelial cells as principal compartments for *MICB* and *NOTCH4* activity, suggesting that therapeutic strategies targeting fibroblast–endothelial interactions may offer novel approaches for early intervention. Recent scRNA-seq studies of SSc blood and lung tissues similarly confirm fibroblast and endothelial dysregulation as central drivers of disease, reinforcing the relevance of our findings across organ systems. eQTL analyses validated functional impacts at key loci, demonstrating convergence of common and RVs on immune activation and ECM dysregulation pathways. These findings support a model wherein genetic risk variants promote fibrosis and immune dysfunction. Integration of independent eQTL data sets further strengthens the biological plausibility of our prioritised risk genes and lays a foundation for translational applications in SSc.

Our study offers several strengths, including the use of whole ES, machine learning–based variant prioritisation, and replication across independent cohorts. Nonetheless, the restriction to European ancestry limits generalisability, highlighting the need for future multiancestry validation.

In summary, using exome-wide association analysis (ExWAS) and an EA method, we identified novel loci and missense mutations contributing to SSc pathogenesis, with replication in independent genomic and transcriptomic data sets. Importantly, while polygenic risk scores (PRS) are not yet clinically implemented in SSc, incorporation of loci such as *MICB* and rare IFN pathway variants identified via EAML could enhance the predictive accuracy of PRS models, particularly for individuals with early or nonspecific disease features. Our findings offer insights into the genetic architecture of SSc and guide prioritisation of future functional and translational studies.

## Competing interests

All authors declare they have no competing interests.

## Acknowledgements

This work has been presented at the following: (1) the American Society of Human Genetics 2023 meeting poster session (https://www.ashg.org/wp-content/uploads/2023/10/ASHG2023-PosterAbstracts.pdf); (2) the American College of Rheumatology 2023 Convergence Conference as an oral presentation (https://acr23.eventscribe.net/fsPopup.asp?PresentationID=1300725&mode=sessionInfo); and (3) the National Institute of General Medical Sciences training grant T32GM139801-03.

## Contributors

BHL, SA, and MDM conceived and designed the study. Regeneron Genetics Center performed exome sequencing in an academic-industry partnership. SK, HD, DM, MA-H, JM, KW, JKA, and OL performed the experiments. BHL, MDM, SA, LB, and BD provided input or key resources. SK, KW, JKA, and OL analysed the data. SK and BHL wrote the manuscript. All authors read, revised, and approved the final manuscript. BHL is the guarantor of this study.

## Funding

This study was funded by the National Institutes of Health 1R01AG074009 and 1U01AG068214 and by National Institute of Arthritis, Musculoskeletal and Skin Diseases (NIAMS) of the National Institutes of Health (NIH) [P50-AR044888, P50-AR054144, N01-AR-02251, and R01-AR-055258]; the University of Texas Health Science Center NIH-funded Clinical and Translational Science Award (CTSA) Clinical Research Unit [UL1 RR024148]; and the Department of Defense (DoD) Congressionally Directed Medical Research Program [W81XWH-07-1-011, WX81XWH-13-1-0452, W81XWH22-1-0372, and WX81XWH-18-1-0423].

## Patient consent for publication

All study participants provided written informed consent, and healthy control participants had no history of autoimmune rheumatologic disease and were not related to enrolled patients with systemic sclerosis.

## Ethics approval

The study was approved by the Institutional Review Board (Committee for the Protection of Human Subjects) at the University of Texas Health Science Center at Houston.

## Provenance and peer review

Not commissioned; externally peer reviewed.

## Data availability statement

The data that support the findings of this study are available on request from the corresponding author. The data are not publicly available due to privacy or ethical restrictions.

## Supplementary materials

Supplementary material associated with this article can be found in the online version at doi:10.1016/j.ard.2025.05.009.

## Orcid

Shamika Ketkar: http://orcid.org/0000-0001-8799-0729
David Murdock: http://orcid.org/0000-0002-8536-3091
Marialbert Acosta-Herrera: http://orcid.org/0000-0002-9868-6535
Jennifer Kay Asmussen: http://orcid.org/0000-0002-9280-0333
Olivier Lichtarge: http://orcid.org/0000-0003-4057-7122
Brendan H. Lee: http://orcid.org/0000-0001-8573-4211

## REFERENCES

[1] Barnes J, Mayes MD. Epidemiology of systemic sclerosis: incidence, prevalence, survival, risk factors, malignancy, and environmental triggers. Curr Opin Rheumatol 2012;24:165–70. doi: 10.1097/BOR.0b013e32834ff2e8.
[2] Li JX. Secular trends in systemic sclerosis mortality in the United States from 1981 to 2020. Int J Environ Res Public Health 2022;19:15088. doi: 10.3390/ijerph192215088.
[3] Scleroderma: practice essentials, background, pathophysiology [Internet]. Medscape [updated 2023 Mar 1; cited 2023 Jul 19]. Available from: https://emedicine.medscape.com/article/331864-overview#a5
[4] Mayes MD, Lacey JV, Beebe-Dimmer J, Gillespie BW, Cooper B, Laing TJ, et al. Prevalence, incidence, survival, and disease characteristics of systemic sclerosis in a large US population. Arthritis Rheum 2003;48:2246–55. doi: 10.1002/art.11073.
[5] Villanueva-Martín G, Martín J, Bossini-Castillo L. Recent advances in elucidating the genetic basis of systemic sclerosis. Curr Opin Rheumatol 2022;34:295–301. doi: 10.1097/BOR.0000000000000897.
[6] Zhou X, Lee JE, Arnett FC, Xiong M, Park MY, Yoo YK, et al. HLA-DPB1 and DPB2 are genetic loci for systemic sclerosis: a genome-wide association study in Koreans with replication in North Americans. Arthritis Rheum 2009;60:3807–14. doi: 10.1002/art.24982.
[7] Reveille JD, Durban E, MacLeod-St Clair MJ, Goldstein R, Moreda R, Altman RD, et al. Association of amino acid sequences in the HLA-DQB1 first domain with antitopoisomerase I autoantibody response in scleroderma (progressive systemic sclerosis). J Clin Invest 1992;90:973–80. doi: 10.1172/JCI115974.
[8] Rueda B, Broen J, Simeon C, Hesselstrand R, Diaz B, Suárez H, et al. The STAT4 gene influences the genetic predisposition to systemic sclerosis phenotype. Hum Mol Genet 2009;18:2071–7. doi: 10.1093/hmg/ddp119.
[9] Sharif R, Mayes MD, Tan FK, Gorlova OY, Hummers LK, Shah AA, et al. IRF5 polymorphism predicts prognosis in patients with systemic sclerosis. Ann Rheum Dis 2012;71:1197–202. doi: 10.1136/annrheumdis-2011-200901.
[10] Radstake TRDJ, Gorlova O, Rueda B, Martin JE, Alizadeh BZ, Palomino-Morales R, et al. Genome-wide association study of systemic sclerosis identifies CD247 as a new susceptibility locus. Nat Genet 2010;42:426–9. doi: 10.1038/ng.565.
[11] Gao L, Emond MJ, Louie T, Cheadle C, Berger AE, Rafaels N, et al. Identification of rare variants in ATP8B4 as a risk factor for systemic sclerosis by whole-exome sequencing. Arthritis Rheumatol 2016;68:191–200. doi: 10.1002/art.39449.
[12] Arnett FC, Cho M, Chatterjee S, Aguilar MB, Reveille JD, Mayes MD. Familial occurrence frequencies and relative risks for systemic sclerosis (scleroderma) in three United States cohorts. Arthritis Rheum 2001;44:1359–62.
[13] Zuk O, Hechter E, Sunyaev SR, Lander ES. The mystery of missing heritability: genetic interactions create phantom heritability. Proc Natl Acad Sci U S A 2012;109:1193–8. doi: 10.1073/pnas.1119675109.
[14] Bourquard T, Lee K, Al-Ramahi I, Pham M, Shapiro D, Lagisetty Y, et al. Functional variants identify sex-specific genes and pathways in Alzheimer's disease. Nat Commun 2023;14:2765. doi: 10.1038/s41467-023-38374-z.
[15] Shapiro D, Lee K, Asmussen J, Bourquard T, Lichtarge O. Evolutionary action −machine learning model identifies candidate genes associated with early-onset coronary artery disease. J Am Heart Assoc 2023;12:e029103. doi: 10.1161/JAHA.122.029103.
[16] Katsonis P, Lichtarge O. A formal perturbation equation between genotype and phenotype determines the evolutionary action of protein-coding variations on fitness. Genome Res 2014;24:2050–8. doi: 10.1101/gr.176214.114.
[17] Lichtarge O, Bourne HR, Cohen FE. An evolutionary trace method defines binding surfaces common to protein families. J Mol Biol 1996;257:342–58. doi: 10.1006/jmbi.1996.0167.
[18] Masi AT. Preliminary criteria for the classification of systemic sclerosis (scleroderma). Subcommittee for scleroderma criteria of the American Rheumatism Association Diagnostic and Therapeutic Criteria Committee. Arthritis Rheum 1980;23:581–90. doi: 10.1002/art.1780230510.
[19] Assassi S, Del Junco D, Sutter K, McNearney TA, Reveille JD, Karnavas A, et al. Clinical and genetic factors predictive of mortality in early systemic sclerosis. Arthritis Rheum 2009;61:1403–11. doi: 10.1002/art.24734.
[20] Van Den Hoogen F, Khanna D, Fransen J, Johnson SR, Baron M, Tyndall A, et al. 2013 classification criteria for systemic sclerosis: an American College of Rheumatology/European League Against Rheumatism Collaborative Initiative. Ann Rheum Dis 2013;72:1747–55. doi: 10.1136/annrheumdis-2013-204424.
[21] Howie B, Fuchsberger C, Stephens M, Marchini J, Abecasis GR. Fast and accurate genotype imputation in genome-wide association studies through pre-phasing. Nat Genet 2012;44:955–9. doi: 10.1038/ng.2354.
[22] 1000 Genomes Project Consortium, Auton A, Abecasis GR, Altshuler DM, Durbin RM, Bentley DR, et al. A global reference for human genetic variation. Nature 2015;526:68–74. doi: 10.1038/nature15393.
[23] 1000 Genomes Project Consortium, Abecasis GR, Altshuler D, Auton A, Brooks LD, Durbin RM, et al. A map of human genome variation from population-scale sequencing. Nature 2010;467:1061–73. doi: 10.1038/nature09534.
[24] Purcell S, Neale B, Todd-Brown K, Thomas L, Ferreira MAR, Bender D, et al. PLINK: a tool set for whole-genome association and population-based linkage analyses. Am J Hum Genet 2007;81:559–75. doi: 10.1086/519795.
[25] López-Isac E, Acosta-Herrera M, Kerick M, Assassi S, Satpathy AT, Granja J, et al. GWAS for systemic sclerosis identifies multiple risk loci and highlights fibrotic and vasculopathy pathways. Nat Commun 2019;10:4955. doi: 10.1038/s41467-019-12760-y.
[26] Yang J, Ferreira T, Morris AP, Medland SE. Genetic Investigation of ANthropometric Traits (GIANT) Consortium, DIAbetes Genetics Replication And Meta-analysis (DIAGRAM) Consortium, et al. Conditional and joint multiple-SNP analysis of GWAS summary statistics identifies additional variants influencing complex traits. Nat Genet 2012;44:369–75. doi: 10.1038/ng.2213.
[27] Yang J, Lee SH, Goddard ME, Visscher PM. GCTA: a tool for genome-wide complex trait analysis. Am J Hum Genet 2011;88:76–82. doi: 10.1016/j.ajhg.2010.11.011.
[28] Rothwell S, Chinoy H, Lamb JA, Miller FW, Rider LG, Wedderburn LR, et al. Focused HLA analysis in Caucasians with myositis identifies significant associations with autoantibody subgroups. Ann Rheum Dis 2019;78:996–1002. doi: 10.1136/annrheumdis-2019-215046.
[29] Manichaikul A, Mychaleckyj JC, Rich SS, Daly K, Sale M, Chen WM. Robust relationship inference in genome-wide association studies. Bioinformatics 2010;26:2867–73. doi: 10.1093/bioinformatics/btq559.
[30] McLaren W, Gil L, Hunt SE, Riat HS, Ritchie GRS, Thormann A, et al. The Ensembl variant effect predictor. Genome Biol 2016;17:122. doi: 10.1186/S13059-016-0974-4.
[31] Szklarczyk D, Kirsch R, Koutrouli M, Nastou K, Mehryary F, Hachilif R, et al. The STRING database in 2023: protein-protein association networks and functional enrichment analyses for any sequenced genome of interest. Nucleic Acids Res 2023;51:D638–46. doi: 10.1093/NAR/GKAC1000.
[32] Pham M, Lichtarge O. Graph-based information diffusion method for prioritizing functionally related genes in protein-protein interaction networks. Pac Symp Biocomput 2020;25:439–50. doi: 10.1142/9789811215636_0039.
[33] Watanabe K, Taskesen E, Van Bochoven A, Posthuma D. Functional mapping and annotation of genetic associations with FUMA. Nat Commun 2017;8:1826. doi: 10.1038/S41467-017-01261-5.
[34] Povysil G, Petrovski S, Hostyk J, Aggarwal V, Allen AS, Goldstein DB. Rare-variant collapsing analyses for complex traits: guidelines and applications. Nat Rev Genet 2019;20:747–59. doi: 10.1038/S41576-019-0177-4.
[35] Cock PJA, Antao T, Chang JT, Chapman BA, Cox CJ, Dalke A, et al. Biopython: freely available Python tools for computational molecular biology and bioinformatics. Bioinformatics 2009;25:1422–3. doi: 10.1093/BIOINFORMATICS/BTP163.

[36] Ashburner M, Ball CA, Blake JA, Botstein D, Butler H, Cherry JM, et al. Gene ontology: tool for the unification of biology. The Gene Ontology Consortium. Nat Genet 2000;25:25–9. doi: 10.1038/75556.
[37] Gene Ontology Consortium. The Gene Ontology resource: enriching a GOld mine. Nucleic Acids Res 2021;49:D325–34. doi: 10.1093/NAR/GKAA1113.
[38] Gillespie M, Jassal B, Stephan R, Milacic M, Rothfels K, Senff-Ribeiro A, et al. The reactome pathway knowledgebase 2022. Nucleic Acids Res 2022;50: D687–92. doi: 10.1093/nar/gkab1028.
[39] Jumper J, Evans R, Pritzel A, Green T, Figurnov M, Ronneberger O, et al. Highly accurate protein structure prediction with AlphaFold. Nature 2021; 596:583–9. doi: 10.1038/S41586-021-03819-2.
[40] Varadi M, Anyango S, Deshpande M, Nair S, Natassia C, Yordanova G, et al. AlphaFold Protein Structure Database: massively expanding the structural coverage of protein-sequence space with high-accuracy models. Nucleic Acids Res 2022;50:D439–44. doi: 10.1093/nar/gkab1061.
[41] Mihalek I, Reš I, Yao H, Lichtarge O. Combining inference from evolution and geometric probability in protein structure evaluation. J Mol Biol 2003;331:263–79. doi: 10.1016/S0022-2836(03)00663-6.
[42] Wilkins AD, Lua R, Erdin S, Ward RM. Lichtarge O. Sequence and structure continuity of evolutionary importance improves protein functional site discovery and annotation. Protein Sci 2010;19:1296–311. doi: 10.1002/PRO.406.
[43] Skaug B, Khanna D, Swindell WR, Hinchcliff ME, Frech TM, Steen VD, et al. Global skin gene expression analysis of early diffuse cutaneous systemic sclerosis shows a prominent innate and adaptive inflammatory profile. Ann Rheum Dis 2020;79:379–86. doi: 10.1136/annrheumdis-2019-215894.
[44] Tabib T, Huang M, Morse N, Papazoglou A, Behera R, Jia M, et al. Myofibroblast transcriptome indicates SFRP2$^{hi}$ fibroblast progenitors in systemic sclerosis skin. Nat Commun 2021;12:4384. doi: 10.1038/s41467-021-24607-6.
[45] Dai B, Ding L, Zhao L, Zhu H, Luo H. Contributions of immune cells and stromal cells to the pathogenesis of systemic sclerosis: recent insights. Front Pharmacol 2022;13:826839. doi: 10.3389/fphar.2022.826839.
[46] Allanore Y, Saad M, Dieudé P, Avouac J, Distler JHW, Amouyel P, et al. Genome-wide scan identifies TNIP1, PSORS1C1, and RHOB as novel risk loci for systemic sclerosis. PLoS Genet 2011;7:e1002091. doi: 10.1371/journal.pgen.1002091.
[47] Ramos PS. Epigenetics of scleroderma: integrating genetic, ethnic, age, and environmental effects. J Scleroderma Relat Disord 2019;4:238–50. doi: 10.1177/2397198319855872.
[48] Zhou X, Li H, Guo S, Wang J, Shi C, Espitia M, et al. Associations of multiple NOTCH4 exonic variants with systemic sclerosis. J Rheumatol 2019;46:184–9. doi: 10.3899/jrheum.180094.
[49] Morris DL, Taylor KE, Fernando MMA, Nititham J, Alarcón-Riquelme ME, Barcellos LF, et al. Unraveling multiple MHC gene associations with systemic lupus erythematosus: model choice indicates a role for HLA alleles and non-HLA genes in Europeans. Am J Hum Genet 2012;91:778–93. doi: 10.1016/j.ajhg.2012.08.026.
[50] Barcellos LF, May SL, Ramsay PP, Quach HL, Lane JA, Nititham J, et al. High-density SNP screening of the major histocompatibility complex in systemic lupus erythematosus demonstrates strong evidence for independent susceptibility regions. PLoS Genet 2009;5:e1000696. doi: 10.1371/journal.pgen.1000696.
[51] Zhan X, Hu Y, Li B, Abecasis GR, Liu DJ. RVTESTS: an efficient and comprehensive tool for rare variant association analysis using sequence data. Bioinformatics 2016;32:1423–6. doi: 10.1093/bioinformatics/btw079.
[52] Hanson AL, Sahhar J, Ngian GS, Roddy J, Walker J, Stevens W, et al. Contribution of HLA and KIR alleles to systemic sclerosis susceptibility and immunological and clinical disease subtypes. Front Genet 2022;13:913196. doi: 10.3389/fgene.2022.913196.
[53] Ota Y, Kuwana M. Updates on genetics in systemic sclerosis. Inflamm Regen 2021;41:17. doi: 10.1186/s41232-021-00167-6.
[54] Barnes J, Agarwal SK. Targeting STAT4 in systemic sclerosis: a promising new direction. Expert Rev Clin Immunol 2011;7:445–8. doi: 10.1586/eci.11.31.
[55] Blondel VD, Guillame JL, Lambiotte R, Lefebvre E. Fast unfolding of communities in large networks. J Stat Mech: Theory Exp 2008;2008.
[56] Groh V, Steinle A, Bauer S, Spies T. Recognition of stress-induced MHC molecules by intestinal epithelial gammadelta T cells. Science 1998;279:1737–40. doi: 10.1126/science.279.5357.1737.
[57] Seguro Paula F, Delgado Alves J. The role of the Notch pathway in the pathogenesis of systemic sclerosis: clinical implications. Expert Rev Clin Immunol 2021;17:1257–67. doi: 10.1080/1744666X.2021.2000391.
[58] Higashi-Kuwata N, Jinnin M, Makino T, Fukushima S, Inoue Y, Muchemwa FC, et al. Characterization of monocyte/macrophage subsets in the skin and peripheral blood derived from patients with systemic sclerosis. Arthritis Res Ther 2010;12:R128. doi: 10.1186/AR3066.
[59] Gruschwitz M, Sepp N, Kofler H, Wick G. Expression of Class II-MHC antigens in the dermis of patients with progressive systemic sclerosis. Immunobiology 1991;182:234–55. doi: 10.1016/S0171-2985(11)80660-1.
[60] Gorlova O, Martin JE, Rueda B, Koeleman BPC, Ying J, Teruel M, et al. Identification of novel genetic markers associated with clinical phenotypes of systemic sclerosis through a genome-wide association strategy. PLoS Genet 2011;7:e1002178. doi: 10.1371/journal.pgen.1002178.
[61] Bergmann C, Chenguiti Fakhouri S, Thuong T, Filla T, Rigau AR, Ekici AB, et al. Mutual amplification of GLI2 /Hedgehog and cJUN/AP1 signaling in fibroblasts in Systemic sclerosis (SSc) – potential implications for combined therapies. Arthritis Rheumatol 2025;77:92–8. doi: 10.1002/ART.42979/ABSTRACT.
[62] Kerick M, González-Serna D, Carnero-Montoro E, Teruel M, Acosta-Herrera M, Makowska Z, et al. Expression quantitative trait locus analysis in systemic sclerosis identifies new candidate genes associated with multiple aspects of disease pathology. Arthritis Rheumatol 2021;73:1288–300. doi: 10.1002/art.41657.
[63] Hartmann S, Yasmeen S, Jacobs BM, Denaxas S, Pirmohamed M, Gamazon ER, et al. ADRA2A and IRX1 are putative risk genes for Raynaud's phenomenon. Nat Commun 2023;14:6156. doi: 10.1038/s41467-023-41876-5.
[64] Haque A, Hughes M. Raynaud's phenomenon. Clin Med (Lond) 2020;20:580–7. doi: 10.7861/clinmed.2020-0754.
[65] Ishikawa Y, Terao C. Genetics of systemic sclerosis. J Scleroderma Relat Disord 2020;5:192–201. doi: 10.1177/2397198320913695.
[66] Kim D, Peck A, Santer D, Patole P, Schwartz SM, Molitor JA, et al. Induction of interferon-alpha by scleroderma sera containing autoantibodies to topoisomerase I: association of higher interferon-alpha activity with lung fibrosis. Arthritis Rheum 2008;58:2163–73. doi: 10.1002/art.23486.
[67] Eloranta ML, Franck-Larsson K, Lövgren T, Kalamajski S, Rönnblom A, Rubin K, et al. Type I interferon system activation and association with disease manifestations in systemic sclerosis. Ann Rheum Dis 2010;69:1396–402. doi: 10.1136/ard.2009.121400.
[68] Morand EF, Furie R, Tanaka Y, Bruce IN, Askanase AD, Richez C, et al. Trial of anifrolumab in active systemic lupus erythematosus. N Engl J Med 2020;382:211–21. doi: 10.1056/NEJMoa1912196.

Ann Rheum Dis 84 (2025) 1375–1386

Contents lists available at ScienceDirect

Annals of the Rheumatic Diseases

journal homepage: https://www.sciencedirect.com/journal/annals-of-the-rheumatic-diseases

Myositis

# Mitochondria-centred metabolomic map of inclusion body myositis: sex-specific alterations in central carbon metabolism

Elie Naddaf[1,*], Ibrahim Shammas[1], Surendra Dasari[2], Xuan-Mai T. Petterson[3], Wolfdieter Springer[4], Eugenia Trushina[1,5], Ian R. Lanza[3,6]

[1] *Department of Neurology, Mayo Clinic, Rochester, MN, USA*
[2] *Department of Quantitative Health Sciences, Mayo Clinic, Rochester, MN, USA*
[3] *Mayo Metabolomics Core Laboratory, Rochester, MN, USA*
[4] *Department of Neuroscience, Mayo Clinic, Jacksonville, FL, USA*
[5] *Department of Molecular Pharmacology and Experimental Therapeutics, Mayo Clinic, Rochester, MN, USA*
[6] *Division of Endocrinology, Nutrition, and Metabolism, Mayo Clinic, Rochester, MN, USA*

ARTICLE INFO

*Article history:*
Received 17 January 2025
Received in revised form 15 April 2025
Accepted 4 May 2025

ABSTRACT

*Objectives:* To benchmark metabolomic signatures of inclusion body myositis (IBM) in muscle tissue, highlighting sex-specific differences and the correlation with clinical parameters.
*Methods:* A total of 37 IBM patients and 22 controls without myopathy were included. All participants had bulk RNA sequencing performed previously. Clinical parameters included disease duration and manual muscle test (MMT) scores. Discovery metabolite screening and quantitative targeted metabolomics platforms were used. Levels of metabolites and RNA-metabolomic integrated modules were correlated with clinical parameters and the mitophagy marker, p-S65-Ubiquitin (p-S65-Ub).
*Results:* IBM muscle samples showed elevated citric acid (TCA) cycle intermediates and anaplerotic amino acids. Proximal glycolytic intermediates were decreased, while pentose phosphate pathway (PPP) metabolites were increased. Short-chain acylcarnitines were lower in IBM males but not in females. Lastly, nucleic acid bases were increased, and nucleotides were decreased. MMT correlated with PPP metabolites and nucleic acid bases, and inversely correlated with glycolysis metabolites and mono/diphosphate nucleotides. MMT also correlated with several amino acids, including cysteine, taurine, carnosine, and sarcosine. Acylcarnitines correlated with disease duration only in males. Four RNA-metabolomic integrated modules demonstrated significant correlations. The strongest correlations were observed between the pink module and both sexes and p-S65-Ub. MMT and p-S65-Ub correlated with 3 and 2 modules, respectively. The enriched pathways were related to central carbon metabolism, cytokine/chemokine signalling, neurotransmission, and mitogen-activated protein kinase (MAPK)/RAS signalling. Males had relatively similar correlations to the combined-sex analysis, while females had no significant correlation with any module.
*Conclusions:* IBM is associated with clinically significant alterations in central carbon metabolism, with the strongest RNA-metabolomic-clinical correlations observed in males. Further research is needed to explore the role of these metabolic changes in IBM pathogenesis and their progression over time.

*Correspondence to Dr Elie Naddaf, Department of Neurology, Mayo Clinic, 200 First Street SW, Rochester, MN 55905, USA.
*E-mail address:* Naddaf.elie@mayo.edu (E. Naddaf).
**Handling editor** Josef S. Smolen.

https://doi.org/10.1016/j.ard.2025.05.003

0003-4967/© 2025 The Author(s). Published by Elsevier B.V. on behalf of European Alliance of Associations for Rheumatology (EULAR). This is an open access article under the CC BY-NC-ND license (http://creativecommons.org/licenses/by-nc-nd/4.0/)

**WHAT IS ALREADY KNOWN ON THIS TOPIC**

Inclusion body myositis (IBM) is a disease that sits at the intersection of ageing, mitochondrial dysfunction, and chronic inflammation. Limited studies have evaluated the underlying metabolic disturbances in IBM.

**WHAT THIS STUDY ADDS**

IBM is associated with sex-specific clinically significant alterations in central carbon metabolism, with the strongest correlation observed in males.

**HOW THIS STUDY MIGHT AFFECT RESEARCH, PRACTICE OR POLICY**

This study provides the foundation for future research to develop metabolomic-based diagnostic and outcome biomarkers in IBM. It highlights shared pathways with ageing and sarcopenia that are potentially amenable to therapeutic interventions.

## INTRODUCTION

Inclusion body myositis (IBM) is a disease of ageing, characterised by progressive muscle loss, which eventually leads to the loss of mobility [1]. Skeletal muscles are a major consumer of energy and play a central role in metabolism. Metabolomic studies on human muscles in myopathies are scarce, partly due to the limited access to human samples. IBM sits at the intersection of ageing, chronic inflammation, and mitochondrial dysfunction, making it an ideal candidate for metabolomic studies [2]. Despite being the most common muscle disease, only a few studies have evaluated the metabolomic profile in IBM, and only 1 study reported metabolomics from muscle tissue [3]. In this study by Murakami et al [3], untargeted metabolomic analysis was performed on samples from 14 IBM patients, 10 males and 4 females, and 6 controls [3]. The top 20 metabolites were associated with histamine biosynthesis, glycosaminoglycan metabolism, carnitine metabolism, and creatine metabolism, and transcriptomics analysis using 5 samples was focused on the genes related to the identified metabolic pathways [3]. In a study by Buzkova et al [4], 94 metabolites were evaluated in blood samples from 6 IBM patients and patients with mitochondrial diseases and other neuromuscular disorders. IBM shared 39% of altered metabolites with progressive external ophthalmoplegia, a mitochondrial disease, vs only 23% with other neuromuscular disorders [4]. Lastly, Cantó-Santos et al [5] evaluated organic acid levels in fibroblasts and urine samples and nucleotide precursors in urine samples from IBM patients and controls. Five out of 19 organic acid alterations in fibroblasts reached statistical significance, with 2-hydroxyglutaric acid having the highest fold change. Only 1 organic acid (orotic acid) reached statistical significance in urine. Among nucleic acids, orotidine and pseudouridine were significantly elevated. Furthermore, the authors evaluated metabolism-related genes using RNA data and assessed their correlation with the observed changes in organic acids. To date, sex-specific differences in IBM metabolism, correlation with clinical parameters, and unsupervised transcriptomic-metabolomic integration have not been done.

Our recently published study [6] on a cohort of 38 IBM patients and 22 controls reported NOD-like receptor family pyrin domain-containing (NLRP) 3 inflammasome activation and altered mitophagy in the muscle tissue of IBM patients. There was a significant elevation of p-S65-Ubiquitin (p-S65-Ub), a mitophagy marker, in muscle lysates from male patients, whereas females had only mildly elevated levels that did not reach statistical significance [6]. In histopathology, we demonstrated the accumulation of p-S65-Ub aggregates in cytochrome c oxidase (CCO)-negative fibres that were strictly type II fibres. Indeed, CCO-negative fibres in IBM muscles, with or without aggregates, were mainly type II [6]. Type II fibres are more prone to mitochondrial dysfunction and have a different metabolic signature than type I [7]. Furthermore, mitochondria play a central and multifaceted role in cellular metabolism, expanding beyond adenosine triphosphate (ATP) synthesis to include the production and breakdown of metabolites and the regulation of metabolic pathways through signalling [8].

Given the central role of mitochondria in metabolism and the distinct vulnerability of type II muscle fibres in IBM, we aimed to address the critical gaps in understanding the metabolomic landscape of IBM via a comprehensive approach that includes sex-specific analyses, unsupervised integration of metabolomic and transcriptomic data, and correlations with clinical parameters and p-S65-Ub.

## METHODS

### *Study population*

The study population consisted of 37 patients with IBM and 22 age- and (biological) sex-matched controls without a myopathy. Patients with IBM fulfilled the 2011 European Neuromuscular Centre (ENMC) diagnostic criteria for IBM. As patients had a typical pattern of weakness and pathologically confirmed diagnosis, they would also fulfil the recently published revision of these criteria [9]. Controls consisted of patients without a myopathy, who underwent a muscle biopsy to rule out a muscle disorder and had an unremarkable workup. This is the same population as in our recently published study [6], which included 38 patients with IBM and 22 controls. However, 1 IBM male patient had insufficient leftover frozen muscle tissue to perform metabolomic analysis. All muscle biopsies were originally obtained for clinical purposes, and residuals were used for this project. Per our clinical practice standards, an open biopsy was performed in the operating room under conscious sedation after fasting overnight for all patients. The harvested muscle tissue was frozen in isopentane, cooled in liquid nitrogen, and stored at −80°C according to our muscle laboratory protocols. About 30 to 50 mg of frozen tissue was used for the metabolomics experiments. Target muscles are shown in the Table.

### *Clinical parameters*

Clinical parameters were obtained via chart review and included age at biopsy, (biological) sex, disease duration (time from symptom onset until biopsy date), manual muscle test (MMT) score, and modified Rankin Scale (MRS). The MMT score is a summated motor exam of the bilateral shoulder abduction, elbow flexion, elbow extension, finger flexion, hip flexion, knee extension, and ankle dorsiflexion. Each muscle is graded from 0 (normal) to 4 (complete paralysis), and the total score ranges from 0 (normal strength) to 56 (complete paralysis) as previously described [10]. The MRS, used to assess a patient's level of disability, ranges from 0 (no symptoms) to 6 (dead) as follows: MRS 1: symptoms without disability; 2: slight disability

Table
**Baseline characteristics and patient demographics**

| Variable | Inclusion body myositis (n = 37) | Controls (n = 22) |
|---|---|---|
| **Age at biopsy (y)** | 62.7 (9.2) | 59.7 (10) |
| **Sex** | | |
| Females | 19 (51) | 11 (50) |
| Males | 18 (49) | 11 (50) |
| **Race** | | |
| American Indian/Alaskan Native | 1 (2.7) | 1 (4.5) |
| Black | 1 (2.7) | 0 |
| White | 31 (83.8) | 19 (86.4) |
| Unknown/not disclosed | 4 (10.8) | 2 (9.1) |
| **Biopsy target** | | |
| Quadriceps | 14 (37.9) | 8 (36.4) |
| Biceps brachii | 9 (24.3) | 5 (22.7) |
| Triceps brachii | 9 (24.3) | 3 (13.6) |
| Others | 5 (13.5) | 6 (27.3) |
| **Disease characteristics** | | |
| Disease duration at time of the biopsy (y) | 6.3 (3.9) | NA |
| Manual motor test score | 17 (9.3) | 0 |

NA, not applicable.
Continuous variables are displayed as mean (SD) and categorical variables are displayed as the number of patients (percentage).

with the ability to perform baseline activities; 3: moderate disability requiring some help, but able to walk unassisted; 4: moderately severe disability with the inability to walk unassisted (wheelchair bound); and 5: severe disability with a need for constant nursing care and bedridden.

## *Metabolomics*

### *Untargeted metabolomics*

Untargeted metabolomics was performed as previously described (see Supplementary Methods for details) [11,12]. Briefly, metabolites were extracted from frozen muscle samples and analysed on a quadrupole time-of-flight mass spectrometer (MS) (Agilent 6550 Q-TOF) coupled with an ultrahigh-pressure liquid chromatograph (LC) (Agilent 1290 Infinity UHPLC). Metabolites were profiled under both positive and negative electrospray ionisation conditions and separated using a hydrophilic interaction (hilic) and reverse-phase C18 columns (C18) (4 modes: positive hilic, negative hilic, positive C18, and negative C18). Metabolites with a log fold change > |0.58| (fold change > 1.5) and a false discovery rate (FDR)-adjusted $P$ value < .05 were considered significantly different between groups.

### *Central carbon metabolism*

Focused profiling of metabolites related to central carbon metabolism was performed using the Agilent Metabolomics Dynamic Multiple Reaction Monitoring (dMRM) Database and Method. Central carbon metabolites (219 compounds) were monitored and measured in muscle tissue homogenates using an Agilent 6460 Triple Quadrupole MS coupled with an Agilent 1290 Infinity II Quaternary Pump [13]. Analytes were searched and confirmed against a curated dMRM database with retention time provided by Agilent. Relative abundances between sample sets were derived via multivariate analysis using the Agilent Mass Profiler Professional (MPP) software. Metabolites with a log fold change > |0.58| (fold change > 1.5) and an FDR-adjusted $P$ value < .05 were considered significantly different between groups.

### *Targeted metabolomics*

Targeted metabolite assays were performed on muscle tissue homogenates for the absolute quantitation of 11 citric acid (TCA) cycle analytes measured by gas chromatography-MS (GC-MS), 10 glycolysis and pentose phosphate pathway (PPP) metabolites measured by GC-MS, 42 amino metabolites measured by LC-MS, carnitine and 13 acyl carnitines (specifically, C0-C18:1) measured by LC-MS, and acetyl coenzyme A (acetyl-CoA) measured by LC-MS. Detailed methods are provided in the Supplementary Methods. Metabolite measurements were normalised to the sample protein measurement by bicinchoninic acid (BCA) assay. Two-group comparisons were performed via an independent samples $t$-test or a Wilcoxon rank-sum test, as appropriate, using BlueSky Statistics v.7.10 software and GraphPad Prism v.9.3.1.

## *Transcriptomics*

The raw gene-level count data from our recently published transcriptomics data on the same patient population were utilised for metabolomics-transcriptomics data integration [6].

## *Correlation between metabolite concentrations, clinical parameters, and p-S65-Ub*

Metabolite data from the central carbon metabolism platform were normalised using the trimmed means of the M-values method and log2 transformation. Metabolites from the targeted metabolomics and central carbon metabolism platform were pooled together. P-S65-Ub levels were measured in 22 IBM patients using a sandwich enzyme-linked immunosorbent assay performed via the Meso Scale Discovery platform, which uses electrochemiluminescence, as described and recently reported for this same cohort of patients [6]. Correlation analysis of clinical parameters and p-S65-Ub levels was performed using Spearman correlation, with $P$ values < .05 considered statistically significant.

## *Integration of RNA-metabolomics data and correlation with clinical parameters and p-S65-Ub levels*

The gene expression count data were normalised using the trimmed mean of M-values method and log2 transformation. Processed data were filtered to retain genes with a >20% coefficient of variation (CV) of expression across the entire cohort. Filtered genes were z-score transformed. Independently, the pooled metabolite data (described above) were filtered, like gene expression data, using a CV filter of >20% and z-score transformed. Scaled gene expression and metabolite data were combined for weighted coexpression network analysis [14]. This process identifies modules of genes and/or metabolites that have a strong association (by expression) with each other. The relationship between each module (via eigenvalues) and various continuous outcomes was measured using Spearman correlation. Biological sex was coded as: female = 1 and male = 0. Module outcome correlation $P$ values were adjusted using the Benjamini-Hochberg method. MetaboAnalyst 6.0 was used for joint pathway analysis in each module. Enrichment analysis was performed via a hypergeometric test, with degree centrality as a topology measure and combining queries as integration methods. An FDR q value < .05 was considered statistically significant.

## RESULTS

### *Study population*

Patients' demographics and disease characteristics are provided in the Table. The IBM group and controls had relatively similar ages at biopsy. There were no significant differences in baseline characteristics between the 2 groups.

### *Untargeted metabolomics*

Results of untargeted metabolomics are shown in Figure 1. Metabolites with the top variable importance in projection (VIP) scores included the TCA cycle, D-glycerate 2-phosphate and D-fructose (glycolysis), 3-deoxyguanosine and isoguanosine (nucleic acids), and phospholipids. A complete list of metabolites is shown in Supplementary Table S1. We then performed analysis by sex. Complete results are shown in Supplementary Figures S1 and S2 and Supplementary Table S2. After removing duplicates and unidentifiable compounds, there were 111 metabolites in females (65 up and 46 down) and 107 metabolites in males (70 up and 37 down), which were significantly different between IBM patients and controls. Males and females shared 44 metabolites with similar regulation (up or down) and 2 metabolites with opposite regulation (phosphatidyl serine [18:0/18:1{9Z}]) and phosphatidyl inositol [16:1{9Z}/22:2{13Z,16Z}]). Several sex-specific metabolites were phospholipids related to cell membrane structure and signalling.

### *Central carbon metabolism*

Given the fragmented nature of the results from the untargeted metabolomics, which is expected due to the exploratory nature of the platform, we followed with the semitargeted platform focusing on central carbon metabolism. It revealed 41 metabolites that were significantly different between IBM samples and controls (Fig 1 and Supplementary Table S3). Metabolites with top VIP scores consisted largely of nucleic acids and metabolites related to glucose metabolism. IBM samples had elevated levels of nucleic acid bases but decreased monophosphate and diphosphate nucleotides compared with controls. Furthermore, there was an increase in PPP metabolites with a decrease in glycolysis pathway metabolites in IBM samples. These findings were also observed when the analysis was stratified by sex. Additional results by sex are shown in Supplementary Figures S1 and S2 and Supplementary Table S4.

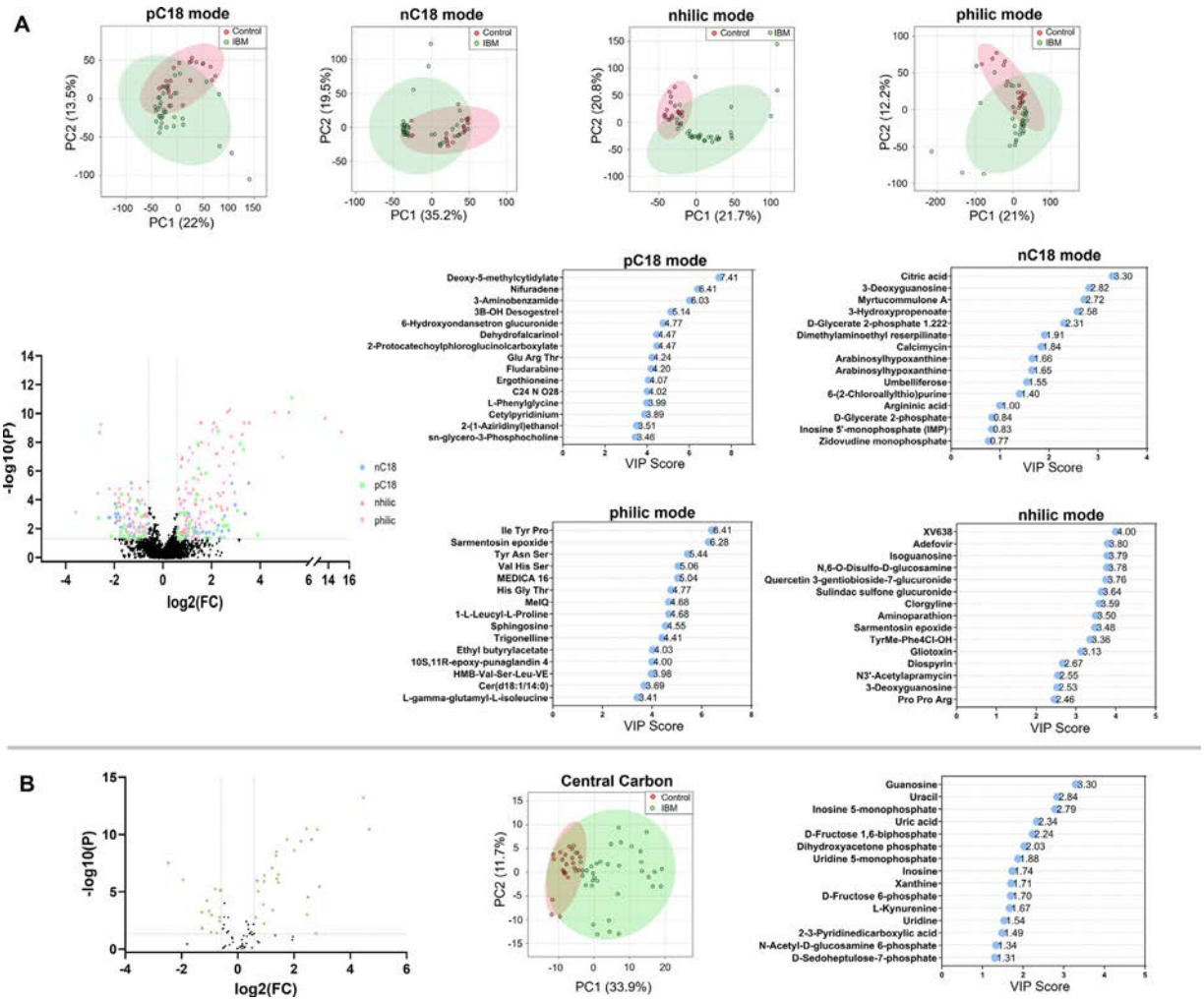



**Figure 1.** Results of untargeted metabolomics and central carbon metabolism platform. (A) Untargeted metabolomics in 4 modes: positive C18 (pC18), negative C18 (nC18), negative hydrophilic interaction (nhilic), and positive hydrophilic interaction (philic), and (B) central carbon metabolism platform. Volcano plots with $\log_2$-fold change (FC) of metabolites on the *x*-axis and $-\log_{10}P$ value (P) on the *y*-axis. Principal component (PC) analysis scatter plots and the top 15 metabolites according to the variable importance in projection (VIP) scores are shown. IBM, inclusion body myositis.

### *Targeted metabolomics*

Lastly, we focused on mitochondria-related metabolites through a combination of targeted quantitative assays. First, several TCA cycle metabolites were increased in IBM samples, with no difference in the lactate level between IBM samples and controls (Fig 2). The observed changes in some of the glycolysis metabolites suggest a decrease in proximal glycolysis. Simultaneously, most of the PPP metabolites were increased in IBM samples, indicating a shift to the PPP (Fig 3). The PPP is one of the main pathways that generate nicotinamide adenine dinucleotide phosphate (NADPH), which is involved in suppressing oxidative stress, and ribose-5-phosphate, used for nucleotide synthesis [15]. These results were relatively similar between males and females (Supplementary Figs S3 and S4).

In the acylcarnitine profile, carnitine and short-chain acylcarnitine levels (C2 and C3) were decreased in IBM samples in the combined-sex analysis, but only in males when stratifying by sex (Fig 4). There was no significant difference in acetyl-CoA levels between IBM samples and controls.

In the amino acid profile, 22 out of 42 amino acids were altered in IBM samples. Notably, there was an anaplerotic increase in amino acids serving the TCA cycle (Fig 2). Several amino acids demonstrated sex-specific changes, such as cysteine and threonine, which were increased only in females, and carnosine, anserine, and citrulline, which were decreased only in males (Supplementary Fig S5).

### *Association between metabolite concentrations, clinical parameters, and p-S65-Ub*

Results of the correlation of clinical parameters with targeted and central carbon metabolites are shown in Figure 5. For simplification, we displayed all the correlations from targeted assays, but only included the correlations of central carbon platform metabolites that reached statistical significance in any analysis. The MMT score had a significant positive correlation with 22 metabolites and an inverse correlation with 16 metabolites. The metabolite with the strongest positive correlation (higher levels are associated with more severe weakness) was

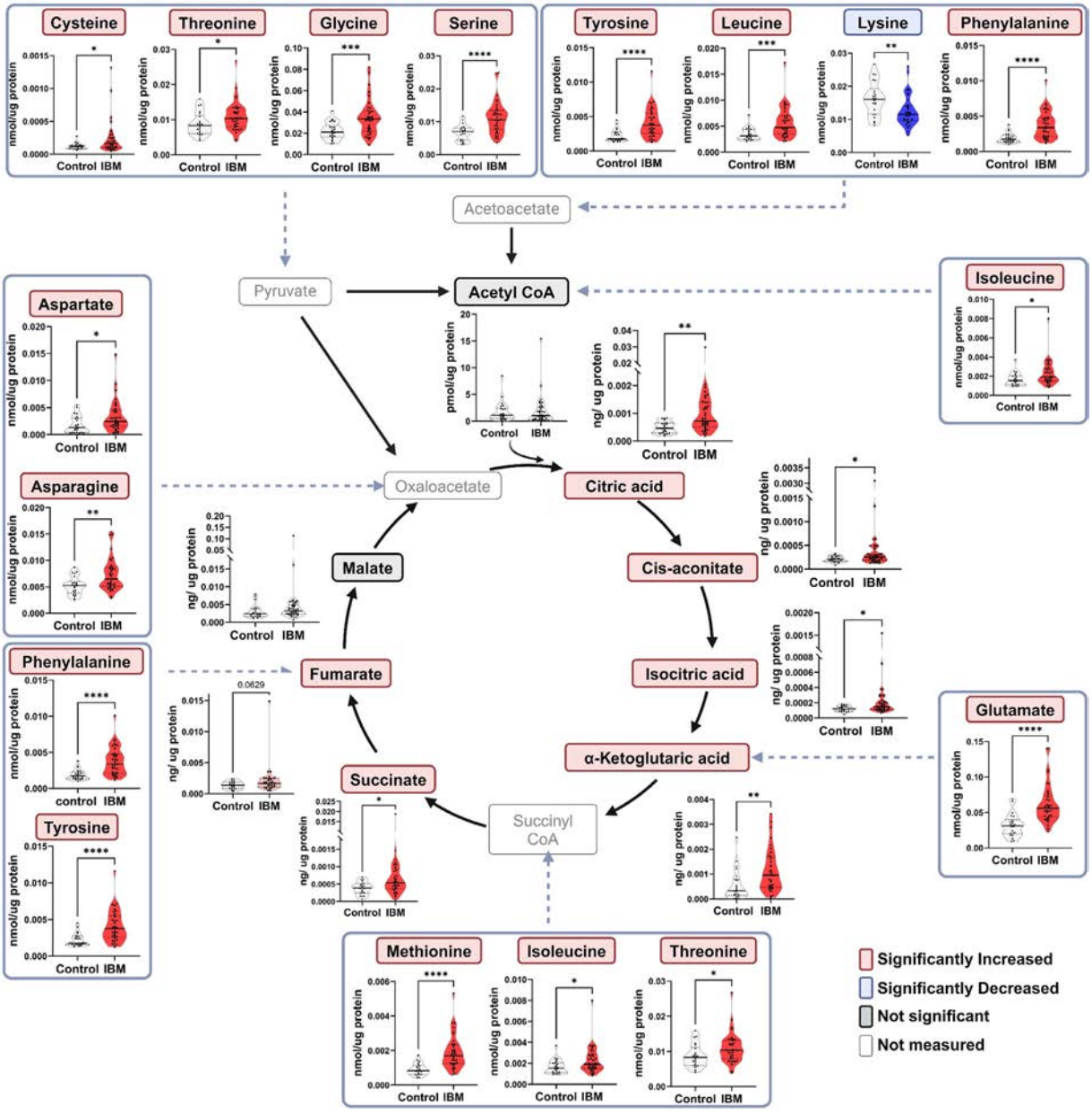



**Figure 2.** Targeted metabolomics results for the citric acid cycle and anaplerotic amino acids levels. Individual data are presented as truncated violin plots. *P* values < .05 are marked with an asterisk (*). ***P* < .01; ****P* < .001; *****P* < .0001. IBM, inclusion body myositis. CoA: coenzyme A.

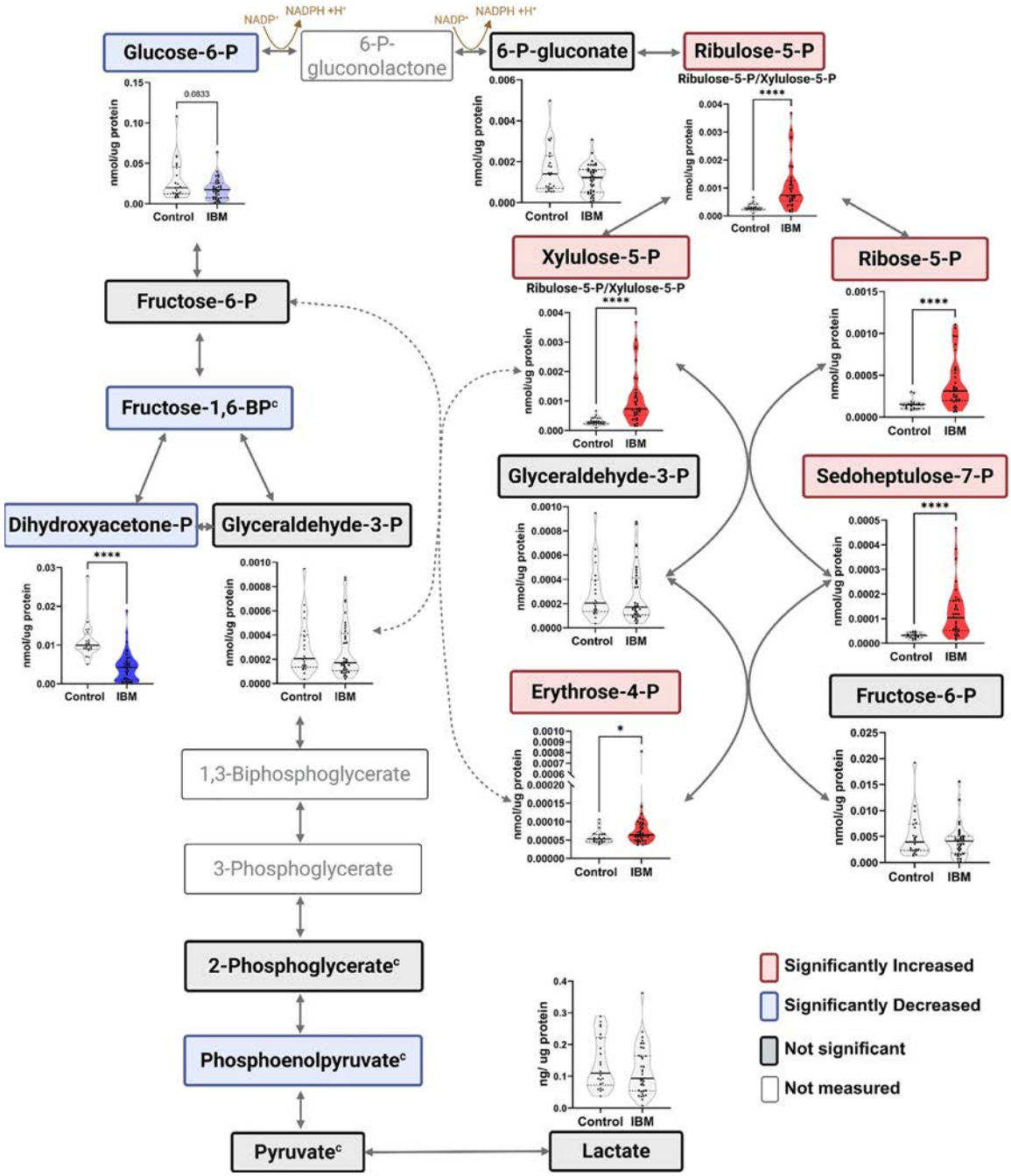



**Figure 3.** Glycolysis-pentose phosphate (P) pathway. Metabolites from the central carbon metabolism platform are marked with (c). Individual data are presented as truncated violin plots. *P* values < .05 are marked with an asterisk (*). **$P < .01$; ***$P < .001$; ****$P < .0001$. IBM, inclusion body myositis; BP: biphosphate.

cysteine. A PPP metabolite (sedoheptulose-7-phosphate) and a glycolysis inhibitor (2-deoxy-D-glucose-6-phosphate) positively correlated with MMT, whereas glycolysis metabolites inversely correlated with MMT. MMT had a negative correlation with carnosine and sarcosine and a positive correlation with taurine levels. Furthermore, MMT correlated with the levels of nucleic acid bases and inversely correlated with monophosphate and diphosphate nucleotides. Thirteen metabolites correlated with MRS. Most were nucleic acids, in addition to L-cystathione and S-5-adenosyl-L-homocysteine (related to antioxidation). Guanosine-3′,5′-cyclic monophosphate (cGMP) inversely correlated with MRS. Decreased cGMP levels have been associated with ageing and ageing-related disorders [16]. Three metabolites, including $\alpha$-aminoadipic acid, were positively correlated with disease duration. $\alpha$-Aminoadipic acid is considered a marker of glucose metabolism and diabetes and has a potential role in glutamatergic neurotransmission and oxidative stress [17,18]. Eight metabolites were inversely correlated with disease duration, including creatinine. Age at biopsy (positively) correlated with 3 TCA cycle metabolites and inversely correlated with thiamine, among others. P-S65-Ub had a significant positive correlation with 12 metabolites, including glycolysis intermediates, several amino acids, and riboflavin. P-S65-Ub inversely correlated with 5 metabolites, including $\alpha$-ketoglutarate, $\beta$-nicotinamide adenine dinucleotide (NAD+), and glutathione.

When stratifying by sex, there were sex-specific differences. For MMT, males shared metabolites with those observed in the combined-sex analysis related to PPP, glycolysis, and nucleosides. Cysteine had the strongest correlation with MMT in males. In contrast, MMT in females had the strongest correlation with

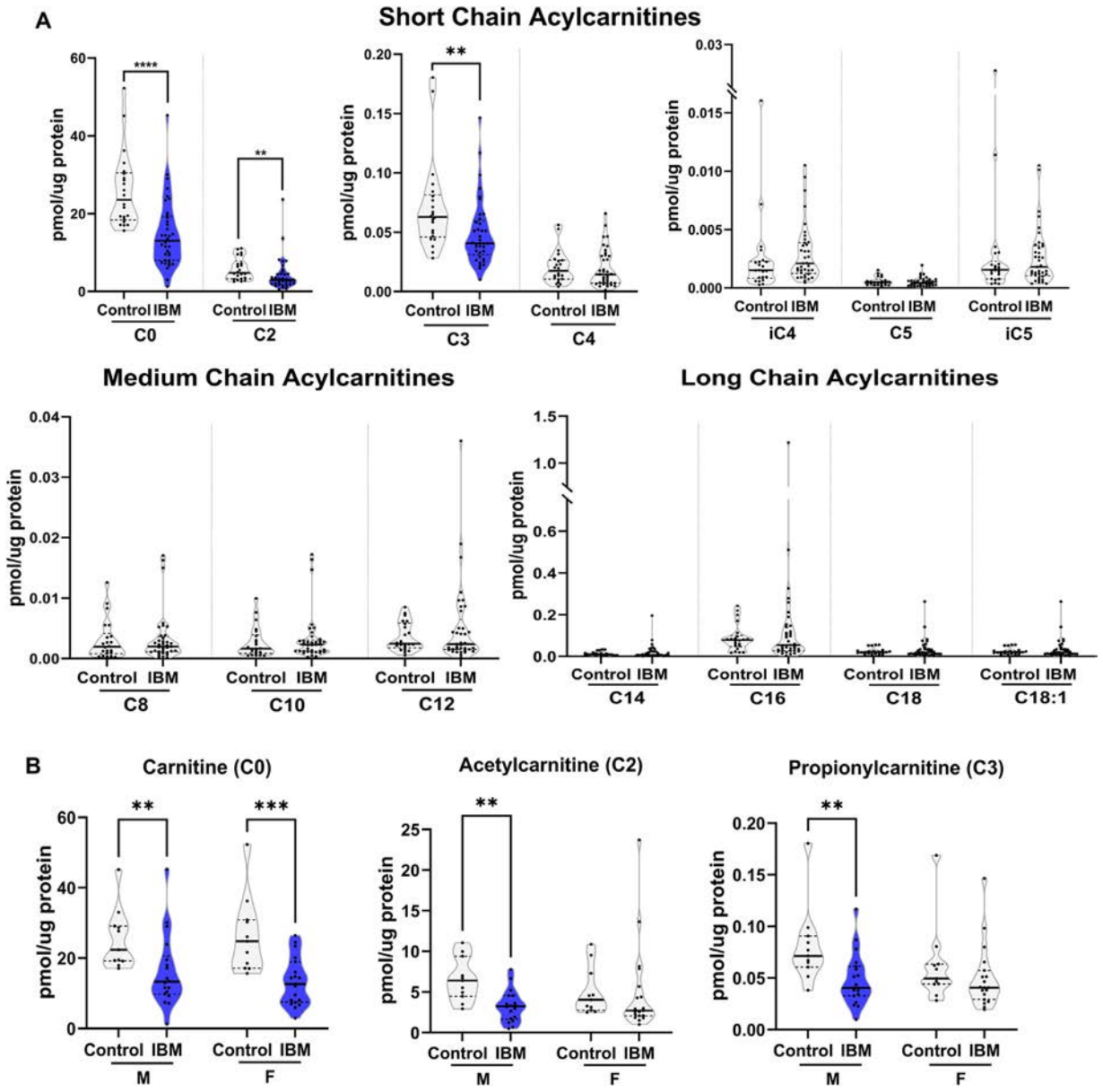



**Figure 4.** Acylcarnitine profile. (A) Combined-sex analysis. (B) Results by sex for C0 to C3 acylcarnitines. Acylcarnitines are displayed according to the number of carbon atoms. Individual data are presented as truncated violin plots. *P* values < .05 are marked with an asterisk (*). *$P < .01$; ***$P < .001$; ****$P < .0001$. F, female; IBM, inclusion body myositis; M, male.

taurine, and there were fewer correlations that reached statistical significance in females. Males and females shared only one common metabolite that correlated with MMT: 3-(2-hydroxyethyl)indole, which had the opposite correlation: positive in males and negative in females. Its role in human biology is unclear. For MRS, a similar pattern was observed with only 1 common metabolite between males and females (isocitrate with an opposite correlation). Again, taurine in females had the strongest correlation with MRS. The most striking sex-specific differences were observed in the metabolomic correlates of disease duration, where most acylcarnitines had a strong correlation with disease duration only in males. A small number of metabolites had a significant correlation with disease duration in females. However, 30 metabolites had significant correlations in males, including 10 acylcarnitines and TCA cycle intermediates, all of which had inverse correlations (higher levels with shorter disease duration). P-S65-Ub levels had the strongest correlation coefficients among the variables and correlated with 11 metabolites in males and 40 metabolites in females. Several glycolysis intermediates had a positive correlation in both sexes. Three TCA cycle intermediates had an inverse correlation with p-S65-Ub in females. Furthermore, ribose-5-phosphate and ribulose-5-phosphate/xylulose-5-phosphate, PPP intermediates, had significant correlations with p-S65-Ub only in females. $\beta$-Nicotinamide mononucleotide (NMN), a precursor of NAD+, was the only metabolite with opposite correlations; it had a positive correlation with p-S65-Ub in males and an inverse correlation in females.

### *RNA-metabolomics integration and correlation with clinical parameters and p-S65-Ub*

Unsupervised integration of bulk RNA sequencing data with metabolites from the targeted analysis and central carbon metabolism platform yielded RNA/metabolite colour-coded modules (Fig 6). The strongest correlations were between sex and the pink module, followed by p-S65-Ub and the pink module. MMT correlated with the yellow module and inversely with the brown and green modules. P-S65-Ub correlated with the pink module and inversely correlated with the brown module.

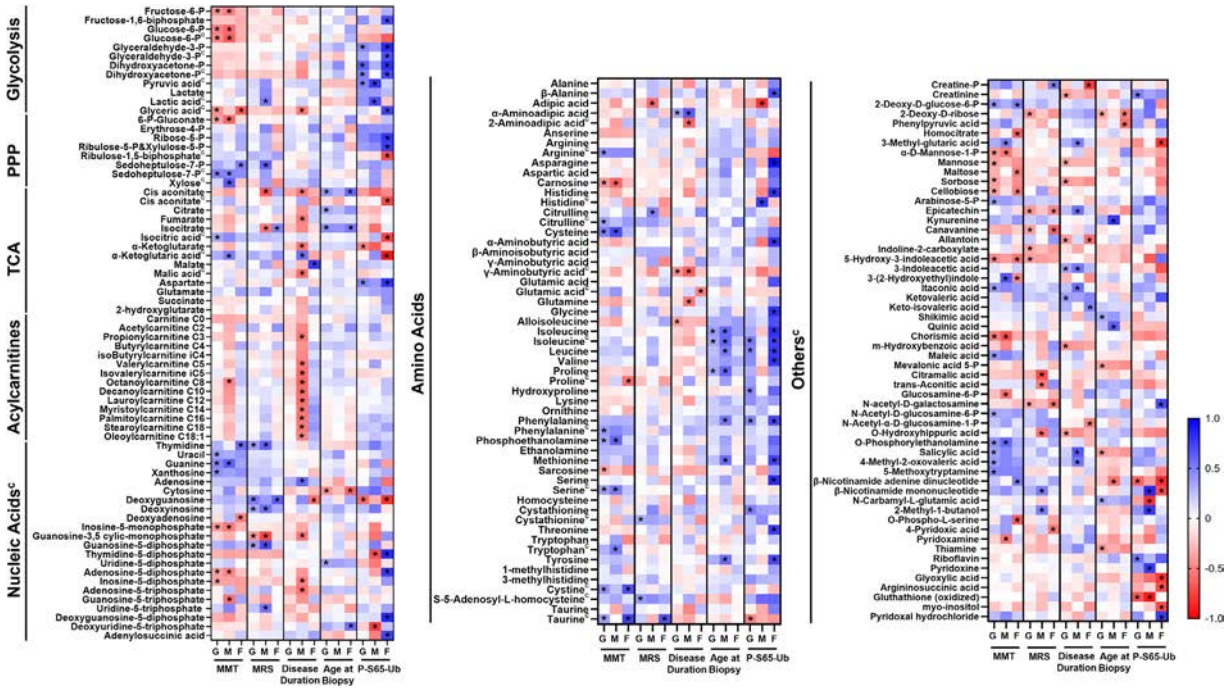
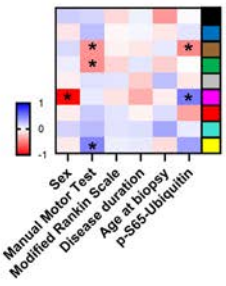



**Figure 5.** Correlation of metabolites with clinical parameters. Correlations that reached statistical significance are marked with an asterisk (*). Metabolites from the central carbon metabolism platform are marked with (c). F, females; G, grouped (both sexes); M, males; MMT, manual motor test; MRS, modified Rankin Scale; PPP, pentose phosphate pathway; p-S65-Ub, p-S65-Ubiquitin; TCA, citric acid cycle. *P* values < .05 are marked with an asterisk (*).

Age at biopsy, disease duration, and MRS had no significant correlation with any of the modules. The pink module contained 3 metabolites. Hydroxyproline is a critical component of collagen and essential for muscle elasticity and repair; trans-4-hydroxy L-proline is the isomer found in collagen [19]. Pyridoxic acid (vitamin B6) is essential for glycogenolysis and muscle contraction, and vitamin B6 deficiency has been associated with sarcopenia [20]. Although no particular pathway was enriched in the 39 genes of the pink module, there were several long noncoding RNAs and Y chromosome genes. Among these genes, *UTY* is thought to contribute to sex-specific phenotypes and disease risks [21]. In addition, there were several genes related to the regulation of gene expression, protein homeostasis, vesicular trafficking, and NADPH. The yellow module included 16 metabolites and 351 genes (Fig 6). Metabolites included 3 related to tryptophan metabolism, ornithine, and 5 nucleic acids, among




**Module: Pink**

| Genes | Metabolites |
|---|---|
| No statistically signficant enriched pathways | Hydroxyproline |
| 39 genes, many related to long noncoding RNAs and Y chromosome | Trans-4-Hydroxy-L-proline |
| | 4-Pyridoxic acid |

**Module: Green**

| Pathways | Metabolites | | | | |
|---|---|---|---|---|---|
| Synaptic vesicle cycle | Histidine | D-Glyceraldehyde 3-P | N-Carbamyl-L-glutamic acid | AMP | dCDP |
| Cholinergic synapse | Anserine | Phosphogluconate | S-2-Aminoethyl-L-cysteine | IMP | dGMP |
| Nicotine addiction | L-Homoserine | Succinic semialdehyde | α-Aminoadipic acid | UMP | Adipic acid |
| | Pyridoxamine | Prephenic acid | α-Amino-N-butyric acid | ATP | Folinic acid |
| | Ketobutyrate | Chorismic acid | β-Aminoisobutyric acid | CMP | |
| | Carnitine C0 | L-Dihydroorotic acid | 3-Hydroxyanthranilic acid | dCTP | |
| | Ribose-5-P | O-Phospho-L-Serine | c-di-GMP | dAMP | |

**Module: Yellow**

| Pathways | Metabolites | |
|---|---|---|
| Viral protein interaction with cytokine and cytokine receptor | Ornithine | Uricacid |
| Cytokine-cytokine receptor interaction | Tryptophan | Oxamic acid |
| Epithelial cell signaling in Helicobacter pylori infection | 5-Methoxytryptamine | Cytosine |
| African trypanosomiasis | Guanidobutyric acid | UTP |
| Mineral absorption | L-Arabinose | dCMP |
| Chemokine signaling pathway | N-Formyl-L-Tyrosine | GDP |
| Malaria | Hydroxy-DL-kynurenine | UDP-galactose |
| IL-17 signaling pathway | N-carbamoyl-DL-aspartic acid | UDP-glucose |

**Module: Brown**

| Pathways | Metabolites | | | |
|---|---|---|---|---|
| Alanine, aspartate and glutamate metabolism | Acylcarnitines: C2, C4, iC4, C5, iC5, C8, C10, C12, C14, C16, C18, C18:1 | | | |
| Central carbon metabolism in cancer | Arginine | Ketoglutarate | Adenylosuccinic acid | Cytidine |
| Butanoate metabolism | Carnosine | Sedoheptulose-7P | trans-Aconitic acid | cAMP |
| Serotonergic synapse | Glutamine | 4-Hydroxyphenylpyruvic acid | D-Glucosamine-6-P | IDP |
| Arginine biosynthesis | Fumarate | 5-Hydroxy-3-indoleacetic acid | γ-Aminobutyric acid | GTP |
| Glutamatergic synapse | L-Cystathionine | 5-Deoxymethylthioadenosine | Dihydroxyacetone-P | dCTP |
| Ras signaling pathway | L-homocystine | Flavin adenine dinucleotide | m-Hydroxybenzoic acid | |
| MAPK signaling pathway | Glucose-6-P | trans,trans-Muconic.acid | 2-Deoxyadenosine | |
| Protein digestion and absorption | Fructose-6-P | 3-Dihydroxyisovalerate | 2-Hydroxyglutarate | |
| GABAergic synapse | D-Fructose-6-P | 2-Methyl-1-butanol | N-acetyl-D-galactosamine | |

**Figure 6.** Correlation of clinical parameters with RNA-metabolomics integrated modules. Heatmap showing the correlation coefficient for each colour-coded module. Correlations that reached statistical significance (*q* value < 0.5) are marked with an asterisk (*), and corresponding modules are displayed as tables. AMP, adenosine monophosphate; ATP, adenosine triphosphate; cAMP, cyclic adenosine monophosphate; c-di-GMP, cyclic di guanosine monophosphate; CMP, cytidine monophosphate; dAMP, deoxyadenosine monophosphate; dCDP, deoxycytidine diphosphate; dCMP, deoxycytidine monophosphate; dCTP, deoxycytidine triphosphate; dGMP, deoxyguanosine monophosphate; GDP, guanosine diphosphate; GTP, guanosine triphosphate; IDP, inosine diphosphate; IL, interleukin; IMP, inosine monophosphate; MAPK, mitogen-activated protein kinase; P, phosphate; UDP, uridine diphosphate; UMP, uridine monophosphate; UTP, uridine triphosphate.

others. Tryptophan is a precursor of serotonin and vitamin B3 and is important for skeletal muscle energy production and metabolism. It is essential for the kynurenine pathway that is related to sarcopenia, ageing, and ageing-related inflammation [22]. Ornithine, a nitrogenous amino acid, is important for nitrogen metabolism and counteracting fatigue [23]. Enriched pathways were related to cytokines/chemokines, interleukin (IL)-17 signalling, and neuroactive-ligand-receptor interaction. Many of the listed pathways had overlapping genes related to cytokines and chemokine receptors: *CXCR1, CXCR2, CXCL1, CXCL8* (IL-8)*, PF4* (ie, *CXCL4*)*, IL6,* and *CCL21*. In addition to the listed pathways, we note that 4 genes were related to the NLRP inflammasomes (*NLRP12, MEFV, CCL21,* and *CXCL8*) and *GDF15*. GDF15 is a myokine, considered a mitochondrial marker and a diagnostic biomarker for IBM and mitochondrial disorders [24]. In the green module, there were 32 metabolites and 195 genes. Metabolites included carnitine, $\beta$-aminoisobutyric acid, $\alpha$-aminoadipic acid, 3 related to the PPP, 2 to vitamin B6 metabolism, 3 to histidine metabolism, and 9 nucleic acids, among others. $\beta$-Aminoisobutyric acid is produced by skeletal muscle during exercise and acts like a myokine that regulates metabolism, oxidative stress, and inflammation [25]. Similarly, pathways enriched in the green module were mostly related to neurotransmission. Lastly, the brown module had 44 metabolites and 369 genes. Metabolites included several related to glycolysis, the TCA cycle, the PPP, nucleic acids, acylcarnitines, in addition to carnosine, L-cystathionine, and others. Enriched pathways were related to central carbon metabolism, mitogen-activated protein kinase (MAPK) signalling, RAS signalling, neurotransmission, and others. MAPK and RAS signalling pathways are regulatory pathways linked to cell growth, survival, and response to oxidative stress, invoked in neurodegenerative diseases and considered therapeutic targets in these disorders [26,27].

Finally, we correlated clinical parameters and p-S65-Ub with the modules from RNA-metabolomics integration for each sex separately. In females, none of the modules significantly correlated with any of the clinical parameters. The strongest correlation in females was with the navy module, but it did not reach statistical significance ($\rho = 0.61$, $P = .058$). The navy module included 84 metabolites and 717 genes related to cytokines and chemokines, such as IL-1B, IL-6, and TNF, as well as the Toll-like receptor signalling pathway. In males, 3 modules correlated with MMT (black, blue, and red) and 3 with p-S65-Ub (black, turquoise, and orange) (Supplementary Fig S6). The black module shared similar enriched pathways with the yellow module, as did the red module with the green module. The turquoise module contained 79 metabolites and 900 genes with top pathways related to central carbon metabolism, including the TCA cycle and anaplerotic amino acids, in addition to purine metabolism and MAPK signalling.

## DISCUSSION

In this study, we provided a mitochondria-centred metabolomic map of the skeletal muscle of IBM using various analytical platforms, underscoring common and sex-specific metabolic changes. We also demonstrated the correlation of metabolites and metabolite-RNA modules with clinical parameters, indicating their clinical significance, and with p-S65-Ub, a mitophagy marker that reflects the accumulation of damaged mitochondria. Additionally, we highlighted pathways shared with ageing, sarcopenia, and muscle disorders, identifying potential targets for therapeutic interventions.

The majority of the TCA cycle intermediates were elevated in the skeletal muscles of IBM patients, without any changes in lactate or acetyl-CoA levels. Cantó-Santos et al [5] reported an elevation in some of the TCA cycle intermediates in fibroblasts from IBM patients. There are limited studies evaluating TCA cycle metabolites in human muscle tissue in general and muscle diseases in particular, as most studies have been performed in cellular or animal models [28,29]. In a study evaluating sarcopenia in patients with hip fractures, serum from those patients had elevated TCA cycle metabolites [30]. The pattern was different from the one observed in our samples (decreased $\alpha$-ketoglutarate and increased malate, fumarate, and succinate), and the authors postulated it was related to complex I deficiency and subsequent buildup of NADH. Many of the TCA cycle-related amino acids were increased in our study, suggesting augmented anaplerosis in IBM that should be further explored in future studies. In a study by Motori et al [31], anaplerosis was reported to play a role in offsetting oxidative phosphorylation defects in neurodegenerative diseases. Lastly, the TCA cycle metabolites had a significant correlation with clinical parameters, with remarkable sex-specific changes, indicating the findings are of clinical significance. Most notable was the correlation with disease duration in males and p-S65-Ub in females, where higher levels of all the TCA cycle metabolites were associated with shorter disease duration in males and lower p-S65-Ub levels in females. From the integrated RNA-metabolomics modules, the brown module, which inversely correlated with the MMT score and p-S65-Ub levels, contained several TCA cycle intermediates. The increase in several central carbon metabolites raises the question of whether a hypermetabolic state exists in IBM. The "energy constraint model" is a recently proposed innovative concept, where underlying defects in mitochondrial oxidative phosphorylation drive an energetically costly hypermetabolic state that is detrimental to the cell and could cause accelerated ageing [32].

The other main finding in our study was the decrease in proximal glycolysis metabolites and an increase in PPP metabolites, suggestive of a shift from glycolysis to the PPP. The shift to the PPP has been attributed to 2 potential reasons: generation of NADPH to defeat oxidative stress, and synthesis of nucleotides through ribose-5-phosphate [33]. Cysteine, a rate-limiting substrate for glutathione synthesis, had the strongest correlation with MMT, and nucleic acid metabolism was markedly perturbed in our study. Activation of PPP is thought to play a protective role in neurodegenerative diseases [34]. Interestingly, abnormal glucose metabolism has also been linked to other diseases of ageing, including Alzheimer's disease, where decreased glucose metabolism on 18-F fluorodeoxyglucose positron emission tomography is one of the first manifestations of this disorder. Studies on the PPP in human skeletal muscle are rare, and to the best of our knowledge, a shift to the PPP has not been addressed in musculoskeletal disease. The decrease in glucose-6-phosphate and fructose-6-phosphate was associated with higher MMT scores. Although it did not reach statistical significance, the pattern was consistent for the majority of metabolites, with decreased levels of glycolysis metabolites and increased levels of PPP metabolites associated with more severe MMT scores. Likewise, the RNA-metabolomics modules that correlated with the MMT contained several PPP and glycolysis metabolites.

Similar to a previous report, decreased carnitine levels were seen in IBM [3]. We also show a decrease in short-chain acylcarnitines (C2 and C3), which were only significantly decreased in males. The decrease in short-chain acylcarnitines could reflect

increased reliance on oxidative lipid metabolism, consistent with decreased glycolysis and increased TCA metabolites. A fibre type shift in IBM is also plausible with the loss of type 2 glycolytic fibres [6,7]. The sex differences in acylcarnitine metabolism were also prominent in the correlation analysis, as there was a strong inverse correlation between disease duration and most acylcarnitine levels observed only in males. Although it did not reach statistical significance, almost all acylcarnitines had an inverse correlation with the MMT in males and a positive (but weak) correlation in females. Likewise, the brown module included several acylcarnitines. Moreover, many sex-specific altered metabolites on untargeted analysis were phospholipids. Alterations in phospholipids have been associated with longevity in females [35]. These sex-specific alterations in lipid metabolism in IBM are intriguing and require further investigation.

Several amino acids were altered in IBM samples, such as taurine, carnosine, citrulline, and anserine, in addition to those related to the TCA cycle. Decreased taurine levels have been associated with ageing, whereas elevated levels, as in our samples, were suggested to help alleviate oxidative stress and sarcopenia [36,37]. Carnosine, formed by $\beta$-alanine and L-histidine, and its analogue, anserine, are essential for muscle health and play a role during exercise and in pH buffering of skeletal muscle [38]. Increasing intramuscular carnosine is considered a therapeutic target to enhance exercise performance [39]. Similarly, citrulline supplementation is thought to increase L-arginine bioavailability, nitric oxide production, and exercise performance [40]. When stratifying by sex, carnosine, citrulline, and anserine were significantly decreased only in males. Additionally, branched chain amino acids (BCAAs), leucine and isoleucine, were elevated in IBM. Increased BCAAs are thought to promote oxidative stress and inflammation in human mononuclear cells by mTORC1 activation [41]. Serine, methionine, and sarcosine are connected through the one-carbon cycle, disturbances of which have been closely linked to mitochondrial dysfunction [42]. Several amino acids correlated with disease severity. Cysteine had the strongest correlation with the MMT. Cysteine is a rate-limiting substrate for the synthesis of glutathione, an antioxidant that neutralises reactive oxygen species. Sarcosine and carnosine had an inverse correlation with the MMT. Sarcosine, a derivative of creatine metabolism, is an autophagy activator modulated by ageing and is essential for muscle health [43,44].

As captured by the central carbon metabolism platform, there were remarkable nucleic acid alterations with an increase in nucleotide synthesis precursors and a decrease in mono- and diphosphate nucleotides, both of which correlated with the severity of muscle weakness in the combined-sex analysis and males, and with disease duration in males only. An increase in nucleotide synthesis precursors has been reported in the sera and urine of IBM patients [4,5]. The reason for these changes is unclear, and they may indicate increased purine and pyrimidine breakdown or decreased synthesis. It could also indicate disrupted cellular energy metabolism, where the high demand for ATP is not being met. Decreased electron transport chain activity has been linked to the activation of the PPP, decreased de novo purine synthesis, and increased uptake of extracellular bases [45]. The central carbon metabolism platform also revealed several altered lipids that require further investigation via a lipidomics platform.

The existing literature on sex-specific metabolomic changes in health and disease is limited [46–48]. In this study, there was a uniform pattern when evaluating sex-specific changes: in general, males consistently had several correlations with clinical parameters, whether with metabolites only or RNA-metabolomics integrated modules. In contrast, fewer correlations between clinical parameters and metabolites were observed in females, and none of the RNA-metabolomics integrated modules correlated with clinical parameters. The reason for this remains elusive. It could be that females are more resilient to metabolic changes caused by the disease. It could also be that the interaction between metabolic disturbances and clinical parameters is more variable in females, so that none is significant when evaluated at a group level. Of note, the pink module, which had the strongest correlation with the clinical parameter biological sex, consisted of several long noncoding RNAs and Y chromosome-related genes. Understanding the regulatory role of noncoding RNAs is a growing field [49]. The role of gonosomal genes in metabolic regulation in musculoskeletal and neurodegenerative diseases is not well explored.

Lastly, we linked these metabolic alterations with the accumulation of damaged mitochondria in IBM, reflected by p-S65-Ub levels. Similar to our previous study, sex-specific differences in mitophagy were reaffirmed in the present study [6]. Among the various metabolites, NAD+ levels inversely correlated with p-S65-Ub levels in the grouped sex analysis. NAD+ is a critical coenzyme in redox reactions and an endogenous mitophagy inducer [50]. However, its precursor, NMN, had an opposite correlation in males and females. Boosting NAD+ levels is being investigated as a therapeutic intervention in various neurodegenerative disorders and primary mitochondrial myopathies. P-S65-Ub levels also correlated with riboflavin, an essential factor for complex I and II function, and inversely correlated with glutathione (oxidised), a major antioxidant. In the RNA-metabolomics integrated modules, p-S65-Ub levels and sex strongly correlated with the pink module. Additionally, p-S65-Ub and the MMT correlated with the brown module. Likewise, when stratifying by sex, p-S65-Ub strongly correlated with various modules only in males. Taken together, these findings further support the association between the accumulation of damaged mitochondria, loss of muscle strength, and alterations in central carbon metabolism in IBM in a sex-specific manner.

Our cross-sectional study provides a thorough evaluation of central carbon metabolism in IBM performed on frozen samples obtained from IBM patients. Inherent to this design and the nature of the specimens, we cannot determine which alterations are mechanistically linked to dysfunction vs adaptive/compensatory, and we cannot perform interventions on the specimens to further explore pathomechanisms or determine fluxes. IBM does not have a valid disease model, as the commonly used mouse models in the literature are deemed not representative of the disease [9,51]. On the other hand, especially in metabolomics, performing experiments on samples derived from patients offers a direct window into disease pathogenesis, which would facilitate bench-to-bedside translation [51]. Furthermore, if diagnostic or prognostic biomarkers are to arise from these studies, this could be directly applied to samples obtained from clinical practice. Of note, correlation analysis does not imply a causative relationship between the identified metabolomic abnormalities and the clinical parameters. Additional limitations include the retrospective nature of the chart review, limiting the clinical parameters that can be abstracted, and the relatively small sample size compared with the number of comparisons. Furthermore, the variability in the muscles that were biopsied, the patients' medications at the time of the biopsy, and the quality of the tissue could have contributed to the findings. However, IBM does not have any known effective treatment; the variability in muscle biopsies was in both groups, and the samples were obtained and handled in the same manner in

both groups, which would help offset these limitations to some extent. Unlike *in vivo* and *in vitro* studies, there will always be variability in the conditions of the samples obtained from patients.

Future studies are needed to further evaluate the role of the detected metabolic alterations in IBM pathogenesis and to further explore the various metabolites identified in the untargeted metabolomics platforms. Furthermore, assessing the longitudinal changes in metabolites over the disease course would be of interest.

## Competing interests

Mayo Clinic and WS have filed a patent related to PRKN mitophagy activators. All other authors report no conflicts of interest related to this manuscript.

## Acknowledgements

The authors acknowledge the Mayo Clinic Metabolomics Core, directed by Ian Lanza, PhD, and managed by Xuan-Mai T Petterson, for the performance and primary analysis of the metabolomics experiments.

## Contributors

Conceptualisation of the study: EN. Study design: EN, WS, ET, and IRL. Performance of metabolomics experiments: XTP and the Mayo Clinic Metabolomics Core. Data analysis, biostatistics, and bioinformatics: EN, SD, and the Mayo Clinic Metabolomics Core. Writing of the first manuscript draft and preparation of the figures: EN and IS. Data interpretation: all authors. Revision of the manuscript for intellectual content: all authors. Study supervision: EN, ET, and IRL. All authors have agreed to the published version of the manuscript.

## Funding

This research was supported by grants from the National Institute of Arthritis, Musculoskeletal and Skins Diseases (NIAMS, K08-AR78254), the American Neuromuscular Foundation (ANF #2, career development grant), and the Mayo Clinic Center for Clinical and Translational Sciences (small project grant and Team Science pilot award, UL1TR002377 from the National Center for Advancing Translational Sciences to EN). The study contents are solely the responsibility of the authors and do not necessarily represent the official view of the National Institutes of Health and other funding organisations. The funders had no role in the study design, data collection and analysis, the decision to publish, or the preparation of the manuscript.

## Ethics approval

The study was approved by the Mayo Clinic Institutional Review Board (IRB# 21-003004). The study was considered a minimal risk; therefore, the requirement for informed consent was waived. However, medical records of any patient who had not provided authorisation for their use in research, in accordance with Minnesota statute 144.335, were not reviewed. The use of clinical residual muscle biopsy tissue was also approved by the Mayo Clinic Biospecimens Subcommittee.

## Data availability statement

The datasets used and/or analysed during the current study are available from the corresponding author on reasonable request. Detailed analysis results are provided in the Supplementary Material.

Provenance and peer review

Patient consent for publication

Not applicable.

Peer reviewed.

Patient and public involvement

Patients or the public were not involved in the study design, or conduct, or reporting, or dissemination plans of our research.

## Supplementary materials

Supplementary material associated with this article can be found in the online version at doi:10.1016/j.ard.2025.05.003.

## Orcid

Elie Naddaf: http://orcid.org/0000-0001-6212-1236

## REFERENCES

[1] Naddaf E, Shelly S, Mandrekar J, Chamberlain AM, Hoffman EM, Ernste FC, et al. Survival and associated comorbidities in inclusion body myositis. Rheumatology (Oxford) 2022;61(5):2016–24.

[2] Guglielmi V, Cheli M, Tonin P, Vattemi G. Sporadic inclusion body myositis at the crossroads between muscle degeneration, inflammation, and aging. Int J Mol Sci 2024;25(5):2742.

[3] Murakami A, Noda S, Kazuta T, Hirano S, Kimura S, Nakanishi H, et al. Metabolome and transcriptome analysis on muscle of sporadic inclusion body myositis. Ann Clin Transl Neurol 2022;9(10):1602–15.

[4] Buzkova J, Nikkanen J, Ahola S, Hakonen AH, Sevastianova K, Hovinen T, et al. Metabolomes of mitochondrial diseases and inclusion body myositis patients: treatment targets and biomarkers. EMBO Mol Med 2018;10(12):e9091.

[5] Cantó-Santos J, Valls-Roca L, Tobías E, García-García FJ, Guitart-Mampel M, Esteve-Codina A, et al. Unravelling inclusion body myositis using a patient-derived fibroblast model. J Cachexia Sarcopenia Muscle 2023;14(2):964–77.

[6] Naddaf E, Nguyen TKO, Watzlawik JO, Gao H, Hou X, Fiesel FC, et al. NLRP3 inflammasome activation and altered mitophagy are key pathways in inclusion body myositis. J Cachexia Sarcopenia Muscle 2025;16(1):e13672.

[7] Wischnewski S, Thäwel T, Ikenaga C, Kocharyan A, Lerma-Martin C, Zulji A, et al. Cell type mapping of inflammatory muscle diseases highlights selective myofiber vulnerability in inclusion body myositis. Nat Aging 2024;4(7):969–83.

[8] Spinelli JB, Haigis MC. The multifaceted contributions of mitochondria to cellular metabolism. Nat Cell Biol 2018;20(7):745–54.

[9] Lilleker JB, Naddaf E, Saris CGJ, Schmidt J, de Visser M, Weihl CC, et al. 272nd ENMC international workshop: 10 Years of progress - revision of the ENMC 2013 diagnostic criteria for inclusion body myositis and clinical trial readiness 16-18 June 2023, Hoofddorp, The Netherlands Neuromuscul Disord 2024;37:36–51.

[10] Pinto MV, Laughlin RS, Klein CJ, Mandrekar J, Naddaf E. Inclusion body myositis: correlation of clinical outcomes with histopathology, electromyography and laboratory findings. Rheumatology (Oxford) 2022;61(6):2504–11.

[11] Trushina E, Dutta T, Persson XM, Mielke MM, Petersen RC. Identification of altered metabolic pathways in plasma and CSF in mild cognitive impairment and Alzheimer's disease using metabolomics. PloS One 2013;8(5):e63644.

[12] Dutta T, Chai HS, Ward LE, Ghosh A, Persson XM, Ford GC, et al. Concordance of changes in metabolic pathways based on plasma metabolomics and skeletal muscle transcriptomics in type 1 diabetes. Diabetes 2012;61(5):1004–16.

[13] Lee HJ, Kremer DM, Sajjakulnukit P, Zhang L, Lyssiotis CA. A large-scale analysis of targeted metabolomics data from heterogeneous biological samples provides insights into metabolite dynamics. Metabolomics 2019;15(7):103.

[14] Langfelder P, Horvath S. WGCNA: an R package for weighted correlation network analysis. BMC Bioinformatics 2008;9(1):559.

[15] TeSlaa T, Ralser M, Fan J, Rabinowitz JD. The pentose phosphate pathway in health and disease. Nat Metab 2023;5(8):1275–89.

[16] Kelly MP. Cyclic nucleotide signaling changes associated with normal aging and age-related diseases of the brain. Cell Signal 2018;42:281–91.
[17] Wang TJ, Ngo D, Psychogios N, Dejam A, Larson MG, Vasan RS, et al. 2-Aminoadipic acid is a biomarker for diabetes risk. J Clin Invest 2013;123 (10):4309–17.
[18] da Silva JC, Amaral AU, Cecatto C, Wajner A, Dos Santos Godoy K, Ribeiro RT, et al. $\alpha$-Ketoadipic acid and $\alpha$-aminoadipic acid cause disturbance of glutamatergic neurotransmission and induction of oxidative stress in vitro in brain of adolescent rats. Neurotox Res 2017;32(2):276–90.
[19] Xu S, Gu M, Wu K, Li G. Unraveling the role of hydroxyproline in maintaining the thermal stability of the collagen triple helix structure using simulation. J Phys Chem B 2019;123(36):7754–63.
[20] Kato N, Kimoto A, Zhang P, Bumrungkit C, Karunaratne S, Yanaka N, et al. Relationship of low vitamin B6 status with sarcopenia, frailty, and mortality: a narrative review. Nutrients 2024;16(1):177.
[21] Rock KD, Folts LM, Zierden HC, Marx-Rattner R, Leu NA, Nugent BM, et al. Developmental transcriptomic patterns can be altered by transgenic overexpression of Uty. Sci Rep 2023;13(1):21082.
[22] Ballesteros J, Rivas D, Duque G. The role of the kynurenine pathway in the pathophysiology of frailty, sarcopenia, and osteoporosis. Nutrients 2023;15 (14):3132.
[23] Sahu B, Pani S, Swalsingh G, Senapati U, Pani P, Pati B, et al. Long-term physical inactivity induces significant changes in biochemical pathways related to metabolism of proteins and glycerophospholipids in mice. Mol Omics 2024;20(1):64–77.
[24] De Paepe B, Verhamme F, De Bleecker JL. The myokine GDF-15 is a potential biomarker for myositis and associates with the protein aggregates of sporadic inclusion body myositis. Cytokine 2020;127:154966.
[25] Yi X, Yang Y, Li T, Li M, Yao T, Hu G, et al. Signaling metabolite $\beta$-aminoisobutyric acid as a metabolic regulator, biomarker, and potential exercise pill. Front Endocrinol (Lausanne) 2023;14:1192458.
[26] Ahmed T, Zulfiqar A, Arguelles S, Rasekhian M, Nabavi SF, Silva AS, et al. Map kinase signaling as therapeutic target for neurodegeneration. Pharmacol Res 2020;160:105090.
[27] Gravandi MM, Abdian S, Tahvilian M, Iranpanah A, Moradi SZ, Fakhri S, et al. Therapeutic targeting of Ras/Raf/MAPK pathway by natural products: a systematic and mechanistic approach for neurodegeneration. Phytomedicine 2023;115:154821.
[28] Li H, Uittenbogaard M, Navarro R, Ahmed M, Gropman A, Chiaramello A, et al. Integrated proteomic and metabolomic analyses of the mitochondrial neurodegenerative disease MELAS. Mol Omics 2022;18(3):196–205.
[29] Garvey SM, Dugle JE, Kennedy AD, McDunn JE, Kline W, Guo L, et al. Metabolomic profiling reveals severe skeletal muscle group-specific perturbations of metabolism in aged FBN rats. Biogerontology 2014;15(3):217–32.
[30] Hintze S, Baber L, Hofmeister F, Jarmusch S, Todorow V, Mehaffey S, et al. Exploration of mitochondrial defects in sarcopenic hip fracture patients. Heliyon 2022;8(10):e11143.
[31] Motori E, Atanassov I, Kochan SMV, Folz-Donahue K, Sakthivelu V, Giavalisco P, et al. Neuronal metabolic rewiring promotes resilience to neurodegeneration caused by mitochondrial dysfunction. Sci Adv 2020;6(35):eaba8271.
[32] Sercel AJ, Sturm G, Gallagher D, St-Onge MP, Kempes CP, Pontzer H, et al. Hypermetabolism and energetic constraints in mitochondrial disorders. Nat Metab 2024;6(2):192–5.
[33] Stincone A, Prigione A, Cramer T, Wamelink MM, Campbell K, Cheung E, et al. The return of metabolism: biochemistry and physiology of the pentose phosphate pathway. Biol Rev Camb Philos Soc 2015;90(3):927–63.
[34] Tang BL. Neuroprotection by glucose-6-phosphate dehydrogenase and the pentose phosphate pathway. J Cell Biochem 2019;120 (9):14285–95.
[35] Gonzalez-Covarrubias V, Beekman M, Uh HW, Dane A, Troost J, Paliukhovich I, et al. Lipidomics of familial longevity. Aging Cell 2013;12(3):426–34.
[36] Scicchitano BM, Sica G. The beneficial effects of taurine to counteract sarcopenia. Curr Protein Pept Sci 2018;19(7):673–80.
[37] Singh P, Gollapalli K, Mangiola S, Schranner D, Yusuf MA, Chamoli M, et al. Taurine deficiency as a driver of aging. Science 2023;380(6649):eabn9257.
[38] de Souza Gonçalves L, Pereira WR, da Silva RP, Yamaguchi GC, Carvalho VH, Vargas BS, et al. Anserine is expressed in human cardiac and skeletal muscles. Physiol Rep 2023;11(19):e15833.
[39] Perim P, Marticorena FM, Ribeiro F, Barreto G, Gobbi N, Kerksick C, et al. Can the skeletal muscle carnosine response to beta-alanine supplementation be optimized? Front Nutr 2019;6:135.
[40] Gonzalez AM, Trexler ET. Effects of citrulline supplementation on exercise performance in humans: a review of the current literature. J Strength Cond Res 2020;34(5):1480–95.
[41] Zhenyukh O, Civantos E, Ruiz-Ortega M, Sánchez MS, Vázquez C, Peiró C, et al. High concentration of branched-chain amino acids promotes oxidative stress, inflammation and migration of human peripheral blood mononuclear cells via mTORC1 activation. Free Radic Biol Med 2017;104:165–77.
[42] Bao XR, Ong SE, Goldberger O, Peng J, Sharma R, Thompson DA, et al. Mitochondrial dysfunction remodels one-carbon metabolism in human cells. Elife 2016;5:e10575.
[43] Walters RO, Arias E, Diaz A, Burgos ES, Guan F, Tiano S, et al. Sarcosine is uniquely modulated by aging and dietary restriction in rodents and humans. Cell Rep 2018;25(3) 663-76.e6.
[44] Gu X, Wang W, Yang Y, Lei Y, Liu D, Wang X, et al. The effect of metabolites on mitochondrial functions in the pathogenesis of skeletal muscle aging. Clin Interv Aging 2022;17:1275–95.
[45] Wu Z, Bezwada D, Cai F, Harris RC, Ko B, Sondhi V, et al. Electron transport chain inhibition increases cellular dependence on purine transport and salvage. Cell Metab 2024;36(7) 1504-20.e9.
[46] Krumsiek J, Mittelstrass K, Do KT, Stückler F, Ried J, Adamski J, et al. Gender-specific pathway differences in the human serum metabolome. Metabolomics 2015;11(6):1815–33.
[47] Mittelstrass K, Ried JS, Yu Z, Krumsiek J, Gieger C, Prehn C, et al. Discovery of sexual dimorphisms in metabolic and genetic biomarkers. PLoS Genet 2011;7(8):e1002215.
[48] Arnold M, Nho K, Kueider-Paisley A, Massaro T, Huynh K, Brauner B, et al. Sex and APOE $\varepsilon$4 genotype modify the Alzheimer's disease serum metabolome. Nat Commun 2020;11(1):1148.
[49] Statello L, Guo CJ, Chen LL, Huarte M. Gene regulation by long non-coding RNAs and its biological functions. Nat Rev Mol Cell Biol 2021;22 (2):96–118.
[50] Zhang T, Liu Q, Gao W, Sehgal SA, Wu H. The multifaceted regulation of mitophagy by endogenous metabolites. Autophagy 2022;18(6):1216–39.
[51] Skolka MP, Naddaf E. Exploring challenges in the management and treatment of inclusion body myositis. Curr Opin Rheumatol 2023;35(6):404–13.

Ann Rheum Dis 84 (2025) 1387–1400

Contents lists available at ScienceDirect

Annals of the Rheumatic Diseases

journal homepage: https://www.sciencedirect.com/journal/annals-of-the-rheumatic-diseases

Vasculitis

# The IL-6 axis in vascular inflammation: effects of IL-6 receptor blockade on vascular lesions from patients with giant-cell arteritis

Marc Corbera-Bellalta[1], Farah Kamberovic[1], Roser Alba-Rovira[1], Ester Planas-Rigol[1], Sergio Prieto-González[1], Núria Farran-Centelles[1], Ester Tobías[2], Anna Jordán[3], Marco A. Alba[1], Eduard Quintana[4], Georgina Espígol-Frigolé[1], Maria C. Cid[1,*]

[1] *Vasculitis Research Unit, Department of Autoimmune Diseases, Hospital Clínic (member of European Reference Network [ERN]-for rare diseases RITA), University of Barcelona, Centre de Recerca biomèdica (CRB)-CELLEX, Institut d'Investigacions Biomèdiques August Pi i Sunyer (IDIBAPS), Barcelona, Spain*

[2] *Muscle Research and Mitochondrial Function Group, IDIBAPS, University of Barcelona School of Medicine, Hospital Clínic of Barcelona, and Rare Diseases Networking Biomedical Research Center (CIBERER), Barcelona, Spain*

[3] *Department of Internal Medicine, Hospital Clínic, Barcelona, Spain*

[4] *Department of Cardiovascular Surgery, Hospital Clínic, University of Barcelona, Barcelona, Spain*

ARTICLE INFO

ABSTRACT

*Objectives:* Blocking interleukin (IL)-6-receptor with tocilizumab has been a major advance in the treatment of giant-cell arteritis (GCA), supporting a crucial role of IL-6 receptor signalling. However, nearly half of the patients are not able to maintain glucocorticoid- free remission with tocilizumab. The impact of tocilizumab on vascular lesions of GCA is largely unknown since conflicting results have been obtained by imaging. The expression and functional role of IL-6-receptor in GCA immunopathology has not been previously investigated. This study aimed to investigate expression of IL-6 receptor in GCA and control arteries and to assess the impact of tocilizumab on *ex vivo*–cultured temporal arteries and aortic tissue from patients with GCA.

*Methods:* This study used a hypothesis-driven, candidate molecule transcriptomic approach using *ex vivo* temporal artery and aortic tissue culture, quantitative real-time polymerase chain reaction, immunofluorescence, Western Blot, immunoassay, adhesion, and chemotaxis assays.

*Results:* IL-6 receptor protein expressed intensively in GCA compared with that in control arteries. Tocilizumab decreased expression/phosphorylation of STAT3 and reduced expression of STAT3-dependent molecules including suppressor of cytokine signalling 3, CCL-2, and ICAM-1 in cultured GCA-involved arteries and patients' peripheral blood mononuclear cells (PBMCs). A similar trend was observed in aortic tissue. Consistently, tocilizumab reduced PBMC adhesiveness to vascular smooth muscle cells and human umbilical vein endothelial cells and chemotaxis towards supernatants of tocilizumab-treated GCA arteries. In some specimens, tocilizumab increased STAT1 phosphorylation and expression of STAT1-dependent chemokines including CXCL9 and CXCL10.

*Correspondence to Dr. Maria C. Cid, Department of Autoimmune Diseases, Hospital Clínic Barcelona, Barcelona, Spain.

*E-mail address:* mccid@clinic.cat (M.C. Cid).

MC-B, FK, and RA-R contributed equally to this work.

**Handling editor** Josef S. Smolen.

https://doi.org/10.1016/j.ard.2025.02.008

0003-4967/© 2025 European Alliance of Associations for Rheumatology (EULAR). Published by Elsevier B.V. All rights are reserved, including those for text and data mining, AI training, and similar technologies.

*Conclusions:* Tocilizumab has a significant impact on vascular lesions by reducing, but not abrogating, key molecules involved in PBMC recruitment. About half of the patients may activate alternative inflammatory pathways in their lesions as a potential escape mechanism to tocilizumab that deserves further investigation.

### WHAT IS ALREADY KNOWN ON THIS TOPIC

- Blocking IL-6 receptor with tocilizumab (TCZ) has improved the management of patients with giant-cell arteritis (GCA) by increasing rates of sustained remission, sparing glucocorticoids, and improving quality of life.
- Although TCZ provides clinical benefit, its effects on vascular inflammation are unknown since no functional preclinical studies have been performed and changes induced on imaging findings are equivocal.

### WHAT THIS STUDY ADDS

- This study demonstrates expression of interleukin (IL)-6 receptor (the target of TCZ) in vascular lesions from patients with GCA which has not been explored before. The study also reveals effects of IL-6 on vascular inflammation, not previously evidenced in GCA, and unravels mechanisms through which TCZ impacts vascular inflammation.
- We demonstrate a reduction in vascular expression and phosphorylation of the strongly proinflammatory transcription factor STAT3 and consequent downregulation of STAT3-dependent genes.
- Among selected molecules investigated, TCZ diminishes expression of molecules involved in leucocyte recruitment in the artery wall (ie, CCL2 and ICAM-1), resulting in decreased adhesion and chemotaxis of mononuclear cells towards the artery wall and reduced vascular inflammation.
- The transcriptomic effects of TCZ are inferior to those induced by high-dose glucocorticoids. Moreover, our study reveals activation of STAT1-dependent alternative inflammatory pathways in about half of the patients.

### HOW THIS STUDY MIGHT AFFECT RESEARCH, PRACTICE OR POLICY

- This study demonstrates that TCZ has an impact on key inflammatory pathways in peripheral blood mononuclear cells, temporal arteries, and aortic tissue from patients with GCA.
- This impact is inferior to that achieved by high-dose glucocorticoids, suggesting caution in excessively minimising glucocorticoid exposure in the remission-induction phase.
- The increase in STAT1 activation induced by TCZ in a patient subset may indicate persistence of inflammatory activity in some patients and suggests that concomitant or sequential additional targeted therapies may benefit some individuals and deserve further investigation.

## INTRODUCTION

Giant-cell arteritis (GCA) is a granulomatous vasculitis affecting large-sized and medium-sized arteries in individuals older than 50 years [1]. Glucocorticoids (GCs) remain the cornerstone of remission-induction in GCA. However, about 40% to 60% of patients relapse when GC are tapered, and prolonged treatment results in significant side effects [2]. Tocilizumab (TCZ), a humanised monoclonal antibody against interleukin (IL)-6 receptor, is more effective than placebo in maintaining remission and sparing GC according to phase 2 and phase 3 clinical trials [3,4] and is recommended and widely used for the treatment of GCA [5–8]. However, >40% of patients receiving TCZ do not tolerate GC tapering or withdrawal without relapse [4,9], indicating a need for better understanding of pathogenic mechanisms in GCA and the specific contribution of the IL-6/IL-6-receptor pathway.

GCA has been classically considered a T helper ($T_H$)1–mediated disease based on its granulomatous nature and the expression of interferon (IFN)$\gamma$ and IFN$\gamma$-induced products in vascular lesions [1,10–13]. Data generated over the past decades indicate that $T_H$17-mediated mechanisms are also relevant to GCA [13,14]. IL-6 is a multifunctional cytokine promoting $T_H$17 differentiation, monocyte/macrophage activation, B cell differentiation, and endothelial cell responses [15–19]. IL-6 has also systemic effects beyond the immune system: it regulates haematopoiesis and is a major trigger of the acute phase response [15–19]. The IL-6 receptor system comprises a specific IL-6 binding molecule, the IL-6R, and a signal transducer molecule, gp130 [15–19]. Binding of IL-6/IL-6R complex to gp130 receptor leads to the activation of Janus kinase (JAK)1, JAK2 and Tyk2 which phosphorylate tyrosine residues in the cytoplasmic domain of gp130 [15–19]. STAT transcription factors, mainly STAT3, are then phosphorylated by JAKs, dimerise and travel to the nucleus where they promote expression of target genes [15–19]. Excessive IL-6 mediated signalling is suppressed by suppressor of cytokine signalling (SOCS)3, that also impacts other cytokine pathways [16,20]. While gp130 is ubiquitously expressed, the expression of IL-6R is limited to a few cell types including hepatocytes, neutrophils, monocytes/macrophages and lymphocyte subsets [15,16]. IL-6R can be also produced as a soluble molecule and can interact with IL-6 and transduce signals via gp130 in cells that do not express membrane IL-6R, a process called trans-signalling [16–19]. Classical signalling would mediate physiological roles of IL-6 whereas transignalling would be more prominent in the context of inflammation [16–19]. A third signalling modality named transpresentation occurs when the IL-6/membrane IL-6R complex on dendritic cells interacts with gp130 on T lymphocytes and activates $T_H$17 differentiation [21,22].

Elevated serum concentrations of IL-6 have been repeatedly demonstrated in patients with GCA, particularly in those with a strong systemic inflammatory response and those with relapsing disease [23–26]. IL-6 is expressed in normal arteries, but its expression is increased in vascular lesions from patients with GCA [27,28]. Increased expression in tissue is also associated with a strong systemic inflammatory response [28]. Although the therapeutic efficacy of TCZ proves the relevance of the IL-6 pathway in GCA, expression of IL-6R and its functional role in the development of vascular inflammatory lesions has not been investigated [8,18]. By blocking the IL-6 pathway, TCZ abrogates the systemic inflammatory response (fever, malaise, and weight loss), which is a major source of discomfort in patients with GCA and suppress the hepatic synthesis of acute phase proteins commonly used to monitor disease activity [29]. The effects of TCZ on vascular inflammation have been assessed by imaging in small studies performed in patients receiving also high/moderate doses of GC, with variable results [30–35]. Imaging assessment is also limited by the fact that distinction between inflammation and vascular remodelling is not perfect

with available techniques. In general, there is an improvement of imaging signs of vascular involvement, but persistent abnormalities can be found in a substantial proportion of patients [30–36]. A necropsy study of a patient with GCA who died from myocardial infarction while receiving TCZ revealed active lesions in his coronary arteries [37], and silent progression of large vessel involvement has also been reported [38]. Consequently, there is some concern about whether TCZ really impacts vascular inflammation or just produces a valuable symptomatic relief [39].

In this study, we explored the functional contribution of the IL-6 pathway to vascular inflammation by exposing *ex vivo*–cultured arteries from patients with GCA to TCZ.

## METHODS

### *Patient samples*

The study was performed with biological samples (frozen temporal arteries, peripheral blood mononuclear cells [PBMCs], fresh temporal arteries, and aortic tissue) obtained from patients with biopsy-proven GCA and controls. Characteristics of patients and controls as well as the experimental use of their samples are depicted in Supplementary Table S1. The study was approved by the ethics committee of Hospital Clínic (Barcelona, Spain), and patients signed informed consent.

### *Temporal artery biopsies*

Temporal artery biopsies (TABs) were performed in 198 consecutive patients with suspected GCA for diagnostic purposes during the study period (2016–2024). Sixty-six biopsies disclosed histopathologic features of GCA, and the remaining 132 showed no inflammatory infiltrates. Fifty-one negative-result biopsies from patients with low clinical suspicion of GCA were selected as controls. In these patients, an alternative diagnosis was achieved, or symptoms were considered nonspecific or attributable to comorbidities, and none of them were treated as GCA (Supplementary Tables S2 and S3).

### *Aortic specimens*

Fresh aortic fragments were obtained from surgical repair of thoracic aortic aneurysms from 6 patients. Four of them had been previously diagnosed with GCA and treated as such and histopathology examination disclosed slight persistent inflammatory infiltrates, mainly in the adventitia, along with extensive disorganisation of elastic fibres. In the additional 2 patients, mild aortic inflammatory infiltrates were serendipitously discovered at histopathologic examination of the specimens.

### *Reagents*

The details of reagents used are given in Supplementary Methods.

### *Arterial tissue culture*

TAB sections (1-mm thick) from patients with GCA and controls and aortic sections were cultured on Matrigel (BD Biosciences) as described [40], with or without TCZ (Ro-Actemra; Roche) at 10 $\mu$g/mL for temporal artery sections and at 20 $\mu$g/mL for aortic sections, human immunoglobulin G (IgG) isotype control (10 $\mu$g/mL; Sigma) or dexamethasone (0.5 $\mu$g/mL; Sigma). Each condition was tested in 2 to 3 replicate wells. After 5-day culture, sections were recovered, pooled, and processed for RNA or protein extraction. Supernatants were also collected and preserved at −80 °C for detection of soluble proteins.

### *Cell culture*

Primary vascular smooth muscle cells (VSMCs) were isolated from TABs as previously described [41] and, except when otherwise indicated, were used between passage 3 and 8 for *in vitro* experiments. PBMCs were obtained from whole blood of healthy donors and 17 patients with GCA using Ficoll-Lymphoprep (Histopaque-1077; Sigma Diagnostics). For coculture experiments, VSMCs were seeded at 90% confluence into 6-well plates and cultured alone or with $1 \times 10^6$ PBMC/well. After 24 hours, PBMCs were isolated from supernatants by centrifugation. The underlying VSMCs were separately recovered after gentle treatment with ethylenediaminetetraacetic acid (EDTA) (Versene; Invitrogen) to remove attached PBMC. Cocultures were also performed with transwell inserts of 0.4-$\mu$m pore size (NuncTM).

Human umbilical vein endothelial cells (HUVECs) were isolated from freshly delivered human umbilical cords [42] and used between passages 3 and 5 for *in vitro* experiments. Cell culture protocols are detailed in Supplementary Methods.

### *Immunofluorescence*

Immunofluorescence staining was performed in fresh-frozen temporal artery (TA) sections. Antibodies used, dilutions, and detailed steps are depicted in Supplementary Methods.

### *Gene expression analysis*

Total RNA was extracted from cultured arteries or cells using TRIzol Reagent (Life Technologies). cDNAs were obtained by reverse transcription (Supplementary Methods). Candidate transcripts were measured by quantitative real-time polymerase chain reaction (PCR). Specific predeveloped TaqMan probes (Applied Biosystems) were used for PCR amplification (Supplementary Table S2).

Fluorescence was detected using ViiA 7 Real-Time PCR System, and results were analysed with the QuantSudio Real-Time PCR software, v1.1 (both from Applied Biosystems). Gene expression was normalised to the expression of the endogenous control gene *GUSB* using comparative ΔCt method.

### *Western blot*

Protein extracts from frozen arteries, cocultured cells or cultured arteries were resolved by SDS-PAGE and transferred onto nitrocellulose membranes. Antibodies used, dilution, and detailed methods are depicted in Supplementary Methods.

### *Immunoassay*

CCL2, CXCL9, and CXCL10 were measured in supernatants of cultured arteries with Quantikine ELISA Kit (R&D Systems).

### *Chemotaxis assay*

PBMC chemotaxis was assessed using Boyden chambers with 5-$\mu$m pore polyester membranes (Poretics; Osmonics; see specific details in Supplementary Methods).

### Cell adhesion assays

VSMCs or HUVECs were seeded into 96-well plates. HUVECs were previously stimulated with IFN$\gamma$ (100 ng/mL; R&D Systems) and tumour necrosis factor $\alpha$ (20 ng/mL; R&D Systems) for 24 hours, before the addition of PBMCs. After 24 hours, $1 \times 10^5$ PBMCs, preincubated with or without 10 $\mu$g/mL of TCZ (Roche) or an IgG control (Sigma) for 1 hour, were added and incubated for 30 minutes at 37 °C. Wells were gently rinsed with phosphate-buffered saline and cells were fixed and stained with 0.2% crystal violet in 20% methanol for 10 minutes. Plates were extensively washed, and crystal violet was solubilised with 1% sodium dodecyl sulfate. Optical density was assessed by spectrophotometry at 580 nm wavelength. Each condition was tested in 8 to 10 different wells. Results were confirmed by counting attached cells/field at 100× magnification.

### Statistical analysis

Mann-Whitney U test and Student *t* test, when applicable, were used for independent or paired data using the IBM SPSS Statistics software (version 20.0). Fisher exact test was applied to qualitative variables. Heatmaps of transcripts analysed were generated using heatmapper.ca online software.

## RESULTS

### Expression of IL-6 and its receptor in GCA lesions

Both IL-6 and IL-6R mRNAs were constitutively present in control arteries. IL-6 mRNA levels were higher in temporal arteries from patients with GCA compared with those in controls but differences did not reach statistical significance, as previously observed in different cohorts [11,28] (Fig 1A). By contrast, IL-6R mRNA was significantly less abundant in GCA lesions than that in control arteries (Fig 1A). Expression of IL-6 and IL-6R mRNA was confirmed in primary VSMC, the main cell component of normal arteries (Fig 1B). A decrease in IL-6R mRNA in GCA-derived VSMC at passage 0 (recently exposed to the GCA inflammatory microenvironment) was consistent with findings in GCA-involved arteries.

However, IL-6R protein content was low in normal artery lysates and markedly increased in GCA arteries (Fig 1C). This result agreed with the observations made in immunofluorescence-stained biopsies where IL-6R protein was intensively expressed in GCA-involved arteries (Fig 1D). IL-6R staining was especially intense in areas with clusters of infiltrating inflammatory cells (Fig 1D). Contrarily, a very slight expression of both IL-6 and its receptor IL-6R was observed in organised VSMCs in the media and in the luminal endothelium of control arteries (Fig 1E).

Specific cell markers were used to further characterise the cell types positively stained for IL-6 and/or IL-6R in GCA lesions. Macrophages, identified as CD68+ cells, showed the most intense staining for IL-6 and IL-6R. Some CD3+ T cells and CD20+ B cells, localised mostly in the adventitia, also expressed IL-6 and IL-6R (Fig 1F). IL-6 and IL-6R were also detected in endothelial cells (CD31+ cells), both in adventitial vessels as well as in the luminal endothelium. To a lesser extent, VSMCs, identified as smooth muscle actin–positive cells, also showed positive staining for both IL-6 and its receptor (Fig 1F). IL-6R and IL-6 expression markedly colocalised.

### Effect of IL-6R blockade with TCZ on STAT3 phosphorylation and expression in PBMCs from patients with GCA, cultured GCA arteries, and PBMC cocultured with VSMC

Next, we investigated whether blocking IL-6R with TCZ interfered with IL-6–mediated signalling by exploring the phosphorylation status of transcription factor STAT3 in *ex vivo*–cultured temporal arteries from patients with GCA. IL-6R blockade significantly decreased phosphorylation of STAT3 (Fig 2A). TCZ virtually abrogated STAT3 phosphorylation in PBMCs from patients with GCA (Fig 2B). In addition to reducing STAT3 phosphorylation, treatment with TCZ also decreased *STAT3* mRNA in cultured GCA arteries (Fig 2C).

We subsequently analysed the specific impact of TCZ on STAT3 phosphorylation in inflammatory cells versus resident cells (VSMCs). Coculture of donor PBMCs with temporal artery–derived VSMCs were used to mimic the inflammatory milieu in GCA-involved arteries [43]. Coculture strongly increased phosphorylated STAT3 (pSTAT3) in both PBMCs and VSMCs, but no effect of TCZ was observed on VSMC. In contrast, TCZ completely abrogated STAT3 phosphorylation in PBMCs when cultured alone. This inhibitory effect decreased when PBMCs were cocultured with VSMCs (Fig 2D). Same results were obtained when PBMCs were cocultured with VSMCs using transwells to avoid cell–cell contact (Fig 2E), indicating a role for soluble factors in the protective role of the vascular niche against TCZ effect on STAT3 phosphorylation of PBMCs.

### Blocking IL-6R with TCZ impacts expression of inflammatory and remodelling molecules in GCA lesions

We further investigated the effects of TCZ on mRNA expression of a variety of candidate molecules relevant to the pathogenesis of vascular inflammation and remodelling in cultured GCA arteries. Molecules investigated included transcription factors involved in T cell functional differentiation, proinflammatory cytokines, chemokines/chemokine receptors, adhesion molecules, growth factors, and extracellular matrix proteins (Table).

In general, and despite potential compensation by other mediators, TCZ decreased transcripts of a variety of proinflammatory molecules and increased transcripts encoding matrix proteins although to a much lesser magnitude than dexamethasone, as visualised in Figure 3. Subanalysis of data according to previous treatment with GC suggests a stronger TCZ impact on samples from treatment-naive patients, possibly because GC treatment decreases IL-6 production [24] (Supplementary Fig). Transcripts significantly reduced by TCZ included suppressor of cytokine signalling *(SOCS)3*, also confirmed at the protein level (Fig 4A); *CD163*, a macrophage scavenger receptor; matrix metalloprotease *(MMP)3*; and adhesion molecule *ICAM-1*, along with several chemokines detailed in more depth in the next section (Fig 5 and Table). *IL-17A* and *IL-21* were undetectable or detected at low levels, and relative fold decrease could not be calculated. All significantly modulated genes have binding sites for STAT3 based on chromatin immunoprecipitation/sequencing studies [44].

### Modulation of chemokine expression by TCZ: exploratory assessment in additional GCA-involved cells and tissues

Under our experimental conditions, TCZ did not significantly modify expression of chemokine (*CCL5*, *CXCL8*, *CXCL11*, and *CXCL12*) or chemokine receptor (*CXCR4* or *CXCR5*) mRNAs (Table). By contrast, TCZ significantly decreased *CCL2* mRNA

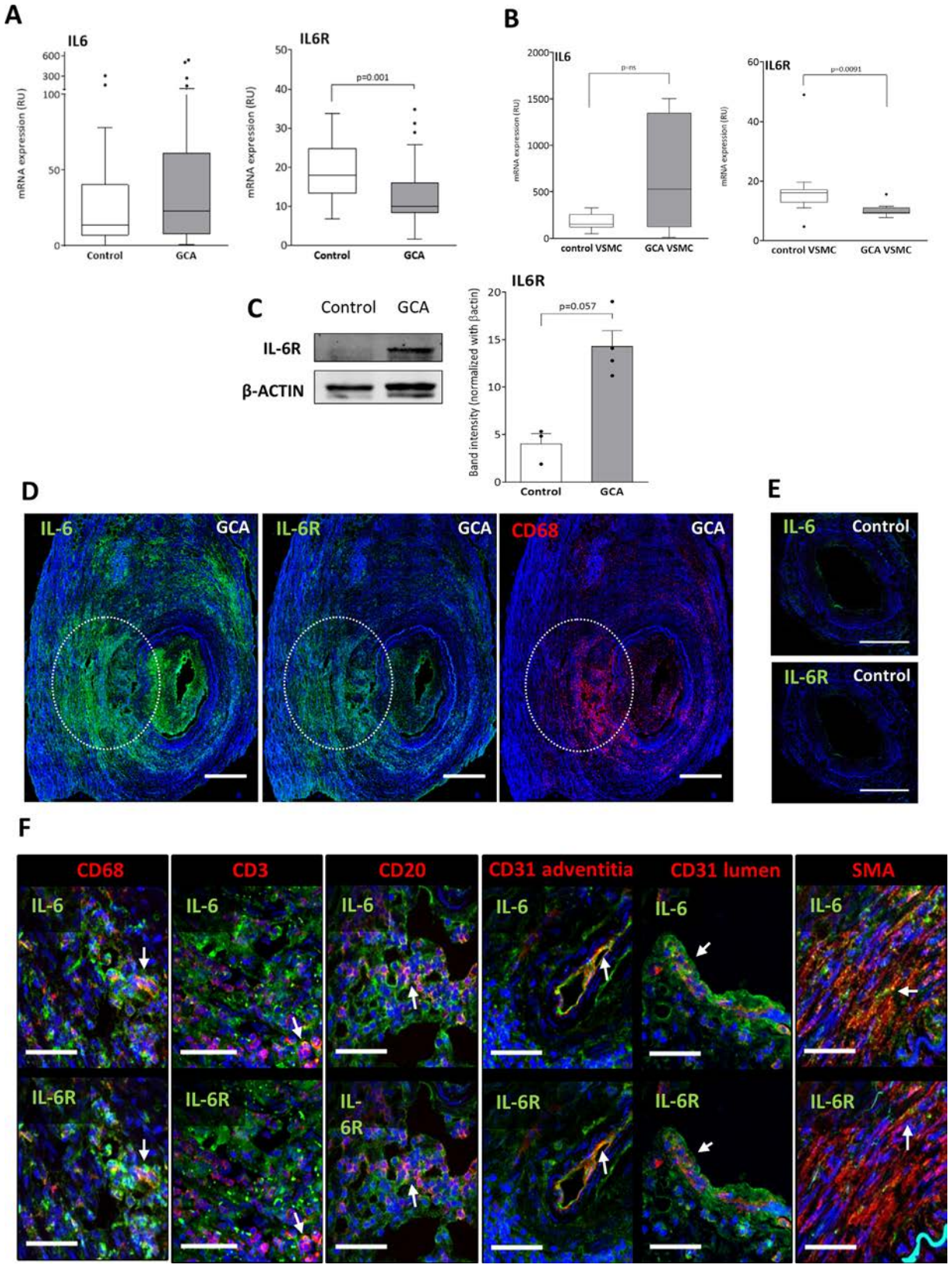



**Figure 1.** Interleukin (IL)-6 and IL-6R expression in temporal arteries from patients with giant-cell arteritis (GCA). (A) Concentrations of IL-6 (left) and IL-6R mRNA (right) measured by quantitative real-time polymerase chain reaction (qRT-PCR) in fresh-frozen histologically negative arteries (controls) (n = 24) versus GCA-positive arteries (n = 28). Results are expressed as relative units normalised to the housekeeping transcript *GUSB*. (B) Concentrations of IL-6 (left) or IL-6R (right) mRNA in primary cultures of vascular smooth muscle cells (VSMCs) at passage zero derived from GCA (n = 8) or control (n = 11) temporal arteries measured by qRT-PCR. (C) Representative image of IL-6R protein expression measured by immunoblot in a GCA biopsy compared with a control artery. IL-6R protein expression was measured in 4 GCA biopsies and 3 control arteries. $\beta$-Actin was used as a loading control. Densitometric analysis of all samples is shown in the bottom plot. Bars represent the mean of all samples ± SEM. (D) Immunostaining of IL-6 or IL-6R (green) and nuclei (blue) in a GCA temporal artery. White circles delimit an area with dense inflammatory infiltrates by CD68+ cells (red), intensively stained for IL-6 and IL-6R. Scale bar represents 500 $\mu$m in all images. (E) Immunostaining of IL-6 or IL-6R (green) and nuclei (blue) in a control artery. Scale bar represents 500 $\mu$m in both images. (F) Immunostaining of IL-6 or IL-6R (green) along with CD68, CD3, CD20, CD31, or smooth muscle actin (red) in GCA lesions. Nuclei are stained blue with 4',6-diamidino-2-phenylindole (DAPI). White arrows highlight cells positively stained for IL-6 or IL-6R and the corresponding cell marker. Scale bar represents 50 $\mu$m in all images.

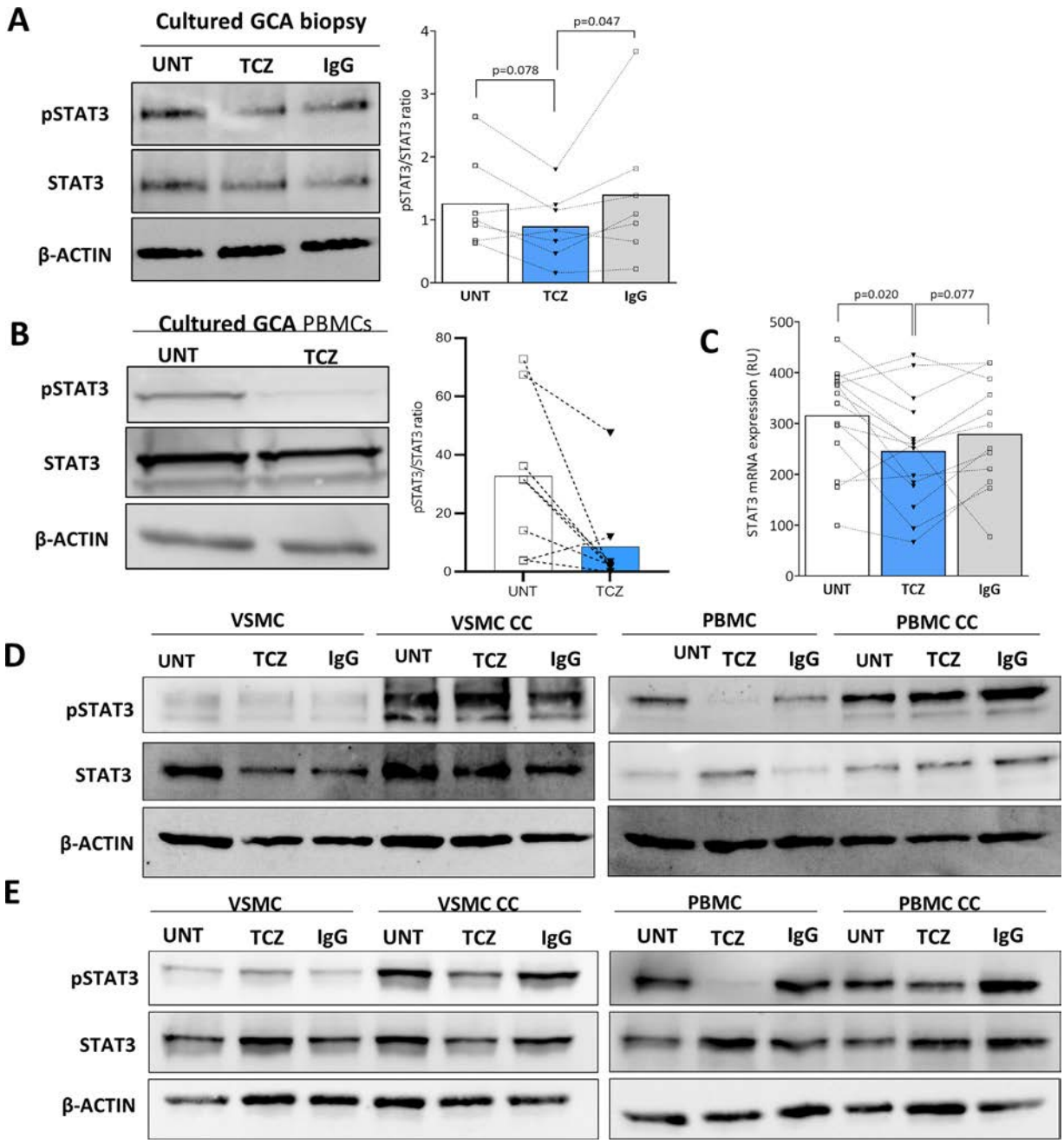



**Figure 2.** Interleukin (IL)-6R blocking with tocilizumab (TCZ) reduces STAT3 phosphorylation and expression in peripheral blood mononuclear cells (PBMCs) and in *ex vivo*–cultured arteries from patients with giant-cell arteritis (GCA). (A) Illustrative immunoblot of phosphorylated STAT3 (pSTAT3) and total STAT3 measured in a cultured GCA temporal artery untreated, treated with TCZ or a control IgG (both at 10 $\mu$g/mL) for 5 days. Proteins were measured by densitometry in 6 cultured arteries. Results are represented as fold increase ± SEM (right plot). $\beta$-Actin was used as a loading control. (B) Representative immunoblot of pSTAT3 and total STAT3 in PBMC from 8 patients with GCA untreated, exposed to TCZ or to a control IgG (both at 20 $\mu$g/mL) for 24 hours. Proteins were measured by densitometry. Results are represented as fold increase ± SEM (right plot). $\beta$-Actin was used as a loading control. (C) Effect of TCZ blockade on STAT3 mRNA expression in cultured GCA arteries with or without exposure to TCZ or to a control IgG (both at 10 $\mu$g/mL) for 5 days measured by quantitative real-time polymerase chain reaction. Results are expressed as relative units normalised to the housekeeping transcript *GUSB*. A total of 15 cultured arteries were analysed. (D) Characteristic immunoblot of pSTAT3 and total STAT3 in isolated or cocultured vascular smooth muscle cells (VSMC CC) (left) or isolated or cocultured PBMC (PBMC CC) (right). Cells were untreated or exposed to TCZ or control IgG (both at 10 $\mu$g/mL) for 24 hours. The experiment was performed 3 times with similar results. (E) Same experiment as in (D), but, in this case, cocultures were performed using transwell supports. Protein expression was measured in 3 independent experiments with similar results. IgG, immunoglobulin G; UNT, untreated.

expression in GCA-cultured arteries and CCL2 concentrations in the supernatant fluid. Surprisingly, TCZ significantly increased expression of *CXCL9* and *CXCL10* and the release of the protein into the supernatant fluid (Fig 4B,C).

Transcripts regulated by TCZ were also assessed in additional samples from patients with GCA (Fig 5A,B). In general, these exploratory results paralleled those found in TA tissue. TCZ significantly reduced expression of *STAT3*, *SOCS3*, and *CCL2* in PBMCs from patients with active GCA (Fig 5A). In aortic tissue, TCZ significantly decreased *CD163, ICAM-1*, *STAT1*, and *MMP3* mRNAs (Fig 5B).

### *Functional impact of chemokine modulation by TCZ*

To assess the net effect of the changes in chemokine expression induced by TCZ in GCA lesions, chemotaxis of PBMC

Table

**Transcriptional differences between cultured GCA and control temporal arteries and changes induced by tocilizumab, control IgG, or dexamethasone in *ex vivo*–cultured arteries from patients with GCA**

| Transcripts investigated | GCA biopsies | | | |
|---|---|---|---|---|
| | GCA/control | TCZ/UNT | TCZ/IgG | DXA/UNT |
| Cell markers | | | | |
| CD68 | 1.63** | 1.11 | 1.10 | 0.79* |
| CD163 | 1.41 | 0.83* | 0.74** | 7.04* |
| CD3 | 8.92** | 1.04 | 1.14 | 0.54* |
| CD20 | 10.61** | 1.09 | 1.34 | 0.75 |
| Transcription factors | | | | |
| TBX21 | 2.38* | 0.94 | 0.91 | 6.05 |
| GATA3 | 1.99* | 1.19 | 1.14 | 0.90 |
| RORC | 3.65** | 1.15 | 1.82 | 0.51 |
| FOXP3 | 2.63** | 1.26 | 1.13 | 0.54 |
| BCL6 | 1.03 | 0.92 | 0.86 | 1.48 |
| Cytokines and cytokine receptor | | | | |
| IL-6 | 2.82** | 0.93 | 0.86 | 0.09* |
| IL-6R | 0.71 | 1.07 | 0.98 | 0.75 |
| IL-1B | 3.85** | 0.93 | 0.95 | 0.12* |
| TNF$\alpha$ | 1.37 | 0.98 | 1.05 | 0.78* |
| IFN$\gamma$ | 17.06** | 0.99 | 0.95 | 0.39 |
| IL-17A | — | — | — | — |
| IL-12A | 0.23* | 1.09 | 0.94 | 0.66 |
| IL-12B (p40) | — | — | — | — |
| IL-23A (p19) | 2.13 | 1.18 | 0.93 | 0.70 |
| IL-10 | 0.99 | 0.89 | 1.03 | 1.00 |
| IL-21 | — | — | — | — |
| Chemokines and chemokine receptors | | | | |
| CCL5 | 7.13** | 1.15 | 1.03 | 0.42* |
| CXCL8 | 1.81 | 1.12 | 0.79 | 0.46 |
| CXCR4 | 1.13 | 1.12 | 0.94 | 0.47* |
| CXCL12 | 0.36* | 0.92 | 1.00 | 0.42* |
| CXCR5 | 3.35* | 0.94 | 0.84 | 0.31* |
| CXCL11 | 0.45 | 2.15 | 1.82 | 0.88 |
| Negative regulators of cytokine signalling | | | | |
| SOCS3 | 0.97 | 0.87* | 0.88* | 0.43* |
| Adhesion molecules | | | | |
| ICAM1 | 1.72 | 1.09 | 0.89* | 0.55 |
| VCAM1 | 1.41 | 1.06 | 1.13 | 0.14* |
| Growth factors | | | | |
| VEGFA | 1.92** | 0.95 | 0.98 | 0.69 |
| TGFB1 | 0.79 | 0.94 | 0.90 | 0.95 |
| Extracellular matrix proteins | | | | |
| COL1A1 | 0.89 | 1.03 | 1.25 | 0.96 |
| COL3A1 | 0.90 | 0.91 | 1.10 | 1.24 |
| Metalloproteases | | | | |
| MMP3 | 1.98 | 1.05 | 0.88* | 0.70 |
| Apoptosis regulators | | | | |
| BCL2 | 0.56* | 1.15 | 0.98 | 1.00 |

DXA, dexamethasone; GCA, giant-cell arteritis; IgG, immunoglobulin G; MMP, matrix metalloprotease; SOCS, suppressor of cytokine signalling; TCZ, tocilizumab; UNT, untreated.

Analysis of transcripts related to GCA pathogenesis in cultured GCA temporal arteries (expressed as fold change compared with control biopsies) or in cultured GCA arteries treated with TCZ for 5 days (expressed as fold change compared with untreated or control IgG), or treated with DXA (0.5 $\mu$g/mL) (expressed as fold change compared with untreated. A total of 17 cultured arteries were analysed.

*$P < .05$; **$P < .01$.

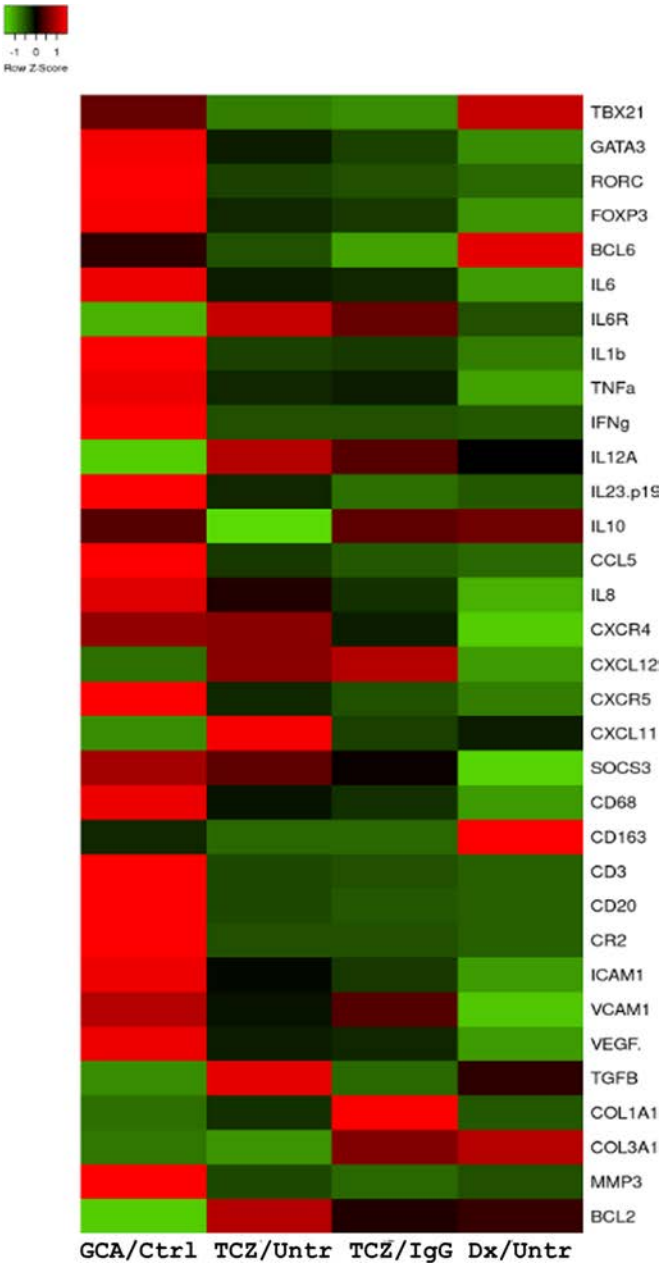



**Figure 3.** Heatmap representing mRNA expression of GCA pathogenesis–related genes listed in the table, in cultured GCA temporal arteries expressed as fold change in GCA versus control biopsies or fold change between untreated GCA arteries or GCA arteries treated with TCZ, control IgG (both at 10 $\mu$g/mL), or dexamethasone (0.5 $\mu$g/mL), all measured by quantitative real-time polymerase chain reaction. IgG immunoglobulin G; TCZ, tocilizumab; Untr, untreated.

towards supernatants of cultured GCA arteries in the presence or absence of TCZ or nonimmune IgG was explored. Overall, a significant decrease in chemotaxis of PBMC towards TCZ-treated artery supernatants was observed (Fig 6A).

Interestingly, brief exposure to TCZ reduced PBMC adhesion to cytokine-stimulated HUVECs and VSMCs (Fig 6B), indicating that TCZ interaction with IL-6R may drive rapid inhibitory signalling on PBMCs adhesiveness even in the absence of significant IL-6 in the microenvironment. Overall, decreased adhesion and chemotaxis induced by TCZ resulted in a reduction of inflammatory infiltrates in cultured arteries (Fig 6C).

### *IL-6R blockade with TCZ increases STAT1 expression and phosphorylation*

The impact of IL-6 and IL-6R blockade by TCZ on STAT1-dependent chemokines CXCL9 and CXCL10 was explored in cocultures of PBMCs and VSMCs. TCZ-induced increase in CXCL9 and CXCL10 expression was mostly at the expense of PBMCs where IL-6 acts through its membrane-bound receptor (Fig 7A). Contrarily, TCZ reduced CXCL9 and CXCL10

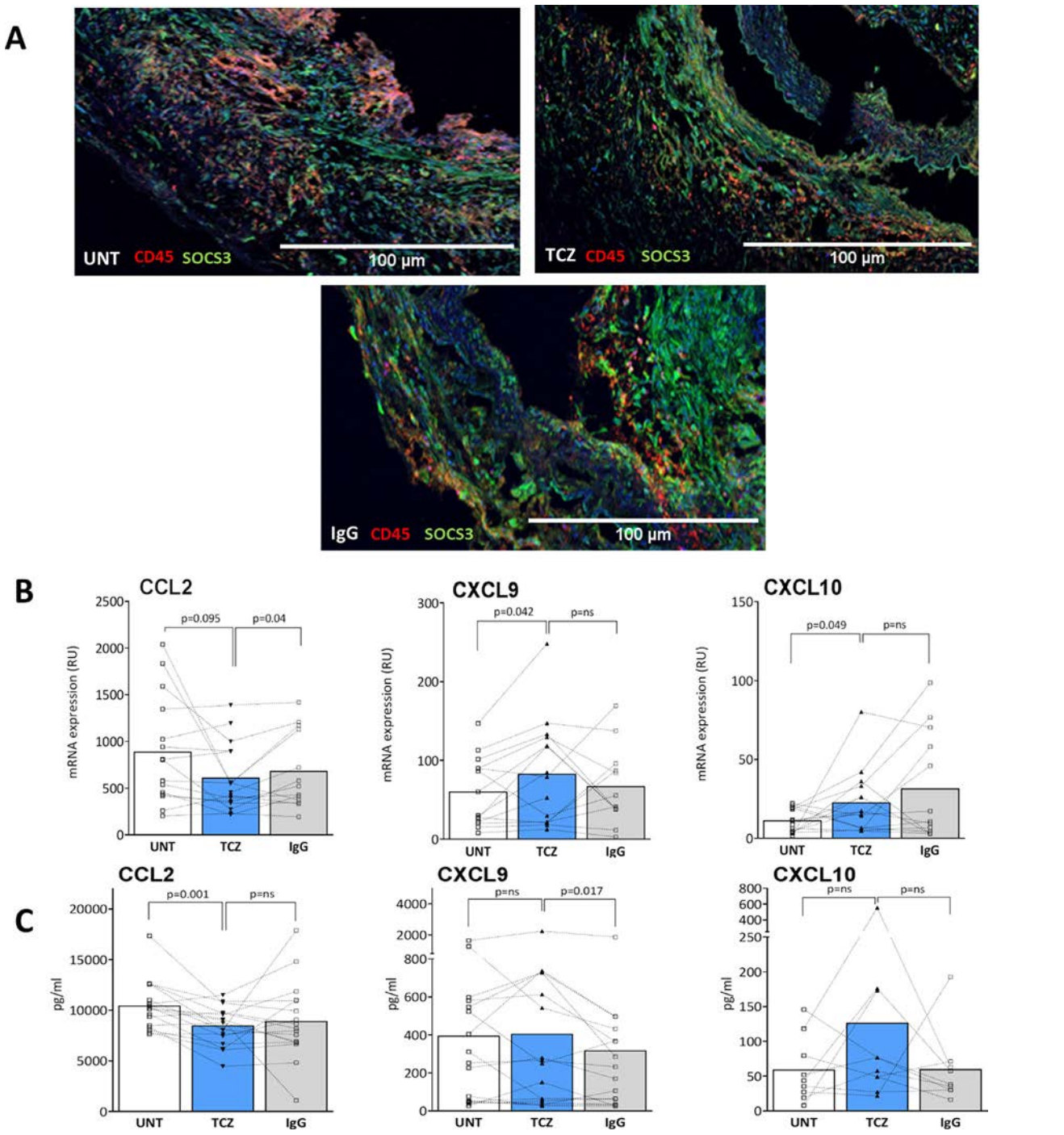



**Figure 4.** Changes induced by blocking interleukin (IL)-6R with tocilizumab (TCZ) on SOCS3 and chemokine expression in *ex vivo*–cultured arteries from patients with giant-cell arteritis (GCA). (A) Immunostaining of SOCS3 (green), CD45 (red), and nuclei (blue) in a GCA-involved temporal artery. Areas with co-immunostaining of SOCS3 and CD45 (orange) in an untreated section and sequential sections exposed to TCZ or control IgG are displayed. (B) CCL2, CXCL9, and CXCL10 mRNA expression in GCA-cultured arteries treated with or without TCZ or a control IgG (both at 10 $\mu$g/mL) for 5 days measured by quantitative real-time polymerase chain reaction. A total of 17 cultured arteries were analysed. (C) CCL2, CXCL9, and CXCL10 concentration (pg/mL) in the supernatant of cultured temporal arteries treated with or without TCZ or an IgG control (both at 10 $\mu$g/mL) for 5 days. Chemokines were measured by immunoassay in 17 GCA-cultured arteries. SOCS, suppressor of cytokine signalling; IgG, immunoglobulin G; UNT, untreated.

production by HUVECs or by primary temporal artery–derived VSMC where IL-6 acts mainly through transignalling (Fig 7B). CCL-2 decreased in all cell types.

While *CCL-2* expression is regulated by both STAT3 and STAT1 transcription factors, *CXCL9* and *CXCL10* are 2 chemokine mRNAs mainly regulated by STAT1 [44], typically activated by IFN$\gamma$ in GCA [12]. Based on the above-described results, we postulated that blocking IL-6R signalling and the corresponding decrease in STAT3 expression and activation elicited by TCZ might result in an increase in STAT1 expression and activation. To check this hypothesis STAT1 expression was analysed in GCA temporal arteries treated with TCZ. Although differences were not statistically significant, *STAT1* mRNA showed an overall tendency to increase upon TCZ treatment when compared with the untreated section of the same biopsy ($P$ = .053) (Fig 7C) However, this was at the expense of a subset of samples only (Fig 7D). Similarly, when we analysed the effect of TCZ treatment on STAT1 phosphorylation in cultured GCA arteries, opposite results were found depending on the sample (Fig 7E).

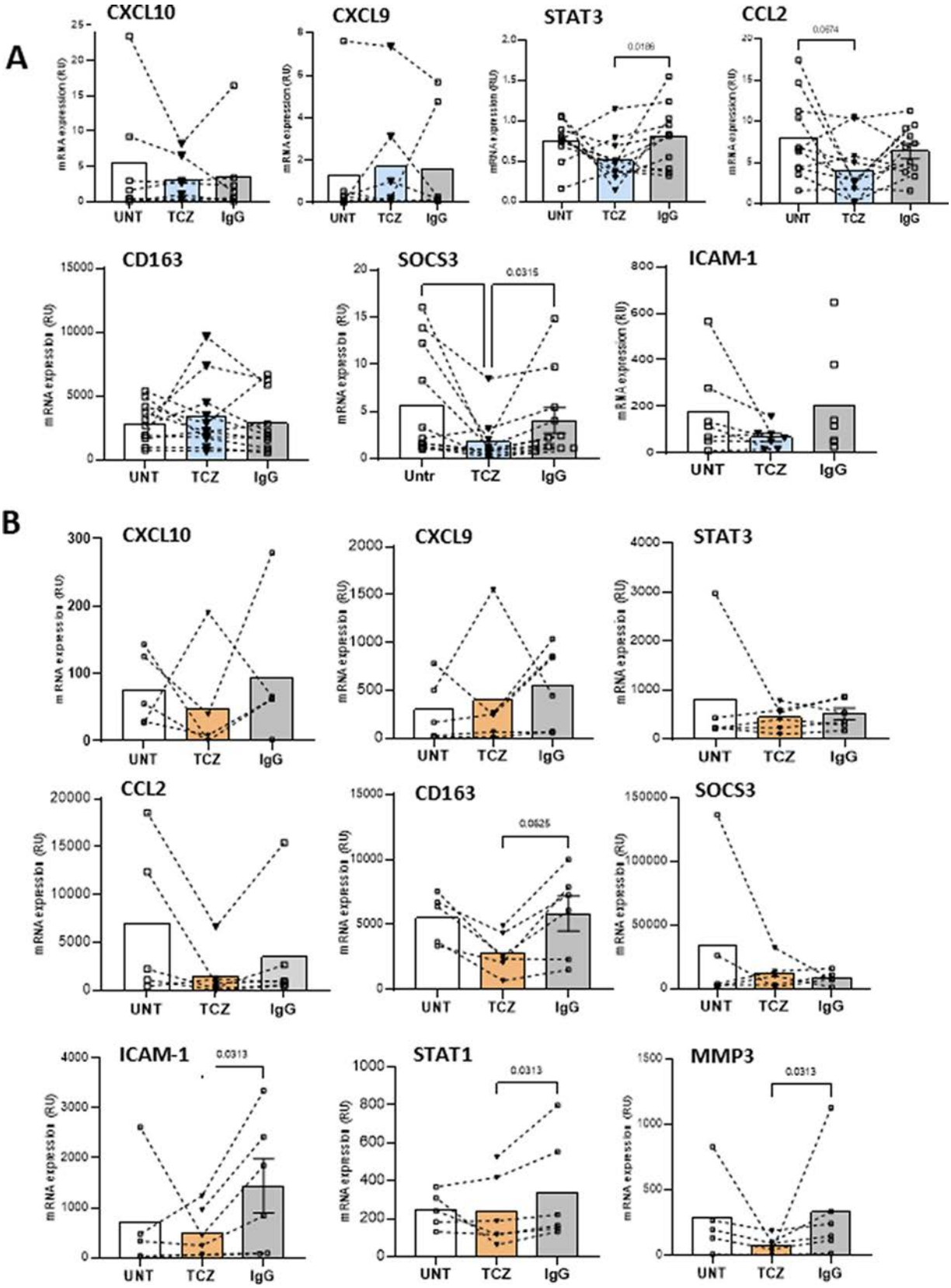



**Figure 5.** Transcriptional changes induced by blocking interleukin (IL)-6 receptor with tocilizumab (TCZ) on additional cells and tissues from patients with giant-cell arteritis (GCA). (A) *CXCL9*, *CXCL10*, *ICAM-1*, *STAT3*, *CCL2*, *CD163*, and *SOCS3* mRNA concentrations in PBMCs from 9 patients with active GCA untreated or exposed to TCZ or control IgG for 24 hours. Samples were obtained at the time of the TAB and transcripts measured by quantitative real-time polymerase chain reaction (qRT-PCR). (B) *CCL2*, *CXCL9*, *CXCL10*, *STAT1*, *STAT3*, *SOCS3*, *MMP3*, *CD163*, and *ICAM-1* mRNA concentrations in cultured aortic sections from 6 patients, 4 with GCA and 2 with idiopathic aortitis, untreated or treated with TCZ or control IgG for 5 days and measured by qRT-PCR. A total of 6 cultured arteries were analysed. IgG, immunoglobulin G; TAB, temporal artery biopsy; UNT, untreated.

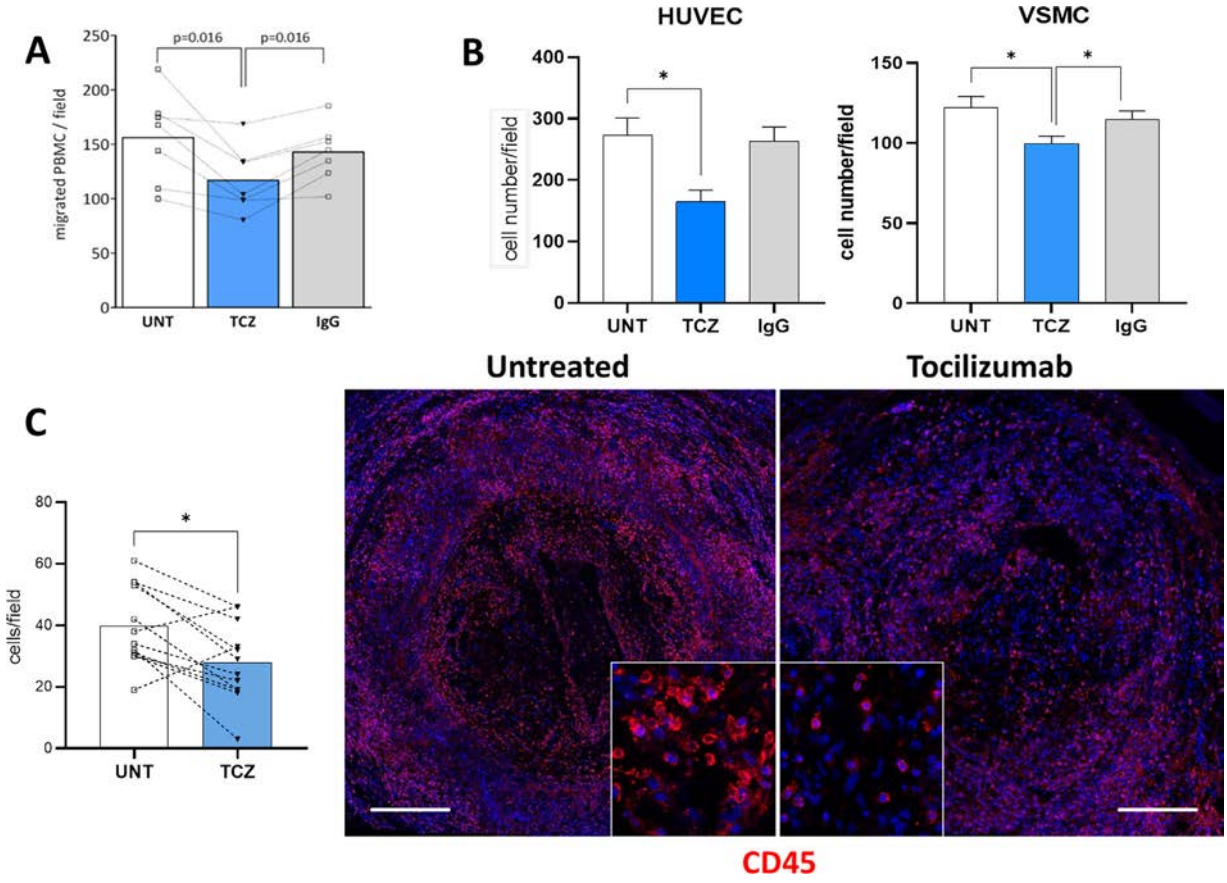



**Figure 6.** Effect of blocking interleukin (IL)-6 receptor with tocilizumab (TCZ) on cell adhesion, chemotaxis and temporal artery inflammation. (A) Chemotaxis of peripheral blood mononuclear cells (PBMCs) towards the supernatant of cultured giant-cell arteritis (GCA) temporal arteries. Diluted supernatants of cultured arteries (untreated or previously treated with TCZ or control IgG for 5 days) were placed in the lower wells of a Boyden chamber. PBMCs, from a healthy donor, were placed in the upper wells of the chamber and allowed to migrate for 2.5 hours. The migration assay was repeated with supernatants from 7 cultured GCA temporal arteries and each condition was performed in quadruplicate wells. (B) PBMCs from patients with GCA untreated or preincubated with TCZ or control IgG for 1 hour, were added on top of human umbilical vein endothelial cells (HUVECs; left) or vascular smooth muscle cells (VSMCs; right). After 30 minutes, the wells were washed, and adherent cells were stained with crystal violet. Cells were counted in 10 replicate wells at ×100 magnification. (C) Immunofluorescence of the pan-leukocyte marker CD45 (red) and nuclei (blue) in a GCA temporal artery cultured with or without TCZ (20 $\mu$g/mL) for 5 days. Scale bar represents 500 $\mu$m in both images. Quantification of CD45+ cells (10 fields per section) is disclosed in the left part of the panel. UNT, untreated.

## DISCUSSION

As expected, but not previously demonstrated, IL-6R, the target of TCZ, was remarkably expressed in GCA lesions. Interestingly, IL-6 and IL-6R transcripts were constitutively expressed by resident cells in normal temporal arteries, particularly by VSMCs, the main cellular component of the artery wall. However, in normal arteries, IL-6R mRNA was hardly translated into protein, indicating that protein expression may be repressed by inhibitory mechanisms in homeostatic conditions. IL-6 mRNA expression by VSMCs was confirmed in primary cells obtained from GCA-involved arteries.

Interestingly, while IL-6R protein expression increased in GCA lesions, IL-6R mRNA decreased in GCA arteries as well as in primary VSMCs previously exposed to inflammation. This dissociation has been observed in other transcripts expressed by both inflammatory cells and VSMCs in GCA [43] and may result from negative feedback mechanisms, possibly mediated by microRNAs, deeply dysregulated in GCA [45,46]. Moreover, VSMC damage or loss, typical of GCA, may decrease their contribution to IL-6R mRNA.

Blocking endogenous IL-6R with TCZ led to a significant reduction in STAT3 expression and phosphorylation in cultured arteries from patients with GCA. TCZ completely abrogated STAT3 phosphorylation in PBMC isolated from active patients. However, when PBMCs were cocultured with VSMCs, simulating the inflammatory environment of the artery wall, the impact of TCZ on pSTAT3 was much reduced, possibly due to the production of other cytokines able to activate STAT3. These results suggest that, in GCA lesions, the effects of IL-6 on STAT3 phosphorylation may be partially compensated by other stimuli present in the microenvironment. Additional members of the IL-6 family or the IL-12/IL-6 family of heterodimeric cytokines may activate STAT3 [16,47]. Among them, IL-22 and IL-23p19, are known to be expressed in GCA [13,48,49]. Other cytokines present in GCA, including IL-21, IL-10, and even IFN$\gamma$, may also activate STAT3 under certain conditions [50]. These findings suggest that TCZ may have a greater impact on circulating cells than in tissue-infiltrating cells.

The effect of TCZ on the expression of key candidate molecules thought to be relevant to GCA pathogenesis was modest, compared with dexamethasone at concentrations equivalent to high-dose prednisone used in patients. Contrarily to blocking granulocyte-macrophage colony-stimulating factor (GM-CSF) receptor $\alpha$ with mavrilimumab [51], there was no apparent impact on cell markers at the mRNA level. There was no effect on expression of transcription factors involved in T cell differentiation in tissue. Several studies have shown a decrease in

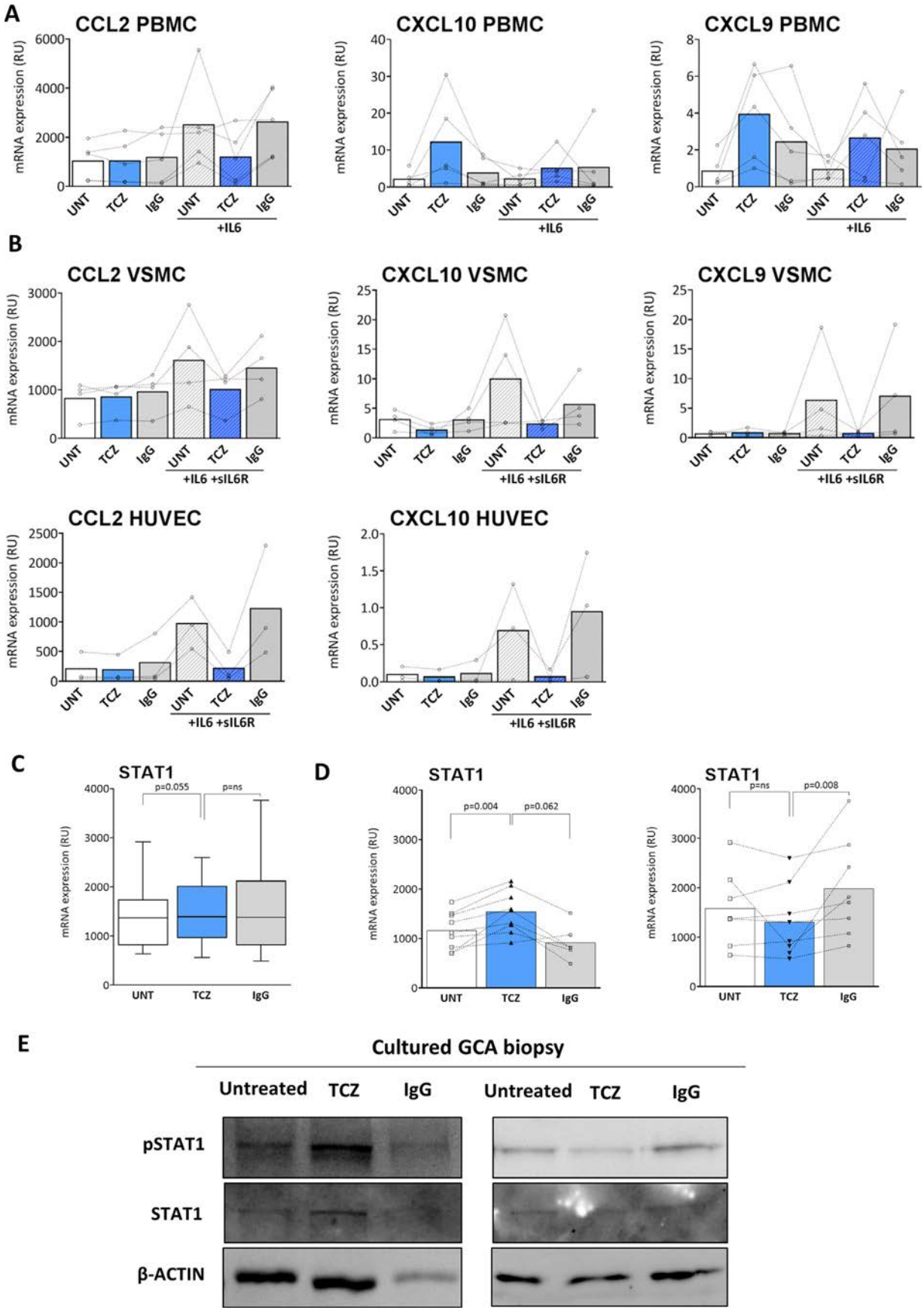



**Figure 7.** Diverse effects of blocking interleukin (IL)-6R with tocilizumab (TCZ) on chemokine expression by inflammatory and resident cells. Impact of TCZ on STAT1 phosphorylation and expression in cultured giant-cell arteritis (GCA) arteries. (A) *CCL2*, *CXCL10*, and *CXCL9* mRNAs measured by quantitative real-time polymerase chain reaction (qRT-PCR) in PBMC. Cells were cultured for 24 hours untreated or treated with TCZ or control IgG (both at 10 $\mu$g/mL), with or without exposure to recombinant IL-6 (10 ng/mL). The figure summarises the results of 5 independent experiments. (B) *CCL2*, *CXCL10*, and *CXCL9* mRNAs determined by qRT-PCR in vascular smooth muscle cells (VSMCs; top panels) or human umbilical vein endothelial cells (HUVECs; bottom panels). Cells were cultured for 24 hours untreated or exposed to TCZ or control IgG (both at 10 $\mu$g/mL), with or without exposure to recombinant IL-6 (10 ng/mL) combined with recombinant soluble IL-6R (100 ng/mL). CXCL9 was not detected in HUVEC in any condition.

FOXP3 expressing regulatory T cells in peripheral blood, particularly those expressing an isoform with deleted exon 2 with lower suppressor activity, in patients with active GCA, and these abnormalities are partially reversed by TCZ [52,53]. However, under our experimental conditions, no changes in global *FOXP3* expression induced by TCZ were observed in GCA tissue. We cannot exclude that longer exposure might modulate expression.

Despite the potential partial compensation by other cytokines, the decrease in STAT3 phosphorylation induced by TCZ had a significant impact on the expression of several STAT3 regulated transcripts including *STAT3* itself, *CD163*, *SOCS3*, *CCL2*, *ICAM-1*, and *MMP3* mRNAs[44]. These results were validated in PBMCs from patients with active GCA and in aortic tissue from patients with GCA.

The decrease in SOCS3, an inhibitor of IL-6 signalling may reflect a reduced need of a counter-regulatory mechanism avoiding excessive IL-6–mediated effects [16]. Moreover, a decrease in SOCS3 may lead to a SOCS1/SOCS3 imbalance, leading to activation of $T_H1$ mechanisms and production of the anti-inflammatory cytokine IL-10 [15,54]. The impact of TCZ on SOCS3 inhibition was absent in some patient samples. This could reflect a persistent impact of other SOCS3-inducing cytokines, such as GM-CSF or IL-1$\beta$, both produced in GCA [11,28,51], or a deficient response to IL-6R blockade as observed in carriers of the Asp358Ala polymorphism who are naturally protected from excessive IL-6–mediated effects [55].

TCZ produced a decrease in CCL2, a relevant cytokine-mediating lymphocyte and monocyte recruitment into arterial walls as demonstrated in other experimental settings [56]. CCL2 is also induced by IFN$\gamma$ [12] and chemoattracts mainly $T_H1$ lymphocytes and macrophages. CCL2 and its receptor CCR2 are expressed by infiltrating cells in GCA and increased production of CCL2 in lesions is associated with relapsing disease [57].

TCZ decreased expression of ICAM-1, and important molecule in T cell activation and in interactions between leukocytes and endothelial cells or with VSMC, leading to arterial inflammation, in spite of the presence in lesions of other inducer cytokines such as IFN$\gamma$ or IL-1$\beta$ [11,12,28]. Interestingly, besides decreasing expression of ICAM-1, TCZ seems to impair adhesion through additional mechanisms: short exposure to TCZ resulted in rapid reduction of PBMC adhesion to cytokine-activated VSMCs or HUVECs in the absence of exogenous IL-6. In addition to its major signalling cascade leading to STAT3-mediated transcriptional regulation, IL-6R signalling can activate Src kinases and PI3kinases [16], which regulate integrin activation and leukocyte adhesion and migration [43]. Our findings suggest that binding of TCZ to IL-6R may send rapid negative signals even in the absence of significant IL-6.

Surprisingly, when we expanded the array of chemokines explored, an increase in STAT1-dependent chemokines CXCL9 and CXCL10 was observed. This effect seemed to mainly occur in mononuclear cells, and, therefore, possibly mediated by classical signalling through the membrane receptor. In spite of the opposite regulation of different chemokines, overall PBMC chemotaxis towards supernatants of TCZ-treated arteries was reduced. CXCL9 and CXCL10 are STAT1-dependent chemokines, typically induced by IFN$\gamma$ [12,44]. It has been shown that STAT1-induced expression of CXCL9 and CXCL10 decreased after STAT3 activation [58], at least partially by preventing STAT1 to form homodimers in myeloid cells [59]. Therefore, in a highly inflammatory microenvironment, such as in GCA lesions, reduction of STAT3 signalling by TCZ might result in STAT1 activation as a compensatory mechanism. Treatment with TCZ resulted, indeed, in increased *STAT1* mRNA expression and STAT1 phosphorylation in about half of the samples, suggesting that TCZ may elicit activation of alternative pathways in some individuals. These findings are in accordance with the results of clinical trials where TCZ is able to maintain GC-free remission in about 50% of patients [4,9].

Our study has some limitations. The *ex vivo* artery culture system, as the mice xenograft model [40,60], explores the target tissue of GCA isolated from a functional immune system. In both models, inflammation decreases over time [40,60] and, in the artery culture, results in decreased production of some cytokines compared with that in the corresponding fresh-frozen tissue [40]. It is likely that the observed effect of TCZ on leukocyte recruitment mechanisms has higher impact in vivo where white blood cells are in continuous circulation. Moreover, experiments were performed at a particular time point, and it cannot be excluded that longer exposure to TCZ would have generated additional changes. Furthermore, we designed a hypothesis-driven, candidate molecule approach, based on known GCA pathophysiology but unbiased large-scale analysis, especially spatial transcriptomics, may have provided a wider appraisal of cell-specific or region-specific changes within the artery wall. In spite of these limitations, our findings demonstrate that TCZ has a relevant impact on vascular inflammation and indicate that TCZ has an important role in cell recruitment into the vessels affected by GCA. Our findings also indicate that TCZ effects differ among tissue donors and that, upon TCZ exposure, STAT1 activation may occur in a patient subset and may partially compensate for STAT3 inhibition. As suggested by clinical trial results, our findings support that molecular responses to TCZ may be variable among patients. A better understanding of the molecular effects of IL-6 and IL-6 blockade with TCZ on GCA immunopathology may facilitate personalised medicine for patients with GCA.

## Competing interests

SP-G received conference attending support from Boehringer-Ingelheim and CSL-Vifor. MAA received conference attending support from CSL-Vifor. EQ received speaker honoraria from Edwards Life Sciences and Medtronics and conference attending support from Cardiva SL; is member of EACTS Francis Fontan Foundation board, SEIVAC Board of Directors, and European Board Thoracic and Cardiovascular Surgery (Secretary); and is an EACTS clinical guidelines committee member. GE-F has received consulting/lecturing fees from GSK and CSL-Vifor and a research grant from GSK. MCC has received consulting/lecturing fees from GSK, AbbVie, Astrazeneca, and CSL-Vifor; conference attending support form CSL-Vifor; a research grant from Kiniksa pharmaceuticals Ltd; and royalties from UpToDate.

Results were consistent in 4 independent experiments for VSMCs and 3 for HUVECs. (C) *STAT1* mRNA expression in GCA-cultured arteries untreated or exposed to TCZ or control IgG (both at 10 $\mu$g/mL) for 5 days measured by qRT-PCR. A total of 16 cultured arteries were analysed. (D) Same results as in (C), with samples separated according to whether IL-6 blockade increased (left) or decreased (right) *STAT1* mRNA levels. (E) Protein expression of phosphorylated STAT1 (pSTAT1) and total STAT1 measured by immunoblot in a GCA-cultured temporal artery untreated or treated with TCZ or control IgG (both at 10 $\mu$g/mL) for 5 days. Variable results were found depending on the sample. A total of 5 cultured arteries were analysed and an increase in pSTAT1 after TCZ treatment was found in 1 of them. $\beta$-Actin was used as a loading control. IgG, immunoglobulin G; UNT, untreated.

## Acknowledgements

The authors are grateful to Mrs Elisenda Coll, Mrs Gemma Martin and Dr Maria Calvo from the Advanced Microscopy Platform for their advice. This work was previously presented at the 21st International Vasculitis Workshop, April 7-10, 2024, Barcelona, Spain, and at the Annual European Congress of Rheumatology (EULAR) 2024, June 12-15, 2024, Vienna, Austria. Part of the results of this manuscript were included in the Doctoral Thesis defended by Nekane Terrades García (https://hdl.handle.net/2445/145702).

## Contributors

MC-B, FK, RA-R, EP-R, and MCC designed the study. MC-B, FK, RA-R, EP-R, ET, and NF-C performed the experimental work. SP-G, MAA, and GE-F collected relevant clinical data and performed biopsies in appropriate conditions for the experiments. AJ contributed to sample collection. EQ provided aortic tissue from aneurysm surgery in the conditions required by our experiments. FK, RA-R, and MCC wrote the manuscript draft. All authors provided intellectual input and revised and approved the manuscript. MCC serves as guarantor.

## Funding

This study was supported by Ministerio de Ciencia e Innovación AEI/10.13039/501100011033 (PID2020-114909RB-I00) and Ministerio de Ciencia, Innovación y Universidades/AEI/FEDER (EU) PID2023-152265OB-I00, the International Vasculitis Foundation, CERCA programme and Agència per la gestió d'Ajuts Universitaris i de Recerca (AGAUR) 2021 SGR 01561. FK was supported by the European Union's Horizon 2020 research and innovation programme under the Marie Sklodowska-Curie grant agreement No.813545 (ITN-MSCA-HELICAL), and MAA by Biomedicine International Training Research for Excellent Clinician-Scientists, co-funded by the European Union's Horizon 2020 research and innovation programme under the Marie Sklodowska-Curie grant agreement No 754550 and from 'La Caixa' Foundation.

## Patient consent for publication

Not applicable

## Ethics approval

The study was approved by the Ethics Committee of Hospital Clínic of Barcelona (HCB/2018/0397), and patients signed informed consent.

## Provenance and peer review

Not comissioned; externally peer reviewed.

## Data availability statement

Data will be made available on reasonable request.

## Patient and public involvement

Patients kindly and conscientiously donated samples to the research content of this article. Part of this study was reviewed and funded by the International Vasculitis Foundation. There was no public involvement.

## Supplementary materials

Supplementary material associated with this article can be found in the online version at doi:10.1016/j.ard.2025.02.008.

## Orcid

Roser Alba-Rovira: http://orcid.org/0000-0003-3308-5787
Sergio Prieto-González: http://orcid.org/0000-0003-3179-597X
Maria C. Cid: http://orcid.org/0000-0002-4730-0938

## REFERENCES

[1] Pugh D, Karabayas M, Basu N, Cid MC, Goel R, Goodyear CS, et al. Large-vessel vasculitis. Nat Rev Dis Primers 2022;7(1):93.
[2] Alba MA, García-Martínez A, Prieto-González S, Tavera-Bahillo I, Corbera-Bellalta M, Planas-Rigol E, et al. Relapses in patients with giant cell arteritis: prevalence, characteristics, and associated clinical findings in a longitudinally followed cohort of 106 patients. Medicine (Baltimore) 2014;93(5):194–201.
[3] Villiger PM, Adler S, Kuchen S, Wermelinger F, Dan D, Fiege V, et al. Tocilizumab for induction and maintenance of remission in giant cell arteritis: a phase 2, randomised, double-blind, placebo-controlled trial. Lancet 2016;387(10031):1921–7.
[4] Stone JH, Tuckwell K, Dimonaco S, Klearman M, Aringer M, Blockmans D, et al. Trial of tocilizumab in giant-cell arteritis. N Engl J Med 2017;377(4):317–28.
[5] Maz M, Chung SA, Abril A, Langford CA, Gorelik M, Guyatt G, et al. 2021 American College of Rheumatology/Vasculitis Foundation guideline for the management of giant cell arteritis and Takayasu arteritis. Arthritis Rheumatol 2021;73(8):1349–65.
[6] Hellmich B, Agueda A, Monti S, Buttgereit F, de Boysson H, Brouwer E, et al. 2018 Update of the EULAR recommendations for the management of large vessel vasculitis. Ann Rheum Dis 2020;79(1):19–30.
[7] Matza MA, Dagincourt N, Mohan SV, Pavlov A, Han J, Stone JH, et al. Outcomes during and after long-term tocilizumab treatment in patients with giant cell arteritis. RMD Open 2023;9(2):e002923.
[8] Samson M, Dasgupta B, Sammel AM, Salvarani C, Pagnoux C, Hajj-Ali R, et al. Targeting interleukin-6 pathways in giant cell arteritis management: a narrative review of evidence. Autoimmun Rev 2025;24(2):103716.
[9] Stone JH, Han J, Aringer M, Blockmans D, Brouwer E, Cid MC, et al. Long-term effect of tocilizumab in patients with giant cell arteritis: open-label extension phase of the Giant Cell Arteritis Actemra (GiACTA) trial. Lancet Rheumatol 2021;3(5):e328–36.
[10] Cid MC, Campo E, Ercilla G, Palacin A, Vilaseca J, Villalta J, et al. Immunohistochemical analysis of lymphoid and macrophage cell subsets and their immunologic activation markers in temporal arteritis. Influence of corticosteroid treatment. Arthritis Rheum 1989;32(7):884–93.
[11] Weyand CM, Hicok KC, Hunder GG, Goronzy JJ. Tissue cytokine patterns in patients with polymyalgia rheumatica and giant cell arteritis. Ann Intern Med 1994;121(7):484–91.
[12] Corbera-Bellalta M, Planas-Rigol E, Lozano E, Terrades-García N, Alba MA, Prieto-González S, et al. Blocking interferon γ reduces expression of chemokines CXCL9, CXCL10 and CXCL11 and decreases macrophage infiltration in ex vivo cultured arteries from patients with giant cell arteritis. Ann Rheum Dis 2016;75(6):1177–86.
[13] Visvanathan S, Rahman MU, Hoffman GS, Xu S, García-Martínez A, Segarra M, et al. Tissue and serum markers of inflammation during the follow-up of patients with giant-cell arteritis—a prospective longitudinal study. Rheumatology (Oxford) 2011;50(11):2061–70.
[14] Espígol-Frigolé G, Corbera-Bellalta M, Planas-Rigol E, Lozano E, Segarra M, García-Martínez A, et al. Increased IL-17A expression in temporal artery lesions is a predictor of sustained response to glucocorticoid treatment in patients with giant-cell arteritis. Ann Rheum Dis 2013;72(9):1481–7.
[15] Rincon M. Interleukin-6: from an inflammatory marker to a target for inflammatory diseases. Trends Immunol 2012;33(11):571–7.
[16] Murakami M, Kamimura D, Hirano T. Pleiotropy and specificity: insights from the interleukin 6 family of cytokines. Immunity 2019;50(4):812–31.

[17] Garbers C, Heink S, Korn T, Rose-John S. Interleukin-6: designing specific therapeutics for a complex cytokine. Nat Rev Drug Discov 2018;17(6):395–412.
[18] Choy EH, De Benedetti F, Takeuchi T, Hashizume M, John MR, Kishimoto T. Translating IL-6 biology into effective treatments. Nat Rev Rheumatol 2020;16(6):335–45.
[19] Rose-John S, Jenkins BJ, Garbers C, Moll JM, Scheller J. Targeting IL-6 transsignalling: past, present and future prospects. Nat Rev Immunol 2023;23 (10):666–81.
[20] Tamiya T, Kashiwagi I, Takahashi R, Yasukawa H, Yoshimura A. Suppressors of cytokine signaling (SOCS) proteins and JAK/STAT pathways: regulation of T-cell inflammation by SOCS1 and SOCS3. Arterioscler Thromb Vasc Biol 2011;31(5):980–5.
[21] Grebenciucova E, Van Haerents S. Interleukin 6: at the interface of human health and disease. Front Immunol 2023;14:1255533.
[22] Swaroop AK, Negi P, Kar A, Mariappan E, Natarajan J, Namboori P K K, et al. Navigating IL-6: from molecular mechanisms to therapeutic breakthroughs. Cytokine Growth Factor Rev 2024;76:48–76.
[23] Dasgupta B, Panayi GS. Interleukin-6 in serum of patients with polymyalgia rheumatica and giant cell arteritis. Br J Rheumatol 1990;29(6):456–8.
[24] Roche NE, Fulbright JW, Wagner AD, Hunder GG, Goronzy JJ, Weyand CM. Correlation of interleukin-6 production and disease activity in polymyalgia rheumatica and giant cell arteritis. Arthritis Rheum 1993;36(9):1286–94.
[25] Hernández-Rodríguez J, García-Martínez A, Casademont J, Filella X, Esteban MJ, López-Soto A, et al. A strong initial systemic inflammatory response is associated with higher corticosteroid requirements and longer duration of therapy in patients with giant-cell arteritis. Arthritis Rheum 2002;47(1):29–35.
[26] García-Martínez A, Hernández-Rodríguez J, Espígol-Frigolé G, Prieto-González S, Butjosa M, Segarra M, et al. Clinical relevance of persistently elevated circulating cytokines (tumor necrosis factor alpha and interleukin-6) in the long-term followup of patients with giant cell arteritis. Arthritis Care Res (Hoboken) 2010;62(6):835–41.
[27] Wagner AD, Goronzy JJ, Weyand CM. Functional profile of tissue-infiltrating and circulating CD68+ cells in giant cell arteritis. Evidence for two components of the disease. J Clin Invest 1994;94(3):1134–40.
[28] Hernández-Rodríguez J, Segarra M, Vilardell C, Sánchez M, García-Martínez A, Esteban MJ, et al. Tissue production of pro-inflammatory cytokines (IL-1beta, TNFalpha and IL-6) correlates with the intensity of the systemic inflammatory response and with corticosteroid requirements in giant-cell arteritis. Rheumatology (Oxford) 2004;43(3):294–301.
[29] Stone JH, Tuckwell K, Dimonaco S, Klearman M, Aringer M, Blockmans D, et al. Glucocorticoid dosages and acute-phase reactant levels at giant cell arteritis flare in a randomized trial of tocilizumab. Arthritis Rheumatol 2019;71(8):1329–38.
[30] Martín-Gutiérrez A, Loricera J, Narváez J, Aldasoro V, Maiz O, Vela P, et al. Effectiveness of tocilizumab in aortitis and aneurysms associated with giant cell arteritis. Eur J Intern Med 2024;129:78–86.
[31] Muratore F, Marvisi C, Cassone G, Boiardi L, Mancuso P, Besutti G, et al. Treatment of giant cell arteritis with ultra-short glucocorticoids and tocilizumab: the role of imaging in a prospective observational study. Rheumatology (Oxford) 2024;63(1):64–71.
[32] Reichenbach S, Adler S, Bonel H, Cullmann JL, Kuchen S, Bütikofer L, et al. Magnetic resonance angiography in giant cell arteritis: results of a randomized controlled trial of tocilizumab in giant cell arteritis. Rheumatology (Oxford) 2018;57(6):982–6.
[33] Quinn KA, Dashora H, Novakovich E, Ahlman MA, Grayson PC. Use of 18F-fluorodeoxyglucose positron emission tomography to monitor tocilizumab effect on vascular inflammation in giant cell arteritis. Rheumatology (Oxford) 2021;60(9):4384–9.
[34] Schönau V, Roth J, Tascilar K, Corte G, Manger B, Rech J, et al. Resolution of vascular inflammation in patients with new-onset giant cell arteritis: data from the RIGA study. Rheumatology (Oxford) 2021;60(8):3851–61.
[35] Tomelleri A, Campochiaro C, Farina N, Mariotti L, Baldissera E, Grayson PC, et al. Effectiveness of a two-year tapered course of tocilizumab in patients with giant cell arteritis: a single-centre prospective study. Semin Arthritis Rheum 2023;59:152174.
[36] Christ L, Bonel HM, Cullmann JL, Seitz L, Bütikofer L, Wagner F, et al. Magnetic resonance imaging to monitor disease activity in giant cell arteritis treated with ultra-short glucocorticoids and tocilizumab. Rheumatology (Oxford) 2024:keae378. doi: 10.1093/rheumatology/keae378.
[37] Unizony S, Arias-Urdaneta L, Miloslavsky E, Arvikar S, Khosroshahi A, Keroack B, et al. Tocilizumab for the treatment of large-vessel vasculitis (giant cell arteritis, Takayasu arteritis) and polymyalgia rheumatica. Arthritis Care Res (Hoboken) 2012;64(11):1720–9.
[38] Elfishawi M, Kaymakci M, Koster MJ, Warrington KJ. Progression of large-vessel giant cell arteritis despite tocilizumab treatment. Clin Exp Rheumatol 2023;41(4):985–6.
[39] Keser G, Aksu K, Direskeneli H. Discrepancies between vascular and systemic inflammation in large vessel vasculitis: an important problem revisited. Rheumatology (Oxford) 2018;57(5):784–90.
[40] Corbera-Bellalta M, García-Martínez A, Lozano E, Planas-Rigol E, Tavera-Bahillo I, Alba MA, et al. Changes in biomarkers after therapeutic intervention in temporal arteries cultured in Matrigel: a new model for preclinical studies in giant-cell arteritis. Ann Rheum Dis 2014;73(3): 616–23.
[41] Lozano E, Segarra M, García-Martínez A, Hernández-Rodríguez J, Cid MC. Imatinib mesylate inhibits in vitro and ex vivo biological responses related to vascular occlusion in giant cell arteritis. Ann Rheum Dis 2008;67(11):1581–8.
[42] Kleinman HK, Cid MC. Preparation of endothelial cells. Curr Protoc Cell Biol 2001 Chapter 2:Unit 2.3.
[43] Planas-Rigol E, Terrades-Garcia N, Corbera-Bellalta M, Lozano E, Alba MA, Segarra M, et al. Endothelin-1 promotes vascular smooth muscle cell migration across the artery wall: a mechanism contributing to vascular remodelling and intimal hyperplasia in giant-cell arteritis. Ann Rheum Dis 2017;76 (9):1624–34.
[44] Diamant I, Clarke DJB, Evangelista JE, Lingam N, Ma'ayan A. Harmonizome 3.0: integrated knowledge about genes and proteins from diverse multi-omics resources. Nucleic Acids Res 2025;53(D1):D1016–28.
[45] Croci S, Zerbini A, Boiardi L, Muratore F, Bisagni A, Nicoli D, et al. MicroRNA markers of inflammation and remodelling in temporal arteries from patients with giant cell arteritis. Ann Rheum Dis 2016;75(8):1527–33.
[46] Bolha L, Hočevar A, Jurčić V. Current state of epigenetics in giant cell arteritis: focus on microRNA dysregulation. Autoimmun Rev 2025;24(3):103739. doi: 10.1016/j.autrev.2024.103739.
[47] Hasegawa H, Mizoguchi I, Chiba Y, Ohashi M, Xu M, Yoshimoto T. Expanding diversity in molecular structures and functions of the IL-6/IL-12 heterodimeric cytokine family. Front Immunol 2016;7:479.
[48] Zerbini A, Muratore F, Boiardi L, Ciccia F, Bonacini M, Belloni L, et al. Increased expression of interleukin-22 in patients with giant cell arteritis. Rheumatology (Oxford) 2018;57(1):64–72.
[49] Espígol-Frigolé G, Planas-Rigol E, Lozano E, Corbera-Bellalta M, Terrades-García N, Prieto-González S, et al. Expression and function of IL12/23 related cytokine subunits (p35, p40, and p19) in giant-cell arteritis lesions: contribution of p40 to Th1- and Th17-mediated inflammatory pathways. Front Immunol 2018;9:809.
[50] Ramana CV, Kumar A, Enelow R. Stat1-independent induction of SOCS-3 by interferon-gamma is mediated by sustained activation of Stat3 in mouse embryonic fibroblasts. Biochem Biophys Res Commun 2005;327(3):727–33.
[51] Corbera-Bellalta M, Alba-Rovira R, Muralidharan S, Espígol-Frigolé G, Ríos-Garcés R, Marco-Hernández J, et al. Blocking GM-CSF receptor $\alpha$ with mavrilimumab reduces infiltrating cells, pro-inflammatory markers and neoangiogenesis in ex vivo cultured arteries from patients with giant cell arteritis. Ann Rheum Dis 2022;81(4):524–36.
[52] Miyabe C, Miyabe Y, Strle K, Kim ND, Stone JH, Luster AD, et al. An expanded population of pathogenic regulatory T cells in giant cell arteritis is abrogated by IL-6 blockade therapy. Ann Rheum Dis 2017;76 (5):898–905.
[53] Samson M, Greigert H, Ciudad M, Gerard C, Ghesquière T, Trad M, et al. Improvement of Treg immune response after treatment with tocilizumab in giant cell arteritis. Clin Transl Immunology 2021;10(9):e1332.
[54] Yasukawa H, Ohishi M, Mori H, Murakami M, Chinen T, Aki D, et al. IL-6 induces an anti-inflammatory response in the absence of SOCS3 in macrophages. Nat Immunol 2003;4(6):551–6.
[55] Cai T, Zhang Y, Ho YL, Link N, Sun J, Huang J, et al. Association of interleukin 6 receptor variant with cardiovascular disease effects of interleukin 6 receptor blocking therapy: a phenome-wide association study. JAMA Cardiol 2018;3(9):849–57.
[56] Germano DB, Oliveira SB, Bachi ALL, Juliano Y, Novo NF, Bussador do Amaral J, et al. Monocyte chemokine receptors as therapeutic targets in cardiovascular diseases. Immunol Lett 2023;256-257:1–8.
[57] Cid MC, Hoffman MP, Hernández-Rodríguez J, Segarra M, Elkin M, Sánchez M, et al. Association between increased CCL2 (MCP-1) expression in lesions and persistence of disease activity in giant-cell arteritis. Rheumatology (Oxford) 2006;45(11):1356–63.
[58] Regis G, Pensa S, Boselli D, Novelli F, Poli V. Ups and downs: the STAT1:STAT3 seesaw of interferon and gp130 receptor signalling. Semin Cell Dev Biol 2008;19(4):351–9.
[59] Ho HH, Ivashkiv LB. Role of STAT3 in type I interferon responses. Negative regulation of STAT1-dependent inflammatory gene activation. J Biol Chem 2006;281(20):14111–8.
[60] Brack A, Rittner HL, Younge BR, Kaltschmidt C, Weyand CM, Goronzy JJ. Glucocorticoid-mediated repression of cytokine gene transcription in human arteritis-SCID chimeras. J Clin Invest 1997;99(12):2842–50.

Ann Rheum Dis 84 (2025) 1401–1411

Contents lists available at ScienceDirect

Annals of the Rheumatic Diseases

journal homepage: https://www.sciencedirect.com/journal/annals-of-the-rheumatic-diseases

Vasculitis

# A coding single nucleotide polymorphism in the interleukin-6 receptor enhances IL-6 signalling in CD4 T cells and predicts treatment response to tocilizumab in giant cell arteritis

Robert Zorc[1], Christopher Redmond[1], McKella Sylvester[1], Mary Maclean[1], Luciana Yamamoto de Almeida[1], Kaitlin A. Quinn[1], Alessandro Tomelleri[2], Corrado Campochiaro[2], Lorenzo Dagna[2], Fernanda Gutierrez-Rodrigues[3], Kristina V. Wells[1], Cameron Rankin[1], Sabrina Helmold Hait[1], Chloe Palmer[1], Robert Corty[4], Alexander Bick[4], Kathi Lambert[5], Jane H. Buckner[5], John J. O'Shea[1], Jin Kyun Park[1,6], Massimo Gadina[1], Peter C. Grayson[1,*]

[1] *National Institute of Arthritis and Musculoskeletal and Skin Diseases, National Institutes of Health, Bethesda, MD, USA*
[2] *Unit of Immunology, Rheumatology, Allergy and Rare diseases, IRCCS San Raffaele Scientific Institute, Milan, Italy*
[3] *National Heart, Lung, Blood Institute, National Institutes of Health, Bethesda, MD, USA*
[4] *Department of Medicine, Vanderbilt University, Nashville, TN, USA*
[5] *Center for Translational Immunology, Benaroya Research Institute at Virginia Mason, Seattle, WA, USA*
[6] *Division of Rheumatology, Department of Internal Medicine, Seoul National University College of Medicine, Seoul, Korea*

ARTICLE INFO

ABSTRACT

*Objectives:* The study objective was to determine if a common single nucleotide polymorphism in the interleukin 6 (IL-6) receptor (rs2228145, p.Asp358Ala) predicted treatment response to tocilizumab in giant cell arteritis (GCA).

*Methods:* Genetic sequencing of the rs2228145 locus was performed in 2 independent cohorts of patients with GCA. Peripheral blood mononuclear cells (PBMCs) from patients and controls were evaluated for expression of the interleukin 6 receptor (IL-6R) and its coreceptor, gp130, using flow cytometry. The same PBMCs were stimulated with IL-6 and evaluated for downstream targets of IL-6: STAT3 phosphorylation (pSTAT3) and IL-17A expression.

*Results:* In total, 100 patients with GCA were included (derivation cohort n = 58; validation cohort n = 42). The rs2228145 variant predicted tocilizumab response in each cohort. In the derivation cohort, a gene dose-dependent response was observed with a 36% response rate in the homozygous patients and 95% response rate in patients without the variant ($P$ = .003). In the validation cohort, tocilizumab response rates were 50% for homozygotes and 85% for patients without the variant ($P$ = .04). pSTAT3 levels were significantly increased in response to IL-6 stimulation in a gene dose-dependent manner in CD4 T cells from patients with GCA but not controls. CD4 T cells from patients with GCA had significantly higher membrane expression

*Correspondence to Dr. Peter C. Grayson, National Institute of Arthritis and Musculoskeletal and Skin Diseases, National Institutes of Health, Bethesda, MD, USA.
*E-mail address:* peter.grayson@nih.gov (P.C. Grayson).
RZ, CR, and MS contributed equally as first authors.
JKP, MG, and PCG contributed equally as senior authors.
**Handling editor** Josef S. Smolen.

https://doi.org/10.1016/j.ard.2025.01.049

0003-4967/Published by Elsevier B.V. on behalf of European Alliance of Associations for Rheumatology (EULAR).

of gp130 than healthy controls, and response to IL-6 correlated with gp130 expression. IL-17 producing CD4 T cells were increased in a gene dose-dependent response to IL-6 ($P < .01$).
*Conclusions:* The rs2228145 variant is associated with decreased treatment response to tocilizumab and worse outcomes in GCA by enhancing CD4 T cell response to IL-6.

**WHAT IS ALREADY KNOWN ON THIS TOPIC**

- Tocilizumab, a humanised anti-interleukin-6 receptor antibody, is an effective treatment for giant cell arteritis (GCA). A substantial proportion of patients do not achieve sustained remission despite treatment with tocilizumab, and clinical factors do not reliably predict treatment response.

**WHAT THIS STUDY ADDS**

- This study identifies a common genetic polymorphism in the interleukin-6 receptor (rs2228145; p.Asp358Ala) that predicts which patients with GCA are most likely to achieve sustained remission when treated with tocilizumab. Signalling response to interleukin-6 is enhanced in CD4 T cells from patients who carry this polymorphism, and these patients are more susceptible to vascular damage. Greater inhibition of the interleukin-6 signalling pathway or alternate treatment approaches in this subset of patients may be needed to establish clinical remission.

**HOW THIS STUDY MIGHT AFFECT RESEARCH, PRACTICE OR POLICY**

- The rs2228145 (p.Asp358Ala) polymorphism is a genetic biomarker may enable precision medicine approaches to treatment in GCA.

## INTRODUCTION

Despite the pivotal role of interleukin-6 (IL-6) in the pathogenesis of giant cell arteritis (GCA), a significant number of patients with GCA do not achieve sustained clinical remission on tocilizumab, a monoclonal antibody directed against the IL-6 receptor (IL-6R) [1,2]. Two randomised controlled trials demonstrated that tocilizumab is effective in GCA to induce and sustain clinical remission [3,4]. However, approximately 20% to 30% of GCA patients in the therapeutic trials and in subsequent observational cohort studies do not achieve sustained clinical remission despite treatment with tocilizumab [5,6]. The data to support alternative steroid sparing options beyond tocilizumab are very limited [7−11], and the few clinical factors that predict treatment response to tocilizumab in GCA have not been validated [12]. Identification of reliable biomarkers that accurately predict clinical response to tocilizumab in GCA and elucidate the mechanisms which underlie treatment failure may advance the development of more precise and comprehensive management strategies and prevent life-threatening complications in one of the most common forms of systemic vasculitis.

A single nucleotide polymorphism in the *IL-6R*, p.Asp358Ala (rs2228145A>C), can affect leukocyte response to IL-6 [13]. This polymorphism, which is prevalent in 30% to 40% of general population [14], renders the membrane-bound IL-6R more susceptible to cleavage by proteases, resulting in increased levels of the soluble form of the IL-6R (sIL-6R) [15]. In classical IL-6 signalling, IL-6 binds membrane-bound IL-6R at the cell surface and forms a complex with gp130 to initiate downstream signalling [16,17]. By promoting cleavage of the IL-6R on leukocytes and hepatocytes, the primary cells where the IL-6R is expressed, the rs2228145 variant can reduce IL-6 classical signalling. In line with this observation, several genetic association studies have shown this polymorphism is protective against the development of certain diseases, including rheumatoid arthritis, inflammatory bowel disease, and atherosclerosis [18−20].

Classical signalling, however, is not the only way in which IL-6 functions. IL-6 trans-signalling occurs when sIL-6R binds circulating IL-6 and the resultant IL-6/IL-6R complex directly engages any cell with a gp130 receptor, which is ubiquitously present on immune and non-immune cells [21]. Compared to classical signalling, trans-signalling contributes more towards inflammatory responses by enhancing the downstream effects of IL-6 signalling on a wider array of cells and promotes chronic inflammation through multiple mechanisms, including activation of the Janus kinase (JAK)−signal transducer and the activator of the transcription (STAT) pathway and differentiation of IL-17 producing T helper cells [22,23].

Although the rs2228145 variant may be protective against the development of specific diseases by reducing IL-6 classical signalling, in diseases where IL-6 is chronically and substantially elevated, the same polymorphism may be associated with worse clinical outcomes via promotion of increased IL-6 trans-signalling. The aim of this study was to determine if the rs2228145 variant is associated with treatment response to tocilizumab and other clinical features in patients with GCA, a disease strongly mediated by IL-6, and to understand the mechanisms that may underlie any clinical associations.

## METHODS

### *Study population*

Patients with GCA who fulfilled the 2022 American College of Rheumatology (ACR)/European League Against Rheumatism (EULAR) Classification Criteria for GCA were recruited into the study [24,25]. Data from 2 independent cohorts were included. A derivation cohort was comprised of patients with GCA enrolled in an ongoing observational cohort study at the National Institutes of Health (NIH). All patients provided written informed consent, and the study was approved by the local institutional review board (#14-AR-0200). A validation cohort was recruited from Milan, Italy within a single arm prospective therapeutic trial in which all study participants with GCA received tocilizumab per treatment protocol. Healthy controls were recruited from the NIH healthy volunteer programme and from a genotyped database at the Benaroya Institute. Patients with Takayasu arteritis (TAK) who fulfilled the 2022 ACR/EULAR Classification Criteria for this disease were also recruited from the NIH cohort as comparator patients.

### *Clinical assessments*

A standardised set of clinical variables was recorded at the study enrolment visit in the derivation and validation cohorts. Clinical remission was defined as the absence of any clinical features attributable to active vasculitis in the judgement of the treating physician. Treatment response to tocilizumab was

defined as achieving and sustaining clinical remission on ≤5 mg daily prednisone for the duration of tocilizumab therapy under observation without the need to increase glucocorticoids or add additional steroid sparing therapies once remission was achieved. Patients who did not meet the definition of treatment response were considered treatment failures. Large vessel involvement was defined as luminal damage (stenosis, occlusion, or aneurysm) in the aorta or a primary arterial branch.

### *IL-6R genotyping*

In the derivation cohort, genomic DNA from peripheral blood was screened for the *IL-6R* p.Asp358Ala (rs2228145A>C) polymorphism using a customised targeted panel (Variant Plex, Archard) as previously described [26,27]. In the validation cohort, rs2228145 genotyping was performed with the TaqMan SNP Genotyping Assay. Custom primers were designed using NCBI BLAST for a region of interest in the *IL-6R* gene. Patients were either homozygous (CC), heterozygous (AC), or wild type (AA) for the rs2228145 polymorphism.

### *UK Biobank analysis*

To determine if the rs2228145 variant was a risk factor for the development of GCA, genetic data from the UK Biobank, a large-scale biomedical database, were used to study patients with GCA and controls. Patients with GCA were identified in the UK Biobank by presence of 2 or more occurrences of ICD10 codes M31.5 or M31.6. Genotype calls were extracted at rs2228145 using plink1.9. We conducted generalised linear regression analysis using in R 4.2.3 using package {stats} version 4.2.3 after data preparation with {tidy verse} version 2.0.0. We modelled case-control status as a binary outcome and modelled genetic effects as additive, specifically with values of 0, 1, and 2 for participants homozygous for A, heterozygous, and homozygous for C, respectively. For sensitivity analysis, we also trialled a model with both additive and dominance effects, with the additive design matrix as before and additionally with a dominance design matrix where participants with the homozygous A, heterozygous, and homozygous C genotypes were assigned values of 0, 1, and 0, respectively. Covariates in the regression analysis included age at recruitment, the square of the age at recruitment, reported sex, and the first 5 principal components of genetic ancestry.

### *Enzyme-linked immunosorbent assay studies*

Serum was prepared by centrifugation of whole blood collected from patients at routine visits. The supernatant was collected and analysed for circulating cytokine levels. IL-6 as well as its soluble receptors glycoprotein 130 (sgp130) and interleukin-6 receptor subunit alpha (sIL-6R) were analysed using commercially available immunoassay kits per the manufacturer's guidelines (R&D systems Inc).

### *Cell isolation and phospho-STAT measurement*

Peripheral blood mononuclear cells (PBMCs) from patients were isolated using Ficoll separation and Leukosep tubes. Cells were collected and stored in liquid nitrogen at −150°C until ready for use. To assess how rs2228145 affects downstream intracellular signalling, we measured *in vitro* STAT3 phosphorylation. Frozen PBMCs from patients and healthy donors were thawed in complete Roswell Park Memorial Institute (RPMI) and stained with eBioscience Fixable Viability Dye and surface markers (CD3, CD8a, CD19, CD14) for 30 minutes. Cells were then rested for 30 minutes in plain RPMI at room temperature (RT), followed by 15-minute cytokine stimulation at 37°C (100 ng/mL IL-6; 1 $\mu$g/mL hyper-IL-6). Cells were then fixed with 3% formaldehyde for 10 minutes at RT and permeabilised with ice cold Phosflow Perm Buffer III (87.7% methanol) (BD cat #558052) for 30 minutes (4°C). Cells were stained for intracellular phospho-STAT proteins (pSTAT1 Tyr 701; pSTAT3 Tyr705) as well as membrane-bound proteins (CD4, gp130, IL-6R (CD126)) overnight (18 hours) before analysis by flow cytometry (FACSymphony A5).

For CD4 T cell subset analysis in a randomly chosen subset of patients, frozen PBMCs were thawed in complete RPMI, washed with phosphate-buffered saline (PBS), and stained with eBioscience Fixable Viability Dye (LIVE/DEAD Blue) for 15 minutes at RT. Staining for surface makers was performed sequentially, with staining for CCR7 following viability staining for 10 minutes at 37°C with BioLegend Human TruStain FcX Fc receptor blocking solution. Next, antibodies for membrane-bound proteins CD3, CD8a, CD19, CD14, and IL-6R (CD126) were added with BD Brilliant Violet Buffer and incubated for 30 minutes at RT. Cells were washed with plain RPMI followed by stimulation with 100 ng/mL IL-6 for 15 minutes at 37°C. Cells were then fixed with 3% formaldehyde for 10 minutes at RT and permeabilised with ice cold BD Phosflow Perm Buffer III (87.7% methanol) (BD cat #558052) for 30 minutes (4°C). Cells were stained for intracellular phospho-STAT proteins (pSTAT1 Tyr701; pSTAT3 Tyr705) and membrane-bound proteins CD4, CD45RA, and gp130 overnight (18 hours) before analysis by flow cytometry (Cytek Aurora 5L UV-V-B-YG-R). CD4 T cells were defined as naïve (CDR45RA+ CCR7+), central memory (CD45RA- CCR7+), effector memory (CD45RA- CCR7-), and terminal effector memory (TEMRA, CD45RA+ CCR7-) populations (see gating strategy in Supplementary Fig S1). Fluorescence minus one controls were prepared for IL-6R and gp130 to define cell positivity.

### *Cell stimulation experiments*

Cells were thawed and rested for 12 to 16 hours at 37°C in media (X-Vivo 15). A 96-well flat bottom plate was coated with CD3 (5 $\mu$/mL) for 12 to 24 hours at 4°C and then warmed for 60 minutes prior to cell transfer. The cells were transferred to the CD3-coated 96-well flat bottom plate with increasing concentrations of IL-6 (0 ng/mL to 50 ng/mL). Costimulatory molecules [anti-CD28 (10 $\mu$g/mL), and TGF-$\beta$ (5 ng/mL)] and inhibitory antibodies [α-IFNγ (20 $\mu$g/mL) and α-IL4 (20 $\mu$g/mL)] were used to optimise IL-17 response. Cells were incubated for 72 hours and then restimulated with phorbol myristate acetate (PMA) (20 ng/mL), ionomycin (1 mM), and brefeldin (10 $\mu$g/mL) for 4 to 6 hours. Following restimulation, cells were washed with fluorescence-activated cell sorting (FACS buffer [PBS with 1% bovine serum albumin and sodium azide]). Viability stain was added (Live/DEAD) and cells were incubated for 30 minutes at RT. Cells were washed twice in 100 $\mu$L of FACS buffer, with centrifugation at 771 × *g* for 2 minutes for each wash, and fixed and permeabilised with FoxP3 fixation/permeabilisation kit (Invitrogen) at RT for 45 minutes. The samples were then washed twice in the FOXP3 Perm wash buffer (Invitrogen) and intracellular/intranuclear stain was added and incubated for 12 hours at 4°C. The samples were washed twice with FACS buffer and analysed by flow cytometry (FACSAurora 5). The cells were gated for singlets, then live T cells (viability negative,

CD3+). Subsequent T cell populations CD4 (CD4+CD8-) and CD8 (CD8+CD4-). Memory T cells were defined by CD45RO expression. Th17 cells were defined primarily by IL-17 expression (see gating strategy in Supplementary Fig S2).

### *Statistical analysis*

Categorical variables were compared between groups using Fisher exact test. Continuous variables were compared between groups using Mann–Whitney test or Kruskal–Wallis test as appropriate. Spearman correlations were used, as applicable. Logistic regression was performed to identify clinical factors associated with treatment response to tocilizumab. All analyses were performed using GraphPad Prism (GraphPad Software Inc) or SPSS Statistics software (v.27.0 IBM Corp, Armonk) and considered statistically significant at $P < .05$. For the functional studies, samples from patients with GCA were matched by genotype for age, sex, disease activity, and treatment status. No patients were treatment naïve at the time of sampling.

## RESULTS

### *Patient characteristics*

One hundred patients with GCA were included in the study, including 58 patients in the derivation cohort and 42 patients in the validation cohort. Baseline characteristics for both cohorts are summarised in Table 1. Patients in the derivation cohort were younger (70 vs 73 years, $P < .01$) with longer disease duration (14.8 versus 10.5 months, $P = .04$) and a higher relapse rate (62% versus 24%, $P < .01$). C-reactive protein (CRP) levels at diagnosis were lower in the derivation cohort compared to the validation cohort (44 [16-105] vs 80 [42-106] mg/L, $P = .04$). Tocilizumab was administered to 64% of the patients in the derivation cohort for a median of 761 days (IQR, 592-921) and 100% patients in the validation cohort for a median of 669 days (IQR, 316-854). In the derivation cohort, 31 of 37 patients received weekly 162 mg subcutaneous tocilizumab. Intravenous dosing was used in 2 patients, and every other week subcutaneous dosing was used in 4 patients. In the derivation cohort, each patient received subcutaneous tocilizumab 162 mg weekly for the first year of treatment with subsequent dose reduction to every other week. Both cohorts demonstrated similar response rates to tocilizumab (78% vs 81%, $P = .79$). All patients in clinical remission tapered completely off glucocorticoids, except 3 patients in the derivation cohort who remained on 5 mg daily prednisone throughout the study period. No patient experienced a significant side effect leading to discontinuation of tocilizumab, including diverticulitis or major infections.

Table 1
**Clinical characteristics of the derivation and validation cohorts**

| Item | Derivation cohort (N = 58) | Validation cohort (n = 42) | *P* value |
|---|---|---|---|
| Age at diagnosis (y, IQR) | 70 (62-75) | 73 (68-79) | <.01 |
| Female sex | 42 (72%) | 30 (71%) | .91 |
| Disease duration (mo, IQR) | 14.8 (6-34) | 10.5 (3-18) | .04 |
| White | 51 (88%) | 42 (100%) | .07 |
| Cranial symptoms | 42 (72%) | 37 (88%) | .08 |
| Ischaemic retinopathy | 5 (9%) | 7 (17%) | .35 |
| Polymyalgia rheumatica | 26 (45%) | 18 (43%) | 1.00 |
| Large vessel GCA[a] | 32 (55%) | 11/20 (55%) | .99 |
| TAB performed | 44 (76%) | 7 (14%) | <.01 |
| TAB positive | 32/45 (71%) | 6/7 (86%) | .66 |
| CRP at diagnosis (mg/L, IQR) | 44 (16-105) | 80 (42-106) | .04 |
| Treated with tocilizumab | 37 (64%) | 42 (100%) | <.01 |
| Tocilizumab response | 29/37 (78%) | 34/42 (81%) | .79 |
| History of relapse | 36 (62%) | 10 (24%) | <.01 |

CRP, C-reactive protein; GCA, giant cell arteritis; TAB, temporal artery biopsy.
[a] Large vessel GCA defined by luminal damage to aorta or branch artery.

The distribution of patients homozygous for the p.Asp358Ala variant was similar in both cohorts (17% versus 19%); however, there were significantly more wild type patients (59% vs 31%) and fewer heterozygous patients (24% vs 50%) in the derivation cohort compared to the validation cohort ($P = .01$) (Fig 1A; Supplementary Tables S1 and S2).

### *Association of IL-6R polymorphism and clinical response to tocilizumab*

Treatment response to tocilizumab differed significantly according to rs2228145 variant status in each cohort (Fig 1B). In the derivation cohort, a gene dose-dependent response was observed with a 33% response rate in the homozygous GCA patients, a 67% response in heterozygous patients, and a response rate of 95% in the wild type patients ($P = .003$). In the validation cohort, tocilizumab response rates were 50% for homozygotes and 85% for wild type patients ($P = .04$), but a gene dose response was not observed due to a 90% response rate in the heterozygous patients. Time to tocilizumab failure differed significantly by variant in the combined cohorts ($P < .0001$) (Fig 1C) and in each independent cohort (Supplementary Fig S3). For comparison, an association of rs2228145 variant status and clinical response to tocilizumab was not observed in 16 patients with TAK (33% response in heterozygous/homozygous vs 57% response in wild type, $P = .61$).

Given the modest sample size in each GCA cohort, additional clinical factors associated with tocilizumab response or failure were studied in the combined cohorts. Clinical characteristics by IL-6R variant status significantly differed in terms of prevalence of ischaemic retinopathy (homozygous 0%, heterozygous 26%, wild type 6%, $P < .01$) and damage to the large arteries of the aorta and its primary branches (homozygous 75%, heterozygous 29%, wild type 45%, $P = .03$) (Table 2).

IL-6R polymorphism status (odds ratio [OR], 4.98 [1.30-19.06]; $P = .02$) and female sex (OR, 7.62; [0.94-61.56]; $P = .06$) were most strongly associated with tocilizumab treatment failure on univariable logistic regression analyses. Factors such as age at diagnosis, large vessel involvement, cranial symptoms, history of relapse, concurrent polymyalgia rheumatica, and CRP levels were not associated with tocilizumab failure. Multivariable logistic regression analysis, adjusting for sex, confirmed that rs2228145 variant status was the sole factor significantly associated with tocilizumab response (Fig 1D, Supplementary Table S3).

### *IL-6R polymorphism status and risk for GCA in UK Biobank*

To investigate whether the IL-6R SNP is both a diagnostic and prognostic risk factor for GCA, we assessed the incidence of this SNP among 1217 GCA patients identified in the UK Biobank with available genotype data, including 376 (30.9%) who had concurrent polymyalgia rheumatica. Additive and additive + dominant logistic regression models adjusted for age, sex, and 5 principal components of genetic ancestry, demonstrated that variant status was not associated with a diagnosis of GCA, confirming that the rs2228145 variant is not a risk factor for the development of GCA but rather a prognostic risk

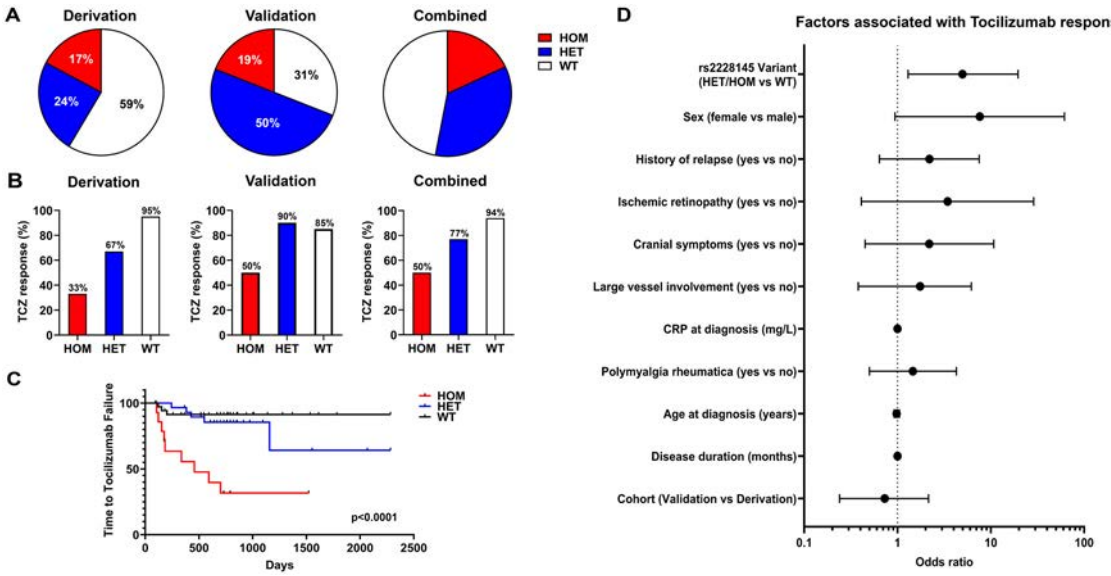



**Figure 1.** Treatment response to tocilizumab by IL-6R Asp358Ala variant status. (A) Distribution of variant status in the derivation, validation, and combined cohorts. (B) Tocilizumab (TCZ) response by IL-6R variant status in the derivation, validation, and combined cohorts. (C) Time to tocilizumab failure was compared between the variants. Survival curves were compared using log rank test. (D) Odds ratio (OR) and 95% confidence intervals of factors for TCZ response were examined using univariable logistic regression analyses in the combined cohort. CRP, C-reactive protein; HET, heterozygous; HOM, homozygous; IL-6R, interleukin 6 receptor; WT, wild type.

factor for treatment response in patients with established disease (Supplementary Table S4).

### *T cell responses upon IL-6 stimulation by IL-6R polymorphism status*

To assess the impact of the rs2228145 polymorphism on IL-6 signalling in GCA patients, PBMCs from patients with GCA were stimulated with IL-6 or hyper-IL-6, which directly binds gp130 [28] and activates downstream signalling. Only CD4 T cells displayed differential pSTAT3 levels by rs2228145 status in response to IL-6 or hyper-IL-6 stimulation (Fig 2). CD4 T cells, but not CD8 T cells, from GCA patients with the homozygous variant exhibited higher pSTAT3 levels than those from heterozygous and wild type patients with GCA, in response to IL-6 or hyper-IL-6 (Fig 3A-C). pSTAT3 levels in CD4 T cells did not vary by variant status in healthy controls or in patients with TAK in response to IL-6 or hyper-IL-6 stimulation (Fig 3B). Differences in pSTAT1 levels were not observed by variant status in GCA in these same experiments (Supplementary Fig S4). With either IL-6 or hyper-IL-6 stimulation, pSTAT3 levels in CD4 T cells from patients with GCA correlated with gp130 expression levels (IL-6: $r = 0.22$, $P = .02$, hyper-IL-6: $r = 0.28$, $P = .007$) but not with IL-6R expression levels (Fig 3D). A similar correlation with gp130 expression was not observed in CD4 T cells from healthy controls or TAK (Fig 3D). IL-6R correlation between pSTAT3 levels and gp130 expression levels was not observed in CD8 T cells from patients with GCA, TAK, or controls (Fig 3E). These results suggest that differences in pSTAT3 signalling by rs2228145 status in patients with GCA were mediated by IL-6 or hyper-IL-6 stimulation through surface gp130 expression in CD4 T cells via trans-signalling. Among T cells, naïve and central effector CD4 T cells displayed the most robust pSTAT3 response to IL-6 stimulation, although there was no difference in abundance of naïve, central effector, central memory, or TEMRA among patients with GCA by rs2228145 status (Supplementary Fig S5).

Table 2
**Clinical characteristics by variant status in the combined cohort**

| Variables | Homozygous N = 18 | Heterozygous N = 35 | Wild type N = 47 | *P* value |
|---|---|---|---|---|
| Age at diagnosis (y, IQR) | 69.5 (59-76.5) | 73 (67-78) | 70 (62-76) | .16 |
| Female sex | 14 (78%) | 27 (77%) | 31 (66%) | .44 |
| Disease duration (mo, IQR) | 19 (10-34) | 8 (5-18) | 13 (6-27) | .07 |
| White | 18 (100%) | 35 (100%) | 40 (85%) | .01 |
| Cranial symptoms | 13 (72%) | 31 (89%) | 35 (74%) | .22 |
| Ischaemic retinopathy | 0 (0%) | 9 (26%) | 3 (6%) | <.01 |
| Large vessel GCA[a] | 9 (75%) | 7 (29%) | 19 (45%) | .03 |
| Polymyalgia rheumatica | 6 (33%) | 17 (49%) | 21 (45%) | .56 |
| CRP at diagnosis (mg/L, IQR) | 44 (14-186) | 72 (35-104) | 55 (33-110) | .58 |
| TAB performed | 7 (39%) | 14 (40%) | 29 (62%) | .09 |
| TAB positive | 7 (100%) | 12 (86%) | 19 (66%) | .10 |
| Treated with tocilizumab | 14 (78%) | 30 (86%) | 35 (75%) | .46 |
| History of relapse | 13 (72%) | 21 (60%) | 20 (43%) | .07 |

CRP, C-reactive protein; GCA, giant cell arteritis; TAB, temporal artery biopsy.
[a] Large vessel GCA defined by luminal damage to aorta or branch artery.

### *IL-6 and IL-6R expression by IL-6R polymorphism status*

To verify, as previously reported [1], that patients with GCA have increased levels of circulating IL-6, we measured serum levels of the cytokine by enzyme-linked immunosorbent assay. As expected, IL-6 levels were significantly higher in patients with GCA compared to healthy controls (Fig 4A); however, we did not observe any difference in IL-6 levels by variant status within patients with GCA. Although sIL-6R levels were comparable between GCA and healthy controls, they were significantly higher in homozygotes compared to wild type within patients with GCA (Fig 4B). Soluble gp130 levels did not differ between GCA and healthy controls, and there were no differences by

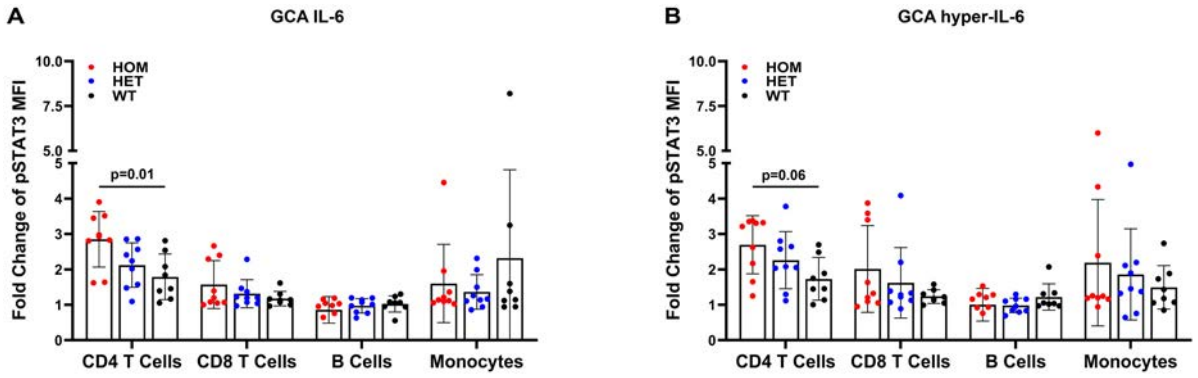



**Figure 2.** Signalling response to IL-6 stimulation in different cell populations. Peripheral blood mononuclear cells obtained from patients with giant cell arteritis (GCA - HOM: n = 9; HET: n = 9; WT: n = 8) were stimulated with IL-6 (100 ng/mL) (A) or Hyper-IL-6 (1 μg/mL) (B) for 15 minutes and phosphor STAT3 levels were measured by flow cytometry. Significant differential expression by variant status was only observed for CD4 T cells. *P* values were calculated using the Kruskal–Wallis test. HET, heterozygous (blue); HOM, homozygous (red); IL-6, interleukin 6; MFI, mean fluorescence intensity; pSTAT3, STAT3 phosphorylation; WT, wild type (black).

variant status (Fig 4C). In CD4 T cells from patients with GCA, membrane expression of gp130 was greatest in patients who were homozygous for rs2228145 variant compared to wild type (Fig 4D) and the inverse was observed for membrane expression of IL-6R (Fig 4E).

### *CD4 T cell production of IL-17A in association with IL-6R polymorphisms*

Given the role of IL-6 in the differentiation of T helper (Th) 17 cells [29], cytokine production by CD4 T cells was also

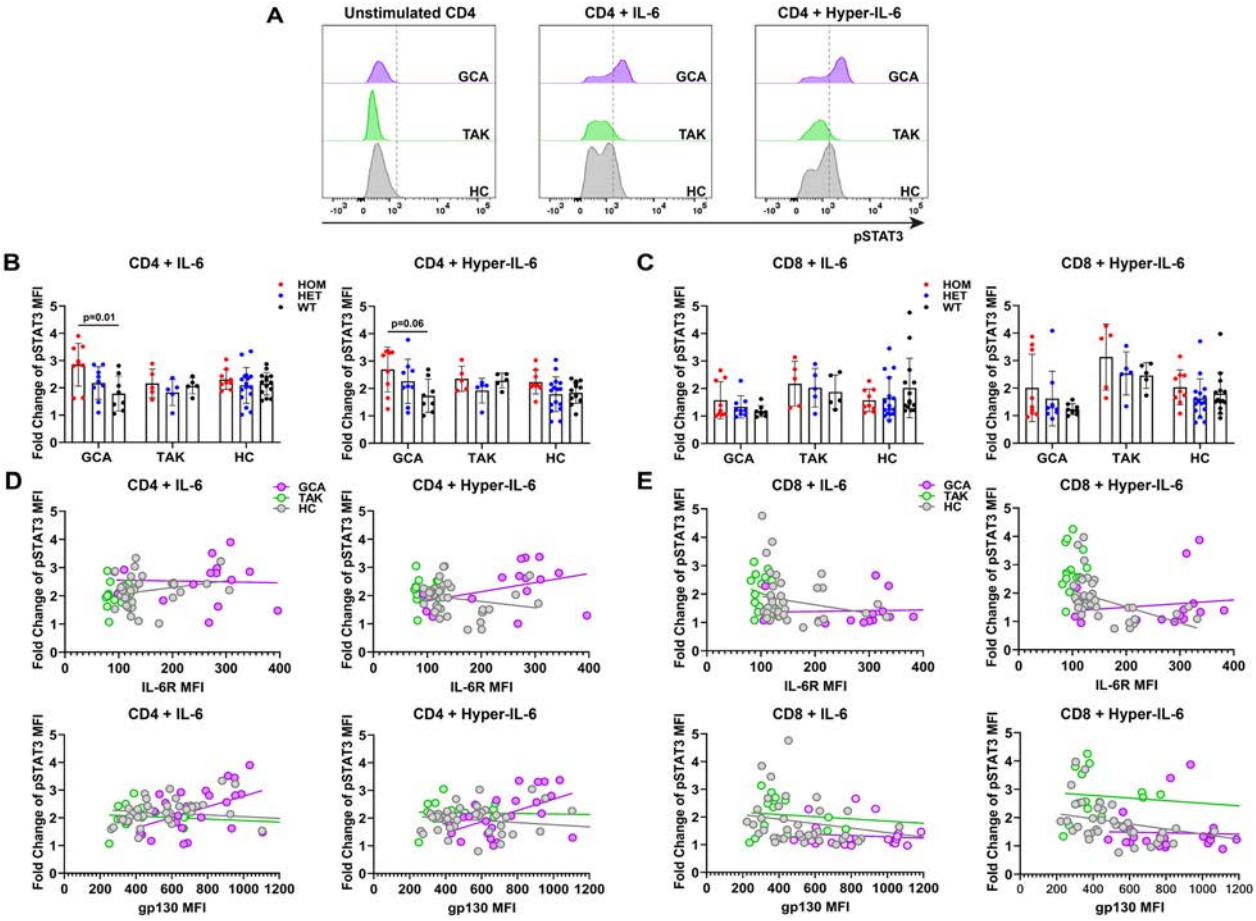



**Figure 3.** Asp358Ala variant is associated with STAT3 phosphorylation in GCA. T cells were stimulated with IL-6 (100 ng/mL) or Hyper-IL-6 (1 μg/mL) for 15 min and phosphor STAT3 levels were measured. Representative flow cytometry plots of the fold change in the pSTAT3 levels in response to IL-6R and Hyper-IL-6 in GCA, TAK, and healthy control CD4 T cells were depicted (A). Fold change in the pSTAT3 levels after stimulation with IL-6 and Hyper-IL-6 in CD4 T cells (B) and CD8 T cells (C) were compared within each group by the variant status (GCA - HOM: n = 9; HET: n = 9; WT: n = 8 / TAK - HOM: n = 5; HET: n = 5; WT: n = 5 / HC - HOM: n = 9; HET: n = 16; WT: n = 14) using the Kruskal–Wallis test. The correlation between the membrane expression of IL-6R and gp130 and fold change of pSTAT3 MFI in GCA,TAK, and healthy CD4 T cells (D) and CD8 T cells (E) were examined after stimulation with IL-6 and Hyper-IL-6 (GCA: n = 26/ TAK: n = 15 / HC: n = 39). Bar represents mean ± SD. GCA, giant cell arteritis; HC, healthy control; HET, heterozygous (blue); IL-6, interleukin 6; IL-6R, interleukin 6 receptor; MFI, mean fluorescence intensity; pSTAT3, STAT3 phosphorylation; TAK, Takayasu arteritis; WT, wild type (black).

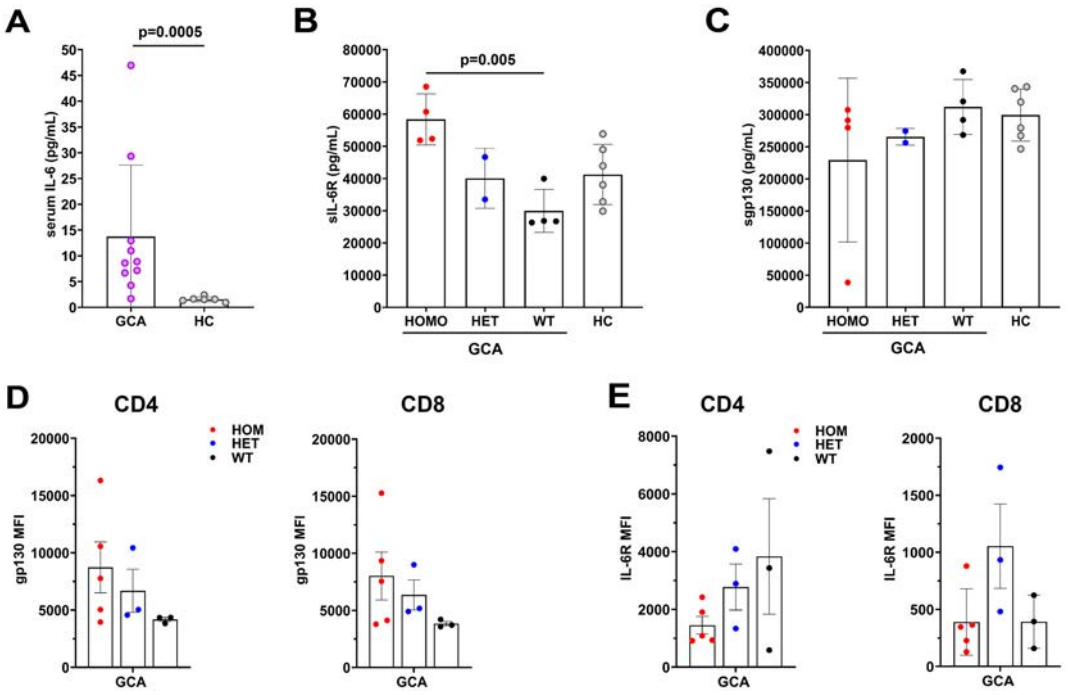



**Figure 4.** IL-6, IL-6R, and sgp130 expression by IL-6R Asp358Ala variant status. Serum levels of IL-6 (A), soluble IL-6R (sIL-6R) (B), and soluble gp130 (sgp130) (C) were measured in GCA patients (HOM: n = 4; HET: n = 2; WT: n = 4; total n = 10) and healthy controls. gp130 expression (D) and IL-6R expression (E) on GCA CD4 and CD8 T cells were assessed (HOM: n = 5; HET: n = 3; WT: n = 3). Groups were compared using the Mann–Whitney test for (A) and the Kruskal–Wallis test for (B, C). Bar represents mean ± SD. GCA, giant cell arteritis; HC, healthy controls; HOM, homozygous (red); HET, heterozygous (blue); IL-6, interleukin 6; IL-6R, interleukin 6 receptor; WT, wild type (black).

assessed by intracellular staining, particularly IL-17A production (Supplementary Fig S6). At baseline (day 0), there were no differences in the frequencies of CD4+ T cells producing IFN-$\gamma$ (Th1), IL-4 (Th2), and IL-17 (Th17) according to rs2228145 status (Fig 5A). However, following 3 days of *in vitro* CD3/CD28 bead activation and IL-6 stimulation, the frequency of IL-17 producing CD4+ T cells was significantly higher in homozygous rs2228145 patients with GCA (Fig 5B).

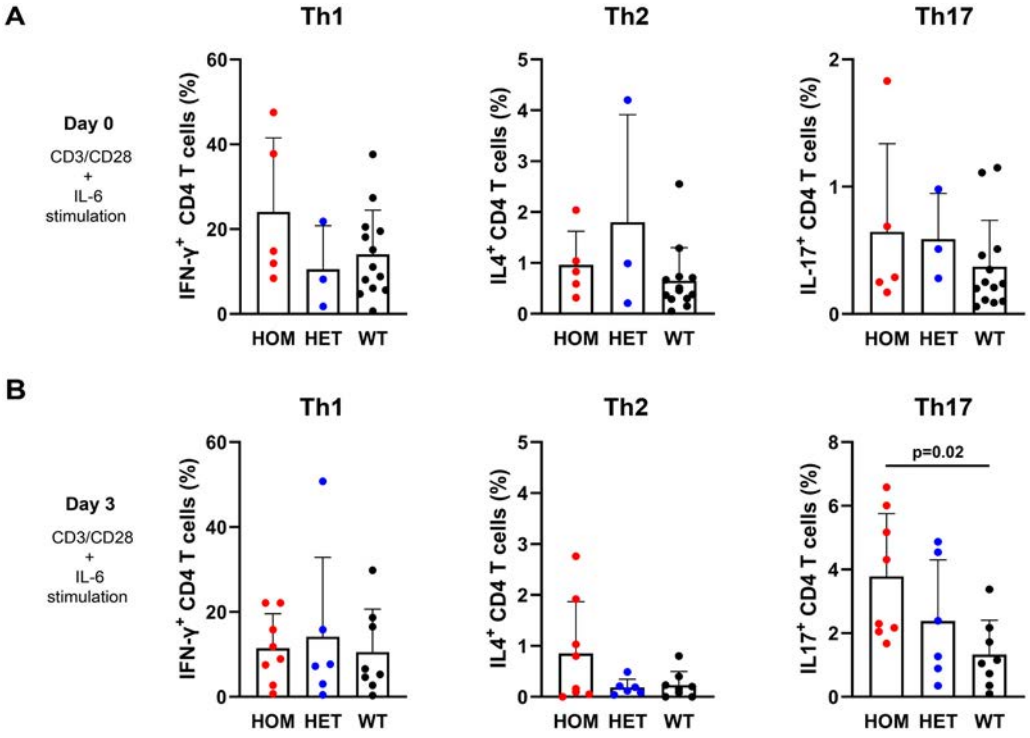



**Figure 5.** Generation of IL-17 producing T cells in GCA stratified by the IL-6R Asp358Ala variant. Frequencies of IFN-$\gamma$ (Th1), IL-4 (Th2), and IL-17 (Th17) producing CD4 T cells between the variants were assessed at baseline (Day 0) (A – HOM: n = 5; HET: n = 3; WT: n = 13) and following 3 days of activation with CD3/CD28 beads and stimulation with IL-6 (B - HOM: n = 8; HET: n = 6; WT: n = 8). Groups were compared using the Kruskal–Wallis test. Bar represents mean ± SD. HC, healthy controls; HET, heterozygous (blue); HOM, homozygous (red); IL-6, interleukin 6; IL-6R, interleukin 6 receptor; WT, wild type (black).

## DISCUSSION

We report that a common genetic polymorphism in the *IL-6R* is associated with altered CD4 T cell responses to IL-6 and predicts clinical response to tocilizumab among patients with GCA. We validated this clinical association in 2 independent cohorts from North America and Europe. Patients with GCA who are homozygous for the rs2228145 variant are less likely to achieve sustained clinical remission on tocilizumab and are more likely to have vascular complications, including damage to the aorta and branch arteries. Further, CD4 T cells from patients with GCA, but not healthy comparators or patients with TAK, display enhanced response to IL-6 stimulation in association with rs2228145 variant status. These findings provide insight into the mechanisms that underpin the variability of clinical response to tocilizumab in GCA and may inform future precision medicine strategies to disease management.

Selecting effective steroid sparing therapy is a major unmet need in GCA to minimise glucocorticoid-related complications and improve clinical outcomes. To date, no clinical or genetic biomarkers have been identified that predict treatment response to tocilizumab in GCA. In this study, treatment response to tocilizumab was observed in 76% of the derivation cohort and 81% of the validation cohort, which is in line with response rates reported in prior randomised clinical trials [3,4]. In the derivation cohort, we demonstrate a gene dose-dependent response rate to tocilizumab by variant status, with the lowest response rates seen in patients who are homozygous for the rs2228145 variant. In the validation cohort, we confirm similar reduced response rates to tocilizumab among homozygotes. There were, however, differences in the frequency of patients who were heterozygous for the rs2228145 variant in the derivation versus validation cohort, and we did not observe similar reduced response rates among heterozygotes in the validation compared to the derivation cohort. Whether patients who are heterozygous for the rs2228145 polymorphism are truly at increased risk for tocilizumab failure will need to be studied further at larger sample sizes. Despite differences in patient selection and clinical management between the cohorts which may have contributed to selection bias, we were able to validate rs2228145 polymorphism as a predictive genetic biomarker of treatment response, even at modest sample sizes, highlighting that this association is robust for patients who are homozygous for the rs2228145 polymorphism. Strikingly, we show that time to tocilizumab failure was also associated with variant status in a gene dose-dependent relationship. Previous gene-association studies have focused primarily on the identification of genetic risk factors to develop GCA [30]. Importantly, we show that the rs2228145 variant is a prognostic biomarker and not a diagnostic risk factor for GCA.

In addition to incomplete treatment response to tocilizumab, patients with GCA with the rs2228145 variant had a higher prevalence of vascular complications, evidenced by the higher proportion of damage to the large arteries of the aorta and its primary branches. Additionally, there was a statistical association with variant status and risk for ischaemic retinopathy, although this was only observed in patients who were heterozygous for the rs2228145 polymorphism. These findings align with previous reports that GCA patients with involvement of the large arteries are at increased risk for treatment refractory disease and clinical relapse [31−33]. IL-6 classical signalling occurs through the membrane-bound IL-6R, which is expressed primarily by hepatocytes and leukocytes [34]. Trans-signalling of IL-6 occurs when sIL-6R binds IL-6 in circulation and subsequently engages membrane gp130, thereby potentiating the effect of IL-6 on a wider array of cells, including vascular endothelial cells which otherwise do not express membrane-bound IL-6R. The clinical association of vascular complications and the rs22228145 polymorphism may therefore be mediated in part by the known effect of the variant to promote shedding of the membrane IL-6R into its soluble form and promote trans-signalling in endothelial cells and stromal cells within the vascular wall.

These data provide mechanistic rationale to test a set of specific medications in future therapeutic trials in GCA. Although patients with GCA who were homozygous for the rs2228145 variant were less likely to achieve sustained clinical remission on tocilizumab, these patients often had at least partial response to this medication. Future studies to investigate the clinical effect of dose-dependent IL-6 blockade using tocilizumab or to investigate the clinical utility of selective inhibition of IL-6 trans-signalling (eg, olamkicept [35]) are warranted in patients with GCA stratified by rs2228145 variant status. In addition, these data provide supporting rationale to test the clinical utility of JAK inhibitors in GCA, which block factors downstream of IL-6 signalling, and to test blockade of the IL-17 pathway, since increased abundance of IL-17 producing CD4 T cells was observed in response to IL-6 stimulation in association with rs2228145 variant status. Accordingly, cohort studies and early phase therapeutic trials have demonstrated that both JAK inhibitors and secukinumab, a monoclonal antibody against IL-17A, may be effective in GCA [36−39].

In previous reports, the rs2228145 variant has been considered anti-inflammatory and protective against certain conditions. Healthy individuals with this variant exhibit lower levels of CRP and fibrinogen and are less susceptible to several inflammatory conditions, including rheumatoid arthritis, inflammatory bowel disease, and atherosclerosis [13,18,40]. In contrast, the same variant was also associated with worse disease activity and treatment response in rheumatoid arthritis [41]. The seemingly paradoxical effect of the rs2228145 variant on disease outcomes is likely dependent on disease-associated levels of IL-6. In situations where circulating IL-6 levels are not markedly elevated (eg, atherosclerosis) [42], the rs2228145 variant may be protective by reducing IL-6 classical signalling via shedding of the membrane IL-6R. In these scenarios, there are likely adequate levels of endogenous sgp130 to neutralise any increases in the IL-6/IL-6R complex and prevent IL-6 trans-signalling [43]. However, in clinical situations where IL-6 levels are markedly elevated, there is likely insufficient sgp130 to buffer against increased IL-6/IL-6R complexes and prevent resultant trans-signalling (Fig 6). Indeed, our findings confirm the presence of high levels of circulating IL-6 and sIL-6R, but not sgp130, in GCA and show a direct correlation between pSTAT3 responses and membrane-bound gp130 in CD4 T cells from patients with GCA, suggesting that these effects could be mediated in part by increased trans-signalling. Strikingly, this correlation was not observed in GCA CD8 T cells or CD4 and CD8 T cells from healthy subjects, indicating that this enhanced response to IL-6 is specific to GCA CD4 T cells.

Although we demonstrated that CD4 T cells, which play a pivotal role in GCA, exhibit enhanced response to IL-6 in association with the rs22228145variant, we did not address a mechanism by which GCA CD4 T cells upregulate membrane-bound gp130 expression. In addition, we did not investigate the effects of trans-signalling on non-immune cells, such as endothelial cells or hepatocytes. The clinical associations were, however, robust and validated in 2 independent cohorts of patients with GCA. Whether similar effects of the rs22228145 variant on IL-6

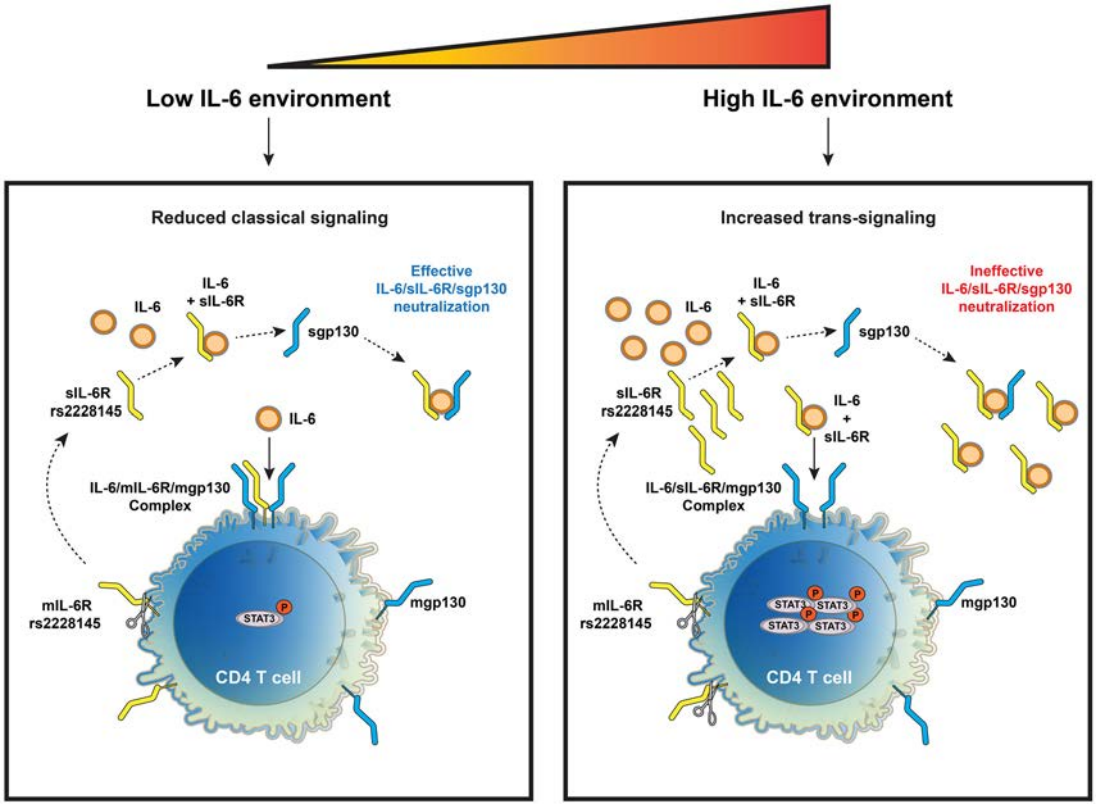



**Figure 6.** Effect of the rs2228145 variant on interleukin 6 (IL-6) signalling is likely dependent on the IL-6 environment. The rs23228145 variant is associated with increased cleavage of the membrane-bound IL-6 receptor (mIL-6R) by metalloproteinases into its soluble form (sIL-6R). In a low IL-6 environment, there is sufficient soluble gp130 to neutralise a resultant increase in the IL-6/sIL-6R complex. Thus, cleavage of mIL-6R would lead to reduced classical IL-6 signalling in leukocytes without a resultant increase in trans-signalling (left panel). Conversely, in an environment where IL-6 is substantially elevated (eg, active disease in giant cell arteritis), there is likely insufficient soluble gp130 to neutralise the IL-6/sIL-6R complex generated in association with the rs2228145 variant. In this scenario, there would be a shift towards greater trans-signalling with activation of the downstream signalling cascade Janus kinase (JAK)/signal transducer and the activator of the transcription (STAT) pathway and increased levels of phosphorylated STAT3 (pSTAT3) in CD4 T cells (right panel). Figure made with BioArt (bioart.niaid.nih.gov).

signalling and clinical response to tocilizumab are observed in other diseases that are strongly mediated by IL-6, beyond GCA, is not yet determined.

In conclusion, a common polymorphism in the IL-6R p.Asp358Ala (rs2228145A>C) predicts treatment response to tocilizumab in GCA. Identifying germline genetic biomarkers that can guide treatment decisions and are not susceptible to confounding by treatment or disease activity status is a major need within the field of rheumatology. This proposed biomarker should be further validated in other prospective observational cohorts of patients with GCA and incorporated into future therapeutic trial designs with the ultimate goal of potential application in routine clinical practice.

## CONTRIBUTORS

RZ, CR, MS, MM, LYA, KQ, JKP, MG, PCG conceptualised and designed the study. KAQ, AT, CC, LD, KL, JHB, PCG provided patient samples. RZ, CR, MS, MM, LYA, KW, SHH, and JKP performed functional experiments. FG-R, CR, and CP performed genetic sequencing. RC and AB performed UK Biobank analyses. All authors were involved in critical review and editing of final manuscript and approved the final version. PCG (guarantor) accepts full responsibility for the work and conduct of the study, had access to the data, and controlled the decision to publish.

## FUNDING

This research was funded by the Intramural Research Program of the National Institute of Arthritis and Musculoskeletal and Skin Diseases and the National Heart, Lung, and Blood Institute.

## Competing interests

All authors declare that they have no competing interests.

## Patient consent for publication

Not applicable.

## Ethics approval

This work was approved by the Institutional Review Board at the National Institutes of Health (#14-AR-0200).

## Provenance and peer review

Not commissioned; externally peer reviewed.

## Data availability statement

Data are available on reasonable request.

## Patient and public involvement

Patients or the public were not involved in the design, or conduct, or reporting, or dissemination plans of our research.

## Supplementary materials

Supplementary material associated with this article can be found in the online version at doi:10.1016/j.ard.2025.01.049.

## REFERENCES


[1] Roche NE, Fulbright JW, Wagner AD, Hunder GG, Goronzy JJ, Weyand CM. Correlation of interleukin-6 production and disease activity in polymyalgia rheumatica and giant cell arteritis. Arthritis Rheum 1993;36(9):1286–94. doi: 10.1002/art.1780360913.

[2] Pugh D, Karabayas M, Basu N, Cid MC, Goel R, Goodyear CS, et al. Large-vessel vasculitis. Nat Rev Dis Primers 2022;7(1):93. doi: 10.1038/s41572-021-00327-5.

[3] Villiger PM, Adler S, Kuchen S, Wermelinger F, Dan D, Fiege V, et al. Tocilizumab for induction and maintenance of remission in giant cell arteritis: a phase 2, randomised, double-blind, placebo-controlled trial. Lancet 2016;387(10031):1921–7. doi: 10.1016/S0140-6736(16)00560-2.

[4] Stone JH, Tuckwell K, Dimonaco S, Klearman M, Aringer M, Blockmans D, et al. Trial of tocilizumab in giant-cell arteritis. N Engl J Med 2017;377(4):317–28. doi: 10.1056/NEJMoa1613849.

[5] Stone JH, Tuckwell K, Dimonaco S, Klearman M, Aringer M, Blockmans D, et al. Glucocorticoid dosages and acute-phase reactant levels at giant cell arteritis flare in a randomized trial of tocilizumab. Arthritis Rheumatol 2019;71(8):1329–38. doi: 10.1002/art.40876.

[6] Unizony S, McCulley TJ, Spiera R, Pei J, Sidiropoulos PN, Best JH, et al. Clinical outcomes of patients with giant cell arteritis treated with tocilizumab in real-world clinical practice: decreased incidence of new visual manifestations. Arthritis Res Ther 2021;23(1):8. doi: 10.1186/s13075-020-02377-8.

[7] Maz M, Chung SA, Abril A, Langford CA, Gorelik M, Guyatt G, et al. 2021 American College of Rheumatology/Vasculitis Foundation Guideline for the Management of Giant Cell Arteritis and Takayasu Arteritis. Arthritis Rheumatol 2021;73(8):1349–65. doi: 10.1002/art.41774.

[8] Hoffman GS, Cid MC, Hellmann DB, Guillevin L, Stone JH, Schousboe J, et al. A multicenter, randomized, double-blind, placebo-controlled trial of adjuvant methotrexate treatment for giant cell arteritis. Arthritis Rheum 2002;46(5):1309–18. doi: 10.1002/art.10262.

[9] Langford CA, Cuthbertson D, Ytterberg SR, Khalidi N, Monach PA, Carette S, et al. A randomized, double-blind trial of abatacept (ctla-4ig) for the treatment of giant cell arteritis. Arthritis Rheumatol 2017;69(4):837–45. doi: 10.1002/art.40044.

[10] Seror R, Baron G, Hachulla E, Debandt M, Larroche C, Puéchal X, et al. Adalimumab for steroid sparing in patients with giant-cell arteritis: results of a multicentre randomised controlled trial. Ann Rheum Dis 2014;73(12):2074–81. doi: 10.1136/annrheumdis-2013-203586.

[11] Matza MA, Fernandes AD, Stone JH, Unizony SH. Ustekinumab for the treatment of giant cell arteritis. Arthritis Care Res (Hoboken) 2021;73(6):893–7. doi: 10.1002/acr.24200.

[12] Unizony SH, Bao M, Han J, Luder Y, Pavlov A, Stone JH. Treatment failure in giant cell arteritis. Ann Rheum Dis 2021;80(11):1467–74. doi: 10.1136/annrheumdis-2021-220347.

[13] Ferreira RC, Freitag DF, Cutler AJ, Howson JM, Rainbow DB, Smyth DJ, et al. Functional IL6R 358Ala allele impairs classical IL-6 receptor signaling and influences risk of diverse inflammatory diseases. PLoS Genet 2013;9(4):e1003444. doi: 10.1371/journal.pgen.1003444.

[14] Chen S, Francioli LC, Goodrich JK, Collins RL, Kanai M, Wang Q, et al. A genomic mutational constraint map using variation in 76,156 human genomes. Nature 2024;625(7993):92–100. doi: 10.1038/s41586-023-06045-0.

[15] Garbers C, Monhasery N, Aparicio-Siegmund S, Lokau J, Baran P, Nowell MA, et al. The interleukin-6 receptor Asp358Ala single nucleotide polymorphism rs2228145 confers increased proteolytic conversion rates by ADAM proteases. Biochim Biophys Acta 2014;1842(9):1485–94. doi: 10.1016/j.bbadis.2014.05.018.

[16] Heinrich PC, Behrmann I, Haan S, Hermanns HM, Müller-Newen G, Schaper F. Principles of interleukin (IL)-6-type cytokine signalling and its regulation. Biochem J 2003;374(Pt 1):1–20. doi: 10.1042/BJ20030407.

[17] Rose-John S. Blocking only the bad side of IL-6 in inflammation and cancer. Cytokine 2021;148:155690. doi: 10.1016/j.cyto.2021.155690.

[18] Zhang M, Bai Y, Wang Y, Cui H, Tang M, Wang L, et al. Cumulative evidence for associations between genetic variants in interleukin 6 receptor gene and human diseases and phenotypes. Front Immunol 2022;13:860703. doi: 10.3389/fimmu.2022.860703.

[19] Parisinos CA, Serghiou S, Katsoulis M, George MJ, Patel RS, Hemingway H, et al. Variation in interleukin 6 receptor gene associates with risk of Crohn's disease and ulcerative colitis. Gastroenterology 2018;155(2) 303-6.e2. doi: 10.1053/j.gastro.2018.05.022.

[20] Eyre S, Bowes J, Diogo D, Lee A, Barton A, Martin P, et al. High-density genetic mapping identifies new susceptibility loci for rheumatoid arthritis. Nat Genet 2012;44(12):1336–40. doi: 10.1038/ng.2462.

[21] Baran P, Hansen S, Waetzig GH, Akbarzadeh M, Lamertz L, Huber HJ, et al. The balance of interleukin (IL)-6, IL-6·soluble IL-6 receptor (sIL-6R), and IL-6·sIL-6R·sgp130 complexes allows simultaneous classic and trans-signaling. J Biol Chem 2018;293(18):6762–75. doi: 10.1074/jbc.RA117.001163.

[22] Scheller J, Chalaris A, Schmidt-Arras D, Rose-John S. The pro- and anti-inflammatory properties of the cytokine interleukin-6. Biochim Biophys Acta 2011;1813(5):878–88. doi: 10.1016/j.bbamcr.2011.01.034.

[23] Mitsuyama K, Sata M, Rose-John S. Interleukin-6 trans-signaling in inflammatory bowel disease. Cytokine Growth Factor Rev 2006;17(6):451–61. doi: 10.1016/j.cytogfr.2006.09.003.

[24] Ponte C, Grayson PC, Robson JC, Suppiah R, Gribbons KB, Judge A, et al. 2022 American College of Rheumatology/EULAR Classification Criteria for Giant Cell Arteritis. Arthritis Rheumatol. 2022;74(12):1881–9. doi: 10.1002/art.42325.

[25] Ponte C, Grayson PC, Robson JC, Suppiah R, Gribbons KB, Judge A, et al. 2022 American College of Rheumatology/EULAR classification criteria for giant cell arteritis. Ann Rheum Dis 2022;81(12):1647–53. doi: 10.1136/ard-2022-223480.

[26] Gutierrez-Rodrigues F, Kusne Y, Fernandez J, Lasho T, Shalhoub R, Ma X, et al. Spectrum of clonal hematopoiesis in VEXAS syndrome. Blood 2023;142(3):244–59. doi: 10.1182/blood.2022018774.

[27] Gutierrez-Rodrigues F, Wells KV, Jones AI, Hironaka D, Rankin C, Gadina M, et al. Clonal haematopoiesis across the age spectrum of vasculitis patients with Takayasu's arteritis, ANCA-associated vasculitis and giant cell arteritis. Ann Rheum Dis 2024;83(4):508–17. doi: 10.1136/ard-2023-224933.

[28] Fischer M, Goldschmitt J, Peschel C, Brakenhoff JP, Kallen KJ, Wollmer A, et al. I. A bioactive designer cytokine for human hematopoietic progenitor cell expansion. Nat Biotechnol 1997;15(2):142–5. doi: 10.1038/nbt0297-142.

[29] Bettelli E, Carrier Y, Gao W, Korn T, Strom TB, Oukka M, et al. Reciprocal developmental pathways for the generation of pathogenic effector TH17 and regulatory T cells. Nature 2006;441(7090):235–8. doi: 10.1038/nature04753.

[30] Carmona FD, Vaglio A, Mackie SL, Hernández-Rodríguez J, Monach PA, Castañeda S, et al. A genome-wide association study identifies risk alleles in plasminogen and P4HA2 associated with giant cell arteritis. *Am J* Hum Genet 2017;100(1):64–74. doi: 10.1016/j.ajhg.2016.11.013.

[31] Liozon E, Dumonteil S, Parreau S, Gondran G, Bezanahary H, Palat S, et al. Risk profiling for a refractory course of giant cell arteritis: the importance of age and body weight: "risk profiling for GC resistance in GCA". Semin Arthritis Rheum 2020;50(6):1252–61. doi: 10.1016/j.semarthrit.2020.09.009.

[32] Moreel L, Betrains A, Molenberghs G, Vanderschueren S, Blockmans D. Epidemiology and predictors of relapse in giant cell arteritis: a systematic review and meta-analysis. Joint Bone Spine 2023;90(1):105494. doi: 10.1016/j.jbspin.2022.105494.

[33] Moreel L, Betrains A, Boeckxstaens L, Molenberghs G, Van Laere K, De Langhe E, et al. Large vessel vasculitis is a risk factor for relapse only in giant cell arteritis patients without polymyalgia rheumatica. Rheumatology (Oxford) 2024 in press. doi: 10.1093/rheumatology/keae456.

[34] Garbers C, Heink S, Korn T, Rose-John S. Interleukin-6: designing specific therapeutics for a complex cytokine. Nat Rev Drug Discov 2018;17(6):395–412. doi: 10.1038/nrd.2018.45.

[35] Zhang S, Chen B, Wang B, Chen H, Li Y, Cao Q, et al. Effect of induction therapy with olamkicept vs placebo on clinical response in patients with active ulcerative colitis: a randomized clinical trial. JAMA 2023;329(9):725–34. doi: 10.1001/jama.2023.1084.

[36] Koster MJ, Crowson CS, Giblon RE, Jaquith JM, Duarte-García A, Matteson EL, et al. Baricitinib for relapsing giant cell arteritis: a prospective open-label 52-week pilot study. Ann Rheum Dis 2022;81(6):861–7. doi: 10.1136/annrheumdis-2021-221961.

[37] Loricera J, Tofade T, Prieto-Peña D, Romero-Yuste S, de Miguel E, Riveros-Frutos A, et al. Effectiveness of Janus kinase inhibitors in relapsing giant cell arteritis in real-world clinical practice and review of the literature. Arthritis Res Ther 2024;26(1):116. doi: 10.1186/s13075-024-03314-9.

[38] Eriksson P, Skoglund O, Hemgren C, Sjöwall C. Clinical experience and safety of Janus kinase inhibitors in giant cell arteritis: a retrospective case series from Sweden. Front Immunol 2023;14:1187584. doi: 10.3389/fimmu.2023.1187584.

[39] Venhoff N, Schmidt WA, Bergner R, Rech J, Unger L, Tony HP, et al. Safety and efficacy of secukinumab in patients with giant cell arteritis (TitAIN): a randomised, double-blind, placebo-controlled, phase 2 trial. Lancet Rheumatol 2023;5(6):e341–50. doi: 10.1016/S2665-9913(23)00101-7.

[40] Interleukin-6 Receptor Mendelian Randomisation Analysis (IL6R MR) Consortium, Swerdlow DI, Holmes MV, Kuchenbaecker KB, Engmann JE, Shah T, et al. The interleukin-6 receptor as a target for prevention of coronary heart disease: a mendelian randomisation analysis. Lancet. 2012;379(9822):1214–24. doi: 10.1016/S0140-6736(12)60110-X.

[41] Lopez-Lasanta M, Julià A, Maymó J, Fernández-Gutierrez B, Ureña-Garnica I, Blanco FJ, et al. Variation at interleukin-6 receptor gene is associated to joint damage in rheumatoid arthritis. Arthritis Res Ther 2015;17(1):242. doi: 10.1186/s13075-015-0737-8.

[42] Pearson TA, Mensah GA, Alexander RW, Anderson JL, Cannon 3rd RO, Criqui M, et al. Markers of inflammation and cardiovascular disease: application to clinical and public health practice: a statement for healthcare professionals from the Centers for Disease Control and Prevention and the American Heart Association. Circulation 2003;107(3):499–511. doi: 10.1161/01.cir.0000052939.59093.45.

[43] Rose-John S, Jenkins BJ, Garbers C, Moll JM, Scheller J. Targeting IL-6 trans-signalling: past, present and future prospects. Nat Rev Immunol 2023;23(10):666–81. doi: 10.1038/s41577-023-00856-y.

Ann Rheum Dis 84 (2025) 1412–1424

Contents lists available at ScienceDirect

Annals of the Rheumatic Diseases

journal homepage: https://www.sciencedirect.com/journal/annals-of-the-rheumatic-diseases

Paediatric rheumatology

# Identification and validation of interferon-driven gene signature as a predictor of response to methotrexate in juvenile idiopathic arthritis

Melissa Kartawinata[1,2,3], Wei-Yu Lin[4], Beth Jebson[1,2,3], Kathryn O'Brien[1,2,3], Elizabeth Ralph[1,2,3], Emma Welsh[1,2,3], Restuadi Restuadi[1,2,3], Elizabeth C. Rosser[3,5], Claire T. Deakin[1,2,3], Lucy R. Wedderburn[1,2,3], Chris Wallace[4,6,7,*], on behalf of the CLUSTER Consortium

[1] *Infection, Immunity and Inflammation Research and Teaching Department, University College London (UCL) Great Ormond Street Institute of Child Health, London, UK*
[2] *National Institute for Health and Care Research (NIHR) Biomedical Research Centre at Great Ormond Street Hospital, London, UK*
[3] *Centre for Adolescent Rheumatology Versus Arthritis at University College London, University College London Hospital and Great Ormond Street Hospital, London, UK*
[4] *Medical Research Council (MRC) Biostatistics Unit, University of Cambridge, Cambridge, UK*
[5] *University College London Division of Medicine, UCL, London, UK*
[6] *Cambridge Institute of Therapeutic Immunology and Infectious Disease, University of Cambridge, Cambridge, UK*
[7] *Department of Medicine, University of Cambridge, Cambridge, UK*

ARTICLE INFO

ABSTRACT

*Objectives:* To identify and validate gene expression biomarkers of response to methotrexate (MTX) treatment in peripheral blood of children with juvenile idiopathic arthritis (JIA) measured before starting MTX treatment.
*Methods:* RNA sequencing was performed on sorted CD4+, CD8+, CD14+, and CD19+ cells, as well as peripheral blood mononuclear cells (PBMC) taken pre-treatment in a discovery cohort (n = 97) and 2 validation cohorts (n = 26 and n = 47, respectively) of patients with non-systemic JIA. Clinical data were recorded at baseline (timepoint 1) prior to treatment and 6 months (timepoint 2) of MTX treatment. Analysis tested the association of gene expression in specific cell types with treatment response using limma-voom, gene set enrichment analysis, and a novel 51-gene score against response to treatment. Parallel analysis, also using pre-treatment gene expression data, was performed in adult rheumatoid arthritis (RA) data (n = 240).
*Results:* In patients with JIA, the baseline expression of genes driven by interferon (IFN) alpha (type-I) or gamma (type-II) was associated with response to treatment at 6 months in 3 independent JIA cohorts. The direction of the association indicated that children with higher baseline expression of IFN-stimulated genes prior to MTX were more likely to be good responders. Comparison with adult RA indicated differences between PBMC and whole blood gene expression associations with response.

*Correspondence to Dr Chris Wallace.
*E-mail address:* cew54@cam.ac.uk (C. Wallace).
Melissa Kartawinata and Wei-Yu Lin contributed equally as co-first authors.
Lucy R. Wedderburn and Chris Wallace are joint senior authors.
**Handling editor** Josef S. Smolen.

https://doi.org/10.1016/j.ard.2025.03.007

0003-4967/© 2025 The Author(s). Published by Elsevier B.V. on behalf of European Alliance of Associations for Rheumatology (EULAR). This is an open access article under the CC BY license (http://creativecommons.org/licenses/by/4.0/)

*Conclusions:* In children with JIA, a high IFN-driven gene signature is associated with a better response to MTX than those with a low IFN-driven gene signature. These data could pave the way to clinically validated tools to identify those most likely to require medications in addition to MTX to control inflammation.

**WHAT IS ALREADY KNOWN ON THIS TOPIC**

- Methotrexate (MTX) is the first line of treatment for most forms of non-systemic juvenile idiopathic arthritis (JIA) before biologic agents are used; however, adequate response to treatment is achieved in only 50% of patients, yet most patients suffer side effects from the use of MTX.
- Achievement of early clinical remission is correlated with better long-term outcomes in JIA.
- There are no validated biomarker tests yet that are used in clinical practice to predict children who need early escalation to biologic agents.

**WHAT THIS STUDY ADDS**

- This study shows that genes in the interferon (IFN) alpha (IFN$\alpha$, type-I) and gamma (IFN$\gamma$, type-II) response pathways are associated with response to treatment with MTX in JIA.
- This finding was replicated in 2 validation cohorts of JIA, and the association was confirmed using a score of only 5 IFN-driven genes.
- The association between IFN-driven pathways and response differs between children with JIA and adults with rheumatoid arthritis (RA).

**HOW THIS STUDY MIGHT AFFECT RESEARCH, PRACTICE OR POLICY**

- An IFN-gene score detected in a small blood test could be built into models to develop a tool to define the risk of nonresponse to MTX and inform treatment decisions early in JIA.
- Accurate prediction of non-response to medication would enable 'patient-precise' medicine and prevent disability.
- This study emphasises the need for age-specific research in inflammatory arthritis, and that results in RA cannot be extrapolated to JIA.

## INTRODUCTION

Juvenile idiopathic arthritis (JIA) is a group of conditions presenting with inflammation of synovial joints in children and young people starting before the 16$^{th}$ birthday. JIA continues to be a major cause of childhood pain, morbidity, and disability [1–3]. When active inflammation remains uncontrolled or children suffer repeated flares of disease, JIA significantly lowers children's quality of life, impacting education, development, and mental health during vital formative years [4]. Despite an increasing number of treatments available, the choice of medication remains largely by historical precedent rather than through an evidence base since there are no validated robust biomarkers that reliably predict response to specific therapeutics. This 'trial-and-error' method of prescribing can result in years of ineffective drug treatment and unpleasant side effects, during which time uncontrolled arthritis causes irreversible joint damage.

Methotrexate (MTX) remains the first-line disease-modifying agent of choice for many types of JIA [5], where a simple intra-articular steroid joint injection does not control the disease. However, typically, 50% of patients have a poor response to MTX at 6 months of treatment [6]; these children may benefit from earlier intervention with biologic agents if they could be reliably identified early. We have shown that the JIA subtype cannot predict a good response to MTX [7]. The CLUSTER (Childhood arthritis and its associated uveitis: stratification through endotypes and mechanism to deliver benefit) Consortium, a UK-wide multidisciplinary collaborative network, was established to address this urgent need for stratifiers to enable a precision approach to treatment for children and young people with JIA [8].

In this study, we aimed to define blood biomarkers that are associated with response to MTX in JIA, with the ultimate goal of generating predictive biomarkers to help guide treatment choice. We took a hypothesis-free approach and interrogated transcriptome data from sorted peripheral blood immune cells and total peripheral blood mononuclear cells (PBMC), taken just prior to MTX start, against treatment response after 6 months in patients with JIA. We identified pathways that are associated with response, with interferon (IFN)-driven pathways being the most significant pathways identified. We generated a univariate gene score of 51 transcripts that were robustly associated with response in JIA and showed that this score was also associated with response. We validated these findings in 2 further JIA replication cohorts. We looked at the relationship between IFN-driven pathways and MTX response at 6 months in adult rheumatoid arthritis patients and found an association in the opposite direction to the results seen in JIA.

This large, comprehensive study which set out to define specific immune cell biomarkers measured by gene expression to predict outcomes in response to MTX treatment, provides a significant step towards the possibility of precision medicine in JIA.

## METHODS

Detailed methods are provided in the Supplementary Methods. In brief, we recruited a discovery cohort of 97 non-systemic JIA patients, naive to disease-modifying antirheumatic drugs (DMARDs), and recorded core outcome variables at baseline (timepoint 1 [t1]) and again after MTX treatment (timepoint 2 [t2], median follow-up 6.6 months). We quantified gene expression in sorted immune cell populations from blood using RNA sequencing (RNAseq). We examined the association between gene expression and change in outcome variables using limma-voom [9–11] and gene set enrichment analysis [12]. We used false discovery rates (FDR) to adjust for multiple hypothesis testing. We attempted to replicate findings in 2 external validation cohorts (1 UK and 1 USA) of JIA patients [13]. We used 2 measures of replication: the correlation between effect estimates in discovery and validation cohorts ($\rho$) and an overall measure of association ($\lambda$, which captures the deviation of a set of $P$ values from their expected distribution if the null hypothesis is true for all tests, defined fully in the Supplementary Methods). We also compared the results with those of the RA-MAP (Rheumatoid Arthritis MRC–ABPI consortium) study of adult rheumatoid arthritis (RA) patients [14]; all 3 cohorts included patients naive to DMARDs and treated with MTX for approximately 6 months.

## RESULTS

### *Study overview*

An overview of the study is shown in Figure 1A. Patients with all categories of JIA other than systemic JIA (sJIA) were

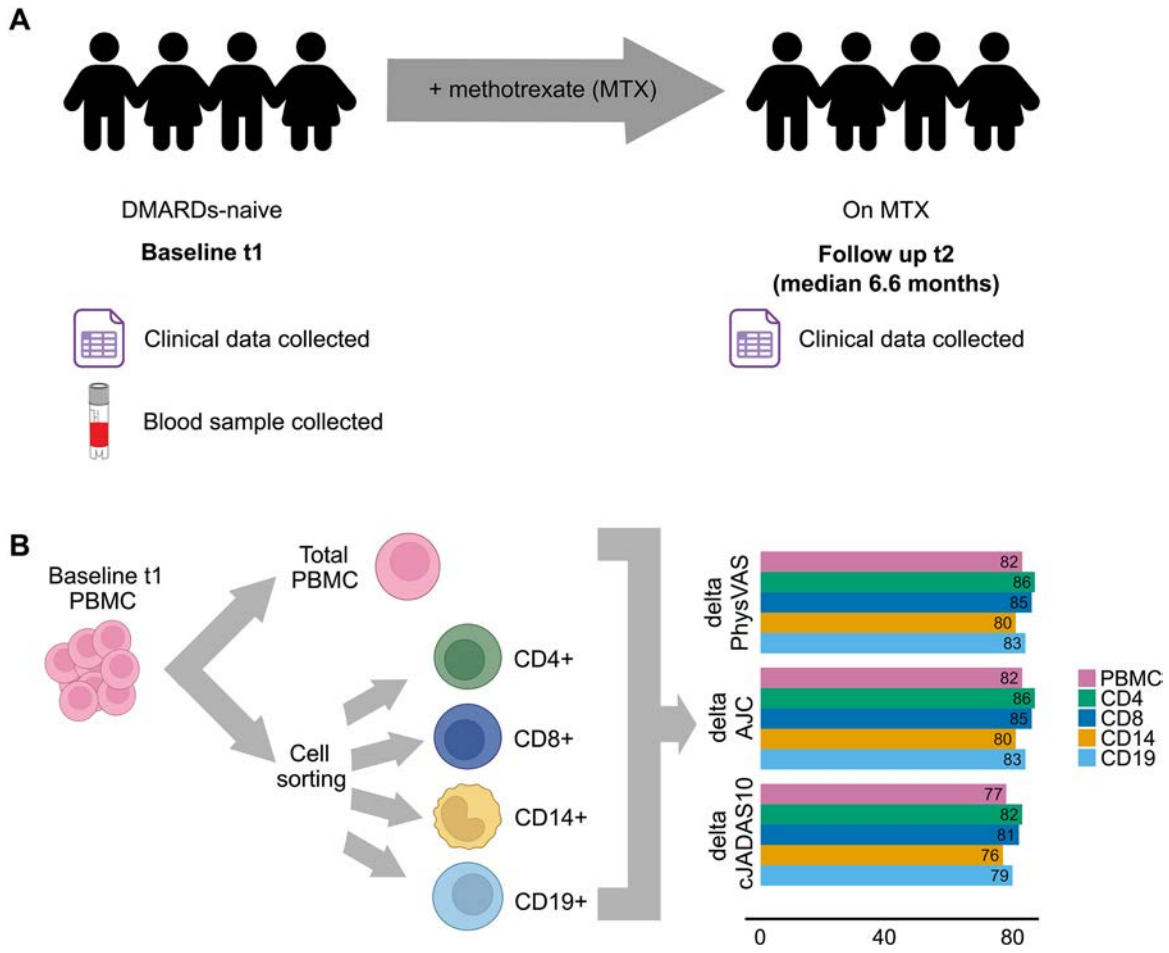



**Figure 1.** Study design and RNA sequencing (RNAseq) data generation. (A) A total of 97 juvenile idiopathic arthritis (JIA) patients with active JIA (excluding systemic JIA) who were about to start methotrexate (MTX) were included. Blood samples were collected at the time of diagnosis (baseline timepoint 1 [t1]), prior to receiving MTX (pre-MTX). Clinical data were collected at baseline t1 and follow-up timepoint 2 (t2) to calculate the response. (B) Peripheral blood mononuclear cells (PBMC) were isolated from whole blood and sorted into 4 different immune cell types. Sorted immune cells and total PBMC were sequenced. The final number of available RNAseq data for each cell type and each outcome variable is shown in the bar plot. delta-AJC, change in active joint count; delta-cJADAS10, change in clinical Juvenile Arthritis Disease Activity Score 10; delta-PhysVAS, change in Physician Visual Analogue Score (VAS); DMARDs, disease-modifying antirheumatic drugs.

recruited when they were about to start MTX for active arthritis. sJIA was excluded since MTX alone is no longer the standard of care for sJIA. A total of 416 RNAseq data files from 97 patients were included in the discovery analysis, as illustrated in Figure 1B. Patients were predominantly in the polyarticular rheumatoid factor-negative and oligoarticular categories of JIA, with smaller numbers in other categories (Table) [15]. PBMC isolated from blood samples collected prior to starting MTX treatment (naive) were sorted into 4 immune cell types: CD4+ T cells, CD8+ T cells, CD14+ monocytes, and CD19+ B cells (Fig 1B). To define predictors of response to MTX in JIA, we performed RNAseq on these sorted immune cell populations and total PBMC.

Our recent study exploring the complexity of available tools for assessing response to treatment in 2 large JIA cohorts showed that an American College Rheumatology (ACR) definition of improvement (DOI) [16] or ACR paediatric DOI may be reached despite disparate changes in the core set variables of the tool [7]. Therefore, for initial analyses, we considered the core variables, the physician's Visual Analogue Score (PhysVAS), active joint count (AJC), and the disease activity score tool, clinical Juvenile Arthritis Disease Activity Score (cJADAS) 10 [15], as continuous variables over time. After thorough quality control, n = 76 to 86 cases had data per cell type across the different measures of response to treatment (Fig 1B). Subsequent analyses also used the ACR-DOI tool [16] in this study.

### *Analysis of gene expression across all cell types against outcome measures*

Our first aim was to identify genes whose expression at baseline in specific cell types or total PBMC was significantly associated with MTX treatment response at 6 months. Gene expression analysis found a limited number of genes that were individually significantly associated with treatment response (FDR < 0.05) in any cell type (Fig 2A-C). In all, 14 genes across all cell types were significantly associated with a change in 1 or more outcome measures, 13 of which were significantly associated with monocytes (Fig 2D). Genes that reached significance with 1 measure of response (change in PhysVAS [delta-PhysVAS], AJC, or cJADAS10) generally had the same direction of association with other outcomes (Fig 2D). However, interestingly, some genes reaching significance in one cell type had a heterogeneous pattern of association across other cell types (Fig 2D).

Table
**Demographic data of JIA patients in CLUSTER cohort**

| Characteristics | JIA patients (n = 97) |
|---|---|
| Age (y) at baseline, median (IQR) | 8.5 (4.9-12.8) |
| Female, n (%) | 61 (62.9) |
| Disease duration (y) at MTX start (t1), median (IQR) | 0.9 (0.5-2.5) |
| Time to follow-up time point t2 (mo), median (IQR) | 6.6 (5.8-7.4) |
| JIA subtype by ILAR classification, n (%) | |
| Oligoarthritis, persistent | 18 (18.6) |
| Oligoarthritis, extended | 19 (19.6) |
| Polyarthritis, RF negative | 37 (38.1) |
| Polyarthritis, RF positive | 7 (7.2) |
| Psoriatic arthritis | 5 (5.2) |
| Enthesitis-related arthritis | 11 (11.3) |
| Clinical variables | |
| Active joints t1, median (IQR) | 5 (3-9) |
| Active joints t2, median (IQR) | 0 (0-3) |
| Change in active joints, delta, median (IQR) | −4 (−7 to −1) |
| Physician global score t1, median (IQR) | 4.4 (2.3-6) |
| Physician global score t2, median (IQR) | 1.1 (0.5-2.7) |
| Change in physician global score delta, median (IQR) | −2.1 (−4.5 to −0.9) |
| cJADAS10 t1, median (IQR) | 13.3 (8.2-19)[a] |
| cJADAS10 t2, median (IQR) | 4.3 (1.5-8.9)[a] |
| Change in cJADAS10 score delta, median (IQR) | −7.7 (−13.6 to −3.1)[b] |

cJADAS, clinical Juvenile Arthritis Disease Activity Score (range, 0-30) [15]; Delta, t2 − t1; ILAR, International League of Associations for Rheumatology; JIA, juvenile idiopathic arthritis; MTX, methotrexate; RF, rheumatoid factor; t1, baseline timepoint; t2, follow-up timepoint.
Summary of demographics and clinical characteristics of patients in the discovery analysis; IQR (25%, 75%).
[a] cJADAS10 available in n = 94 JIA patients.
[b] Delta-cJADAS10 available in n = 92 JIA patients.

## *Expression of IFN-driven genes at baseline is associated with response to MTX*

Because the power to detect association with individual genes can be limited by the large multiple testing burden, we next used gene set enrichment analysis (GSEA) to ask whether particular pathways showed enrichment for association signals. First, we compared 2 popular methods: GSEA, as originally proposed [12], and the more recent fastGSEA (fGSEA) [17], using simulated traits in an independent set of JIA cases (US cohort). We found that fGSEA produced a large number of false positive results, whereas GSEA, as originally proposed, controlled the false positive rate well while maintaining similar power (Supplementary Fig S1A). Therefore, we used GSEA rather than fGSEA to explore biological drivers of response-associated gene expression in our data.

Using Molecular Signatures Database (MSigDB) Hallmark as a database reference [18], we found significant enrichment of genes in the IFN alpha (IFN$\alpha$, type-I) and gamma (IFN$\gamma$, type-II) response pathways associated with delta-PhysVAS across PBMC, CD8, and CD19 cell types (FDR < 0.05 or FDR < 0.01; Fig 3A), with consistent direction of effect across the cell types and other outcome measures (Fig 3B). Specifically, higher expression of type-I and type-II IFN-driven genes prior to starting MTX was associated with a better response at 6 months. Of note, parallel analyses using PhysVAS at baseline and t2 showed higher expression of type-I IFN and type-II IFN-driven genes associated with higher PhysVAS at baseline and lower PhysVAS at t2, although enrichment was only significant in PBMC (IFN$\alpha$ and IFN$\gamma$) at t2 and in CD19 (IFN$\gamma$) at baseline (Supplementary Fig S1B). Interestingly, having defined IFN-stimulated genes as being associated with response to MTX in JIA, we then reanalysed the 14 significant genes initially identified by differential gene expression analysis (Fig 2D) using the Interferome database [19]; 12 of these 14 genes are associated with IFN-driven pathways (Supplementary Table S1).

To identify a set of IFN response genes for further analysis, we identified genes that drive enrichment (leading-edge genes) of these 2 IFN pathways (type-I and type-II IFN) from cell types (PBMC, CD8, and CD19) that were significantly associated with delta-PhysVAS and took these 127 genes for further analysis (Fig 4A, top table and Venn diagram). We also included *SIGLEC1* (CD169) since this gene has been reported in multiple autoimmune studies [20–23] to be associated with type-I IFN, but it is not annotated in MSigDB Hallmark IFN pathways. Of these 128 genes, 51 were nominally associated ($P < .05$) with PBMC from the CLUSTER cohort (Fig 4A, lower plot), which led to our definition of a 51-gene IFN-driven gene set (Supplementary Table S2) for further analysis in validation cohorts. We confirmed that the baseline expression of these 51 genes, expressed as the 51-IFN-gene score, correlated significantly with response at 6 months by delta-PhysVAS (Fig 4B) and change in cJADAS10 (delta-cJADAS10) (Supplementary Fig S2). Analysis of these 51 genes, annotated as type-I or type-II IFN-driven genes, showed that there was considerable overlap, with 30 of the 51 genes being annotated by the Hallmark database as both (Fig 4A, lower Venn diagram).

We next investigated whether we could replicate these findings in an independent cohort of JIA patients (Childhood Arthritis Response to Medication Study [CHARMS]) who were also naive to treatment and about to start MTX; demographics are shown in Supplementary Table S3. In this replication cohort (26 children), gene expression levels of the 51 genes were associated with delta-PhysVAS ($\lambda = 2.1$, $P = .043$; Fig 4C and Supplementary Fig S3A), with 15 reaching a nominal $P$ value of $\leq .05$. The estimated log-fold changes for these 51 genes were significantly correlated between the replication CHARMS cohort and those from the primary CLUSTER dataset ($\rho = 0.765$, $P = .037$; Fig 4D and Supplementary Fig S3B).

## *Comparison with adult RA*

Higher expression of genes in IFN response pathways at baseline was associated with an improved response to MTX in our JIA cohorts. This is in contrast to reports in adult RA where higher expression of IFN response genes in whole blood (WB) in treatment-naive patients has been observed to be associated with poor response to MTX treatment [24–26]. Previous analysis in RA WB samples was based on a 5-gene score (IGS5) comprised of the average expression of 5 canonical IFN response genes: *MX1, IFI44L, OAS1, ISG15*, and *IFI6*, only 2 of which were on our list of 51 genes. We, therefore, compared the expression of all these genes (the 51 genes we defined and the 5 genes comprising IGS5) in RA samples at baseline (RA-MAP cohort, N = 240) with change in DAS28 after MTX treatment in all cell types, PBMC, and WB, and across several time points (3, 6, 9, 12, 15, and 18 months) using data released by the RA-MAP consortium [14] (Fig 5A, Supplementary Table S4). We found that effect directions in the RA-MAP cohort were consistent across time points (3-18 months; Fig 5A), so differences in the timing of recording treatment response were unlikely to be responsible for the contrasting directions between JIA and RA. On the other hand, we did see heterogeneity between cell types

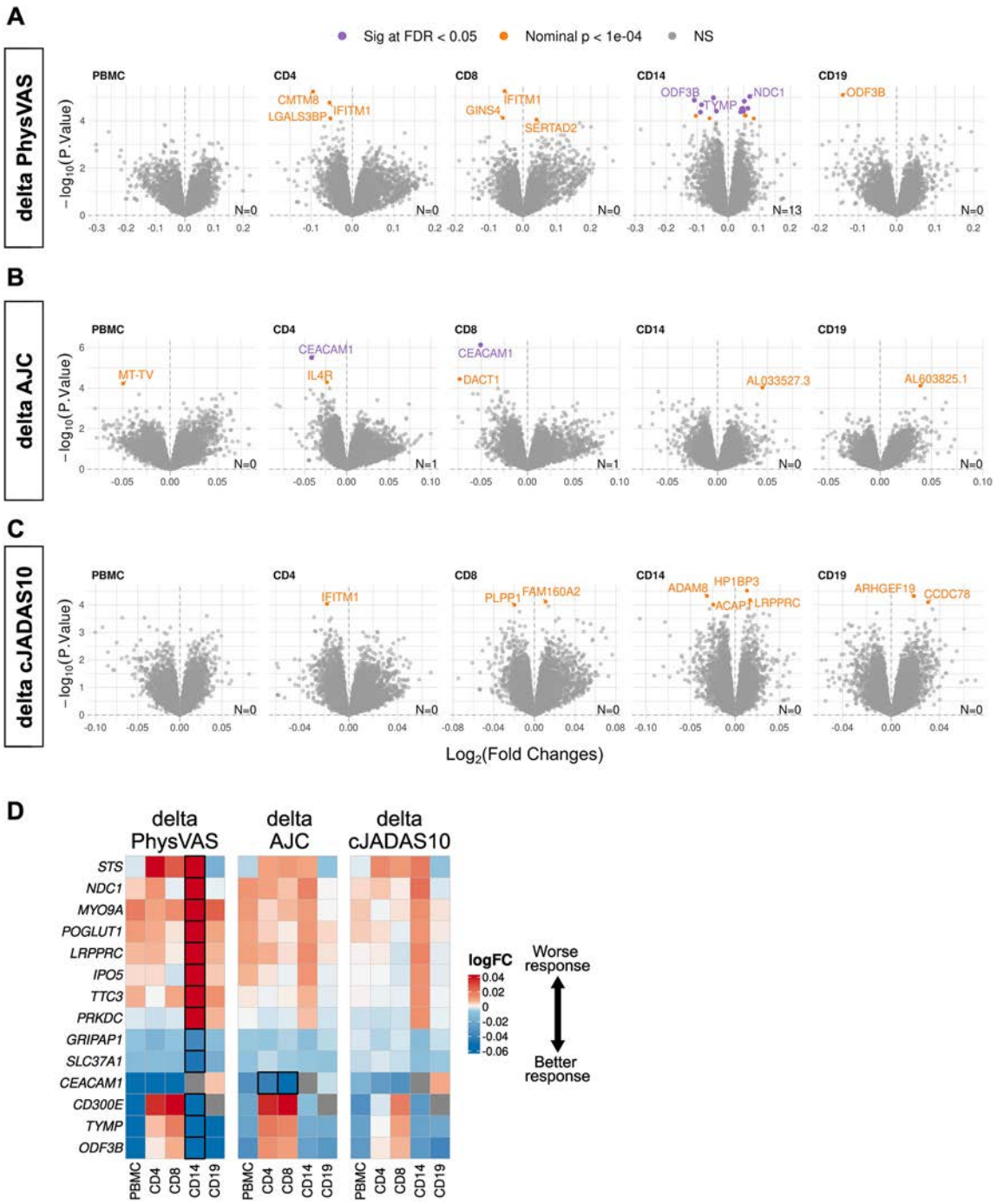



**Figure 2.** Analysis of gene expression across cell types and outcome measures. Gene expression was measured using RNA sequencing in sorted cell types and total peripheral blood mononuclear cells (PBMC) taken prior to starting methotrexate (MTX). Gene expression was analysed for associations with response to MTX treatment, with outcome assessed by change in Physician Visual Analogue Score (delta-PhysVAS), change in active joint count (delta-AJC), or change in the clinical Juvenile Arthritis Disease Activity Score 10 (delta-cJADAS10) in patients with juvenile idiopathic arthritis. Analysis was conducted in parallel within cell types, and we highlight genes that are significant in any one cell type. Results for (A) delta-PhysVAS, (B) delta-AJC, and (C) delta-cJADAS10 are shown as volcano plots for each cell type with nominally ($P < 10^{-4}$) and false discovery rate (FDR < 0.05) significant genes, which are highlighted in orange and purple, respectively. Gene names are shown for the top 3 genes either by FDR or *P* value significance. (D) Results across all outcomes for significant genes and cell types are summarised in a heatmap showing fold change (FC; colour) and significance (FDR < 0.05, solid box). A negative delta value (calculated as value at timepoint 2 − value at timepoint 1) indicates a decreasing measure of disease activity and, hence, a good response to treatment. NS, not significant.

for RA-MAP data, with the most consistently positive associations seen for WB and the least for PBMC.

We performed univariate comparisons of DAS28 in RA and PhysVAS in JIA at baseline (ie, t1), 6 months (ie, t2), and the change in each measure (delta-DAS28 and delta-PhysVAS, respectively) against the IGS5 previously defined in RA studies [24]. We saw that disease activity tends to correlate positively with the IGS5 in PBMC at baseline in both RA and JIA, but while this correlation was maintained in RA at 6 months, the IGS5 in PBMC at baseline was negatively correlated with disease activity at 6 months in JIA. This led to positive or negligible correlations of the IGS5 at baseline with increasing DAS28 at 6 months in

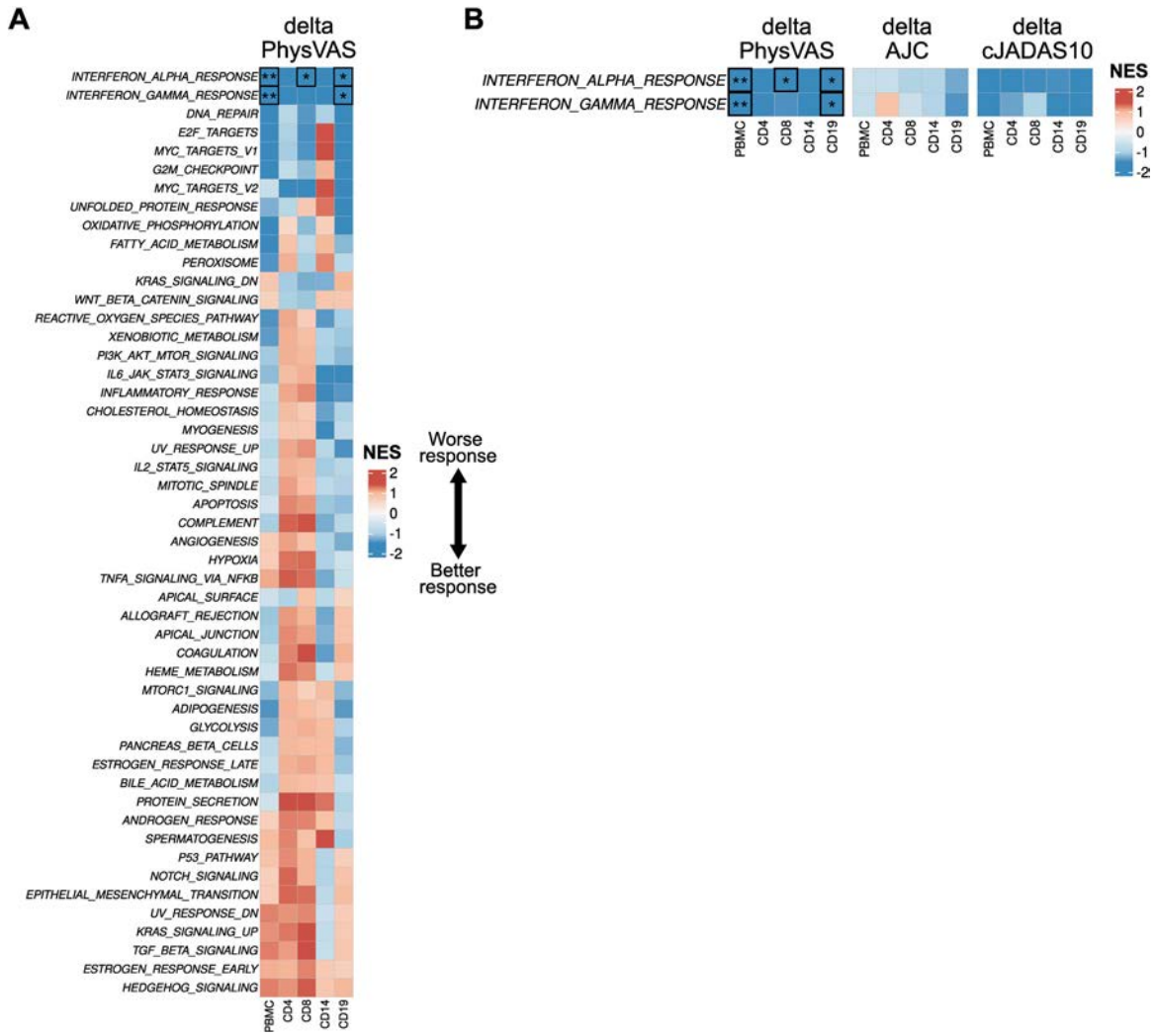



**Figure 3.** Gene Set Enrichment Analysis (GSEA) identifies the association of interferon (IFN) response gene pathways with response to methotrexate. (A) GSEA analysis in the CLUSTER JIA dataset identified type-I (IFN$\alpha$) and type-II (IFN$\gamma$) response gene pathways as robustly associated with a change in Physician Visual Analogue Score (delta-PhysVAS). The heat map shows the enrichment score (colour) and significance (*false discovery rate [FDR] < 0.05, **FDR < 0.01) of Molecular Signatures Database (MSigDB) Hallmark pathways across delta-PhysVAS over 5 cell types. (B) Both type-I (IFN$\alpha$) and type-II (IFN$\gamma$) response pathways showed consistent directions of effect with other outcomes, change in active joint count (delta-AJC), or change in the clinical Juvenile Arthritis Disease Activity Score 10 (delta-cJADAS10). JIA, juvenile idiopathic arthritis; NES, normalised enrichment score; PBMC, peripheral blood mononuclear cells.

RA. In JIA, this gave a positive correlation of the IGS5 with PhysVAS at baseline and with response, as assessed by a decrease in PhysVAS (Fig 5B). We also saw the same direction of effect when we analysed these measures against the 51-gene score in JIA (Supplementary Fig S4).

The pattern in Figure 5B could suggest that the effect on treatment response, as marked by IFN response gene expression at baseline, is mediated by disease severity at baseline, although this would be in contrast to the pathway analyses conducted independently at baseline and t2. To examine this in more detail, we compared models for delta-PhysVAS with and without adjustment for baseline measures in the CLUSTER and CHARMS cohorts. We found that association with treatment response was maintained even after adjustment for disease severity at baseline and saw no significant interaction effects with baseline measures (Fig 6A-D), suggesting that the effect marked by IFN response gene expression at baseline is not mediated by disease severity at baseline. We found a similar pattern using AJC in CLUSTER, CHARMS, and a second validation cohort, US JIA (Supplementary Fig S5); note that PhysVAS was not available in the US cohort. These results suggest that even though there is an association between IFN-driven gene expression and disease activity prior to treatment, after adjusting for this effect, there remains an association between response and the baseline expression of the IFN-driven signature.

In these analyses, both gene scores were nominally associated with delta-PhysVAS and AJC in the validation cohorts, where they were measured in the baseline-adjusted models, providing further support for the validation of our results in these independent cohorts.

### *IFN response genes show a consistent direction of association with the ACR-DOI in JIA*

The majority of clinical trials in JIA have used the ACR paediatric DOI tool to define response to treatment [16]. Therefore, we wished to confirm that our findings were consistent when the treatment response outcome was defined by ACR-DOI. The distribution of delta-PhysVAS by the ACR group in the CLUSTER cohort is shown in Figure 7A. As expected, children with a good response to MTX (here defined as reaching American College Rheumatology (ACR) 50 (ACR50) or above) have a more

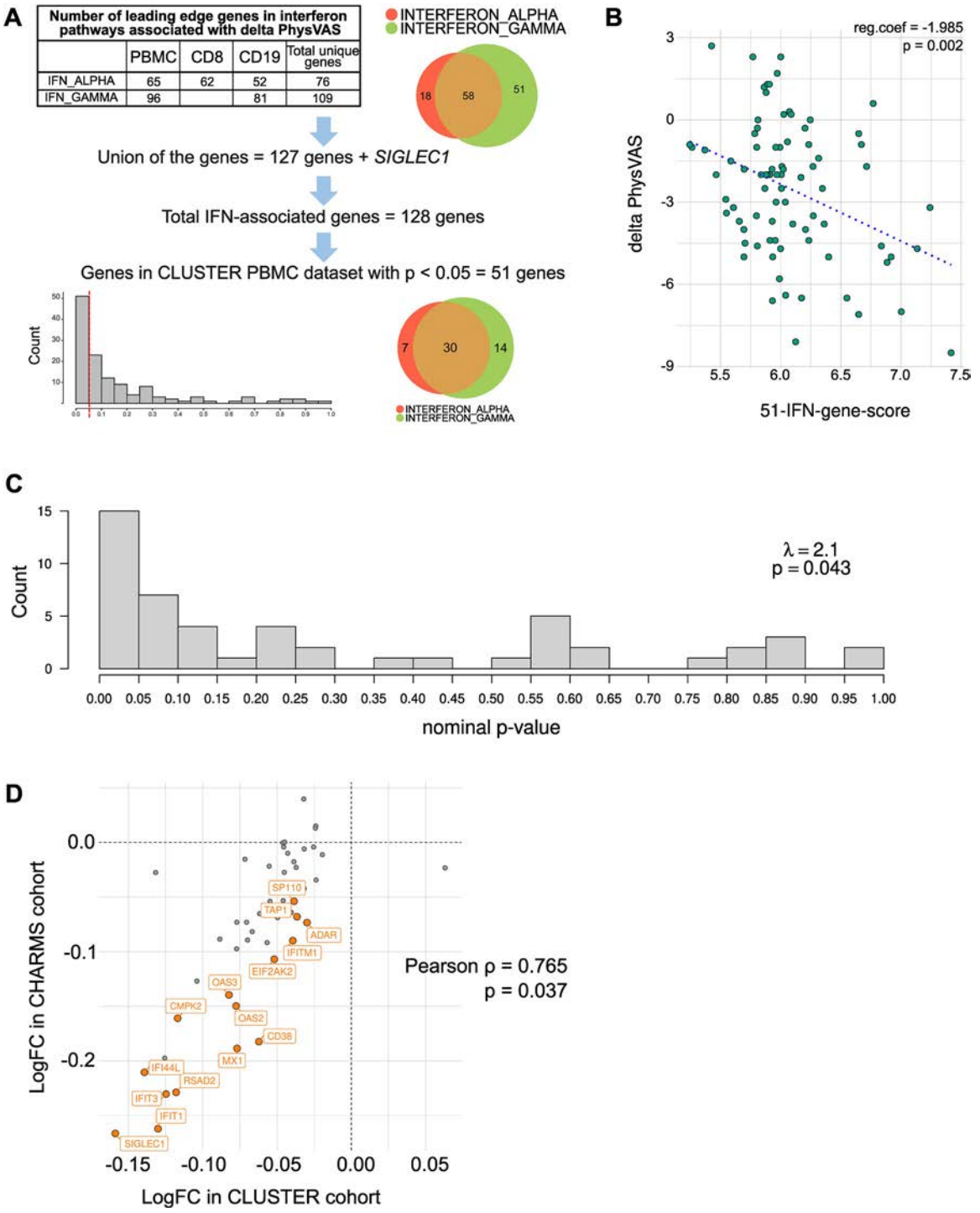



**Figure 4.** Validation of the association between interferon (IFN) response gene expression and treatment response. (A) The table shows the number of leading-edge genes in each cell type (peripheral blood mononuclear cells [PBMC], CD8, and CD19) where response was significantly associated with type-I and type-II IFN pathways. The union of leading-edge genes (127 genes) from both pathways across different cell types showed a substantial overlap (n = 58 genes) in gene membership between type-I and type-II pathways (upper Venn diagram). Including *SIGLEC1*, a total of 128 interferon-related genes were considered as marking the interferon response pathways, of which 51 were found to be nominally significant ($P < .05$) in the PBMC dataset. The bottom Venn diagram shows overlapped gene membership between the 2 IFN pathways for those 51 genes (lower plot). (B) A 51-IFN-gene score was generated using the mean log2 expression of the 51 significant genes. The dot plot shows the correlation of the 51-IFN-gene score in PBMC with a change in Physician Visual Analogue Score (delta-PhysVAS) in the CLUSTER dataset ($P = .002$). (C) Regression of delta-PhysVAS on PBMC gene expression in the independent CHARMS dataset of 26 children showed significant enrichment of small $P$ values among the 51 IFN response genes ($\lambda = 2.1$, $P = .043$). (D) Estimated effect sizes for 51 IFN response genes in the CHARMS replication dataset were significantly correlated with those estimated in the CLUSTER dataset ($\rho = 0.765$, $P = .037$). Genes highlighted in orange represent the 15 genes reaching a nominal $P$ value of <.05 in the CHARMS JIA cohort. CHARMS, Childhood Arthritis Response to Medication Study; FC, fold change; JIA, juvenile idiopathic arthritis.

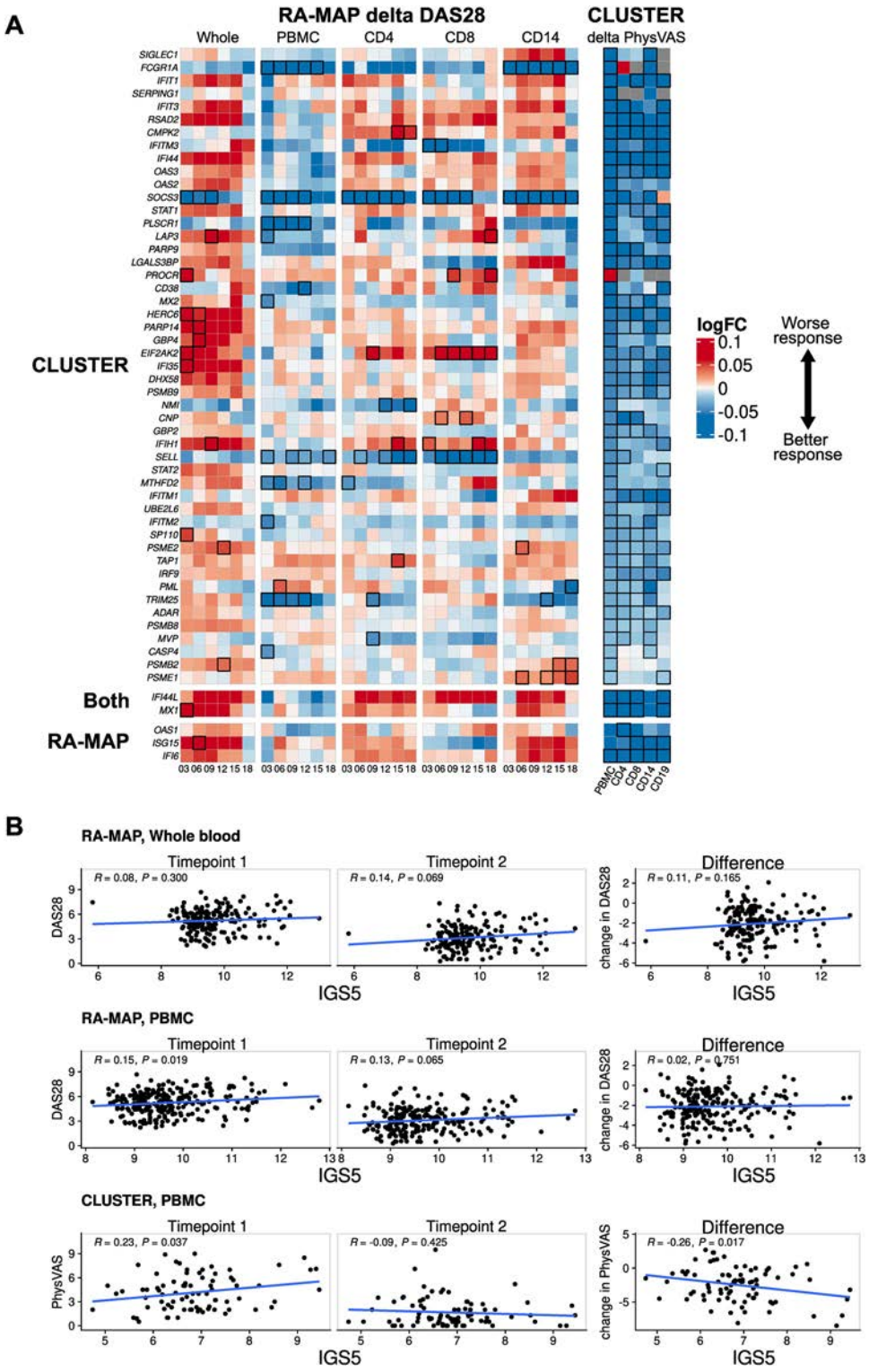



**Figure 5.** Comparative analysis between juvenile idiopathic arthritis (JIA) and adult Rheumatoid Arthritis (RA) for association of gene expression with response to methotrexate. (A) Heatmap of log-fold changes (FCs) estimated in expression analysis of the 54 interferon response genes (51 from our study and 5 from the RA-MAP study, including 2 in both RA samples [RA-MAP] and JIA samples [CLUSTER]) across all available time points and cell types for delta-DAS28 (RA) and a change in Physician Visual Analogue Score (delta-PhysVAS, in JIA). For all plots, genes are shown in rows. Columns in RA show the time point at which delta-DAS28 was calculated, with sets of columns split by cell type. In CLUSTER, columns show different cell types. The value of logFC is represented by colour, and a black square indicates nominal significance ($P < .05$). (B) Comparison of the 5-gene score (IGS5) with measures of disease activity (DAS28 in RA and PhysVAS in JIA) at baseline (timepoint 1), 6 months (timepoint 2), and differences between the time points. For RA, the IGS5 is shown for whole blood and peripheral blood mononuclear cells (PBMC), and in JIA, only in PBMC.

negative value for delta-PhysVAS. We conducted further analysis of the baseline expression of the 51 IFN-driven genes against ACR status at follow-up in both the CLUSTER and US JIA cohorts. Note that only 3 children in CHARMS had a response of American College Rheumatology (ACR) 30 (ACR30) or below, so we were not powered to perform this analysis in the CHARMS cohort. We again saw a significant positive correlation between the effect size (log-fold change) for delta-PhysVAS and the effect

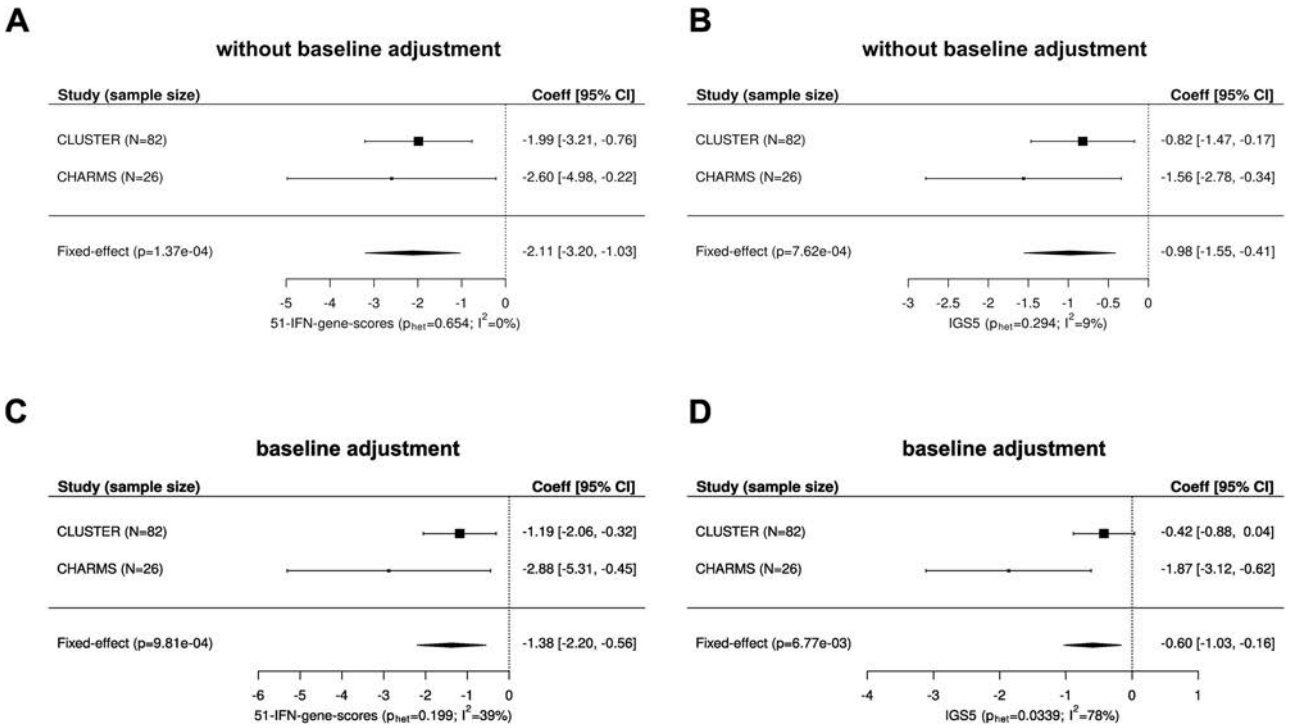



**Figure 6.** The association of change in Physician Visual Analogue Score (delta-PhysVAS) with both gene scores remains after adjustment for baseline. (A) Meta-analysis of the estimated effect of the 51 gene score on delta-PhysVAS across the CLUSTER and CHARMS cohorts. The bottom row shows the fixed effects meta-analysis result. (B) Meta-analysis of the estimated effect of the 5-gene score (IGS5) on delta-PhysVAS across the CLUSTER and CHARMS cohorts. (C) Same model as A, adjusted for baseline PhysVAS at timepoint 1. (D) Same model as B, adjusted for baseline PhysVAS at timepoint 1. Across all plots, phet is the *P* value for testing the significance of Cochran's Q statistic, and heterogeneity index, I2 (0-100), is the proportion of the total variation due to heterogeneity. CHARMS, Childhood Arthritis Response to Medication Study; IFN, interferon.

size for ACR across the 51 IFN genes in the CLUSTER JIA dataset ($\rho = 0.853$, $P = .019$; Supplementary Fig S6A). The same direction of correlation was observed with the US JIA dataset compared with the CLUSTER cohort, although this did not reach significance ($\rho = 0.40$, $P = .298$; Supplementary Fig S6B).

We also tested the 51-IFN-gene score as a univariate measure for association with response at 6 months in the CLUSTER cohort using the ACR-DOI outcome, with cases dichotomised into responders (defined as reaching ACR50 or above) and non-responders (those reaching ACR30 or below). Figure 7B shows that the 51-IFN-gene score, calculated from baseline PBMC gene expression (n = 118 cases), was significantly higher ($P = .00556$) in responders than in non-responders.

Next, we chose to use the IGS5 as a further univariate summary of IFN response, defined independently of our data, to support the most robust analyses. We compared the IGS5 between ACR outcome groups in the CLUSTER cohort and saw a nominally significant difference across all cell types ($P < .03$) between responders (defined as reaching ACR50 or above) and nonresponders (those reaching ACR30 or below), with a higher IGS5 in responders in all cell types (Fig 7C).

Finally, as we have previously observed that the serum concentration of the protein MRP8/14 (also known as S100A8/9), measured before treatment with MTX, in nonsystemic cases of JIA [27] correlates with response to MTX, we asked how this protein relates to the IFN score measured here. We found that serum MRP8/14 concentration correlates weakly with the 51-IFN-gene score ($\rho = 0.27$, $P < .09$; Supplementary Figs S7 and S8). The weak association is perhaps unsurprising given that cell sources of this serum protein include blood monocytes and neutrophils, as well as synovial tissue itself, while the 51-IFN-gene score derives from PBMC. The direction of the association, however, is consistent, meaning that in this study, children with a higher inflammatory signal by both measures were more likely to respond to MTX.

## DISCUSSION

Reliable biomarkers that predict response to medication in inflammatory arthritis would offer a major step towards personalised treatment. In this large study of JIA, we took an unbiased approach to define genes and pathways whose expression in blood mononuclear cells prior to the start of treatment is associated with response to MTX. Within our discovery cohort, we found that genes whose transcription is driven by IFN$\alpha$ or IFN$\gamma$ are expressed at higher levels prior to treatment in those who then achieve a good response to MTX. We validated this finding in 2 further JIA cohorts, one from the same centre (n = 26) and a second independent cohort (n = 47). To our knowledge, this is the first study to analyse how the pre-treatment transcriptome of both PBMC and separated major mononuclear cell types (T cells, B cells, and monocytes) are associated with response in JIA.

Our initial analyses to identify genes that were significantly associated with treatment response in each specific cell type or total PBMC yielded relatively few associated genes with an FDR < 0.05. This concurs with previous studies, all of which were on total PBMC, where few individual genes were identified as predictive of response to MTX [13,28]. However, GSEA analysis demonstrated a significant association of both IFN$\alpha$ (type-I) and IFN$\gamma$ (type-II) pathways with response to MTX. Notably, we used the original GSEA method, including performing permutations on raw data to generate *P* values rather than gene labels in summary data, to minimise the risk of false positives and provide the greatest confidence in our results. The observation that the direction of this effect was the same across all cell types

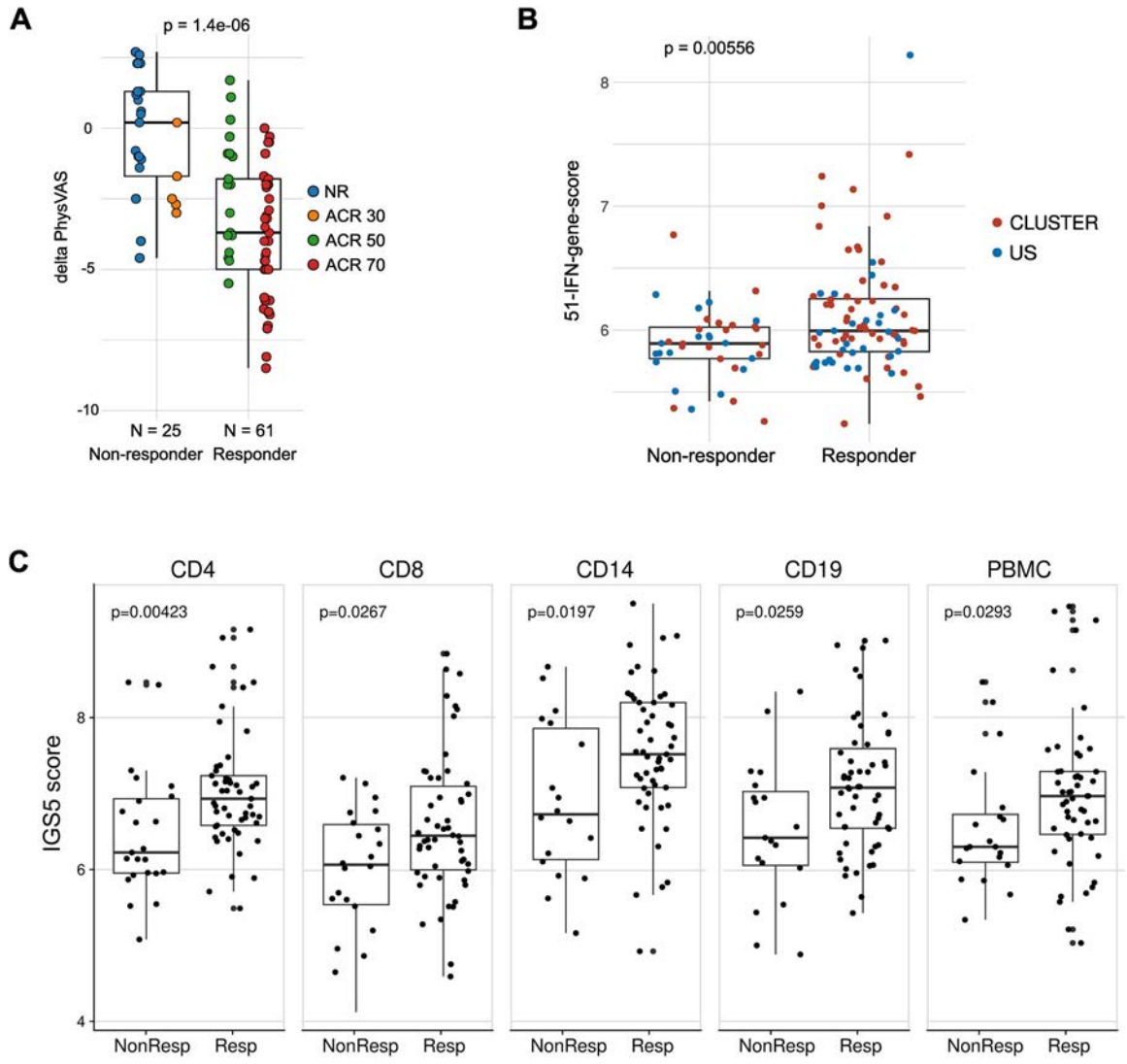



**Figure 7.** The association of treatment response with interferon (IFN) genes is recapitulated using American College Rheumatology (ACR) status. (A) Measures of change in Physician Visual Analogue Score (delta-PhysVAS) were higher in non-responders (Non-responder; NR [Non-responder] and ACR30) than in responders (Responder; ACR ≥ 50), $P = 1.4e10^{-6}$. N = 86 cases had full ACR status determined. (B) The 51-IFN-gene score calculated in peripheral blood mononuclear cells (PBMC) was higher in Responder (ACR ≥ 50) than in Non-responder (NR and ACR30). N = 71 cases of the CLUSTER cohort (blue dots) and n = 47 cases of the US cohort (red dots) had full ACR status determined and 51-IFN-gene scores calculated. (C) Mean log2 expression of the 5 genes, *MX1, IFI44L, OAS1, ISG15, and IFI6,* were used to provide a univariate summary (5-gene score [IGS5]) of the IFN response gene signature. The IGS5 was calculated in all 5 cell types (from left to right: CD4, CD8, CD14, CD19, and PBMC, as shown) and was significantly higher in Resp (ACR ≥ 50) than in NonResp (NR and ACR30) in all cell types. All data in this figure are from the CLUSTER cohort except for B, which includes data from the US cohort as shown.

suggests that this could be translatable to a meaningful clinical biomarker test in the future. In another study of response to MTX in JIA, 5 (*SOCS3, B2M, CASP3, IL4R,* and *CD40*) of 94 genes implicated in the association with response [28] overlapped with our list of 128 leading genes. Interestingly, other pathways that have previously been implicated in response to MTX, such as interleukin-6/JAK/STAT3 signalling, showed opposite directionality of effect in T cells to those in monocytes or B cells, although these did not reach significance. This cell-specific discrepancy is perhaps unsurprising given the known complexity of mechanisms of MTX, which affect many immune cell types [29] and may contribute to the challenge of finding robust biomarkers of response using PBMC or WB samples.

Given our ultimate goal to develop biomarker tests with clinical utility, we focused on significant pathways that were consistently associated across all cell types and PBMC. By selecting the IFN-pathway genes from cell types that reached significance, we developed a robust gene score of 51 IFN-driven genes to take forward for validation. We confirmed that this score correlated with change in 3 individual outcome measures used and the ACR-DOI outcome, and we then validated our results in an independent cohort of patients ($P = .037$). We also replicated this result using the ACR-DOI tool as a dichotomous outcome in a separate independent cohort across all the cell types.

Previous studies have shown raised IFN$\alpha$- and IFN$\gamma$-driven signatures in PBMC, T cells, and monocytes from treatment-naive JIA patients, and enhanced IFN signalling in these cells taken prior to treatment, as well as greater development of Th1 or Th17 cells *in vitro*, but this signal varies between patients [30–32]. It is possible that MTX treatment is more effective in a distinct immunophenotype (present across many International League of Associations for Rheumatology subtypes), where IFN-driven processes are dominant early in the disease. New studies where the single-cell transcriptome of JIA synovial tissue is analysed and compared with matched blood will reveal whether this holds true for the tissue site itself [8,33].

We were intrigued to compare JIA with adult RA because an IFN IGS5 has been proposed as a predictor of response to DMARD treatment in RA [24]. In contrast to our study, a high baseline IFN score in RA has been shown to predict non-response to MTX [24,26] and rituximab [25]. Importantly, these RA studies were performed on WB samples; in RA, the greatest contributor to the baseline IFN score in WB prior to treatment has been shown to come from the neutrophils [34], while WB or neutrophils were not examined in our JIA cohorts. Our comparative analysis of expression of the 51-IFN-gene score and the RA IGS5 across all cell types revealed that certain genes showed the same direction of effect across time and cell types in RA as in JIA, including *FCGR1A, SOCS3,* and *SELL* (CD62L and L-selectin). However, for other genes, differences in the direction of association were observed in adult arthritis, even in the parallel cell type. These differences between adult and child arthritis may relate to underlying pathological differences between the 2 conditions, different disease duration at the start of treatment (itself a known predictor of response in JIA [35]), different magnitude of disease burden at the time of treatment start, the fact that adult RA patients frequently have a combination of DMARD therapies (MTX with hydroxychloroquine or other medications), or technical differences between these studies. This highlights the need for further investigations of treatment efficacy for children rather than extrapolation of data from adults to children with inflammatory arthritis.

Despite these differences, our findings in JIA were further confirmed when using the ACR-DOI measure to dichotomise JIA patients into responders (≥ACR50) and non-responders (Non-responder [NR] and ACR30), both for the 51 genes and the independent IGS5. For both tools, a higher score was associated with JIA responders (≥ACR50) in the discovery and validation cohorts.

Our study has some limitations. Despite the large discovery cohort and 2 replication cohorts, the analyses and necessary corrections for multiple testing mean that the study may have been underpowered to detect pathways that have a small but biologically important impact on response. Power considerations also precluded subanalyses based on the JIA subtype. In addition, WB RNA samples were not available to test whether the 51-IFN-gene score in WB is associated with response. Given the differences seen in the expression of these 51 genes between WB and PBMC in adult RA samples and prior evidence of a dysregulated neutrophil transcriptome in both pre-treatment and on-treatment JIA [36], this is an important limitation that will be key to consideration in future studies. Future studies will include not only WB and neutrophil analysis but also analysis from the tissue site, the inflamed synovium. Finally, we have shown that response to treatment can fluctuate over time [7], while this study analysed outcomes only at 1 time point (6 months).

Since we took a hypothesis-free approach at the start of this analysis, we have not yet interrogated these data for signals related to pathways known to be mechanistically impacted by MTX or those involved in the metabolism of MTX. Our previous studies [37,38] have shown that these may have effects on treatment response to MTX in JIA, meaning that such ‘candidate pathway’ analyses will be valuable to explore within these data.

Here, we have systematically interrogated the transcriptional profile of PBMC and their major constituent mononuclear cell populations for genes or pathways that may be useful in building treatment-response predictive biomarkers. Given that parents and patients report uncertainty about treatment response as a major burden and that MTX intolerance is very prevalent in JIA [4,39], the clinical value of a biomarker measured in a small blood sample that could predict response to MTX and aid clinical choices of medication would be high. Further studies are warranted to define the most cost-effective assay, using a small non-redundant gene set derived from our 51 genes, investigate if this test has utility if measured in WB, and then test such a tool in new prospective studies of JIA patients treated with MTX. Our study provides proof of principle that carefully designed analyses can yield hope for a more precision-based approach to treatment in the future for children and families living with arthritis.

## Competing interests

LRW declares consultancies with Pfizer Inc and Cabaletta unrelated to this work and research funding from Pfizer Inc for a completely separate project. The CLUSTER Consortium has had support through contributions-in-kind from GSK, Pfizer, and UCB, as well as research funding from AbbVie Inc, Lilly, and SOBI. CW receives funding from MSD and GSK and is a part-time employee of GSK. These organisations did not contribute to the planning or analysis of this work. All the other authors declare no competing interests.

## Acknowledgements

We thank all of the families, patients, parents, and carers who contributed to the study and allowed us to use their samples and data for this work. We thank the UCL Genomics Facility for sequencing, specifically Paola Niola and Tony Brooks, and the UCL Flow Cytometry Facility for cell sorting, specifically Ayad Eddaoudi, Machaela Palor, and Panagiota Constandinou. We thank the Roth Lab (Munster) for their help with quantifying the MRP8/14 protein. We acknowledge the Childhood Arthritis Response to Medication Study (CHARMS) at GOSH for the use of samples and data. We thank the clinical study team for their support in recruitment and data collection, including Klaudia Kupiec, Serena Cruickshank-Hull, Charlene Foley, and everyone in the CHARMS study group. We thank Dr Faye Cooles (University of Newcastle) and Professor Michael Barnes (QMUL) for helpful discussion and advice about IFN in response to treatment in RA and Sandra Ng (QMUL) for support with data management. We thank Dr S Thompson and Dr G Schulert (Cincinnati Children’s Hospital USA) and the team for the generation of sequence data on the CHARMS validation cohort. We are grateful to the CLUSTER champions and members of the CLUSTER Consortium, who have provided invaluable input and feedback for this work and the future dissemination of this work to patients and parents.

The data presented here have not been published before; however, some of the data formed part of a recent conference abstract at the Paediatric Rheumatology European Society Congress, 2024 [40].

## Members of the CLUSTER Consortium

Prof Lucy R Wedderburn, Ms Zoe Wanstall, Ms Vasiliki Alexiou, Mr Fatjon Dekaj, Ms Bethany R Jebson, Dr Melissa Kartawinata, Ms Aline Kimonyo, Ms Eileen Hahn, Ms Genevieve Gottschalk, Ms Freya Luling Feilding, Ms Alyssia McNeece, Ms Fatema Merali, Ms Elizabeth Ralph, Ms Emily Robinson, Ms Emma Welsh (UCL GOS Institute of Child Health, London); Prof Andrew Dick, (UCL Institute of Ophthalmology, London); Prof Michael W Beresford, Dr Emil Carlsson, Dr Joanna Fairlie, Dr Jenna F Gritzfeld, Dr Oliver McClurg, Dr Karen Rafferty (University of Liverpool); Prof Athimalaipet V Ramanan, Ms Teresa Duerr (University Hospitals Bristol and Weston NHS Foundation

Trust); Prof Michael Barnes, Ms Sandra Ng, (Queen Mary University, London); Prof Kimme Hyrich, Prof Stephen Eyre, Prof Soumya Raychaudhuri, Prof Wendy Thomson, Dr John Bowes, Ms Jeronee Jennycloss, Ms Saskia Lawson-Tovey, Dr Paul Martin, Prof Andrew Morris, Dr Stephanie Shoop-Worrall, Dr Samantha Smith, Mr Michael Stadler, Dr Damian Tarasek, Dr Melissa Tordoff, Dr Annie Yarwood (University of Manchester); Dr Chris Wallace, Dr Wei-Yu Lin (University of Cambridge); Prof Nophar Geifman (University of Surrey); Dr Sarah Clarke (School of Population Health Sciences and MRC Integrative Epidemiology Unit, University of Bristol); Dr Thierry Sornasse (AbbVie Inc); Dr Robert J Benschop, Dr Rona Wang (Eli Lilly); Daniela Dastros-Pitei MD, PhD, Sumanta Mukherjee, PhD (GlaxoSmithKline Research and Development Limited); Dr Michael McLean, Dr Anna Barkaway (Pfizer); Dr Peyman Adjamian (Swedish Orphan Biovitrum AB [Sobi]); Dr Helen Neale (UCB Biopharma SRL); The CLUSTER Champions (patient and parent representatives).

## Members of the CHARMS study group

Eslam Al-Abadi, Vicky Alexiou, Cherelle Allen, Kate Armon, Rehana Begum, Rumena Begum, Mariejennelynn Bostock, Katrin Buerkle, Charlotte Busby, Maryam Butt, Nga Sze (Emily) Cheng, Chia-Ping Chou, Joanna Cobb, Louise Coke, Julie Cook, Jenny Crook, Serena Cruickshank-Hull, Karen Davies, Lucinda Dawson, Fatjon Dekaj, Monika Dimitrova, Julie Enright, Angela Etheridge, Elizabeth (Lizzie) Fofana, Sara Foster, Sophie Foxall, Paul Gilbert, Genevieve Gottschalk, Eileen Hahn, Jeannette Hall, Daniel Hawley, Anne Hinks, Shashi Hirani, Ruth Howman, Alisha Hussein, Fatema Jeraj, Melissa Kartawinata, Laura Kassoumeri, Aline Kimonyo, Klaudia Kupiec, Sham Lal, Alice Leahy, Freya Luling Feilding, Ian MacDonald, Alyssia McNeece, Laura Melville, Halima Moncrieffe, Gudrun Moore, Kathleen Mulligan, Stanton Newman, Lucy Nguyen, Fiona Patrick, Hannah Peckham, Chadwick Pils, Elizabeth Ralph, Rachel Rikunenko, Emily Robinson, Jennie Sharp, Taunton Southwood, Jason Sowter, Mohammed Zaffar Ullah, Wendy Thomson, Simona Ursu, Hemlata Varsani, Kishore Warrier, Lucy R Wedderburn, Emma Welsh, Pamela Whitworth, Rachel Wiffen, Alexis Wormall, Patricia Woo, Brogan Wrest, and patient/parent representatives.

## Contributors

MK, W-YL, LRW, and CW conceptualised the study, analysed data, and co-wrote the manuscript. MK and W-YL contributed equally to this paper. LRW and CW led and supervised the study under the CLUSTER Consortium and obtained funding. MK, BJ, KOB, EW, and ER performed the wet laboratory experiments. MK, BJ, and EW curated the clinical data. W-YL and RR established the RNAseq pipeline. W-YL, MK, and RR performed data quality control. W-YL and CW led the statistical analyses. ECR and CTD designed and supervised parts of the study. All authors critically reviewed the manuscript and approved the final draft for submission.

## Funding

CLUSTER and this work are supported by grants from the Medical Research Council (MRC) [MR/R013926/1] and Versus Arthritis [Grant: 22084], Great Ormond Street Hospital Children's Charity [VS0518], and Olivia's Vision. This work is supported by the Wellcome Trust [WT220788], the MRC [MC UU 00002/4], the NIHR Cambridge BRC [BRC-1215-20014], and the NIHR GOSH BRC [BRC-1215-20012]. The views expressed are those of the author(s) and not necessarily those of the NHS, the NIHR, or the Department of Health. LRW is supported by Versus Arthritis [Grant: 21593] at the Centre for Adolescent Rheumatology Versus Arthritis at UCL UCLH and GOSH and an NIHR Senior Investigator award. ECR is supported by a Senior Fellowship from the Kennedy Trust for Rheumatology Research [KENN 21 22 09] and by a research prize from the Lister Institute for Preventive Medicine. BJ was supported by Fight 4 Sight Versus Arthritis PhD studentship U/24VA22 awarded to LRW and ECR. Sample and data collection were supported through the CHARMS study, funded by Sparks UK [reference 08ICH09] and the MRC [references MR/M004600/1 and MR/R013926/1]. The validation of the CHARMS JIA cohort was in part supported by the National Institute of Arthritis and Musculoskeletal and Skin Diseases of the National Institutes of Health [Grant Award Number P01AR048929]. The CLUSTER Consortium has had support through contributions-in-kind from GSK, Pfizer, and UCB, as well as research funding from AbbVie Inc, Lilly, and SOBI. These organisations did not contribute to the planning or analysis of this work.

## Patient consent for publication

Not applicable, consent provided through recruitment through ethically proved study.

## Ethics approval

This study involves human participant and ethics were approved by London-Bloomsbury Research Ethics Committee 05/Q0508/95. All participants gave informed consent and age-appropriate assent, in accordance with the Declaration of Helsinki.

## Provenance and peer review

Not commissioned; externally peer reviewed.

## Data availability statement

Data are available upon reasonable request. RNAseq FASTQ files and full core set clinical variables at t1 and t2 are available by request for data access through EGA. The EGA datasets can be found in here: EGAS50000000995 and the access request can be found here: EGAC50000000426.

Notes: EGAD50000001457 is for PBMC dataset, EGAD50000001455 is for CD4 dataset, EGAD50000001456 is for CD8 dataset, EGAD50000001458 is for CD14 dataset, and EGAD50000001459 is for CD19 dataset.

## Supplementary materials

Supplementary material associated with this article can be found in the online version at doi:10.1016/j.ard.2025.03.007.

## Orcid

Melissa Kartawinata: http://orcid.org/0000-0002-9432-393X
Wei-Yu Lin: http://orcid.org/0000-0002-9267-7988
Elizabeth Ralph: http://orcid.org/0000-0002-7955-7084
Restuadi Restuadi: http://orcid.org/0000-0001-8434-4465
Elizabeth C. Rosser: http://orcid.org/0000-0003-4800-4695
Claire T. Deakin: http://orcid.org/0000-0002-7044-5801
Lucy R. Wedderburn: http://orcid.org/0000-0002-7495-1429
Chris Wallace: http://orcid.org/0000-0001-9755-1703

## REFERENCES


[1] Petty RE, Southwood TR, Manners P, Baum J, Glass DN, Goldenberg J, et al. International League of Associations for Rheumatology Classification of juvenile idiopathic arthritis: second revision, Edmonton, 2001. J Rheumatol 2004;31(2):390–2.

[2] Glerup M, Rypdal V, Arnstad ED, Ekelund M, Peltoniemi S, Aalto K, et al. Long-term outcomes in juvenile idiopathic arthritis: eighteen years of follow-up in the population-based Nordic juvenile idiopathic arthritis cohort. Arthritis Care Res 2020;72(4):507–16. doi: 10.1002/acr.23853.

[3] Guzman J, Oen K, Huber AM, Watanabe Duffy K, Boire G, Shiff N, et al. The risk and nature of flares in juvenile idiopathic arthritis: results from the ReACCh-Out cohort. Ann Rheum Dis 2016;75(6):1092–8. doi: 10.1136/annrheumdis-2014-207164.

[4] Livermore P, Ainsworth S, Beesley R, Douglas S, Earle E, Wilson D, et al. 'The current mental health status of children and young people with JIA, and their wider family': a charity partner collaboration survey. Pediatr Rheumatol Online J 2023;21(1):111. doi: 10.1186/s12969-023-00898-5.

[5] Martini A, Lovell DJ, Albani S, Brunner HI, Hyrich KL, Thompson SD, et al. Juvenile idiopathic arthritis. Nat Rev Dis Primers 2022;8(1):5. doi: 10.1038/s41572-021-00332-8.

[6] Hinze C, Gohar F, Foell D. Management of juvenile idiopathic arthritis: hitting the target. Nat Rev Rheumatol 2015;11(5):290–300. doi: 10.1038/nrrheum.2014.212.

[7] Shoop-Worrall SJW, Lawson-Tovey S, Wedderburn LR, Hyrich KL, Geifman N, CLUSTER Consortium. Towards stratified treatment of JIA: machine learning identifies subtypes in response to methotrexate from four UK cohorts. EBioMedicine 2024;100:104946. doi: 10.1016/j.ebiom.2023.104946.

[8] Wedderburn LR, Ramanan AV, Croft AP, Hyrich KL, Dick AD, CLUSTER Consortium. Towards molecular-pathology informed clinical trials in childhood arthritis to achieve precision medicine in juvenile idiopathic arthritis. Ann Rheum Dis 2023;82(4):449–56. doi: 10.1136/ard-2022-222553.

[9] Law CW, Alhamdoosh M, Su S, Dong X, Tian L, Smyth GK, et al. RNA-seq analysis is easy as 1-2-3 with limma, Glimma and edgeR. F1000Res. 2016;5 ISCB Comm J-1408. doi: 10.12688/f1000research.9005.1.

[10] Ritchie ME, Phipson B, Wu D, Hu Y, Law CW, Shi W, et al. limma powers differential expression analyses for RNA-sequencing and microarray studies. Nucleic Acids Res 2015;43(7):e47. doi: 10.1093/nar/gkv007.

[11] Law CW, Chen Y, Shi W, Smyth GK. Voom: precision weights unlock linear model analysis tools for RNA-seq read counts. Genome Biol 2014;15(2):R29. doi: 10.1186/gb-2014-15-2-r29.

[12] Subramanian A, Tamayo P, Mootha VK, Mukherjee S, Ebert BL, Gillette MA, et al. Gene set enrichment analysis: a knowledge-based approach for interpreting genome-wide expression profiles. Proc Natl Acad Sci U S A 2005;102 (43):15545–50. doi: 10.1073/pnas.0506580102.

[13] Moncrieffe H, Bennett MF, Tsoras M, Luyrink LK, Johnson AL, Xu H, et al. Transcriptional profiles of JIA patient blood with subsequent poor response to methotrexate. Rheumatology (Oxford) 2017;56(9):1542–51. doi: 10.1093/rheumatology/kex206.

[14] RA-MAP Consortium. RA-MAP, molecular immunological landscapes in early rheumatoid arthritis and healthy vaccine recipients. Sci Data 2022;9(1):196. doi: 10.1038/s41597-022-01264-y.

[15] McErlane F, Beresford MW, Baildam EM, Chieng SE, Davidson JE, Foster HE, et al. Validity of a three-variable Juvenile Arthritis Disease Activity Score in children with new-onset juvenile idiopathic arthritis. Ann Rheum Dis 2013;72(12):1983–8. doi: 10.1136/annrheumdis-2012-202031.

[16] Giannini EH, Ruperto N, Ravelli A, Lovell DJ, Felson DT, Martini A. Preliminary definition of improvement in juvenile arthritis. Arthritis Rheum 1997;40(7):1202–9. doi: 10.1002/1529-0131(199707)40:7<1202::AID-ART3>3.0.CO;2-R.

[17] Korotkevich G, Sukhov V, Sergushichev A. fgsea: fast gene set enrichment analysis. 2023. doi: https://doi.org/10.1101/060012.

[18] Liberzon A, Birger C, Thorvaldsdóttir H, Ghandi M, Mesirov JP, Tamayo P. The Molecular Signatures Database (MSigDB) hallmark gene set collection. Cell Syst 2015;1(6):417–25. doi: 10.1016/j.cels.2015.12.004.

[19] Samarajiwa SA, Forster S, Auchettl K, Hertzog PJ. INTERFEROME: the database of interferon regulated genes. Nucleic Acids Res 2009;37(database issue):D852–7. doi: 10.1093/nar/gkn732.

[20] Lerkvaleekul B, Veldkamp SR, van der Wal MM, Schatorjé EJH, Kamphuis SSM, van den Berg JM, et al. Siglec-1 expression on monocytes is associated with the interferon signature in juvenile dermatomyositis and can predict treatment response. Rheumatology (Oxford) 2022;61(5):2144–55. doi: 10.1093/rheumatology/keab601.

[21] Graf M, von Stuckrad SL, Uruha A, Klotsche J, Zorn-Pauly L, Unterwalder N, et al. SIGLEC1 enables straightforward assessment of type I interferon activity in idiopathic inflammatory myopathies. RMD Open 2022;8(1):e001934. doi: 10.1136/rmdopen-2021-001934.

[22] Stuckrad SLV, Klotsche J, Biesen R, Lieber M, Thumfart J, Meisel C, et al. SIGLEC1 (CD169) is a sensitive biomarker for the deterioration of the clinical course in childhood systemic lupus erythematosus. Lupus 2020;29 (14):1914–25. doi: 10.1177/0961203320965699.

[23] Sakumura N, Yokoyama T, Usami M, Hosono Y, Inoue N, Matsuda Y, et al. CD169 expression on monocytes as a marker for assessing type I interferon status in pediatric inflammatory diseases. Clin Immunol 2023;250:109329. doi: 10.1016/j.clim.2023.109329.

[24] Cooles FAH, Anderson AE, Lendrem DW, Norris J, Pratt AG, Hilkens CMU, et al. The interferon gene signature is increased in patients with early treatment-naive rheumatoid arthritis and predicts a poorer response to initial therapy. J Allergy Clin Immunol 2018;141(1) 445-8.e4. doi: 10.1016/j.jaci.2017.08.026.

[25] Cooles FAH, Isaacs JD. The interferon gene signature as a clinically relevant biomarker in autoimmune rheumatic disease. Lancet Rheumatol 2022;4(1): e61–72. doi: 10.1016/S2665-9913(21)00254-X.

[26] Plant D, Maciejewski M, Smith S, Nair N, Maximising Therapeutic Utility in Rheumatoid Arthritis Consortium, the RAMS Study Group, et al. Profiling of gene expression biomarkers as a classifier of methotrexate nonresponse in patients with rheumatoid arthritis. Arthritis Rheumatol. 2019;71(5):678-84. doi:10.1002/art.40810

[27] Moncrieffe H, Ursu S, Holzinger D, Patrick F, Kassoumeri L, Wade A, et al. A subgroup of juvenile idiopathic arthritis patients who respond well to methotrexate are identified by the serum biomarker MRP8/14 protein. Rheumatology (Oxford) 2013;52(8):1467–76. doi: 10.1093/rheumatology/ket152.

[28] Moncrieffe H, Hinks A, Ursu S, Kassoumeri L, Etheridge A, Hubank M, et al. Generation of novel pharmacogenomic candidates in response to methotrexate in juvenile idiopathic arthritis: correlation between gene expression and genotype. Pharmacogenet Genomics 2010;20(11):665–76. doi: 10.1097/FPC.0b013e32833f2cd0.

[29] Brown PM, Pratt AG, Isaacs JD. Mechanism of action of methotrexate in rheumatoid arthritis, and the search for biomarkers. Nat Rev Rheumatol 2016;12 (12):731–42. doi: 10.1038/nrrheum.2016.175.

[30] Throm AA, Moncrieffe H, Orandi AB, Pingel JT, Geurs TL, Miller HL, et al. Identification of enhanced IFN-$\gamma$ signaling in polyarticular juvenile idiopathic arthritis with mass cytometry. JCI Insight 2018;3(15):e121544. doi: 10.1172/jci.insight.121544.

[31] De Nardi L, Pastore S, Rispoli F, Tesser A, Pin A, Taddio A, et al. Type I interferon signature as a possible new marker for stratification of patients with juvenile idiopathic arthritis. Clin Exp Rheumatol 2023;41(7):1548–52. doi: 10.55563/clinexprheumatol/b37xbd.

[32] Patrick AE, Shoaff K, Esmond T, Patrick DM, Flaherty DK, Graham TB, et al. Increased development of Th1, Th17, and Th1.17 cells under T1 polarizing conditions in juvenile idiopathic arthritis. Front Immunol 2022;13:848168. doi: 10.3389/fimmu.2022.848168.

[33] Bolton C, Mahony C, Smith C, Alexiou V, Nguyen H, Reis-Nisa P, et al. Inflammatory arthritis across the age-spectrum: single-cell profiling of the inflamed synovium in children with juvenile idiopathic arthritis. Arthritis Rheumatol 2023;75(Suppl 9).

[34] de Jong TD, Lübbers J, Turk S, Vosslamber S, Mantel E, Bontkes HJ, et al. The type I interferon signature in leukocyte subsets from peripheral blood of patients with early arthritis: a major contribution by granulocytes. Arthritis Res Ther 2016;18:165. doi: 10.1186/s13075-016-1065-3.

[35] Albers HM, Wessels JA, van der Straaten RJ, Brinkman DM, Suijlekom-Smit LW, Kamphuis SS, et al. Time to treatment as an important factor for the response to methotrexate in juvenile idiopathic arthritis. Arthritis Rheum 2009;61(1):46–51. doi: 10.1002/art.24087.

[36] Du N, Jiang K, Sawle AD, Frank MB, Wallace CA, Zhang A, et al. Dynamic tracking of functional gene modules in treated juvenile idiopathic arthritis. Genome Med 2015;7:109. doi: 10.1186/s13073-015-0227-2.

[37] Hinks A, Moncrieffe H, Martin P, Ursu S, Lal S, Kassoumeri L, et al. Association of the 5-aminoimidazole-4-carboxamide ribonucleotide transformylase gene with response to methotrexate in juvenile idiopathic arthritis. Ann Rheum Dis 2011;70(8):1395–400. doi: 10.1136/ard.2010.146191.

[38] Hawwa AF, Albawab A, Rooney M, Wedderburn LR, Beresford MW, McElnay JC. A novel dried blood spot-LCMS method for the quantification of methotrexate polyglutamates as a potential marker for methotrexate use in children. PLoS One 2014;9(2):e89908. doi: 10.1371/journal.pone.0089908.

[39] Mulligan K, Kassoumeri L, Etheridge A, Moncrieffe H, Wedderburn LR, Newman S. Mothers' reports of the difficulties that their children experience in taking methotrexate for juvenile idiopathic arthritis and how these impact on quality of life. Pediatr Rheumatol Online J 2013;11(1):23. doi: 10.1186/1546-0096-11-23.

[40] Kartawinata M, Lin W-Y, Jebson B, O'Brien K, Ralph E, Restuadi R, et al. P180 Interferon pathways are associated with the response to methotrexate treatment in juvenile idiopathic arthritis. In: Proceedings of the 31st European Paediatric Rheumatology Congress: part 2. Pediatr Rheumatol. 2024;22 Suppl 2:PReS24-ABS-1280. https://doi.org/10.1186/s12969-024-01005-y.

Ann Rheum Dis 84 (2025) 1425–1436

Contents lists available at ScienceDirect

Annals of the Rheumatic Diseases

journal homepage: https://www.sciencedirect.com/journal/annals-of-the-rheumatic-diseases

Paediatric rheumatology

# Physician's global assessment of disease activity in juvenile idiopathic arthritis: consensus-based recommendations from an international task force

Veronika Rypdal[1,2,*], Hermine I. Brunner[3], Brian M. Feldman[4], Nicolino Ruperto[5,6], Amita Aggarwal[7], Sheila T. Angeles-Han[3], Maria Backström[8,9], Erin Balay-Dustrude[10,11], Claudia Bracaglia[12], Fabrizio De Benedetti[12], Pavla Doležalová[13,14], Marco Garrone[15], Jaime Guzman[16], Daniel B. Horton[17,18,19], Ronald M. Laxer[4], Daniel J. Lovell[3], Tonje Løvli[1], Silvia Magni-Manzoni[20], Francesca Minoia[21], Esi M. Morgan[10,11], Jane Munro[22], Ellen B. Nordal[1,2], Christophe Normand[23], Nancy Pan[24], Elisa Patrone[15], Angelo Ravelli[25,26], Claudia Saad Magalhães[27], Rashmi Sinha[28], Joost F. Swart[29], Maarit Tarkiainen[30], Marinka Twilt[31], Paula Vähäsalo[32], Sebastiaan Vastert[29], Jelena Vojinovic[33], Pamela F. Weiss[34,35], Beth Gottlieb[36], Alessandro Consolaro[26,37], For the Pediatric Rheumatology European Society, the Paediatric Rheumatology International Trials Organisation, the Pediatric Rheumatology Care & Outcome Improvement Network, and the Pediatric Rheumatology Collaborative Study Group

[1] *Department of Pediatrics, University Hospital of North Norway, Tromsø, Norway*
[2] *Department of Clinical Medicine, UIT the Arctic University of Norway, Tromsø, Norway*
[3] *Division of Rheumatology, Cincinnati Children's Hospital Medical Center, Department of Pediatrics University of Cincinnati, Cincinnati, OH, USA*
[4] *The Hospital for Sick Children, University of Toronto, Toronto, ON, Canada*
[5] *Università Milano Bicocca, Milan, Italy*
[6] *IRCCS Fondazione San Gerardo dei Tintori, Clinica Pediatrica Fondazione PRINTO, Monza, Italy*
[7] *Department of Clinical Immunology and Rheumatology, Sanjay Gandhi Postgraduate Institute of Medical Sciences, Lucknow, India*
[8] *Department of Pediatrics, The Wellbeing Services County of Ostrobothnia, Vaasa, Finland*
[9] *Research Unit of Clinical Medicine, University of Oulu, Oulu, Finland*
[10] *Department of Pediatrics, Division of Rheumatology, University of Washington, Seattle, WA, USA*
[11] *Department of Pediatric Rheumatology, Seattle Children's Hospital and Research Center, Seattle, WA, USA*
[12] *Division of Rheumatology, IRCCS Ospedale Pediatrico Bambino Gesù Roma, Rome, Italy*
[13] *Centre for Paediatric Rheumatology and Autoinflammatory Diseases ERN-RITA, Department of Paediatrics and Inherited Metabolic Disorders, General University Hospital, Prague, Czech Republic*
[14] *1st Faculty of Medicine, Charles University in Prague, Prague, Czech Republic*

*Correspondence to Dr Veronika Rypdal, Department of Pediatrics, University Hospital of North Norway; Department of Clinical Medicine, UIT the Arctic University of Norway, Tromsø, Norway.

*E-mail address:* veronika.rypdal@unn.no (V. Rypdal).

**Handling editor** Josef Smolen.

https://doi.org/10.1016/j.ard.2025.01.013

0003-4967/© 2025 European Alliance of Associations for Rheumatology (EULAR). Published by Elsevier B.V. All rights are reserved, including those for text and data mining, AI training, and similar technologies.

[15] IRCCS Istituto Giannina Gaslini, UOC Gaslini Trial Centre/Servizio di Sperimentazioni Cliniche Pediatriche, Genoa, Italy
[16] Division of Pediatric Rheumatology, University of British Columbia, Vancouver, BC, Canada
[17] Division of Pediatric Rheumatology, Department of Pediatrics, Rutgers Robert Wood Johnson Medical School, New Brunswick, NJ, USA
[18] Center for Pharmacoepidemiology and Treatment Science, Institute for Health, Health Care Policy and Aging Reaserch, New Brunswick, NJ, USA
[19] Department of Biostatistics and Epidemiology, Rutgers School of Public Health, Piscataway, NJ, USA
[20] Division of Rheumatology, Istituto di Ricovero e Cura a Carattere Scientifico Ospedale Pediatrico Bambino Gesù, Rome, Italy
[21] Pediatric Immuno-Rheumatology Unit, Fondazione IRCSS Ca' Granda Ospedale Maggiore Policlinico, Milan, Italy
[22] Rheumatology Service, Department of General Medicine, Royal Children's Hospital, Melbourne Victoria and Murdoch Children's Research Institute, Melbourne, VIC, Australia
[23] ENCA, The Global Foundation for Children, and Families, with Rheumatic and Musculoskeletal Conditions, and KOURIR, Paris, France
[24] Division of Pediatric Rheumatology, Hospital for Special Surgery, Department of Pediatrics, Weill Medical College of Cornell University, New York, NY, USA
[25] Dipartimento di Neuroscienze, Riabilitazione, Oftalmologia, Genetica e Scienze Materno Infantili (DINOGMI), Università degli Studi di Genova, Genoa, Italy
[26] IRCCS Istituto Giannina Gaslini, Genoa, Italy
[27] São Paulo State University (UNESP), Botucatu, São Paulo, Brazil
[28] Systemic JIA Foundation, Cincinnati, OH, USA
[29] Wilhelmina Children's Hospital, University Medical Center Utrecht and University of Utrecht, Utrecht, The Netherlands
[30] Pediatric Research Center, Helsinki University Hospital and University of Helsinki, New Children's Hospital, Helsinki, Finland
[31] Department of Pediatrics, Alberta Children's Hospital, Cumming School of Medicine, University of Calgary, Calgary, AB, Canada
[32] Research Unit of Clinical Medicine, University of Oulu; Department of Children and Adolescents, Oulu University Hospital; and Medical Research Center, Oulu University Hospital and University of Oulu, Oulu, Finland
[33] University of Nis, Faculty of Medicine, Clinic for Pediatrics, University Clinical Center Nis, Nis, Serbia
[34] Division of Rheumatology and Clinical Futures, Children's Hospital of Philadelphia, Philadelphia, PA, USA
[35] Center for Clinical Epidemiology and Biostatistics, Perelman School of Medicine at the University of Pennsylvania, Philadelphia, PA, USA
[36] Northwell Health, Cohen Children's Medical Center, Division of Pediatric Rheumatology, New Hyde Park, NY, USA
[37] Università degli Studi di Genova, Genova, Italy

ARTICLE INFO

ABSTRACT

*Objectives:* To develop consensus-based recommendations for physician's global assessment of disease activity (PhGA) scoring and to standardise definitions of disease activity.
*Methods:* An international task force of 34 members was assembled, and recommendations were developed in 3 phases: (1) 2 preliminary surveys of paediatric rheumatologists and a literature review; (2) 14 videoconference meetings, informed by multicriteria decision analysis and formal anonymous voting; and (3) a 2-day in-person consensus conference using structured nominal group technique discussions and formal voting. The threshold for achieving consensus was ≥78% of voting task force members. Agreement with the final statements was rated using a numerical rating scale from 0, strongly disagree, to 10, strongly agree.
*Results:* Eighteen points to consider were agreed upon. All statements achieved consensus (≥78%), with a level of agreement ≥9.2. Points included the definition of disease activity in juvenile idiopathic arthritis (JIA), factors to assess in nonsystemic JIA and systemic JIA, consideration of available imaging and laboratory tests, the role of extra-articular manifestations, the evaluation of treatment, and the timing of PhGA scoring.
*Conclusions:* The task force developed consensus-based recommendations when scoring the PhGA in nonsystemic and systemic JIA. These recommendations will lead to more reliable scoring of disease activity in patients with JIA.

## INTRODUCTION

Juvenile idiopathic arthritis (JIA) is the most common rheumatic disease in childhood [1]. The treatment goal for JIA is inactive disease or at least minimal disease activity. To assess disease activity and treatment efficacy, standardised and validated JIA disease activity measures are needed [2]. The physician's global assessment of disease activity (PhGA) is a frequently used outcome measure in JIA for which a physician scores the level of the child's overall disease activity on a 10-cm linear visual analogue scale (VAS) or on a 21-circle numeric rating scale [3,4], with anchors of '0 = no activity', and '10 = maximum activity'. The PhGA can be used as a single outcome measure or in a composite disease activity score [5,6]. The PhGA is also used for defining clinical inactive disease in JIA [2,5,7–9]. Moreover, it is part of the American College of

**WHAT IS ALREADY KNOWN ON THIS TOPIC**

- The physician's global assessment of disease activity (PhGA) is a commonly used tool by paediatric rheumatologist for the evaluation of disease activity in patients with juvenile idiopathic arthritis (JIA).
- Studies have shown that the PhGA lacks standardisation in its scoring.
- Currently, there are not any available recommendations for the treating physician on how to score the PhGA.

**WHAT THIS STUDY ADDS**

- An international task force was convened with the aim to develop and validate guidelines for a more standardised way of scoring the physician global in JIA.
- The main objective for our task force was to help the worldwide paediatric rheumatology community to use this tool consistently with the purpose of enhancing the comparability of disease activity measures obtained by different physicians and international clinical trials in JIA.

**THIS STUDY MIGHT AFFECT RESEARCH AND PRACTICE**

- We identified 18 points to consider when scoring the PhGA, including disease activity definition in JIA and factors affecting the scoring of the PhGA in nonsystemic JIA and systemic JIA.
- The work might need to be refined along with the improvement of our knowledge of what disease activity in JIA is, and we will need to validate the recommendations to see if they improve the consistency of the PhGA scoring.

Rheumatology (ACR) JIA response criteria [10], which is the primary outcome in clinical trials of Disease-modifying antirheumatic drugs (DMARDs) in JIA [11].

The PhGA is the physician's subjective appraisal of the patient's disease activity at the time of the visit. Until now, there are no guidelines on which information should be considered and integrated when scoring the PhGA. Studies have shown that physicians often avoid scoring a PhGA as 0 and that the score may be influenced by patient symptoms other than inflammation [12,13]. A multinational survey among members of the Pediatric Rheumatology International Trials Organisation (PRINTO) and the Pediatric Rheumatology Care & Outcome Improvement Network (PR-COIN) identified features of JIA considered when scoring the PhGA and showed that the PhGA is not scored reliably [14–16], emphasising the need for establishing guidance on how to score the PhGA.

Standardised definitions of disease activity, extra-articular manifestations, and comorbidities are necessary to assess the efficacy of treatment in clinical settings, trials, and observational studies and may improve the consistency of the PhGA scoring. An international task force was launched in June 2023 with the aim of securing a more reliable and standardised scoring of disease activity in JIA.

## METHODS

The task force leads (VR and AC) assembled the group by inviting experienced clinicians and researcher's members of paediatric rheumatology associations involved in outcome measures research (Table 1). Delegates from the United States, Canada, Australia, Brazil, India, and 7 countries in Europe were represented. A patient representative (CN), a paediatric rheumatology nurse (TL), and 2 research assistants also participated. The standardised operating procedure recommendations provided by the European Alliance of Associations for Rheumatology (EULAR) were followed where applicable for this task [17,18].

Table 1
**Paediatric rheumatology associations represented by the task force members**

| |
|---|
| Childhood Arthritis and Rheumatology Research Alliance (CARRA) |
| Canadian Alliance of Pediatric Rheumatology Investigators (CAPRI) |
| European Network for Children with Arthritis (ENCA) |
| Outcome measures in Rheumatology (OMERACT) JIA Working group |
| Pediatric Rheumatology Care & Outcome Improvement Network (PR-COIN) |
| Pediatric Rheumatology Collaborative Study Group (PRCSG) |
| Pediatric Rheumatology European Association (PReS) |
| JIA, sJIA, and imaging working parties |
| Pediatric Rheumatology International Trials Organization (PRINTO) |

JIA, juvenile idiopathic arthritis; sJIA, systemic juvenile idiopathic arthritis.

Work proceeded in 3 phases described below and summarised in Figure 1.

### *Phase 1*

Through web-based surveys of PRINTO and PR-COIN members, rheumatology clinicians were asked to (1) identify factors considered when scoring the PhGA, (2) score clinical patient vignettes, and (3) rank factors influencing PhGA in order of importance [14]. The results from these 2 surveys are published [14,16].

A literature review in PubMed with the search strings ('physician global assessment' or 'MD global assessment') and 'arthritis' was performed in Autumn 2023 by task force members (EBD, MTa, AC).

### *Phase 2*

Between November 2023 and February 2024, regular task force online meetings were held (Fig 1). After discussion of literature review results by the task force, the first aim was to agree on a consensus working definition of disease activity in JIA, and on the use of multicriteria decision analysis (MCDA) with the 1000minds software (1000minds Ltd) [19]. MCDA rank factors considered when scoring the PhGA and calculates the relative importance of each factor weighted in relation to the others [20,21]. Figure 2 shows an example of one MCDA trade-off question generated by the software. A subgroup of the task force developed 2 1000minds surveys, including 1 for nonsystemic JIA and 1 for systemic JIA. The process was discussed with the whole task force, and surveys were refined based on feedback. The whole task force was asked to complete each survey.

Factors obtaining a relative importance >5% in MCDA (Tables 2 and 3) were voted on by the task force before the in-person consensus conference, whereas factors with ranks ≤4 by ≥78% of the task force were proposed for voting on exclusion.

During subsequent online meetings, drafted statements based on the results of the 1000minds exercise were discussed, refined, and then voted upon by the task force. Statements with >80% agreement were considered final; statements that did not achieve consensus in the preliminary votes, or factors that had a high variability of the mean rank or considered controversial, were discussed at the in-person consensus conference.

### *Phase 3*

At the consensus conference in Tromsø, Norway, on March 14 and 15, 2024, 30 task force members were randomly divided

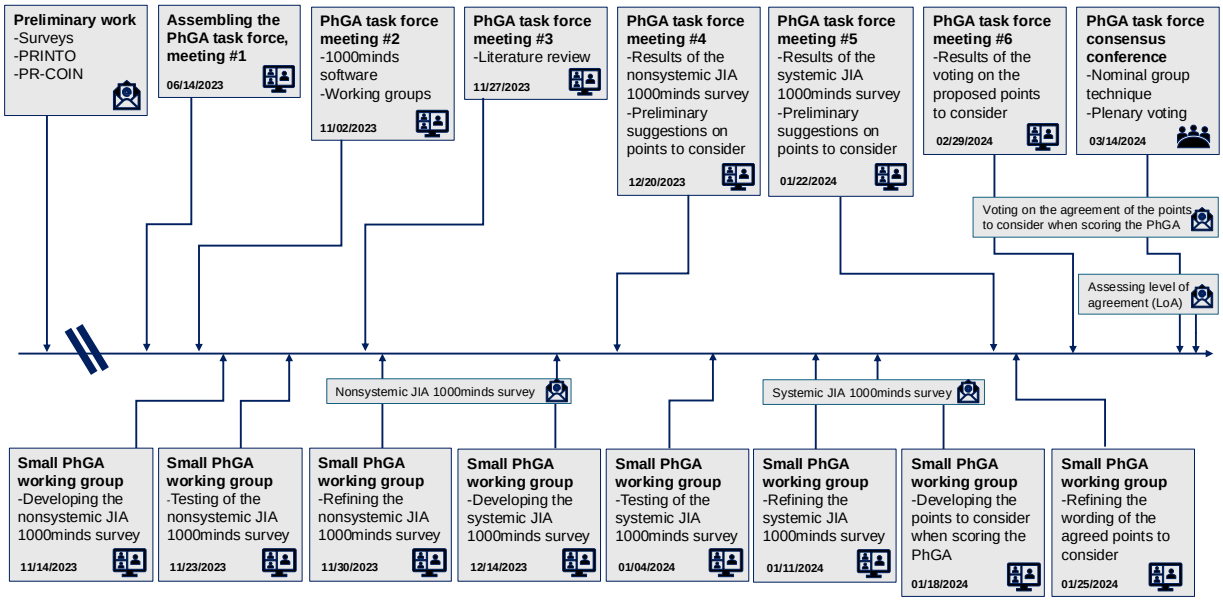



**Figure 1.** Timeline for the working process towards a more standardised way of scoring the physician's global assessment of disease activity (PhGA). From the fall of 2023 to the spring of 2024 the PhGA task force systematically worked towards the achievement of consensus-based statements when scoring the PhGA in juvenile idiopathic arthritis (JIA). PR-COIN, Pediatric Rheumatology Care & Outcome Improvement Network; PRINTO, Pediatric Rheumatology International Trials Organisation.

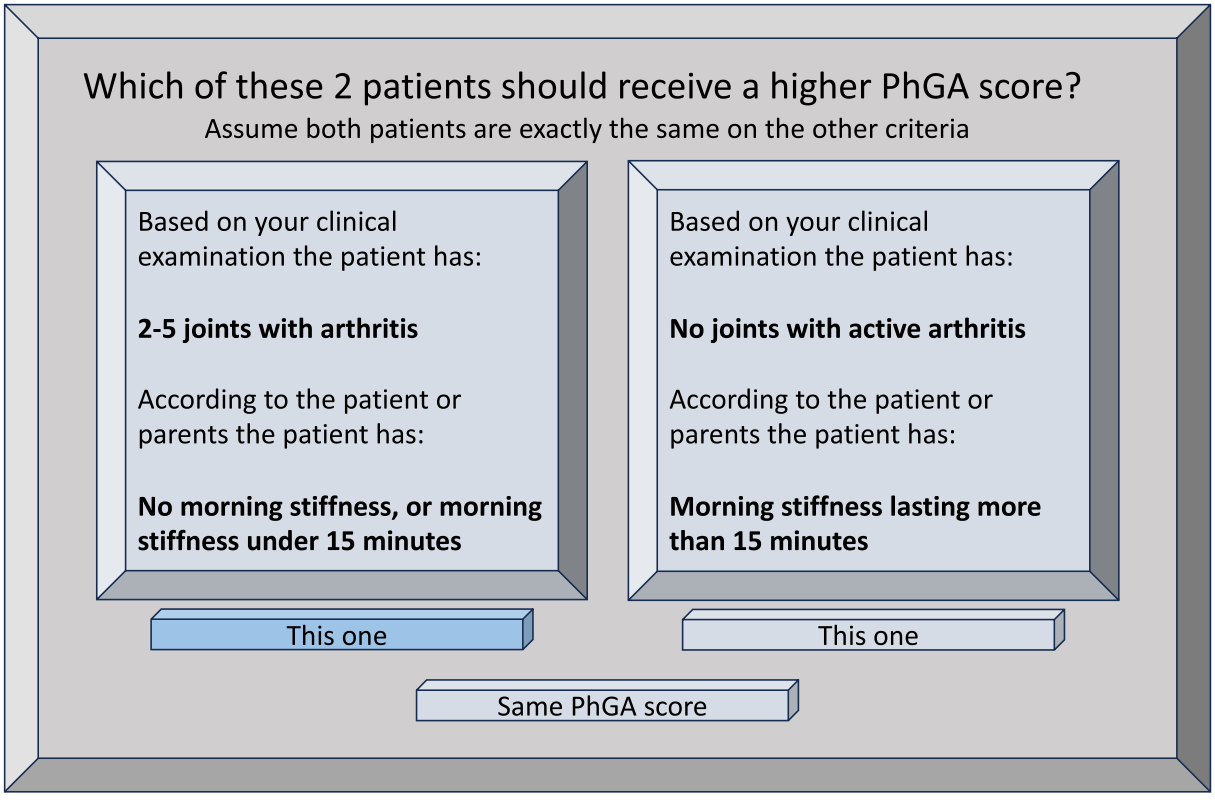



**Figure 2. Illustration of a possible trade-off question generated by the 1000minds software.** The 1000minds software uses the Potentially All Pairwise Rankings of all possible Alternatives (PAPRIKA) method for multiple-criteria decision making. PAPRIKA involves participants making a series of choices between 2 hypothetical alternatives that contrast the trade-offs between 2 features at the time. In our case, which of the 2 case vignettes presented should have a higher score in the physician's global assessment of disease activity (PhGA)? The questions are repeated with different pairs of hypothetical alternatives defined on different combinations of the criteria and levels until preferences are captured. The composition of trade-offs is selected adaptively by the 1000minds software as they are answered, with the number of trade-offs per responder being variable depending on the consistency of the answers. For the current task, criteria were the factors to be considered when scoring the PhGA and alternatives where the increasing levels of disease activity according to a criterion. In this example: 'Based on your clinical examination the patient has 2 to 5 joints with arthritis' is a Criterion A and Level 3, whereas 'According to the patient or parents the patient has no morning stiffness, or morning stiffness under 15 minutes' is a Criterion B and a Level 1. 'Based on your clinical examination the patient has no joints with active arthritis' is a Criterion A and Level 1, and 'According to the patient or parents the patient has morning stiffness lasting more than 15 minutes' is a Criterion B and Level 2.

Table 2
**The task force assessment of the relative importance and ranking of factors evaluated for the scoring of the physician's global assessment of disease activity (PhGA) in nonsystemic juvenile idiopathic arthritis (JIA) using multicriteria decision analysis (n = 31)**

| Factors | Relative importance of the factors (%)[a] | Median rank | Mean ± SD | Ranked 1st to 4th, n (%) | Ranked 8th to 11th, n (%) | Ranked 1 | Ranked 2 | Ranked 3 | Ranked 4 | Normalised factors weights[b] |
|---|---|---|---|---|---|---|---|---|---|---|
| Number of active joints | 25.3 | 1.5 | 1.7 ± 0.9 | 30 (96.8) | 0 | 16 | 12 | 1 | 1 | 0.253 |
| Imaging | 23.4 | 2.0 | 2.0 ± 1.1 | 30 (96.8) | 0 | 14 | 8 | 7 | 1 | 0.234 |
| Degree of joint inflammation | 11.8 | 4.0 | 3.9 ± 1.8 | 22 (71.0) | 2 (6.5) | 1 | 7 | 7 | 7 | 0.118 |
| Active uveitis | 7.9 | 5.5 | 6.0 ± 3.2 | 15 (48.4) | 10 (32.3) | 3 | 2 | 5 | 5 | 0.079 |
| Activity limitations[c] | 7.5 | 6.0 | 5.7 ± 2.0 | 12 (38.7) | 6 (19.4) | 0 | 1 | 2 | 9 | 0.075 |
| Enthesitis | 5.4 | 6.0 | 6.3 ± 2.0 | 10 (32.3) | 7 (22.6) | 0 | 1 | 2 | 7 | 0.054 |
| Tenosynovitis | 5.3 | 6.0 | 6.4 ± 1.8 | 5 (16.1) | 7 (22.6) | 0 | 0 | 1 | 4 | 0.053 |
| Psoriasis | 4.5 | 8.5 | 7.8 ± 2.7 | 5 (16.1) | 18 (58.1) | 0 | 3 | 1 | 1 | 0.045 |
| Patients' disease course | 3.6 | 9.0 | 8.4 ± 2.3 | 2 (6.5) | 20 (64.5) | 0 | 0 | 1 | 1 | 0.036 |
| Laboratory markers[d] | 2.8 | 9.5 | 8.9 ± 1.9 | 1 (3.2) | 23 (74.2) | 0 | 0 | 0 | 1 | 0.028 |
| Morning stiffness | 2.6 | 9.0 | 8.9 ± 1.7 | 0 | 23 (74.2) | 0 | 0 | 0 | 0 | 0.026 |

[a] Relative importance of the factors based on the mean values summed up to 100.
[b] Relationship between the relative importance of the factor, and the degree of performance (ie, the weights on the criteria sum to 1).
[c] Activity limitations due to active arthritis.
[d] Laboratory markers of inflammation.

into 3 nominal group technique (NGT) tables (to avoid grouping bias), each led by a moderator experienced in conducting clinical trials and consensus conferences in JIA (HIB, BMF, NR). The moderators were not allowed to vote at the consensus conference due to their role; therefore, the number of voting members at the meeting was 27. For each table, the threshold for consensus was set at 7 of 9 (78%), and 21 of 27 (78%) for plenary votes with the entire task force. Discussion according to the NGT [22] took place at each table regarding the specific topic to address; in cases where consensus on an initial statement was not achieved, the wording was reformulated, with majority votes if controversy arose. The results from the NGT tables were reported to the whole task force in plenary sessions where discussions of the proposals were followed by voting on the revised statements using an anonymised poll software [23]. Statements that achieved an agreement of at least 78% were accepted as final; statements that did not reach consensus were rediscussed, reformulated, and revoted on, until a ≥78% consensus was attained. If after several attempts consensus was not achieved, the statement was discarded. After the consensus conference, all task force members were asked to adjudicate, via e-mail, their level of agreement (LoA) with each recommendation on a 0 to 10 scale (0 = no agreement at all; 10 = full agreement).

## RESULTS

### *Literature review*

The PhGA was originally adopted as an outcome measure in rheumatoid arthritis (RA) and JIA clinical trials in the early 1980s [24–29]. The initial version consisted of a 5-point ordinal scale measuring disease activity from 'asymptomatic' to 'very severe'. Later, a linear VAS (100 mm) became the most widely adopted form, based on the work of Huskisson [30]. More recently, a horizontal scale of 21 squares or circles in 0.5-unit increments was suggested to replace the linear scale to avoid the need for a ruler and the possible distortion of the line length [3,4]. The PhGA became a key outcome measure; included in the RA ACR preliminary core set of disease activity measures for clinical trials in 1993 [31] and in the JIA ACR paediatric core set in 1997 [10,32].

The PhGA in its different formats include a statement such as 'What is your assessment of the patient's current disease activity?' However, various versions of this statement were adopted in different studies and the literature review failed to yield guidelines on how to complete the PhGA. In most recent JIA clinical trials, the standard PRINTO/Pediatric Rheumatology Collaborative Study Group (PRCSG) joint assessment form uses the 21-circle VAS and the anchors no activity (0), maximum activity (10). In other studies, the statement introducing the tool was 'considering the whole signs and symptoms of the disease at the time of the present visit, please rate the overall level of disease activity by marking a circle'.

Because there were no published recommendations on how to score the PhGA in JIA and the level of evidence for the development of the PhGA was scarce, the task force agreed to present the recommendations as points to consider when scoring the PhGA.

### *Points to consider when scoring the PhGA in patients with JIA*

The factors included in the general statement on disease activity and the statements for nonsystemic JIA and systemic JIA are shown in Tables 2 and 3, respectively. Table 4 lists the

Table 3

**The task force assessment of the relative importance and ranking of factors evaluated for the scoring of the physician's global assessment of disease activity (PhGA) in systemic juvenile idiopathic arthritis (JIA) using multicriteria decision analysis (n = 32)**

| Factors | Relative importance of the factors (%)[a] | Median rank | Mean ± SD | Ranked 1st to 4th, n (%) | Ranked 13th to 17th, n (%) | Ranked 1 | Ranked 2 | Ranked 3 | Ranked 4 | Normalised factors weights[b] |
|---|---|---|---|---|---|---|---|---|---|---|
| MAS | 19.1 | 1.0 | 1.1 ± 0.3 | 32 (100) | 0 | 30 | 2 | 0 | 0 | 0.191 |
| Interstitial lung disease | 9.9 | 3.0 | 3.9 ± 2.6 | 25 (78.1) | 0 | 2 | 14 | 6 | 3 | 0.099 |
| Imaging | 8.7 | 5.0 | 5.6 ± 2.7 | 15 (46.9) | 0 | 1 | 6 | 6 | 2 | 0.087 |
| Number of active joints | 8.4 | 5.0 | 5.6 ± 2.3 | 16 (50.0) | 1 (3.1) | 0 | 4 | 4 | 8 | 0.084 |
| Fever | 7.2 | 5.8 | 6.0 ± 2.7 | 12 (37.5) | 0 | 0 | 4 | 3 | 5 | 0.072 |
| Degree of joint inflammation | 7.1 | 6.5 | 7.3 ± 3.8 | 12 (37.5) | 2 (6.3) | 0 | 2 | 5 | 5 | 0.071 |
| Serositis | 6.8 | 7.0 | 7.0 ± 3.3 | 13 (40.6) | 0 | 0 | 4 | 4 | 5 | 0.068 |
| Laboratory markers[c] | 5.7 | 8.2 | 8.0 ± 2.6 | 7 (21.9) | 0 | 0 | 1 | 2 | 4 | 0.057 |
| Activity limitations[d] | 5.5 | 9.0 | 8.5 ± 3.6 | 8 (25.0) | 2 (6.3) | 1 | 2 | 2 | 3 | 0.055 |
| Hepatomegaly and/or splenomegaly | 5.5 | 9.2 | 8.6 ± 3.8 | 10 (31.3) | 5 (15.6) | 0 | 4 | 2 | 4 | 0.055 |
| Rash | 4.5 | 9.2 | 9.3 ± 2.7 | 2 (6.3) | 3 (9.4) | 0 | 0 | 0 | 2 | 0.045 |
| Generalised lymphadenopathy | 4.3 | 10.5 | 10.0 ± 3.0 | 1 (3.1) | 6 (18.8) | 0 | 1 | 0 | 0 | 0.043 |
| Patient's disease course | 2.2 | 13.5 | 12.8 ± 2.6 | 0 | 20 (62.5) | 0 | 0 | 0 | 0 | 0.022 |
| Morning stiffness | 1.8 | 13.0 | 13.6 ± 2.0 | 0 | 23 (71.9) | 0 | 0 | 0 | 0 | 0.018 |
| History of interstitial lung disease | 1.5 | 15.5 | 14.6 ± 2.4 | 0 | 26 (81.3) | 0 | 0 | 0 | 0 | 0.015 |
| History of MAS | 1.1 | 16.0 | 15.2 ± 1.8 | 0 | 31 (96.9) | 0 | 0 | 0 | 0 | 0.011 |
| Therapy | 0.8 | 16.0 | 15.8 ± 1.1 | 0 | 30 (93.8) | 0 | 0 | 0 | 0 | 0.008 |

MAS, macrophage activation syndrome.

[a] Relative importance of the factors based on the mean values summed up to 100.

[b] Relationship between the relative importance of the factor, and the degree of performance (ie, the weights on the criteria sum to 1).

[c] Laboratory markers of inflammation.

[d] Activity limitations due to active arthritis.

Table 4
**Recommendations for scoring of the physician's global assessment of disease activity (PhGA) in juvenile idiopathic arthritis (JIA)**

| Points to consider when scoring the PhGA | Participants voting (n) | Agreement votes (%) | Mean ± SD level of agreement[a] |
|---|---|---|---|
| 1. Disease activity definition in JIA | | | |
| 1.1 Disease activity reflects the aspects of the disease related to the pathophysiology that can be reversible with treatment and can worsen with a disease flare. | 27 | 81.5 | 9.8 ± 0.6 |
| 1.2 Disease activity is different from disease damage, with the latter reflecting long-standing, potentially irreversible changes. | 27 | 100 | 9.9 ± 0.4 |
| 1.3 Evaluation of disease activity should not include findings known or suspected to be due to another disease process, eg, comorbidities[b], or side effects of JIA treatment. | 27 | 92.6 | 9.5 ± 1.0 |
| 2. Nonsystemic JIA | | | |
| 2.1 The PhGA quantifies JIA activity based on the number of joints with arthritis and their degree of inflammation, the number of sites with tenosynovitis and/or enthesitis, and resultant activity limitations due to inflammation. | 32 | 87.5 | 9.8 ± 0.5 |
| 2.2 The PhGA should be scored at the end of the clinical evaluation, and all information available at that time, including imaging results, should be considered. | 27 | 85.2 | 9.6 ± 1.0 |
| 2.3 The PhGA should be scored at the end of the clinical evaluation, and all information available at that time, including relevant laboratory test results, should be considered. | 27 | 81.5 | 9.8 ± 0.5 |
| 2.4 The clinical evaluation should be completed on the day of the visit. | 27 | 88.9 | 9.3 ± 1.5 |
| 2.5 Uveitis may be an extra-articular manifestation of JIA. When this is the case, the presence and extent of active uveitis should be considered when scoring the PhGA. | 27 | 100 | 9.4 ± 1.7 |
| 2.6 Psoriasis may be an extra-articular manifestation of JIA. When this is the case, the presence and extent of active psoriasis should be considered when scoring the PhGA. | 27 | 88.9 | 9.3 ± 1.7 |
| 2.7 When scoring the PhGA, consider only the current patient presentation, and not the prior disease activity or disease course. | 32 | 96.9 | 9.8 ± 0.5 |
| 2.8 Treatment should not be considered when scoring the PhGA in nonsystemic JIA. | 19[c] | 100 | 9.7 ± 1.6 |
| 3. Systemic JIA | | | |
| 3.1 The PhGA quantifies systemic JIA activity based on the presence and extent of systemic features such as fever, serositis, hepatosplenomegaly, generalised lymphadenopathy, rash, and on the number of joints with arthritis, their degree of inflammation, and resultant activity limitations due to inflammation. | 31[d] | 83.9 | 9.6 ± 0.7 |
| 3.2 The PhGA should be scored at the end of the clinical evaluation, and all information available at that time, including imaging results, should be considered. | 27 | 85.2 | 9.6 ± 0.8 |
| 3.3 The PhGA should be scored at the end of the clinical evaluation, and all information available at that time, including relevant laboratory test results, should be considered. | 27 | 81.5 | 9.9 ± 0.3 |
| 3.4 The clinical evaluation should be completed on the day of the visit. | 27 | 88.9 | 9.2 ± 1.4 |
| 3.5 The presence of MAS and/or active ILD should be considered when scoring the PhGA. | 31[d] | 96.8 | 9.8 ± 0.5 |
| 3.6 When scoring the PhGA, consider only the current patient presentation, and not the prior disease activity or disease course or history of MAS and/or ILD. | 31[d] | 93.5 | 9.7 ± 0.5 |
| 3.7 Treatment should not be considered when scoring the PhGA in systemic JIA. | 31[d] | 93.5 | 9.5 ± 1.5 |

JIA, juvenile idiopathic arthritis; MAS, macrophage activation syndrome; ILD, interstitial lung disease; PhGA, physician's global assessment of disease activity.
[a] The total number answering to the e-mail regarding the level of agreement on a 0 to 10 scale (0 = no agreement at all; 10 = full agreement) on the points to consider when scoring the PhGA was 33.
[b] Definition of comorbidities (coexisting diseases) as opposed to extra-articular manifestations.
[c] Voting performed at an online task force meeting with 19 members present.
[d] Voting performed at an online task force meeting with 31 members present.

final points to consider, the proportion of task force members approving each statement and the final LoA.

1. Disease activity definition in JIA

1.2 Disease activity reflects the aspects of the disease related to the pathophysiology that can be reversible with treatment and can worsen with a disease flare.

1.3 Disease activity is different from disease damage, with the latter reflecting long-standing, potentially irreversible changes.

1.4 Evaluation of disease activity should not include findings known or suspected to be due to another disease process, eg, comorbidities, or side effects of JIA treatment.

Statement 1.3 raised the most discussion regarding the term 'comorbidities'. The task force agreed that a definition of comorbidities was needed to distinguish them from extra-articular manifestations of JIA. A comorbidity was considered a concurrent disease, coexisting with JIA in time, eg, metabolic disease, asthma, psychiatric disorder or infection [33]. The term comorbidity generally refers to the presence of 2 or more health conditions that exist independently of each other but co-occur within the same person [34]. The impact that a comorbidity may have in addition to the impact of JIA could be substantial, but the occurrence of that comorbidity should not affect the PhGA score. The task force recognised the challenge in differentiating the term comorbidities and extra-articular manifestations because both coexist at the same time in the patient, and the terms are sometimes used interchangeably. An extra-articular manifestation should be a sign or symptom of the disease occurring outside of the joint that may partly have a shared pathophysiology with the joint disease. Suggested extra-articular manifestations were systemic features of systemic JIA, macrophage activation syndrome (MAS), interstitial lung disease (ILD), psoriasis, and uveitis. Indeed, systemic features and psoriasis are classifying factors according to the International League of Association for Rheumatology classification criteria [35]. Uveitis was considered an extra-articular manifestation because its high incidence among patients with JIA [36], and its

inclusion in the 2011 ACR definition of clinical inactive disease [9].

Inflammatory bowel disease (IBD) was discussed as a possible extra-articular manifestation of JIA. After consideration and voting at the consensus conference, consensus was achieved on not including IBD as an extra-articular manifestation of JIA. A history of IBD in a first-degree relative is a minor criterion for the JIA category of enthesitis-related arthritis (ERA) [35]. IBD in the patient is not a part of the ERA criteria and the presence of gastrointestinal symptoms should raise suspicion of IBD-related arthritis as an alternative diagnosis instead of JIA [37].

2. Nonsystemic JIA

2.1. The PhGA quantifies JIA activity based on the number of joints with arthritis and their degree of inflammation, the number of sites with tenosynovitis and/or enthesitis, and resultant activity limitations due to inflammation.

The most debated part of this statement was 'activity limitations due to inflammation'. The final task force consensus is that the physician should estimate the impact of joint inflammation on the patient's activity limitations based on the information obtained with the clinical examination. Considering this factor, the PhGA score should be higher if the patient has more severe activity limitations due to the degree of inflammation and which joints are affected.

2.2. and 2.3. The PhGA should be scored at the end of the clinical evaluation, and all information available at that time, including imaging and relevant laboratory test results, should be considered.

*Imaging* received the second highest ranking and weight of the factor (Table 2). However, the inclusion of imaging findings was extensively discussed. The general opinion of the task force was that imaging is an important supplement to clinical assessment and results of imaging need to be considered in conjunction with the clinical findings of disease activity. The final statement regarding imaging was agreed upon by 85.2% of the task force members. Information from any imaging modality may be considered, though currently musculoskeletal ultrasound (MSUS) and magnetic resonance imaging (MRI) are considered the most reliable modalities for assessing inflammation in JIA [38]. It was argued that the PhGA is a subjective global assessment of disease activity scored by the treating physician based on clinical examination. However, we cannot ignore available imaging information or laboratory exam at the time of the PhGA scoring. In respect to imaging, over time, this may both increase and decrease the PhGA score based on the availability of this information. However, based on the 2 large surveys sent to PRINTO and PR-COIN members and the discussions among the task force, imaging is so important to be excluded from its appraisal. The task force discussed several proposed time limits with respect to imaging but in the end decided to leave this to the judgement of the physician. There was agreement that the imaging results should be available at the time of the visit, performed recently or concurrently, and in a clinical acceptable timeframe to be associated with current disease activity at the time of PhGA scoring. Ideally, imaging information should be collected within the day of the visit, which is often required for clinical trials. With respect to observational studies and trials, it is important to recognise the potential bias of including imaging results in the scoring of the PhGA. For research purpose, it may be necessary to state the inclusion of imaging in the evaluation.

The importance of the PhGA being based on clinical judgement was emphasised; therefore, precise indication of timing in this statement may not be applicable. It was highlighted that for the temporomandibular and sacroiliac joints, imaging by MRI, is of major importance for disease activity assessment. If imaging results are available at the visit for the PhGA scoring they should be considered. Conversely, if only available after the visit, the physician should score the PhGA with the available information at the time. If the imaging results are valid for the next clinical assessment, then this should inform a subsequent patient evaluation and a new PhGA scoring.

*Laboratory tests* were considered of minor importance for the scoring of the PhGA in nonsystemic JIA. As in the case of imaging, the test results should be available at the time of the visit, they should be recent enough to reflect the patient's current disease activity state, and other causes of abnormal results should be ruled out.

2.4. The clinical evaluation should be completed on the day of the visit.

There was consensus (88.9%) for this statement, emphasising the time frame of the assessment.

2.5. and 2.6. Uveitis and psoriasis may be extra-articular manifestations of JIA. When this is the case, the presence and extent of active uveitis and active psoriasis should be considered when scoring PhGA.

Active *uveitis* achieved a high mean rank and weight in MCDA but had the largest variation in ranking. During the consensus conference 2 major points of view emerged. First, most task force members argued that since the PhGA is a global measure that aims to capture every aspect of disease activity in JIA, and uveitis is considered an extra-articular manifestation of JIA, it should be included in the score. Second, uveitis activity deserves a separate disaggregated assessment scale to provide more precise information, especially since the assessment of uveitis activity is usually done by an ophthalmologist and not the physician scoring the PhGA. After several rounds of discussion, the task force agreed unanimously (100%) on the final statement. The timing of the uveitis assessment was discussed. The assessment should be recent and validated measures for assessing uveitis activity should be used [39]. A maximum time frame of 3 months was proposed, as this is a common screening interval [40], although children with active uveitis will often have more frequent ophthalmology visits. The scoring physicians must judge the adequacy and timing of the uveitis information available. If active uveitis but no other signs of disease activity are present, the PhGA score *should not be 0*.

Regarding *psoriasis,* the main discussion was whether psoriasis should be considered an extra-articular manifestation or a comorbid condition in JIA. After extensive discussions, there was consensus (88.9%) for the final statement shown in Table 4. The task force stated that the presence and degree of psoriasis activity should be considered when scoring the PhGA, and a standardised psoriasis activity assessment tools, such as the Psoriasis Area and Severity Index, should be used [41]. However, this tool has not been validated in children, posing a challenge for an objective evaluation. If suspected to be a medication adverse event, psoriasis should not be considered in the PhGA score. When evaluating activity of nail lesions, the physician should keep in mind that changes in the nails may persist for a long time and not be a sign of currently active psoriasis.

2.7. When scoring the PhGA, consider only the current patient presentation, and not the prior disease activity or disease course.

The task force members agreed that the PhGA should quantify the *current* level of disease activity. The PhGA score *should be the same* in 2 patients with the same clinical picture at the time of the visit, independent of JIA category, prior disease activity trajectory, and whether there is an improvement or worsening since the previous visit.

If imaging and laboratory exams that may inform the PhGA score are not available at the time of the scoring, these should not inform your PhGA at that time. If the patient is in for a new clinical evaluation and these tests are performed in a clinically relevant time frame to be valid for your next PhGA score, and the treating physician consider them as relevant, these may then inform your next PhGA score.

Treatment should not be considered when scoring the PhGA in nonsystemic JIA. Accordingly, the PhGA score *should be the same* for 2 patients with the same clinical picture at the visit, independent of whether one patient is receiving treatment and the other is not and independent of whether they are receiving different medications. Discussion was raised regarding the role of glucocorticoids; in line with current treat-to-target recommendations [33], patients' care must aim towards steroid-free remission; in a patient with a PhGA indicating no disease activity but receiving systemic glucocorticoids, the treatment should be tapered and possibly withdrawn.

3. Systemic JIA

3.1. The PhGA quantifies systemic JIA activity based on the presence and extent of systemic features such as fever, serositis, hepatosplenomegaly, generalised lymphadenopathy, and rash, and on the number of joints with arthritis, their degree of inflammation, and resultant activity limitations due to inflammation.

The rank and weight of the factors in this statement are shown in Table 3. The task force had the same discussion and conclusion about activity limitations due to active arthritis as for nonsystemic JIA: the impact of joint inflammation on patient's activity is assessed by the physician based on the information obtained during the clinical examination.

3.2. and 3.3. The PhGA should be scored at the end of the clinical evaluation, and all information available at that time, including imaging and relevant laboratory test results, should be considered.

For systemic JIA, additional imaging besides conventional MRI and MSUS may be relevant, such as a computed tomography (CT) scan for evaluation of ILD activity. As for nonsystemic JIA, all imaging information should be available within the day of the visit; a new patient evaluation and a new PhGA scoring should be performed if results are available after the visit. It is left to the physician to discern whether the results of an imaging exam performed before the visit are still reflective of disease activity at the time of PhGA scoring.

*Laboratory tests* relevant for evaluation of level of inflammation, which for systemic JIA may comprise a broader set of tests, should be considered for the scoring of the PhGA. Laboratory tests should have high sensitivity and specificity and be associated with the inflammatory process. Research biomarker results may be used when available; this was felt to be particularly applicable for systemic JIA. The issue of timing of tests relative to the clinical visit and PhGA scoring are the same as for nonsystemic JIA. The treating physician should score the PhGA at the visit with the currently available results.

3.4. The clinical evaluation should be completed on the day of the visit.

The discussion and voting on this statement were held jointly for systemic and nonsystemic JIA (see above).

3.5. The presence of macrophage activation syndrome (MAS) and/or active ILD should be considered when scoring the PhGA.

MAS and ILD obtained high ranks and weights in MCDA with the complete statement approved at an online task force meeting by 31 voters (96.8%). It was suggested to also use a specific measure of MAS severity.

3.6. When scoring the PhGA, consider only the current patient presentation, and not the prior disease activity or disease course or history of MAS and/or ILD.

The PhGA should quantify the level of disease activity, ie, the PhGA score should *be the same* in 2 patients with the same clinical picture at the visit, independent of JIA category, independent on whether they have experienced a mild or a severe disease course, and independent of whether they have improved or worsened since the previous visit. Prior MAS events or ILD should lead to a more thorough assessment of the patient than in a patient without such history, but it should not influence the PhGA if currently absent. There were also discussions regarding disaggregating the systemic features into separate VAS. However, again the decision was that the PhGA aim is to give an *overall score of the global disease activity* in JIA assessed by the treating physician.

3.7. Treatment should not be considered when scoring the PhGA in systemic JIA.

The discussion and voting on this statement were held jointly for systemic and nonsystemic JIA (see above).

### *Adjudication of the LoA after the consensus conference*

The LoA on the recommendations was assessed with a survey after the consensus conference; 33 task force members responded to the survey. The LoA was in general high, with all statements achieving a LoA greater than 9 (Table 4).

## DISCUSSION

We report the systematic work of an international task force to develop recommendations for scoring the PhGA in children and youth with nonsystemic and systemic JIA. The PhGA is an essential measure embedded into multiple disease activity assessment tools that impact care and research in JIA. This work resulted in the first clear guideline for PhGA scoring, which is expected to markedly increase its consistency and validity.

After detailed deliberations using multiple consensus building methods, 18 points to consider were approved, 3 articulating an operational definition of disease activity in JIA, 8 detailing what should and should not be considered when scoring the PhGA in nonsystemic JIA, and 7 detailing the PhGA scoring in systemic JIA. Five statements were the same for nonsystemic JIA and systemic JIA.

The task force first agreed that it was necessary to provide an unequivocal definition of disease activity for JIA. It was agreed that joint inflammatory disease is central in the evaluation of a patient with JIA and that changes from disease damage or medications side effects are outside the disease

activity domain. However, greater uncertainty was evident when or whether to consider extra-articular manifestations of JIA disease in the PhGA. To ensure compatibility with current JIA classification criteria and definition of clinically inactive disease, the task force concluded that disease activity of extra-articular manifestations should be considered when scoring the PhGA, including systemic manifestations, uveitis, and psoriasis, if relevant.

There was a crucial discussion about how and whether imaging and laboratory tests should be considered in the PhGA scoring. The task force reached consensus that imaging and relevant laboratory information available at the time of PhGA scoring should be considered but that the time frame of the information should be left to the discretion of the physician. We acknowledge that this might introduce a bias in clinical studies and trials, when imaging is not available in every evaluation or in every setting. However, this bias could be comparable to other biases, such as those that can arise from different experience of the physicians or different amount of time spent performing the physical examination. There was also agreement that 2 patients with the same findings at the time of the PhGA scoring should receive the same score, irrespective of disease history, whether they have improved or worsened relative to the previous assessment, and irrespective of their current treatment.

Once the points to consider when scoring the PhGA are identified, their efficacy in achieving a more consistent use of the tool should be demonstrated. The research agenda for the task force include a validation phase, reassessing clinical cases in PRINTO/PR-COIN surveys by a large group of stakeholders in JIA, using the newly developed points to consider.

In conclusion, the consensus statements lay the foundation for a more homogeneous scoring of the PhGA, a key outcome measure in JIA. Although we anticipate further refinement of the statements as the knowledge of mechanisms of disease activity in JIA improves, the agreements on how to score the PhGA constitutes, in our opinions, a major step towards enhancing the comparability of disease activity measurement for clinical care and international clinical trials in JIA.

## Competing interests

None of the authors received any support from commercial entities for the work reported in the current submitted manuscript. VR and AC reports that the project was supported by the 2022 Paediatric Rheumatology European Association (PReS)/ Paediatric Rheumatology International Trials Organisation (PRINTO) grant, The Systemic JIA Foundation, the University Hospital of North Norway, the University of Tromsø, The Arctic University of Norway, and Grete Harbitz legacy against rheumatic diseases, Norway. All the authors of the paper attending the PhGA consensus conference in Tromsø, Norway, received reimbursement of travel expenses covered by the PRes/PRINTO grant, and the Systemic JIA Foundation. The accomodation in Tromsø and meeting facilities expenses were covered by funding from Grete Harbitz legacy, the University Hospital of North Norway and the University of Tromsø - The Arctic University of Norway. CB has received consulting fees from Swedish Orphan Biovitrum AB (SOBI) and Novartis. AC has an investigator initiated grant from Pfizer. AC has received payment or honoraria for lectures, presentations, speakers bureaus, manuscript writing or educational events from Pfizer. BF has received grants from Canadian Institutes of Health Research (CIHR) and the institution. BF has received royalties or licenses from Hemophilia Joint Health Score (HJHS) and the institution. BF has received consulting fees from Pfizer, Cabaletta, and Data Safety and Monitoring Board (DSMB). BF reports participation on a data safety monitoring board or advisory board for Pfizer. JG reports that the project was funded by a competitive grant as stated in the manuscript. JG is the co-lead of the American College of Rheumatology Disease Criteria Subcommittee. DBH reports grant funding from Childhood Arthritis and Rheumatology Research Alliance-Arthritis Foundation and Danisco USA, Inc. DBH reports receiving payment or honoraria for lectures, presentations, speakers bureaus, manuscript writing or educational events from American College of Rheumatology and honorarium for participating in JIA treatment guidelines. DBH reports support for attending meetings and/or travel from Childhood Arthritis and Rheumatology Research Alliance and American College of Rheumatology. DBH reports leadership or fiduciary role in other board, society, committee or advocacy group, paid or unpaid from Childhood Arthritis and Rheumatology Research Alliance and membership of the steering committee. RML reports royalties and license from UpToDate and Elsevier. RML reports consulting fees from SOBI, Novartis, Sanofi, Akros Pharma, and Eli Lilly Canada. RML reports Participation on a Data Safety Monitoring Board or Advisory Board for Novartis, Eli Lilly, Sanofi, and Children's Hospital of Philadelphia. FM reports consulting fees from SOBI. FM reports payment or honoraria for lectures, presentations, speakers bureaus, manuscript writing or educational events from SOBI and Novartis. FM reports support for attending meetings and/or travel from SOBI. FM reports participation on a data safety monitoring board or advisory board for SOBI. EMM reports grants or contracts from Pfizer and Agency for Healthcare Research and Quality. EMM reports payment or honoraria for lectures, presentations, speakers bureaus, manuscript writing or educational events from American College of Rheumatology. EMM reports support for attending meetings and/or travel from American College of Rheumatology and Systemic JIA Foundation. EMM reports leadership or fiduciary role in other board, society, committee or advocacy group, paid or unpaid, for the Pediatric Rheumatology Care and Outcomes Improvement Network. JM reports payment or honoraria for lectures, presentations, speakers bureaus, manuscript writing or educational events for Pfizer excite meeting Sept 2023 Melbourne speaker. CN reports PReS as support for the present manuscript. CN reports support for attending meetings and/or travel from PReS. AR reports payment or honoraria for lectures, presentations, speakers bureaus, manuscript writing or educational events from AbbVie, Alexion, Novartis, Pfizer, SOBI, and Galapagos. AR is the President of the Pediatric Rheumatology European Society. JFS reports receiving a small Research grant from Pfizer. JFS reports Payment or honoraria for lectures, presentations, speakers bureaus, manuscript writing or educational events from Pfizer. MTw reports receiving travel support to attend the Consensus meeting. MTw is a committee chair of Childhood Arthritis and Rheumatology Research Alliance (CARRA) JIA. PV reports Support for attending meetings and/or travel from Pfizer, Novartis, and Orion. PV reports Participation on a Data Safety Monitoring Board or Advisory Board for Novartis. SJV reports grants from Dutch Arthritis Society Grant: InSyST (systemic JIA), Dutch Arthritis Society Grant: Longitudinal Research Support line 10 (LLP10), and PReS PRINTO Grant: Metaphor project, co-PI. SJV reports consulting fees from SOBI and Novartis. SJV reports Payment or honoraria for lectures, presentations, speakers bureaus, manuscript writing or educational events from SOBI and Novartis. SJV reports Patents planned, issued or pending (PCT/EP2023/066764). SJV reports being Chair Kawasaki Disease Coronary Artery Aneurysm

Prevention (KD CAAP) Trial Steering Committee, Co-principal investigator for Canada-Netherlands Personalized Medicine Network in Childhood Arthritis and Rheumatic Diseases (UCAN CAN-DU), and Chair Clinical Guideline Committee The European Reference Network-Rare Immunological Disorders (ERN-RITA). JV reports Payment or honoraria for lectures, presentations, speakers bureaus, manuscript writing or educational events from Novartis and Eli Lily. JV reports Support for attending meetings and/or travel from Abbvie and Novartis. JV is a member of the PRES executive committee. PW reports grants from Patient-Centered Outcomes Research Institute, National Institutes of Health (NIH), National Institute of Arthritis and Muskuloskeletal and Skin Diseases (NIAMS) (1R01AR074098), and Spondylitis Association of America. PW reports Royalties or licenses from UpToDate. PW reports Consulting fees from Pfizer and Cerecor. PW is a Site investigator for Pfizer and Abbvie Clinical Trials. PW is an advisory board member of Lily, Biogen, and Novartis. PW reports payment or honoraria for lectures, presentations, speakers bureaus, manuscript writing or educational events from Rheum Now Speaker (2022) and Spondyloarthritis Research and Treatment Network. The following authors have no conflicts of interest to disclose: AA, SA-H, MB, EB-D, MG, DJL, TL, SM-M, EN, NP, EP, CSM, RS, MTa.

## Acknowledgements

We wish to thank Giulia de Angelis, PRINTO research assistant, and Federico Serra, PRINTO IT Unit, for their help in the project. We thank Nils Thomas Songstad, the head of the Department of Pediatrics at the University Hospital of North Norway, and Hilde B. Hansen, research assistant, for the help in organizing the consensus conference. We thank the Childhood Arthritis and Rheumatology Research Alliance (CARRA), European Network for Children with Arthritis (ENCA), Outcome measures in Rheumatology (OMERACT) JIA Working group, Pediatric Rheumatology Care and Outcomes Improvement Network (PR-COIN), Pediatric Rheumatology Collaborative Study Group (PRCSG), Paediatric Rheumatology European Association (PReS), PRINTO and Canadian Alliance of Pediatric Rheumatology Investigators (CAPRI) for supporting this initiative and all PRINTO and PR-COIN members who answered the Delphi surveys. We also want to thank The European Reference Network that aims at improving the care of patients with Rare immunological disorders (ERN-RITA) for the endorsement of these recommendations.

## Contributors

All authors have contributed to the development of the recommendations and the manuscript.

## Funding

The project was supported by the 2022 PReS/PRINTO grant, the Systemic JIA Foundation, the University Hospital of North Norway, the University of Tromsø – The Arctic University of Norway and Grete Harbitz legacy against rheumatic diseases.

## Patient consent for publication

Not applicable.

## Ethics approval

Not applicable.

## Patient and public involvement

We have included a parent of a JIA patient representative in the PhGA task force (CN). CN has participated in the working process towards achieving consensus-based recommendation for scoring the PhGA (including research planning, execution of the consensus process, drafting and revising of the manuscript).

## Orcid

Veronika Rypdal: http://orcid.org/0000-0003-3476-305X
Hermine I. Brunner: http://orcid.org/0000-0001-9478-2987
Brian M. Feldman: http://orcid.org/0000-0002-7813-9665
Sheila T. Angeles-Han: http://orcid.org/0000-0002-9552-6464
Maria Backström: http://orcid.org/0000-0002-8632-8634
Erin Balay-Dustrude: http://orcid.org/0000-0001-6235-1947
Marco Garrone: http://orcid.org/0000-0001-9543-7915
Daniel B. Horton: http://orcid.org/0000-0002-1831-1339
Daniel J. Lovell: http://orcid.org/0000-0003-1604-0130
Silvia Magni-Manzoni: http://orcid.org/0000-0002-5714-1141
Nancy Pan: http://orcid.org/0000-0001-7884-3751
Elisa Patrone: http://orcid.org/0000-0002-3177-8347
Angelo Ravelli: http://orcid.org/0000-0001-9658-0385
Maarit Tarkiainen: http://orcid.org/0000-0002-1569-5349
Paula Vähäsalo: http://orcid.org/0000-0002-2712-3903
Beth Gottlieb: http://orcid.org/0000-0002-2559-7793

## REFERENCES

[1] Ravelli A, Martini A. Juvenile idiopathic arthritis. Lancet 2007;369 (9563):767–78.
[2] Consolaro A, Giancane G, Schiappapietra B, Davi S, Calandra S, Lanni S, et al. Clinical outcome measures in juvenile idiopathic arthritis. Pediatr Rheumatol Online J 2016;14(1):23.
[3] Filocamo G, Davi S, Pistorio A, Bertamino M, Ruperto N, Lattanzi B, et al. Evaluation of 21-numbered circle and 10-centimeter horizontal line visual analog scales for physician and parent subjective ratings in juvenile idiopathic arthritis. JRheumatol 2010;37(7):1534–41.
[4] Pincus T, Bergman M, Sokka T, Roth J, Swearingen C, Yazici Y. Visual analog scales in formats other than a 10 centimeter horizontal line to assess pain and other clinical data. J Rheumatol 2008;35(8):1550–8.
[5] Consolaro A, Ruperto N, Bazso A, Pistorio A, Magni-Manzoni S, Filocamo G, et al. Development and validation of a composite disease activity score for juvenile idiopathic arthritis. Arthritis Rheum 2009;61(5):658–66.
[6] McErlane F, Beresford MW, Baildam EM, Chieng SE, Davidson JE, Foster HE, et al. Validity of a three-variable Juvenile Arthritis Disease Activity Score in children with new-onset juvenile idiopathic arthritis. Ann Rheum Dis 2013;72(12):1983–8.
[7] Consolaro A, Ruperto N, Bracciolini G, Frisina A, Gallo MC, Pistorio A, et al. Defining criteria for high disease activity in juvenile idiopathic arthritis based on the juvenile arthritis disease activity score. Ann Rheum Dis 2014;73(7):1380–3.
[8] Wallace CA, Ruperto N, Giannini E, Childhood A, Rheumatology Research A, Pediatric Rheumatology International Trials O. Preliminary criteria for clinical remission for select categories of juvenile idiopathic arthritis. J Rheumatol 2004;31(11):2290–4.
[9] Wallace CA, Giannini EH, Huang B, Itert L, Ruperto N, Childhood Arthritis Rheumatology Research A. American College of Rheumatology provisional criteria for defining clinical inactive disease in select categories of juvenile idiopathic arthritis. Arthritis Care Res (Hoboken) 2011;63(7):929–36.

[10] Giannini EH, Ruperto N, Ravelli A, Lovell DJ, Felson DT, Martini A. Preliminary definition of improvement in juvenile arthritis. Arthritis Rheum 1997;40(7):1202–9.
[11] Ruperto N, Martini A. Current and future perspectives in the management of juvenile idiopathic arthritis. Lancet Child Adolesc Health 2018;2(5):360–70.
[12] Alongi A, Giancane G, Naddei R, Natoli V, Ridella F, Burrone M, et al. Drivers of non-zero physician global scores during periods of inactive disease in juvenile idiopathic arthritis. RMD Open 2022;8(1).
[13] Rypdal V, Glerup M, Rypdal M, Arnstad E, Aalto K, Berntson L, et al. Disease activity trajectories from childhood to adulthood in the population-based Nordic juvenile idiopathic arthritis cohort. RMD Open 2024;10(1).
[14] Backstrom M, Tarkiainen M, Gottlieb BS, Trincianti C, Qiu T, Morgan E, et al. Paediatric rheumatologists do not score the physician's global assessment of juvenile idiopathic arthritis disease activity in the same way. Rheumatology (Oxford) 2023;62(10):3421–6.
[15] Giancane G, Campone C, Gicchino MF, Alongi A, Bava C, Rosina S, et al. Determinants of Discordance Between Criteria for Inactive Disease and Low Disease Activity in Juvenile Idiopathic Arthritis. Arthritis Care Res (Hoboken) 2021;73(12):1722–9.
[16] Tarkiainen M, Balay-Dustrude E, Consolaro A, Morgan EM, Ruperto N, Rypdal V, et al. Factors for Consideration by Pediatric Rheumatologists When Scoring the Physician Global Assessment (PhGA) of Disease Activity in Juvenile Idiopathic Arthritis: First Step Toward an Internal Consensus. Arthritis Care Res (Hoboken) 2024. Epub ahead of print. PMID: 39387125. doi: 10.1002/acr.25447.
[17] Dougados M, Betteridge N, Burmester GR, Euller-Ziegler L, Guillemin F, Hirvonen J, et al. EULAR standardised operating procedures for the elaboration, evaluation, dissemination, and implementation of recommendations endorsed by the EULAR standing committees. Ann Rheum Dis 2004;63(9):1172–6.
[18] van der Heijde D, Aletaha D, Carmona L, Edwards CJ, Kvien TK, Kouloumas M, et al. 2014 Update of the EULAR standardised operating procedures for EULAR-endorsed recommendations. Ann Rheum Dis 2015;74(1):8–13.
[19] 1000minds Ltd. 1000minds decision-making and conjoint analysis software: 1000minds Ltd; 03/15/24, 2024. Available from: https://www.1000minds.com.
[20] Weistroffer HR, Li Y. Multiple Criteria Decision Analysis Software. In: Greco S, Ehrgott M, Figueira JR, editors. Multiple Criteria Decision Analysis: State of the Art Surveys. New York, NY: Springer New York; 2016. p. 1301–41.
[21] Hansen P, Ombler F. A new method for scoring additive multi-attribute value models using pairwise rankings of alternatives. Journal of Multi-Criteria Decision Analysis 2008;15(3-4):87–107.
[22] McMillan SS, King M, Tully MP. How to use the nominal group and Delphi techniques. Int J Clin Pharm 2016;38(3):655–62.
[23] Vyduna J, Gessler B, Eby S. Poll Everywhere® Audience response systems software; 03/15/24, 2024. Available from: https://www.polleverywhere.com.
[24] Ward JR, Williams HJ, Egger MJ, Reading JC, Boyce E, Altz-Smith M, et al. Comparison of auranofin, gold sodium thiomalate, and placebo in the treatment of rheumatoid arthritis. A controlled clinical trial. Arthritis Rheum 1983;26(11):1303–15.
[25] Williams HJ, Ward JR, Reading JC, Egger MJ, Grandone JT, Samuelson CO, et al. Low-dose D-penicillamine therapy in rheumatoid arthritis. A controlled, double-blind clinical trial. Arthritis Rheum 1983;26(5):581–92.
[26] Kvien TK, Hoyeraal HM, Sandstad B. Assessment methods of disease activity in juvenile rheumatoid arthritis–evaluated in a prednisolone/placebo double-blind study. J Rheumatol 1982;9(5):696–702.
[27] Williams HJ, Willkens RF, Samuelson Jr. CO, Alarcon GS, Guttadauria M, Yarboro C, et al. Comparison of low-dose oral pulse methotrexate and placebo in the treatment of rheumatoid arthritis. A controlled clinical trial. Arthritis Rheum 1985;28(7):721–30.
[28] Kvien TK, Hoyeraal HM, Sandstad B. Azathioprine versus placebo in patients with juvenile rheumatoid arthritis: a single center double blind comparative study. J Rheumatol 1986;13(1):118–23.
[29] Brewer EJ, Giannini EH, Kuzmina N, Alekseev L. Penicillamine and hydroxychloroquine in the treatment of severe juvenile rheumatoid arthritis. Results of the U.S.A.-U.S.S.R. double-blind placebo-controlled trial. N Engl J Med 1986;314(20):1269–76.
[30] Huskisson EC. Measurement of pain. Lancet 1974;2(7889):1127–31.
[31] Felson DT, Anderson JJ, Boers M, Bombardier C, Chernoff M, Fried B, et al. The American College of Rheumatology preliminary core set of disease activity measures for rheumatoid arthritis clinical trials. The Committee on Outcome Measures in Rheumatoid Arthritis Clinical Trials. Arthritis Rheum 1993;36(6):729–40.
[32] Ringold S, Wallace CA. Measuring clinical response and remission in juvenile idiopathic arthritis. CurrOpinRheumatol 2007;19(5):471–6.
[33] Ravelli A, Consolaro A, Horneff G, Laxer RM, Lovell DJ, Wulffraat NM, et al. Treating juvenile idiopathic arthritis to target: recommendations of an international task force. Ann Rheum Dis 2018;77(6):819–28.
[34] Valderas JM, Starfield B, Sibbald B, Salisbury C, Roland M. Defining comorbidity: implications for understanding health and health services. Ann Fam Med 2009;7(4):357–63.
[35] Petty RE, Southwood TR, Manners P, Baum J, Glass DN, Goldenberg J, et al. International League of Associations for Rheumatology classification of juvenile idiopathic arthritis: second revision, Edmonton, 2001. JRheumatol 2004;31(2):390–2.
[36] Rypdal V, Glerup M, Songstad NT, Bertelsen G, Christoffersen T, Arnstad ED, et al. Uveitis in Juvenile Idiopathic Arthritis: 18-year Outcome in the Population-based Nordic Cohort Study. Ophthalmology 2020.
[37] Petty RE, Laxer RM, Lindsley CB, Wedderburn L, Fuhlbrigge FC, Mellins ED. Textbook of pediatric rheumatology. 8th ed. Amsterdam, The Netherlands: Elsevier; 2020. p. 768.
[38] Colebatch-Bourn AN, Edwards CJ, Collado P, D'Agostino MA, Hemke R, Jousse-Joulin S, et al. EULAR-PReS points to consider for the use of imaging in the diagnosis and management of juvenile idiopathic arthritis in clinical practice. Ann Rheum Dis 2015;74(11):1946–57.
[39] Jabs DA, Nussenblatt RB, Rosenbaum JT. Standardization of uveitis nomenclature for reporting clinical data. Results of the First International Workshop. AmJOphthalmol 2005;140(3):509–16.
[40] ST Angeles-Han, Ringold S, Beukelman T, Lovell D, Cuello CA, Becker ML, et al. 2019 American College of Rheumatology/Arthritis Foundation Guideline for the Screening, Monitoring, and Treatment of Juvenile Idiopathic Arthritis-Associated Uveitis. Arthritis Care Res (Hoboken) 2019;71(6):703–16.
[41] Feldman SR, Krueger GG. Psoriasis assessment tools in clinical trials. Ann Rheum Dis 2005;64(Suppl 2):ii65–8 Suppl 2. discussion ii9-73.

Ann Rheum Dis 84 (2025) 1437–1438

Contents lists available at ScienceDirect

Annals of the Rheumatic Diseases

journal homepage: https://www.sciencedirect.com/journal/annals-of-the-rheumatic-diseases

Images in rheumatology

# IgG4-related pulmonary disease presenting as a solid pulmonary mass

Shuyun Wang, Binglin Lai *

*Ganzhou Key Laboratory of Medical Imaging and Artificial Intelligence, Medical Imaging Center, Ganzhou Institute of Medical Imaging, Ganzhou People's Hospital, Ganzhou Hospital-Nanfang Hospital, Southern Medical University, Ganzhou, Jiangxi, China*

A 20-year-old man was incidentally found to have a mass in his left lung on a routine chest X-ray. He was asymptomatic and had no relevant medical history. Laboratory tests revealed an elevated serum immunoglobulin (Ig) G4 level of 3030 mg/L. Computed tomography (CT) scanning of the chest (Fig 1A,B) showed a spherical soft tissue density mass adjacent to the hilum of the left lower lobe, measuring approximately 7.3 cm × 5.5 cm × 5.8 cm. The mass had mildly lobulated edges, clear boundaries, and multiple small calcified foci, with mild compression of the adjacent bronchi. After contrast enhancement (Fig 1C,D), the mass showed inhomogeneous mild enhancement during the arterial phase and more uniform enhancement during the venous phase. Enlarged lymph nodes were noted below the carina. The initial CT diagnosis was

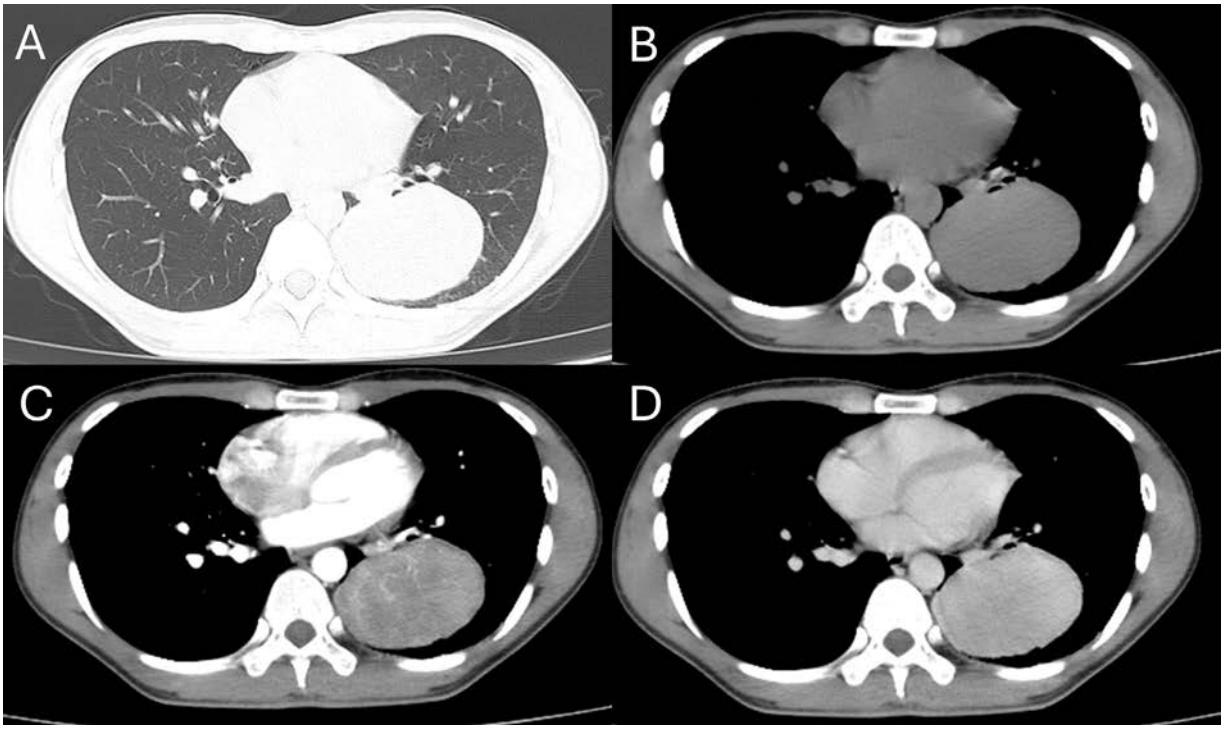



**Figure 1.** Computed tomography (CT) images of a 20-year-old man with immunoglobulin (Ig) G4-related lung disease. A plain CT scan (A, B) shows a spherical soft tissue mass adjacent to the hilum of the left lower lobe, with mildly lobulated edges and clear boundaries. Contrast-enhanced CT (C, D) demonstrates inhomogeneous mild enhancement during the arterial phase (C) and more uniform enhancement during the venous phase (D).

* **Correspondence to** Dr Binglin Lai, Department of Medical Imaging, Ganzhou People's Hospital, Ganzhou, Jiangxi, China.
*E-mail address:* binglin723.lai@outlook.com (B. Lai).
**Handling editor** Josef S. Smolen.

https://doi.org/10.1016/j.ard.2025.03.011
Received 22 January 2025; Revised 22 February 2025; Accepted 20 March 2025

0003-4967/© 2025 Published by Elsevier B.V. on behalf of European Alliance of Associations for Rheumatology (EULAR).

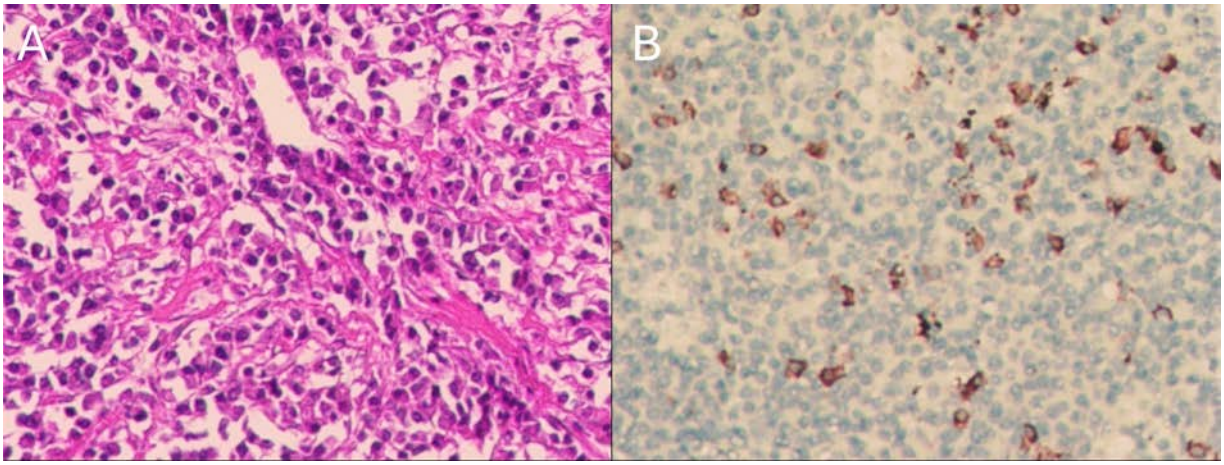



Figure 2. Histopathological findings. (A) Hematoxylin and eosin (HE) staining (× 200 magnification) reveals extensive plasma cell infiltration within the fibrous septa. (B) Immunoglobulin (Ig) G4 staining (× 200 magnification) shows abundant IgG4-positive plasma cells, with more than 30 cells per high-power field and an IgG4/IgG ratio greater than 40%.

inflammatory pseudotumor. Postsurgical pathological examination (Fig 2A,B) confirmed the diagnosis of IgG4-related lung disease (IgG4-RLD). Histological examination revealed extensive plasma cell infiltration within the fibrous septa, with abundant IgG4-positive plasma cells. The IgG4/IgG ratio was greater than 40%, with more than 30 IgG4-positive cells per high-power field.

IgG4-RLD is a rare manifestation of IgG4-related disease (IgG4-RD), a systemic fibroinflammatory condition that can affect multiple organs, including the lungs. Pulmonary manifestations of IgG4-RD typically include nodules or masses, ground-glass opacities, interstitial lung disease, and pleural involvement. According to classification [1], the lesion was categorised as a solid nodular subtype of IgG4-RD. Histological examination of the pulmonary lesion revealed dense plasma cell infiltration consistent with IgG4-related pseudotumor. Compared with other pseudotumor types, the plasma cell infiltration in IgG4-related pseudotumor was distinctive. Elevated serum IgG4 levels, combined with characteristic imaging findings, should raise suspicion for this diagnosis. Histopathological examination, showing dense IgG4-positive plasma cell infiltration, is essential for confirmation.

In our patient, the large pulmonary mass with calcifications and inhomogeneous enhancement on CT imaging is consistent with previously reported cases of IgG4-RLD. The diagnosis was confirmed by histological examination, which revealed high IgG4-positive plasma cell infiltration and an elevated IgG4/IgG ratio. Although corticosteroids are the first-line treatment for IgG4-RD, surgical resection may be considered for large or symptomatic lesions [2]. No extrapulmonary organ involvement was identified in this patient with confirmed IgG4-RLD. Surgical resection was performed, followed by maintenance prednisone therapy (5 mg/d) for 1 year. Serial follow-up over 3 years demonstrated persistently normal serum IgG4 levels. IgG4-RD is recognised as a systemic inflammatory disorder with potential multiorgan involvement. Nonspecific manifestations in pulmonary, orbital, and abdominal inflammatory pseudotumors may pose diagnostic challenges [3]. Therefore, heightened clinical awareness of IgG4-RD is recommended when encountering lesions in these anatomical regions to prevent misdiagnosis or oversight. Our case highlights the importance of considering IgG4-RLD in the differential diagnosis of pulmonary masses, especially when serum IgG4 levels are elevated.

## Contributors

SW contributed to the conception and design of the study; BL contributed to the acquisition and analysis of data, drafting the text, and preparing the figures.

## Funding

Clinical Research Center for Medical Imaging in Jiangxi Province [Grant number 20223BCG7400199].

## Competing interests

The authors disclose no conflicts of interest.

## Patient consent for publication

Consent obtained directly from patient(s).

## Ethics approval

Not applicable.

## Provenance and peer review

Not commissioned; externally peer reviewed.

## Orcid

Binglin Lai: http://orcid.org/0009-0003-4690-8241

## REFERENCES

[1] Inoue D, Zen Y, Abo H, Gabata T, Demachi H, Kobayashi T, et al. Immunoglobulin G4-related lung disease: CT findings with pathologic correlations. Radiology 2009;251(1):260–70.
[2] Dragos C, Joseph C, Elwell H, Dey M, Kouranloo K. Pulmonary manifestations, treatments and outcomes of IgG4-related disease-a systematic literature review. Rheumatol Int 2024;44(10):1875–86.
[3] Muller R, Ebbo M, Habert P, Daniel L, Briantais A, Chanez P, et al. Thoracic manifestations of IgG4-related disease. Respirology 2023;28(2):120–31.

Ann Rheum Dis 84 (2025) 1439–1441

Contents lists available at ScienceDirect

Annals of the Rheumatic Diseases

journal homepage: https://www.sciencedirect.com/journal/annals-of-the-rheumatic-diseases

Letter

# Anticitrullinated caspase 14 peptide antibody is a novel biomarker for seronegative rheumatoid arthritis

Rheumatoid arthritis (RA) is a chronic autoimmune disease characterised by joint damage, systemic inflammation, and early mortality. Early diagnosis and effective treatment are crucial for averting or slowing the progression of joint damage and disability in patients with RA [1,2]. Anticyclic citrullinated peptide antibody (anti-CCP) and rheumatoid factor (RF) serve as routinely used diagnostic biomarkers for RA, but their diagnostic accuracy remains limited [3–5]. There is an unmet need to identify novel and effective biomarkers for diagnosis of anti-CCP/RF-negative (seronegative) RA. Our previous study of RA serum autoantigenome revealed that caspase 14 was a potential autoantigen in anti-CCP–negative RA [6], which was similarly observed in our unpublished data of the proteome of RA-enriched citrullinated autoantigens.

Caspase 14, a unique member of the evolutionarily conserved family of cysteinyl aspartate–specific proteinases, mediates cleavage of profilaggrin into filaggrin and subsequent degradation into free amino acids. Although implicated in retinal dysfunction, malignancies, and skin conditions [7], its association with RA and other rheumatic diseases remains poorly investigated.

In this study, we identified the autoantigenic B cell epitopes of caspase 14 by Immune Epitope Database. The amino acid residues of 132 to 146 (RGEQRDPGETVGGDE) was chosen as the potential candidate. Since citrullination is particularly important for the autoantigenicity of peptides in RA [8], the corresponding citrullinated peptide was synthesised for the detection of autoantibodies, with the sequence of Cit-GEQ-Cit-DPGETVGGDE. Our tentative study revealed that the serum levels of anticitrullinated caspase 14 peptide, named anticitrullinated caspase 14 peptide antibody (anti-CCPP), were significantly elevated in patients with RA, while serum antibodies to non-citrullinated caspase 14 peptide (anti-NCCPP) revealed similar levels between patients with RA and healthy controls (HCs), further suggesting the importance of citrullination to the autoantigenicity (Fig A,B). The specificity of the detected anti-CCPP was further validated by competitive enzyme linked immunosorbent assay (ELISA) analysis (Fig C). Thereafter, the diagnostic value of anti-CCPP for RA was assessed in 416 patients with RA (anti-$CCP^+$ RA:anti-$CCP^-$ RA = 2:1), 210 HCs, and 445 patients with other common rheumatic diseases, including 149 patients with Sjögren's syndrome (SS), 148 patients with systemic lupus erythematosus (SLE), and 148 patients with osteoarthritis (OA). All patients with RA fulfilled the 2010 American College of Rheumatology (ACR)/European League against Rheumatism (EULAR) classification criteria, while patients with SS (ACR 2012), SLE (Systemic Lupus International Collaborating Clinics Revision of ACR 2009), and OA (ACR 1995) fulfilled their classification criteria, respectively. The results showed that anti-CCPP was specifically elevated in RA. A pool of 10 positive serum samples from patients with RA was included on each plate as a positive control and reference to correct interassay variations. The level of anti-CCPP was expressed as arbitrary units and quantified as follows: arbitrary unit = ([Optical density $(OD)_{\text{anti-CCPP}}$ - $OD_{\text{nonspecific background}}$] test serum/[$OD_{\text{anti-CCPP}}$ - $OD_{\text{nonspecific background}}$] positive control serum) × 100, as commonly used in similar studies [5,9,10]. All ELISA experiments were repeated for 3 times, which demonstrated similar results.

Based on the optimal cutoff value of 33.17, set as 2 SD above the mean value of the HCs, the sensitivity of anti-CCPP for RA diagnosis was 40.38%, with the specificity of 93.13%, revealing as a novel biomarker. As shown in Figure D-L, anti-CCPP was especially useful for diagnosis of seronegative RA, with the sensitivity of 39.52% in anti-CCP–negative RA, 37.74% in RF-negative RA, and 37.04% in (anti-CCP and RF)–double-negative RA (for all, specificity was 93.13%). There was no significant difference of anti-CCPP between seronegative RA and seropositive RA, further suggesting its superior diagnostic advantage. Moreover, anti-CCPP combination significantly improved the diagnostic power of anti-CCP, increasing the sensitivity by ~10% while maintaining high specificity (Table). These results were further confirmed in a validation cohort including 60 (anti-CCP and RF)–double-negative patients with RA, 30 patients with SS, 30 patients with OA, 30 patients with SLE, and 60 HCs, with the sensitivity of 36.67% and specificity of 94.67% (Fig N,O).

In conclusion, our study identified anti-CCPP as a novel and clinically applicable biomarker for seronegative RA, offering a promising tool to improve diagnostic precision and early discrimination.

XW and CW contributed equally to this work.

https://doi.org/10.1016/j.ard.2025.03.019
Received 4 February 2025; Revised 16 March 2025; Accepted 31 March 2025

0003-4967/© 2025 European Alliance of Associations for Rheumatology (EULAR). Published by Elsevier B.V. All rights are reserved, including those for text and data mining, AI training, and similar technologies.

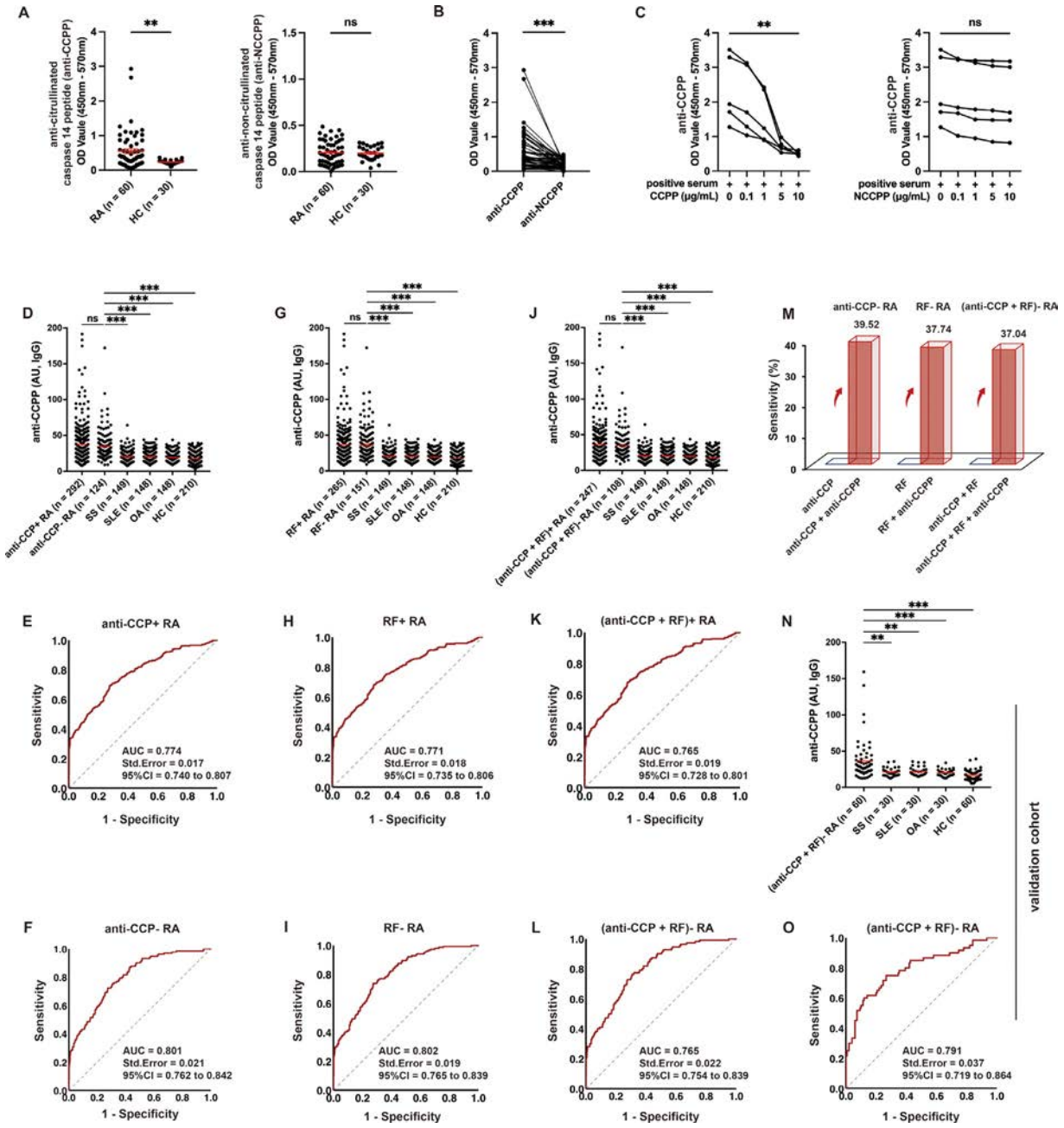



**Figure.** The prevalence and diagnostic value of anti-CCPP in anti-CCP and/or RF-negative RA. The serum levels of antibody to anti-CCPP (left) and anti-NCCPP (right) in patients with RA (n = 60) (A) and HCs (n = 30) (B) were detected. (C) Preincubation of RA serum (n = 5) with increased concentrations (0-10 $\mu$g/mL) of CCPP, but not NCCPP, significantly decreased the detected level of anti-CCPP. (D) The serum concentrations of anti-CCPP in patients with anti-CCP−positive (n = 292) and anti-CCP−negative RA (n = 124). The ROC curves of anti-CCPP in patients with anti-CCP−positive RA (E) and patients with anti-CCP−negative RA (F). (G) The serum concentrations of anti-CCPP in patients with RF-positive (n = 265) and RF-negative RA (n = 151). The ROC curves of anti-CCPP in patients with RF-positive RA (H) and RF-negative RA (I). (J) The serum concentrations of anti-CCPP in patients with (anti-CCP and RF)−double-positive (n = 247) and (anti-CCP and RF)−double-negative RA (n = 108). The ROC curve of anti-CCPP in patients with (anti-CCP and RF)−double-positive RA (K) and (anti-CCP and RF)−double-negative RA (L). (M) Anti-CCPP partially closed the seronegative gap of RA. (N,O) The serum concentrations of anti-CCPP and the corresponding ROC curves in patients with (anti-CCP and RF)−double-negative RA of another independent validation cohort. *$P < .05$; **$P < .01$; ***$P < .001$; ns, not significant (Kruskal−Wallis test followed by Dunn posttest for multiple comparisons). Red horizontal lines, means; error bars, SEMs. AUC, area under the curve; CCP, cyclic citrullinated peptide; CCPP, citrullinated caspase 14 peptide; HC, healthy control; NCCPP, noncitrullinated caspase 14 peptide; RA, rheumatoid arthritis; RF, rheumatoid factor; ROC, receiver operating characteristic.

Table
**Diagnostic value of anti-CCPP, anti-CCP, and their combination for RA**

| Biomarkers | Sensitivity (%) | Specificity (%) | PPV (%) | NPV (%) |
|---|---|---|---|---|
| Anti-CCPP | 40.38 | 93.13 | 78.87 | 71.10 |
| Anti-CCP | 70.19 | 96.79 | 93.29 | 83.64 |
| Anti-CCPP or anti-CCP | 81.97 | 90.23 | 84.20 | 88.74 |
| Anti-CCPP and anti-CCP | 28.60 | 99.69 | 98.35 | 68.74 |

CCP, cyclic citrullinated peptide antibody; CCPP, citrullinated caspase 14 peptide; NPV, negative predictive value; PPV, positive predictive value; RA, rheumatoid arthritis.

## Competing interests

The authors declare that they have no competing interests.

## Contributors

XW, CW, HL, and YX performed the experiments and analysed the data. HL and YX provided reagents, materials, and analysis tools. XW and CW wrote the original draft of the manuscript. ZL and FH revised the manuscript. FH designed the study and defined the final version of the manuscript. FH is the guarantor.

## Funding

This study was supported by grants from the National Natural Science Foundation of China (32441099, 82371807, and 82171773 to FH; 92374202 and 32141004 to ZL), the Beijing Natural Science Foundation (7252143 to FH), Beijing Medical Science and Technology Promotion Center Excellence Plan (YC202401QX0364 to FH), the Beijing Nova Program (Z181100006218044 and Z211100002121163 to FH), and the Peking University People's Hospital Research and Development Funds (RZG2024-01 to FH).

## Patient consent for publication

Not applicable.

## Ethics approval

The study protocol was approved by the ethics committees of Peking University People's Hospital.

## Provenance and peer review

Not commissioned; externally peer reviewed.

## Data availability statement

The data underlying this article are available in the article or available from the authors upon reasoned request.

## Supplementary materials

Supplementary material associated with this article can be found in the online version at doi:10.1016/j.ard.2025.03.019.

## Orcid

Fanlei Hu: http://orcid.org/0000-0002-3892-3164

## REFERENCES

[1] Aletaha D, Smolen JS. Diagnosis and management of rheumatoid arthritis: a review. JAMA 2018;320(13):1360–72.
[2] Holers VM, Kuhn KA, Demoruelle MK, Norris JM, Firestein GS, James EA, et al. Mechanism-driven strategies for prevention of rheumatoid arthritis. Rheumatol Autoimmun 2022;2:109–19.
[3] Nishimura K, Sugiyama D, Kogata Y, Tsuji G, Nakazawa T, Kawano S, et al. Meta-analysis: diagnostic accuracy of anti–cyclic citrullinated peptide antibody and rheumatoid factor for rheumatoid arthritis. Ann Intern Med 2007;146(11):797–808.
[4] Hu F, Jiang X, Guo C, Li Y, Chen S, Zhang W, et al. Scavenger receptor-A is a biomarker and effector of rheumatoid arthritis: a large-scale multicenter study. Nat Commun 2020;11(1):1911.
[5] Xie Y, Wei C, Fu D, Zhang W, Du Y, Huang C, et al. Large-scale multicenter study reveals anticitrullinated SR-A peptide antibody as a biomarker and exacerbator for rheumatoid arthritis. Sci Adv 2025;11(1):eadr8078.
[6] Han P, Hou C, Zheng X, Cao L, Shi X, Zhang X, et al. Serum antigenome profiling reveals diagnostic models for rheumatoid arthritis. Front Immunol 2022;13:884462.
[7] Denecker G, Ovaere P, Vandenabeele P, Declercq W. Caspase-14 reveals its secrets. J Cell Biol 2008;180(3):451–8.
[8] Wegner N, Lundberg K, Kinloch A, Fisher B, Malmström V, Feldmann M, et al. Autoimmunity to specific citrullinated proteins gives the first clues to the etiology of rheumatoid arthritis. Immunol Rev 2010;233(1):34–54.
[9] Himbert M, Jourde-Chiche N, Chapart L, Charles N, Baumstarck K, Daugas E. Anti-dsDNA IgE: a potential non-invasive test for prediction of lupus nephritis relapse. RMD Open 2024;10(2):e004255.
[10] Li YN, Guo JP, He J, Liu X, Yin FR, Ding Y, et al. Serum IgA against type 3 muscarinic acetylcholine receptor is a novel marker in diagnosis of Sjögren's syndrome. Chin Med J (Engl) 2011;124(16):2490–5.

Xihua Wei[1], Chaonan Wei[1], Hongying Lin[1], Yang Xie[1], Zhanguo Li[1,2,3], Fanlei Hu[1,3,4,*]
[1] *Department of Rheumatology and Immunology, Peking University People's Hospital & Beijing Key Laboratory for Rheumatism Mechanism and Immune Diagnosis, Beijing, China*
[2] *Peking-Tsinghua Center for Life Sciences, Peking University, Beijing, China*
[3] *State Key Laboratory of Natural and Biomimetic Drugs, School of Pharmaceutical Sciences, Peking University, Beijing, China*
[4] *Department of Integration of Chinese and Western Medicine, School of Basic Medical Sciences, Peking University, Beijing, China*
*__Correspondence to__ Prof. Fanlei Hu, Department of Rheumatology and Immunology, Peking University People's Hospital, Beijing, China.
*E-mail address:* fanleihu@bjmu.edu.cn (F. Hu).

Ann Rheum Dis 84 (2025) 1442–1444

Contents lists available at ScienceDirect

Annals of the Rheumatic Diseases

journal homepage: https://www.sciencedirect.com/journal/annals-of-the-rheumatic-diseases

Letter

# The immune response to the dermatomyositis-specific autoantigen nuclear matrix protein 2 can result in experimental autoimmune myositis

Dermatomyositis (DM) is a subtype of idiopathic inflammatory myopathy characterised by myositis and specific rashes, and its aetiology remains unclear. Several myositis-specific autoantibodies (MSAs) have been detected in DM patients, with each MSA reportedly related to distinct pathogenesis and clinical phenotypes [1]. Antinuclear matrix protein 2 (NXP2) autoantibody-positive DM is characterised by severe muscular involvement and subcutaneous calcinosis [1]. In recent years, several murine models mimicking idiopathic inflammatory myopathies characterised by MSAs have been reported [2–5]. Here, we show that experimental autoimmune myositis can develop following immunisation with NXP2 peptides.

There are 3 conserved domains within NXP2: the GHKL-type ATPase domain, a CW-type zinc finger domain, and a coiled-coil dimerisation domain [6]. Two corresponding human NXP2 peptide sequences, aa 1 to 455 and aa 455 to 939, were chosen for active immunisation (Fig, A, Supplementary Fig S1). Dot blot assays revealed that the 2 peptides were recognised by sera from DM patients with anti-NXP2 autoantibodies separately (Supplementary Fig S2). To investigate the pathogenic properties of anti-NXP2 autoantibodies, we injected wild-type C57BL/6 mice with 2 different NXP2 peptides separately once a week for 4 weeks (Supplementary Materials). The production of autoantibodies to the corresponding NXP2 peptides, body weight, grip strength, serum creatine kinase levels, and histological changes in each group were investigated 2 weeks after the fourth immunisation. Dot blot assays revealed that the sera from the mice injected with each NXP2 peptide presented signals for the corresponding peptides, whereas the sera from the control individuals presented no signals (Fig, B). Compared with the control mice, the peptide-1 (aa 1-455)–injected mice and peptide-2 (aa 455-939)–injected mice presented significantly decreased body weight and grip strength (Fig, C,D). Our results also revealed that the serum creatine kinase levels in the peptide-1–injected group and peptide-2–injected group were greater than those in the control group, but a significant difference was detected only between the peptide-1–injected group and the control group (Fig, E). Histological analysis of muscles from the peptide-1–injected mice and peptide-2–injected mice revealed atrophic myofibers (dotted box), necrotic myofibers (arrowhead), increased infiltration of inflammatory cells, overexpression of major histocompatibility complex class I, and capillary C5b-9 deposition (triangles) (Fig, F). Typical perifascicular atrophy was not detected in the present study, but a trend towards perifascicular atrophy was detected only in 1 peptide-2–injected mouse (arrow in Fig, F). No inflammation was observed in other organs, including the skin or lungs. The histological scores of the hamstrings and quadriceps of the peptide-1–injected group and peptide-2–injected group were significantly greater than those of the control group (Fig, G). Our quantitative real-time polymerase chain reaction analyses revealed that messenger RNA (mRNA) expression of the type I interferon-related gene *IFIT1* was significantly upregulated in the muscle tissues of the peptide-1–injected group compared with those of the controls (Fig, H). Further, the mRNA expression levels of *ISG15, Mx1, RSAD2,* and *SIGLEC1* in the peptide-1–injected group and peptide-2–injected group showed increased trends (Supplementary Fig S3).

Our findings indicate that immunity to NXP2 can contribute to the development of myositis in mice, which is consistent with previous reports showing that muscle and/or lung inflammation could be induced by immunisation with other DM-specific autoantigens (transcriptional intermediary factor 1$\gamma$ and melanoma differentiation-associated protein 5) in mice [2,3]. There are several limitations to this murine model, including the lack of several DM-like phenomena (skin rashes, joint contractures, perifascicular atrophy, and upregulation of some type I interferon-related genes in the muscle). The immunogenicity of the full-length NXP2 protein or other shorter peptides was also not evaluated. In summary, our new model, which is based on autoimmunity against the ubiquitous intracellular autoantigen NXP2, provides a useful tool for investigating the pathologic mechanisms of anti-NXP2 autoantibody-positive DM.

## Competing interests

The authors have declared no conflicts of interest.

## Acknowledgements

The authors thank all participants and/or their parents for participating in this study. The authors also acknowledge Y Zuo and J Liu (Peking University First Hospital) for their work in preparing the pathological sections.

https://doi.org/10.1016/j.ard.2025.02.016
Received 11 October 2024; Revised 19 February 2025; Accepted 19 February 2025

0003-4967/© 2025 Published by Elsevier B.V. on behalf of European Alliance of Associations for Rheumatology (EULAR).

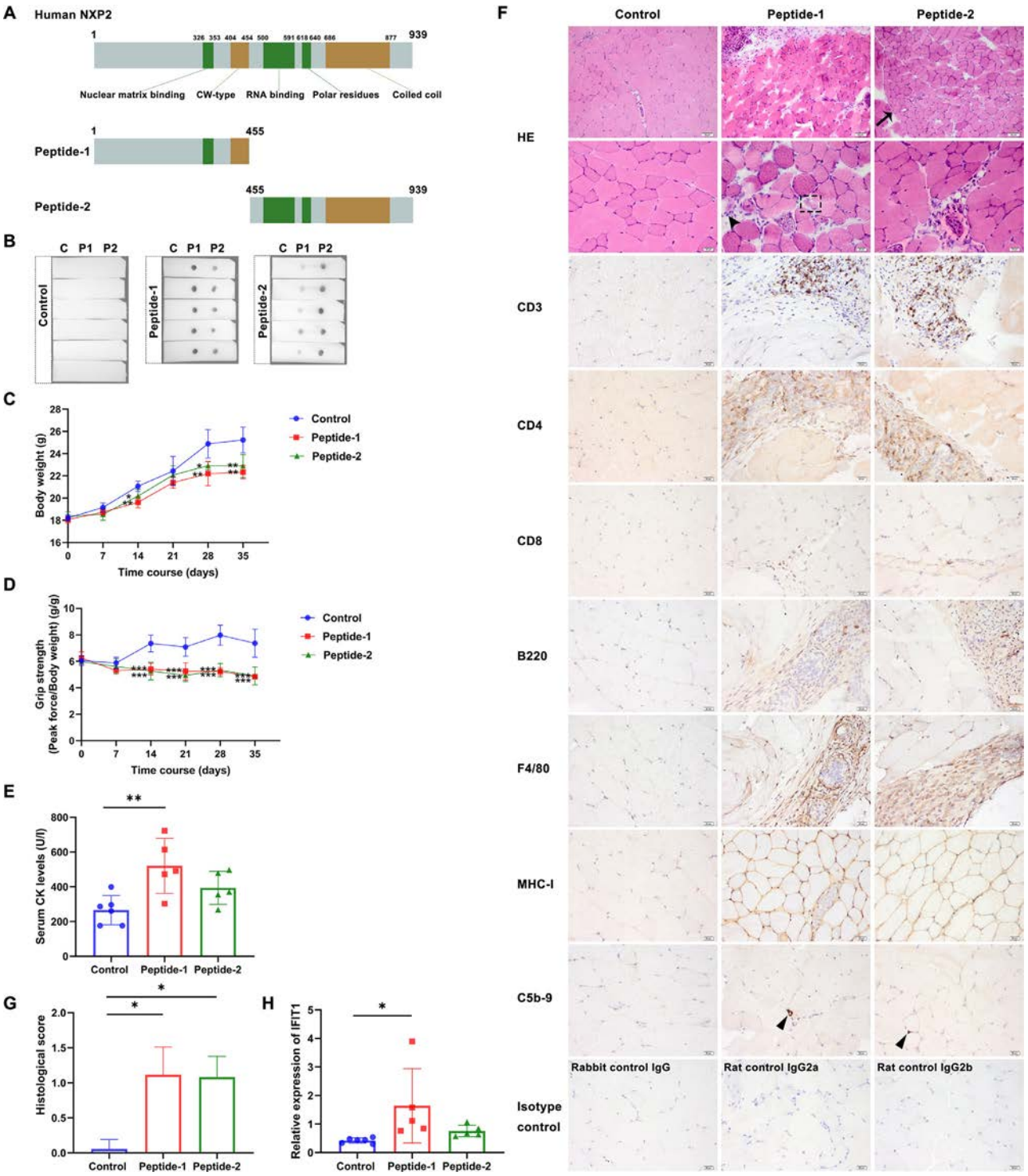



**Figure.** Sequences of the peptides used for active immunisation and evaluation of immunised mice. A, Schematic representation of the peptides used for active immunisation. B, Dot blot of peptide solution (P1 or P2) or RIPA buffer (C) probed with sera from the mice injected with complete Freund's adjuvant alone (control) (n = 6), peptide-1 (n = 5) or peptide-2 (n = 5). C, Body weight of the control (n = 6), peptide-1−injected (n = 5), and peptide-2−injected (n = 5) mice. *$P < 0.05$, ** $P < 0.01$ according to one-way ANOVA with Bonferroni correction. D, Four-limb grip strength of the control (n = 6), peptide-1−injected (n = 5), and peptide-2−injected (n = 5) mice. ***$P < 0.001$ according to one-way ANOVA with Bonferroni correction. E, Serum CK levels of the control (n = 6), peptide-1−injected (n = 5), and peptide-2−injected (n = 5) mice were measured 2 weeks after the fourth immunisation. Dots and bars represent individuals and the mean ± SD, respectively. **$P < 0.01$ according to one-way ANOVA with Bonferroni correction. F, Representative HE staining and immunohistochemistry results for CD3, CD4, CD8, B220, F4/80, MHC-I, and C5b-9 in the hamstrings and quadriceps of the control (n = 6), peptide-1−injected (n = 5), and peptide-2−injected (n = 5) mice. Histological analysis of muscles from the peptide-1−injected mice and/or peptide-2−injected mice revealed a trend towards perifascicular atrophy (arrow), atrophic myofibers (dotted box), necrotic myofibers (arrowhead), increased infiltration of inflammatory cells, overexpression of MHC-I, and capillary C5b-9 deposition (triangles). Bars in the first panels represent 50 μm; bars in the other panels represent 20 μm. G, Histological scores for experimental myositis in the hamstrings and quadriceps of the control (n = 6), peptide-1−injected (n = 5), and peptide-2−injected (n = 5) mice 2 weeks after the fourth immunisation. Bars represent the mean ± SD. *$P < 0.05$ according to the Kruskal-Wallis test with Dunn's multiple comparisons test. H, Fold changes in the messenger RNA levels of *IFIT1*, which were normalised to *β-actin* messenger RNA levels, in skeletal muscle tissues from the control (n = 6), peptide-1−injected (n = 5), and peptide-2−injected (n = 5) mice 2 weeks after the fourth immunisation. Dots and bars represent individuals and the mean ± SD, respectively. *$P < 0.05$ according to one-way ANOVA with Bonferroni correction. RIPA, radioimmunoprecipitation assay; CK, creatine kinase; HE, hematoxylin and eosin; MHC-1, major histocompatibility complex class I; *IFIT1*, interferon-induced protein with tetratricopeptide repeats 1; IgG, immunoglobulin G; NXP2, antinuclear matrix protein 2; ANOVA, analysis of variance.

## Contributors

YW and QY performed the *in vivo* and *ex vivo* experiments and data analysis. Y Zhao, QG, HH, FG, JD, and WZ provided technical help and expertise. YW and Y Zheng contributed to the study concept and design and drafted the manuscript. ZW, YY, and Y Zheng revised the final version of the manuscript for intellectual content. YY and Y Zheng are responsible for the overall content as the guarantors. All authors discussed the results, commented on the article, and gave final approval to the publication.

## Funding

This work was supported by the National Natural Science Foundation of China (grant number 82201550).

## Patient consent for publication

Not applicable.

## Ethics approval

All participants provided written informed consent for inclusion before they participated in the study. The study was approved by the Ethics Committee of Peking University First Hospital (2021[061]) and was conducted in accordance with the guidelines established in the World Medical Association Declaration of Helsinki. All the animal experiments were reviewed and approved by the Institutional Animal Care and Use Committee of Peking University First Hospital (approval ID: J2022145) and were conducted in strict compliance with their guidelines.

## Provenance and peer review

Not commissioned; externally peer reviewed.

## Data availability statement

All data relevant to the study are included in the article or uploaded as supplementary information.

## Patient and public involvement

Patients and/or the public were not involved in the design or conduct or reporting or dissemination plans of this research.

## Supplementary materials

Supplementary material associated with this article can be found in the online version at doi:10.1016/j.ard.2025.02.016.

## REFERENCES

[1] Lundberg IE, Fujimoto M, Vencovsky J, Aggarwal R, Holmqvist M, Christopher-Stine L, et al. Idiopathic inflammatory myopathies. Nat Rev Dis Primers 2021;7(1):86. doi: 10.1038/s41572-021-00321-x.

[2] Okiyama N, Ichimura Y, Shobo M, Tanaka R, Kubota N, Saito A, et al. Immune response to dermatomyositis-specific autoantigen, transcriptional intermediary factor 1$\gamma$ can result in experimental myositis. Ann Rheum Dis 2021;80(9):1201–8. doi: 10.1136/annrheumdis-2020-218661.

[3] Ichimura Y, Konishi R, Shobo M, Tanaka R, Kubota N, Kayama H, et al. Autoimmunity against melanoma differentiation-associated gene 5 induces interstitial lung disease mimicking dermatomyositis in mice. Proc Natl Acad Sci U S A. 2024;121(16):e2313070121. doi: 10.1073/pnas.2313070121.

[4] Katsumata Y, Ridgway WM, Oriss T, Gu X, Chin D, Wu Y, et al. Species-specific immune responses generated by histidyl-tRNA synthetase immunization are associated with muscle and lung inflammation. J Autoimmun 2007;29(2-3):174–86. doi: 10.1016/j.jaut.2007.07.005.

[5] Bergua C, Chiavelli H, Allenbach Y, Arouche-Delaperche L, Arnoult C, Bourdenet G, et al. *In vivo* pathogenicity of IgG from patients with anti-SRP or anti-HMGCR autoantibodies in immune-mediated necrotising myopathy. Ann Rheum Dis 2019;78(1):131–9. doi: 10.1136/annrheumdis-2018-213518.

[6] Groh S, Milton AV, Marinelli LK, Sickinger CV, Russo A, Bollig H, et al. Morc3 silences endogenous retroviruses by enabling Daxx-mediated histone H3.3 incorporation. Nat Commun 2021;12(1):5996. doi: 10.1038/s41467-021-26288-7.

Yikang Wang[1,2], Qingyue Yuan[1], Yawen Zhao[1], Qiang Gang[1], Yuanyuan Ma[3], Hongjun Hao[1], Feng Gao[1], Jianwen Deng[1,4], Wei Zhang[1,4], Zhaoxia Wang[1,4], Yun Yuan[1,4,†,*], Yiming Zheng[1,†,*]

[1] *Department of Neurology, Peking University First Hospital, Beijing, China*

[2] *Department of Neurology, The First Affiliated Hospital of Zhengzhou University, Zhengzhou, China*

[3] *Animal Center, Peking University First Hospital, Beijing, China*

[4] *Beijing Key Laboratory of Neurovascular Disease Discovery, Beijing, China*

*Correspondence to Dr Yun Yun and Yiming Zheng.

*E-mail addresses:* yuanyun2002@126.com (Y. Yuan), 804067836@qq.com (Y. Zheng).

[†]Yun Yuan and Yiming Zheng contributed equally to this paper, and they are co-corresponding authors.

Ann Rheum Dis 84 (2025) e36–e37

Contents lists available at ScienceDirect

Annals of the Rheumatic Diseases

journal homepage: https://www.sciencedirect.com/journal/annals-of-the-rheumatic-diseases

Response

# Correspondence to: 'CD19-CAR T-cell therapy induces deep tissue depletion of B cells' by Tur et al

We read with interest the recent paper from Tur et al [1] detailing changes in lymph node cell populations in autoimmune disease patients before and after CAR T-cell therapy in comparison with B-cell-directed biologic therapy with rituximab.

We had a few additional questions and points to raise for consideration. The authors show the ablation of B-cell populations in lymph nodes after CAR T-cell therapy, during a period of peripheral B-cell depletion, with general preservation of B-cell populations in lymph nodes after rituximab therapy. To help tie this contrasting histologic finding between CAR T-cell therapy and B-cell-directed biologic therapy, it would be interesting to investigate evidence of active CAR T-cell presence and surveillance in lymph nodes during the period of B-cell aplasia. Better access, persistence, and efficacy of infiltrating T cells in target tissues compared with monoclonal antibodies may be a salient feature of this novel therapeutic modality.

Another interesting aspect that is unanswered is how the lymph nodes would appear after B-cell reconstitution. Data from such peripheral B-cell reconstitution after CAR T-cell therapy from the same centre [2] showed peripheral recovery of B cells after a mean of 112 days, with a naive B-cell phenotype, implying an immunologic reset. Would the lymph node cell populations, after such peripheral B-cell recovery, in particular dendritic cells and T helper follicular cells, reflect a histologic reset, or might there be some histologic features of autoimmune activity despite peripheral quiescence of disease? Conversely, the altered architecture of these nodes may be associated with a delay or absence of immunological reset, and this could have adverse implications for long-term outcomes.

Regarding the immunohistochemical staining of the data, we note that the authors had used only CD23 to mark follicular dendritic cells (Fig 2A in Tur et al [1]). However, CD23 is a B-cell antigen and not a specific marker for follicular dendritic cells. Thus, the staining observed may be on B cells rather than follicular dendritic cells. More clarity is required on this front, either by exploring the morphology of the stained cells or through the use of specific follicular dendritic cell markers [3]. These findings may significantly impact the hypotheses regarding why CD19 CAR T cells may be more effective than rituximab.

Lastly, while the authors compare pre- and post-CAR T-cell findings with rituximab-treated patients as a control, it may be interesting to see what lymph node changes are observed with plasma cell-directed therapies, such as daratumumab (CD38 targeting biologic). Data from recent studies suggest plasma cell-directed therapy may also induce significant clinical improvement, as well as a decline in autoantibody production [4]. Would such plasma cell-directed therapy (with anti-CD38 also targeting plasmablasts) produce broader changes in lymph nodes, such as impacting follicular dendritic cell and T helper follicular cells, as well as reaching plasma cell (CD138+) populations in lymph nodes? Alternatively, one may find that targeting these cells at an earlier stage when they express CD19 but not CD38 may be a more effective approach to depleting tissue-resident plasma cells.

Nevertheless, the overall model implied, with the focused targeting of B cells with anti-CD19 CAR T cells, that inducing loss of follicular dendritic cells and T helper follicular cells in lymph nodes suggests that autoreactive B cells act as a central driver of autoimmunity, with follicular dendritic cell and T helper follicular cell activity and survival secondary to B-cell presence and activity. Deep B-cell depletion, including within lymph nodes, with anti-CD19 CAR T-cell therapy clearly represents a new frontier and paradigm for autoimmune disease. We look forward to further translational results that help explain the mechanisms behind such clinical findings.

## Competing interests

All authors declare they have no competing interests.

## CRediT authorship contribution statement

**Rahul K Patel:** Conceptualization, Writing – original draft, Writing – review & editing. **Chandra Mohan:** Conceptualization, Writing – original draft, Writing – review & editing.

## Funding

This research did not receive any specific grant from funding agencies in the public, commercial, or not-for-profit sectors.

## Patient consent for publication

Not applicable.

## Ethics approval

Not applicable.

## Provenance and peer review

Not commissioned; externally peer reviewed.

https://doi.org/10.1016/j.ard.2025.02.015
Received 19 February 2025; Accepted 22 February 2025

0003-4967/© 2025 European Alliance of Associations for Rheumatology (EULAR). Published by Elsevier B.V. All rights are reserved, including those for text and data mining, AI training, and similar technologies.

## Orcid

Rahul K Patel: http://orcid.org/0000-0003-4337-0696

## REFERENCES

[1] Tur C, Eckstein M, Velden J, Rauber S, Bergmann C, Auth J, et al. CD19-CAR T-cell therapy induces deep tissue depletion of B cells. Ann Rheum Dis 2025;84 (1):106–14.

[2] Müller F, Taubmann J, Bucci L, Wilhelm A, Bergmann C, Völkl S, et al. CD19 CAR T-cell therapy in autoimmune disease - a case series with follow-up. N Engl J Med 2024;390(8):687–700. doi: 10.1056/NEJMoa2308917.

[3] van Nierop K, de Groot C. Human follicular dendritic cells: function, origin and development. Semin Immunol 2002;14(4):251–7.

[4] Alexander T, Ostendorf L, Zernicke J, Klotsche J, Schneider U, Biesen R, et al. Safety and efficacy of daratumumab in systemic lupus erythematosus - a single-center phase 2 open-label trial. Ann Rheum Dis 2024;83:237–8.

Rahul K Patel[1,*], Chandra Mohan[2]
[1] *AyurBio Consulting, Coppell, TX, USA*
[2] *Science & Engineering Research Center, University of Houston, Houston, TX, USA*
*__Correspondence to__ Dr. Rahul K. Patel, AyurBio Consulting, Coppell, TX, USA.
*E-mail address:* rpatel@ayurbiocs.com (R.K. Patel).

Ann Rheum Dis 84 (2025) e38–e39

Contents lists available at ScienceDirect

Annals of the Rheumatic Diseases

journal homepage: https://www.sciencedirect.com/journal/annals-of-the-rheumatic-diseases

Response

# Response to the correspondence on "CD19-CAR T-cell therapy induces deep tissue depletion of B cells"

We appreciate the insightful comments by the authors regarding our recent paper [1]. We agree that detecting CAR T cells within the lymph nodes would have been interesting. However, the anti-CAR antibodies have been specifically developed for flow cytometry and are not suitable for recognising dehydrated and cross-linked epitopes in formalin-fixed paraffin-embedded (FFPE) sections. We have tested the available antibodies in our laboratory and found no specific staining in FFPE sections despite confirming positive results in flow cytometry assays. As we have focused on the assessment of lymph node architecture, we did not have enough biopsy material to perform additional flow cytometry in these samples.

We also agree that investigating lymph node architecture after B-cell reconstitution is of great interest. To explore this, we performed sequential lymph node analyses before and after CD19-CAR T-cell therapy in 3 patients (2 systemic lupus erythematosus and 1 systemic sclerosis) in whom the follow-up lymph node biopsy was done when B cells in the periphery were depleted (60 days after CAR T-cell infusion) and when B cells were repopulated (1-year after CAR T-cell infusion). Our observations revealed the reconstitution of normal follicular structures with B cells, follicular dendritic cells (FDCs), and T follicular helper (TFH) cells, suggesting a complete histological reset of the B-cell zone (Fig, described below).

Regarding the authors' concern about the specificity of CD23 as a marker for FDCs, several aspects should be considered. Among the commonly used FDC markers in immunohistochemistry (CD21, CD35, and CD23), CD21 and CD35 are generally expressed in both primary and secondary (activated) follicles,

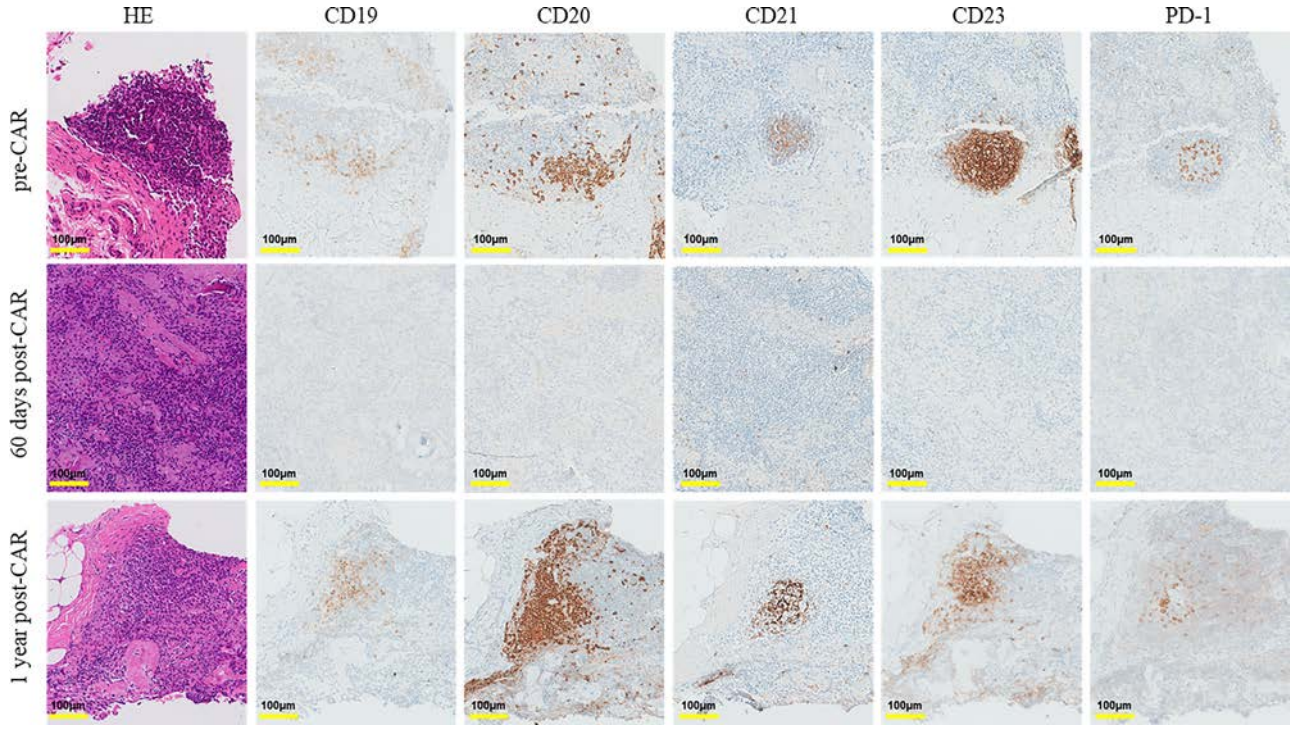



**Figure.** Representative haematoxylin and eosin (HE) images of lymph node biopsy specimens taken from a patient with systemic lupus erythematosus before (pre) and 60 days and 1 year after anti-CD19 CAR T-cell therapy (post), alongside representative immunohistochemistry images showing CD19+ and CD20+ B cells, CD21+ and CD23+ follicular dendritic cells (FDCs), and PD-1+ T follicular helper (TFH) cells.

https://doi.org/10.1016/j.ard.2025.03.006
Received 13 March 2025; Accepted 17 March 2025

0003-4967/© 2025 European Alliance of Associations for Rheumatology (EULAR). Published by Elsevier B.V. All rights are reserved, including those for text and data mining, AI training, and similar technologies.

whereas CD23 is more specifically associated with FDCs within germinal centre structures of secondary follicles [2,3]. Using haematoxylin and eosin (HE) staining and immunohistochemistry, we focused on germinal centre structures in pretreatment biopsies, where CD23+ FDCs were present. However, as shown in the HE staining (Fig 2A in the study by Tur et al [1]), no germinal centres were identified after treatment, and consequently, CD23+ FDCs were also absent. Additionally, while CD21 is also expressed by B cells, raising a similar specificity concern as CD23, we performed CD21 staining at multiple time points (before treatment, 60 days after treatment, and 1 year after treatment). This approach further confirmed the absence of FDCs following CD19-CAR T-cell therapy and their reappearance after 1 year (Fig, described above).

We concur with the authors that lymph node assessment could substantially improve our understanding of the tissue effects of drugs other than CD19 CAR T cells. Daratumumab, a therapeutic monoclonal antibody targeting CD38, is an excellent example, as the expression of CD38 differs from that of CD19 and includes the plasma cell compartment. Therefore, treatment with daratumumab might induce reduction or even depletion of CD138+ plasma cells in the lymph nodes. Notably, CD38 is also expressed by germinal centre B cells [4], which could point to an effect of daratumumab on the follicular structures of the lymph nodes. Depth of depletion, however, would also depend on the efficacy of monoclonal antibodies, such as daratumumab, to reach sufficient concentrations in the target tissue.

Taken together, we think that analysis of the lymph nodes of patients with autoimmune disease provides an exciting and feasible opportunity to understand the effects of therapeutic interventions on the human immune system and to better understand the phenomenon of immune reset [5].

## Competing interests

GS reports speaking and lecture fees from Novartis, Janssen, Kyverna, and Cabaletta.

## CRediT authorship contribution statement

**Carlo Tur:** Data curation, Methodology. **Markus Eckstein:** Data curation, Methodology. **Georg Schett:** Writing – review & editing. **Maria Gabriella Raimondo:** Data curation, Writing – original draft, Writing – review & editing.

## Funding

This research did not receive any specific grant from funding agencies in the public, commercial, or not-for-profit sectors.

## Patient consent for publication

Consent obtained directly from patient.

## Ethics approval

All procedures were performed in accordance with the Good Clinical Practice guidelines of the International Council for Harmonization and covered by license 334_18 B and 24-13-B of the Institutional Review Board (IRB). All participants gave written informed consent according to CARE guidelines and in compliance with the Declaration of Helsinki principles. No commercial sponsor was involved.

## Provenance and peer review

Not commissioned; externally peer reviewed.

## Orcid

Carlo Tur: http://orcid.org/0009-0003-6241-6116
Markus Eckstein: http://orcid.org/0000-0001-5418-3349
Georg Schett: http://orcid.org/0000-0001-8740-9615
Maria Gabriella Raimondo: http://orcid.org/0000-0003-2020-6711

## REFERENCES

[1] Tur C, Eckstein M, Velden J, Rauber S, Bergmann C, Auth J, et al. CD19-CAR T-cell therapy induces deep tissue depletion of B cells. Ann Rheum Dis 2025;84(1):106–14.
[2] Allen CDC, Cyster JG. Follicular dendritic cell networks of primary follicles and germinal centers: phenotype and function. Semin Immunol 2008;20(1):14–25.
[3] Kurshumliu F, Sadiku-Zehri F, Qerimi A, Vela Z, Jashari F, Bytyci S, et al. Divergent immunohistochemical expression of CD21 and CD23 by follicular dendritic cells with increasing grade of follicular lymphoma. World J Surg Oncol 2019;17(1):115.
[4] Zeng F, Zhang J, Jin X, Liao Q, Chen Z, Luo G, et al. Effect of CD38 on B-cell function and its role in the diagnosis and treatment of B-cell-related diseases. J Cell Physiol 2022;237(7):2796–807.
[5] Junt T, Calzascia T, Traggiai E, da Costa AN, Gergely P, Schett G, et al. Defining immune reset: achieving sustained remission in autoimmune diseases. Nat Rev Immunol 2025 Mar 5. doi: 10.1038/s41577-025-01141-w. Online ahead of print.

Carlo Tur
*Department of Internal Medicine 3 - Rheumatology and Immunology, Friedrich-Alexander-Universität (FAU) Erlangen-Nürnberg and Universitätsklinikum Erlangen, Erlangen, Germany*
*Deutsches Zentrum Immuntherapie (DZI), Friedrich-Alexander-Universität (FAU) Erlangen-Nürnberg and Universitätsklinikum Erlangen, Erlangen, Germany*
*Division of Rheumatology-Fondazione Policlinico Universitario A. Gemelli IRCCS - Università Cattolica del Sacro Cuore, Rome, Italy*

Markus Eckstein
*Institute of Pathology and Comprehensive Cancer Center EMN, Friedrich-Alexander Universität (FAU) Erlangen-Nürnberg and Universitätsklinikum Erlangen, Erlangen, Germany*

Georg Schett
*Department of Internal Medicine 3 - Rheumatology and Immunology, Friedrich-Alexander-Universität (FAU) Erlangen-Nürnberg and Universitätsklinikum Erlangen, Erlangen, Germany*
*Deutsches Zentrum Immuntherapie (DZI), Friedrich-Alexander-Universität (FAU) Erlangen-Nürnberg and Universitätsklinikum Erlangen, Erlangen, Germany*
*Division of Rheumatology-Fondazione Policlinico Universitario A. Gemelli IRCCS - Università Cattolica del Sacro Cuore, Rome, Italy*

Maria Gabriella Raimondo *
*Department of Internal Medicine 3 - Rheumatology and Immunology, Friedrich-Alexander-Universität (FAU) Erlangen-Nürnberg and Universitätsklinikum Erlangen, Erlangen, Germany*
*Deutsches Zentrum Immuntherapie (DZI), Friedrich-Alexander-Universität (FAU) Erlangen-Nürnberg and Universitätsklinikum Erlangen, Erlangen, Germany*
***Correspondence to** Dr Maria Gabriella Raimondo
*E-mail address:* mariagabriella.raimondo@uk-erlangen.de (M.G. Raimondo).